



Seroprevalence of Fasciolosis in Sheep in the Alkut City

Thuraya .Kh.Abdul-Wahed* and Amer.M. Al-Amery

Department of Parasitology, College of Veterinary Medicine, University of Baghdad, Baghdad,Iraq.

Received: 22 Sep 2018

Revised: 24 Oct 2018

Accepted: 27 Nov 2018

*Address for Correspondence

Thuraya .Kh.Abdul-Wahed

Department of Parasitology,
College of Veterinary Medicine,
University of Baghdad,Baghdad,Iraq.
Email: Thuraya1155@gmail.com



This is an Open Access Journal / article distributed under the terms of the **Creative Commons Attribution License** (CC BY-NC-ND 3.0) which permits unrestricted use, distribution, and reproduction in any medium, provided the original work is properly cited. All rights reserved.

ABSTRACT

The study was conducted to investigate the prevalence of ovine fasciolosis in Alkut slaughter house. A total number of the examined sheep was 360 (205 males and 155 females). Results revealed that the prevalence was 21.94%. The effect of sex on the infection rate was not significant. Also, results showed that the infection rate of females (50%) in autumn was significantly ($P<0.05$) higher than infection rate in male (25.92%). For serological examination using ELISA applied on 200 blood samples which were collected from suspected sheep from Alkut slaughterhouse in different ages and sexes results showed that the total positive samples was 41 % (82/200).

Keywords: ovine fasciolosis, ELISA, sheep,

INTRODUCTION

Fasciolosis, or fascioliasis, is one of the most important helminth infections of ruminants in the world caused by digenean trematodes belonged to the Phylum Platyhelminthes of Class Trematoda, and the genus *Fasciola* spp. which are a common liver flukes and the common species are *F. gigantica* and *F. hepatica* (1). Mas-Coma *et al.*, (2) reported that *F. hepatica* can be found in temperate zones and *F. gigantica* in tropical areas, and that both species may be overlapped in subtropical zones. Fasciolosis in animal cause severe and enormous economic losses all over the world due to the mortality, morbidity, susceptibility to secondary infections, cost of treatment and control, decrease in weight gain of animal reduced carcass quality, besides the condemnation of infected liver,(3).

In Iraq, there are many studies of *Fasciola* infection, some of these studies recorded infection percentage about 3.3% in females and 0.82 % in males(4). The prevalence of animal fasciolosis has been carried out in different parts of KSA (5). Between all serologic procedures ELISA method is usually have a high sensitivity, specificity, accuracy and easy to perform for paraclinical goals in parasitic infections in endemic areas (6,7). Therefore, the present study was carried out to estimate the prevalence of *Fasciolosis* in sheep in alkut slaughter house and to use the serological diagnosis of *Fasciolosis* by ELISA.





Thuraya.Kh.Abdul-Wahed and Amer.M.AI-Amery

MATERIALS AND METHODS

Samples Collection

In this study, three hundred and sixty livers of sheep were examined in the Alkut slaughter house. A weekly visit was made to the slaughter house at the period of the examination that extended from January to December 2017. The age of animals ranged between less than year month to up 3 year for both sexes.

Post-Mortem examination

For each slaughtered sheep, The infected livers were thoroughly examined alongside, it was located on a plank and the livers and bile ducts were firstly inspected to identify existence of *Fasciola sp.* to apply the routine inspection procedures to the internal organs. If there is a sign of fasciolid flukes is found, the case was classified as immature and mature worms and the gross lesions were recognized (8). The primary examination included visualization and palpation of the organs, while secondary examination included make more incision of liver and bile duct opening. For generalized fasciola infection (liver fluke), we have made incision in different parts of the liver to confirm the presence of fluke in liver parenchyma. The cut liver was pressed in order to flukes squeeze out from the tissue and smaller bile ducts. Each collected flukes from animal was examined and classified on the basis of shape and size (9).

Blood samples and Separation of serum

Two hundred blood samples were collected from suspected sheep before slaughtering. After collection of blood through the jugular vein, blood was transferred into gel tube (without anticoagulant) and allowed to stand in refrigerator for 15 minutes and centrifuged at speed of up to 3500 RPM for 5 minutes. Serum was aspirated by a pipette and transferred into Eppendorf tubes kept frozen in (-20 C°) until use.

Procedure Indirect IgG-ELISA

Commercial versions of MM3-SERO (BIO K 211) are available from Bio-X Diagnostics. The samples were performed in this test according to the instructions of the company.

Statistical analysis

The Statistical Analysis System-SAS (2012) program was used to explain the differences factors in this study parameters. For significant comparison between percentages, Chi-square test has been used to explain results of this study.

RESULTS

Epidemiological study

All samples collected were recorded under different condition, like; season, age and sex. The total number of the examined sheep was (360) included 205,155 male and female respectively, while the total number of infected sheep was (n= 79) with percentage (21.94%) . table (1).





Infection percentage of Fascioliosis according to the sex

The total infection rate of fascioliosis was 18.53% in the males and 26.49% in the females. The statistical analysis showed that however, the infection rate was higher in females as compared with males but there was no significant differences ($P > 0.05$) (Table 2).

Infection percentage of Fascioliosis according to age

Results showed that the highest infection percentage were recorded in female sheep > 3 years of age with percentage (36.73 %) on the other hand, In male results showed that highest infection percentage were in age (2-3)year with percentage (28.07%) .Statistically results confirmed that the association between Age groups and sex for infection rate was significant ($P = 0.001$) table (3).

Infection percentage of fascioliosis according to the seasons

According to the season of this study, the highest infection rate was recorded in female with percentage (50%) in Autumn, and highest infection rate in male was in winter with percentage (34.78%). Statistically, the differences in the infection rates of males and females due to season were significant ($P < 0.0001$). Table (4)

Serological examination

Two hundred blood samples were collected from suspected sheep from Al-Kut slaughter house in different ages and sexes. All samples were subjected to ELISA. The results showed that 82 serum samples (41 %) were positive.

Infection percentage of Fascioliosis according to the sex by using ELISA

The total percentage % of infection by ELISA according to sex in sheep was between (29.89 % to 59.55%) for male and female, respectively. The statistical analysis showed that there were significant differences ($P < 0.0001$) between them. Table (5).

Infection percentage of Fascioliosis according to age by using ELISA

Results showed that the highest infection percentage were recorded in female sheep > 3 years of age with percentage (36.73 %) on the other hand, In male results showed that highest infection percentage were in age (2-3)year with percentage (28.07%) . Statistically results confirmed that the association between Age groups and sex for infection rate was significant ($P = 0.001$) (table 6).

DISCUSSION

The total percentage infection in sheep was (18.53%, 26.49%) for male and female, the incidence of Fasciola in female sheep was higher than that of male. This result coincided with all previous studies that conducted field surveys in the massacres to detect parasitic diseases that need a long time to appear (10) this because of the fact of that females are rarely slaughtered except at old ages and consequently the chances of being infected with parasitic infections are higher than that of males which are often slaughtered in young ages (4). %. A study of Al-juboury, (11) in holly karbala province' slaughter house recorded that the percentage of fascioliosis in sheep and was (1.62). While, Dakhil (12) documented that the infection with *F. gigantica* in sheep in slaughters of Al-Amara abattoir about 1.62%. In contrast, other researcher observed that the prevalence of fascioliosis in sheep in Baghdad city was 40.8% (13). Wajdi and Nassir (14) at Baghdad slaughter house showed that the percentage of infection with *F. gigantica* was 9.1, in



**Thuraya.Kh.Abdul-Wahed and Amer.M.AI-Amery**

sheep. However, Al-Obaidy (15) noted the prevalence of *F.gigantica* ova from sheep's feces was (4.4 %) in Mousl province. In 2017, in Karbala city the study showed that the percentage was (2.27 to 3.5%) for male and female, respectively. (16). the prevalence of animal fasciolosis has been carried out in different parts of KSA (5).

Statistical analysis of infection rates on the basis of age indicated a significant difference ($P < 0.05$) among different age groups. The decrease in infection rate (prevalence rate) as age increase is the result of acquired immunity which is manifested by humoral response and tissue reaction in bovine liver due to previous challenge (17). The incidence of fasciolosis during this study in male sheep was high in Autumn months (September, October and November) and this was disagree with (16) who found that the highest infection rate of fasciolosis in spring months (March and April) and the lowest infection rate of present study was in summer months this was disagree with Mahdi and Al-Baldawi (18) who found that the highest percentage was in summer months reaching 4.06 % followed by the spring months 3.33% while the infection rate decreased to 2.66% in winter months.

Several studies conducted have shown that the incidence of fasciolosis is high along the months of year, however, is relatively higher in autumn and winter than in the rest of the year (19). the present study serum sample 82 (41%) samples were seropositive in the applied ELISA test this was higher than oliewi (20) who recorded 28 (12.73) percentage in sheep in Abu Ghriab district in Baghdad this may be because of this areas had more wet than other, the result is represented to the disease in area since the higher sensitivity of applied test which can reach to 98% (21) As well as there is lack of strategically control measures in area .

While our study was lower than that recorded by Al-khafajy, (22)(67.7%) who used 43 sheep in his study as well as the environmental changing that happen in present study area and Hussain, (16) ,in karbala city recorded (69.89%) in sheep. The sensitivity and specificity of all serologic assays are varying according to the population on which they are tested (23,24) and the season at which samples are being tested (25).

CONCLUSION

The statistical analysis showed that there were a no significant differences under ($P < 0.05$) between the percentage of infection in male and female sheep (0.07). According to seasons the highly percentage of infection was in autumn (4.12%), while the lowest percentage was in summer (0.00%). The statistical analysis showed that there were a no significant differences under ($P < 0.05$) between percentage of infection in male and female cow (0.28). In sheep the highly percentage of infection was in march (6.84) while the low percentage was also in November (0.00%). The results showed that the infection of sheep with fasciolosis in sheep more than in cattle, and infection in female more than male, also infection occur in spring season.

REFERENCES

1. Massoud, A.M., Shalaby, H.A., El Khateeb, R.M., Mahmoud, M.S., Kutkat, M.A., 2012. Effects of Mirazid and myrrh volatile oil on adult *Fasciola gigantica* under laboratory conditions. Asian. Pac. J. Trop. Biomed. 2, 875–884.
2. Mas-Coma, S., Bargues, M.D., Valero, M.A., 2005. Fasciolosis and other plant-borne trematode zoonoses. Inter. J. Parasitol. 35, 1255–1278.
3. Tadele T. and worku T. (2007). The Prevalence and Economic Significance of Bovine Fasciolosis at Jimma, Abattoir, Ethiopia. Int.J.Vet. Med. 3:15.
4. Farhan H.S. (2016) Morphological and Molecular Study of *Fasciola gigantica* in Buffaloes and Cows. University of Basrah College of Veterinary Medicine.
5. Khanjari, A., Bahonar, A., Fallah, S., Bagheri, M., Alizadeh, A., Fallah, M., Khanjari, Z., (2014). Prevalence of fasciolosis and dicrocoeliosis in slaughtered sheep and goats in Amol Abattoir, Mazandaran, northern Iran. Asian Pac. J. Trop. Dis. 4, 120–124.





Thuraya.Kh.Abdul-Wahed and Amer.M.AI-Amery

6. Anderson, N., Luong, T.T., Vo, N.G., Bui, K.L., Smooker, P.M., Spithill, T.W., 1999. The sensitivity and specificity of two methods for detecting Fasciola infections in cattle. *Vet. Parasitol.* 83, 15–24.
7. Kralova-Hramadova, I., Spakulova, M. Horackova, E. Turcekova, L. Novobilsky, A. Beck, R. Koudela, B. Marinculic, A. Rajskey, D., Pybus, M.(2008) Sequences analysis of ribosomal and mitochondrial genes of the giant liver fluke *Fascioloides magna* (Trematoda: Fasciolidae): intraspecific variation and differentiation from *Fasciola hepatica*. *Journal of Parasitology*, 98, 58-67.
8. Sohair IB, Eman MN. Histopathological and bacteriological studies on livers affected with fascioliasis in cattle. *Egy.J.comp.path. and clinic. Path.* 2009; 22(1):19-45.
9. Soulsby, E.J.L. (1982). *Helminths, Arthropods and Protozoan's of Domesticated Animals*. 7th Ed. Bailliemre Jindal, London.
10. AL-Fattlawi,M.A.A. (2002). Study in the epidemiology and biology of hydatid cysts in kadesia province M.sc. thesis. College of Vet. Med., Baghdad. University.
11. Al-Juboury, M.M.O. (2008). Epidemiological study vitality about infection final and intermediate hosts of *Fasciola gigantica* in Karbala. , M.Sc. Thesis, Educ.Coll. Unvi. Karbala. 79pp.
12. Dakhil , H. G. (2012). Epidemiology of *Fasciola gigantica* infection in cattle, sheep and intermediate host in Missan / southern Iraq.M.Sc. Thesis , Educ.Coll. Basrah. univ. 66pp.
13. AL-Nammy, R.A.S. (1978). Studies on some aspects of bovine fasciolias In Iraq with particular reference to pathology and hematology of the disease due to *Fasciola gigantica* infection. M SC. Thesis College of Vet. Medicine Univ. Baghdad.
14. Wajdi, N. and Nassir, J. K. (1983). Studies on the parasitic helminths of slaughtered animals in Iraq. Parasitic helminthes of livers of herbivores. *Ann. Trop. Med. Parasitol.*, 77: 583-585.
15. Al-Obaidy, W.A. A. (2001). Epidemiological study satisfactory for the liver worms *Fasciola gigantica* of the sheep in Nineveh Governorate. M.Sc. Thesis, Veterinary Coll. Mosul Unvi. 81pp.
16. Hussain K. L. and Zghair Z. R. (2017). Serological and pathological study of fascioliosis in cattle, sheep and human in karbala province.M.Sc. Thesis.Zoonosis, Coll. of Vet. Med./ Baghdad University, Iraq.
17. Ogunrinade AF, Okan ED, Fasan M (1982). The prevalence of Bovine fasciolosis in Nigeria. *Trop. Anim. Health Afr.* 29:381-397.
18. Mahdi, N. K. and Al-Baldawi , F. A. K. (1987). Hepatic fascioliasis in the abattoirs of Basrah. *Ann. Trop. Med. Parasitol.*, 81: 377-379.
19. Arafa, M.I. (2007). Liver fluke (fascioliosis) and their effect on national economy. *Assiut J. Environ.studies*,33:23-46.
20. Oliewi kh.I. (2017). Eidemiological study on fascioliosis in sheep in Abu Ghraib district/ Baghdad . M SC. Thesis College of Vet. Medicine Univ. Baghdad.
21. salimi-Begestani, M. R.; McGarry, J. W.; Felstead, S.; Ortiz, P.; Akca, A. and Williams, D. J. (2005). Development of an antibody- detection ELISA for *Fasciola hepatica* and its evaluation against a commercially available test. *Res.in Vet.Sci.*,78:177-181.
22. Al-khafajy, A.M.A. (2011). Detection of fascioliosis in sheep and cattle by using of ELISA technique . *Al-Qadisiya J.Vet. Med. Sci.*, 10(1):131-135.
23. Whiting, P., Rutjes, A.W., Reitsma, J.B., Glas, A.S.,Bossuyt, P.M., Kleijnen, J. (2004) Sources of variation and bias in studies of diagnostic accuracy: a systematic review. *Annals of Internal Medicine*, 140, 189–202.
24. Leeflang, M.G., Bossuyt, P.M.M. (2005) Test accuracy is likely to vary depending on the population it is used in. *Veterinary Parasitology* 134, 189.
25. Charlier, J., De Meulemeester, L. Claerebout Williams, E.D., Vercruysse, J. (2008) Qualitative and quantitative evaluation of coprological and serological techniques for the diagnosis of fasciolosis in cattle. *Veterinary Parasitology*, 153, 44–51.





Thuraya.Kh.Abdul-Wahed and Amer.M.AI-Amery

Table 1: The total number of examined and infected sheep with *Fasciolosis* with percentage of infection:

Total No.	No. of Positives samples	Percentage (%)	No. of Negatives samples	Percentage (%)
360	79	(21.94%)	281	(78.05%)

Table 2 : Infection percentage of *Fasciola spp.* in sheep according to the sex

sex	No. of examined	No. of infected	Percentage of infection (%)
Male	205	38	(18.53%)
Female	155	41	(26.49%)
Total No.	360	79	(21.94%)
Chi-Square value	3.22		
P	0.07		

Table 3 : Percentage of infection of *fasciolosis* in sheep according to the age

Age	No. of examined		Total no.	No. of infected and percentage(%)		Total percentage (%)
	Male	Female		Male	Female	
<1 year	44	29	73	2 (4.54%)	1 (3.44%)	3 (4.1%)
1-2 year	59	32	91	10 (16.94%)	9 (28.12%)	19 (20.87%)
2-3 year	57	45	102	16 (28.07%)	13 (28.88%)	29 (28.34%)
3<	45	49	94	10 (22.22%)	18 (36.73 %)	28 (29.78)
Total no.	205	155	360	38	41	79
Chi-Square value	23.91					
P	0.001					

*No significant difference between male and female at level of (P<0.05).





Thuraya.Kh.Abdul-Wahed and Amer.M.AI-Amery

Table 4| Infection percentage of *fascioliosis* according to the seasons

Season	No. of examined		No. of infected		Percentage of infection (%)		Chi square value	P
	Male	Female	Male	Female	Male	Female	Chi square value	P
Spring	56	34	8	8	26.45%	23.52%	1.23	0.26
Summer	49	41	0	0	0 %	0%	-	-
Autumn	54	36	14	18	25.92%	50%	5.46	<0.05
Winter	46	44	16	15	34.78%	34.09 %	0.005	0.94
Total no.	205	155	38	41	18.53%	26.45%	3.22	0.07
Chi square value			21.81	26.47				
P			<0.0001	<0.0001				

**Results confirmed that the association between Age groups and sex for infection rate was significant (P=0.001).

Table 5: Infection percentage of *Fascioliosis* according to sex by using ELISA

Sex	No. of examined	No. of infected	Percentage of infection (%)
Male	97	29	(29.89 %)
Female	89	53	(59.55%)
Total No.	200	82	(41 %)
Chi square value			15.36
P			<0.0001

**Significant difference between male and female at level of (<0.0001).

Table6 : Infection percentage of *Fascioliosis* according to age by using ELISA

Age	No. of examined	No. of infected	Percentage of infection (%)
<1 year	32	9	28.12 %
1-2 year	53	19	35.84 %
2-3 year	56	25	44.64 %
3<	45	29	64.44 %
Total no.	200	82	41 %
Chi square value			12.37
P			<0.01

The differences in the infection rates between age groups were significant (P <0.01)





Genotyping of *Cryptosporidium* Spp. Isolated from Human and Cattle in Baghdad Province, Iraq

Maysoon A. Merdaw^{1*}, Mohammed Th. S. Al-Zubaidi², Dalya B. Hanna³, Ilham A. Khalaf⁴ and Huda S. Jassim²

¹College of Pharmacy, University of Baghdad, Baghdad, Iraq

²College of Veterinary Medicine, University of Baghdad, Baghdad, Iraq

³College of Pharmacy, University of Al-Mustansiyria, Baghdad, Iraq

⁴Al-Razi Center for Research and Diagnostic Kits, Ministry of Industry and Minerals, Baghdad, Iraq

Received: 18 Sep 2018

Revised: 22 Oct 2018

Accepted: 27 Nov 2018

*Address for Correspondence

Maysoon A. Merdaw

College of Pharmacy,
University of Baghdad,
Baghdad, Iraq

Email: MaysoonA.Merdaw@copharm.uobaghdad.edu.iq



This is an Open Access Journal / article distributed under the terms of the **Creative Commons Attribution License** (CC BY-NC-ND 3.0) which permits unrestricted use, distribution, and reproduction in any medium, provided the original work is properly cited. All rights reserved.

ABSTRACT

Cryptosporidiosis is an intestinal protozoan parasitic disease that infects human and animals, caused by apicomplexan parasite belong to the genus of *Cryptosporidium*. The current study was done to record the infection rate of cryptosporidiosis in human and cattle, and genotype the clinical isolates of *Cryptosporidium* in Baghdad Province. A total of 265 stool sample were collected (150 from human and 115 from cattle) during the period from December 2016 to the May 2017. Cryptosporidial infection was detected using modified acid fast stain. DNA of the parasite was extracted from oocysts of positive fecal samples and nested PCR method was used for partial 60 kDa glycoprotein (*gp60*) gene amplification then sequence analysis for selected samples. The total infection rates of *Cryptosporidium* in human and cattle were 47.33% (71/150), 35.63% (41/115) respectively. The results of this study record that *Cryptosporidium parvum* was found in all positive samples of human and cattle except two human samples which were *Cryptosporidium hominis*, and all were belonging to the common allele family IIa. The prevalent zoonotic subtype of *C. parvum* species (IIa) in this study highlights the significance of zoonotic transmission of cryptosporidiosis in the country.

Keywords: *Cryptosporidium*, human, cattle, genotyping.



**Maysoon A. Merdaw et al.**

INTRODUCTION

Cryptosporidium spp. are apicomplexan parasites that have a wide occurrence in developed and developing countries and infecting humans and various animal hosts (Liu et al., 2014). *Cryptosporidium* species infect different sites including intestine, stomach, and respiratory system (Plutzer and Karanis, 2009). At least five genotypes/species of *Cryptosporidium* infect humans: a human genotype (*C. hominis*) found only in humans and 4 zoonotic genotypes: bovine genotype in cattle (*C. parvum*), avian (*C. meleagridis*), cat (*C. felis*) and dog (*C. canis*) found mainly in animals. Cattle cryptosporidiosis is usually associated with four main species, i.e., *C. parvum*, *C. andersoni*, *C. ryanae*, and *C. bovis* (Robertson et al., 2014; Chen F and Huang, 2012 and Xiao, 2009). *Cryptosporidium parvum* cause changes in mucosubstances secreted from goblet cells of mucosal villi and submucosal glands (Al-Kennany et al., 2012), also resulting in villus atrophy, microvillus shortening, and destruction in the intestine (De-Graaf et al., 1999). Severity of the disease ranges from asymptomatic or mild to severe, intractable diarrhea with wasting depending on immune status, nutrition, and age. Transmission is fecal-oral with both human and animal reservoirs (Stefan and Honorine, 2010). Although diarrhea in livestock results in economic loss, symptomatic and asymptomatic infections in animals have the potential for transmission and are a threat to public health (Bowman and Forster, 2010).

The most common methods for diagnosis of the parasite oocysts in feces of infected man or animals is by staining with modified acid fast stain (Chalmers and Katzer, 2013; Al-Zubaidi, 2017). The molecular methods are essentially used for the identification of the species, genotype, and subtype of *Cryptosporidium* because the oocysts of many species are indistinguishable from one another. In this way the identification of the organism which is responsible for the infection and the source and routes of transmission becomes more applicable (Ryan et al., 2014). According to previous studies the molecular investigations to define the parasite species used genetic marker, the gene encoding the glycoproteins GP60 which is the single most polymorphic marker identified so far in the *Cryptosporidium* genome (Widmer G and Sullivan., 2010).

MATERIALS AND METHODS

Collection of Stool samples

A total of 265 fecal samples from both sexes were collected during the period from early December 2016 to the end of May 2017. Selected geographic regions of Baghdad city were (Al-Hurria, Al-Gazaliya, Al-Shuala and Al-Chcok). 150 sample from human (49 handlers and 101 non handlers) in different ages from less than 1 year to more than 40 year, visited government hospitals for treatment because of gastrointestinal symptoms. 115 samples were collected from randomly selected cattle aged from less than 1 year to more than 3-4 years (age of the cattle was determined by their owners). Fecal samples were collected in two aliquots; one of them concentrated by formalin-ethyl-acetate sedimentation method and stained by Modified Ziehl-Neelsen stain to identify *Cryptosporidium* oocysts microscopically as explained previously by (Biderouni and Salehi., 2014), and another aliquot was suspended in a storage medium composed of aqueous potassium dichromate (2.5% w/v, final concentration) and kept at 4 °C for molecular study. The presence of other intestinal parasites detected in some of the samples using various methodologies was not considered in the present study.

DNA isolation and molecular analysis

Prior DNA isolation, positive fecal samples with staining method were washed with distilled water for three times to remove potassium dichromate by centrifugation, and then were subjected to thermal shock to weaken the active oocyst cell walls. A total of five freeze-thaw cycles of 15 minutes at -80°C in a freezer followed by 15 minutes at 65-70°C in a metal bead bath were conducted on each sample (Jiang et al., 2005). Total DNA was extracted from a



**Maysoon A. Merdaw et al.**

quantity of about 200 mg of feces using a DNA isolation kit (Accuprep stool DNA extraction kit, Bioneer Corp. Korea) following the manufacturer's suggested protocols. Purified DNA was stored at -20°C .

Nested polymerase chain reaction and sequencing

Nested polymerase chain reaction was used to amplify a fragment of 400 bp in the *gp60* gene from DNA samples as described (Abe et al., 2006). PCR was conducted in 20 μL volumes using the primers: 5'-ATA GTC TCC GCT GTA TTC-3' and 5'-GCA GAG GAA CCA GCA TC-3' in the first round of PCR employing the following thermal cycling protocol: one cycle of initial denaturation at 94°C for 3 min, followed by 32 cycles of: denaturation at 94°C for 30 s, annealing at 42°C for 30 s, and extension at 72°C for 1 min, then followed by a final extension at 72°C for 7 min. In the second round, 1 μL of the primary amplicon was subjected to the PCR using primers 5'-TCC GCT GTA TTC TCA GCC-3' and 5'-GAG ATATAT CTT GGT GCG -3' employing the same cycling protocol. A positive control and a negative control (DNA free sample) were included in each set of PCR of this study. The PCR products were sent to Macrogen Co./ Korea where they were subjected to direct sequencing. *Cryptosporidium* species and subtypes were identified by using the BLAST search against the GenBank database.

Ethical issues

This research project was approved by the Ethics Committee of the University of Baghdad-College of Pharmacy (No. 112016-A1).

RESULTS

Cryptosporidium parvum was found in all positive samples of human and cattle except two human samples which were *Cryptosporidium hominis*. The *Cryptosporidium* infection rate was 47.33% in human (46% *C. parvum* and 1.33% *C. hominis*) and 35.63% in cattle (all were *C. parvum*). The peak of human positive rates were seen among children less than 1 year old which was 68 % when it compared with other age groups (table 1), and the higher cattle infection, 43.75% appeared also in age (< 1) year (table 2). The infection rate of *Cryptosporidium spp.* in human was higher in handlers than non- handlers as shown in table 3.

***Cryptosporidium* genotypes**

Figure 1 showed the nested PCR analysis of the *gp60* gene DNA preparations of all 112 specimens yielded products of the expected size (400 bp) on the gel electrophoresis.

PCR products were sequenced for 10 human samples and 16 cattle samples, and the analyses of the partial *gp60* sequence data were aligned with sequences obtained from previous studies allowed the genotypic classification of isolates. The genotyping of most of the remaining isolates was failed due to very small amounts of fecal materials that were available. Moreover, the extraction technique used has reduced DNA productivity. *GP60* subtypes were identified according to the number of serine-coding trinucleotide repeats (TCA or TCG) in the 5' region of the gene. The subtype name usually starts with the designation of subtype family, followed by the TCA number (represented by the letter A) and TCG (represented by the letter G). Some subtypes have one copy of the sequence ACATCA immediately after the trinucleotide repeats whereas others have two, therefore R1 and R2 are used to differentiate the two types of sequences (Sulaiman et al., 2005). All isolates of *C. parvum* and *C. hominis* were belonged to the previously described subtype family IIa and all were R1 except the two *C. hominis* isolates which were undecided subtype (Table 3). Two subtypes of human isolates were recognized within the *C. parvum* subtype family IIa including IIaA15G2R1 (2/10) and IIaA22G1R1 (6/10) (Table 3), while the subtypes of cattle isolates were six including IIaA15G2R1 (4/16), IIaA16G2R1 (2/16), IIaA16G3R1 (4/16), IIaA17G2R1 (2/16), IIaA19G3R1 (2/16) and





Maysoun A. Merdaw et al.

IlaA22G1R1 (2/16) as shown in Table 4. Representative sequences of *C. parvum* subtypes of human isolates in this study submitted to the GenBank under accession numbers LC383634 to LC383637, and the one of *C. hominis* under submission. Cattle subtypes are under accession numbers LC383638 to LC383645.

DISCUSSION

Cryptosporidium parvum is responsible for most of the diarrheic outbreaks. Results of the study have shown a predominance in human of *C. parvum*, and it is in a higher percentage for handlers than the non-handlers, indicating that zoonotic pathway is expected due to close contact with cattle. *C. parvum* is responsible for zoonotic and anthroponotic infections in both urban and rural settings worldwide (Xiao et al., 2000). The common occurrence of zoonotic subtypes of *C. parvum* in cattle highlights the potential role of these animals as significant reservoirs of infection to humans (Ehsan et al., 2015; Nget et al., 2012; Adam et al., 2014). *C. parvum* and *C. hominis* found in 46% and 1.33% of positive samples respectively in human. Previous Iraqi studies reported a prevalence of 72.9% and 24.3% human samples in Mid-Euphrates Area (Abdul-Sada, 2015), while Salman found *C. parvum* percentage 16.28 in Kirkuk (Salman et al., 2015). These findings also supported by some studies in Iran, indicating that *C. parvum* and *C. hominis* are the most prevalent species in humans and that *Cryptosporidium parvum* is the dominant species (Ryan et al., 2016; Xiao, 2010). The predominance of *C. parvum* and the low proportion of infections due to *C. hominis* in a population has been considered the result of zoonotic transmission (Sulaiman et al., 2005). Thus, anthroponotic transmission was possibly less important in human in current study.

In Baghdad, the tap water is the major source of drinking water, and this can indicate the low importance of water-borne transmission in Baghdad province and this agrees with a study done by AL-Waridin in the north of Baghdad that all tap water samples were free of *Cryptosporidium* (AL-Warid, 2010). The higher infection of *C. parvum* was appeared in age younger than 1 year for both human and cattle. This agrees with the data from less severe management systems in different regions of the world (Rahiet et al., 2013; Benhouda et al., 2017 and Budu-Amoako et al., 2012). A previous study confirmed that the high molecular subtyping resolve of the GP60 an immune dominant antigen which is recognized by almost all infected individuals and animals, especially in outbreak surveys or transmission-dynamics studies (Cama et al., 2007). The present study is considered the first regarding genotyping and subtyping of *Cryptosporidium* in human and cattle in Iraq. Subtypes in the allele family Ila are commonly seen in both humans and cattle in the current study. Allele Ila is almost exclusively the only allele family found in cattle (Alves et al., 2003; Penget et al., 2003). In Baghdad, *C. parvum* IlaA22G1R1 was the most endemic subtype for human, while for cattle both IlaA15G2R1 and IlaA16G3R1. The most common allele for human in a city in northern of Iran was the zoonotic subtype IId A17G1d (Sharbatkhoriet al., 2015). In France, IlaA16G3R1 genotype was the most frequent subtype for cattle with no geographic clustering (Sharbatkhoriet al., 2015).

Sequencing of a fragment of the GP60 locus revealed an undecided subtype Ila belonging to *Cryptosporidium hominis* in two non-handlers human samples referred also to age less than 1 year group. An undecided subtype may be because the presence of mixed subtypes or several genotypes (Sulaiman et al., 2005; Razakandrainibe et al., 2018). IlaA15G2R1 and IlaA22G1R1 *C. parvum* subtypes were isolated from both humans and animals in our study, while in Egypt the subtype IIdA20G1 within *C. parvum* was isolated from both animals and humans (Ibrahim et al., 2016). In a rural area in the north of Tunisia, two subtypes, *C. parvum* IIdA16G1 and IlaA15G2R1 were identified in children and calves respectively (Rahmouniet al., 2014). IlaA15G2R1 was the most endemic subtype reported in China for cattle (Gong et al., 2017) and in Kuwait for the children, also found in Jordanian human samples (Hijawiet al., 2016). That indicates the subtype IlaA15G2R1 of *C. parvum* is more prevalent in cattle but it can transmit to human, and this mentioned in Fayer study that both human and bovine genotypes may be transmitted from person-to-person (Fayer et al., 2000). Consumption of raw milk and its products by most people of the studied areas is known to be a risk factor, also supported the zoonotic transmission of cryptosporidiosis.





Maysoon A. Merdaw et al.

CONCLUSION

Cryptosporidium parvum was the most common species found in Iraqi human and cattle for current study. Subtype family IIa was the only one found for of *C. parvum* and *C. hominis* in all studied samples suggest that zoonotic transmission play an important role in human Cryptosporidiosis in our country. Biosafety measures of personal hygiene and food hygiene, may reduce the levels of cryptosporidiosis infections and environmental contamination. More studies are needed on *Cryptosporidium* isolates to improve knowledge in subtype analysis and transmission of cryptosporidiosis in other provinces in Iraq.

ACKNOWLEDGMENTS

Authors would like to thank Al-Razi center of medical research for the technical assistance. This work was private financially supported, and the authors declare that there is no conflict of interests.

REFERENCES

- 1- Abe N, Matsubayashi M, Kimata I, Iseki M. (2006). Subgenotype analysis of *Cryptosporidium parvum* isolates from humans and animals in Japan using the 60-kDa glycoprotein gene sequences. *Parasitol Res.* 99 (3):303–05.
- 2- Abdul-Sada K M. (2015). Molecular and Epidemiological Study of *Cryptosporidium* spp. in Mid-Euphrates Area. *Kufa Journal for Nursing Sciences.* 5 (1): 102-112.
- 3- Adamu H, Petros B, Zhang G, Kassa H, Amer S, Ye J, Feng Y and Xiao L. (2014). Distribution and clinical manifestations of *Cryptosporidium* species and subtypes in HIV/AIDS patients in Ethiopia. *PLoS Neglected Tropical Diseases.* 8, e2831.
- 4- Alves M, Xiao L, Sulaiman I, Lal A A, Matos O and Antunes F. (2003). Subgenotype analysis of *Cryptosporidium* isolates from humans, cattle, and zoo ruminants in Portugal. *J. Clin. Microbiol.* 41:2744–2747.
- 5- Al-Kennany E R, Rahawi A M and Al-Jabori S A. (2012). Histopathological and Histochemical Study of Intestinal Cryptosporidiosis in Mice. *Kufa journal For Veterinary Medical Sciences.* 3 (2): 36-44.
- 6- AL-Warid H S. (2010). Study in Epidemiology and PCR Detection of Cryptosporidiosis in North of Baghdad. College of Science, University of Baghdad. Ph.D. thesis.
- 7- Al-Zubaidi, M.Th.S. (2017). Molecular and microscopic detection of *Cryptosporidium* spp. *International J of Science and Nature.* 8 (2) 372-376.
- 8- Benhouda D, Hakem A, Sannella A R, Benhouda A and Cacciò S M. (2017). First molecular investigation of *Cryptosporidium* spp. in young calves in Algeria. *Parasite.* 24: 15.
- 9- Biderouni FT and Salehi N. (2014). Detection of *Cryptosporidium* infection by modified ziehl-neelsen and PCR methods in children with diarrheal samples in pediatric hospitals in Tehran. *Gastroenterol Hepatol Bed Bench.* 7(2): 125–130.
- 9- Bowman DD and Forster AL. (2010). Cryptosporidiosis and giardiasis in dogs and cats: veterinary and public health importance. *Exp Parasitol.* 124: 121–127.
- 10- Budu-Amoako E, Greenwood SJ, Dixon BR, Barkema HW and McClure JT. (2012). *Giardia* and *Cryptosporidium* on dairy farms and the role these farms may play in contaminating water sources in Prince Edward Island, Canada. *Journal of Veterinary and Internal Medicine.* 26: 668–673.
- 11- Cama V A, Ross J M, Crawford S, Kawai V, Chavez-Valdez R, Vargas D, Vivar A, Ticona E, Navincopa M, Williamson J, Ortega Y, Gilman R H, Bern C and Xiao L. (2007). Differences in Clinical Manifestations among *Cryptosporidium* Species and Subtypes in HIV-Infected Persons. *The Journal of Infectious Diseases.* 196 (5): 684–691.
- 12- Chalmers RM and Katzer F. (2013). Looking for *Cryptosporidium*: the application of advances in detection and diagnosis. *Trends Parasitol.* 29: 237-251.
- 13- Chen F and Huang K. (2012). Prevalence and molecular characterization of *Cryptosporidium* spp. in dairy cattle from farms in China. *Journal of Veterinary Science.* 13(1), 15–22.





Maysoon A. Merdaw et al.

- 14- De-Graaf DC, Vanopdenbosch E, Ortega-Mora LM, Abbassi H and Peeters JE. (1999). A review of the importance of cryptosporidiosis in farm animals. *International Journal for Parasitology*.29(8), 1269–1287.
- 15- Ehsan AM, Geurden T, Casaert S, Parvin SM, Islam TM, Ahmed UM, Levecke B, Vercruyse J and Claerebout E. (2015). Assessment of zoonotic transmission of *Giardia* and *Cryptosporidium* between cattle and humans in rural villages in Bangladesh. *PLoS One*.10(2), 1–11.
- 16- Fayer R, Morgan U and Upton SJ. (2000). Epidemiology of *Cryptosporidium*: transmission, detection and identification. *Int J Parasitol*. 30: 1305–1322.
- 17- Gong Ch, Cao X, Deng L, Li W, Huang X, Lan J, Xiao Q, Zhong Z, Feng F, Zhang Y, Wang W, Guo P, Wu K. and Peng G. (2017). Epidemiology of *Cryptosporidium* infection in cattle in China: a review. *Parasite*.24: 1.
- 18- Hijjawi N, Mukbel R, Yang R, Ryan U. (2016). Genetic characterization of *Cryptosporidium* in animal and human isolates from Jordan. *Vet Parasitol*. 228: 116-20.
- 19- Ibrahim MA, Abdel-Ghany AE, Abdel-Latef GK, Abdel-Aziz SA and Aboelhadid SM. (2016). Epidemiology and public health significance of *Cryptosporidium* isolated from cattle, buffaloes, and humans in Egypt. *Parasitology Research*.115: 2439–2448.
- 20- Jiang, J.; Alderisio, K. A.; Singh, A.; Xiao, L. (2005). Development of procedures for direct extraction of *Cryptosporidium* DNA from water concentrates and for relief of PCR inhibitors. *Appl Environ Microbiol*. 71, 1135-1141.
- 21- Liu H, Shen Y, Yin J, Yuan Z, Jiang Y, Xu Y, Pan W, Hu Y and Cao J. (2014). Prevalence and genetic characterization of *Cryptosporidium*, *Enterocytozoon*, *Giardia* and *Cyclospora* in diarrheal outpatients in China. *BMC Infectious Diseases*.14(1), 290–292.
- 22- Ng JSY, Eastwood K, Walker B, Durrheim DN, Massey PD, Porigneaux P, Kemp R, Mckinnon B, Laurie K and Miller D. (2012). Evidence of *Cryptosporidium* transmission between cattle and humans in northern New South Wales. *Experimental Parasitology*.130(4), 437–441.
- 23- Peng M M, Wilson M L, Holland R E, Meshnick S R, Lal A A and Xiao L. (2003). Genetic diversity of *Cryptosporidium* spp. in cattle in Michigan: implications for understanding the transmission dynamics. *Parasitology Research*. 90:175–180.
- 24- Plutzer J and Karanis P. (2009). Genetic polymorphism in *Cryptosporidium* species: an update. *Veterinary Parasitology*.165(3–4), 187–199.
- 25- Rahi A A, Ali M A and Al-Charrakh A H. (2013). Prevalence of *Cryptosporidium parvum* among children in Iraq. *American Journal of Life Sciences*.1(6): 256-260.
- 26- Rahmouni I, Essid R, Aoun K and Bouratbine A. (2014). Glycoprotein 60 diversity in *Cryptosporidium parvum* causing human and cattle cryptosporidiosis in the rural region of Northern Tunisia. *American Journal of Tropical Medicine and Hygiene*.90: 346–350.
- 27- Razakandrainibe R, Diawara E I, Costa D, Goff L L, Lemeteil D, Ballet J J, Gargala G, Favennec L. (2018). Common occurrence of *Cryptosporidium hominis* in asymptomatic and symptomatic calves in France. *PLoS Negl Trop Dis*. 12(3):e0006355.
- 28- Robertson LJ, Bijorkman C, Axen C and Fayer R. (2014). *Cryptosporidiosis in farmed animals*, in *Cryptosporidium: parasite and disease*. Cacciò SM, Widmer G, Editors. Springer-Verlag: Wien.149–235.
- 29- Ryan U, Fayer R and Xiao L. (2014). *Cryptosporidium* species in humans and animals: current understanding and research needs. *Parasitology*. 141: 1667-1685.
- 30- Ryan U, Zahedi A and Paparini A. (2016). *Cryptosporidium* in humans and animals-a one health approach to prophylaxis. *Parasite Immunol*. 38: 535-47.
- 31- Salman Y J, Sadek W S and Rasheed Z K. (2015). Prevalence of *Cryptosporidium parvum* among Iraqi displaced people in Kirkuk city using direct microscopy, flotation technique and ELISA-copro antigen test. *Int.J.Curr.Microbiol.App.Sci*. 4(11): 559-572.
- 32- Sharbatkhori M, Mojarad E N, Taghipour N, Pagheh A and Mesgarian F. (2015). Prevalence and Genetic Characterization of *Cryptosporidium* Spp. In Diarrheic Children from GonbadKavoos City, Iran. *Iran J Parasitol*. 10 (3): 441–447.





Maysoon A. Merdaw et al.

- 33- Sulaiman IM, Hira PR, Zhou L, Al-Ali FM, Al-Shelahi FA, Shweiki HM, Iqbal J, Khalid N and Xiao L. (2005). Unique endemicity of cryptosporidiosis in children in Kuwait. *J Clin Microbiol*.43 (6):2805–09.
- 34- Stefan C A and Honorine D W.(2010). Cryptosporidiosis: Environmental, therapeutic, and preventive challenges. *Eur J Clin Microbiol Infect Dis*. 29(8):927–935.
- 35- Widmer G and Sullivan S. (2010). Genomics and population biology of *Cryptosporidium* species. *Parasite Immunol*.34: 61–71.
- 36- Xiao L. (2009). Molecular epidemiology of cryptosporidiosis: an update. *Experimental Parasitology*.124(1), 80–89.
- 37- Xiao L. (2010). Molecular epidemiology of cryptosporidiosis: an update. *Exp Parasitol*. 124: 80-9.
- 38- Xiao L, Morgan UM, Fayer R, Thompson RCA, Lal AA. (2000). *Cryptosporidium* systematics and implications for Public Health. *Parasitol Today*. 16: 287–292.

Table 1: Prevalence of *Cryptosporidium* in human according to the age groups in Baghdad-Iraq 2017.

Age groups (Year)	Number of cases	Positive	Percentage%
< 1	25	17	68
1-10	25	12	48
11-20	25	13	52
21-30	25	10	40
31-40	24	11	44
>40	26	8	32
Total	150	71	47.33

Table 2: Prevalence of *Cryptosporidium* in cattle according to the age groups in Baghdad-Iraq 2017.

Age groups (Year)	Number of cases	Positive	Percentage%
<1	32	14	43.75
1 – 2	29	10	34.48
2-3	28	10	35.71
3-4	26	7	26.92
Total	115	41	35.65

Table 3: prevalence of *Cryptosporidium* in human according to the host in Baghdad-Iraq 2017.

Host	No of examined samples	No of Positive	Percentage%
Handlers	49	33	67.34
Non handlers	101	38	37.62
Total	150	71	47.33





Maysoon A. Merdaw et al.

Table 4: Distribution of *Cryptosporidium* spp. subtypes in Iraqi human isolates from Baghdad Province.

Species	Subtype	No. of isolates	Accession numbers	Reference
<i>C.parvum</i>	IlaA15G2R1	2	LC383634	IranMG787320
<i>C.parvum</i>	IlaA22G1R1	6	LC383635 LC383636 LC383637	Norway MF062698
<i>C.hominis</i>	Ila*	2	Under submission	Saudi Arabia AJ973149

*an undecided subtype

Table 5: Distribution of *Cryptosporidium parvum* subtypes in Iraqi cattle isolates from Baghdad Province.

Subtype	No. of isolates	Accession numbers	Reference
IlaA15G2R1	4	LC383645	MexicoKY990891
		LC383642	IranMG787320
IlaA16G2R1	2	LC383640	JordanMF770734
IlaA16G3R1	4	LC383639	ChinaKF128741
		LC383641	ChinaKF128741
IlaA17G2R1	2	LC383644	AustraliaMG738818
IlaA19G3R1	2	LC383643	AustraliaFJ839880
IlaA22G1R1	2	LC383638	NorwayMF062698

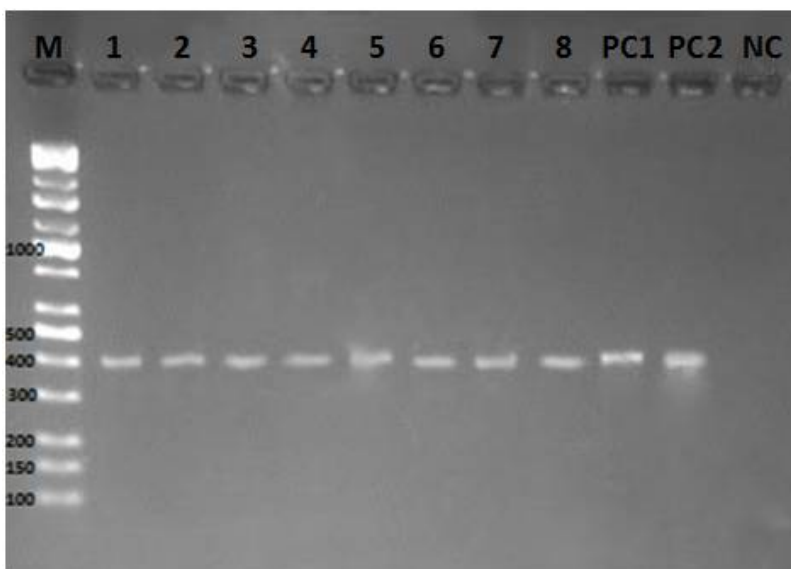


Fig. 1: PCR of *Cryptosporidium* isolates based on partial *gp60* gene. Lanes 1-8 *Cryptosporidium* isolates, PC1: positive control of *C. parvum*, PC2: positive control of *C. hominis*, NC: negative control, M: DNA size marker.





Effects of Sodium Nitroprusside (SNP) on Newcastle Disease Virus in the Infected Broilers.

Aws El-Muntasir H^{1*} and Emad J. Khammas²

¹Department of Pathology and Poultry Diseases, College of Veterinary Medicine, University of Baghdad. Baghdad, Iraq.

²Department of Pathology and Poultry Diseases, college of veterinary medicine, University of Dyala. Iraq.

Received: 23 Sep 2018

Revised: 25 Oct 2018

Accepted: 27 Nov 2018

* Address for Correspondence

Aws El-Muntasir H

Department of Pathology and Poultry Diseases,
College of Veterinary Medicine University of Baghdad,
Baghdad, Iraq.



This is an Open Access Journal / article distributed under the terms of the **Creative Commons Attribution License** (CC BY-NC-ND 3.0) which permits unrestricted use, distribution, and reproduction in any medium, provided the original work is properly cited. All rights reserved.

ABSTRACT

The present work study the therapeutic effects of Sodium Nitroprusside (SNP) on Newcastle disease virus NDV on 20 day old broilers, and compare this material with other antiviral (Amantidine and Verkon®S) and the effects of this therapeutic material on the growth, blood, immune status, histopathology, blood volume in immune organs and body Wight parameters of the infected broilers. The experiment design included one hundred (80) broilers chick (ROSS 308) were used from day one till 45 days.

The chicks were weighted and divided randomly into four groups; 20 birds for each group. All three groups were infected intratracheally with NDV 0.1 ml (50ELD₅₀ 1×10⁷) at 20 day old, the 1st group received SNP in dose (3mg/ml) orally, the 2nd group received the Amantidine in dose (1gm /10L), the 3rd group received the Virkon® S in dose (1gm/L), while the 4th group was control without any treatment or infection. All groups were vaccinated against Newcastle diseases on 5 and 15 day and against Gumboro disease on day 10 of age. The results referred to the antiviral effects of SNP on the NDV and have ability to reduce the loses in poultry in case of Newcastle diseases infection when was used or administrated with other medications to elevate the antibodies titer and increase the ability to resist the diseases.

The SNP group shows vasodilation and highly vascularization with blood vessels filled with erythrocytes and very low inflammatory reactions in the tissues in the different organs (spleen , liver , kidney, thymus, ileum and bursa of fabricious) while the Amantidine and Verkon® S groups shows vacuolation and sever haemorrhages in these organs as compared with the SNP. As a conclusion, the results indicated the antiviral positive effect of SNP on the infected birds with NDV as it reducing mortality and inducing

15933



**Aws El-Muntasir H and Emad J. Khammas**

less pathological lesions, and also increase body performance and increase the immunity of broilers against virus.

Keywords: Sodium Nitroprusside (SNP), Newcastle disease virus, broilers (comet assay).

INTRODUCTION

At present, viral and bacterial diseases represent a considerable problem in medicine, which despite significant progress in the field of biophysics, biochemistry, molecular biology, pharmacology and medicine has not been satisfactorily coped with. Influenza, in comparison with other viral diseases, however the opposite is true. Every year, thousands of people die of influenza or connected complications all over the world (Iramet *et al.*, 2014) . Newcastle disease can affect many species of birds. In addition to poultry, more than 230 species from more than one-half of the 50 orders of birds have been found to be susceptible to natural or experimental infections with avian paramyxoviruses. Chickens are mainly affected by Newcastle disease. Turkeys and pigeons, ducks , geese, as well as parrots and wild cormorants may also develop generalized disease, but clinical signs are rarely reported in geese and ducks. (Capua and Alexander, 2009).

Conventional antiviral agents can interfere successfully with viral proteins and functions (declercq,2004). Nitric oxide has been shown antibacterial and antiviral activity(Vargaet *al.*, 2013)NO is produced by the nitric oxide synthase (NOS) protein family.(Li *et al.*, 2009).Sodium nitroprusside(SNP) Potent vasodilator working through releasing NO spontaneously in blood. Potent vasodilating effects in arterioles and venules. Breaks down in circulation to release nitric oxide (NO).(Vargaet *al.*, 2013).The aim of current study explain the therapeutic effects of Sodium Nitroprusside (SNP) on Newcastle disease virus infected broilers.

MATERIALS AND METHODS

Viruses used in this study were propagated in fertile chicken's eggs. The Allantoic fluid was processed for Hemagglutination assay to detect the viruses. The presence of viruses in the Allantoic fluid was confirmed using the Hemagglutination assay (Alexander & Senne, 2008). The chicken antiserum that has been prepared against one of the strains of NDV is used.Nine-day-old chicken embryonated eggs were prepared from a local hatchery. Sodium Nitroprusside (SNP) materials were ground to a fine powder diluted with distilled water and were mixed with virulent NDV strain (10^7 EID₅₀/mL) and maintained at a room temperature for one hour.A more accurate indication of the true pathogenicity of ND viruses for a susceptible species could come from experimental infection of a statistically significant number (≥ 10) of young and adult birds with a viral standard dose (10^5 EID₅₀) administered via natural routes (intra tracheal route).(Sustaet *al.*.2013).Eighty Broiler (Breed: Rose 308, Origin: Belgium) were brought in good condition from (hatchery in Baghdad) . The chicks were divided randomly into 4 groups, each group contained 20 birds reared in poultry field distance of 10 x 5 m. All management requirements as poultry hygiene standardization were done. Blood samples were collected from jugular vein randomly from 10 chicks in 15 days old for measuring of maternal immunity against Newcastle disease virus (NDV) using ELISA test.Birds bodies weight was done on day 18. The birds inoculated intra tracheally with NDV and some drops of the virus were dropped in the eyes and nostrils, after 24 hrs. the birds divided into 4 groups treated with sodium Nitroprusside , amantadine , verkon®S , and the fourth group was control without treatment.After 7 days the blood samples were collected from the birds .The body weight for each group was measured. The samples of serum were collected to evaluate the Antibody titers against Newcastle disease.





Aws El-Muntasir H and Emad J. Khammas

Statistical analysis

The data were subjected to analysis using SAS software. One way ANOVA was applied and post hoc test least significant differences was done. $P < 0.05$ is considered significant.

RESULTS

The body weight in the experimental groups that supplied SNP was increased significantly ($P < 0.05$) as compared with Amantadine and Verkon® Sin. And the Feed Conversion Ratio (FCR) in the experimental groups that supplied SNP was increased significantly ($P < 0.05$) and it was different than the increase due to Amantadine and Verkon® Sin which it was less.

H/L ratio of broilers during the experiment

According to the results shown in the table below the therapeutic material (SNP) shows same and no significant in different groups.

Blood Volume (ml/gm) in Broilers

The blood volume in immune organs (liver, bursa and thymus) increased significantly ($P < 0.05$) in group treated by SNP if compared with other groups.

DISCUSSION

All birds which were treated with the Sodium Nitroprusside (SNP) or amantadine against Newcastle disease virus showed low neurologic clinical signs after infection if compared with Verkon®S or the control groups. Agree with the neurologist, the exposure of neural cells with NO donors may cause the release of Nervous Nitric Oxide (nNOS), leading to a positive feedback loop in the NO production and subsequently decreasing proliferation and increasing differentiation of neurons (Cheng *et al.* 2003). and obtained good results in weight parameters increase body weight and FCR because of vasodilator effects of SNP which increase the transporting the nutrition leading to increase weights, and high blood volume measured in immune organs of the SNP group compared with the other groups, that showed high mortality and morbidity. After challenge at 20 days old, the statistical analysis showed that (tables) the treated groups with the Sodium Nitroprusside kept their normal Body Weight (BW), Body Weight Gain (BWG), Feed Intake (FI) and Food Conversion Ratio (FCR), this proved protection against the Newcastle disease virus and against the *E. coli* after challenge infections, comparing with the other groups which suffered from weights loss, severe anorexia. The SNP was the efficiency of food utilisation adversely affected (Table). Similarly there was a progressive and significant increase in plasma thiocyanate concentration. It would normally be expected that high plasma thiocyanate would lead to thyroid hypertrophy. This has been observed in an experiment with chicks in which potassium thiocyanate was included in the diet (Elzubeir, 1986). However, because dietary potassium thiocyanate does not depress growth comparisons can be made between birds of similar size. In the present experiment there was a large disparity in body weight and this may have served to obscure effects upon thyroid size. (Fournoux *et al.* 2000).

Treatment with Sodium Nitroprusside (SNP) showed significant ($P < 0.05$) increase in feed intake in certain treated groups as table (2). This may presumably be one of the motives for high body weights. This result is explained by Calignano *et al.*, (1993) who reported that L-arginine-NO pathway had effect on feeding behavior in mammalian species. The results on body weight showed an increase in the live body measurements indicating a direct positive effect in group of Sodium





Aws EI-Muntasir H and Emad J. Khammas

Nitroprusside (SNP) .this resulted in effects of nitric oxide on the intestine muscles as reported in recent studies Bulbul *et al* 2013 mention ,the effect of NO on contractile activity of the small intestine of chickens during different feeding periods. (Bulbul *et al.* 2007).There are some reports of increased NO levels in blood and other tissues after oral administration of NO donors (Rytlewski *et al.* 2005). It has been reported that arginine, a NO donor, either stimulates the immune system or inhibits pulmonary hypertension by increasing NO levels(Hampl and Herget 2000). It is known that NO inhibitors decrease the efficiency of NO *in vitro* (Vapaatalo *et al.* 2000, Bulbul *et al.* 2007).Therefore, we suggest that SNP did not alter the neural NOS expression and nNOS did not exist throughout the nerve fibres of the small intestine and that the intensity of nNOS expression changed during growth of the chickens. The absorption activity of the small intestine and the contraction/relaxation of smooth muscle in the small intestine are the major factors in promoting and regulating the transport and absorption of nutrients (Thompson and Applegate, 2006).

In this study, the effect of SNP on the antibody titers of ND, H/L ratio, organ development, and frequency of mid colon contractions of broilers were investigated during the infection with Newcastle disease . SNP improves the immune defence mechanism of the body against infectious agents (Lee *et al.* 2002). Moreover, SNP modulates or boosts humoral and cellular immune response to experimental infection challenges (Abdulkalykova and Ruiz-Feria 2006).

Previous reports mentioned the exact mechanism of antiviral response of NO against avian viruses as well as *in vivo* activity of LPS against avian viruses are still not defined adequately. Thus, the current observation and previous two observations might indicate that the LPS is indeed a useful antiviral agent that could be used *in vivo* for poultry viral diseases control. Although, there are limitations in the use of LPS in mammals, the chickens are less sensitive to toxic effects of LPS. The fact that chickens are more tolerant towards detrimental effects of LPS (Bercziet *et al.*, 1966) Present study, suggests that Sodium Nitroprusside (SNP) supplementation affect antibody synthesis after challenge and the result showed significance increase in antibodies titer in group of Sodium Nitroprusside (SNP) if compared with other groups .Sodium Nitroprusside (SNP) supplements increase the proliferation of lymphocytes in the blood, boost suppressor T-cell counts (Barbulet *et al.* 1981), phagocytic activity of alveolar macrophages (Tachibana *et al.* 1985). In this study significant difference in H/L ratio was observed . (Cengiz and Kucukersan, 2010).

Treatment with Sodium Nitroprusside (SNP) loading dose showed significant increase in blood volume of immune organs especially thymus , bursa of fabricius and liver through indirect effect on blood vessels vasodilation activity during metabolic production nitric oxide potent vasodilator. It had been implied that nitric oxide exerts part of its physiological actions in the body blood flow, possibly by facilitating an increase or maintenance of local nitric oxide is an important mediator for the maintenance of local blood perfusion as well as the regulation of blood pressure (Zackrisson *et al.*, 1998). Modulating blood perfusion in the liver might be one of the significant mechanisms by which NO can affect various aspects of hepatic function by increase blood volume (Bonello *et al.*, 1996 :Rosselliet *et al.*, 1998).

The main objectives of the research described in this study showed the antiviral antibacterial effects of the Sodium Nitroprusside (SNP) against the Newcastle disease virus *in-vitro* and *in vivo* and against the *Escherichia coli* after challenge.

REFERENCES

1. Abdulkalykova S, Ruiz-Feria CA (2006) Arginine and vitamin E improve the cellular and humoral immune response of broiler chickens. Int J Poultry Sci 5: 121-127.





Aws EI-Muntasir H and Emad J. Khammas

2. Alexander D.J. & Senne D.A. (2008). Newcastle Disease, Other Avian Paramyxoviruses, and Pneumovirus Infections. *In: Diseases of Poultry*, Twelfth Edition, Saif Y.M., Fadly A.M., Glisson J.R., McDougald L.R., Nolan L.K. & Swayne D.E., eds. Iowa State University Press, Ames, Iowa, USA, 75–116.
3. Barbul A, Sisto DA, Wasserkrug HL, Efron G (1981) Arginine stimulates lymphocyte immune response in healthy human beings. *Surgery* 90: 244-251.
4. Berczi, I., Bertok, L., Bereznai, T., 1966. Comparative studies on the toxicity of Escherichia coli lipopolysaccharide endotoxin in various animal species. *Can J Microbiol* 12, 1070-1071.
5. Bonello, N. Mckie, K. Jasper, M. Andrew, L. Ross, N. Braybon, E. and Brannstron, M. (1996). Inhibition of nitric oxide: effects of interleukin-1 β - enhanced ovulation rate, steroid hormones, and ovarian leukocyte distribution at ovulation in the rat. *Biol. Reprod.*; 54:436-445.
6. Bulbul A ,Altunbas K Sevimli A , Ya ğ c ı A , Akdag E , Celik HA (2007) The effects of ovarian steroids on myometrial contractions in ovariectomized rats . *Rev. Med. Vet* .158 : 556 – 561 .
7. Calignano, A., P. Persico, F. Mancuso, and L. Sorrentino, 1993. Endogenous nitric oxide modulates morphine-induced changes in locomotion and food intake in mice. *Eur. J. Pharmacol.* 231:415–419.
8. Caupa I, Alexander DJ (2009) Avian Influenza and Newcastle Disease. A Field and Laboratory Manual. Milan: Springer-Verlag.
9. Cengiz O, Kuc, ukersan S (2010) Effects of graded contents of arginine supplementation on growth performance, haematological parameters and immune system in broilers. *Revue Med Vet* 161: 409-417.
10. Cheng A, Wang S, Cai J, Rao MS and Mattson MP 2003 Nitric oxide acts in a positive feedback loop with BDNF to regulate neural progenitor cell proliferation and differentiation in the mammalian brain. *Dev. Biol.* 258 319–333.
11. De clerq E. antiviral and antiviral strategies *Nat. Rev. microbial* 2004 ;2:704-720.
12. Elzubeir, E.A. (1986) Interactions of dietary cyanide with sulphur amino acids and with selenium in the domestic fowl *Gallus domesticus*. *Ph.D. Thesis*, University of London .
13. Fafournoux P, Bruhat A, Jousse C. 2000. Amino acid regulation of gene expression. *The Biochemical Journal.* 351(Pt 1): 1-12.
14. Hamp IV ,Hergert J (2000) Role of nitric oxide in the pathogenesis of chronic pulmonary hypertension . *Physiol. Rev.*80 : 1337 – 1372 .
15. Iram N, Shah MS, Ismat F, Habib M, Iqbal M, et al. (2014) Heterologous expression, characterization and evaluation of the matrix protein from Newcastle disease virus as a target for antiviral therapies. *Appl Microbiol Biotechnol.* 98: 1691-1701.
16. Lee JE, Austic RE, Naqi SA, Golemboski KA, Dietert RR (2002) Dietary arginine intake alters avian leukocyte population distribution during infectious bronchitis challenge. *Poult Sci* 81: 793-798.
17. Li X, Qiu Y, Yu A, Chai T, Zhang X, et al. (2009) Degenerate primers based RT-PCR for rapid detection and differentiation of airborne chicken Newcastle disease virus in chicken houses. *J Virol Methods.* 158: 1-5.
18. Roselli, M., Keller, P. J. and Dubey, R. K. (1998). Role of nitric oxide in biology, physiology and pathophysiology of reproduction. *Hum. Reprod. Update*, 4,3–24.
19. Rytlewski K , Olszanecki R , Korbut R , Zdebski Z (2005) Effects of prolonged oral supplementation with L-arginine on blood pressure and nitric oxide synthesis in pre-eclampsia . *Eur. J. Clin. Invest.* 35 : 32 – 37.
20. Susta L, Cornax I, Diel DG, Garcia SC, Miller PJ, et al. (2013) Expression of interferon gamma by a highly virulent strain of Newcastle disease virus decreases its pathogenicity in chickens. *Microb Pathog* 61-62: 73-83.
21. Thompson KL , Applegate TJ (2006) Feed withdrawal alters small-intestinal morphology and mucus of broilers. *Poult. Sci.*85 : 1535 – 1540 .
22. Vapaatalo H ,Mervaala E , Nurminen ML (2000) Role of endothelium and nitric oxide in experimental hypertension . *Physiol. Rev.* 49 : 1 – 10 .
23. Varga J., Bátor J., Pap M., ifj.Sétáló G., Szeberényi J.: PC12 cells expressing a mutant p53 protein are more susceptible to the cytotoxic effects of sodium nitroprusside, 2nd International Doctoral Workshop on Natural Sciences, Pécs, 2013.





Aws El-Muntasir H and Emad J. Khammas

24. Zackrisson, U., Mikuni, M., Wallin, A., Delbro, D., Hedin, L. and Brännström, M. (1996). Cell-specific localization of nitric oxide synthases (NOS) in the rat ovary during follicular development, ovulation and luteal formation. Hum. Reprod., 11, 2667–2673.

Table 1. body weight of broilers during the experiment

Group	Mean ± SE of Body weight (g)						
	d 0	d 7	d 14	d 21	d 28	d 35	d 42
SNP	44.8 ± 2.19 a	157 ± 6.71 a	454 ± 9.57 ab	967 ± 16.72 a	1210 ± 19.63 a	1305 ± 18.42 ab	2113 ± 18.94 a
VER	41.1 ± 1.84 a	150 ± 5.07 a	423 ± 11.24 b	856 ± 13.96 b	1037 ± 17.87 a	1005 ± 16.35 c	1902 ± 20.08 b
AMA	42.5 ± 2.63 a	155 ± 5.37 a	475 ± 9.89 a	908 ± 17.61 ab	1029 ± 14.02 a	1255 ± 18.13 b	1899 ± 20.61 b
CTRL	42.1 ± 2.55 a	158 ± 7.18 a	463 ± 9.36 a	895 ± 12.53 b	1200 ± 23.09 a	1378 ± 25.26 a	2053 ± 21.67 a
Level of sig.	NS	NS	*	*	NS	*	*

* (P<0.05), NS: Non-Significant.

Means with the different letters in same column differed significantly

And the Feed Intake (FI) in the groups that supplied SNP was increased significantly (P<0.05) as compared with Amantadine and Verkon® Sin which it was less.

Table 2 .The Feed Intake (FI) of broilers during the experiment

Group	Mean ± SE of feed intake (gm)		
	From 0–21 days old	From 21–42 days old	From 0–42 days old
SNP	1091 ± 15.78 a	3545 ± 35.86 ab	4636 ± 43.07 a
AMA	1122 ± 13.27 a	3533 ± 38.72 ab	4655 ± 39.51 a
VER	1081 ± 13.09 a	3572 ± 41.98 a	4653 ± 44.08 a
-VE CTRL	1085 ± 14.55 a	3475 ± 36.05 b	4560 ± 32.61 b
Level of sig.	NS	*	*

* (P<0.05), NS: Non-Significant.

Means having with the different letters in same column differed significantly





Aws EI-Muntasir H and Emad J. Khammas

Table 3. The Feed Conversion Ratio (FCR) of broilers during the experiment.

Group	Mean ± SE of FCR		
	From 0–21 days old	From 21–42 days old	From 0–42 days old
SNP	1.279 ± 0.04 a	3.527 ± 0.08 a	2.468 ± 0.04 a
AMA	1.289 ± 0.06 a	3.487 ± 0.07 a	2.472 ± 0.05 a
VER	1.326 ± 0.06 a	3.259 ± 0.05 ab	2.434 ± 0.06 a
-VE CTRL	1.258 ± 0.03 a	3.165 ± 0.07 b	2.343 ± 0.06 a
Level of sig.	NS	*	NS

* (P<0.05), NS: Non-Significant.
Means with the different letters in same column differed significantly

Table 4. The H/L ratio of broilers during the experiment

Group	Before challenge	After challenge
	D15	D30
SNP	0.401 ± 0.05 a	0.412 ± 0.05 a
VER	0.400 ± 0.05 a	0.407 ± 0.03 a
AMA	0.404 ± 0.06 a	0.409 ± 0.03 a
POS+	0.398 ± 0.03 a	0.394 ± 0.02 a
NEG-	0.401 ± 0.05 a	0.472 ± 0.07 a
Level of sig.	NS	NS

NS: Non-Significant.
Means with the similar letters in same column non- significantly

Table 5. The Antibodies Titer of broilers during the experiment

Groups	Before challenge	After challenge and treatment
SNP	645 ± 16.78 a	5919 ± 88.35 a
VER	598 ± 12.97 a	5550 ± 71.97 a
AMA	634 ± 15.24 a	3545 ± 52.66 b
POS+	645 ± 15.07 a	3454 ± 64.91 b
NEG-	655 ± 17.37 a	--
Level of sig.	NS	*





Aws El-Muntasir H and Emad J. Khammas

Table 6. The effect of Sodium Nitroprusside blood volume (ml/gm) in broilers.

	Sodium Nitroprusside	Amantadine	Verkon S	Control	Level of sig.
Liver blood volume	0.22 ± 0.04 a	0.20 ± 0.03a	0.18 ± 0.01 a	0.11 ± 0.02 b	*
Bursa blood volume	0.24 ± 0.06 a	0.21 ± 0.05 a	0.11 ± 0.02 a	0.14 ± 0.02 b	*
Thymus blood volume	0.26 ± 0.06 a	0.19 ± 0.02 ab	0.12 ± 0.02 b	0.17 ± 0.02 b	*
* (P<0.05), Means with the different letters in same row differed significantly					





Isolation and Molecular Identification of *Histoplasma capsulatum* from Respiratory Samples of Horses in Iraq

Rami S.Owaid* and Zainab A.A. Al-Hadad.

Unit of Zoonotic Diseases, College of Veterinary Medicine, University of Baghdad, Iraq.

Received: 17 Sep 2018

Revised: 23 Oct 2018

Accepted: 27 Nov 2018

*Address for Correspondence

Rami S.Owaid

Unit of Zoonotic Diseases,
College of Veterinary Medicine,
University of Baghdad, Iraq.



This is an Open Access Journal / article distributed under the terms of the **Creative Commons Attribution License** (CC BY-NC-ND 3.0) which permits unrestricted use, distribution, and reproduction in any medium, provided the original work is properly cited. All rights reserved.

ABSTRACT

This research was carried out to isolate *Histoplasma capsulatum* from respiratory samples of horses in Iraq using genomic detection. A total numbers of one hundred (100) nasal swabs and one hundred (100) blood samples were collected from equestrian clubs in Baghdad, DhiQar, Addiwaniya and Najaf provinces. All samples cultured on sabouraud dextrose agar (SDA) and brain heart infusion agar (BHIA) with chloramphenicol and cycloheximide and incubated at (25°C and 37°C) for (4 weeks). The samples were examined macroscopically depending on shape, texture and color of the fungal growth and microscopically by preparing a mount smear with lactophenol cotton blue and examined under (40X). The diagnosis confirmed by molecular techniques for the detection of *Histoplasma capsulatum* by using conventional PCR. So, the isolation of *Histoplasma capsulatum* was (4%) in both conventional examination and molecular detection in nasal swabs, but in case of blood samples, the *Histoplasma capsulatum* isolated by conventional methods was 3%, whereas the molecular detection appeared as 2%.

Keywords: *Histoplasma capsulatum*, Horses, Conventional PCR, Sequences analysis

INTRODUCTION

Histoplasmosis was first described in (1906) by Darling among the workers of the Panama Canal (Darling, 1909). The *H. capsulatum* is thought to cause approximately 500,000 respiratory infections a year in the central river valleys in the Midwestern and south-central United States (Chang, 2007). *Histoplasma capsulatum* is a fungal pathogen that can result in a wide range of clinical presentations, from asymptomatic to fatal infection. It usually causes lung disease called Histoplasmosis or Darling's disease, according to Samuel Darling who found the pathogenic fungi in histopathologic specimens about a century ago, (Chang, 2007). *Histoplasma capsulatum* is a biologically interesting inhabitant of soil and mammalian hosts, a clinically significant cause of respiratory and systemic infection, and an excellent fungal



**Rami S.Owaid and Zainab A.A. Al-Hadad**

model of dimorphic cell development and facultative intracellular pathogenesis(Heitman.*et al*, 2006). *Histoplasma capsulatum* is unique in its dimorphism.

This fungus also causes Epizootic lymphangitis in equids and most common form of this disease is an ulcerative, suppurative, spreading dermatitis and lymphangitis; however, other forms including pneumonia or ulcerative conjunctivitis also occurs. Epizootic lymphangitis spreads most readily where large numbers of animals are assembled, and it was a serious problem during the early twentieth century, when large numbers of horses were stabled together. This disease continues to be a significant concern in some countries, where the prevalence in carthorses is nearly (19%), and economic losses from this disease are high. (Ameni and Terefe 2004).

MATERIALS AND METHODS

The collected samples

A total of one hundred(100) nasal swabs and one hundred (100) blood samples of the horses were collected from equestrian clubs in Baghdad, Dhi Qar, Ad diwaniya and Najaf provinces, during the period from October 2017 to the end of March 2018. The samples were kept in a cold until and processed in the laboratory, the nasal swabs inoculated in transport media before processed in laboratory.

Laboratory tests

All samples from horses were inoculated in Sabouraud dextrose agar with Chloramphenicol; incubated in (25° C for 2-4 weeks) , as well as they were inoculated in Brain heart infusion agar with Chloramphenicol 0.05 mg/ml and Cycloheximide (1%) ; incubated in (37° C for 2-4 weeks).

Isolated strains examined macroscopically according to their shape, texture and color of the fungal colonies on SDA and BHIA and microscopically by preparing a mount of smear with lactophenol cotton blue to identify fungal elements. So, the suspected isolated strains were inoculated in a new BHIA to proceed to a molecular detection by conventional PCR(Alexander and Street, 2001).

Molecular diagnosis

PCR techniques were performed on isolated strains of the horses for the four provinces to detect of the *Histoplasma capsulatum* based on 18SrRNA gene. The method was carried out according to a description obtained by Wang *et al.*,(2014).The DNA extraction was done from isolated suspected strains by using EZ-10 Spin Column Fungal Genomic DNA Mini-Preps Kit(DNA Extraction Kit), (Bioneer, Korea). PCR master mix preparation by using primer pair: forward (5- TTGTCTACCGGACCTGTTGC-3) and reverse (5-CCTGGTGTGAAAAGGGGGTT-3) (Maxime™ PCR PreMix Kit (*i*-Taq)), then placed in PCR Thermocycler (MyGene. Bioneer. Korea).

Sequence analysis

The genetic analysis done by phylogenetic tree method between local *Histoplasma capsulatum* horse isolates and NCBI-Blast submission *Histoplasma capsulatum*. Then the identification species isolates were submitted into of NCBI-GenBank.The DNA sequencing analysis was conducted by using Molecular Evolutionary Genetics Analysis version 6.0 (Mega 6.0) and Multiple sequence alignment analysis of the partial small subunit rRNA gene based on ClustalW alignment analysis and the evolutionary distances were computed using the Maximum Composite Likelihood method by phylogenetic tree UPGMA method (Wang *et al.*, 2014).





Rami S.Owaid and Zainab A.A. Al-Hadad

RESULTS

Conventional macroscopic method recorded 4 (4%) positive out of 100 swabs, and 3 (3%) positive out of 100 blood samples in horses. Not all microscopy positive specimens were found positive by PCR only one had been negative as in Tab. (1).

Microscopic appearance

Two types of conidia were produced on the hyphae. The macroconidia, or tuberculate conidia, are (8 to 15 μm) in diameter and have distinctive projections on their surface; the microconidia are small (2 to 4 μm) and smooth walled. Fig. (2).

PCR

Genomic DNA samples obtained from suspected isolates were subjected to molecular analysis by PCR, using 18S rRNA gene specific primers in order to identify *Histoplasma capsulatum*. PCR of positive samples employed in the research exhibited distinct band of (476 bp) on agarose gel confirming the presence of *Histoplasma capsulatum* (Fig. 3).

Macroscopic appearance

After four weeks, the mold was grainy to cottony in appearance, and became increasingly brown in color from white over time. Yellow/yellow-orange reverse (Fig. 1). DNA sequence results for *Histoplasma capsulatum* (2-6) showed a close relation to NCBI blast *Histoplasma capsulatum* (AF129547) according to phylogenetic tree analysis between local *Histoplasma capsulatum* isolate and NCBI blast *Histoplasma capsulatum* isolate at homologous sequence identity (100%) and then local *Histoplasma capsulatum* isolate (2-6) were submitted to NCBI GenBank at accession number (MH745422, MH745423, MH745424, MH745425 and MH745426) (Table 2).

DISCUSSION

The results of macroscopic and microscopic appearance of *Histoplasma capsulatum* isolated from nasal swabs and blood samples of horses in four provinces in Iraq, which were Baghdad, Dhi Qar, Addiwaniya and Najaf, revealed (3.5%) with characteristic features of *histoplasma capsulatum* (4/100 from nasal swabs and 3/100 from blood samples) were the fungal colonies appeared with grainy cottony appearance and became increasingly brown in color from white over time, yellow/yellow-orange reverse with two types of conidia. The macroconidia, or tuberculate conidia with distinctive projections on their surface and microconidia which were small and smoothly walled, so it gives the characteristic appearance of *Histoplasma capsulatum* which agrees with Al-Ani *et al.* (1998), Ameni and Siyoum (2002) and Kauffman (2007).

Isolation percent of *Histoplasma capsulatum* in this research was (3.5%), that indicates presence of this dimorphic fungus in horses without any other clinical signs related with *Histoplasma capsulatum*, but it also revealed that there were animals (horses) which were carriers (asymptomatic) to such pathogenic systemic fungi and also have ability to induce the disease related to predisposing factors and this disagrees with (Al-ani and Al-delami in 1986), who were isolated *Histoplasma capsulatum* in conducting with incidence of epizootic lymphangitis with (6.4%) in Iraq, and similar to that was Mesafint *et al.* (2018) whom estimated prevalence of Epizootic lymphangitis (EL) in (23.2%) in carthorses in Ethiopia.

The confirm diagnosis in this research was done by using PCR conventional technique so in all six positive cases, sequencing of the (476-bp amplicons) demonstrated the presence of *Histoplasma capsulatum* DNA, and this was





Rami S.Owaid and Zainab A.A. Al-Hadad

further confirmed by sequencing of a large sample of clones. PCR methods targeting the 18S rRNA region have previously been used to identify *Histoplasma capsulatum* and have the additional advantage of enabling strain sequence variation to be explored, region sequences shown a high degree of conservation, which was agree with the minimal diversity that was reported among *Histoplasma* spp. by Raquelet *et al.* (2013) and Scantlebury *et al.* (2016). In this research fungal cells were used as template for the PCR amplification procedure. Molecular approaches have been developed to provide more rapid and accurate identification of fungi compared with traditional microscopic methods. The 18S rRNA regions have been used extensively for PCR-based systems to detect and identify fungal pathogens. Molecular identification of *Histoplasma capsulatum* can be based on the sequences of the 18S rRNA followed by a similarity search in public databases even though this may be hampered by the poor quality of databases in terms of sequence quality, sequence length and taxonomic group or other updates. (Al-ani *et al.* 1998), recorded the appearance of *Histoplasma capsulatum var farciminosum* in twelve suspected cases of horses suffered from Epizootic lymphangitis, and diagnosed presence of *Histoplasma capsulatum var farciminosum*, in contrast to results in this research which confirmed detection of *Histoplasma capsulatum var capsulatum* from asymptomatic carriers of horses by molecular techniques.

This is the first research depend upon PCR-based detection of *Histoplasma capsulatum* from nasal swabs and blood samples of Iraqi equine. Our data suggests the identification of *Histoplasma capsulatum var. capsulatum* in horses, although further work is required to determine the timing of the development of histoplasmosis and investigate the potential for the early detection of *H. capsulatum* from nasal swabs and blood samples.

Conclusions:

According to results appeared in this research, *Histoplasma capsulatum* was isolated from apparently normal, healthy animals (horses) without clinical signs, so it was suggested carrier animals may appeared infection with any risk factors animals may suffered from them, so continuous observation and periodic inspection must be done to animals by using classical and modified conventional laboratory tests to confirm the devoid of animals from any infection in latent phase.

REFERENCES

1. Al-Ani, F. K., A. H. Ali, H. B. Banna (1998): *Histoplasma farciminosum* infection of horses in Iraq. Vet. arhiv 68, 101-107.
2. Al-Ani, F. K., A. K. Al-Delaimi (1986): Epizootic lymphangitis in horses: clinical, epidemiological and hematological studies. Pakistan Vet. J. 6, 96-99.
3. Alexander S. and Street D. (2001): In microbiology a photographic atlas for the laboratory. Benjamin Cummings, an imprint of Addison Wesley longman, pp.51-52.
4. Ameni G and Terefe W. (2004): A cross-sectional study of epizootic lymphangitis in cart-mules in western Ethiopia. Prev Vet Med. 66(1-4):93-9.
5. Ameni, G. and Siyoum, F., 2002: Study on histoplasmosis (epizootic lymphangitis) in carthorses in Ethiopia. Journal of Veterinary Science, 3, p.135-139.
6. Chang, Ryan. (2007): Histoplasmosis. <http://www.emedicine.com/MED/topic1021.htm>.
7. Collier; Balows L., A. and Sussman M. (1998): Topley & Wilson's Microbiology and Microbial Infections, 9th ed, vol. 4. Arnold, London, Sydney, Auckland, New York.
8. Darling (1909): The morphology of the parasite (*Histoplasma capsulatum*) and the lesions of histoplasmosis, a fatal disease of tropical America. Journal of Experimental Medicine, vol. 11, no. 4, pp. 515-531, 1909.
9. Dodge. H.J. (1965) : The association of bird-roosting site with infection of school children by *Histioplasma capsulatum*. Am J Publ. Health 55:1203-1211.
10. Heitman; Joseph; Scott G. Filler; Aaron P. Mitchell and John E. Edwards. (2006): Molecular Principles of Fungal Pathogenesis. 1st ed. New York: ASM Press. (Heitman et al. 321-331).





Rami S.Owaid and Zainab A.A. Al-Hadad

11. Petrie A. and Watson P. (2006): Statistics for Veterinary and Animal Science, Second Edition. Ames: Blackwell Publishing, Pp: 24-112.
12. Wang Y.; Bo Pan, Jianhua Wu, Xinling Bi, Wanqing Liao, Weihua Pan, and Jun Gu (2014): Short Report: Detection and Phylogenetic Characterization of a Case of Histoplasma capsulatum Infection in Mainland China. Am. J. Trop. Med. Hyg., 90(6), pp. 1180–1183.
13. Mesafint M, Ashenafi A, Askale A, Gashaw E. (2018): Prevalence, associated risk factors and socioeconomic impact of Epizootic lymphangitis (EL) in carthorses in and around Gondar town. J Am Sci;14(2):77-83]. ISSN 1545-1003 (print); ISSN 2375-7264 (online). <http://www.jofamericanscience.org>. 10. doi:10.7537/marsjas140218.10.
14. Kauffman C.A.(2007): Histoplasmosis: a clinical and laboratory update. Clin Microbiol Rev. 20(1):115–32. doi: 10.1128/CMR.00027-06.
15. Scantlebury, C.E., Pinchbeck, G.L., Loughnane, P., Aklilu, N., Ashine, T., Stringer, A.P., Gordon, L., Marshall, M., Christley, R.M., McCarthy, A. (2016):Development and evaluation of a molecular diagnostic method to rapidly detect *Histoplasma capsulatum* var. *farciminosum*, the causative agent of epizootic lymphangitis, in equine clinical samples.J Clin Microbiol.54(12): 2990–2999.
16. Raquel C. T.; Christina M. S.; Mary E. B.; Takao K.; Eduardo B. (2013):PRP8 intein in cryptic species of *Histoplasma capsulatum*: Evolution and phylogeny

Table 1.Number of total and Positive.

Types of samples	Total numbers	Positive by conventional methods	Positive by molecular detecting
Nasal swabs	100	4	4
Blood samples	100	3	2



Fig. 1: Macroscopic appearance of suspected isolates, *Histoplasma capsulatum*.

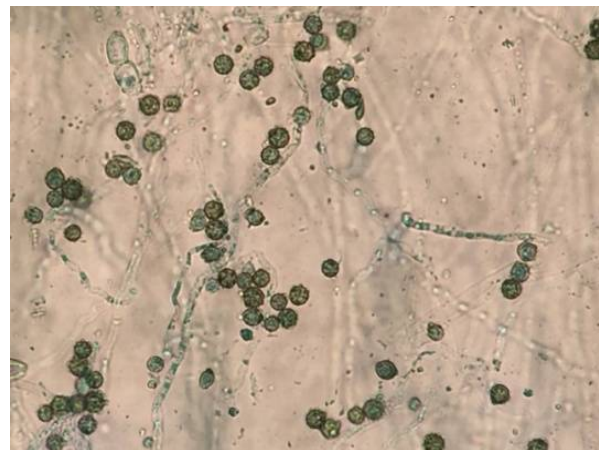


Fig. 2: microscopic appearance of suspected isolates *Histoplasma capsulatum*





Rami S.Owaid and Zainab A.A. Al-Hadad

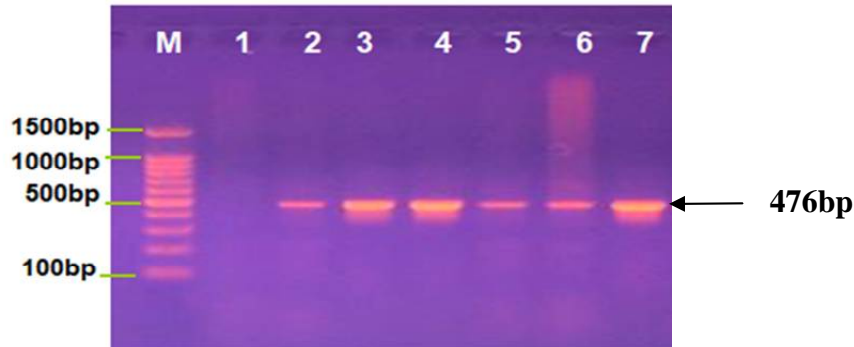


Fig. 3: Agarose gel electrophoresis image that shows the PCR product analysis of 18S ribosomal RNA gene in *H. capsulatum* positive isolates. Where Marker Ladder (1500-100bp), lane (1) negative isolates, and lane (2-7) *H. capsulatum* isolates at PCR product size 476bp. Sequence analysis

Table 2:NCBI-BLAST Homology sequence identity (%) between local *Histoplasma capsulatum* horse isolates and NCBI BLAST *Histoplasma capsulatum* isolates.

Local horse <i>H. capsulatum</i> isolatesNo.	Gen-Bank accession No.	NCBI BLAST Homology sequence identity	
		Genbank isolates	Identity (%)
2	MH745422	AF129547	100%
3	MH745423	AF129547	100%
4	MH745424	AF129547	100%
5	MH745425	AF129547	100%
6	MH745426	AF129547	99%

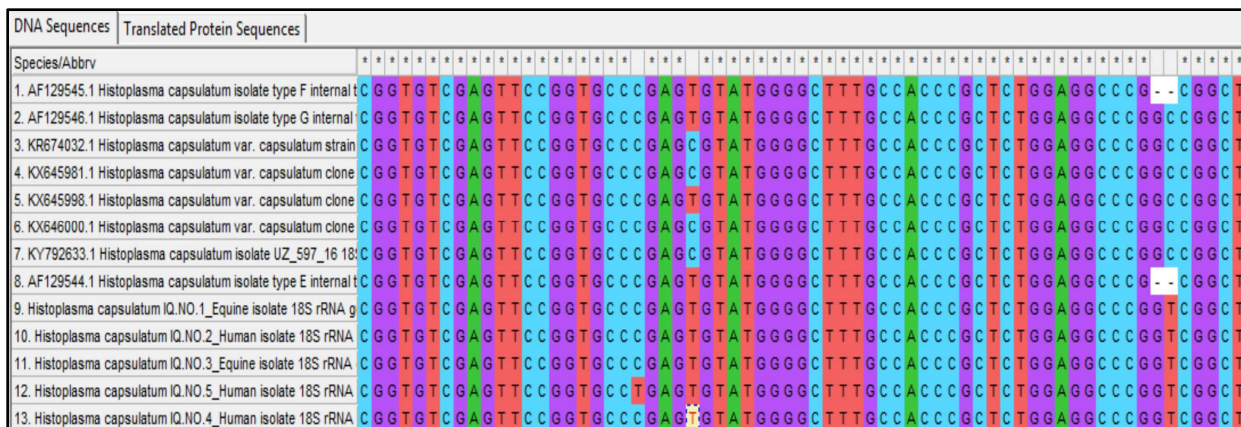


Fig.4: Multiple sequence alignment analysis of the partial 18S ribosomal rRNA gene sequence in local *Histoplasma capsulatum* isolates and NCBI-Genbank *Histoplasma capsulatum* isolates based ClustalW alignment analysis by using (MEGA 6.0, multiple alignment analysis tool). The multiple alignment analysis similarity was shown at (*) in nucleated sequence of 18 ribosomal gene.





Rami S.Owaid and Zainab A.A. Al-Hadad

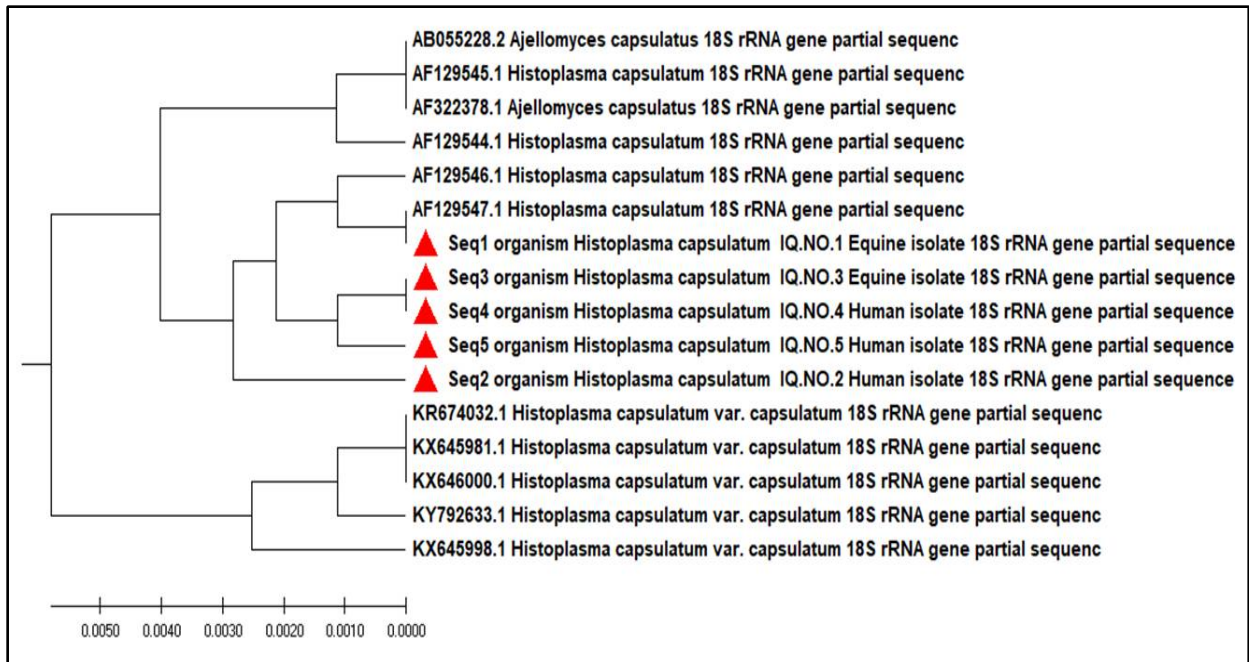


Figure (5): Phylogenetic tree analysis based on the partial sequence of 18S ribosomal rRNA gene in local *Histoplasma capsulatum* isolates that used for genetic confirmative detection analysis. The evolutionary distances were computed using the Maximum Composite Likelihood method by UPGMA phylogenetic tree (MEGA 6.0 version). The local *Histoplasma capsulatum* No.1-No.5 isolates were shown closed related to NCBI-Blast *Histoplasma capsulatum* (AF129547) at total genetic change (0.0010-0.0050).





Comparative Study on Biochemical Profiles between Fertile and Sterile Hydatid Cyst Fluid

Wasan Addai Mahdi^{1*}, Sabaa Taher Mohammed² and Asmaa M. Salih Almohaidi³

²Department of Biology, College of Science, AL-Mustansyria University, Iraq.

^{1,3}Department of Biology, College of Science for Women, University of Baghdad, Baghdad, Iraq.

Received: 20 Sep 2018

Revised: 22 Oct 2018

Accepted: 27 Nov 2018

*Address for Correspondence

Sabaa Taher Mohammed

Department of Biology,

College of Science,

AL-Mustansyria University, Iraq.

Emai.:dr.saba@uomustansiryha.edu.iq



This is an Open Access Journal / article distributed under the terms of the **Creative Commons Attribution License** (CC BY-NC-ND 3.0) which permits unrestricted use, distribution, and reproduction in any medium, provided the original work is properly cited. All rights reserved.

ABSTRACT

Echinococcus granulosus is a causative agent of hydatidosis, a parasitic disease that affects humans and livestock with significant economic and public health impact worldwide. The hydatid disease parasite *E. granulosus* has a restricted lipid metabolism and needs to harvest essential lipids from the host. The aim of the present study was to compare between some biochemical parameters infertile and sterile hydatid cyst fluids obtained from the liver, lung and spleen of human naturally infected with hydatidosis diseases who have a complex clinical management. The current study showed the distribution of hydatid cyst in the infected patients and revealed that a high percentage in liver (100%), followed by lung, spleen and kidney (33.33%). The number of fertile and sterile cysts was (16) and (14) respectively. The biochemical components of the cystic fluid for fertile and sterile types are measured. The results showed that the concentration of glucose, cholesterol and total protein in the fertile cysts fluid was more concentrated than sterile cysts.

Keywords: fertile and sterile cyst, *Echinococcus granulosus*, cystic fluid components

INTRODUCTION

Hydatidosis, a problem of worldwide importance (approximately 2-3 million human cases are thought to occur worldwide) is caused by adult or larval (metacestode) stages of cestodes belonging to the genus *Echinococcus* of the family *Taeniidae* (Brunetti *et al.*, 2010). This disease has serious impacts on human and animal health (Snabel *et al.*, 2009) and public health problem in many parts of the world, especially in rural areas where dogs and livestock are raised together, it is usually asymptomatic, however, it can clinically manifest as a complicated cyst, the most frequent complication is compression or rupture of pericystic structures (Daali *et al.*, 2001). The disease is endemic in



**Wasan Addai Mahdi et al.**

South America, Far East, Middle East and Eastern Europe, as well as in some other parts of the world and the disease is endemic and enzootic in Iraq, it is estimated to have a prevalence in all world of 50-70% and is present in the liver member, the majority of them are single and in the right lobe of the this organ (Ezer *etal.*,2006).The cyst fluids contain biochemical such as proteins, carbohydrates, lipids, vitamins, electrolytes and trace elements that may have role in metabolism and growth of unilocular hydatid, the composition of cyst content may differ in various area and strains (Koudri *et al.*, 2014).The purposes of this study is the assessment and compare the level of biochemical components in the two types liquid hydatid cysts (fertile and sterile) in patients infected.

MATERIALS AND METHODS

The current study included Iraqi patients suffering from hydatid cysts disease in different organs , during the period March 2017 until the end of February 2018, which has been shown to have hydatid cysts disease according to x-ray diagnosis, ultrasound and CT scan programmed by specialized medical surgeons, after their consultation with six major hospital in Baghdad after achieving agreement of the ethical committee (the General Surgery Hospital at Baghdad Teaching Hospital, Al Yarmouk Teaching Hospital, Gastroenterology and liver Hospital, Al Kindi Teaching Hospital, Al Kadhimiya Teaching Hospital, Al Sadr Hospital).

Specimens hydatid cyst

The contents of hydatid cysts were excised from patients who underwent surgery for cystic echinococcosis from different hospitals throughout Iraq previously mentioned. The samples were placed in refrigerated containers and transferred to the laboratory for study. Then washed several times with sterile physiological (PBS) to decrease contamination with host tissue, and they were extensively washed with 70% alcohol.

Preparation protoscoleces

According to Khan *et al.* (2001), the cyst fluid contents were aspirated aseptically via sterile disposable syringes (10 ml) into sterile tubes. Then cysts were opened longitudinal incision and all the remaining fluid were centrifugation at 3000 rpm for 10 minutes at room temperature to get of the protoscoleces to pellet. The supernatant was collected into a sterile tube for measuring some biochemical parameters, stored at (- 20C°) until it is used. The supernatant was discarded and only 2 ml of fluid with precipitate was left in the bottom of the test tube, then after shaking well, one drop was taken by pasture pipette and placed on a microscopic slide, then add one drop of methanol left to dry, covered by cover slip and examined under microscope (40x). Fertility was defined as presence of protoscoleces, the positive sample was an indicator of cyst fertility ,while the absence of it is characterized by sterile samples (Bajalan, 2006).

Estimation chemical components

Cystic hydatid fluid assessment for two types cyst was sterile or fertile, used to measurement the following criteria

- The concentrations of the glucose were estimated by colorimetric method uses glucose liquid color kits (Spinreact, Spanish), according to No. (Bsis 17-1), this test was carried out by the Roche system.
- The cholesterol was determined using an enzymatic colorimetric by test (CHOL2, Cobas cIII ,Germany), according to No. 2017- 01 (V 8.0).
- The concentrations of the total proteins were evaluated by colorimetric method using total proteins liquid color kits (Linear, Spanish), according to No.(B1153-2/0901) by (humalyzer primus human / Germany).



**Wasan Addai Mahdi et al.**

Statistical Analysis

The Statistical Analysis System- SAS (2012) program was used to effect of difference factors in study parameters . Chi-square test was used to significant compare between percentage and Least significant difference –LSD test (ANOVA) t-test was used to significant compare between means.

RESULTS AND DISCUSSION

The current study included 30 patients (16 fertile and 14 sterile hydatid cyst type) suffering from hydatid cysts disease in liver, lung and spleen organ, in ages between 12 - 75 years. The sterile cysts type, most of which were ruptured, the major sources of morbidity are pressure effects from cyst size, location in a sensitive organ (brain, reproductive tract, bone) (Mandal and Mandal, 2012). As shown in (table 1).

As well as that all organs of the body are targeted by parasite embryos except teeth, hair and nails (Prabhakar *et al.*, 2005). The presence of cysts in more than one member depends on the host's body resistance to infection, then parasite evasion to escape from the immune system and spread disease (Derbel *et al.*, 2012). In contrast Al-Ubaidi (2002) noted that the high rate of infection of the hydatid cysts in the lung compared to the proportion of the liver.

The relationship between the number of cysts and the type of infected organ, shows that the liver has a highest rate of infection (15 cases), followed by lung, spleen and kidney (one case for each organ). The liver was the only infected organ in the case of two cysts and three cysts or more in organs with rate of 3 and 12 patients respectively. These relationships showed significant differences ($P < 0.01$) and ($P < 0.05$) (table 2). This may be due to, the liver is the more influenced by cases of hydatid cysts (Mandal and Mandal, 2012), also, because the liver is the first refinery for oncosphere which hold these embryos in the liver in large numbers and attach it to the hooks and begins to form of the cyst. This is called the initial infection (Moro and Schantz, 2009).

Glucose concentration

Glucose present as a component in the cystic fluid, the results showed significant increasing glucose concentration in fertile hydatid cyst (55.71 mmol/L) compared with sterile cysts (24.58 mmol/L) figure (1). This is comparable to Kouidriet *et al.* (2014) who showed a significant differences in glucose concentration between fertile and sterile cysts. Unlike of our results Al-Bayati *et al.* (2010) who found a non-significant differences in this compound for two types of cysts. Biochemical substances of hydatid cysts play a definitive role in the metabolism, physiology and immunology of cysts echinococcosis. The variations in these parameters reflect the relation between intermediate host and parasite (Gruboret *et al.*, 2017).

High rate of glucose in the fertile cysts represent an evident component in hydatid fluid. It has been reported that the parasite contains glycogen as a stored polysaccharide and it serves as an essential source of energy (Pakala *et al.*, 2016). A Chinese group working on *E. granulosus* documented that mebendazole inhibits the transport of exogenous glucose from the host to the cyst wall and subsequently promotes the decomposition of glycogen for energy (Gruboret *et al.*, 2017). The reason for the presence of glucose in the fluid of fertile more than sterile cysts may be due to its transformation from the stored glycogen of the cysts or part of it may be extracted from the host cells (Hoschet *et al.*, 2008).

Cholesterol level

Cholesterol level were also measured in the fluid. His level in fertile cysts was (163.63 mmol/L) higher than in sterile cysts (135.52 mmol/L), also there was a significant differences ($P < 0.05$) between two groups figure (2).





Wasan Addai Mahdi et al.

Present study goes with Al-Bayatiet al. (2010) who showed that there are a significant difference between cholesterol, triglyceride and calcium in liver more than lung of hydatid cysts fluid collected from sheep slaughter in Duhok abattoir. It was reported previously that a large amount of lipid is present in the laminated layer of *E. granulosus* of horse origin, these lipids may be released in the fluid during the degeneration process of the cyst, as evidenced in the literature by the fact that the concentration of cholesterol in the fluid is an indicator of cystic degeneration (Silva-Alvarez et al., 2015).

In contrast, Kouidri et al. (2014) emphasized that non significant differences found for this compound. This difference can be explained the role played of the cyst membrane as a transport border between the hydatid fluid and host serum. Therefore, the quantity of biochemical parameters in hydatid fluid probably relates to the species or subspecies of *E. granulosus* and not to the cyst location (Silva-Alvarez et al., 2015).

Total proteins

The higher concentrations of total protein were found mostly in the fertile cysts (9.79 g/L), while the lower concentrations were in sterile cysts (6.58 g/L) with a significant difference ($P < 0.05$) figure (3). This may indicate that cyst proteins increase during degenerative process, i.e degradation of parasitic membrane or protoscolices in fertile cysts. Therefore, the occurrence of proteins can be regarded as an intracellular pool, part of which may be derived from uptake from surrounding host tissue, produced from protein degradation, or as a result of metabolic transformations occurring within the parasite. This biochemical parameter that may have role in metabolism and growth of unilocular hydatid, and this may be attributed probably due to reduced immunological compatibility of hosts at their old age of infection (Siles-Lucas et al., 2017).

REFERENCES

1. Al-Bayati S., Aziz O., Abdull A. and Abed S. (2010). Biochemical profile of hydatid cyst fluid of *Echinococcus granulosus* of sheep in Duhok area. Iraqi J. of Vete. Med., 34(1): 185-190.
2. Al-Ubaidi A. (2002). Cytogenetic and enzymatic studies on patient with hydatid disease., M. Sc. Thesis, Al-Nahrain Coll. Med., Univ. Al-Nahrain: 70.
3. Bajalan M. M. (2006). Prevalence of Echinococcosis in stray dogs and slaughtered livestock in Kalar district Sulaimaniyah province.
4. Brunetti E., Kern P. and Vuitton D. (2010). Expert concerns for the diagnosis and treatment of cystic and alveolar echinococcosis in human. Acta Trop., 114(1): 1-16.
5. Daali M., Fakir A., Hssaida R., and Had A. (2001). Hydatid cysts of the liver opening in the biliary tract., Ann Chir., 126(3): 242-245.
6. Derbel F., Mabrouk M., Hadj M., Mazhoud J., Youssef S., Ali A., Jemni H., Mama N., Ibtissem H., Nadia A., El Ouni C., Naija W., Mokni M. and Hadj R. (2012). Hydatid cyst of the liver diagnosis, complication and treatment. Abdom. Surg., 5(8): 105-138.
7. Ezer A., Nursal T. Z., Moray G., Yildirim S., Karakayali F., Noyan T. and Haberal M. (2006). Surgical treatment of liver hydatid cysts., W. j. of Gastro., 8(1): 38-42.
8. Grubor N., Jovanova-Nesic K., Shoenfeld Y. (2017). Liver cystic echinococcosis and human host immune and autoimmune follow-up: A review. W. J. Hepatology., 9(30): 1176-1189.
9. Khan A., El-Buni A. and Ali M. (2001). Fertility of the cysts of *Echinococcus granulosus* in domestic herbivores from Benghazi, Libya, and the reactivity of antigens produced from them. Ann. Trop. Med. Parasitol., 95(4): 337-342.
10. Kouidri M., Khoudja F., Boulkaboul A. and Selles S. (2014). Comparative Study on Fertility, Viability and Biochemical Profiles of Hydatid Cyst Fluid from the Lungs and Liver of Sheep in Algeria. W. Appl. Scien.J., 31 (10): 1699-1703.





Wasan Addai Mahdi et al.

11. Mandal S. and Mandal M. (2012). Human cystic echinococcosis epidemiologic, zoonotic, clinical, diagnostic and therapeutic aspects. *Asian Pacific. J. Trop. Med.*, 5(4): 235 – 260.
12. Moro P. and Schantz P. (2009). Echinococcosis: a review. *Int. J. Infect. Dis.*, 13 (2): 125–33.
13. Pakala T., Molina M. and George Y. (2016). Hepatic Echinococcal Cysts: A Review., *J. Clin. Transl. Hepatol.*, 4(1): 39–46.
14. Prabhakar M., Acharya A., Modi D. and Jadav B. (2005). Spinal hydatid disease : A case series., *J. Spin . Cord. Med .*, 28(5): 426 – 431.
15. SAS. (2012). Statistical Analysis System, User's Guide. Statistical. Version 9.1th ed. SAS. Inst. Inc. Cary. N.C. USA.
16. Siles-Lucas M. and Gottesein B. (2001). Molecular tools for diagnosis of cystic and alveolar echinococcosis. *Trop. Med. Int. Health.*, 6(6): 463-475.
17. Silva-Alvarez V., Gisela R., Jorge L., Malcolm W., Ana M. and Corsico B. (2015). Lipid-Free Antigen B Subunits from *Echinococcus granulosus*: Oligomerization, Ligand Binding and Membrane Interaction Properties. *PLOS Negl. Trop. Dis.*, 9(3): 1-23.
18. Snabel V., Altnta D., Amelio S., Sakao M., Romig T., Yolasmaz A. and Dubinsky P. (2009). Cystic echinococcosis in Turkey: genetic variability and first record of the pig strain (G7) in the country., *Parasitol. Res.*, 105(10): 143-154.

Table 1: Numbers of fertile and sterile hydatid cysts

Type of hydatid cyst		
Number of patients	Fertile	Sterile
	16	14

Table 2: Cyst numbers and distribution according to the infected organ

Number of cysts	Members number according to infected organ				
	Liver N=30	Lung N=1	Spleen N=1	Kidney N=1	P-value
One cyst	15	1	1	1	0.01**
Two cyst	3	0	0	0	0.0437*
Three cyst and more	12	0	0	0	0.01**
P-value	0.01**				

** : (P<0.01) , * : (P<0.05)





Wasan Addai Mahdi et al.

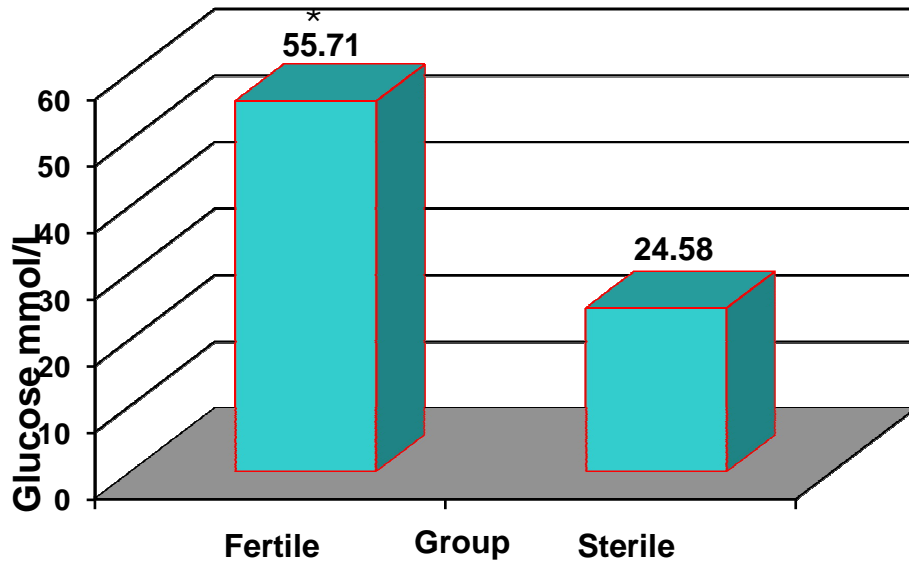


Figure (1): Comparison between fertile and sterile groups in glucose of cyst fluid

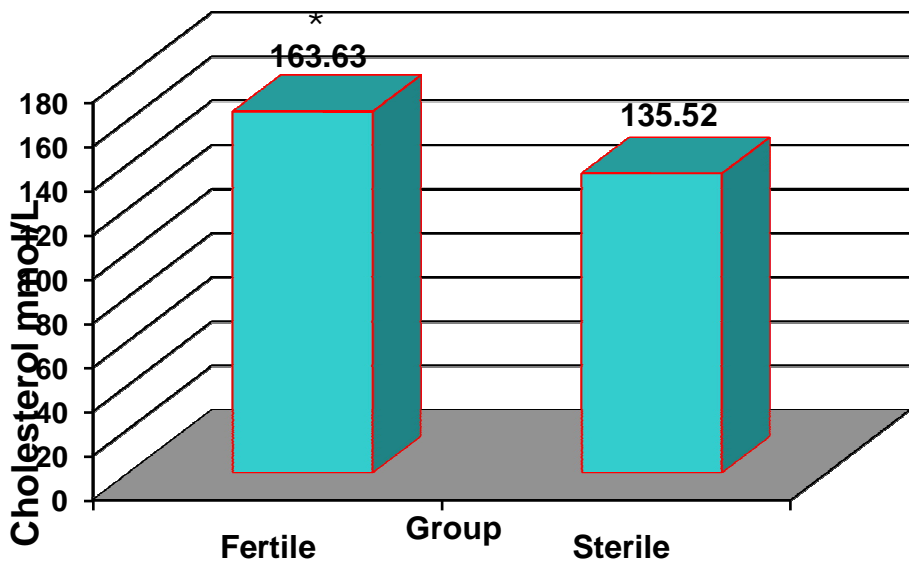


Figure (2): Comparison between fertile and sterile groups in cholesterol level for cyst fluid





Wasan Addai Mahdi et al.

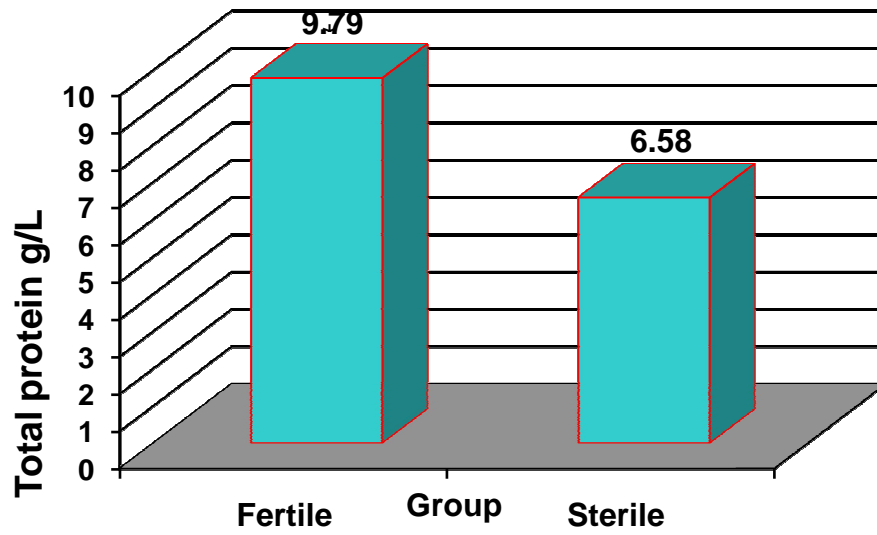


Figure (3) :Comparison between fertile and sterile groups in total protein of cyst fluid





Isolation of *Escherichia coli* O157:H7 from Cloacal Broiler and Feed Samples

Taha H. Al-Yasiri¹ *and Meyada F. Mohammed²

¹Basic College of Education, University of Misan, Misan, Iraq

²Public Health Department, University of Baghdad, Baghdad, Iraq

Received: 21 Sep 2018

Revised: 25 Oct 2018

Accepted: 27 Nov 2018

*Address for Correspondence

Taha H. Al-Yasiri

Basic College of Education,

University of Misan, Misan, Iraq.

Email:aleassery@gmail.com



This is an Open Access Journal / article distributed under the terms of the **Creative Commons Attribution License** (CC BY-NC-ND 3.0) which permits unrestricted use, distribution, and reproduction in any medium, provided the original work is properly cited. All rights reserved.

ABSTRACT

Two hundred sample from cloacal of broiler and one hundred and fifty of broiler feed samples were collected from chicken houses in Amara city in Iraq, they were placed in sterilized and closed bags and were transported by a cooled box to public health laboratories. On sorbitol, and on the chromogen media agar were isolated and demonstrated by a vitike2 assay and confirmed by a latex agglutination test, three positive sample detection from 200 cloacal swabs samples and five positive sample were isolated from 150 samples were tested.

Keywords: broiler; *E. coli* O157:H7; sorbitol, cloaca.

INTRODUCTION

Escherichia coli O157:H7 has showed up as an unused pathogen and it found around the world (1). In Californian at 1975 the primary disconnected of it was from woman with grisly the runs. (2). Riley and co-workers in 1982 recognized it as pathogen amid an examination of two flare-ups of hemorrhagic colitis that were related with utilization of sullied cheeseburgers (3). It has exceedingly harmfulness components, in this manner moo measurements (10-100 life forms) may take put disease and quick clinical signs in people, the tall harmfulness variables of *E.coli* O157:H7, which related with serious sickness of people, was shiga poisons (4). This bacterium can cause hemorrhagic colitis and other infections such as hemolytic uremic disorder and thrombotic thrombocytopenic purpura when utilization of sullied nourishment and water (5) Shiga toxin generation is basic to the pathogenesis of *Escherichia coli* O157:H7 strains. The harmfulness components *E. coli* O157:H7 are encoded by chromosomal pathogenicity islands, phage chromosomes coordinates within the bacterial genome as well as plasmids, which are decided the pathogenicity of Shiga toxin-producing *E.coli* (6). The high virulence of STEC strains like *E.coli* O157:H7 isn't only dependent on harmfulness variables but mostly moreover on the capacity to outlive natural unfavorable



**Taha H. Al-Yasiri and Meyada F. Mohammed**

conditions, such as resistance to low pH levels found within the gastrointestinal tract which contributes to exceptionally low irritable measurements of 50–100 cells or lower (7).

Escherichia coli O157:H7 spreading is regarded negligible compared with other species, especially ruminants. It is disconnected regularly from poultry or poultry handled (8,9). *E. coli* O157:H7 (EHCH) gotten to be determinate in Poultry. Numerous considers have report that 1 day-old chicks are touchy to long period colonization for up 1 year by verbal organization which note a critical number of egg shells is sully but not the connect the substance (10; 11;12;13;14). The distinguished sit of *E. coli* O157:H7 is the epithelial connection of youthful chicken, which cause multifocal enterocyte corruption and degeneration from almost 10-14 day after organization (15). A quick increment of *E.coli* in cecal colonization and diminish in crop structure was apparent all through the essential few hours, when challenge, with a most inside the caeca at six hour. *E. coli* endured in cecal substance in expansion as on cecal dividers all through the course of the tests (14 days), be that as it may at a parcel of lower levels compared with the six h post-challeng (11). Chicks have been appeared tentatively quick infected by little numbers 25 of *E. coli* O157:H7 bacteria cell and will still remove the life form in feces for a least of eight months past immunization (10).

MATERIALS AND METHODS

Source of samples

The samples were taken to isolated *Escherichia coli* O157:H7 bacteria from broiler and feed farms of Amara city in Iraq, they were collected during the period from April to July 2017. All the samples were placed in sterile bags and keeps in a thermos icebox during transfer to the central health laboratories; they were examined after two hours of collection. One gram of the samples were placed in (10) ml of Buffer Peptone Water (BPW) and incubated at 37C°for overnight.

Sample size

A total of (450) samples (cloacal swabs and feed samples) of broiler were collected from farm in Al-amara city.

Preparation

According to company, sorbitol McConke suspends 51.5g in 1 liter of distilled water. Bring to the boiling to break down totally. The suspend was sanitized by autoclaving at 121°C for 15 minutes and permit to cool to 50°C. The agar was pour into sterile Petri dishes. In order to isolate the *Escherichia coli* O157:H7, sorbitol added to the antibiotic was used as cefixime and potassium tellurite, one vial of cefixime, tellurite supplement per 500ml medium, concurring to the informational within the item flyer in which Cefixime is inhibitory to *Proteus* spp bacteria and the potassium tellurite inhibits *Providencia* and *Aeromonas* species. (16).

Sorbitol McConkey agar for selective and differential media for the isolation of *Escherichia coli* O157:H7

After the preparation of the sample, cultured on sorbitol McConkey to purify as well as to test for presence of *E. coli* O157:H7 and the samples were placed in the incubator for 24 hours at 37 C°, the colony of *E. coli* O157:H7, were appears on sorbitol McConkey agar, and the bacteria could not sorbitol fermentation.





Taha H. Al-Yasiri and Meyada F. Mohammed

Eosin Methylene Blue Agar (EMB) Agar

Eosin Methylene Blue Agar was used for the isolation and differentiation of e.coli bacteria from clinical and nonclinical specimens, the characteristics consistent of E. coli (blue-green).

Isolates and Identification of *Escherichia coli* O157:H7 on Chromogenic medium:

Chromogenic medium *ChROMagar™ O157* are used for the isolation and differentiation of *E.coli* O157.

***ChROMagar™* media agar**

Microorganisms appear, as different colonies in different colours that is depended on exist of various chromogenic substrates in the media. The chromogenic substrates are pasted with specific enzymes which are produced by organisms, that gave special colour may be used to identify genus, species, or groups of microorganisms. The colony appear coloured, purveying simple recognition (17).

Composition

The media contain agar, 15 g/l Peptone, yeast extract and salts, 13 g/l Special chromogenic mix, 1 g/l pH 6.8 Classical formula adjusted and/or supplemented as required to meet performance criteria.

Preparation of media

Agreeing to amounts wanted, weigh out powder and utilize within the extent 29 g/l litter of decontaminated water. Bubble the agar (100 °C) by repeated heating, whirling or mixing frequently. Warming utilizing autoclave without weight than cooling the agar in a water shower to 48 °C.

The Vitek 2

The Vitek 2 is an automated microbiology system utilizing growth-based technology.

Reagent Cards

The reagent cards have 64 wells that can each contain an individual test substrate. Substrates measure various metabolic activities such as acidification, alkalisation, enzyme hydrolysis, and growth in the presence of inhibitory substances. An optically clear film present on both sides of the card allows for the appropriate level of oxygen transmission while maintaining a sealed vessel utomatically that prevents contact with the organism-substrate admixtures. Each card has apre-inserted transfer tube used for inoculation (described below). Cards have bar codes that contain information on product type, lotnumber, expiration date, and a unique identifier that can be linked to the sample either before or after loading the card onto the system.

Latex Coagulation Test

Latex testing is a serological test to ensure that the E. coli insulation was used according to the manufacturer's recommendations. Nutrient medium agar used for detection *E.coli* 157 antigen as a sub-culture solid medium for *E.coli* colonies and for discover the location of H7 antigen used blood agar. E.coli was streaked on the 5% blood agar to get one colony. This kit is production of RymelWilcolex Diagnostics kit was imported from Europe ltd clipper boulevard wet.



**Taha H. Al-Yasiri and Meyada F. Mohammed****O157and H7 detection****O157 test latex**

O157 latex composed of suspension buffered of red polystyrene latex coated with rabbit specific IgG to *E. coli* O157:H7.

H7 latex test

H7 latex test composed of suspension buffered of red polystyrene latex coated with rabbit specific IgG to *E. coli* O157:H7. The latex O157, H7, and reagent reaction were brought to 25-30 °C and shaking well, put on reaction card in the 4 circles 40 µl of normal saline (for each test sample two circle for O157 and H7 then by mixing stick pick up adequate bacteria culture and blends with normal saline. Put one drop of either O157 or H7 latex test in the circle for each test sample and one drop for the control latex test of O157 and H7 latex and mixing well carefully and shaking the card slowly and with noticed the agglutination.

RESULTS AND DISCUSSION

Results showed that a total of 3 (1.5%) positive sample of *E. coli* O157:H7 were isolated from 200 cloacal swab samples taken from broiler houses, while 5 (3.33%) samples were isolated from 150 feed sample of broiler shown taken from different market in Al-Amara city, Iraq. Isolation of *E. coli* O157:H7 from poultry was infrequently reported (8). In poultry the prevalence of *Escherichia coli* O157:H7 infection was low compared with other animals (18). The result in table (1) showed positive sample of *E. coli* O157:H7 were isolated from variable sample cloacal swab (1.5%), feed sample (3.33%), and meat chicken (3%). The results were agreement with several studies reported, Baran and Gulmez (19), who reported 2% and 4.4% in Kenya. The prevalence of STEC *E. coli* O157:H7 in domestic chicken is relatively low, ranging from (0 to 1.5%), depending on the geographic location sampled (20). Same results were also obtained in United Kingdom where 1.5% of wild bird samples had the *E. coli* O157:H7 stx1 gene, 7.9% the stx2 gene (21). In turkeys, the incidence was higher than that in chickens, with up to 7.5% of fecal samples testing positive (22). Nielsen *et al.*, (23) identified that 2% of the wild bird dropping samples take it in close proximity to farms contained *E. coli* O157:H7 stx genes.

E. coli O157:H7 isolated in different countries, in Ethiopia, 13.4% were found to be positive for *E. coli* O157:H7 from Poultry farms. Olatoye *et al.*, (24) in Lagos and Ibadan poultry farms 13 and 14% of *E. coli* O157:H7 was isolate. In another study, Ojo *et al.* (25) confirmed *E. coli* O157:H7 strains in the dropping of poultry sample from different farms in Nigeria.

The variations take place due to the low isolation rate of culture methods compared to more sensitive immunological and molecular methods cross contamination with other principal reservoirs, areas and time, different sampling techniques, and lack of strict hygienic measures (26). Shecho *et al.*, (27) observed the prevalence of *E. coli* O157:H7 among the various age of groups, was higher of 18.8% among young birds (less than 6 months) than adult birds. This knowledge was converging with current study where achieved under 6 week of age. Chadran and Mazumder, (28), who isolates 93 *E. coli* of 8 avian birds from cloacal swabs and fresh droppings in British Columbia, Canada were carriers of stx2-gene.

REFERENCES

- 1- Doyle, M. E. (1999). Use of organic acids to control Listeria in meat. *American meat institute Foundation. VV-Madison. Organic Acids*, 6.





Taha H. Al-Yasiri and Meyada F. Mohammed

- 2- Griffin, P. M., & Tauxe, R. V. (1991). The epidemiology of infections caused by Escherichia coli O157: H7, other enterohemorrhagic E. coli, and the associated hemolytic uremic syndrome. *Epidemiologic reviews*, 13(1), 60-98.
- 3- Riley, L. W., Remis, R. S., Helgerson, S. D., McGee, H. B., Wells, J. G., Davis, B. R., ... & Blake, P. A. (1983). Hemorrhagic colitis associated with a rare Escherichia coli serotype. *New England Journal of Medicine*, 308(12), 681-685.
- 4- Paton, A. W., & Paton, J. C. (1998). Detection and Characterization of Shiga Toxigenic Escherichia coli by Using Multiplex PCR Assays for stx 1, stx 2, eaeA, Enterohemorrhagic E. coli hlyA, rfb O111, and rfb O157. *Journal of Clinical Microbiology*, 36(2), 598-602.
- 5- Boyce, T. G., Swerdlow, D. L., & Griffin, P. M. (1995). Escherichia coli O157: H7 and the hemolytic-uremic syndrome. *New England Journal of Medicine*, 333(6), 364-368.
- 6- Newton-Cheh, C., Johnson, T., Gateva, V., Tobin, M. D., Bochud, M., Coin, L., & Papadakis, K. (2009). Genome-wide association study identifies eight loci associated with blood pressure. *Nature genetics*, 41(6), 666.
- 7- Armstrong, G. L., Hollingsworth, J., & Morris Jr, J. G. (1996). Emerging foodborne pathogens: Escherichia coli O157: H7 as a model of entry of a new pathogen into the food supply of the developed world. *Epidemiologic reviews*, 18(1), 29-51.
- 8- Doyle, M. P., & Schoeni, J. L. (1987). Isolation of Escherichia coli O157: H7 from retail fresh meats and poultry. *Applied and Environmental Microbiology*, 53(10), 2394-2396.
- 9- Levine, P., Rose, B., Green, S., Ransom, G., and Hill, W. (2001). Pathogen testing of ready-to-eat meat and poultry products collected at federally inspected establishments in the United States, 1990 to 1999. *Journal of Food Protection* 64:1188-1193.
- 10- Beery, J. T., Doyle, M. P., & Schoeni, J. L. (1985). Colonization of chicken cecae by Escherichia coli associated with hemorrhagic colitis. *Applied and environmental microbiology*, 49(2), 310-315.
- 11- Stavric, S., Buchanan, and T. M. Gleeson. (1993). Intestinal colonization of young chicks with *Escherichia coli* O157:H7 and other verotoxin-producing.
- 12- Schoeni, J. L., & Doyle, M. P. (1994). Variable colonization of chickens perorally inoculated with Escherichia coli O157: H7 and subsequent contamination of eggs. *Applied and Environmental Microbiology*, 60(8), 2958-2962.
- 13- Best, A., La Ragione, R.M., Cooley, W.A., O'Connor, C.D., Velge, P., Woodward, M.J., (2003). Interaction with avian (Div-1) cells and colonisation of specific pathogen free (SPF) chicks by Shiga-toxin negative Escherichia coli O157:H7 (NCTC 12900). *Vet. Microbiol.* 92, 207-222.
- 14- Best, A., La Ragione, R.M., Sayers, A.R., Woodward, M.J., (2005). A role for flagella but not intimin in the persistent infection of the gastro-intestines of specific pathogen free chicks by Stx-negative Escherichia coli O157:H7 (NCTC12900). *Infect. Immun.* 73, in press.
- 15- Sueyoshi, M., Nakazawa, M., 1994. Experimental infection of young chicks with attaching and effacing Escherichia coli. *Infect. Immun.* 62, 4066-4071.
- 16- Food and Drug Administration (1995) Bacteriological Analytical Manual. 8th Edition. AOAC International. Gaithersburg. MD. Chapter 4, 20-23
- 17- Ronald, M.A. (2006). *Handbook of Microbiology Media for Examination of Food*, 2nd ed. CRD press, pp. 64-114.
- 18- La Ragione, R. M., Best, A., Sprigings, K., Liebana, E., Woodward, G. R., Sayers, A. R., & Woodward, M. J. (2005). Variable and strain dependent colonisation of chickens by Escherichia coli O157. *Veterinary Microbiology*, 107(1-2), 103-113.
- 19- Baran and M. Gulmez (2010). "The occurrence of Escherichia coli O157:H7 in the ground beef and chicken drumsticks," *Internet Journal of Food Safety*, vol.2, pp. 13-15, 2010.
- 20- Persad, A. K., & Lejeune, J. T. (2014). Animal reservoirs of Shiga toxin-producing *Escherichia coli*. *Microbiology Spectrum*, 2(4), 1-14. <https://doi.org/10.1128/microbiolspec.EHEC-0027-2014>. Correspondence.
- 21- Hughes, L. A., Bennett, M., Coffey, P., Elliott, J., Jones, T. R., Jones, R. C., Chantrey, J. (2009). Risk factors for the occurrence of Escherichia coli virulence genes eae, stx1 and stx2 in wild bird populations. *Epidemiology and Infection*, 137(11), 1574-1582. <https://doi.org/10.1017/S0950268809002507>.
- 22- Doane, C. a, Pangloli, P., Richards, H. a, Mount, J. R., Golden, D. a, & Draughon, F. a. (2007). Occurrence of Escherichia coli O157:H7 in diverse farm environments. *Journal of Food Protection*. <https://doi.org/10.4315/0362-028X-70.1.6>





Taha H. Al-Yasiri and Meyada F. Mohammed

23- Nielsen, E. M., Skov, M. N., Madsen, J. J., Lodal, J., Jespersen, J. B., & Baggesen, D. L. (2004). Verocytotoxin-producing *Escherichia coli* in wild birds and rodents in close proximity to farms. *Applied and Environmental Microbiology*. <https://doi.org/10.1128/AEM.70.11.6944-6947.2004>.

24- Olatoye, I. O., Amosun, E. A., & Ogundipe, G. A. T. (2012). Multidrug-resistant *Escherichia coli* O157 contamination of beef and chicken in municipal abattoirs of southwest Nigeria. *Nature and Science*, 10(8), 125-132.

25- Ojo, O. E., Oyekunle, M. A., Ogunleye, A. O., & Otesile, E. B. (2009). *E. coli* O157: H7 in food animals in part of S/Western Nigeria: Prevalence and in vitro antimicrobial susceptibility. *Tropical Veterinarian*, 26, 23-30.

26- Hiko, A., Asrat, D., & Zewde, G. (2008). Occurrence of *Escherichia coli* O157: H7 in retail raw meat products in Ethiopia. *The Journal of Infection in Developing Countries*, 2(05), 389-393.

27- Shecho, M., Thomas, N., Kemal, J., & Muktar, Y. (2017). Cloacal Carriage and Multidrug Resistance *Escherichia coli* O157: H7 from Poultry Farms, Eastern Ethiopia. *Journal of veterinary medicine*, 2017.

28- Chandran, A., & Mazumder, A. (2014). Occurrence of Diarrheagenic Virulence Genes and Genetic Diversity in *Escherichia coli* Isolates from Fecal Material of Various Avian Hosts: British Columbia, Canada. *Applied and environmental microbiology*, AEM-03949.

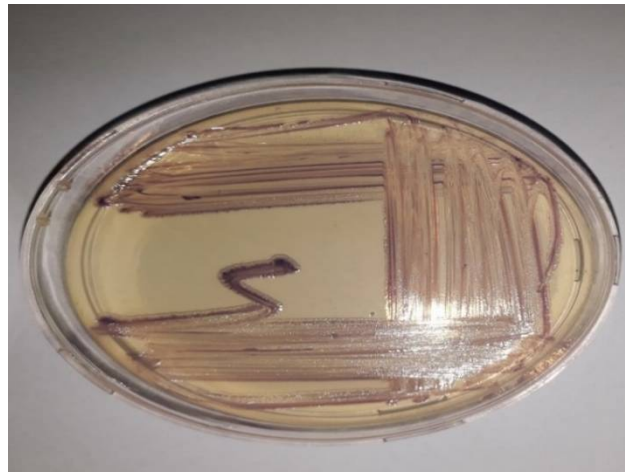


Figure 1 shows the *E. coli* 157:H7 growth colony on Chromogenic medium ChROM agar TM O157

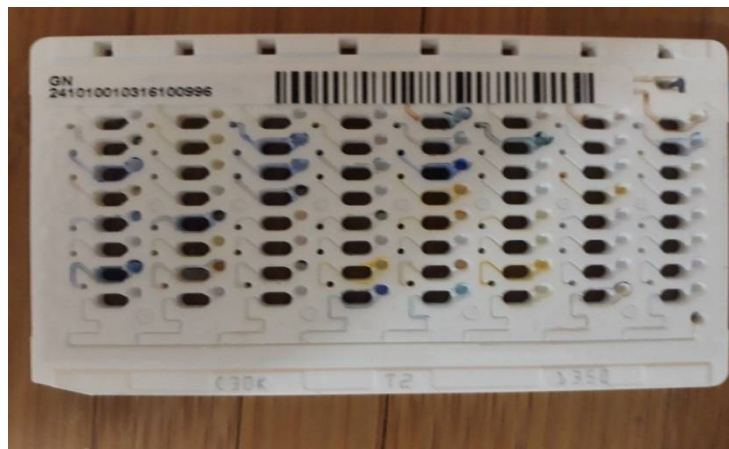


Figure 2. Shows the Reagent Cards card





Taha H. Al-Yasiri and Meyada F. Mohammed

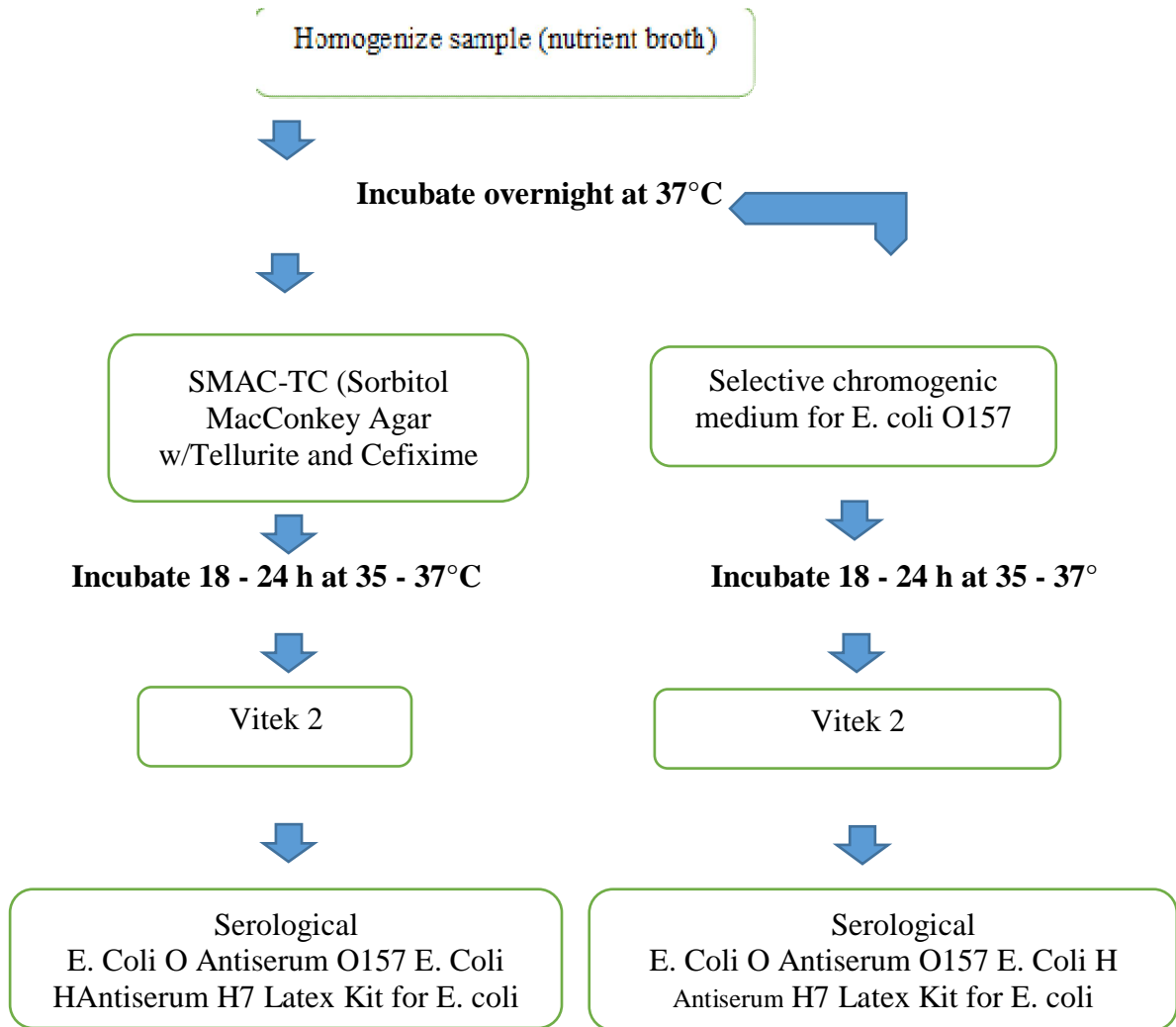


Figure 3. Isolation and Identification of *E. coli* O157:H7 in from cloacal broiler and feed samples.





RESEARCH ARTICLE

Numerical Calculations of Sunspot Growth, Decay Phases and Area Calculations using Matlab

Noor Alhuda Kamel* and Ahmed Abdul-Razzaq Selman

Department of Astronomy and Space, College of Science, University of Baghdad, Baghdad, Iraq.

Received: 05 Sep 2018

Revised: 07 Oct 2018

Accepted: 09 Nov 2018

* Address for Correspondence

Noor Alhuda Kamel

Department of Astronomy and Space,
College of Science,
University of Baghdad,
Baghdad, Iraq.
Email:kamlnwralhdy@gmail.com



This is an Open Access Journal / article distributed under the terms of the **Creative Commons Attribution License** (CC BY-NC-ND 3.0) which permits unrestricted use, distribution, and reproduction in any medium, provided the original work is properly cited. All rights reserved.

ABSTRACT

A study is made about the growth, decay phases and the area of observed Sunspots on the surface of the sun are calculate. Two types of images have been used H-alpha and HMI magnetograms images. Calculations were made in this work focused on the period from 2010 till 2018. The calculations were made by Matlab. Results are divided into two parts ,the first part is the growth rate that found from fitting velocity of sunspots radius variation due to the time of sunspots evolution. The sunspots decayed in the period time (17-27 Aug 2011) and (14-25 Nov 2010) when using H-alpha images more than other years of the study, and the little variation in the sizes of sunspots happened in (03-14 Sep 2016) when using H-alpha images. The results of second part are showed the area of Sunspots that covered the surface of the sun. The area of Sunspot are continues in change during the time of study. The results are give us an indicates about the appearance and disappearance of the Sunspots on the surface of the sun.

Keywords: Sun, Sunspot, Decay , Growth, Evolution, Area, Appearance, Disappearance, Magnetic field.

INTRODUCTION

When concentrated magnetic field lines start to emerge from the photosphere, directed outward in the direction of the solar corona, the sunspots are developed. The umbra of the sunspot is the dark black region of a sunspot. The penumbra may expand on more established sunspots on the outer edge of the umbra. The penumbra appears a little brighter than the umbra. The penumbra still darker than the surrounding solar surface. This is caused by the Evershed effect where magnetic field lines have a larger horizontal component leaving the sunspot, allowing for increased plasma flow and increased convection below the penumbra [1]. So the penumbra has a higher temperature and brighter appearance than in the umbra. The presence of a penumbra is important to distinguish sunspots from





Noor Alhuda Kamel and Ahmed Abdul-Razzaq Selman

the usually smaller pores. Sunspots harbor magnetic fields which inhibit at least partially convection energy transport leading to the darker appearance of the umbra. The most strong plasma flow is observed in the penumbra dominated by the flow which is interpreted as a horizontal outflow pattern with velocities roughly in the range 2-6 km/sec. The magnetic field is almost vertical in the umbra. Forced by the exponential decrease of density and flux conservation the field lines spread out with height giving rise to a magnetic canopy [2]. The sunspot's growth phase is generally much shorter than its decay phase. The sunspots forms in a few days but its typically live for a few weeks and sometimes for several months (several solar rotation periods).

Early studies of the sunspots growth based on the Greenwich photoheliographic. The growth was fastest at the first appearance of a spot [3] , but later found that the growth rate typically increased especially for the largest spots, during the early stages of spot growth. The pores grow into proper spots, growing and separating in longitude within two weeks the group has reached its maximum length with a fairly regular leading spot and a less regular follower together with many smaller spots spread around in the area[6]. The largest that of April (1947) recorded, That covered an area of over 18,000 million square kilometers (7000 million square miles) when at its largest, but they are not enduring. A major group may continue for anything up to six months, though very small spots often have lifetimes of less than a couple of hours. Spots are basically magnetic phenomena and there is a practically predictable cycle of events. Maxima, with many groups on view at the same time[5]. The cycle occur every 11 years or so. After which activity starts to build up once more towards the next maximum ,activity then dies down until at minimum the disk may be free of spots for many successive days or even weeks.

There are a relation between the solar cycle and the number of sunspots. Which the number of sunspots called "The International Sunspot Numbers" (Wolf or Zürich sunspot numbers) have long served as the primary time series defining solar activity since the year 1700[4]. The area of the largest visible sunspot also follows the activity of the solar cycle with a clear rising phase and a slower declining phase[7]. The variation in sunspot area is larger as sunspot sizes have a larger range than the number of spots that are present[7].

The Growth phase and the Decay Phase of Sunspot

In this section the ratio between the variation in sunspots radius due to the variation in time of sunspots evolution calculated. This ratio help us to know how the sunspots growing or decaying during the time of study[5]. This ratio, R_g , is given by :

$$R_g = \frac{\Delta r}{\Delta t} \dots \dots \dots (1)$$

where

R_g :is the ratio between the variation of sunspot radius in km due to the variation in time of sunspot evolution in second. Δr : is the difference between the between the sunspot radius and the radius of next sunspot in km.

Δt : is the difference between the time of sunspot and the time of the next sunspot in sec.

When :

R_g : positive value this mean that the size of sunspot increase by about that value(growing).

R_g :negative value this mean that the size of sunspot decrease by about that value(decay). This ratio calculated and plotted for period of time from 2010 to 2018 . The data taken from the GONG and SDO for two types of images H-alpha image and HMI magnetogram image . The results that we get it from H-alpha image differ from the results that we have it from HMI magnetogram images, this because the difference between the properties of two images that we used it in the program[5].





Noor Alhuda Kamel and Ahmed Abdul-Razzaq Selman

The Area of Largest Visible Sunspots

The area of sunspots that cover the surface of sun calculated. The area of the largest visible sunspot also follows the activity of the solar cycle. The variation is larger as sunspot sizes have a larger range than the number of spots that are present. The sunspots appear as a dark spots (circles) on the photosphere so we used the equation of area of circle to find the area of sunspots[5]. The equation of area of sunspots is given by:

Area of sunspots = πr^2 (2)

where :

r : is the radius of the sunspot in km.

The unit of the area of sunspot is km^2 .

The variation of the area is larger as sunspot sizes have a larger range than the number of spots that are present on the surface of the sun. The area of sunspot when increase and decrease with time this mean that the appearance and disappear of sunspots changed during the time of study. This part used to have a close insight of the changes of magnetic fields of observed sunspots[5].

RESULTS AND DISCUSSION

The Growth and Decay Phases of Sunspots

The ratio between the variation in sunspots radius due to the variation in time of sunspots evolution is calculated. This ratio help us to know how much the sunspots growing or decaying during the time of study. The first results indicated in figure (1-1-a) to figure (1-9-b) for the most suitable values. In this section we calculated and plotted this ratio for period of time from 2010 to 2018. The data taken from the GONG and SDO for two types of images H-alpha image and HMI magnetogram image. The results that we get it from H- alpha image differ from the results that we have it from HMI magnetograms, this because the difference between the properties of two images that we used it in this research. The figure (1-1-a) shows the fitting velocity of the variation of sunspots radius in km due to the variation of time in (sec) using H-alpha images. This variation shows how much the sunspots grow or decay. If the ratio between the difference in radius to the difference in time positive this means the sunspots grow, but if it is negative this means the sunspots decay. From the figure we noticed that the sunspots changed irregularly in the period (14-25 Nov 2010). The values of $R_g = (0.0256, -0.0656, -0.0159, 0.0381, \text{ and } -0.0158)$ km/sec respectively. The first value of $R_g = 0.0256$ km/sec means that the sunspots grow by about 0.0256 from its origin size. Then the $R_g = -0.0656$ km/sec this value means that the sunspots decay by about -0.0656 from its origin size. The other values of R_g that I mentioned above also the positive values are mean the sunspot grow, and the negative are mean the sunspots decay.

When the fitting velocity of the variation of sunspots radius in km due to the variation of time in (sec) for the same time period using HMI magnetogram images as shown in figure (1-1-b) the values of $R_g = 0.1107, -0.0159, 0, -0.0159, -0.0118$ and 0.0167 respectively. In the case of $R_g = 0$ the sunspots radius don't change through the two day that we are study. This means the size of sunspot don't change (still constant). When compared between of R_g for H-alpha images and HMI magnetogram images for period time(2010 to 2018), as shown in the above figurers, Note that the sunspots decayed in the period time (17-27 Aug 2011) when using H-alpha images more than other years that have been studying, and the little variation in the sizes of sunspots happened in (03-14 Sep 2016) when using H-alpha image more than the other years, but when using HMI magnetogram images are show variation in the sizes of sunspots(the sunspots decay or growth) this variation can't be seen in H-alpha images. So the HMI images are the best images for detection and study the sunspots size and activity.



**Noor Alhuda Kamel and Ahmed Abdul-Razzaq Selman****The Area of Observed Sunspots**

The area of the larger visible sunspots on the surface of sun are calculated using the radius of the sunspots that found automatically using a Matlab code. The area of sunspots for period of time from 2010 to 2018 are calculated in this research, as shown in the figures (2-1-a) to (2-18-b) using two types of images H-alpha images and HMI magnetogram images. Figure(2-1-a) shows the relation between the area of the largest visible sunspot with time during time period (14-25 Nov 2010) using H-alpha image and fig(2-1-b) shows the relation between the area of the largest visible sunspot with time during time period (14-25 Nov 2010) using HMI magnetogram image. Fig(2-1-c) and Fig(2-1-d) show the relation between the area of the largest visible sunspot with time during time period (17-27 Aug 2011) using H-alpha and HMI magnetogram images respectively. Fig(2-1-a) shows the area of the sunspot is changed irregular with time.

An interesting feature of this plot is that at the start the area of observed sunspots increased with time this mean that there are more spots beginning to appear and the magnetic field is strong then the area of observed sunspots decreased with time this mean that there are spots beginning to appear but the spot magnetic fields are still weak. Then the area increase and return to decrease with time of evaluation of sunspots that we study. When using HMI magnetogram images for the same time period (14-25 Nov 2010) as shown in Fig(2-1-b) an interesting feature of this plot is that at the start the area of observed sunspots also increased with time, this mean that there are more spots beginning to appear and the magnetic field is strong then the area of observed sunspots decreased with time this mean that there are spots beginning to appear but the spot magnetic fields are still weak.

Then the area of observed sunspots continuous to decreased and then become constant this mean that the sunspots beginning to appear and the magnetic fields doesn't change still weak(constant). Then the area of observed sunspots decreased and increased this mean that appearance and disappear of sunspots changed during the time of study with the magnetic felids of observed sunspots. The behavior of results that have been using H-alpha are similar to the behavior of results that when using HMI magnetogram images. When changes the data and using the data that taken in time period (17-27 Aug 2011) using H-alpha images. The area of the sunspot is continues to change irregular with time as shown in Fig(2-1-c). The sunspots beginning to appear but the spot magnetic fields are still weak then its increased with time this mean that there are more spots beginning to appear and the magnetic field is strong. Then its increase and decrease with time this mean that appearance and disappear of sunspots changed during the time of study with the magnetic felids of observed sunspots. Fig(2-1-d) shows the relation between the area and the time using HMI magnetogram images.

The area of observed sunspots increased with time this mean that there are more spots beginning to appear and the magnetic field is strong then the area of observed sunspots decreased with time this mean that there are spots beginning to appear but the spot magnetic fields are still weak. Then the area of observed sunspots continuous to decreased and then become constant this mean that the sunspots beginning to appear and the magnetic fields doesn't change still weak(constant). Then the area of observed sunspots decreased and increased this mean that appearance and disappearance of sunspots changed during the time of study with the magnetic felids of observed sunspots. The behavior of results that we have using H-alpha are similar to the behavior of results that we have by using HMI magnetogram images.

Figures(2-1-e,2-1-f,2-1-g,2-1-h,2-1-i,2-1-j,2-1-k,2-1-l,2-1-m,2-1-n,2-1-o,2-1-p,2-1-q,2-1-r) show the area of sunspots changed with time of sunspots evolution for the period time (02-11 June 2012, 02-11 April 2013, 10-20 Feb 2014, 13-23 December 2015, 03-14 Sep 2016, 01-12 Aug 2017, 05_16 Feb 2018) respectively. The area of sunspot are continues in change during the time of study. The results are give us an indicates about the appearance and disappearance of sunspots on the surface of the sun. In some figures the behavior of the area with time is approximately constant.





Noor Alhuda Kamel and Ahmed Abdul-Razzaq Selman

CONCLUSIONS

1. The sunspot's are decayed more in 2010 and 2011 than 2012,2013,2014,2015,2016,2017 and 2018.
2. The size of sunspots variation little in 2016 when using H-alpha image more than the other years, but when using HMI magnetogram images are show variation in the sizes of sunspots(the sunspots decay or growth) this variation can't be seen in H-alpha images.
3. From the above results the HMI images are the best images for detection and study the sunspots size, decay of sunspots ,growth of sunspots and activity.
4. The area of sunspot's that cover the suns' surface are changed during the time of study. The area of the largest visible sunspot also follows the activity of the solar cycle. The variation is larger as sunspot sizes have a larger range than the number of spots that are present.
5. The HMI magnetogram images are the best images for studying the sunspots properties than H-alpha images. Because the HMI magnetogram images show the small details, and variations that can't be seen in H-alpha images.

REFERENCES

[1] MacLane A. Townsend, 2016,"Automated Sunspot Classification and Tracking Using SDO/HMI Imagery", Department of Engineering Physics, Air University, Theses and Dissertations 349.

[2] Z. F. Al-Hakeem, 2015 ,"Study and Analysis of Solar Coronal Mass Ejections (CME) from SOHO/LASCO Coronagraph Data", M.Sc. ,University of Baghdad.

[3] Johnh. Thomas and Nigelol. Weiss, 2008,"SUNSPOTS AND STARSPOTS",Cambridge University Press The Edinburgh Building, Cambridge CB2 8RU, UK.

[4] N.K.Hussien, "Automatic detection of sunspots size and activity by Matlab" B.Sc. in Astronomy and Space 2016,university of Baghdad.

[5] Sir Patrick Moore, 2005, "Atlas of the univers ", revised edition The Journal of British Astronomical Association.

[6] S.A.Thabet, 2014, "Study of Solar Magnetic Field Generation using the Dynamo Model", M.Sc. University of Baghdad.

[7] F. T. Watson and L. Fletcher, "Evolution of sunspot properties during solar cycle 23", School of Physics and Astronomy (2011), SUPA, University of Glasgow, Glasgow G12 8QQ, UK.

Table (1) shows the values of $(R_g-\Delta r/\Delta t)$ in (km/sec) for H-alpha images and HMI magnetogram images for period time(2010-2018), as shown in the below figurers ((1-2-a),(1-2-b),(1-3-a),(1-3-b),(1-4-a),(1-4-b),(1-5-a),(1-5-b),(1-6-a),(1-6-b),(1-7-a),(1-7-b),(1-8-a),(1-8-b),(1-9-a) and (1-9-b)).

The date	The values of R_g using H-alpha image	The values of R_g using HMI magnetogram image
(17-27 Aug 2011)	-0.0269 -0.0239 -0.0530 -0.0153 0.2465 -0.0687	0.0263 -0.0299 0.1026 0.0297 -0.2386
(02-11 June 2012)	-0.0078 0 0 0.0126 -0.0252	-0.0296 0.0190 0.0594 0.8836 -0.8245





Noor Alhuda Kamel and Ahmed Abdul-Razzaq Selman

(02-11 April 2013)	-0.0049 0.0359 0 -0.045 -0.0136	0.0134 -0.0485 0 -0.1848 0.1347
(10-20 Feb 2014)	-0.1673 -0.0228 0.0208 -0.0254 0.3952	0 -0.0823 0.0171 0.0456 1.1380
(13-23 Dec 2015)	-0.2071 -0.0060 0.0162 0 0.0065 -0.5961	-1.1697 -0.1542 0.0162 0.0955 -0.5706
(03-14 Sep 2016)	-0.1940 0.0071 0 0 0	0.0803 -0.0561 -0.0647 -0.0708
(01-12 Aug 2017)	-0.1473 0 -0.0154 0 0.0106 0.0944	-0.8783 0.0313 -0.0313 -0.0291 0.0029 0.0233 0.0477
(05-16 Feb 2018)	-0.1948 0 0.0198 -0.0139 0.0624 0.382	-0.1234 0.0074 0.0062 -0.0252

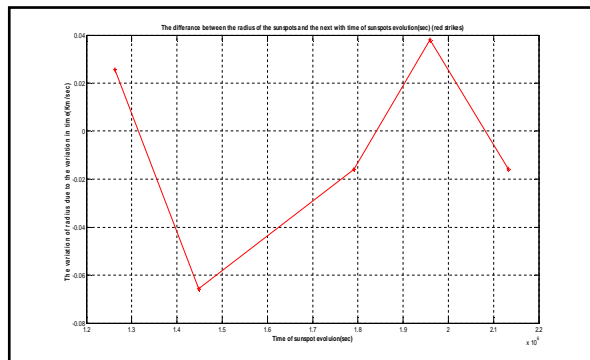


Figure (1-1-a) shows the relation between the variation of sunspots radius to the variation of time in (km/sec) and the time of evolution in (sec) using H-alpha images for period (14_25 Nov 2010).

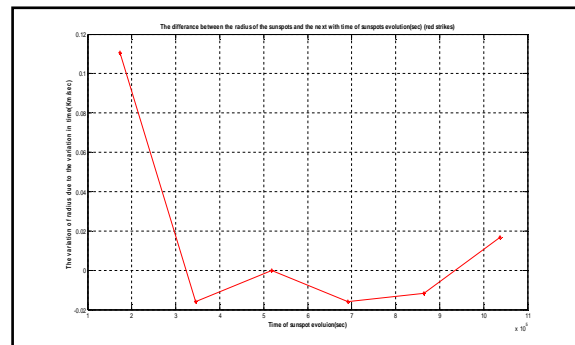


Figure (1-1-b) shows the relation between the variation of sunspots radius to the variation of time in (sec) and the time of evolution in (sec) using HMI magnetogram images for period time from (14-25 Nov 2010).





Noor Alhuda Kamel and Ahmed Abdul-Razzaq Selman

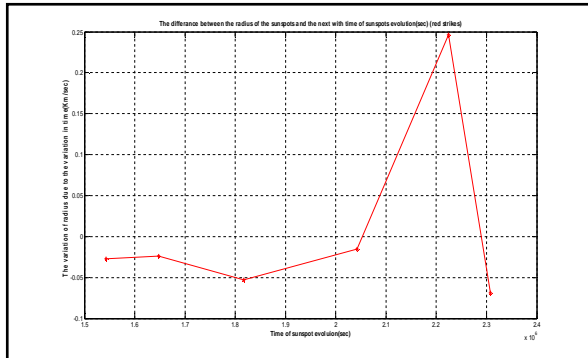


Figure (1-2-a) shows the relation between the variation of sunspots radius to the variation of time in (sec) and the time of evolution in (sec) using H-alpha images for period (17-27 Aug 2011).

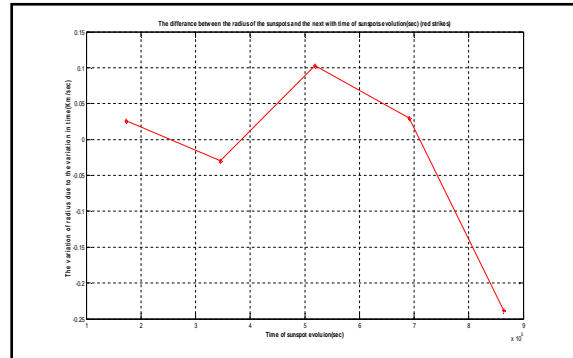


Figure (1-2-b) shows the relation between the variation of sunspots radius to the variation of time in(sec) and the time of evolution in (sec) using HMI magnetogras images for period(17-27 Aug 2011).

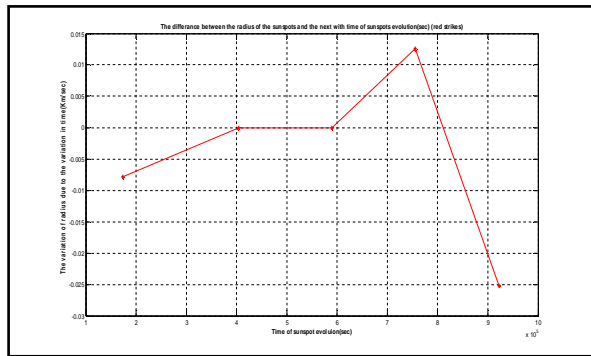
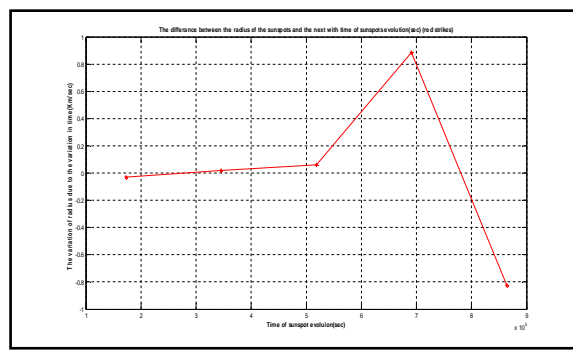


Figure (1-3-a) shows the relation between the variation of sunspots radius to the variation of time in (sec) and the time of evolution in (sec) using H-alpha images for period (02-11 June 2012).



Figure(1-3-b) shows the relation between the variation of sunspots radius to the variation of time in(sec) and the time of evolution in (sec) using HMI magnetogras images for period(02-11 June 2012).

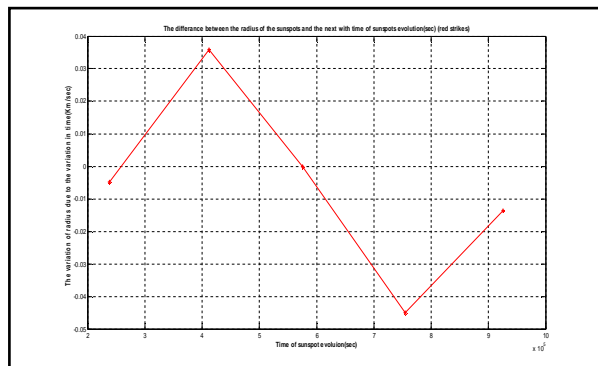


Figure (1-4-a) shows the relation between the variation of sunspots radius to the variation of time in (sec) and the time of evolution in (sec) using H-alpha images for period (02-11 April 2013).

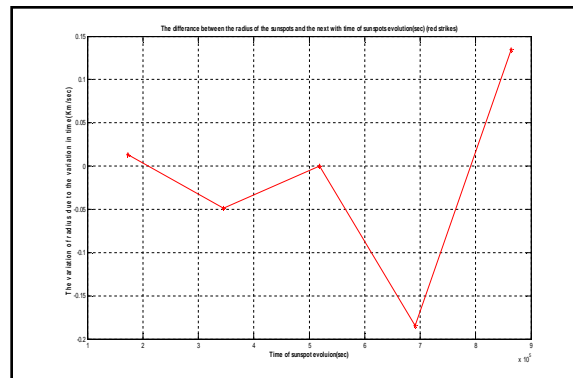


Figure (1-4-b) shows the relation between the variation of sunspots radius to the variation of time in (sec) and the time of evolution in (sec) using HMI magnetogram images for period (02-11 April 2013)





Noor Alhuda Kamel and Ahmed Abdul-Razzaq Selman

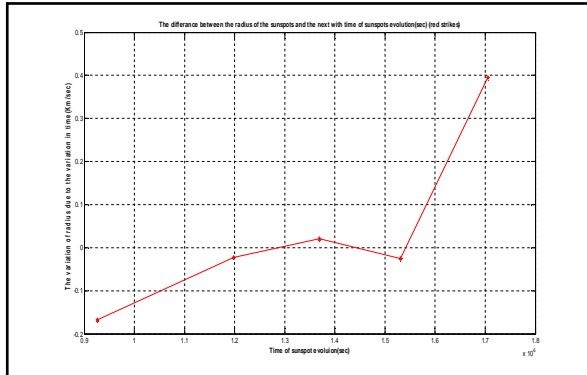


Figure (1-5-a) shows the relation between the variation of sunspots radius to the variation of time in (sec) and the time of evolution in (sec) using H-alpha images for period (10-20 Feb 2014).

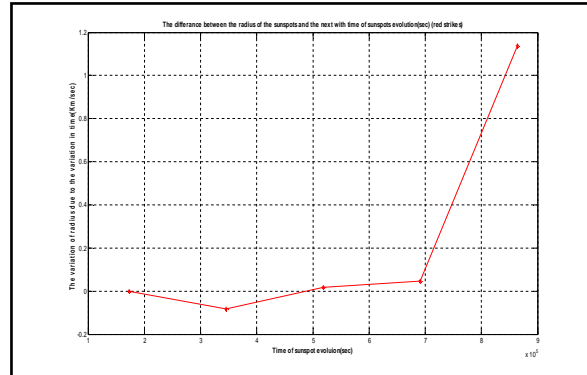


Figure (1-5-b) shows the relation between the variation of sunspots radius to the variation of time in (sec) and the time of evolution in (sec) using HMI magnetogram images for period (10-20 Feb 2014).

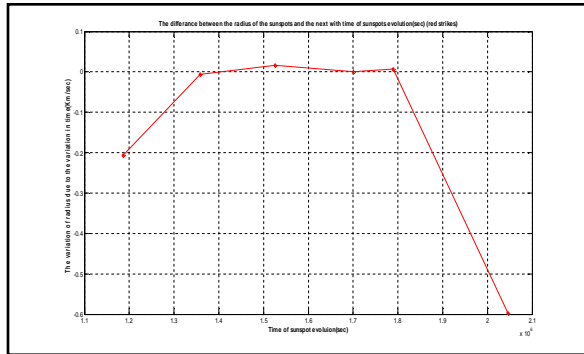


Figure (1-6-a) shows the relation between the variation of sunspots radius to the variation of time in (sec) and the time of evolution in (sec) using H-alpha images for period (13-23 December 2015).

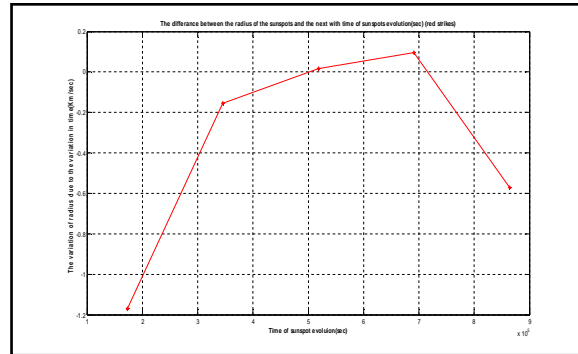
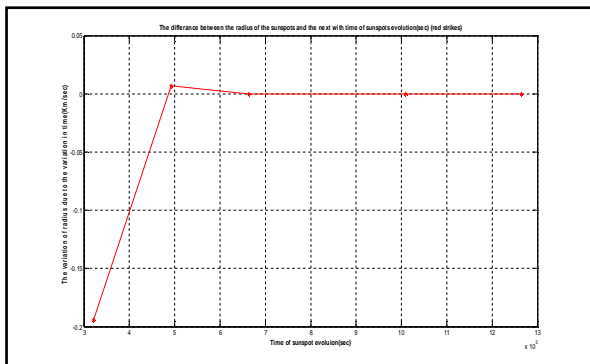
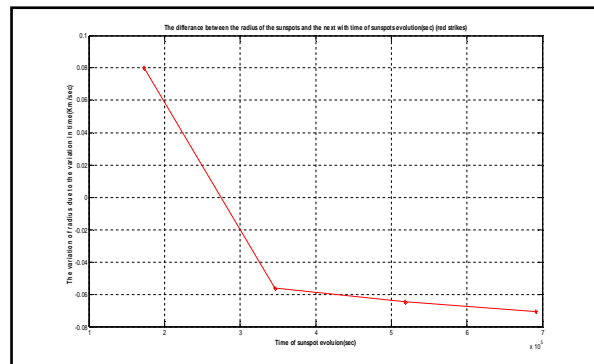


Figure (1-6-b) The relation between the variation of sunspots radius to the variation of time in(sec) and the time of evolution in (sec) using HMI magnetogram images for period (13-23 December 2015).



Figure(1-7-a) shows the relation between the variation of sunspots radius to the variation of time in(sec) and the time of evolution in (sec) using H-alpha images for period(03-14 Sep 2016).

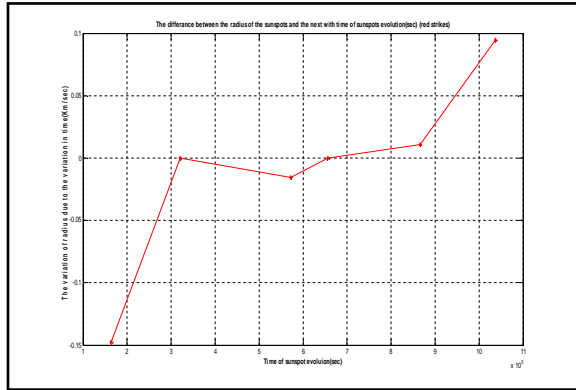


Figure(1-7-b) shows the relation between the variation of sunspots radius to the variation of time in (sec) and the time of evolution in (sec) using HMI magnetogras images for period (03-14 Sep 2016

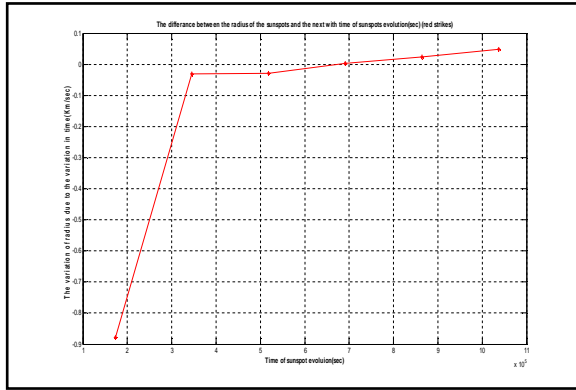




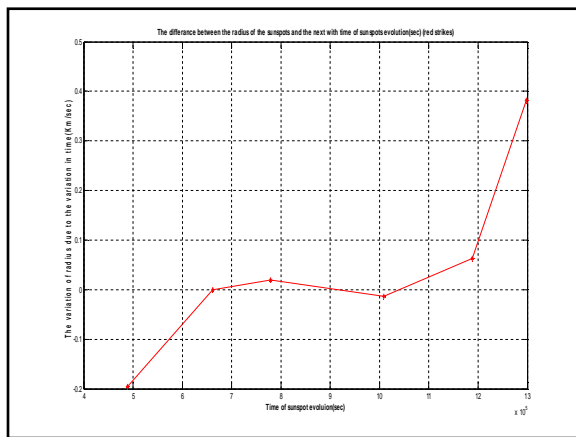
Noor Alhuda Kamel and Ahmed Abdul-Razzaq Selman



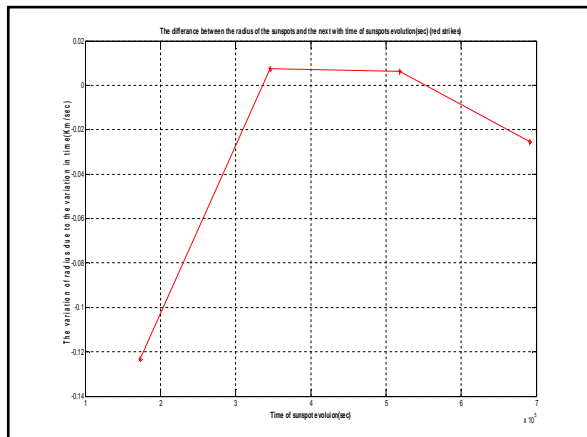
Figure(1-8-a) shows the relation between the variation of sunspots radius to the variation of time in (sec) and the time of evolution in (sec) using H-alpha images for period (01-12 Aug 2017).



Figure(1-8-b) shows the relation between the variation of sunspots radius to the variation of time in (sec) and the time of evolution in (sec) using HMI magnetogram images for period (01-12 Aug 2017).



Figure(1-9-a) shows the relation between the variation of sunspots radius to the variation of time in (sec) and the time of evolution in (sec) using H-alpha images for period (05-16 Feb 2018).



Figure(1-9-b) shows the relation between the variation of sunspots radius to the variation of time in (sec) and the time of evolution in (sec) using HMI magnetogram images for period (05-16 Feb 2018).





An Empirical Analysis of the Relationship between Unemployment and GDP in Iraq

Mustafa Omer Abbas AL-Gburi*

Korea Advanced Institute of Science and Technology, South Korea

Received: 18 Aug 2018

Revised: 20 Sep 2018

Accepted: 22 Oct 2018

*Address for Correspondence

Mustafa Omer Abbas AL-Gburi

Korea Advanced Institute of Science and Technology,
South Korea.

Email: mustafaomar.abbas1@yahoo.com



This is an Open Access Journal / article distributed under the terms of the **Creative Commons Attribution License** (CC BY-NC-ND 3.0) which permits unrestricted use, distribution, and reproduction in any medium, provided the original work is properly cited. All rights reserved.

ABSTRACT

Okun's law is one of the important laws in the macro-economy, which provides for an inverse relationship between unemployment and economic growth, in this sense, my study aims to examine Okun's law and its potential application to the Iraqi economy and whether there is an inverse relationship between them. Approach: For this study, we used time series techniques to estimate Okun's law coefficient and determine the existence of the relationship between the unemployment rate and the economic growth rate by using "ARDL" The Autoregressive Distributed Lag cointegration test. It uses the bound testing approach. Finally, the study showed that the relationship between unemployment and economic growth is inverse, which is a short-run relationship with a weak Okun's coefficient (**-0.052141**). It is negative and statistically significant between the two variables. Therefore, the decision-makers should take the necessary measures to increase employment in Iraq by increasing economic growth rates.

Keywords: empirical results, economic growth, unemployment, okun's law, Iraq economy, OLS, PP, ARDL, Bound test, ECM, Iraq, Arab.

INTRODUCTION

Most developed and developing countries with high unemployment face serious socio-economic problems. This is an economic phenomenon that shows an imbalance in economic activity. The economic and social dimensions of unemployment are complex and require a thorough analysis of the causes and consequences and the identification of responses to this phenomenon. The most important impact positively reflected in the reduction of unemployment is the tendency to increase growth, thereby creating more jobs through investment programs. (Ahmed, A., A. Abdul Kader and R. Ahmed, 1996). The lack of economic growth, population growth, low economic activity due to stagnation and the lack of funding for investment, unskilled labor and changes in demand for consumer goods that are disproportionate to changes in the labor market, and changes in technology as well as the imbalance between



**Mustafa Omer Abbas AL-Gburi**

supply and demand in the market are all factors have led to the emergence of unemployment, which has been witnessed in many countries in the world, especially developing countries (Abdulla,2012).There is a desire for the existence of a labour force in the country's economy and it is affected by production and work. The loss of any part of these forces causes unemployment, which is measured by the difference between working-age category (those who are able to work) in the community and opportunities to work (Abdulla, 2012).The growth rate of GDP in all developing countries has a direct impact on employment and lack of the current economic growth may seriously hinder the basic assumptions in the economy. If the GDP increases, the unemployment rate will decrease and also the employment rate will increase. Therefore, there is a relationship between changing economic growth and changing unemployment rates, which has been confirmed by many studies.

This study is of great importance in determining the relationship between the economic growth rate and the unemployment rate in Iraq, as well as examining the reality witnessed by the Arab countries and Iraq in particular from unemployment. The main idea of this study is to analyze the relevant relationships consistent with the theoretical basis of Okun's test.

Selection of the Topic

The problem of unemployment has become increasingly dangerous in Iraq since the 1980s because of the security and social conditions experienced by the country until now. These events have had a negative impact in the following area:

- 1- The labour force in Iraq.
- 2- Lack of clear policies on the economy and society.
- 3- Lack of job creation opportunities because of the lack of investment and the lack of economic well-being.

Therefore, reducing the unemployment rate is the real task in building a strong economy according to Okun's law, which shows the inverse relationship between the two variables.

The Objectives of the study

The research aims to study the following issues:

1. To understand the relationship between unemployment and economic growth, there is a real law linking them, Okun's law. Okun tried to understand this relationship by studying the economic cycle. Consequently, he found an inverse relation between unemployment rates and economic growth rates. These two factors work inversely: a decrease in GDP by 1% leads to an increase in unemployment by 0.35%, and also an increase in GDP by 1% leads to a decrease in unemployment by 0.35% (Alamro , Al-dalaie, 2014).
2. The phenomenon of unemployment and its analysis in the Iraqi economy.
3. The main causes of unemployment in Iraq.
4. Diagnosis of the stages of unemployment, which has greatly affected the Iraqi economy.
5. Proposals to reduce unemployment in Iraq.

The Problem of the Research

Iraq has fought wars since 1980 until the fall of the regime on April 9, 2003. At the beginning of the third-millennium, unemployment rates increased despite the abundance of economic resources and the state has not sought to develop plans to address it. Thus, this study intends to focus on remedy, so the problem of the study is to answer the following:





Mustafa Omer Abbas AL-Gburi

- To examine Okun's law and its potential application to the Iraqi economy.
- Address the impact of unemployment and mitigate its consequences.

Okun's law

The study attempts to shed light on the concept of Okun's law, which examines the relationship between unemployment and economic growth in Iraq, and that the presence of a high number of unemployed means low income and thus a decline in production leading to the layoffs of workers. Therefore income is a key element in economic growth and economic development.

$$u_t = \alpha + \beta y_t + e_t, \quad \Delta u/u = \alpha + \beta \Delta y/y$$

Where u = unemployment, y = Gross Domestic Product (GDP), α is intercept, β is Okun's coefficient, e = error term. This version is clear and accurate.

RESEARCH METHODOLOGY

Based on the literature and previous studies that have used many statistical analyses, this study focuses on statistical analysis, using "ARDL" The Autoregressive Distributed Lag cointegration test. It uses the bound testing approach. The study is structured into six chapters. Chapter one is the introduction and chapter two is literature review as well as chapter three gives an overview of unemployment in the Arab countries in general and Iraq in particular. It also diagnoses unemployment, which has greatly affected Iraqi economy. Followed chapter four by a review of the theoretical aspect of the Okun's law. Chapter five explains the data and research methodology and discusses the results. Finally, chapter six discusses the conclusions and recommendations.

Data collection and hypotheses and previous studies

For this study, the data consisting of a 40 year time series from 1977 – 2016 were used. It was collected from the Central Bureau of Statistics in the Ministry of Planning, and also the World Bank.

Previous studies

Many literary studies have used the same hypotheses to looking forward for inverse relationship between unemployment and economic growth or not, as well as an examination Okun's law and its potential application to the economy in developed and developing countries. In order to examine this relationship, many researchers have used new econometrics methods, the Hodrick-Prescott filter (HP), the Engle-Granger cointegration technique, the Johansen and Juselius cointegration, the vector error correction model (VECM), the VAR model, the Autoregressive Distributed Lag cointegration "ARDL" approach to co-integration and the Error Correction Model (ECM) (etc..). The results showed that in the developed countries, the Okun's law applies, and the relationship between them has an inverse because of the strong and good economic conditions and political and social environment, either in the case of developing countries including Arab countries, the Okun's law cannot be applied, and many Arab studies have confirmed that, as I mentioned in literary review part because of security, social and economic conditions deteriorating in those countries.

Hypotheses of the Research

H0: There is no relationship between the unemployment rate and the GDP growth rate.

H1: There is a relationship between the unemployment rate and the GDP growth rate.





Mustafa Omer Abbas AL-Gburi

There is an inverse relationship between the rate of unemployment and economic growth in Iraq. To achieve more economic growth, the rate of unemployment must be reduced.

Time series

To assess the validity of Okun's law and the relationship between unemployment and economic growth in Iraq, a time series for 40 years from 1977 –2016 was chosen.

Stationary test

Stationarity

Many of the techniques in the time series required that the data are constant. This means that the average and the variation and the structure of their self-correlation over time is constant and this is a common assumption. The time series is stable if the following 2 characteristics, the variable does not change its probability distribution in case of change of time, the data showed that it does not contain a unit root. Stationarity can usually be determined from a run sequence plot.

Unit root test (non-stationarity test)

Stationarity as defined above is a stable time series where there has been no change in the form of distribution over time. If time series has a unit root, then it is non-stationary. There are many tests for unit root that look for statistical strength as many of these choices indicate a low statistical strength:

- 1- The Augmented Dickey-Fuller (ADF).
- 2- The Dickey-Fuller GLS (ERS).
- 3- The Phillips-Perron (PP) Test.
- 4- The Kwiatkowski-Phillips-Schmidt-Shin.
- 5- The Elliott-Rothenberg-Stock Point-Optimal.
- 6- The Ng-Perron.

To examine the time-series properties of the data, we used an Augmented Dickey-Fuller (ADF) unit root test to check the stationarity of the variables, according to the hypothesis for each time series.

- Stationarity for unemployment rate :
H0: The unemployment rate is non-stationary. "Data contents has a unit root"
H1: The unemployment rate is stationary. "Data contents doesn't have a unit root"
- Stationarity for GDP growth :
H0: The GDP growth is non-stationary. "Data contents has a unit root"
H1: The GDP growth is stationary. "Data contents doesn't have a unit root"

The following table shows the process to select which model we used. As a consequence, the ARDL approach to co-integration, a more reliable and very clear. Based on the ARDL model, it's has one assumption that, it's should be all the variables stationary at level I (0) or I (1) or mix between them. And also it's has one exception is that the variable is stationary at I (2), we can't apply this model.





Cointegration Test

Cointegration presented by Engel-Granger (Engel and Granger (1987)) is a method for addressing instability in time series. If two or more time series are found to be unstable, the linear composition of these time series is stable, (i.e.) the two series will share a common stochastic trend (Drebee, 2016, p.6). And also we can say, If two or more number of time-series variables are integrated of order "1" and there exists a linear combination of these variables which is integrated of order "0", then the collection of variables is said to be cointegrated.

The existence of a long-run equilibrium between the basic economic time series that coincides with the passage of time is a simulation of the concept of cointegration, which is a concept of econometrics. Also cointegration provides the combined short and long-run information and thus establishes an economic and statistical basis, the strongest model among empirical error correction models, one of the cointegration tests prepared by Engel and Granger (1987). Among them is the Autoregressive Distributed Lag cointegration technique or bound cointegration testing technique (Nkoro1 and Uko, 2016, p.75-76).

Autoregressive Distributed Lag Model (ARDL) Approach to bound Testing

"When one cointegrating vector exists, Johansen and Juselius (1990) cointegration procedure cannot be applied. Hence, it becomes imperative to explore Pesaran and Shin (1995) and Pesaran et al (1996) proposed Autoregressive Distributed Lag (ARDL) approach to cointegration or bound procedure for a long-run relationship." (Nkoro1 and Uko, 2016, p.76).

Therefore, for the analyses of the cointegration relationship between unemployment and economic growth in Iraq based on the ARDL approach, the model will be employed based on the following general model.

$$Pun_t = \alpha_0 + \alpha_{1t} GDP_t + \varepsilon_t$$

Where un = unemployment rate GDP = Gross Domestic Product (GDP), α_0 = intercept, α_{1t} = coefficient, ε_t = error term. Moreover, the ARDL modelling approach to cointegration, involves OLS estimation of an unrestricted Error Correction Model (ECM):

$$\Delta Y_t = \alpha_0 + \alpha_1 * T + \theta_1 * Y_{t-1} + \theta_2 * X_{t-1} + \dots + \theta_k * X_{k,t-1} + \sum_{i=1}^{p-1} \beta * \Delta Y_{t-1} + \sum_{i=1}^{q-1} \theta_1 * \Delta X_{1,t-1} + \dots + \sum_{i=1}^{q-1} \delta * K_i * \Delta X_{1,t-1} + \varepsilon_{1t}$$

Where Δ is the difference operator, α_0 is a constant, T is a time trend, Y is the dependent variable, X_i ($i = 1, 2, \dots, k$) are explanatory variables, ε is the error term, p and q are maximum lag orders, and the rest are coefficients.

The ARDL Cointegration Approach Steps

- 1- In the first phase, choosing lag length in Eviews 9 is automatically.
- 2- In the second phase existence of a long-term relationship is identified for the variables where it is tested by the Bound F-statistic.

The hypothesis is the following:

H0: non-existence of a long-run relationship

H1: existence of a long-run relationship

By using bound test, we can decide if there is relationship in long run or not, to test these hypothesis, we need check F-statistic, and compare this value with upper and lower critical bound, so if F-statistic is more than upper critical





Mustafa Omer Abbas AL-Gburi

bound, it's mean reject null hypothesis says non-existence of a long run and accept alternative hypothesis says there is relationship in long run. But if F-statistic is less than lower critical bound, its mean accept null hypothesis says there isn't relationship in long run. But if value of F-statistic between lower and upper critical bound, we can say that uncertain relationship.

- 3- Cointegrating and long run form, at this point, we going to test coefficient in long run and short run. Also estimate (ECM=CointEq) error correction model test, it coefficient should be negative and statistically significant, and this indicate how many years adjustment back to equilibrium relation in long run if there is problem or trouble in short run.

Testing for the Stability of the Model: Using the tests, including the serial correlation (using LM test), and heteroscedasticity (using Breusch-Pagan-Godfrey test) to verify the integrity and goodness of the model. As noted by Pesaran et al. (2001) stability tests (CUSUM) are useful in checking the stability of the coefficients of the regression.

EMPIRICAL RESULTS

The first practice in applying any cointegration technique is to determine the degree of integration of each variable. For this reason, we applied the unit root using the Augmented Dickey-Fuller (ADF) test to check the stationarity of time series, according to the hypotheses below:

-Stationarity for unemployment rate:

H0: The unemployment rate is non-stationary. "Data contents has a unit root"

H1: The unemployment rate is stationary. "Data contents doesn't have a unit root"

-Stationarity for GDP growth:

H0: The GDP growth is non-stationary. "Data contents has a unit root"

H1: The GDP growth is stationary. "Data contents doesn't have a have unit root"

The below table shows the Augmented Dickey-Fuller (ADF) test for the unemployment rate and GDP growth.

Lag Model (ARDL)

And then the eviews 9 has a new version to choose the lag length automatically based on the ARDL. According to Pesaran et al. (2001), implemented (ARDL), to check the existence of a co-integration relationship among the variables in the bound test. The results show that the calculated F-statistics for the model exceeds the upper critical bound at the 5%, 10% levels of significance. All these results support the rejection of the null hypothesis says no long-run relationships exist and this confirm the existence of a long-term equilibrium relationship between variables in this model.

The ARDL modeling approach to cointegration involves OLS estimation of an unrestricted Error Correction Model (ECM) of the following type as:

$$\Delta(Y_t) = c + \gamma y_{t-1} + \delta x_{t-1} + \sum_{i=1}^m a_{1,i} * \Delta(y_{t-1}) + \sum_{i=0}^k a_{2,i} * \Delta(x_{t-i}) + \varepsilon_i$$

Where $c + \gamma y_{t-1} + \delta x_{t-1}$ is Long - run information

$\sum_{i=1}^m a_{1,i} * \Delta(y_{t-1}) + \sum_{i=0}^k a_{2,i} * \Delta(x_{t-i})$ is short - run information

ε_i is error term

Our model is $ut = \alpha + \beta yt + et$





Mustafa Omer Abbas AL-Gburi

$$\alpha = \frac{-c}{\gamma} \quad , \quad \beta = \frac{-\delta}{\gamma}$$

In order to formulate the equation above and detect the presence of the cointegration equation long and short - run order we mentioned the details as below.

FINAL RESULTS

In general, the table above shows that the estimation represents the long-run and the short run relationship between unemployment and GDP. The results show the existence of a long-term equilibrium relationship towards explanatory variables to the dependent variables at the levels of significance 5%, 10%. The finding shows that the GDP does not affect the unemployment rate in the long run as coefficients are negative and not statistically significant. However, it also shows that in the short run the GDP rate affects the unemployment rate by the Okun's coefficient (0.052141*) is negative and statistically significant consistent with the theory. The insignificance of the long run coefficient in conjunction with the significance of the short run coefficient shows that this variable has a weak causal effect. And also the CointEq or ECM is (-0.068073), and it Inverted is equal (1/0.068073=14.6) represented, if there is a problem in a short-term, it takes around 15 years to back to the equilibrium relationship in the long-run. Also the change in the dependent variable is due to the independent variable and the percentage of R-squared = 89%. The rest of the changes are due to random causes, as well as the significance of the model where the value of (F-statistic) is significant < 5%. And also Durbin-Watson statistic is closer to value 2, for this information, we can say this model is good.

Testing for the Stability of the Model

To ensure the good of fit of the model, a number of diagnostic tests were conducted. Specifically, these tests examined the serial correlation (using LM test), and heteroscedasticity (using Breusch-Pagan-Godfrey test) associated with the selected model. As noted by Pesaran et al. (2001) stability tests (CUSUM) are useful in checking the stability of the coefficients of the regression.

- Test examined the serial correlation (using LM test):
The hypothesis is:
H0: Residuals are not correlated
H1: Residuals are correlated
- Test examined the heteroscedasticity (using Breusch-Pagan-Godfrey test):
The hypothesis is:
H0: Residuals are not heteroscedasticity
H1: Residuals are heteroscedasticity

From the diagnostic test results, there is no evidence of serial correlation and heteroscedasticity in the Autoregressive Distributed Lag (ARDL-Bounds) model specified. Test for the Stability of the Model is given by the figures below, which show that the cumulative sum of recursive residuals (CUSUM) are within the critical boundaries for the 5% significance level indicating that the coefficients of the ARDL model in each of the specifications are stable.



**Mustafa Omer Abbas AL-Gburi**

CONCLUSIONS

This study examined the relationship between GDP and unemployment in Iraq during the period of 1977 to 2016 using World Bank and Central Bureau of Statistics in the Ministry of Planning time series data. And then following the literature, we identified the unemployment rate as influenced by GDP. We started the modeling by examining the time series characteristics of the data. Specifically, we conducted the stationarity test using the Augmented Dickey-Fuller (ADF) unit roots test and we applied the bound test using the autoregressive distributed lag (ARDL) cointegration framework.

The results show that Okun's coefficient by (-0.052141^*) is very weak because of the lack of a real recovery in the unemployment rate, and that the Iraqi economy is not integrated. So there isn't a variety of productivity where Iraq depends on oil for more than 90% of its revenues and also industries totally destroyed because of the wars in Iraq, because of above, there is no question about Okun's law valid in Iraq. The achievement of economic growth leads to the creation of new employment opportunities and consequently addresses the problem of unemployment. Iraq aims to address the imbalance in the economy through macroeconomic policies. Okun's law in Iraq shows that there is a short-term relationship between unemployment and economic growth and it is an inverse relationship and it is statistically significant.

Unemployment has affected Iraq for three decades. It has gone through three phases-- behavioral, structural and masked, and then the imported unemployment phase, which accompanied the economic openness that deepened the problems suffered by the Iraqi economy. It is one of the most serious problems facing the Iraqi economy because of its social and political dimensions. Several internal and external factors contributed to the aggravation of unemployment, especially during the period 2003-2016, including the freezing of appointments in state institutions, the replacement of ministries, and the demobilization of a number of workers, which increased the size of unemployment in Iraq.

The relationship between economic growth and the unemployment rate is a short-term phase due to poor correlation between the GDP rate and the rate of unemployment in the Iraqi economy because of dependence on the oil sector in the composition of GDP rate, limiting the ability of the economy to absorb the increase in the supply of work. The Okun's coefficients vary from one country to another and from time to time for many reasons, including social customs, technology, laws, and demographics, etc., where most studies lie between $(-0.20$ to $-0.50)$.

The Iraqi economy is a rentier economy, so its growth is not real growth, and central economic policies have led to weak economic growth and the economy has been following modest steps. Thus it limits its ability to absorb the labor force entering the labor market annually. Iraq is suffering from the exacerbation of the phenomenon of structural unemployment resulting from the imbalance in the productive structure as a result of the cessation of the main production sectors, especially the agriculture sector, the finance industry and most service activities. Privatization of some projects has contributed to the growth rate of unemployment as the management of the companies has been implemented.

Privatization demobilized a large number of employees because of the surplus labor force in these companies, due to a lack of experience and lack of qualifications, which later forced a freeze in activities and a layoff of the rest of its staff. The destruction of the infrastructure of the Iraqi economy and the accompanying resolutions imposed an economic siege. The decisions of the Coalition Authority, led to the abolition of the army, and police forces, the Internal Security Forces, the Military Industrialization, the Ministry of Information. This, in turn, which led to the demobilization of large numbers of employees of these organizations, and increased pressure on the labor market and contributed to the deterioration of the security situation.





Mustafa Omer Abbas AL-Gburi

RECOMMENDATIONS

The finding shows that the GDP does not affect the unemployment rate in the long run as coefficients are negative and not statistically significant, and also in the short run, the relationship between unemployment rate and GDP rate have very weak coefficients, in this case, we need to build our industries, to do that we should be the following steps:

- Improve the investment climate to encourage domestic and foreign investments, to create jobs for graduates, according to their scientific qualifications, and to develop a system of incentives that will attract investors.
- Emphasis on vocational training for the workforce as the main tool of the work structure.
- The liberation of the Iraqi economy from the dominance of the oil sector, and work on the employment of oil revenues in favor of public investment in basic development projects and social services.
- Work on the distribution of the workforce to achieve optimal use of human resources.
- Supporting and developing the private sector in all its activities, and working to remove its fears and give it guarantees to expand its activities, creating job opportunities to absorb redundancy from the needs of the labor market.
- The Ministry of Labor and Social Affairs, in coordination with the Central Organization for Statistics and Information Technology should prepare data on the unemployment in Iraq to identify the size, type, and contents to ensure the development of a national program based on coordination between the various ministries. This will create employment opportunities commensurate with the qualifications of the unemployed, and to achieve social justice.
- To find great coordination between economic policies and employment policies in state institutions and the private sector in the future.
- Paying attention to support programs for Small and medium-sized enterprises, granting them soft loans and exempt them from taxes and duties to enable them to compete with foreign companies to be able to absorb a large part of unemployment.

ACKNOWLEDGMENTS

I express my warm thanks to my advisor, Professor Sungmin Kim, for his continuous and excellent guidance, caring, patience, and providing me with precious advises based on his immense knowledge and experience. I am using this opportunity to express my gratitude to everyone who supported me throughout the course of this MBA project. I am thankful for their aspiring guidance, invaluable constructive criticism, and friendly advice during the project work. I am sincerely grateful to them for sharing their truthful and illuminating views on a number of issues related to the project. Also, I would like to thank KOICA for the foresight and the thoughtfulness to put together such a laudable program to help build the capacity of government officials from developing countries in the field of Finance. I would like to thank all staff faculty in KAIST for deepening and insight into the science and knowledge field, especially in the finance field, I thank them very much. I would like to thank my institution, Central Bank of Iraq, as well as, the Governor of the Central Bank, to give me this opportunity to build my skills and knowledge in field financial.

REFERENCES

1. Abdul, K. Abdulla, (2012), "The Relationship between Economic Growth and Unemployment in Iraq", Iraqi Journal for Economic Sciences, No – 32, pp.193, 196,197.
2. Ahmed, A., A. Abdul Kader and R. Ahmed, (1996). Macroeconomic theory, Faculty of Commerce, Alexandria University, Egypt.
3. Alamro and Al-dalaien, (2014), "Modeling the relationship between GDP and unemployment for Okun's law specific to Jordan", Mut'ah University, Aqaba Special Economic Zone Authority (ASEZA), pp.4,5.




Mustafa Omer Abbas AL-Gburi

4. Al-Habees and Abu Rumman, (2012), "The Relationship Between Unemployment and Economic Growth in Jordan and Some Arab Countries", Faculty of Planning and Management, AL-Balqa Applied University, Jordan, pp.676,677 ,678.
5. Alhdiy & Johari & Daud & Abdul Rahman, (2015), "Short and Long Term Relationship between Economic Growth and Unemployment in Egypt: An Empirical Analysis", Mediterranean Journal of Social Sciences, MCSER Publishing, Rome-Italy, Vol 6 No 4 S3.
6. Al-Husseini, (2004), Economic Policies in Iraq and Social Political Aspirations, Research and Discussion in Iraq and the Region after the War, First Edition, Beirut, Center for Arab Unity Studies.
7. Al-Jabouri, (1997), Policies of activating the private sector and its applications in Iraq, Baghdad, Sixth Scientific Conference, Faculty of Management and Economics.
8. Al-Rawi, (2009), studies in the Iraqi economy after 2003" Baghdad: Al-Mustansiriya Center for Arab and International Studies", p. 20.
9. Arab Monetary Fund, (2010). United Arab Economic Report for 2010, Cairo.
10. Arshad, z., (2010), "The Validity of Okun's Law in the Swedish", master thesis, Stockholm University, Sweden.
11. Central Bureau of Statistics and Information Technology, Statistical Abstract of the years (2005, 2006, 2007, 2008, 2009).
12. Consolidated Arab Economic Report: (2001).
13. Dahmani Driouche, (2013), "Economic Growth and Unemployment in Algeria: An Econometric Study" , Faculty of Economic Sciences, Management and Commercial Sciences, Jialali Lybes University, Sidi Bel Abbes, Algeria, Najah University Research Journal (Humanities) Volume.27 (6).
14. Drebee, Hayder Abbas , (2016) , "The Impact of Financial Depth and Exchange Rate on Inflation in Iraq during the Period (1970-2014),Al-Qadissiya University – College of Agriculture,p.6.
15. Emeka Nkoro1 and Aham Kelvin Uko2,(2016) "Autoregressive Distributed Lag (ARDL) cointegration technique:application and interpretation, Journal of Statistical and Econometric Methods, vol.5, no.4, 2016, 63-91, p.75-76.
16. Fabien.Tripier,(2002)The dynamic correlation between growth and unemployment .Economics bulletin.Vol.5.No.4.pp.(1-9).
17. Faisal Mokhtari, "The relationship between unemployment and economic growth and the effects of economic policies." University Center Mustafa Istanbuli, pp.4, 5.
18. Faten ,(fmohamad@ksu.edu.sahttp://\faculty.ksu.edu.sa/75499/default.aspx),p.6., "Unemployment and harmful effects".
19. Harris. R. and B. Silverstone, (2001), "Testing for asymmetry in Okun's law: A cross-country comparison.Economics Bulletin. Vol. 5. No. 2, pp. 1–13.
20. <http://www.itl.nist.gov/div898/handbook/eda/section3/runseqpl.htm>.
21. Ibrahim, (2009), Unemployment and Job Creation One of the Challenges of the Present Situation, Baghdad College of Economic Sciences Journal, Issue 19.
22. Imad A.Moosa, (2008), "Economic growth and Unemployment in Arab countries: Is Okun's low valid. International conference on "the unemployment crisis in the arab countries". 17-18 march 2008. cairo- Egypt. Journal of Development and Economic Policies.Vol.10.No.2, pp. 7-24.
23. International Monetary Fund Forum (2012).
24. Javed, u., (2005), Okun's law: empirical evidence from Pakistan 1981-2005, master thesis, Södertörn University, School of Social Sciences, Sweden, pp.9, 10.
25. Javeid Umer, (2012), "Validity of Okun's Law Empirical Evidence from Pakistan: 1981-2005" Dept. of Economics Södertörn University, uj_gau@yahoo.com, pp. 10
26. John A. Tatom, (Oct. 1978), "Economic Growth and Unemployment: A Reappraisal of the Conventional View. Federal reserve bank of St. Louis",pp. 16-22.
27. Juda, N. H. & Esa, R. A ,(2010).Relationship between economic growth and unemployment in Iraq using Okun's law and Toda-Yamamoto test.AI-Qadissia Journal of Administrative & Economic Sciences,Volume 12, Issue (3), pp.63-87.





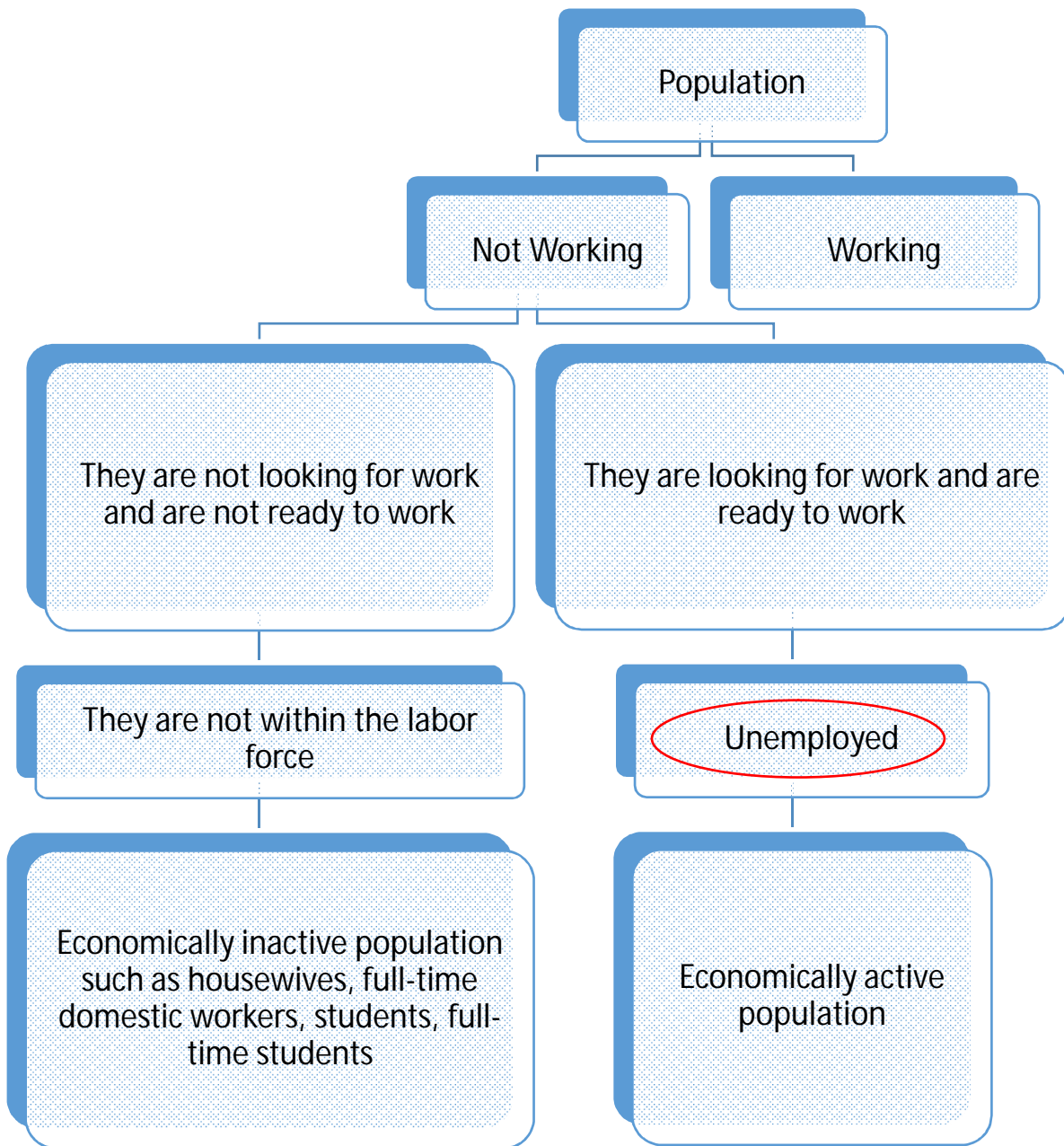
Mustafa Omer Abbas AL-Gburi

28. Kamil, (2010), " Analysis of Unemployment Trends for the period 1996-2008", Master of Science in Economics, Faculty of Management and Economics, University of Basrah.
29. Keller, J. & Nabil, M.K., (2002). The Macroeconomics of Labor Market Outcomes in MENA over the 1990s: How Growth has failed to keep Pace with a Burgeoning Lab our Market. Working Study, the Egyptian Center for Economic Studies.
30. Khalil, S., (1994). Macroeconomic theory: the concepts and theories. AIAhram Agency, Kuwait.
31. M. Kreishan Fuad, 2011, "Economic Growth and Unemployment: An Empirical Analysis " (Journal of Social Sciences 7 (2): 228-231, 2011 - ISSN 1549-3652 - © Science Publications),pp.228-231.
32. Ma'arouf, H., (2005). Macroeconomic analysis, Dar Safa, First Printing.
33. Malik Abdul Hussain Ahmed, (2011) , The unemployment in Iraq, Reasons, results, and treatment" Management Technical College Basra ,pp.3,6,9.
34. Muhammad Nasser Ismail et al., (2008), Employment and Unemployment in Iraq for the Period (1977-2004), Journal of Technology, Research Administrative, vol. 21, No. 6 .
35. Neely Christopher Joseph, (2010), "Okun's Law: Output and Unemployment", Economic SYNOPSES short essays and reports on the economic issues of the day.p.1"
36. Republic of Iraq, Ministry of Planning and Development Cooperation, National Development Plan for (2010-2014), pp. 34-35.
37. Sögner & Alfred, (2002), "An analysis on the structural stability of Okun's law--a cross-country", Applied Economics in 2010, ISSN: 0003-6846 (Print) 1466-4283 (Online) Journal homepage: <http://www.tandfonline.com/loi/raec20>, pp. 1776-1780.
38. Ting and Ling (2011), Okun's law in Malaysia: an autoregressive distributed lag (ARDL) approach with hodrick-prescott (hp) filter, Journal of Global Business and Economics, 2, 1.
39. Villaverde and Adolfo (2007), Okun's law in the Spanish regions, Economics Bulletin, 18, 5, 1-11.
40. World Bank, (2012). Economic Report on indicators of economic performance for the Middle East and North Africa, Washington DC.





Mustafa Omer Abbas AL-Gburi



Source: Author

Figure 1: The economic classifications of the population





Mustafa Omer Abbas AL-Gburi

Table 1: The rates of economic growth and unemployment in some Arab countries

Country	Algeria		Egypt		Jordan		Kuwait		Morocco		KSA		Sudan		Syria		Tunis	
Year	PIB	T.C	PIB	T.C	PIB	T.C	PIB	T.C	PIB	T.C	PIB	T.C	PIB	T.C	PIB	T.C	PIB	T.C
2006	2.0	12.3	6.84	10.92	7.93	14.06	5.26	1.37	7.67	9.7	3.16	12.0	11.29	17.49	5.05	8.3	5.65	12.5
2007	3.0	11.8	7.09	9.21	8.49	13.1	4.46	1.70	2.71	9.8	2.02	11.0	10.16	16.77	5.68	9.2	6.26	12.4
2008	2.4	11.3	7.16	8.91	7.61	12.65	4.97	1.67	5.59	9.6	4.23	9.8	6.84	16.04	4.48	10.9	4.52	12.6
2009	2.38	10.21	4.67	9.45	2.33	12.94	5.19	1.64	4.95	9.1	0.60	10.46	5.98	14.89	6.01	8.1	3.10	13.3
2010	3.33	10.03	5.15	9.2	3.09	12.50	1.97	1.64	3.15	9.0	3.74	10.48	5.07	13.73	3.23	8.4	3.69	13.0
2011	3.62	9.8	1.0	9.15	3.25	12.50	5.29	1.64	3.86	8.85	7.54	n\	4.72	12.56	2.99	n\	1.29	14.7

Source: International Monetary Fund Forum 2012. Where PIB : growth rate , T.C: unemployment rate

Table 2: The required growth percentages to reduce unemployment rates by 1%.

Country	Coefficient Okun (b)	Natural growth rate	Required growth rate
Algeria	3.8-	2.788	.073
Egypt	1.75-	5.391	.017
Jordan	2.37-	5.45	.012
Kuwait	0.527-	2.675	.056
Morocco	1.99-	4.67	.015
KSA	3.04	3.541	2.009-
Sudan	1.61-	7.343	.018
Syria	1.52-	4.573	.019
Tunis	2.78-	4.085	.010

Source : Mahmoud A. Al-Habees and Mohammed Abu Rumman “The Relationship Between Unemployment and Economic Growth in Jordan and Some Arab Countries”, Faculty of Planning and Management, AL-Balqa Applied University, Jordan, 2012.p.677

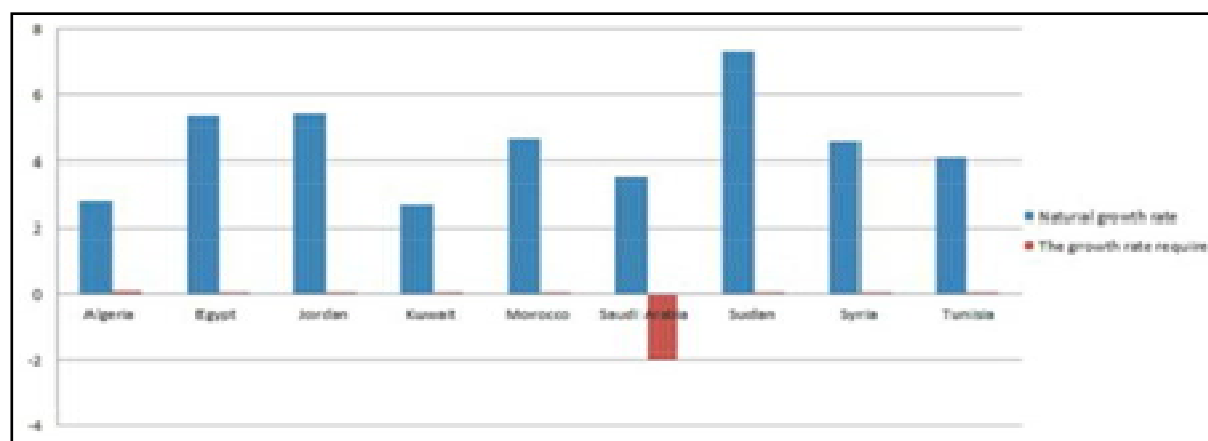


Figure 2: Needed percentages to reduce unemployment rates.

Source: Mahmoud A. Al-Habees and Mohammed Abu Rumman “The Relationship Between Unemployment and Economic Growth in Jordan and Some Arab Countries”, Faculty of Planning and Management, AL-Balqa Applied University, Jordan, 2012.p.678





Mustafa Omer Abbas AL-Gburi

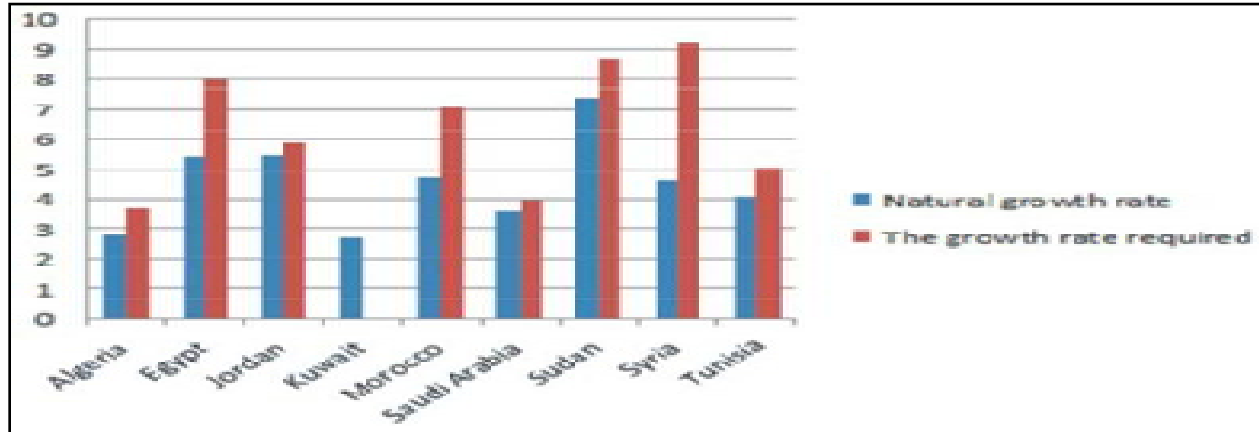


Figure 3: Needed growth percentages to reduce unemployment rates.

Source: Mahmoud A. Al-Habees and Mohammed Abu Rumman “The Relationship Between Unemployment and Economic Growth in Jordan and Some Arab Countries”, Faculty of Planning and Management, AL-Balqa Applied University, Jordan, 2012.p.678

Table 3: Unemployment rates in Arab countries in the last three decades

Description/ years	Averages unemployment rates
1980s	10.6
1990s	14.5
2000s	15.5

Source: United Nations Development Program, the League of Arab States 2009, p 23-24.



Source: Author

Figure4: Unemployment Rates in Iraq



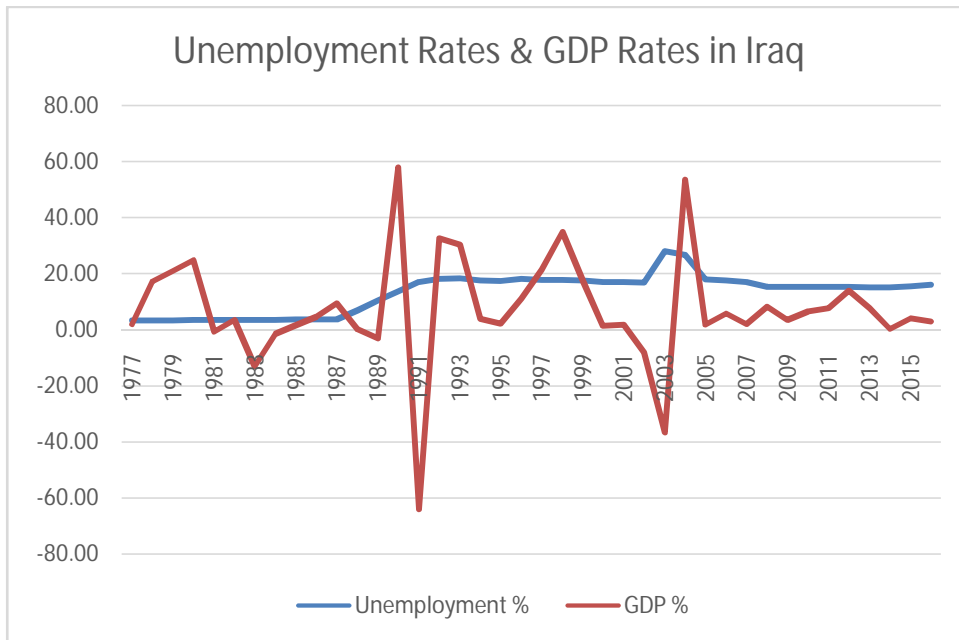


Mustafa Omer Abbas AL-Gburi



Source: Author

Figure 5: GDP Rates in Iraq



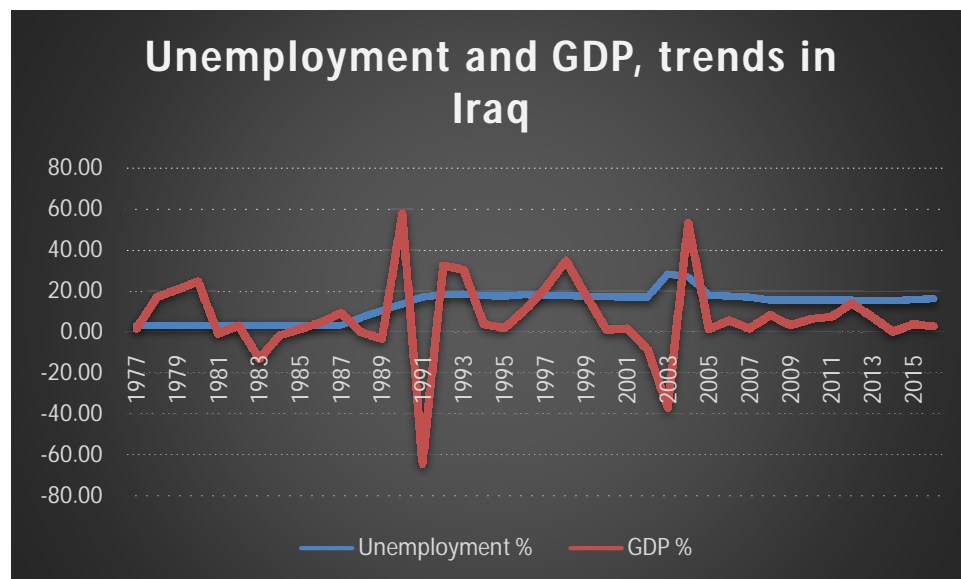
Source: Author

Figure6: Unemployment Rates and GDP Rates in Iraq





Mustafa Omer Abbas AL-Gburi



Source: Author

Figure7: Trends in Unemployment Rates and GDP Rates, in Iraq

Table 4:Percentage of the Distribution of Unemployed Persons by Educational Level for the Years(2003-2008)

Level	Primary		secondary		Preliminary Education		Higher Education		
	Primary	Medium	liedadia	Diploma	Bachelor	Diploma	Master	Doctorate	
2003	55.1	13.48	8.09	9.63	12.45	0.47	0	0	
2004	54.6	15.78	6.93	10.69	11.51	0.12	0.02	0.29	
2005	52.89	15.45	7.09	11.9	12.4	0.08	0.28	0.01	
2006	18.3	18.19	17.15	15.45	19.76	6.66	4.8	0	
2008	12.2	10.4	12.2	13.4	14.3	6.5	3.7	0	

Source: Ministry of Planning and Development Cooperation, the Central Bureau of Statistics and Information Technology, operating and unemployment survey for the years (2003,2004,2005,2006,2008)

Table 5: Registered unemployment rates for the years 1977-2008 by type and environment (%)

Years	Urban Unemployment rates			Rural Unemployment rates			Total Unemployment rates		
	Male	Female	Total	Male	Female	Total	Male	Female	Total
1977	3.1	5.2	3.3	4.1	0.3	3.1	3.5	2.1	3.2
1987	3.5	7.8	3.5	3.6	3.6	3.6	3.1	7.5	3.6
1997	14.7	2.2	13.3	15.3	1.7	14	15	2.1	13.6
2003	31	22.3	30	28.9	6.7	25.4	30.2	16	28.1
2004	28.3	22.4	27.7	31.2	3.1	25.7	29.4	15	26.8
2006	20	37	23	15	8	13	16.16	22.65	17.5





Mustafa Omer Abbas AL-Gburi

2008	15.4	43.6	16.3	14.89	8.26	13.34	14.33	19.64	15.34
------	------	------	------	-------	------	-------	-------	-------	-------

Source:1-Muhammad Nasser Ismail et al., Employment and Unemployment in Iraq for the Period (1977-2004), Journal of Technology, Research Administrative, vol. 21, No. 6, 2008,
 2. Central Bureau of Statistics and Information Technology, Statistical Abstract of the years(2005,2006,2007,2008,2009).

Table 6: Unemployment rates and GDP rates in Iraq (1977-2016)

Year	Unemployment Rate%	GDP Rate%	Year	Unemployment Rate%	GDP Rate%
1977	3.20	1.90	1997	17.69	21.24
1978	3.24	17.06	1998	17.76	34.86
1979	3.28	20.87	1999	17.52	17.58
1980	3.32	24.75	2000	17.03	1.41
1981	3.36	-0.73	2001	16.90	1.77
1982	3.40	3.43	2002	16.78	-8.20
1983	3.44	-13.07	2003	28.10	-36.66
1984	3.48	-1.49	2004	26.80	53.39
1985	3.52	1.45	2005	17.97	1.68
1986	3.56	4.65	2006	17.50	5.64
1987	3.60	9.31	2007	16.90	1.89
1988	6.93	-0.02	2008	15.34	8.23
1989	10.27	-3.12	2009	15.22	3.38
1990	13.60	57.82	2010	15.24	6.40
1991	16.93	-64.05	2011	15.22	7.55
1992	18.15	32.59	2012	15.27	13.94
1993	18.40	30.29	2013	15.14	7.63
1994	17.58	3.85	2014	14.98	0.20
1995	17.33	2.12	2015	15.48	3.99
1996	18.16	11.02	2016	16.05	2.90

Summary Statistics of the Data

Table7: Description statistics: for Unemployment and GDP

	UN	GDP
Mean	13.09088	7.185744
Median	15.30500	3.922230
Maximum	28.10000	57.81783
Minimum	3.200000	-64.04711
Std. Dev.	6.858694	20.17978
Skewness	-0.230698	-0.538756





Mustafa Omer Abbas AL-Gburi

Kurtosis	2.270961	6.709408
Jarque-Bera	1.240641	24.86791
Probability	0.537772	0.000004
Sum	523.6350	287.4298
Sum Sq. Dev.	1834.626	15881.71
Observations	40	40

Table 8: a cross correlation matrix between Unemployment and economic growth.		
	UN	GDP
UN	1	0.036
GDP	0.036	1

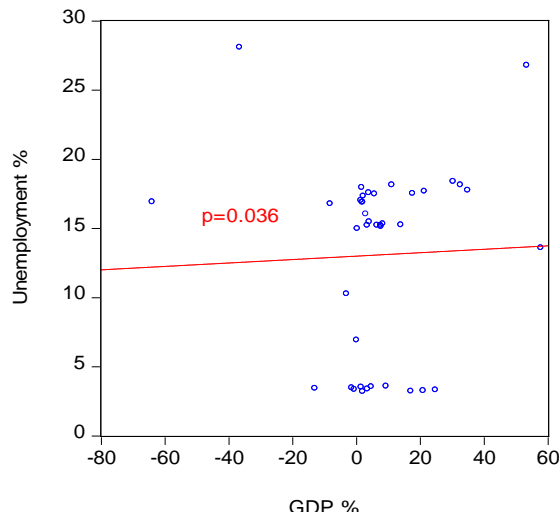
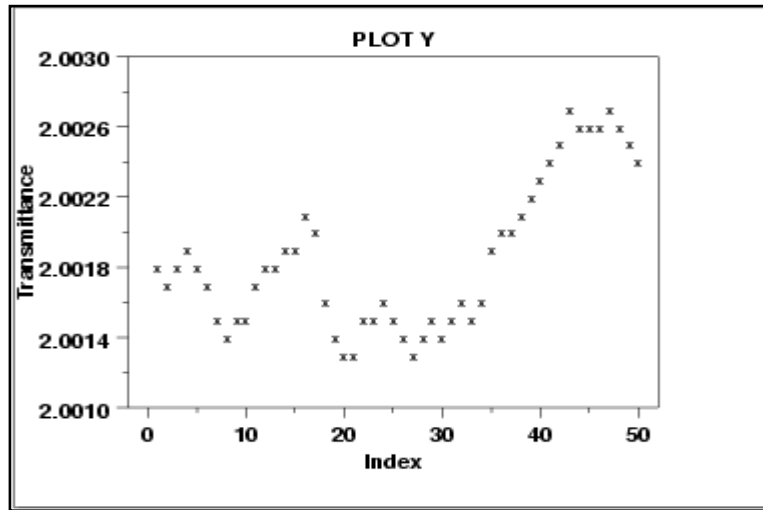


Figure 8: across correlation matrix between Unemployment and economic growth





Mustafa Omer Abbas AL-Gburi



Source: <http://www.itl.nist.gov/div898/handbook/eda/section3/runseqpl.htm>

Figure 9: Run sequence plot

Table 9: Process for unit root

Statistical Model Selection (For time series) on the base of data sationarity						
Unit Root						
step 1	All Variables Stationary at level	If all variables are stationary purely I(0) & I(1)	All variables Stationary at 1st difference		Variables Stationary at I(1) difference and I(2) difference	variables stationary at 1(0),I(0),I(2)
step2	Simple regression (long run)	ARDL	Co-integration		Autoregressive models	Toda and Yamamoto (1995)
step3			Unrestrictied VAR model	Error correction model		
step4				ECM One endogenous	VECM More than one endogenous	





Mustafa Omer Abbas AL-Gburi

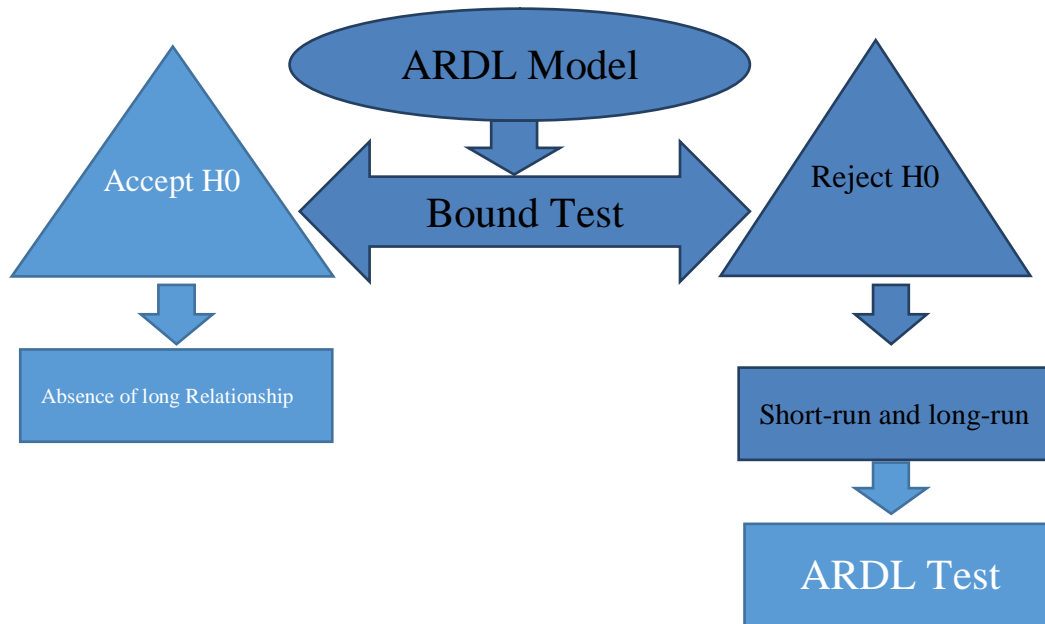


Figure 10: ARDL analysis steps

Variables	ADF test statistics Level		First Difference		Results
	Intercept	Trend and intercept	Intercept	Trend and intercept	
Unemployment rate	-1.596	-1.491	-5.239*	-5.384*	I(1)
GDP Growth	-8.812*	-8.709*	-8.864	-8.733	I(0)

Note: *statistical significance at the 1%, 5% levels.

ARDL Bounds Test

Sample: 1978 2016

Included observations: 39

Null Hypothesis: No long-run relationships exist

Test Statistic	Value	K
F-statistic	4.566	1

Critical Value Bounds

Significance	I0 Bound	I1 Bound
10%	3.02	3.51*





Mustafa Omer Abbas AL-Gburi

Table 13: Breusch-Godfrey Serial Correlation LM Test

Breusch-Godfrey Serial Correlation LM Test:

F-statistic	1.255791	Prob. F(2,33)	0.2981*
Obs*R-squared	2.758302	Prob. Chi-Square(2)	0.2518

Note: * statistical significance at the 5% levels.

Table 14: Heteroskedasticity Test: Breusch-Pagan-Godfrey

Heteroskedasticity Test: Breusch-Pagan-Godfrey

F-statistic	1.173251	Prob. F(3,35)	0.3339*
*Obs*R-squared	3.563635	Prob. Chi-Square(3)	0.3126
Scaled explained SS	9.448783	Prob. Chi-Square(3)	0.0239

Note: * statistical significance at the 5% levels

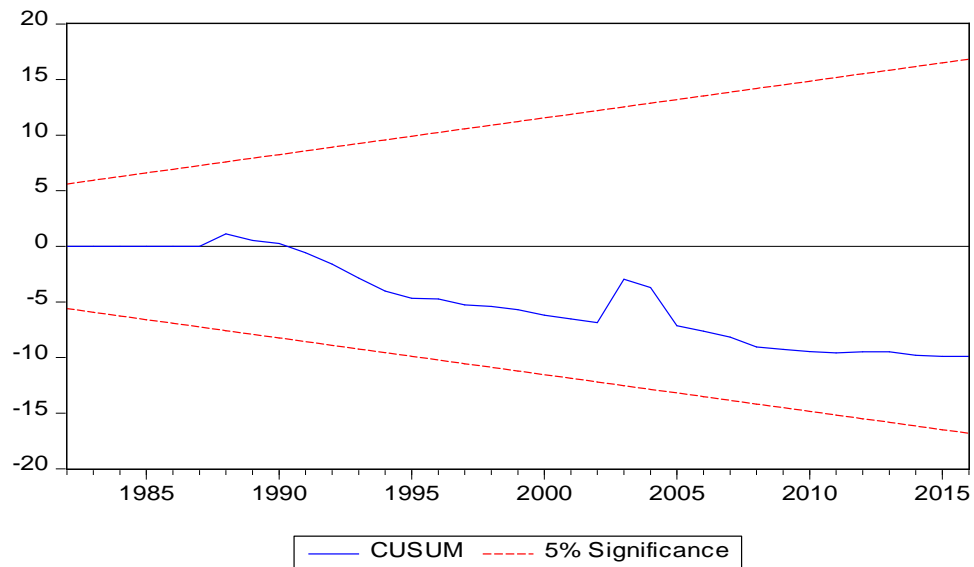


Figure 11: Plot of CUSUM for coefficient stability of Model





A Proper Methodology for Building 3-D Geological Model in High-Heterogeneity Complex Fluid-Phases

Nermein F.Jaffar* and Jalal A.AI – Sudanyi

Department of Petroleum Engineering, University of Baghdad, Baghdad, Iraq.

Received: 17 Sep 2018

Revised: 21 Oct 2018

Accepted: 27 Nov 2018

* Address for Correspondence

Nermein F.Jaffar

Department of Petroleum Engineering,

University of Baghdad,

Baghdad, Iraq.

Email: Near_falih@yahoo.com



This is an Open Access Journal / article distributed under the terms of the **Creative Commons Attribution License** (CC BY-NC-ND 3.0) which permits unrestricted use, distribution, and reproduction in any medium, provided the original work is properly cited. All rights reserved.

ABSTRACT

A geological plan was run on Halfaya field, an Iraqi oil field which shows a high heterogeneity and complicated fluid phases. The geological model has been developed in late cretaceous era. For an analytical study, its formation is divided into multiple layers, KA and KB as the main zones were located within those two layers. Based on processed data from Missan Oil Company, fifty-three datasets including well coordinates, formation tops and well logs were used to develop the geological model of the field including structural model, structural frame work, reservoir isochores, layering, structure grid surface and the petrophysical evaluation model. As a result of this study, initial oil in place was calculated to be certain.

Keywords: geological, Oil, structural, model, evaluation.

INTRODUCTION

3D geological modelling has been constructing for Khasib formation using Petrel 2015 software. The first step in the process of constructing a global reservoir model is constructing a geological framework of the structure and reservoir architecture based on seismic data and well loggings. The geological modelling represents all main geological features (flow barriers, faults, pinch outs, compartments, etc.) that are possible to affect the connectivity of the reservoir. The main important process for geologist is finding an oil-bearing rock and calculate the area or volume of the reservoir[1]. The goal of this paper is to construct 3D geological modelling using Petrel software for fifty-three wells in Khasib formation in Halfaya Oil Field. This model includes structural models and Petrophysical models for each unit and final model of the reservoir.



**Nermein F.Jaffar and Jalal A.AI – Sudanyi**

Area Under Study

Halfaya oil field is located in the south of Iraq, at about 35 kilometers southeast of Amara city as shown in figure 1. The structure of Khasib formation in the Halfaya contract area is an elongated gentle anticline trending NW-SE, 28km long and 9km wide around within contract area. NE flank dip is 2.4° and SW dip is 2.7°. Khasib formation, including three individual reservoirs KA1-2, KA2 and KB, has been proved to be very complicated reservoir with different oil type and strong heterogeneity [2].

Geological Description of Khasib Reservoir

Khasib formation was developed in the Late Cretaceous overlying Mishrif formation, and underlying Sadi & Tanuma formations as shown in figure 2. Structurally, it is a gentle elongated anticline trending NW-SE to NWW-SEE, about 32km long and 8.4km wide, flank dip is 2.3-2.7°. Closure area is 159km² with 150m vertical relief [3]. Stratigraphically Khasib stratum can be divided into KA and KB, and KA can be further divided into KA1 and KA2. There are two sub layers KA1-1 and KA1-2 in KA1, while three sub layers, KB-1, KB-2 and KB-3 in KB. The main pay zones are KA1-2 and KB. The reservoir rock consists of packstone, wackestone and mudstone. And according to core data, log curves, and sedimentary facies; Khasib formation can be divided into good and poor reservoirs. The good reservoir is packstone in KA1-2 and KB with intergranular pore, dissolution pore and intergranular dissolved pore. Poor reservoir is wackestone with a few dissolution pores and intergranular dissolved pore.

METHODOLOGY

Available Data

The present study is based on the data supplied by Missan Oil Company. Totally, the database of fifty three wells is incorporated to construct geological model, including well coordinates, formation tops, sub-layer well tops, raw well logging curves including SP, GR, CAL, LLD, LLS, MSFL, NHPI, DEN and DT, and their interpretations including Vsh, γ , and SW, and core data from three wells.

Structural Model

Identifying and recovering hydrocarbons requires accurate, high resolution geological modeling of the reservoir structure, stratigraphy and rock properties to enhance the geological understanding and provide accuracy throughout the exploration, development and production cycles. The Three-Dimensional (3D) modeling of structure requires incorporation of all available data and interpretation [4]. The (3D) structural model was done through the following steps:

Structural Framework

The geological framework is the basic inputs in the reservoir characterization and then simulation of fluid flow inside the porous media. This provides the structural style and reservoir architecture, the connectivity of the reservoir rock and the gross thickness trends of the pay [1].

Due to no faults finding in Khasib formation, the grid was constructed using the Petrel 'Make Simple Grid' process. The gridding process was finished with the areal grid spacing of 100m* 100m and the grid number is $NX*NY=122*309=37,698$. Layering process was used to define the vertical resolution of the grid by setting each cell value at 0.6m for every oil zone, number of layers is 135. The geological model comprises data from 53 wells.



**Nermein F.Jaffar and Jalal A.AI – Sudanyi**

Vertically the top and the base of the model were constrained by structural map on top of Khasib formations as shown in figure 3.

Reservoir Isochores

The “Make Horizons” process utilized seven input depth surfaces, these having been derived from 2D time mapping. Isochores were generated from interpolation of the vertical zone thicknesses defined by the tops in the 53 field wells. The result of the “Make Horizons” process was thus six ‘Main Zones’, which captured the primary variation in stratigraphic character figure 4

Layering

This process is used to give the final cell resolution, which requires providing the vertical resolution of each zone, cell thickness and corresponding layer properties in the models. Each reservoir unit has been divided into many layers depending on Petrophysical properties. 135 layers were constructed by using ‘layering’ process in Petrel.

Fluid Contacts

The oil water contacts (OWC) shown in table 1 have been incorporated into the geological model.

Structure Grid Surface

The final structural modeling is in the creation of 3D structural grid surfaces, which comprise both the simple grids model and the horizon surfaces. The skeletal framework of the base, mid and top skeletons inputted with the edges which provides the structure frame as Geo-Modeling which serve as simulation grids for dynamic fluids analysis.

Well Logs Scaling Up

Totally, fifty three wells porosity, permeability and water saturation well logging interpretations are up scaled figure 5 and QC work is done for the up scaling on every well.

Petrophysical Modeling

Petrophysical modeling can interpolate and simulate reservoir data such as porosity and water saturation throughout the model grids, and ultimately provide the distribution of these properties continuously in 3D model [5] (petrel manual). The goal of a geological model is to provide a full set of continuous reservoir parameters (i.e. porosity, permeability, and water saturation) for each cell of the grid. Many different methods can be used to distribute these parameters in the model [6] [7].

a.Porosity Model

PHIE (effective porosity) logs from Computer Processed Interpretation results (CPI) were first up-scaled for all reservoir penetrations using arithmetic averaging and ‘as point’ options in Petrel. Porosity was then populated using Gaussian (random function) simulation. The Porosity model which is built for each unit of Khasib formation is shown in Figures (6 to 11). The porosity distribution maps show the favorable reservoir is in the western and central part of the contract area.



**Nermein F.Jaffar and Jalal A.AI – Sudanyi****b.Water Saturation Model**

Water saturation (sw) logs from Computer Processed Interpretation results (CPI) were first up-scaled for all reservoir penetrations using arithmetic averaging and 'as point' options in Petrel. Water saturation was then populated using Gaussian (random function) simulation. The water saturation model was built for each unit of Khasib formation as shown in figures (12 to 17). Net to gross (NTG) model was calculated and generated from porosity and water saturation model with the cut-off value calculated by classical method. NTG assigned in the cellular model by (properties-calculator option in petrel) as shown in figure 18.

OOIP Calculation

On the basis structure maps, logging interpretation data available in Original-Oil-In-Place (OOIP) was calculated oil-bearing formation with based on 3D geological models. Because the fluid property of KA1-2 and KB varies greatly from crest to the flank. The original fluid character should distribute continues because of gravitated differentiation effect, the fluid PVT parameter should also vary from light oil to black oil. Based on this analysis, Bo model was built to calculate OOIP. The Bo model was built by using the correlation [3] as shown in figure 19. Incorporated with the porosity model, water saturation model and NTG model, the OOIP was calculated.

RESULTS AND DISCUSSION

According to the structural map, the Khasib Formation in Halfaya oil Field shows asymmetrical anticlinal fold which contains one dome. The accumulation thickness of KA2 and KA1-2 reservoir is biggest, followed by KB-2 reservoir. The single thickness of KA1-2 is biggest, then KB-2 and KB-3. KB2 and KA1-2, then KB3 which are the highest in terms of Petrophysical properties (porosity values). The porosity distribution maps show the favorable reservoir is in the western and central part of the contract area.

REFERENCES

- [1] Islam, M. R. , Hossain, M. E. , Moussavizadegan, S. H., Mustafiz, S., J. H. and Abou-Kassem." Advanced Petroleum Reservoir Simulation," 2nd ed, 2016, pp. 40-54
- [2] Petro China:" Field Development Plan Revision No.1 of Halfaya Contract Area", MOC, Iraq (Aug. 2017).
- [3] Petro China: "Re-geomodeling and Development Plan Revision of Khasib Reservoir", MOC, Iraq (Jun. 2017).
- [4] Mirta, S. and Leslie: "Three Dimensional Structure Model of the Rhourde el Baguel Field," Algeria, AAPG.Bull, Vol.87, 2003, pp. 231-250.
- [5] Schlumberger: "Petrel Version 2010.1: Reference Manual", 2010.
- [6] Bellorini, J. P., Casas, J., Gilly P., Jannes, P. and Matthews P: " Definition of a 3D Integrated Geological Model in a Complex and Extensive Heavy Oil Field," Oficina Formation, Faja de Orinoco, Venezuela, Sincor OPCO, Caracas, Venezuela, 2003.





Nermein F.Jaffar and Jalal A.AI – Sudanyi

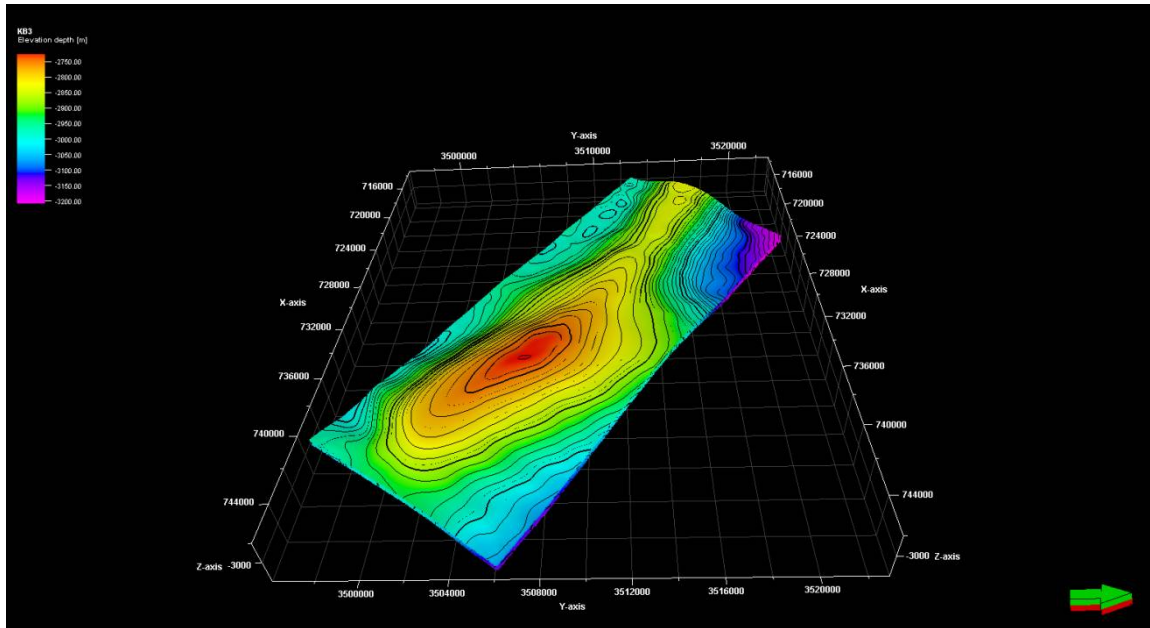


Fig. 3. Structural constraint for geological model

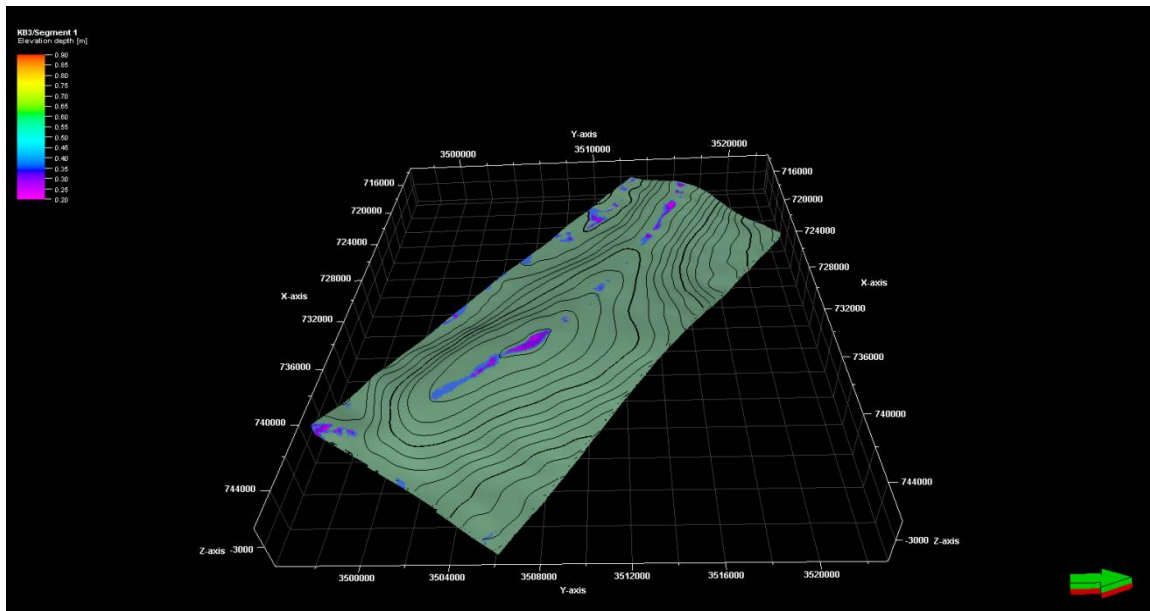


Fig. 4. Main horizons of Khasib reservoir.





Nermein F.Jaffar and Jalal A.AI – Sudanyi

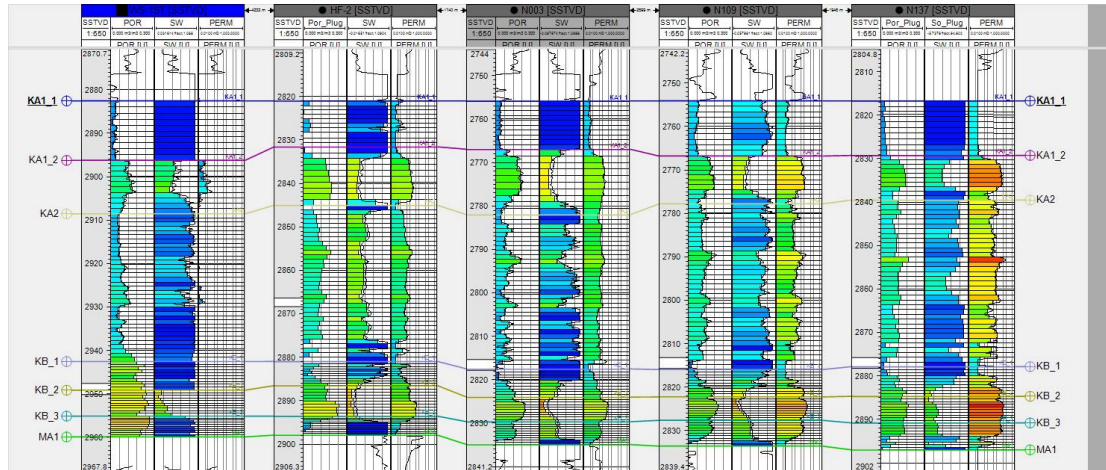


Fig. 5. Well Logs Up Scaling and QC for Khasib

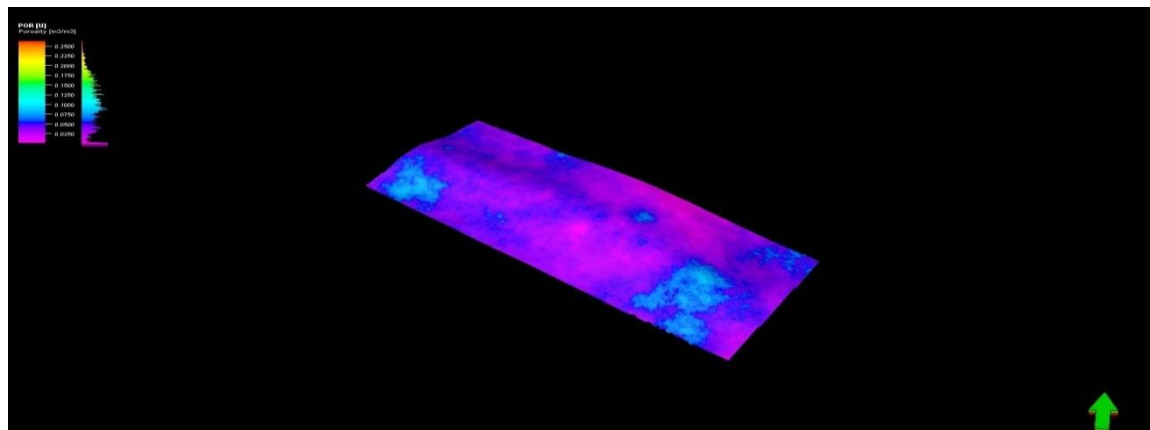


Fig. 6. Porosity model for KA1-1 unit

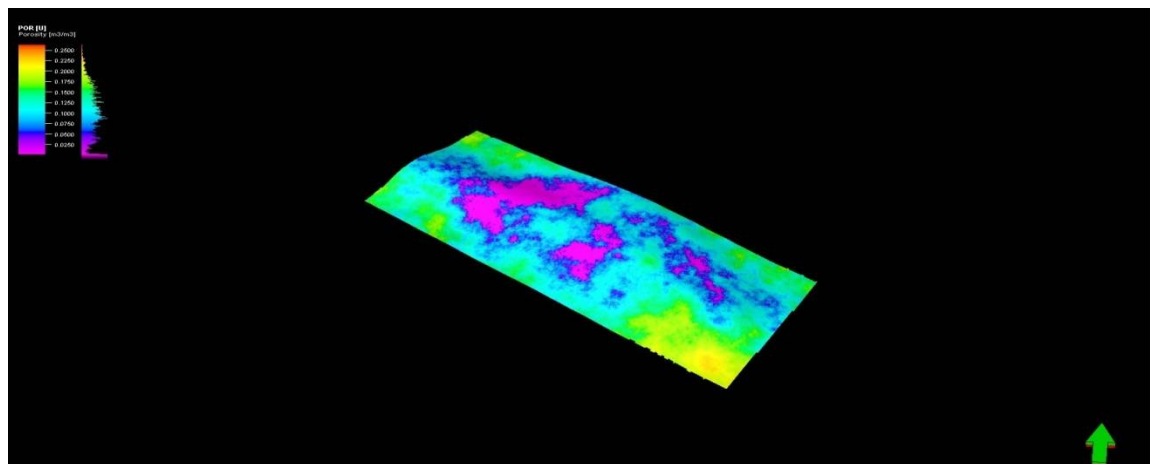


Fig. 7. Porosity model for KA1-2 unit





Nermein F.Jaffar and Jalal A.AI – Sudanyi

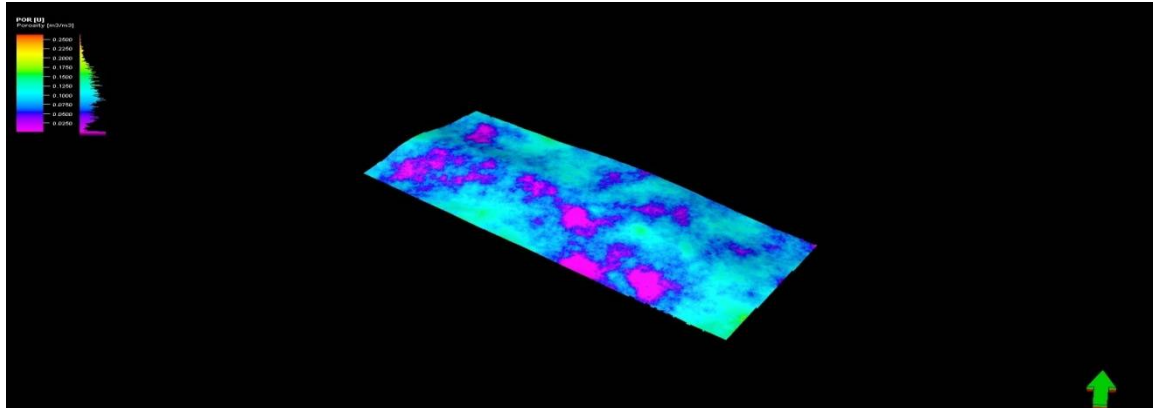


Fig. 8. Porosity model for KA2 unit

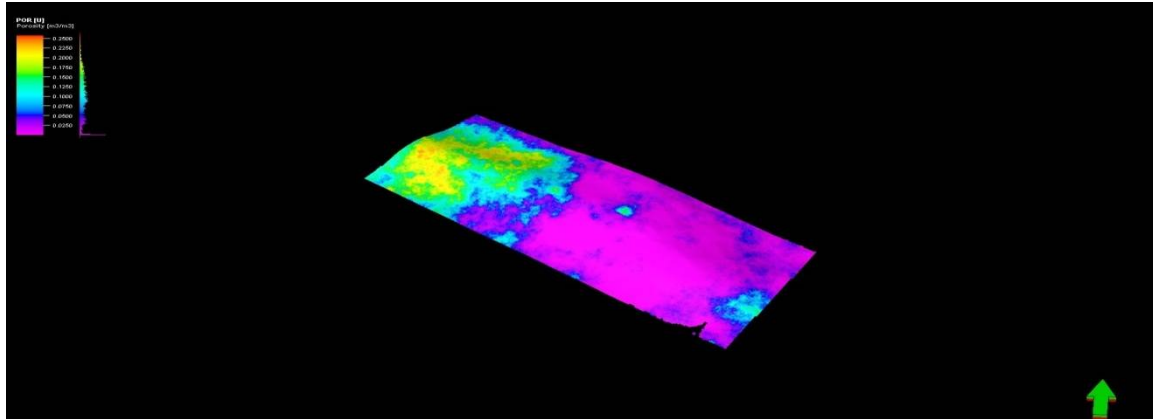


Fig. 9. Porosity model for KB1 unit

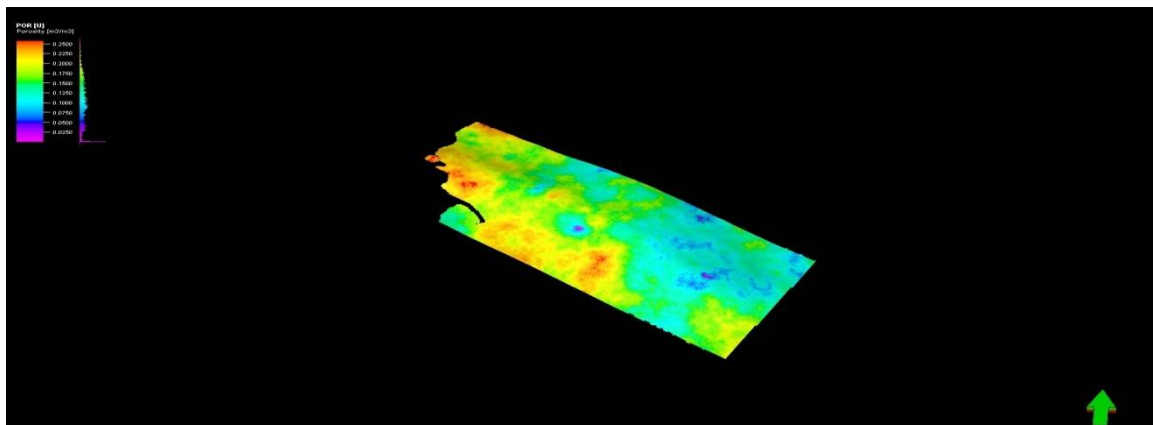


Fig. 10. Porosity model for KB2 unit





Nermein F.Jaffar and Jalal A.AI – Sudanyi

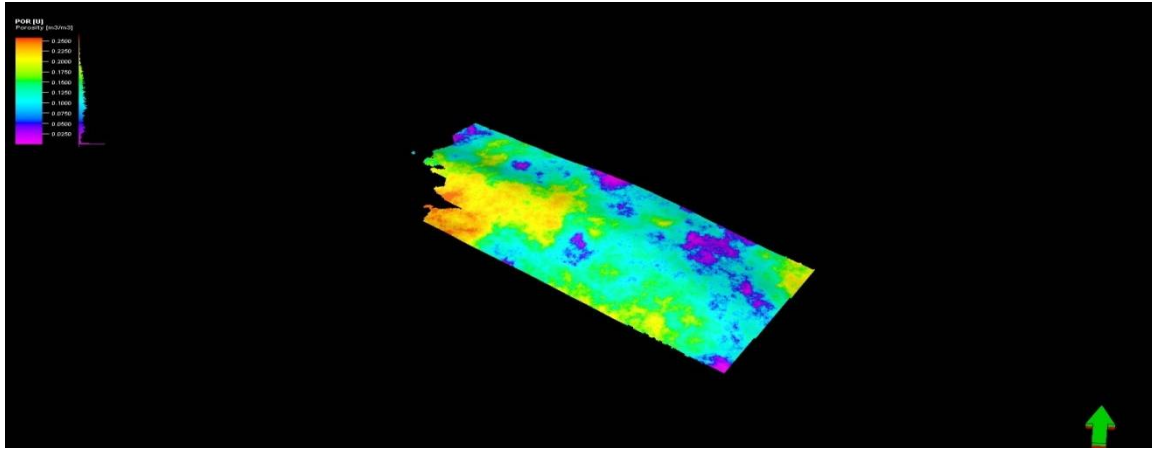


Fig. 11. Porosity model for KB3 unit

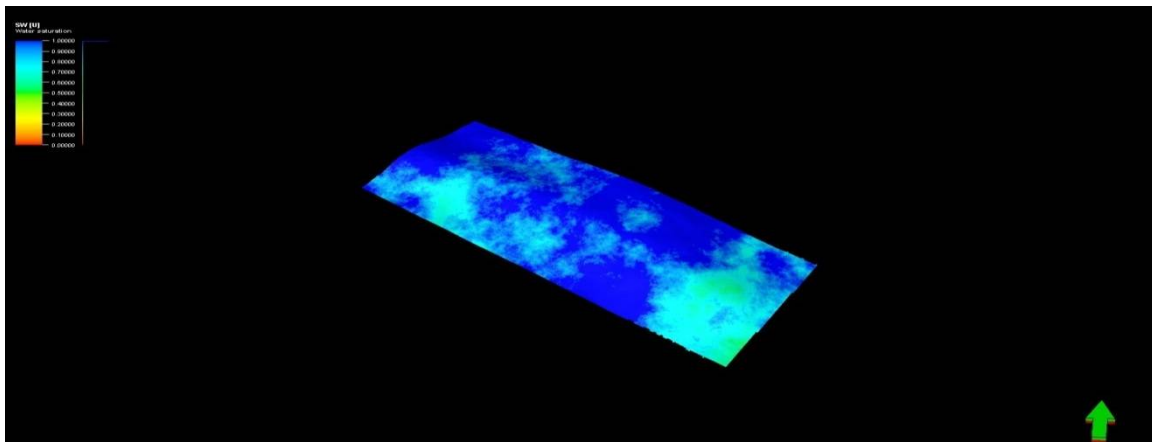


Fig. 12. Water saturation model for KA1-1 unit

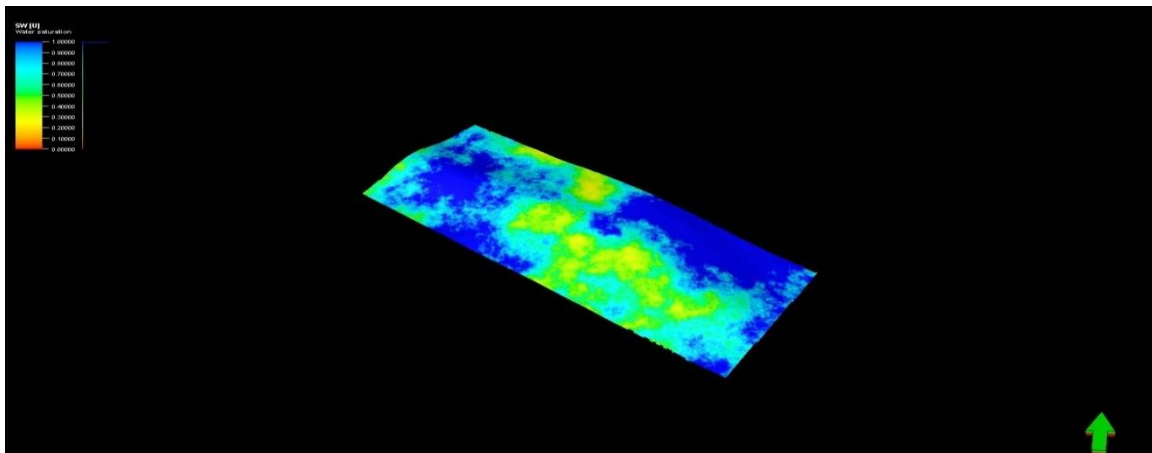


Fig. 13. Water saturation model for KA1-2 unit





Nermein F.Jaffar and Jalal A.AI – Sudanyi

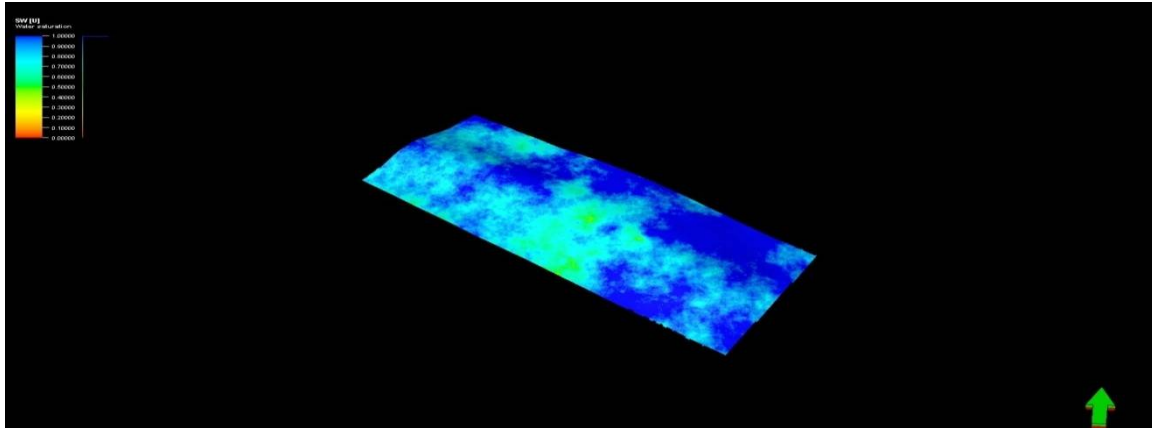


Fig. 14. Water saturation model for KA2 unit

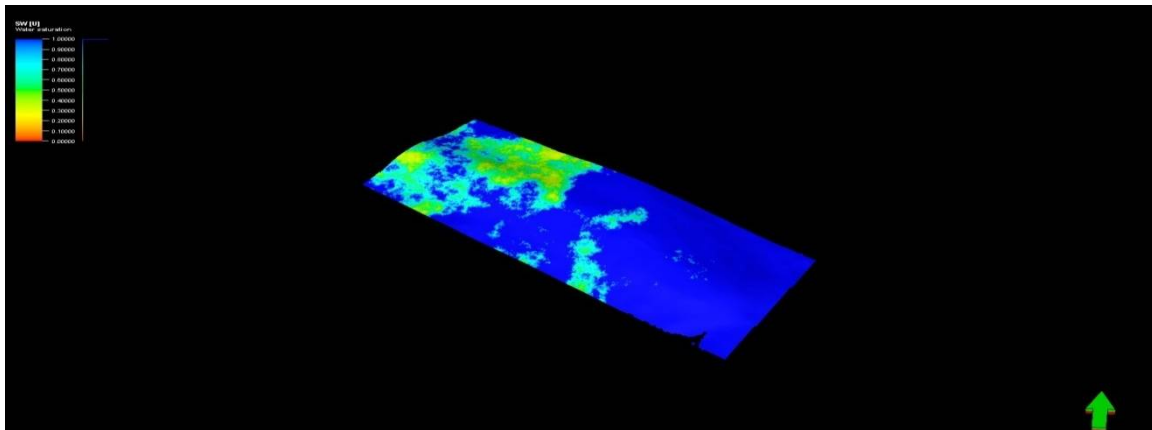


Fig. 15. Water saturation model for KB1 unit

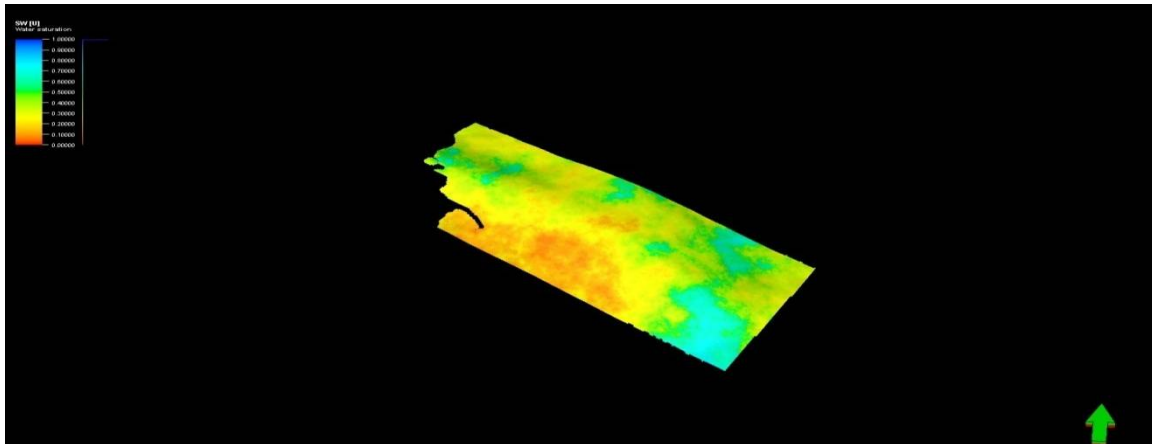


Fig. 16. Water saturation model for KB2 unit





Nermein F.Jaffar and Jalal A.AI – Sudanyi

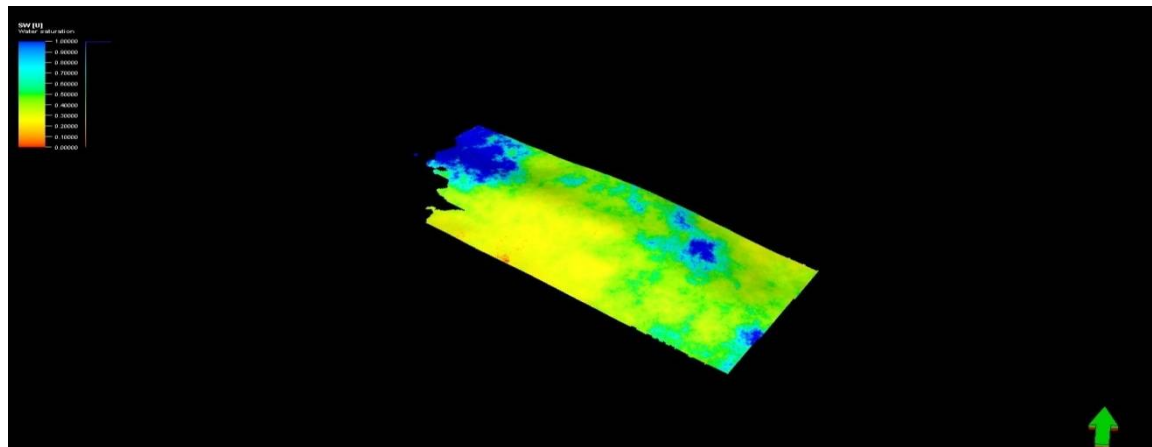


Fig. 17. Water saturation model for KB3 unit

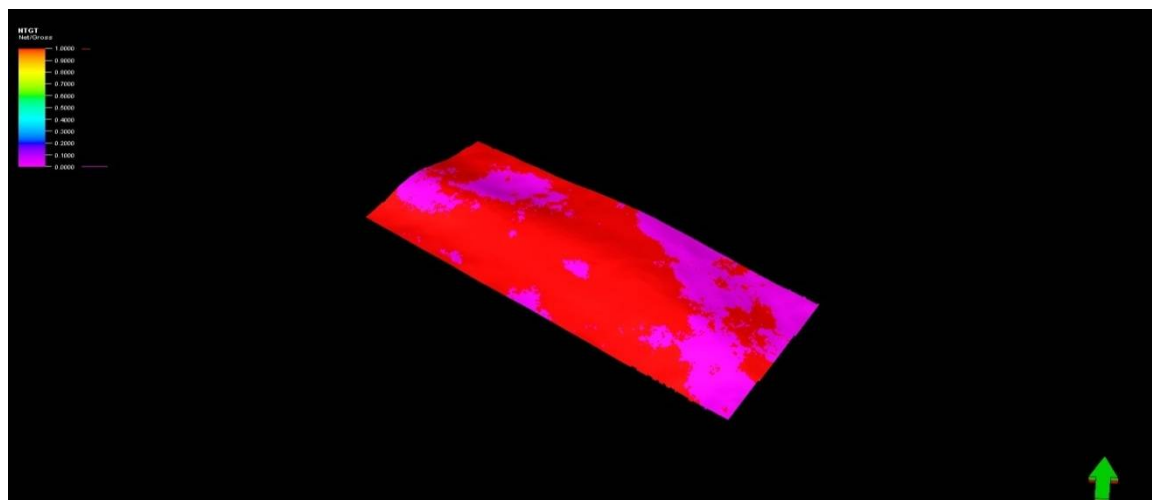


Fig. 18. Net to Gross model for KA1-2 unit





Nermein F.Jaffar and Jalal A.AI – Sudanyi

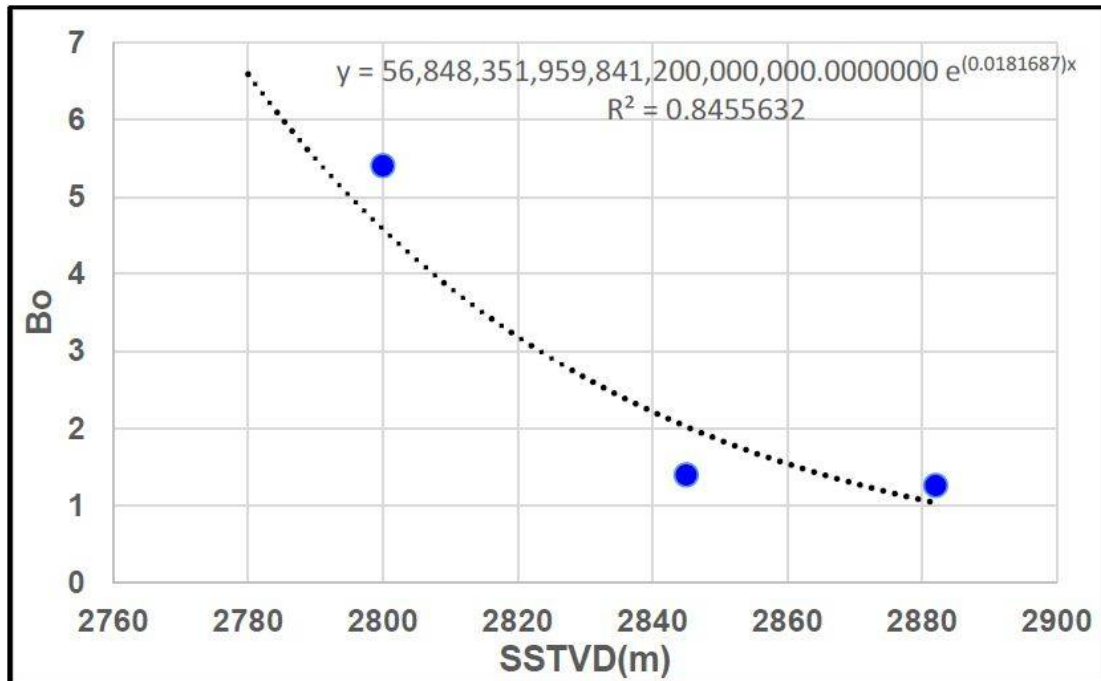


Fig. 19. Correlation regression between Bo and SSTVD





A Review on the Causes, Life Cycle, Pathology and Treatment of *Trypanosoma gambiense* and *Trypanosoma cruzi*

Hwaida Shakir Mustafa Al-Mahdawy*

Community Health Department, College of Health and Medical Technology, Medical Technical University, Iraq.

Received: 19 Sep 2018

Revised: 22 Oct 2018

Accepted: 27 Nov 2018

*Address for Correspondence

Hwaida Shakir Mustafa Al-Mahdawy

Community Health Department,
College of Health and Medical Technology,
Medical Technical University, Iraq.
Email: Mustafa3@gmail.com



This is an Open Access Journal / article distributed under the terms of the **Creative Commons Attribution License** (CC BY-NC-ND 3.0) which permits unrestricted use, distribution, and reproduction in any medium, provided the original work is properly cited. All rights reserved.

ABSTRACT

The current review aims to shedding light on the most important types of pathogenic parasites, trypanosomiasis and its main causes, life cycle and pathogens of *Trypanosoma gambiense* and *Trypanosoma cruzi*. And also presented some charts and images that illustrate these parasitic diseases, which must be taken into consideration for the purpose of avoidance and non-injury.

Keywords: shedding, *Trypanosoma gambiense*, *Trypanosome cruzi*, pathogens.

Introduction to *Trypanosoma*

Pathogens and their families cling to a continuous molecular arms race. In one evolutionary confrontation, the heroes were trypanosomal parasites and a human immune compound based on high-density lipoprotein. Trypanosomiasis parasites that cause African sleeping sickness have been waging a war on humans for thousands of years. The rapidly evolving complex of human lipoproteins in humans and some primates 1 is the focus of this conflict, which mediates the innate immune host response to parasites, but some trypanosomiasis parasites evolved to defeat this defense mechanism and successfully produce long-term infection in humans. In a recent study published in the journal Nature, Ozero and his colleagues described 2 complex combinations of resistance adaptations used by the most common African pathogenic parasites of trypanosomiasis: the Prussian parasitic parasite.

Trypanosomes are single-celled parasites that live freely in their host's blood. In order to avoid destruction by the immune system, these parasites constantly change their outer envelope. Some genes select the gene stock encoded for heterozygous surface sugars, but some primates, including humans, have developed innate immune compounds known as trypanosomiasis (TLFs) (Parasite surface proteins) and kill most types of trypanosomiasis parasites.



**Hwaida Shakir Mustafa Al-Mahdawy**

Trypanosomal analysis agents are high density lipoprotein molecules consisting of two main components: a protein linked to the lipoprotein (HPR) and lipid protein L1. The first protein binds to the hemoglobin protein and then binds it to a receptor on the surface of trypanosomiasis parasites. After that, the parasites swallow the molecule of trypanosomal analysis and transfer it to the cytoplasmic cytoskeletal lysosome to use hemoglobin and its lipid synthesis. During the transition, however, the core of the L1 lipoprotein is released from the Wenger compound by a small lysosome membrane that forms tiny holes in the ions that cause the parasite's explosion and death.

There are three types of human species belonging to this species are *T. gambiense* and *T. rhodesinse* and they are very similar because they are originally a subspecies of the species *T. brucei*, these types fall under the group Salivary Trypanosomes (because they are infected by the saliva of the insect Infected with human bite). The third type is *T. cruzi*, which falls under the group of Stercorarian Trypanosomes (because the infection is transmitted through the emergence of infected insect during the bite of the human after the delivery of insect feces to the wound caused by the bite of the insect).

Trypanosoma gambiense

This parasite was registered in the Gambia in 1901, causing Gambian trypanosomiasis, or sleeping sickness. Parasitic disease caused by this type of trpanosoma transmitted to humans by tsetse fly bites. This parasite is characterized by many wattles (the structures that take the shape of the thread and contribute to the movement of the cell) and confined to the presence of the African continent, specifically in the forest areas and in the bodies of antelopes, where Do not cause any harm to them and are subsequently acquired from the tsetse fly that works on sucking the infected antelope or cattle and then transmitting them to humans.

Symptoms and Signs of *Trypanosoma gambiense*

A tsetse fly bite causes a red sore to appear and, in a few weeks, a person who has been infected can develop symptoms such as fever, swollen lymph nodes, muscle and joint pain, headache and irritation. In the advanced stages of the disease, the disease affects the central nervous system, leading to a change in the personality of the patient, disorder in his biological clock (the day-to-day systems), confusion of things, lack of speech and seizures and difficulty in walking and talking.

Life Cycle

The parasite passes several stages of its life cycle within the fly until it reaches the salivary glands, making it ready for injection into the body of the bloodstream source following the tsetse fly. The first stage of the disease begins once the parasite passes through the host's body through the bloodstream and the lymphatic system, causing the temperature to rise significantly and then return to normal and return to the rise again and suddenly. Fever accompanied by skin rash associated with intestinal itching, headache and mental confusion. In many advanced cases, the virus causes swelling of the lymph nodes and tissues, enlargement of the liver and spleen, and the swelling of the lymph nodes in the area under the ear, specifically above the base of the neck. The second stage of the disease includes the central nervous system, where the brain is affected by a large number of people, causing the implication of the words of the patient, slow mental processes, sleep patient and his body and his skin for long periods. Some symptoms similar to Parkinson's disease may appear to be imbalance during walking, slow walking, limp jitter, muscle tension and increased mental confusion.

The life cycle of both species is similar. The parasite needs two hosts to complete its life cycle: the human host and the transient host, the Tse-Tse flies of the genus *Glossina G. palpalis* and *G. tachinoides* illustrate the life cycle with the following scheme:



**Hwaida Shakir Mustafa Al-Mahdawy****Pathology of *Trypanosoma gambiense***

The incubation period of 1-2 weeks may be chronic and lasts for several years. The initial period of the disease is Parasitaemia, followed by the spread of the parasite in the lymph nodes. The signs are intermittent Fever, Chills and Headache. The liver, hepatosplenomegaly, Lymphadenopathy especially in the area behind the neck. The parasite invasion then the central nervous system occurs several months later as sleeping starts and signs of increased headache, morbidity and sleepiness and the patient falls into a coma long coma followed by death due to Asthenia debility. Other symptoms of the disease include chronic inflammation of the membranes, heavy lymphocytic and plasma lymphocytes, Morula cells, blockage of cerebrospinal fluid, brain and nerve cord dissection, neuronal dissolution, and microglial proliferation.

Trypanosoma cruzi

Chagas disease is also known as American trypanosomiasis disease, the disease may be a threat to the lives of those infected and is contained to a parasite called *Trypanosoma cruzi* protozoan. The estimated number of people infected throughout the world infected with the disease in the range of 6 to millions of 7 million people almost, spread mainly disease in endemic by regions located in 21 countries, from Latin American countries, where it is exposed to vectors where transmitted to humans in the first place The way of mixing with Braz is triatomine, which is known by several names as "kissing bugs", according to geographical region.

Signs and symptoms of *Trypanosoma cruzi*

Chagas' disease can cause a brief illness (acute), or it may be a long-term (chronic) condition. Symptoms range from mild to severe, although many people do not have until the chronic phase

Cute stage

The acute phase of Chagas disease, which lasts for weeks or months, is often symptom-free. When signs and symptoms occur, they are usually mild, and may include: Swelling in place of infection, Fever, Fatigue, rash, body aches, Swollen eyelids, Headaches, Anorexia, Nausea, diarrhea or vomiting, Swollen glands and Enlarged liver or spleen Signs and symptoms that develop during the acute phase usually disappear on their own. If left untreated, the infection will continue and, in some cases, progress to the chronic stage.

Chronic stage

Chronic signs of Chagas's disease and symptoms may occur 10 to 20 years after the initial infection, or may never occur. In severe cases, signs and symptoms of Chagas disease may include:

- Irregular heartbeat
- Congestive heart failure
- Sudden cardiac arrest
- Difficulty swallowing due to enlarged esophagus
- Pain in the abdomen or obstruction due to colon enlargementsymptoms until the chronic stage.

The cause of the Chagas disease is the parasite "keratocytosis" which is transmitted from an insect known as triatomine bug. These insects can become infected with "Crocheted perforation" when the blood is already swallowed by animals infected with these parasites.





Hwaida Shakir Mustafa Al-Mahdawy

Triatomine bugs live mainly in clay, straw and mud-built huts in Mexico, South America and Central America. These insects hide during the day in the cracks of walls or ceilings, and then go out at night - and often feed on sleeping people. The infected insects are excreted after feeding, leaving the corneal peritoneal parasites on the skin. Parasites can enter the body through the eye or mouth, cutting, injuring or scratching from bite bugs. Scratching or scratching at the point of sting helps the parasites enter the body. Once they enter the body, the parasites multiply and spread. You may also be infected in the following ways:

- Non-cooked food contaminated with carboxylic vertebrate parasites found in the bugs bug
- If you are born to a woman with Crocheted Crochet
- Undergo blood transfusion containing contaminated blood
- Perform organ transplantation containing viable peritoneal peritoneal parasite
- Work in laboratories with potential for accidental exposure to parasites
- Spend time in a forest containing infected wild animals such as raccoons and oopsomes

Life Cycle

The parasite's life cycle is very complex, with all four phases. This parasite requires two hosts to complete its life cycle: the human and middle host, the carrier, the Reduviid Bugs of the *Triatoma* species. As we have seen previously, Metacyclic Trypomastigote infections enter the human skin and cause local inflammation and Swelling at the entry site. This is called Chagoma. The parasite is then spread through the lymph and blood to the various tissues and inside the cells of the ventricle. Reticuloendothelial cells Trypomastigote - Epimastigote - Promastigote - Amastigote In the latter phase, the multiplication occurs and then turns back to the stage of Promastigote, then Epimastigote and finally Trypomastigote, which is introduced into the blood outside the cells. When the last stages enter other cells, Cardiomyocytes These phases are transformed into uncontrolled phases and multiply causing serious problems. That the stages of the traitomystectot in the blood of this species do not multiply unlike the previous species, and when feeding the same sex carrier of the disease, the last stages go to the middle intestine Mid Gut and then to the hind gut Hind Gut, where it turns into the stage Epimastigote, which multiply fission and turn in the same place to Metacyclic Trypomastigote, which in turn are contagious stages of the human. The parasitic infection is transmitted by conjunctiva or conjunctiva after contact with the fingers infected with the infected insect pimples where the eyelid swells and is called Romanas sign.

Pathology of *Trypanosoma cruzi*

The period of incubation is 1-2 weeks. Symptoms of the disease are in acute and chronic stages. The acute form, often occurring in children, is Oedema. The acute form may take three to four weeks and may result in death due to myocarditis or membrane inflammation Meningoencephalitis. The chronic form, often found in adults, is neurotrophic, cardiotropic, or viscerotropic, and may persist for many years. The severity of the disease is based on the rate of multiplication of the inhibition stages in the cells of the various organs of the body and thus affected. The common sites of injury are the heart muscle, skeletal muscle, Neuroglial cells and Reticuloendothelial System cells, the damage of the heart muscle leads to failure of blood delivery and nerve damage often What leads to so-called inflationary diseases Megadiseases include enlarged esophageal megaoesophagus, megacolon hypertrophy and enlarged ureter Megaureter.

Treatment of *Trypanosoma cruzi*

To eliminate parasites and treat disease, use benzeneidazole as well as Nephurtimox. Both drugs ensure approximately 100% efficacy in treating the disease if given shortly after infection, ie at the acute stage. However, the efficacy of both drugs is diminishing and the duration of the infection has increased. Treatment is also prescribed for people who have been re-infected (for example by immunosuppression), infants with congenital infection, and





Hwaida Shakir Mustafa Al-Mahdawy

patients at the onset of the chronic stage. Treatment should be provided to infected adults, especially those who have no symptoms. Antiretroviral therapy may prevent or stop the development of the disease and prevent the transmission of the mother-to-child transmission during pregnancy. Weight should be given between the potential benefits of drugs to prevent the development or delay of Chagas disease, between the length of treatment (approximately two months) and potential adverse effects (which occur in about 40% of those treated). Pregnant women or those with renal or hepatic failure should not take benzenezole and naphthimox. People suffering from neurological or psychiatric disorders should also avoid taking Nephurtimox. In addition, specific treatment may be needed for people with heart or digestive symptoms.

REFERENCES

- 1- Abu Habib, Jalil (1978). Medical and veterinary insects. Baghdad University Press, pp. 104-108.
- 2- Abu Hub, Jalil (1982). Vector - borne diseases. Kuwait, World Knowledge Series.
- 3- Al-Rawi, Khasha Mahmoud and Khalafullah, Abdul Aziz (1980). Design and analysis of agricultural experiments. Dar of Books for Printing and Publishing, University of Mosul, 488 pages.
- 4- Altclas J., et al. 2005. Chagas disease in bone marrow transplantation: an approach to preemptive therapy. Bone Marrow Transplant. 36:123–129
- 5- Andrade A. L., et al. 1996. Randomised trial of efficacy of benznidazole in treatment of early Trypanosoma cruzi infection. Lancet 348:1407–1413
- 6- Andrade A. L., et al. 2004. Benznidazole efficacy among Trypanosoma cruzi-infected adolescents after a six-year follow-up. Am. J. Trop. Med. Hyg. 71:594–597
- 7- Andrade M. C., et al. 2009. Nonspecific lymphocytic myocarditis in baboons is associated with Trypanosoma cruzi infection. Am. J. Trop. Med. Hyg. 81:235–239
- 8- Andrade S. G. 1982. The influence of the strain of Trypanosoma cruzi in placental infections in mice. Trans. R. Soc. Trop. Med. Hyg. 76:123–128
- 9- Anonymous 1956. Found: two cases of Chagas disease. Texas Health Bull. 9:11–13
- 10- Arganaraz E. R., et al. 2001. Blood-sucking lice may disseminate Trypanosoma cruzi infection in baboons. Rev. Inst. Med. Trop. Sao Paulo 43:271–276.
- 11- Azogue E., Darras C. 1991. Prospective study of Chagas disease in newborn children with placental infection caused by Trypanosoma cruzi (Santa Cruz-Bolivia). Rev. Soc. Bras. Med. Trop. 24:105–109
- 12- Baroldi, Giorgio; Oliveira, Samuel J.M; Silver, Malcolm D (1997). "Sudden and unexpected death in clinically 'silent' Chagas' disease. A hypothesis". International Journal of Cardiology. 58 (3): 263–8. doi:10.1016/S0167-5273(96) 02878-1
- 13- Chagas, C. 1909b. Nouvelle espèce de trypanosomiase humaine. Bulletin de la Société de Pathologie Exotique, Paris, v. 2, n. 6, p. 304-307
- 14- Chagas, C. 1909c. Nova especie morbida do homem, produzida por um Trypanozoma (Trypanozoma cruzi): nota prévia. Brazil-Medico, Rio de Janeiro, v. 23, n. 16, p. 161.
- 15- Chin,j. (2000).Control of communicable diseases Manual.,17th.Ed. The American Puplic Health Association, New York: 420- 422.
- 16- [https://www.who.int/ar/news-room/fact-sheets/detail/chagas-disease-\(american-trypanosomiasis\)](https://www.who.int/ar/news-room/fact-sheets/detail/chagas-disease-(american-trypanosomiasis))
- 17- Lori Stevens, Patricia L. Dorn, Julia Hobson, Nicholas M. de la Rua, David E. Lucero, John H. Klotz, Justin O. Schmidt, Stephen A. Klotz Vector Blood Meals and Chagas Disease Transmission Potential, United States
- 18- Marin-Neto, Jose Antonio; Cunha-Neto, Edécio; Maclel, Benedito C.; Simões, Marcus V. (2007). "Pathogenesis of Chronic Chagas Heart Disease". Circulation. 115 (9): 1109–23. doi:10.1161/CIRCULATIONAHA.106.624296
- 19- Reis-Cunha JL, Baptista RP, Rodrigues-Luiz GF, Coqueiro-Dos-Santos A, Valdivia HO, de Almeida LV, Cardoso MS, D'Ávila DA, Dias FHC, Fujiwara RT, Galvão LMC, Chiari E, Cerqueira GC5, Bartholomeu DC (2016) Whole genome sequencing of Trypanosoma cruzi field isolates reveals extensive genomic variability and complex aneuploidy patterns within TcII DTU. BMC Genomics 19(1):816





Hwaida Shakir Mustafa Al-Mahdawy

- 20- Samudio F., Ortega-Barria E., Saldana A., Calzada J. 2007. Predominance of *Trypanosoma cruzi* I among Panamanian sylvatic isolates. *Acta Trop.* 101:178–181
- 21- Sarkar S., et al. 2010. Chagas disease risk in Texas. *PLoS Negl. Trop. Dis.* 4:e836.
- 22- Sartori A. M., et al. 2007. Manifestations of Chagas disease (American trypanosomiasis) in patients with HIV/AIDS. *Ann. Trop. Med. Parasitol.* 101:31–50
- 23- Schaffer G. D., Hanson W. L., Davidson W. R., Nettles V. F. 1978. Hematotrophic parasites of translocated raccoons in the southeast. *J. Am. Vet. Med. Assoc.* 173:1148–1151
- 24- Schijman A. G. 2006. Congenital Chagas disease, p. 223–259 *In* Mushahwar I. K., editor. (ed.), *Congenital and other related infectious diseases of the newborn*, vol. 13
- 25- Shaaban, Ibrahim and Bandar, Muhammad (1986). *Parasitology*. Ministry of Higher Education and Scientific Research, pp. 124-142.
- 26- Wood S. F. 1943. Observations on vectors of Chagas' disease in the United States. II. Arizona. *Am. J. Trop. Med. Hyg.* 23:315–320
- 27- Wood S. F. 1975. *Trypanosoma cruzi*: new foci of enzootic Chagas' disease in California. *Exp. Parasitol.* 38:153–160
- 28- Wood S. F., Wood F. D. 1961. Observations on vectors of Chagas' disease in the United States. III. New Mexico. *Am. J. Trop. Med. Hyg.* 10:155–162
- 29- World Health Organization 2007, posting date New global effort to eliminate Chagas disease (pressrelease). <http://www.who.int/mediacentre/news/releases/2007/pr36/en/index.html>
- 30- World Health Organization 2008. The global burden of disease: 2004 update. World Health Organization, Geneva, Switzerland: http://www.who.int/healthinfo/global_burden_disease/2004_report_update/en/index.html
- 31- Yabsley M. J., Noblet G. P. 2002. Seroprevalence of *Trypanosoma cruzi* in raccoons from South Carolina and Georgia. *J. Wildl. Dis.* 38:75–83
- 32- Yoshida N. 2008. *Trypanosoma cruzi* infection by oral route: how the interplay between parasite and host components modulates infectivity. *Parasitol. Int.* 57:105–109.
- 33- Yabsley M. J., Noblet G. P., Pung O. J. 2001. Comparison of serological methods and blood culture for detection of *Trypanosoma cruzi* infection in raccoons (*Procyon lotor*). *J. Parasitol.* 87:1155–1159.
- 34- Young, D. and Duncan, M. (1994). Guide to the identification and geographic distribution of *Lutzomyia* sand flies in Mexico, the west Indies, central and south America (Diptera: psychodidae). *Memoirs of the American Entomological Institute*, 54, associated publishers-American Entomological Institute, Gainesville, FL, USA.
- 35- Yeo M., et al. 2005. Origins of Chagas disease: Didelphis species are natural hosts of *Trypanosoma cruzi* I and armadillos hosts of *Trypanosoma cruzi* II, including hybrids. *Int. J. Parasitol.* 35:225–233
- 36- Zingales B., et al. 2009. A new consensus for *Trypanosoma cruzi* intraspecific nomenclature: second revision meeting recommends TcI to TcVI. *Mem. Inst. Oswaldo Cruz* 104:1051–1054.

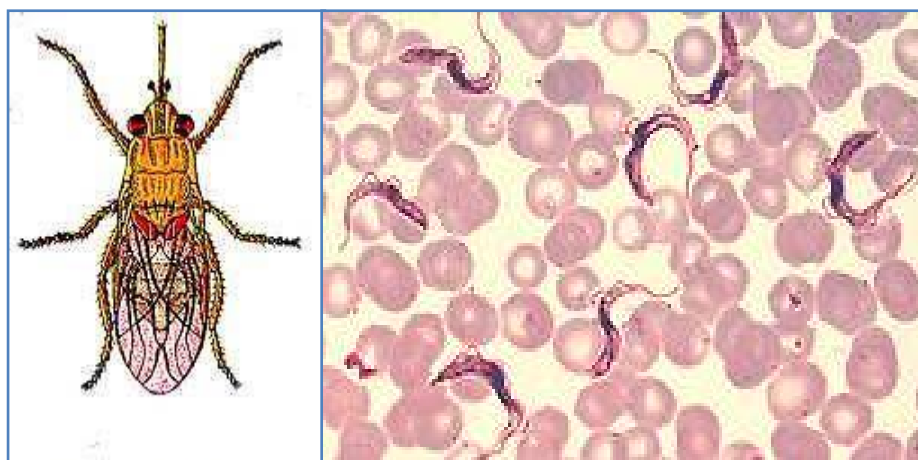


Figure.1: Shows the *Trypanosoma gambiense* and its causes.





Hwaida Shakir Mustafa Al-Mahdawy

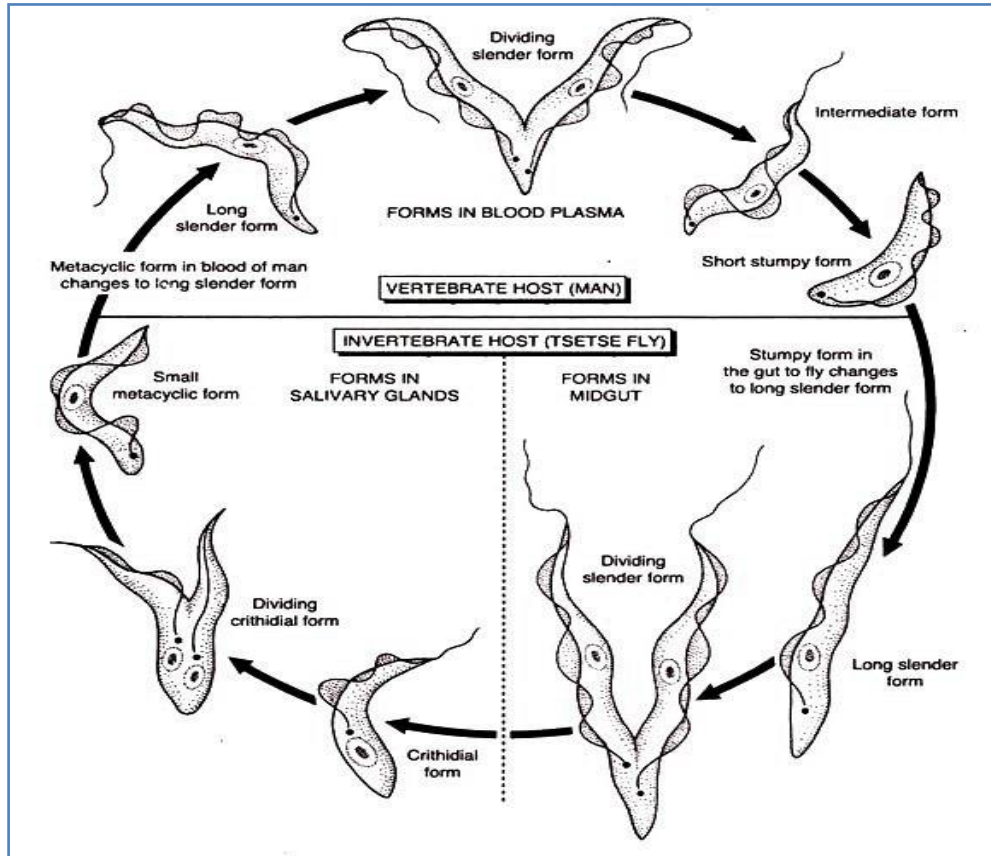


Figure.2: Life Cycle of *Trypanosoma gambiense*

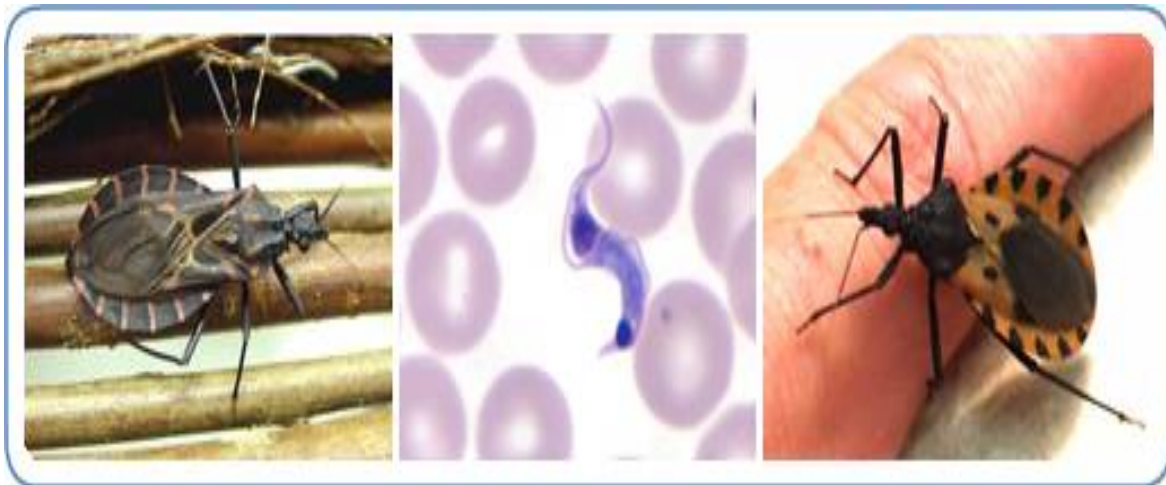


Figure.3: Shows the *Trypanosoma cruzi* and its causes





Hwaida Shakir Mustafa Al-Mahdawy

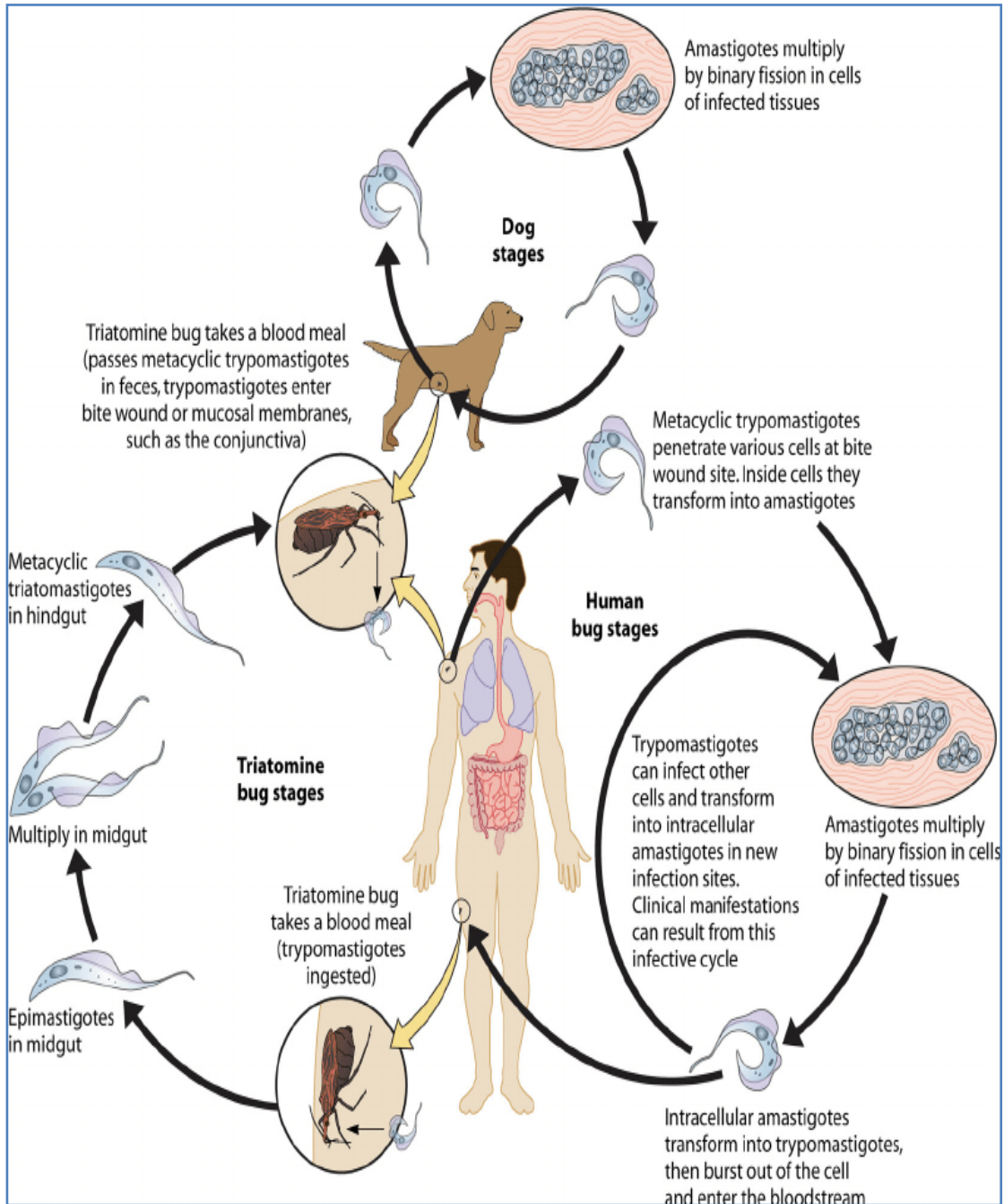


Figure.4: Life Cycle of *Trypanosoma cruzi*





The Role of Cytotoxic T Lymphocyte Associated Protein-4 Gene (-318 C/T) Polymorphism in Type 1 Diabetes Patients in Iraqi Children

Hosam A. A. Al-Issawi^{1*}, AbdulKareem A. Jasim¹ and Dhafer A. F. Al-Koofee²

¹Department of Biochemistry, College of Medicine, University of Kerbala, Kerbala, Iraq.

²Department of Clinical Laboratory Science, Faculty of Pharmacy, University of Kufa, Najaf, Iraq.

Received: 17 Sep 2018

Revised: 20 Oct 2018

Accepted: 27 Nov 2018

*Address for Correspondence

Hosam A. A. Al-Issawi

Department of Biochemistry,

College of Medicine,

University of Kerbala,

Kerbala, Iraq.

Email: hussamkk@yahoo.com



This is an Open Access Journal / article distributed under the terms of the **Creative Commons Attribution License** (CC BY-NC-ND 3.0) which permits unrestricted use, distribution, and reproduction in any medium, provided the original work is properly cited. All rights reserved.

ABSTRACT

Background:Type 1 diabetes mellitus (T1DM) is an insulin-dependent form of diabetes, Cytotoxic T lymphocyte antigen-4 (CTLA-4) is a member of the immunoglobulin superfamily that is expressed by activated T cells and transmits an inhibitory signal to T cells. CTLA-4 coded by CTLA-4 gene on chromosome 2q33. Polymorphisms of CTLA-4 gene belong to the main genetic factors determining the susceptibility to T1DM. **Methods:** A case-control study was designed to include 120 Iraqi children with T1DM and 120 healthy children controls. The patients were diagnosed previously with T1DM by Al-Imam Al-Hassan center for endocrine and diabetes in Al-Imam Al-Hussein medical city in holy Kerbala province. Genotyping was performed using the Tetra-primer amplification refractory mutation system polymerase chain reaction technique (T-ARMS-PCR). The biochemical tests was HbA1c test has been performed at central laboratory of Al-Imam Al-Hussein medical educational city. While the DNA extraction and PCR done at the research laboratory of the biochemistry department of the medical college of Kerbala university. **Results:** Risk factors of T1DM (Family history of diabetes mellitus, age at onset, gender) were found to be an independent risk factor for T1DM. The -318 C/T(rs5742909) polymorphism of CTLA-4 has non-significant differences are revealed for genotype and allele frequencies between T1DM patients and the control group. By calculating the odds ratios, is less than (1), it suggests that a person carrying T allele and C/T genotyping, decreased insusceptibility to be with T1DM. It is evident in the current study that the T allele of the CTLA-4 -318 C/T was not associated with the occurrence of T1DM and could not be considered as a risk factor for the development of the disease. **Conclusion:** Our case-control study suggests that the CTLA-4(-318C/T) gene polymorphism is not associated with T1DM in the Kerbala children.



**Hosam A. A. Al-Issawi et al.****Keywords:** Type 1 diabetes mellitus, Cytotoxic T lymphocyte antigens-4, Kerbala.

INTRODUCTION

Type 1 diabetes is generally thought to be precipitated by an immune-associated by destruction of insulin-producing pancreatic β cells (Atkinson *et al.* 2014; Paschou *et al.* 2018). T1DM is one of the most common chronic illnesses of childhood and requires a complex and demanding treatment regimen (Naranjo and Hood 2013). Whether mortality in T1DM patients is improved by intensive glycemic therapy has not been clarified yet. A number of studies have recently been published claiming that mortality rate is still higher than in age-matched controls without diabetes, despite improvements in management of glucose levels (Livingstone *et al.* 2015; Orchard *et al.* 2015). T1DM represent only 10–15% of cases with diabetes mellitus. Type 2 diabetes mellitus (T2DM) represent the most common form (Diaz-Valencia *et al.* 2015). The incidence of T1DM among children has been confirmed to be increased over the past 50 years in the worldwide, especially among a children of (10–14) years of age (Chen *et al.* 2017). In the Arabs contraries there are approximately (60,000) cases of children less than 15 years old with T1DM. According to recent incidence rates by the International Diabetes Federation (IDF)'s at (2015), Saudi Arabia and Kuwait are featured as among the top 10 list of countries with the highest incidence rates in the world (Robert *et al.* 2018). Although differences in human leukocyte antigen (HLA) genes are a very important genetic risk factor of T1DM incidence, they alone do not account for the disease (Jerram and Leslie 2017). Concannon *et al.* reported the functions of non-HLA-associated loci in T1DM. They appear on important rounds of sites in causing (Fig. 1.3).

They suggests that other dangerous sites for T1DM susceptibility may do their effects through the immune system (Concannon *et al.* 2009). A different levels, the genes act on it including extend self-reactive cells, interfere with immune regulation, and influence β -cell survival (Katsarou *et al.* 2017). Genetic variations may be affect the expression of gene products (Haraksingh and Snyder 2013; Pai *et al.* 2015). many studies have shown the effect of the variations of the *CTLA-4* gene on the function of CTLA-4 protein (Piccioli *et al.* 2010; Haraksingh and Snyder 2013), affecting the pathogenic pathways of autoimmune diseases, such as insulin-dependent diabetes mellitus (Rich and Concannon 2015), Graves' disease, Hashimoto's thyroiditis and other autoimmune diseases (Pastuszak-Lewandoska *et al.* 2012). The CT transition at position 318 of the promoter region (-318 C/T) has a potential role for in the regulation of *CTLA-4* gene expression (Karabon *et al.* 2009), the T allele of -318C/T was associated with a significantly higher promoter activity than the C allele of -318C/T (Murase *et al.* 2011). The T mutation could be considered as protective for autoimmune disease (Wang *et al.* 2002). Several studies was found correlation between the (-318C/T) polymorphism and the onset of pediatric T1DM, There were two studies that evaluated the African population, two studies were conducted in Asia and one study was conducted to investigate the Latino and European population (Bao *et al.* 2016). several studies was found *CTLA-4* (-318C/T) polymorphism does not correlate with autoimmune diseases (Almasi *et al.* 2015; Tanhapour *et al.* 2017)

MATERIALS AND METHODS

Study individuals

A case-control study was designed to include 120 Iraqi children with T1DM and 120 healthy children controls. The collections of samples were achieved during the period from 1st of December 2017 till 30th of March 2018. Patient group: Contained 120 Patients with T1DM (58 male and 62 female). The patient ages were (Mean \pm SD) 11.97 \pm 2.99 Year. The patients were diagnosed previously with T1DM by Al-Imam Al-Hassan center for endocrine and diabetes in Al-Imam Al-Hussein medical city in holy Kerbala province. A structured validated questionnaire would be used consisting of two parts:

1. Socio – demographic characteristics like (Name, age, gender).
2. T1DM related variables (date of first diagnosis, family history of T1DM, family history of T2DM)





Hosam A. A. Al-Issawi et al.

Control group: Included 120 healthy children (63 male and 57 female). Age of control group were (Mean±SD), they were free from T1DM. A permission was taken from all subjects of patient and control groups after they were told about the aim and advantages of this study.

Biochemical measurements

Biochemical measurements included glycated hemoglobin (HbA1c), it was measured as mentioned in the instruction of the manufacturing company of the purchased kits.

Genotypic Measurements

Blood sample of T1DM patients and control group were collected in EDTA anticoagulant tubes. DNA was extracted from whole blood samples using the genomic DNA extraction kit (Promega, USA). The protocol was carried out as recommended in the instruction of the kit. DNA concentration and purity were measured with the use of BioDrop, UK. Genotyping of *CTLA-4-318 C/T* polymorphism was performed by T-ARMS PCR with the use of Thermo cycler (Clever/UK). Primers and its concentrations were selected as described by (Balbi *et al.* 2007; Narooie-Nejad *et al.* 2017). As mention below:

Outer forward:

5'-CAATGAAATGAATTGGACTGGATG-3'(0.5mM)

Outer reverse:

5'-TGCACACACAGAAGGCTCTTGAATA-3'(0.5mM)

Inner forward:

5'-CTCCACTTAGTTATCCAGATC TTC-3'(0.8mM)

Inner reverse:

5'-ACTGAAGCTTCATGTTCCTACTCTA-3'(1mM)

The amplification was performed in a total volume of 25 µl consisted of 12.5 µl Go Taq green master mix (promega, USA), 1.25, 1.25, 2 and 2.5 µl of outer forward, reverse forward, inner forward and inner reverse primers, respectively and 3.1 µl genomic DNA as template. The PCR reaction program protocol was 95°C for 10 min followed by 35 cycles of 94°C for 30 s, 62 °C for 30 s, 72°C for 30 s and a final cycle 72°C for 7 min. The amplification products were 296bp for control band, 201bp for C allele and 141bp for T allele. The product of amplification was analyzed by 2% agarose gel electrophoresis.

Statistical analysis

Student *t*-test and ANOVA test were used to compare numerical data of the patient and control groups using SPSS v.20.0 software (SPSS Inc., Chicago, IL). Genotype distribution and alleles frequency were tested for Hardy–Weinberg equilibrium by using online software, web-Assotest, (www.ekstoem.com).

RESULTS

The characteristics of the study groups were presented in table (1). There is no statistically significant difference concerning the age and sex distribution between diabetic patients and control group ($p > 0.05$). The history of consanguinity marriage was studied, as shown in figure (1), and shows 70% of patients with T1DM have positive





Hosam A. A. Al-Issawi et al.

history of consanguineous marriage. Serum concentration of (HbA1C) was significantly increased in patients with T1DM when compared with control group, As shown in table (2). The deterioration in means of glycemic control in all age of T1DM patients was tested and compared to American Diabetes Association (ADA) goals, as shown in figure (2). The curves show deterioration in mean glycemic control in all ages (except for five years) of patients with T1DM and the proportions was not meeting the ADA. The electrophoretic analysis of the PCR product of *CTLA-4* SNP rs5742909C>T demonstrated two (296,201 bp), three (296, 201,141 bp) and two (296,141 bp) bands for carriers of the CC, CT and TT genotypes respectively figure (3). Results of this SNP were found to be consistent with Hardy-Weinberg equilibrium in control group. The genotyping was non-significant (OR=0.87, CI 95%= 0.34-2.23 & P>0.05) differences of the variant CT genotype in T1DM patients when compared with control group. The TT genotype was not frequent in patients (Table.3).

DISCUSSION

In the current study, a case-control study was conducted to assess the association of *CTLA-4*rs5742909(C/T) polymorphism with the occurrence of T1DM in Iraqi population. The project was also targeted the impact of the intended polymorphisms on studied risk factors of T1DM. Such attempt is essential to perceive the genetic involvement of T1DM in our population. Thus, it is worthy to identify individuals at high risk to occurrence T1DM, aspiring to improve the plan of the management of the disease. The results are shows that chi-square of examined SNPs less than (3.84), while a chi-square (χ^2) value >3.8 is significant at $p < 0.05$ with first degree of freedom (Ganachari et al. 2010). Therefore genotype distributions of the examined SNP was consistent with the Hardy-Weinberg equilibrium (HWE) in the control individuals suggesting constant frequencies of the investigated genotypes between generations (Morra et al. 2016).

The results of the assessment of genotype distribution of the rs5742909 SNP was exhibited a non-significant associations ($P < 0.05$) between C/T genotype and incidence of T1DM patients when compared with those of the control group. By calculating the odds ratios, is less than (1), it is suggest that a person carrying T allele and C/T genotyping, decreased in susceptibility to be with T1DM. It is evident in the current study that the T allele of the *CTLA-4* -318 C/T was not associated with the occurrence of T1DM and could not be considered as a risk factor for the development of the disease. The *CTLA-4* promoter polymorphism at -318 C/T (rs5742909) and its effect on protein expression was investigated (Ghaderi 2011; Naroie-Nejad et al. 2017). The -318 T allele may contribute to increased expression of *CTLA-4* and consequently to the inhibition of excessive immune activity, thus reducing the risk of autoimmune disorders (Ligers et al. 2001; Wang et al. 2002). Several studies on the association of the *CTLA-4* -318 C/T polymorphisms and susceptibility to T1DM in various ethnic populations revealed in concordance with our finding, Lee et al. showed that the frequency of the C allele was higher in patients with T1DM, whereas, the frequency of the T allele was negatively associated with T1DM (Lee et al. 2001). Also, *CTLA-4* -318 C/T SNP was not related to T1DM susceptibility in (South America) Argentina and Chile (Caputo et al. 2007; Balic et al. 2009), (North African) Egypt (Saleh et al. 2013) and (Northeast Asia) Korea (Jung et al. 2009) populations. Furthermore, a meta-analysis of 5637 T1DM patients and 6759 controls demonstrated no association of the -318 variant with T1DM (OR = 0.92; 95% CI = 0.45–1.89) after several confounders were controlled for (Kavvoura and Ioannidis 2005). By contrast results. Steck et al. found that the frequency of the CC genotype at position -318 in the *CTLA-4* promoter was significantly lower in patients with T1DM compared to controls, and they suggested that this polymorphism was associated with T1DM (Steck et al. 2005). Moreover, Benmansour, Jihen, et al. reported a positive association of -318 C/T polymorphism with T1DM in a case-control study of population from Tunisian populations (Benmansour et al. 2010). Furthermore, Balic, Iván, et al. found -318 C/T SNP to be associated with T1DM (Balic et al. 2009).

The table (3.3) shows elevated HbA1c levels significantly in patient with T1DM when compared with control group. Inadequate glycemic control (HbA1c levels >7.0%) in patients with T1DM was observed in 77% of the participants of a study in the USA in 2016 (McCarthy et al. 2016), 74% of the study patients in the region of Castilla-La Mancha, Spain in 2012 (Sastre et al. 2012), 87% of patients surveyed in Venezuela and 84%–90% of the participants of national





Hosam A. A. Al-Issawi et al.

multicentre studies conducted in Brazil in 2010 and 2015 (Mendes *et al.* 2010;Sastre *et al.* 2012). In this study, The curves show deterioration in mean glycemic control in all ages of patients with T1DM and the proportions was not meeting the American Diabetes Association recommend a target values for HbA1c in relation to age as follows: HbA1c<8.5% (<69 mmol/mol) at age <6 years, < 8 % (64mmol/mol) % at 6 to 12 years, 7.5% (< 58 mmol/mol) at 13 to 18 years and < 7% (< 53 mmol/mol) in adults(Association 2012).Results from the T1DM Exchange Clinic Network, including 13,316 participants revealed that overall, only 32% met the ADA targets for their age group and 25% met the ISPAD goals. The proportions meeting the ADA goals were 64% for the under 6 years age group, 43% for (6-12) yearolds, and 21% for the (13-19) year olds (Wood *et al.* 2013).

According to the guidelines of the International Society of Pediatrics and Adolescents (ISPAD) treatment of T1DM should target HbA1c level of <7.5% (<58 mmol/mol), if achieved without severe episodes of hypoglycemia(Rewers *et al.* 2009).Consanguineous marriages, which were more common among the familial patients, may also contribute to an increased genetic predisposition for the development of T1DM as the two parents may share similar susceptibility genes that could be transmitted to their offspring(Lebenthal *et al.* 2010).Although Finland has among the highest global incidence and prevalence rates of T1DM (Federation 2015), compared to Arab nation, they have very low consanguineous mating rates and much lower first-cousin marriage rates, at 0.17% in Finland. Therefore, studying the Arab genome will provide important insights into the molecular pathology of T1DM and help identify rare alleles or haplotypes that might contribute to a better understanding of T1DM pathology (Zayed *et al.* 2016).

CONCLUSION

The *CTLA-4* (-318 C/T) gene polymorphism was nosignificant associated with susceptibility to T1DM in Iraqi children.

ACKNOWLEDGEMENTS

Authors wish to thank participants whom blood samples were taken. Alsothanks to the staff of al-imam al-hassan center for diabetes and endocrinology, at al-imam al-hussain medical city, for help duringblood samples collection.

REFERENCES

1. Almasi, S., M. R. Aliparasti, A. Aliasgarzadeh, B. Abd-Nikfarjam, H. Hyöty, M. Knip, *et al.* (2015). "Investigation of CTLA-4-318C/T gene polymorphism in cases with type 1 diabetes of Azerbaijan, Northwest Iran." *Immunology letters***166**(2): 134-139.
2. Association, A. D. (2012). "Standards of medical care in diabetes--2012." *Diabetes care***35**: S11.
3. Atkinson, M. A., G. S. Eisenbarth and A. W. Michels (2014). "Type 1 diabetes." *The Lancet***383**(9911): 69-82.
4. Balbi, G., F. Ferrera, M. Rizzi, P. Piccioli, A. Morabito, L. Cardamone, *et al.* (2007). "Association of- 318 C/T and+ 49 A/G cytotoxic T lymphocyte antigen-4 (CTLA-4) gene polymorphisms with a clinical subset of Italian patients with systemic sclerosis." *Clinical & Experimental Immunology***149**(1): 40-47.
5. Balic, I., B. Angel, E. Codner, E. Carrasco and F. Pérez-Bravo (2009). "Association of CTLA-4 polymorphisms and clinical-immunologic characteristics at onset of type 1 diabetes mellitus in children." *Human immunology***70**(2): 116-120.
6. Bao, L., M. Chen, Y. Lei, Z. Zhou, H. Shen and L. Feng (2016). "Association of cytotoxic T-lymphocyte-associated antigen 4 genetic polymorphisms with type 1 diabetes in children: A systematic review and meta-analysis." *Meta Gene***10**: 61-66.





Hosam A. A. Al-Issawi *et al.*

7. Benmansour, J., M. Stayoussef, F. A. Al-Jenaidi, M. H. Rajab, C. B. Rayana, H. B. Said, *et al.* (2010). "Association of single nucleotide polymorphisms in cytotoxic T-lymphocyte antigen 4 and susceptibility to autoimmune type 1 diabetes in Tunisians." *Clinical and Vaccine Immunology***17**(9): 1473-1477.
8. Caputo, M., G. E. Cerrone, C. Mazza, N. Cédola, H. M. Targovnik and D. F. Gustavo (2007). "No evidence of association of CTLA-4-318 C/T, 159 C/T, 3' STR and SUMO4 163 AG polymorphism with autoimmune diabetes." *Immunological investigations***36**(3): 259-270.
9. Chen, Y.-l., Y.-c. Huang, Y.-c. Qiao, W. Ling, Y.-h. Pan, L.-j. Geng, *et al.* (2017). "Climates on incidence of childhood type 1 diabetes mellitus in 72 countries." *Scientific reports***7**(1): 12810.
10. Concannon, P., S. S. Rich and G. T. Nepom (2009). "Genetics of type 1A diabetes." *New England Journal of Medicine***360**(16): 1646-1654.
11. Diaz-Valencia, P. A., P. Bougnères and A.-J. Valleron (2015). "Global epidemiology of type 1 diabetes in young adults and adults: a systematic review." *BMC Public Health***15**(1): 255.
12. Federation, I. D. (2015). "IDF DIABETES ATLAS Seventh Edition." from <https://www.idf.org/search.html?searchword=prevalence&ordering=newest&searchphrase=all&limit=100>.
13. Ganachari, M., J. A. Ruiz-Morales, J. C. G. de la Torre, J. Dinh, J. Granados and P. O. Flores-Villanueva (2010). "Joint effect of MCP-1 genotype GG and MMP-1 genotype 2G/2G increases the likelihood of developing pulmonary tuberculosis in BCG-vaccinated individuals." *PloS one***5**(1): e8881.
14. Ghaderi, A. (2011). "CTLA4 gene variants in autoimmunity and cancer: a comparative review." *Iranian Journal of Immunology***8**(3): 127-149.
15. Haraksingh, R. R. and M. P. Snyder (2013). "Impacts of variation in the human genome on gene regulation." *Journal of molecular biology***425**(21): 3970-3977.
16. Jerram, S. T. and R. D. Leslie (2017). "The Genetic Architecture of Type 1 Diabetes." *Genes***8**(8): 209.
17. Jung, M. H., J. Yu, C. H. Shin, B. K. Suh, S. W. Yang and B. C. Lee (2009). "Association of cytotoxic T lymphocyte antigen-4 gene polymorphisms and HLA class II alleles with the development of type 1 diabetes in Korean children and adolescents." *Journal of Korean medical science***24**(6): 1004-1009.
18. Karabon, L., A. Kosmaczewska, M. Bilinska, E. Pawlak, L. Ciszak, A. Jedynak, *et al.* (2009). "The CTLA-4 gene polymorphisms are associated with CTLA-4 protein expression levels in multiple sclerosis patients and with susceptibility to disease." *Immunology***128**(1pt2): e787-e796.
19. Katsarou, A., S. Gudbjornsdottir, A. Rawshani, D. Dabelea, E. Bonifacio, B. J. Anderson, *et al.* (2017). "Type 1 diabetes mellitus." *Nat Rev Dis Primers***3**: 17016.
20. Kavvoura, F. K. and J. P. Ioannidis (2005). "CTLA-4 gene polymorphisms and susceptibility to type 1 diabetes mellitus: a HuGE Review and meta-analysis." *American journal of epidemiology***162**(1): 3-16.
21. Leberthal, Y., L. De Vries, M. Phillip and L. Lazar (2010). "Familial type 1 diabetes mellitus—gender distribution and age at onset of diabetes distinguish between parent-offspring and sib-pair subgroups." *Pediatric diabetes***11**(6): 403-411.
22. Lee, Y.-J., F.-S. Lo, S.-G. Shu, C.-H. Wang, C.-Y. Huang, H.-F. Liu, *et al.* (2001). "The promoter region of the CTLA4 gene is associated with type 1 diabetes mellitus." *Journal of Pediatric Endocrinology and Metabolism***14**(4): 383-388.
23. Ligers, A., N. Teleshova, T. Masterman, W. Huang and J. Hillert (2001). "CTLA-4 gene expression is influenced by promoter and exon 1 polymorphisms." *Genes and immunity***2**(3): 145.
24. Livingstone, S. J., D. Levin, H. C. Looker, R. S. Lindsay, S. H. Wild, N. Joss, *et al.* (2015). "Estimated life expectancy in a Scottish cohort with type 1 diabetes, 2008-2010." *Jama***313**(1): 37-44.
25. McCarthy, M., M. Funk and M. Grey (2016). Ideal cardiovascular health in adults with type 1 diabetes. NURSING RESEARCH, LIPPINCOTT WILLIAMS & WILKINS TWO COMMERCE SQ, 2001 MARKET ST, PHILADELPHIA, PA 19103 USA.
26. Mendes, A. B. V., J. A. S. Fittipaldi, R. C. S. Neves, A. R. Chacra and E. D. Moreira (2010). "Prevalence and correlates of inadequate glycaemic control: results from a nationwide survey in 6,671 adults with diabetes in Brazil." *Acta diabetologica***47**(2): 137-145.





Hosam A. A. Al-Issawi et al.

27. Morra, A., S. Böhringer and A. van der Vaart (2016). "A Goodness-of-fit test for Hardy-Weinberg Equilibrium in the Presence of Covariates."
28. Murase, M., T. Nishida, M. Onizuka, Y. Inamoto, K. Sugimoto, N. Imahashi, *et al.* (2011). "Cytotoxic T-lymphocyte antigen 4 haplotype correlates with relapse and survival after allogeneic hematopoietic SCT." *Bone marrow transplantation***46**(11): 1444.
29. Naranjo, D. and K. Hood (2013). "Psychological challenges for children living with diabetes." *Diabetes Voice***58**(s1): 38-40.
30. Narooie-Nejad, M., O. Taji, D. M. Kordi Tamandani and M. A. Kaykhaei (2017). "Association of CTLA-4 gene polymorphisms-318C/T and+ 49A/G and Hashimoto's thyroiditis in Zahedan, Iran." *Biomedical reports***6**(1): 108-112.
31. Orchard, T. J., D. M. Nathan, B. Zinman, P. Cleary, D. Brillon, J.-Y. C. Backlund, *et al.* (2015). "Association between 7 years of intensive treatment of type 1 diabetes and long-term mortality." *Jama***313**(1): 45-53.
32. Pai, A. A., J. K. Pritchard and Y. Gilad (2015). "The genetic and mechanistic basis for variation in gene regulation." *PLoS genetics***11**(1): e1004857.
33. Pascho, S. A., N. Papadopoulou-Marketou, G. P. Chrousos and C. Kanaka-Gantenbein (2018). "On type 1 diabetes mellitus pathogenesis." *Endocrine connections***7**(1): R38-R46.
34. Pastuszek-Lewandoska, D., E. Sewerynek, D. Domańska, A. Gładys, R. Skrzypczak and E. Brzezińska (2012). "CTLA-4 gene polymorphisms and their influence on predisposition to autoimmune thyroid diseases (Graves' disease and Hashimoto's thyroiditis)." *Archives of medical science: AMS***8**(3): 415.
35. Piccioli, P., G. Balbi, M. Serra, A. Morabito, T. Lamparelli, M. Gobbi, *et al.* (2010). "CTLA-4+ 49A> G polymorphism of recipients of HLA-matched sibling allogeneic stem cell transplantation is associated with survival and relapse incidence." *Annals of hematology***89**(6): 613-618.
36. Rewers, M., C. Pihoker, K. Donaghue, R. Hanas, P. Swift and G. J. Klingensmith (2009). "Assessment and monitoring of glycemic control in children and adolescents with diabetes." *Pediatric diabetes***10**: 71-81.
37. Rich, S. S. and P. Concannon (2015). "Role of Type 1 Diabetes-Associated SNPs on Autoantibody Positivity in the Type 1 Diabetes Genetics Consortium: Overview." *Diabetes care***38**(Supplement 2): S1-S3.
38. Robert, A. A., A. Al-Dawish, M. Mujammami and M. A. A. Dawish (2018). "Type 1 Diabetes Mellitus in Saudi Arabia: A Soaring Epidemic." *International journal of pediatrics***2018**.
39. Saleh, H. M., B. Koeleman, G. Szénási, L. Rosivall and P. Hamar (2013). "Association of CTLA-4 Polymorphisms with Type 1 Diabetes in the Egyptian Population."
40. Sastre, J., P. J. Pinés, J. Moreno, M. Aguirre, B. Blanco, D. Calderón, *et al.* (2012). "Situación de control metabólico y pautas de tratamiento en pacientes con diabetes tipo 1 en Castilla-La Mancha: estudio de diabetes tipo 1 en Castilla-La Mancha." *Endocrinología y Nutrición***59**(9): 539-546.
41. Steck, A. K., T. L. Bugawan, A. M. Valdes, L. M. Emery, A. Blair, J. M. Norris, *et al.* (2005). "Association of non-HLA genes with type 1 diabetes autoimmunity." *Diabetes***54**(8): 2482-2486.
42. Tanhapour, M., A. Vaisi-Raygani, M. Khazaei, Z. Rahimi and T. Pourmotabbed (2017). "Cytotoxic T-lymphocyte associated antigen-4 (CTLA-4) polymorphism, cancer, and autoimmune diseases." *AIMS Med Sci***4**: 395-412.
43. Wang, X., X. Zhao, R. Giscombe and A. Lefvert (2002). "A CTLA-4 gene polymorphism at position- 318 in the promoter region affects the expression of protein." *Genes and immunity***3**(4): 233.
44. Wood, J. R., K. M. Miller, D. M. Maahs, R. W. Beck, L. A. DiMeglio, I. M. Libman, *et al.* (2013). "Most youth with type 1 diabetes in the T1D Exchange Clinic Registry do not meet American Diabetes Association or International Society for Pediatric and Adolescent Diabetes clinical guidelines." *Diabetes care***36**(7): 2035-2037.
45. Zayed, H., A. Ouhtit and R. El Bekay (2016). "An Arab registry for type 1 diabetes: global benefits for type 1 diabetes patients." *Current medical research and opinion***32**(10): 1681-1684.





Hosam A. A. Al-Issawi et al.

Table (1): The study sample characteristics

Parameters	Patient with T1DM	Control group	P-value
Age (Y) (Mean± SD)	11.97 ± 2.99	11.02 ± 2.08	>0.05
Age rang	2 – 15	3 – 15	-
Gender (Male : Female)	58 : 62	63 : 57	>0.05

NS; Non significant, SD; standard deviation, T1DM; Type 1 diabetes mellitus,p-value <0.05

Table (2): HbA1c levels in studies groups

HbA1c data	Patients with T1DM	Control group	P-value
Mean ± SD	9.48±2.60	4.27±0.58	<0.05
(Mini – Max)	(4.3 - 16)	(3.02 – 5.33)	-
Less than 7.5 (good control) No. (%)	28 (23.3 %)	120 (100%)	-
More than 7.5 (bad control) No. (%)	92 (76.7 %)	0 (0%)	-

*S; significant, p-value <0.05 significant, HbA1c; glycated hemoglobin A1c and T1DM;type 1diabetes mellitus.

Table (3): Genotyping of CTLA-4-318 C/T polymorphism with allele frequency

Groups	Gene variation	Genotype			Total	Allele frequency	
		CC (%)	CT (%)	TT (%)		C (%)	T (%)
Patients with T1DM		111	9	0	120	231	9
Control		104	14	2	120	222	18

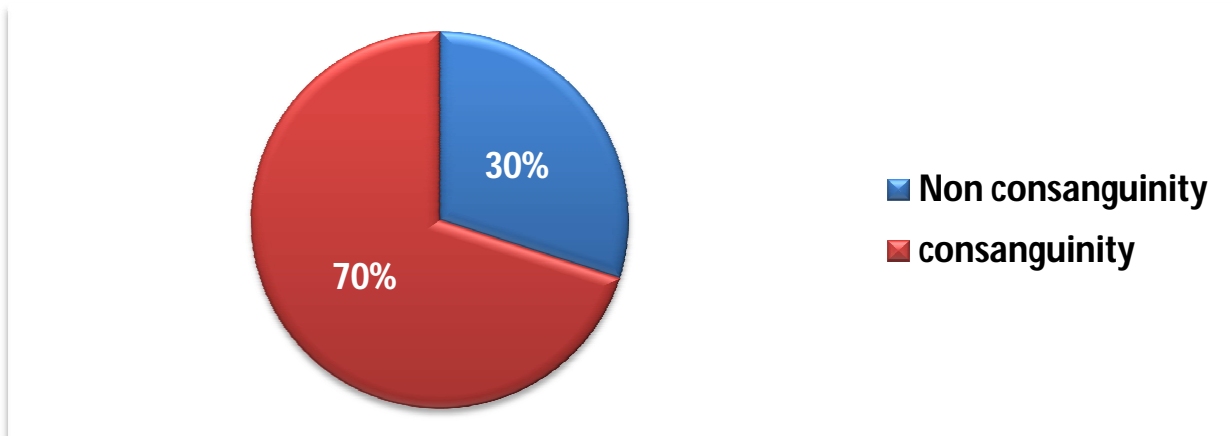
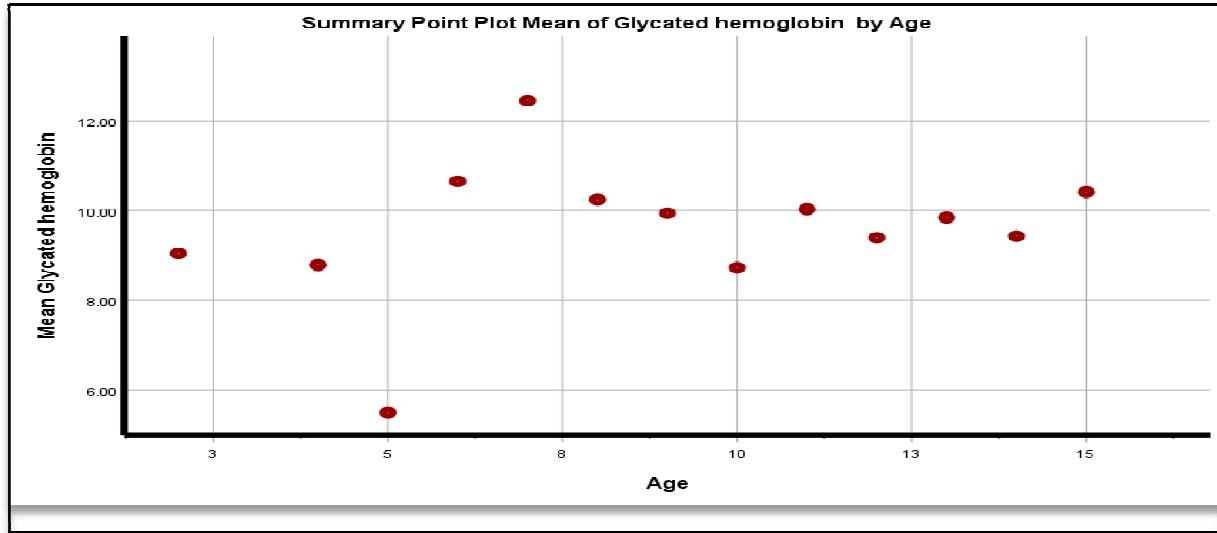


Figure (1): Distribution of parental consanguinity among the patients group





Hosam A. A. Al-Issawi et al.



Figure(2): Mean HbA1c trajectory from 2 to 15 year of age

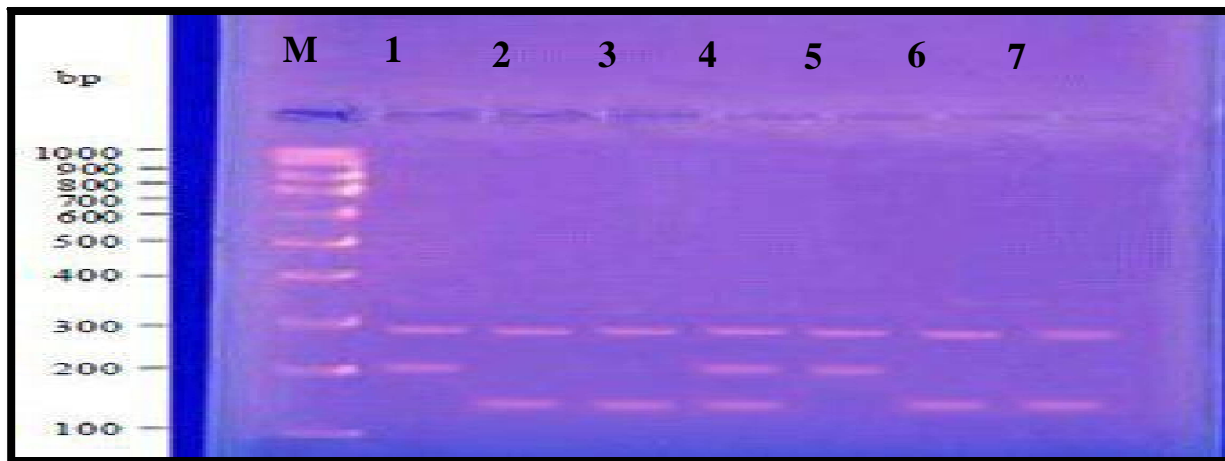


Figure (3):Amplification of *CTLA-4* gene -318 C/T polymorphism by T-ARMS-PCR. Lines MW: Molecular weight marker, Lines 1 and 5: CC wild genotype 296 bp, Lines 4 : CT Heterozygous genotype 201 bp, Lines 2,3 and 7: TT homozygous genotype 141 bp and K band: Non-allele-specific control band.

Abbreviations list

- ADA American Diabetes Association
- bp Base pair
- HbA1c Hemoglobin A1c
- PCR Polymerase chain reaction
- P-value probability value
- SPSS Statistical Package for the Social Sciences
- T1DM Type 1 diabetes mellitus
- T2DM Type 2 Diabetes Mellitus
- T-ARMSTetra- amplification-refractory mutation system





Association of *MTHFR* Gene Polymorphisms and Some Risk Factors with Myocardial Infarction in Baghdad City

Farah Farouk Hassan AL-Haially* and Rasha Abdull-Hussein Mahood

Institute of Genetic Engineering and Biotechnology for Postgraduate Studies, University of Baghdad, Baghdad, Iraq.

Received: 18 Sep 2018

Revised: 23 Oct 2018

Accepted: 27 Nov 2018

* Address for Correspondence

Farah Farouk Hassan AL-Haially

Institute of Genetic Engineering and Biotechnology for Postgraduate Studies,
University of Baghdad,
Baghdad, Iraq.



This is an Open Access Journal / article distributed under the terms of the **Creative Commons Attribution License** (CC BY-NC-ND 3.0) which permits unrestricted use, distribution, and reproduction in any medium, provided the original work is properly cited. All rights reserved.

ABSTRACT

Myocardial infarction (MI) is one of the most prevalent cardiovascular diseases (CVD) worldwide. It has been shown that traditional risk factors, including diabetes, hypertension, , smoking, and the remaining risk is attributed to genetic factors such as mutation of *MTHFR* gene in common C677T (rs1801133) and A1298C (rs1801131) single nucleotide polymorphisms (SNP). This study was conducted on total 100 subject only men included fifty patient with MI at first time were admitted to Cardiac Care Unit (CCU) in Baghdad city, and fifty healthy volunteers, similarly age matched the patient group, with no history of cardiovascular diseases (CVD), diabetes, hypertension, and renal dysfunction. The genomic DNA was extracted from all samples, and used tetra-primer ARMS-PCR method for genotyping two common *MTHFR* gene polymorphisms (C677T and A1298C). The results of this study showed the risk factors that were related with MI patients compared with the control healthy group, and smoking was the higher risk factor in MI patients than other risk factors, it was found that 66% of MI patient were smoker, 30% who infected with diabetes, 18% who have hypertension, 42% who have family history of CVD or MI and 44% who have bad physical activity was significantly increase ($p < 0.01$) than control group. The result of genotype polymorphism (C677T) showed CC wild-type frequency 32(64%), CT heterozygous frequency 16(32%), and TT homozygous frequency 2(4%), respectively in MI patients. The results of polymorphism (A1298C) genotyping recorded AA wild-type frequency 30(60%) in MI patients and 23(46%) in control group, AC heterozygous frequency in 7(14%) MI patients and 17(34%) in control group, and CC homozygous frequency 13(26%) in MI patients and 10(20%) in control group. Smoking represented the higher risk factor of MI, followed by physical activity, family history then diabetes. *MTHFR* gene polymorphisms have relationship with increased the risk to infection with MI, the heterozygous of two polymorphism (C677T and A1298C), and homozygous CC (A1298C) was more frequency in MI patients than control.

Keywords: Myocardial Infarction, Risk Factors, *MTHFR* gene polymorphisms, T-ARMS-PCR.





Farah Farouk Hassan AL-Haially and Rasha Abdull-Hussein Mahood

INTRODUCTION

Myocardial infarction (MI) it is the medical term for an event commonly known as a heart attack, one of the cardiovascular complications is the leading cause of death worldwide (Roffiet *al.*, 2016).MI, occurs as a result of atherosclerotic plaque rupture and emergence of thrombus. Myocardial tissue becomes inflamed and necrotic, it loses contraction and impulse conducting ability with net result of decreased oxygen distribution (Mendis *et al.*, 2011).It is a complex, multifactorial and polygenic disease that involves interaction between genetic predisposition and environmental influences (Dogra *et al.*, 2012). Epidemiological studies reveal a significant environmental contribution to the pathogenesis of MI (Bowron *et al.*, 2005). Well recognized risk factors of CVD such as smoking, hypertension, diabetes, family history, physical activity, age and gender (Myers *et al.*, 1990; Ezzat *et al.*, 2002; Anand *et al.*, 2008; Zethelius *et al.*, 2014; Fox *et al.*, 2015; Steele *et al.*, 2015).

The human *methylene tetra hydro folate reductase (MTHFR)* gene has been localized to chromosome 1p36.3 and is composed of 11 exons (van der Put *et al.*, 1998). There are two common polymorphisms in the *MTHFR* gene as C677T and A1298C (Cristalli *et al.*, 2017). Individual with the 677TT and 677CT genotypes have 30% and 65% of the expected enzyme activity; in turn, in homozygotes of the 1298C allele, the enzyme's activity is decreased to 60% (van der Put *et al.*, 1998). Various association studies have attempted to identify genetic variants that contribute to MI and *MTHFR* gene which has received special attention since it has been implicated in hyperhomocysteinemia that, in turn, has been associated with an increased risk of MI (Slama *et al.*, 2014). A tetra-primer amplification refractory mutation system – PCR (ARMS-PCR) is a technique used for genotype variation from SNPs of interest by running the reaction in a single tube and in one PCR step followed by agarose gel electrophoresis (Ye *et al.*, 2001; Akhrawat *et al.*, 2014; Medrano and de Oliveira, 2014). Tetra-primer amplification refractory mutation system-polymerase chain reaction (T-ARMS-PCR), which was first introduced by Ye *et al.* is the modification of ARMS-PCR which amplifies both wild and mutant alleles, simultaneously is achieved in a single PCR reaction using two outer primers and two allele-specific inner primers (Ye *et al.*, 2001).

MATERIALS AND METHODS

Subject data

This study carried out on 100 subjects only males with age range (20-69) years, 50 patients diagnosed with (MI) at first time with no previous infection. All patients were admitted to Cardiac Care Unit (CCU) of Ibn Al-Nafees Teaching Hospital, Al-Yarmook Teaching Hospital and Ibn Al-Bitar Hospital. Fifty samples of apparently healthy volunteers with no history of cardiovascular disease (CVD), hypertension, diabetes and kidney dysfunction. All samples were collected during the period extended from the last of October (2017) to first of January (2018). Questionnaire was formed for each patients and control group subjects and their descriptive information was comprising: name, age, family history of CVD, smoking, alcohol drinking, coffee intake, physical activity, food system, hypertension, diabetes, kidney dysfunction, weight and height.

Sample collection

Venous blood sample from each patients and healthy control was collected, and transfer the blood sample to EDTA tube with gently mix then stored frozen (-20) until used for molecular study.



**Farah Farouk Hassan AL-Haially and Rasha Abdull-Hussein Mahood****Genomic DNA Isolation**

The genomic DNA was extracted from 200µl aliquots venous blood using a ready-made blood DNA Extraction kit according to the manufacturer instructions (Tonkbio, USA). The horizontal agarose gel electrophoresis was applied to make-sure the presence and integrity of DNA.

Detection of *MTHFR* gene SNPs (C677T and A1298C) by tetra-primer ARMS-PCR method

This method was carried out to genotyping two SNPs of *MTHFR* gene (C677T and A1298C) in a single PCR reaction tube, by using set of four primers (two allele specific primers and common primers) to each SNP. A mismatch at the penultimate or third nucleotide of the 3' terminus was introduced in order to maximize specificity. The sequence of oligonucleotide primers (provided by Alpha DNA company Canada) was designed previously by Lajinet *et al.*, (2012) (Table 3). The total volume of PCR reaction was 20µl containing 100 ng genomic DNA, 5µl of ready-use master-mix (Gold Multiplex PCR Premix, Bioneer company, Korea): *Top* DNA polymerase; dNTPs, reaction buffer with MgCl₂; pyrophosphatase and pyrophosphate; stabilizer and tracking dye. The PCR system (96 wells) Veriti Thermal cycler (Applied Biosystems Company, Germany) was used for the amplification. PCR was commenced with an initial denaturation step at 95°C for 5 min, followed by 40 cycles of denaturation at 95°C for 30 sec, annealing at 52°C for 75 sec, and extension at 72°C for 40 sec. The final extension step was at 72°C for 7 min. The product of PCR reaction was loaded on agarose gel concentrated (2%) stained with ethidium bromide submerged in TBE buffer. After electrophoresis the gel was visualized under UV light by transilluminator and photographed.

Statistical Analysis

The Statistical Analysis System- SAS (2012) program was used to find out the effect of difference factors in study parameters. Chi-square test was used to compare significantly between percentage and Least significant difference – LSD or test was used to significant compare between means in this study.

RESULTS AND DISCUSSION**The Risk Factor for Myocardial Infarction disease in patients and Control**

The table (1) described the risk factors and their prevalence that related with MI patients when compared with control healthy group which does not infected with diabetes and hypertension. The results showed that MI was more prevalent among smokers (66%) than non-smokers, and the smoking was the higher risk factor in MI patients than other risk factors. Fifteen of MI patients (30%) who have had diabetes. Nine of MI patients (18%) who have hypertension. Twenty-one of MI patients (42%) who have family history of CVD or MI was significantly increase ($p < 0.01$) than that of control group (22%). Twenty-two of MI patients who have bad physical activity (44%) was significantly increase ($p < 0.01$) than that of control group (14%). The smoking represent the first risk factor in present study was in accordance with Abdulkaremet *et al.*, (2012) results who reported that smoking was an important risk factor among Libyan male acute myocardial infarction (AMI) patients. Smoking was the second risk factor among male AMI patient (51.2%) (Azab and Elsayed, 2017). A study, conducted by Noeman *et al.*, (2007), showed that smoking was the most prevalent (63.4%) risk factor in young CAD patients.

The results of study applied by Nusier and El-Dwairi, (2007) on Jordan population, found that forty-two percent of the controls were smokers. Eighteen percent of the controls had a family history of IHD, MI 49% were smokers, 48% were diabetics, twenty nine percent of AMI patients had a family history of IHD. Kadhim, (2013) showed in his study that the major risk factor was hypertension (66.4%), followed by smoking (60.7%), and diabetes mellitus (52.1%).



**Farah Farouk Hassan AL-Haially and Rasha Abdull-Hussein Mahood**

Diabetes increases the risk of CVD and mortality by about two folds in men, 30% of patients with an episode of MI had type II Diabetes mellitus (Rafaqat *et al.*, 2016). Azab and Elsayed, (2017) showed in their study that diabetes was the most predominant risk factor among male who have AMI, 70.9% of males were diabetic. Other study, conducted in a rural population of India, cases of AMI were twice as likely to have history of diabetes compared to controls (Patil *et al.*, 2004). Iraqi recent study by Aouda and Hamza, (2017) found that patients who smoked 31(49%) mostly male, the patients who have diabetes 54(86%) and family history of CAD revealed that 28(44%) cases reported that they had family history of CAD and MI. Marković-Boras *et al.*, (2018) found that hypertension noticed in 59 (70%) and it was almost equal among males and females, 43 (71%) and 16 (67%), respectively, smoking habit was noticed in 49 (58%), with a difference between males and females, 39 (63%), and 10 (42%), respectively.

In the study of Mohammed, (2017) who shown that known traditional factors such as male gender, hypertension, diabetes, and smoking were frequently encountered in patients with IHD; there were 21.4% hypertensive patients; 26.8% diabetics, 75% smokers, 48.2% had positive family history of IHD. These findings were similar to other studies after adjustment of age. Ercanet *et al.*, (2008) reported in a case-control study that 28% of IHD patients had hypertension, and 36% had diabetes mellitus. Subjects whose occupation involved either light [multivariable-adjusted odds ratio (OR) 0.78, confidence interval (CI) 0.71–0.86] or moderate (OR 0.89, CI 0.80–0.99) physical activity were at a lower risk of MI, whereas those who did heavy physical labour were not (OR 1.02, CI 0.88–1.19), compared with sedentary subjects, mild exercise (OR 0.87, CI 0.81–0.93) as well as moderate or strenuous exercise (OR 0.76, CI 0.69–0.82) was protective (Held *et al.*, 2011). The effect of physical activity was observed across countries with low, middle, and high income. Subjects who owned both a car and a television (multivariable adjusted OR 1.27, CI 1.05–1.54) were at higher risk of MI compared with those who owned neither. Leisure-time physical activity and mild-to-moderate occupational physical activity, but not heavy physical labour, were associated with a reduced risk, while ownership of a car and TV was associated with an increased risk of MI across all economic regions (Held *et al.*, 2011).

Regular physical activity is associated with a reduced risk of IHD and mortality. Mechanisms are partly through beneficial effects on a number of cardiovascular risk factors, i.e. physical activity reduces blood pressure, improves dyslipidaemia, regulates body weight, improves insulin sensitivity and have a plethora of other beneficial effects (Bull *et al.*, 2004; Sofiet *et al.*, 2008). Physical activity has also been shown to reduce the risk of heart failure developing and one mechanism may be through ischaemic preconditioning (Saevereid *et al.*, 2014).

Tetra primer ARMS-PCR

The current study was applied tetra primer ARMS-PCR method for amplified and genotyped two common *MTHFR* gene polymorphisms (C677T and A1298C). To found the wild and mutant alleles of each polymorphism a set of four primers (two forward and two reverse) were used. The eight primers were used for the amplification of genomic DNA as the template in single PCR reaction tube to each sample. The product of PCR reaction viewed after horizontal gel electrophoresis by UV light (Figure 1). The fragment lengths for the specific amplicons were as follows; 146 bp for the 677T allele, 87 bp for the 677C allele, 281 bp for the 1298A allele, 361 bp for the 1298C allele. For each polymorphism the presence of one specific amplicon indicates homozygosity and two specific amplicons indicates heterozygosity.

The association between *MTHFR* gene polymorphisms and Myocardial Infarction

The results recorded in the table (2) described *MTHFR* gene genotyping of two polymorphism (C677T and A1298C), and their association with MI patients and control group. The result of genotype polymorphism (C677T) showed CC wild-type frequency 32(64%) in MI patients and 42(84%) in control group, CT heterozygous frequency showed significant difference in MI patients 16(32%) compared to control group 8(16%), and TT homozygous frequency 2(4%) in MI patients showed non-significant difference compared with control group 0(0%). The results of polymorphism (A1298C) genotyping recorded AA wild-type frequency 30(60%) in MI patients and 23(46%) in





Farah Farouk Hassan AL-Haially and Rasha Abdull-Hussein Mahood

control group, AC heterozygous frequency in 7(14%) MI patients and 17(34%) in control group, and CC homozygous frequency 13(26%) in MI patients and 10(20%) in control group. The result conducted by Eftychiou *et al.*, (2012) showed no statistically significant differences between patients and controls in *MTHFR* polymorphism (C677T and A1298C), the mutant homozygous 677TT was present in (17.7%) of the patients and in (19.2%) of the controls ($p=0.838$), while mutant homozygous 1298CC was present in (16.1%) of the patients and in (13.5%) of the controls ($p=0.690$).

Another study applied on Egypt population by Hashadet *et al.*, (2016) found that the genotype distribution for *MTHFR* gene was significantly different between AMI patients (CC 55%, CT 34% and TT 11%) and controls (CC 73%, CT 25%, TT 2%) ($p = 0.0083$). Also a recent Iraqi study conducted by Mohammed, (2017) found that, wild *MTHFR* C677T (CC) genotype was present in (50%) patients, heterozygous *MTHFR* C677T (CT) was detected in (35.7%) patients, while homozygous (TT) was detected in (14.3%) patients. Also reported that, homozygosity AA for the *MTHFR* A1298C allele was present in (37.5%) patients. Heterozygous AC state was detected in (44.6%) patients, while homozygous CC state was detected in (17.9%) patients. This mutation was the most common genetic risk factors detected in this study. The result of Al-allawiet *et al.*, (2009), which showed that *MTHFR* C677T heterozygous (CT) and homozygous (TT) states were found in 44% and 8% respectively among 150 healthy blood donors in Duhok (Al-allawiet *et al.*, 2009), and they also found that *MTHFR* C677T (TT) genotype was a significant risk factor for ischemic stroke among Iraqi population. Alizadeh *et al.*, (2016) reported that C677T polymorphism was associated with risk of MI in African, North American, and elderly populations.

Relation between *MTHFR* A1298C and IHD is less studied than C677T; those few studies reported no significant association between the mutant C allele and IHD (Rothenbacher *et al.*, 2002; Kochet *et al.*, 2003). The present study in C677T polymorphism, found the TT genotype was absent in control groups, which is in correlate with the study prepared by Angeline *et al.*, (2007), and it was present in MI patients only, This may be explained by the fact that the occurrence of the 677TT genotype may be deleterious and it might have its impact on fetal viability as suggested by Devi *et al.*, (2004). Some authors have suggested that *MTHFR* C677T and A1298C SNPs with homozygous/heterozygous mutant genotype or combined heterozygous for both the SNPs contribute to CVD (Verhoef *et al.*, 1997; Gemmatiet *et al.*, 1999). Chen *et al.*, (2018), they found among the 123 case-control studies, 93 studies were conducted in CAD patients and 30 in MI patients, no significant association was found between *MTHFR* 1298 polymorphism and IHD risk, the frequencies of the *MTHFR* 677 homozygous (TT) genotype were highest in Hispanic populations (28.90%), followed by East Asian (20.23%), African (12.01%), Caucasian (11.10%), Middle Eastern (10.28%), mixed group (9.78%), and South Asian (3.76%), For pooled analyses in *MTHFR* 1298, the frequencies of the homozygous CC genotype were highest in the mixed group (27.36%), South Asian (16.55%), Caucasian (10.40%), African (6.86%), Middle Eastern (6.4%), and East Asian (3.70%) populations.

REFERENCES

1. Abduelkarem, A.R.; El-Shareif, H.J. and Sharif, S.I. (2012). Evaluation of risk factors in acute myocardial infarction patients admitted to the coronary care unit, Tripoli Medical Centre, Libya. *EMRO Journal Articles (EMHJ)*, 18(4): 332-336.
2. Akhlatwat, S.; Sharma, R.; Maitra, A.; Roy, M. and Tantia, M.S. (2014). Designing, optimization, and validation of tetra primer ARMS PCR protocol for genotyping mutation in caprine Fc genes. *Meta Gene*, 2:439-449.
3. Al-allawi, N.; Jubrael, J.; Baban, N.K. and Gedeon, G.S. (2009). Thrombophilic mutations in blood donors in Duhok-Iraq. *Duhok Medical Journal*, 3(1): 25-32.
4. Alizadeh, S.; Djafarian, K.; Moradi, S. and Shab-Bidar, S. (2016). C667T and A1298C polymorphisms of methylenetetrahydrofolate reductase gene and susceptibility to myocardial infarction: A systematic review and meta-analysis. *International Journal of Cardiology*, 217:99-108.




Farah Farouk Hassan AL-Haially and Rasha Abdull-Hussein Mahood

5. Anand, S.S.; Islam, S.; Rosengren, A.; Franzosi, M.G.; Steyn, K.; Yusufali, A.H.; *et al.* (2008). on behalf of the INTERHEART Investigators, Risk factors for myocardial infarction in women and men: insights from the INTERHEART study. *European Heart Journal*, 29: 932–940.
6. Angeline, T.; Jeyaraj, N. and Tsongalis, G. J. (2007).MTHFR Gene polymorphisms, B-vitamins and hyperhomocystinemia in young and middle-aged acute myocardial infarction patients.*Experimental and Molecular Pathology*, 82 : 227–233.
7. Aouda M. A. and Hamza, A. S. (2017). The Impact Of Smoking And Diabetes On Homocysteine Levels In Patients With Myocardial Infarction..*Journal of Thi-Qar Science*, 6 (2).
8. Azab, A.E. and Elsayed, A.S. (2017).Acute Myocardial Infarction Risk Factors and Correlation of its Markers with Serum Lipids..*Journal of Applied Biotechnology & Bioengineering*, 3(4).
9. Bowron ,A.; Scott, J. and Stansbie, D. (2005). The influence of genetic and environmental factors on plasma homocysteine concentrations in a population at high risk for coronary artery disease..*Annals of Clinical Biochemistry*, 42: 459-462.
10. Bull, F.C.; Armstron ,T.P.; Dixon, T. *et al.* (2004). Physical inactivity. In: Comparative Quantification of Health Risks Global and Regional Burden of Disease Attributable to Selected Major Risk Factors. Geneva: *World Health Organization*, , pp.729–882.
11. Chen, Z.F.; Young, L.; Yu, CH.and Shiao, S.P. (2018). A Meta-Prediction of Methylenetetrahydrofolate-Reductase Polymorphisms and Air Pollution Increased the Risk of Ischemic Heart Diseases Worldwide. *International Journal of Environmental Research and Public Health*, 15(7): 1453.
12. Cristalli, C.P.; Zannini, C.; Comai, G.; Baraldi, O.; Cuna, V.; Cappuccilli, M. *et al.* (2017).Methylenetetrahydrofolatereductase, MTHFR, polymorphisms and prediposition to different multifactorial disorders..*Genes Genomics*, 39:689–699.
13. Devi, R.R.; Govindaiah, V.; Ramakrishnan, G. and Naushad, S.M.(2004). Prevalence of methylene tetrahydrofolatereductase polymorphism in South Indian population..*Current Science* ,89 (3): 440–443.
14. Dogra, R. K.; Das, R.; Ahluwalia, J.; Kumar, R. M. and Talwar, K. K. (2012).Prothrombotic gene polymorphisms and plasma factors in young north Indian survivors of acute myocardial infarction..*Journal of Thrombosis and Thrombolysis*, 34(2), 276–282.
15. Eftychiou, C.; Antoniadou, L.; Makri, L.; Koumas, L.; Costeas, P. A.; Kyriakou, E. *et al.* (2012) .Homocysteine Levels and MTHFR Polymorphisms in Young Patients with Acute Myocardial Infarction: A Case Control Study. *Hellenic Journal of Cardiology*, 53: 189-194.
16. Ercan, B.; Tamer, L .; Sucu, N.; Pekdemir, H .; Çamsar, A. and Atik, U. (2008). Factor V Leiden and Prothromb in G20210A Gene Polymorphisms in Patients with Coronary Artery Disease..*Yonsei Medical Journal*, 49(2):237 – 243.
17. Ezzati, M.; Lopez, A. D.; Rodgers, A.; Vander-Hoorn, S. and Murray, C. J. (2002).Selected major risk factors and global and regional burden of disease. *The Lancet*, 360(9343): 1347–1360.
18. Fox, C.S.; Coady, S.; Sorlie, P.D. , Levy, D.; Meigs, J.B.; D'Agostino, R.B.*et al.* (2004). Trends in cardiovascular complications of diabetes..*JAMA*, 292:2495–2499.
19. Gemmati, D.; Previati, M.; Serino, M.L.; Moratelli, S.; Capitani, S.; Forini, E. *et al.* (1999). Low folate levels and thermolabile methylene tetrahydrofolatereductase as primary determinant of mild hyperhomocystinemia in normal and thromboembolic subjects. *Arteriosclerosis, Thrombosis, and Vascular Biology* , 19:1761–1767.
20. Hashad, I. M.; Abdel Rahman, M. F.; Alenina, N.; Bader, M. and Gad, M. Z. (2016).Investigating the link between MCP-1 A-2518G, RANTES G-403A, CX3CR1 V249I and MTHFR C677T gene polymorphisms and the risk of acute myocardial infarction among Egyptians..*Meta Gene*, 11: 181–188.
21. Held, C.; Iqbal, R.; Lear, S. A.; Rosengren, A.; Islam, S. and Mathew, J. (2012). Physical activity levels, ownership of goods promoting sedentary behaviour and risk of myocardial infarction: results of the INTERHEART study. *European Heart Journal*, 33: 452–466.
22. Kadhim, A. A. (2013). Major Risk Factors For Myocardial Infarction. *American Journal of Political Science*, 13(1).
23. Koch, W.; Ndrepepa, G.; Mehilli, J.; Braun, S.; Burghartz, M.; Lengnick, H.*et al.* (2003). Homocysteine status and polymorphisms of methylenetetrahydrofolatereductase are not associated with restenosis after stenting in coronary arteries. *Arteriosclerosis, Thrombosis, and Vascular Biology* , 23(12):2229-2234.




Farah Farouk Hassan AL-Haially and Rasha Abdull-Hussein Mahood

24. Marković-Boras, M.; Čaušević, A.; Brzić, I.; Mikulić, I.; Vasilj, M. and Jelić-Knezović, N. (2018). A relation of serum homocysteine, uric acid and C-reactive protein level in patients with acute myocardial infarction. *Medicinski Glasnik*, 15 (2):101-108.
25. Medrano, R.F. and de Oliveira, C.A. (2014). Guidelines for the tetra primer ARMS-PCR technique development. *Molecular Biotechnology*, 56: 599-608.
26. Mendis, S.; Thygesen, K.; Kuulasmaa, K.; Giampaoli, S.; Mähönen, M.; NguBlackett, K. and Lisheng, L. (2011). Writing group on behalf of the participating experts of the WHO consultation for revision of WHO definition of myocardial infarction. World health organization definition of myocardial infarction: 2008-09 revision. *Int J Epidemiol* 40:139-46.
27. Mohammed, W. J. (2017). Molecular Assessment of Cardiovascular Genetic Risk Factors among a Sample of Iraqi Patients with Ischemic Heart Diseases. Master thesis. Baghdad University, Baghdad, Iraq.
28. Myers, R.H.; Kiely, D.K.; Cupples, L.A. and Kannel, W.B. (1990). Parental history is an independent risk factor for coronary artery disease: the Framingham study. *American Heart Journal*, 120: 963-969.
29. Nusier, M. K. and El-Dwairi, Q. A. (2007). Effects of Vitamin B12 and Folic Acid on Hyperhomocysteinemia in Patients with Acute Myocardial Infarction. *Journal of Health Science*, 53(1) :16-22.
30. Patil, S.S.; Joshi, R.; Gupta, G.; Reddy, M.V.; Pai, M. and Kalantri, S.P. (2004). Risk factors for acute myocardial infarction in a rural population of central India: a hospital based case control study. *The National Medical Journal of India*, 17(4): 189-194.
31. Rifaqat, M.; Shazma, B.; Muhammad, N.A. (2016). Acute myocardial infarction; frequency of modifiable risk factors. *The Professional Medical Journal*, 23(3): 293-297.
32. Roffi, M.; Patrono, C.; Collet, J.P.; Mueller, C.; Valgimigli, M.; Andreotti, F. *et al.* (2016). 2015 ESC guidelines for the management of acute coronary syndromes in patients presenting without persistent ST-segment elevation: Task Force for the Management of Acute Coronary Syndromes in Patients Presenting Without Persistent ST-Segment Elevation of the European Society of Cardiology (ESC). *European Heart Journal*, 37(3):267-315.
33. Rothenbacher, D.; Fischer, H.G.; Hoffmeister, A.; Hoffmann, M.M.; März, W.G.; Bode, G. *et al.* (2002). Homocysteine and methylenetetrahydrofolate reductase genotype: association with risk of coronary heart disease and relation to inflammatory, hemostatic, and lipid parameters. *Atherosclerosis*, 162 (1): 193-200.
34. Saevereid, H.A.; Schnohr, P. and Prescott, E. (2014). Speed and duration of walking and other leisure time physical activity and the risk of heart failure: a prospective cohort study from the Copenhagen City Heart Study. *PLoS One*, 9: 1-8.
35. Slama, D. B. B.; FekihMrissa, N.; Haggui, A.; Nsiri, B.; Haouala, H. and Gritli, N. (2014). Association of methylenetetrahydrofolate reductase C677T and A1298C polymorphisms with myocardial infarction in Tunisian young patients. *Comparative Clinical Pathology*, 23(5):1633-1638.
36. Sofi, F.; Capalbo, A.; Cesari, F. *et al.* (2008). Physical activity during leisure time and primary prevention of coronary heart disease: an updated meta-analysis of cohort studies. *Eur J Cardiovasc Prev Rehabil*, 15: 247-257.
37. Steele, L.; Lloyd, A.; Fotheringham, J. *et al.* (2015). A retrospective cross-sectional study on the association between tobacco smoking and incidence of ST-segment elevation myocardial infarction and cardiovascular risk factors. *Postgrad Med J*, 91:492-496.
38. van der Put, N.M.; Gabreels, F.; Stevens, E.M.; Smeitink, J.A.; Trijbels, F.J.; Eskes, T.K. *et al.* (1998). A second common mutation in the methylenetetrahydrofolate reductase gene: an additional risk factor for neural-tube defects? *Am J Hum Genet*. 62(5):1044-1051.
39. Verhoef, P.; Kok, F.J.; Kruyssen, D.A.; Schouten, E.G.; Witteman, J.C.; Grobbee, D.E. *et al.* (1997). Plasma total homocysteine, B vitamins, and risk of coronary atherosclerosis. *Arteriosclerosis, Thrombosis, and Vascular Biology*, 17: 989-995.
40. Ye, S.; Dhillon, S.; Ke, X.; Collins, A.R. and Day, I.N. (2001). An Efficient Procedure for Genotyping Single Nucleotide Polymorphisms. *Nucleic Acids Research*, 29: E88-8.
41. Zethelius, B.; Gudbjornsdottir, S.; Eliasson, B.; Eeg-Olofsson, K. and Cederholm, J. (2014). Level of physical activity associated with risk of cardiovascular diseases and mortality in patients with type-2 diabetes: report from the Swedish National Diabetes Register. *Eur J Prev Cardiol*, 21:244-25





Farah Farouk Hassan AL-Haially and Rasha Abdull-Hussein Mahood

Table (1): Risk factors for myocardial infarction disease in patients and control.

Factors		Controls No (%)	MI patients No (%)	P-value
Smoking	Smoker	5 (10%)	33 (66%)	0.0001 **
	Non-Smoker	45 (90%)	17 (34%)	
Diabetes	Yes	--	15 (30%)	0.0001 **
	No	--	35 (70%)	
Hypertension	Yes	--	9 (18%)	0.0001 **
	No	--	41 (82%)	
Family history	Yes	11 (22%)	21 (42%)	0.0001 **
	No	39 (78%)	29 (58%)	
Physical activity	Bad	7 (14%)	22 (44%)	0.0001 **
	Good	43 (86%)	28 (56%)	

** (P<0.01).

Table (2): Distribution of MTHFR gene polymorphisms in MI patients and control.

MTHFR polymorphism	Genotype frequencies		χ ²	P-value
	MI patients N= 50	Control N = 50		
C677T gene				
CC Wild-type	32 (64%)	42 (84%)	7.25 **	0.0089
CT Heterozygous	16 (32%)	8 (16%)	6.74 **	0.0096
TT Homozygous	2 (4%)	0 (0%)	1.05 NS	0.147
A1298C gene				
AA Wild-type	30 (60%)	23 (46%)	5.26 *	0.026
AC Heterozygous	7 (14%)	17 (34%)	7.25 **	0.0089
CC Homozygous	13 (26%)	10 (20%)	2.39 NS	0.072

* (P<0.05), ** (P<0.01), NS: Non-Significant.

Table (3): The primers sequence used to amplified and genotyped of two polymorphisms (C677T and A1298C) of MTHFR gene.

Size	Polymorphisms	Primer Sequence (5'→3')
146 bp	F/ C677T	GAAGGAGAAGGTGTCTGCGGGAAT
	R/ C677T	CCCTCACCTGGATGGGAAAGAT
86 bp	R/ C677T	AGCAAAGCTGCGTGATGATGAAATAGG
	F/ C677T	CCGAAGCAGGGAGCTTTGAGG
281 bp	F/ A1298C	GGCAAAGAACGAAGACTTCAAAGACACATI
	R/ A1298C	GAAGAAGTTTGCATGCTTGTGGTTG
361 bp	R/A1298C	GAGGAGCTGACCAGTGATGC
	F/ A1298C	CAGGCAAGTCACCTGGGAGAGA





Farah Farouk Hassan AL-Haially and Rasha Abdull-Hussein Mahood

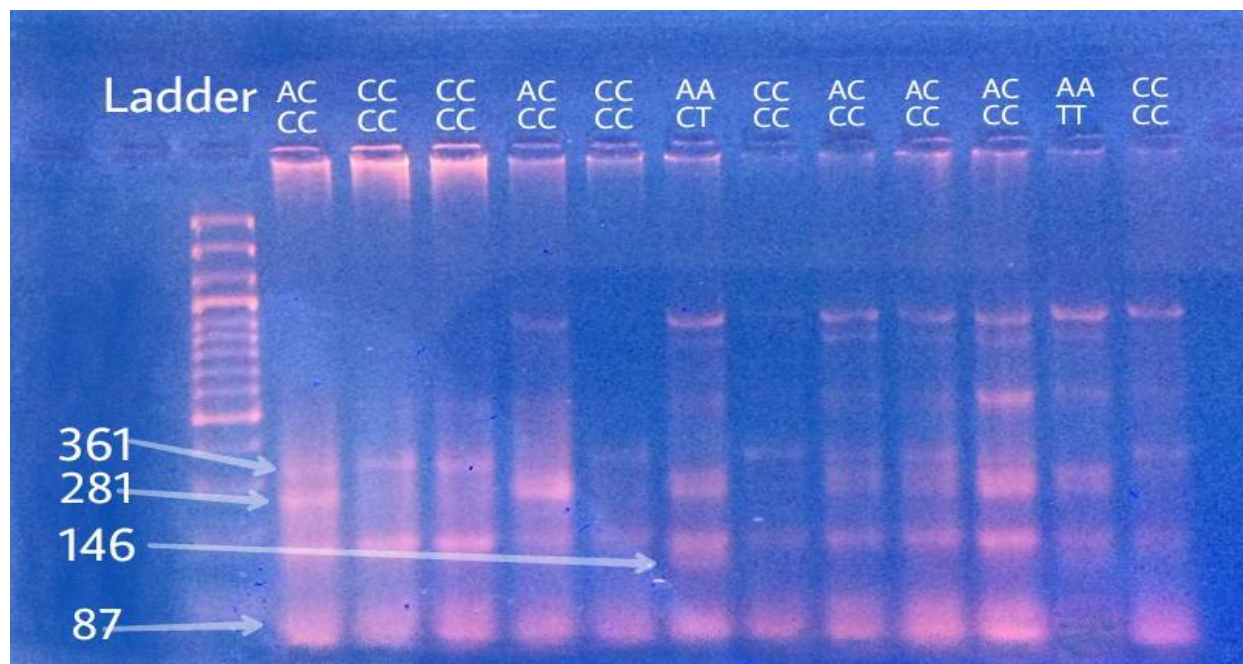


Figure 1 : Agarose gel electrophoresis showing the detection of two *MTHFR* gene polymorphism (C677T and A1298C) by tetra-primer ARMS-PCR.





Association between Glycated Hemoglobin A1C and DRB1*0301 Allele of Human Leukocyte Antigens in Type 1 Diabetes Mellitus of Iraqi Children

Amir F. Al-Tu'ma^{1*}, Zuhair M. Ali² and Hadeef D. Elyassin³

¹Department of Biochemistry, College of Medicine, University of Kerbala, Holy Kerbala, Iraq.

²Department of Medical Microbiology, College of Medicine, University of Kerbala, Holy Kerbala, Iraq.

³Department of Biochemistry, College of Medicine, University of Baghdad, Baghdad, Iraq.

Received: 16 Sep 2018

Revised: 21 Oct 2018

Accepted: 27 Nov 2018

* Address for Correspondence

Amir F. Al-Tu'ma

Department of Biochemistry,

College of Medicine,

University of Kerbala,

Holy Kerbala, Iraq.

Email: amir.altoma@doctor.com



This is an Open Access Journal / article distributed under the terms of the **Creative Commons Attribution License** (CC BY-NC-ND 3.0) which permits unrestricted use, distribution, and reproduction in any medium, provided the original work is properly cited. All rights reserved.

ABSTRACT

Type 1 diabetes mellitus (T1DM) is an autoimmune disease. There are associations between human leukocyte antigen (HLA) complex and T1DM in various populations. The allele of HLA gene polymorphism that affected on T1DM is *DRB1*0301*. Analysis of glycated hemoglobin (HbA1c) in blood provides evidence about an individual's average blood glucose levels during the previous two to three months, which is the predicted half-life of red blood cells (RBCs). To investigate the molecular basis of gene encoding human leukocyte antigens *DRB1*0301* allele and its association with glycated hemoglobin A1c in type 1 diabetes mellitus of children in Kerbala province of Iraq. This is a case-control study, that was conducted in 125 T1DM patients including 66 males (52.8%) and 59 females (47.2%) subjects, and another 100 healthy controls including 57 males (57%) and 43 females (43%), which were randomly recruited from the Kerbala province of Iraq. Genotyping of HLA was performed on genomic DNA extracted by polymerase chain reaction-sequence-specific priming (PCR-SSP). Determination of HbA1c was performed by COBAS HbA1c kit (Roche, Germany). The frequency of *DRB1*0301* in T1DM patients were (66.4%) and apparently healthy control were (18%). Significant results were observed of the association between HbA1c and *DRB1*0301* allele of HLA gene (P value ≤ 0.01). The allele of HLA gene (*DRB1*0301*) was highly affect T1DM pathogenesis. Highly significant correlation between HbA1c with allele HLA gene (*DRB1*0301*).

Keywords: T1DM, HLA gene, *DRB1*0301* allele, HbA1c.





Amir F. Al-Tu'ma et al.

INTRODUCTION

Diabetes mellitus is epidemic in Asia characterized by rapid rates of increasing over short period and onset at a relatively young age and low BMI. The epidemic is heterogeneous, varying according to different ethnic and cultural subgroups, degree of urbanization, and socioeconomic conditions in different Asian populations. In parallel with economic development and nutrition transition, the rates of overweight and obesity have been increasing rapidly in Asian countries. Abdominal or central adiposity, particularly detrimental to type 2 diabetes and other metabolic diseases, is highly prevalent in Asians. The high rates of gestational diabetes, childhood obesity, and over nutrition in later life, may contribute substantially to the increasing diabetes epidemic in Asia (1-3). Diabetes mellitus is characterized by the presence of chronic hyperglycemia accompanied by greater or lesser impairment in the metabolism of carbohydrates, lipids and proteins due to various genetic causes(4). DM were classified into three types(5):

- a. Type 2 diabetes mellitus (T2DM) this form of diabetes, which accounts for 90–95% of those with diabetes, previously referred to as non-insulin-dependent diabetes(5,6), type 2 diabetes or adult onset diabetes. The type 2 diabetes and obesity are associated with insulin resistance (7-9). Most obese individuals, despite being insulin resistant, do not develop hyperglycemia.
- b. Gestational Diabetes Mellitus (GDM) There's any degree of glucose intolerance with onset during pregnancy especially diagnosed in the second or third trimester of pregnancy, which is increasing worldwide(10,11).
- c. Type 1 diabetes mellitus (T1DM) is a chronic autoimmune disease characterized by increased blood glucose levels (hyperglycemia), which are due to the insulin deficiency that occurs as the consequence of the loss of the pancreatic islet β -cells (12,13). T1DM is one of the most common endocrine and metabolic conditions occurring in children and adolescents(14). In the vast majority of patients (70–90%), the loss of β -cells is the consequence T1DM-related autoimmunity (concomitant with the formation of T1DM-associated autoantibodies); these patients have autoimmune T1DM also known as type 1a diabetes mellitus(15,16). Polydipsia, polyphagia, and polyuria, which are the classic trio of symptoms associated with disease onset(17). Complications in T1DM are classified as macrovascular or microvascular(18). Cardiovascular disease is becoming a more common macrovascular complication. The risk for microvascular complications, including retinopathy, nephropathy, and neuropathy, decrease with intensive insulin therapy(19,20).

Human leukocyte antigen (*HLA*) in humans is located on the short arm of chromosome 6 (6p21.3) as shown in figure (1). The classical *HLA* loci are encoded in a region of DNA approximately 4 Mb long, with the class II loci at the centromeric end of the region(21,22). *HLA* genes are coding for cell surface antigen proteins responsible for a major function of the immune system then bind antigenic peptides and present them to T cells, these to detection the foreign or abnormal antigens(23). *HLA* has the most significant effect on susceptibility to T1DM. This region contributes to 50% of the inherited risk for T1DM(24).

The most alleles that affected on T1DM is *DR3 – DQ2 (DRB1*0301, DQA1*0501 and DQB1*0201)*(26), there's another alleles affected on T1DM is *DR4–DQ8 (DRB1*0401, DQA1*030) and DQB1*0302* (23). Analysis of glycated hemoglobin (HbA1c) in blood provides evidence about an individual's average blood glucose levels during the previous two to three months, which is the predicted half-life of red blood cells (RBCs)(27). The HbA1c is now recommended as a standard of care for testing and monitoring diabetes (28). Proteins are frequently glycosylated during various enzymatic reactions when the conditions are physiologically favorable. However, in the case of hemoglobin, the glycosylation occurs by the nonenzymatic reaction between the glucose and the N-terminal end of the β -chain, which forms a Schiff base (29). During the rearrangement, the Schiff base is converted into Amadori products, of which the best known is HbA1c figure (2).

The present study aimed to investigate the molecular basis of gene encoding human leukocyte antigens *DRB1*0301* allele and its association with HbA1c in type 1 diabetes mellitus and in children of Kerbala province : Iraq.



**Amir F. Al-Tu'ma et al.**

MATERIALS AND METHODS

This study was a case-control study. The number of samples 225 subjects divided into 125 of the patients have type 1 diabetes mellitus as cases and 100 apparently healthy as control groups, the sample collected from Al-Hassan Medical Center for Endocrinology in the Al-Hussein Medical City, Kerbala Health Directorate, Iraq. It should be noted that Kerbala is a holy city and one of the biggest cities in Iraq, and thousands of Iraqi and foreign people visit it each day, also the diabetic center is an important center in Iraq and recruits patients from all cities of Iraq, therefore our study population could be representatives for the Iraqi population. The study protocol was approved by the Medical Ethics Committee at College of Medicine/Kerbala University and Kerbala Health Directorate. Written informed consent was obtained from the parents of all the children who participated in this study. All of the authors of this research confirmed that the patients' privacy was protected and the entire process was done with a prior written consent.

Determination of HbA1c was performed by COBAS HbA1c kit (Roche, Germany), the principle is Turbidity: Turbid metric measurements are made with spectrophotometer to determine the concentration of particulate matter in a sample. The amount of light blocked by suspension of particles depends not on concentration but also on size, because particles tend to aggregate and settle out of suspension sample handling becomes critical. Instrument operation is the same as for any spectrophotometer. Blood samples of T1DM patients and the control groups were collected in EDTA anticoagulant tubes. Total genomic DNA was extracted from the peripheral blood cells of study participants using the kit obtained from (Promega USA), the amount of blood that withdrawn from patients and healthy control was 1ml of whole blood. The protocol was carried out as recommended in the instruction of the kit. DNA concentration and purity were measured with the use of BioDrop, UK. Polymerase Chain Reaction-Sequence-Specific Priming (PCR-SSP) technique (Table 1) by a thermocycler was used for *DRB1*0301* allele, as described (31). Sequences of primers are shown in table 2. The PCR products were analyzed by agarose gel electrophoresis using 1.75 gram of agarose gel, and visualized by staining with ethidium bromide (Promega USA).

In each PCR reaction a primer pair was included that amplified the third intron of *HLA* gene. These two primers matched non-allelic sequences and thus functioned as an internal positive amplification control. The forward primer is (5'TGC CAA GTG GAG CAC CCAA3'), and the melting temperature (T_m) is 60°C, complementary to codons 173-179 in the 3' end of exon 3), while the melting temperature (T_m) for reverse primer (5'GCATCT TGC TCT GTG CAG AT3') is 60°C, complementary to codons 193-200 in the 5' end of exon 4) that given rise to a 796 base pair (bp) fragment (32).

The data were expressed as mean \pm SD, student t test and the ANOVA were used for calculating the probability using the PAST version 3.09, 2004 used for calculating probability value (P value), chi-square (χ^2), odd ratio (OR) and confidence interval 95% (CI 95%), where used to express the significance in polymorphisms, biochemical parameters and demographical characteristics between the studied groups. In all statistical analysis the significant p value is (0.05).

RESULTS AND DISCUSSION

The case-control study was conducted on a total of 125 clinically confirmed T1DM subjects and another 100 samples as apparently healthy males as control group. The glycated hemoglobin levels of the study subjects were presented in table 3.

In present study the results indicated in table 4 concerning the correlation between allele of *HLA* gene *DRB1*0301* with T1DM patients as compared with the apparently healthy control.





Amir F. Al-Tu'ma et al.

The *DRB1*0301* allele that correlated with T1DM indicate a significant correlation (P value ≤ 0.01) and ($OR = 9.003$, $95\% CI = 4.79 - 16.92$), these meaning the *DRB1*0301* is higher frequency in T1DM $OR = 9.003$ in $95\% CI (4.79 - 16.92)$ as compared with healthy control. The common occurrence of *DRB1*0301* allele in Asian T1DM patients, and in particular *DR3/DR9*, is due to the high frequency of the *DRB1*0301* allele relative to the predisposing category of another allelesthat are relatively common in the Caucasian populations (33), there was differences in risk of T1DM associated with *HLA-DRB1*0301*(34) and wecould find high risk association between *DR3 (DRB1*0301)* allele with T1DM patients (35).

Amplification *DRB1*0301* allele

The amplification of exon 2 of HLA gene of *DRB1*0301* allele was showed in 151 bp and internal control was showed in 796 bp as in figure 3.

Biochemical parameters compared with allele of HLA gene

Table 3 indicate the relationship between HbA1c (Mean \pm SD) and allele of *HLA* gene(*DRB1*0301*).The results obtained show that the positive resultsof HbA1c with *DRB1*0301* allele was revealed (10.16 ± 2.63) of HbA1c in T1DM patients as compared with the control groups(4.78 ± 1.16) which was a significant result with the observed P value ≤ 0.01 .The negative results were appeared (9.83 ± 2.07) of HbA1c in T1DM patients and (4.59 ± 1.25) of HbA1c in control groups, the results of statistical analysis was appeared significant (P value ≤ 0.01).

Allele of *HLA* gene *DRB1*0301* in T1DM patients ($N = 125$) and control groups ($N = 100$), *DRB1*0301* that shows in table (4) was revealed in positive results ($N = 83$) (66.4%) of T1DM patients and ($N = 42$) (33.6%) of healthy control. The negative results of *DRB1*0301* allele was ($N = 18$) (18%) of T1DM patients and ($N = 82$) (82%) of healthy control. The results of *DRB1*0301* allele was appeared a significant value (P value = ≤ 0.01) and ($OR = 9.003$, $95\% CI = 4.79 - 16.92$).The results of all *HLA* alleles the frequencies had higher in T1DM patients as compared with health control.

In the present study table 4 showed a significant value of HbA1c as compared with allele of *HLA* gene(*DRB1*0301*) these due to elevated of HbA1c in diabetic patients, environmental risk factors are believed to interact with susceptibility genes and thereby contribute to the disease process(36), and the average HbA1c value of (9.3) among the Somali children with T1DM is high in value, poor glycemic control among ethnic minorities has been reported(37).

Demographical characteristics compared with allele HLA gene *DRB1*0301*

The results of present study that showed in table 5, the correlation between demographical characteristics (History of consanguinity and family to T1DM) and allele of *HLA* gene (*DRB1*0301*) in T1DM patients ($No = 125$) and healthy control ($No = 100$).In the current study that correlation between history of consanguinity (cousin relation and no relation) and allele of *HLA* gene (*DRB1*0301*), the positive results of *DRB1*0301* allele in T1DM patients is cousin relation showed (56/125) and no relation (27/125) compared with healthy control homo (15/100) and hetero (3/100), Chi square test used in analysis and appeared non – significant results (P value = 0.18, $\chi^2 = 1.78$).

In negative results of *DRB1*0301* allele in T1DM patients cousin relation (26/125) and no relation (16/125) correlated with healthy control cousin relation (52/100) and no relation (30/100), the statistical analysis used Chi square test was observed non – significant results (P value = 0.87, $\chi^2 = 0.03$).The current study the history of family to T1DM (father and mother) compared with allele of *HLA* gene(*DRB1*0301*) that revealed as following results:

*DRB1*0301* allele was observed the positive results in T1DM patients is father (7/125) and mother (2/125) compared with healthy control father (5/100) and mother (1/100), Chi square test used in statistical analysis and appeared non –





Amir F. Al-Tu'ma et al.

significant results (P value = 0.79, $\chi^2 = 0.07$). In negative results of *DRB1*0301* allele in T1DM patients father (5/125) and mother (9/125) correlated with healthy control father (4/100) and mother (9/100), the statistical analysis used Chi square test was observed non – significant results (P value = 0.79, $\chi^2 = 0.07$). In the present study table (4) the relationship between demographical characteristics with allele of *HLA* gene (*DRB1*0301*), the results were observed as the following:

The history of consanguinity (cousin relation and no relation) was compared with *DRB1*0301*, the current study was shown a non – significant results, the heritability and genetics effect that transfer from parents to offspring and T1DM is autoimmune disease that affected in consanguinity of parents(38) which was disagreed with others (39). Relationship between History of family to T1DM (father and mother) with *DRB1*0301* is non – significant results, T1DM is autoimmune disease that Inherited from parents and other family transfer to the children (33). These results of family history relations with T1DM compared with *DR3 – DQ2* was dis-alignment with other study(40).

CONCLUSION

The allele of *HLA* gene (*DRB1*0301*) was highly affect T1DM pathogenesis. Highly significant correlation between HbA1c levels with allele *HLA* gene (*DRB1*0301*).

ACKNOWLEDGMENTS

Authors wish to thank all the participants' families from whom blood samples were taken. Also we are grateful to thank the staff of the Department of Biochemistry, College of Medicine – University of Kerbala and to the staff of Teaching Hospital for Pediatrics – Kerbala Health Directorate / Iraq for their great help throughout this work.

REFERENCES

1. Heindel JJ, Blumberg B, Cave M, Machtiger R, Mantovani A, Mendez MA, et al. Metabolism disrupting chemicals and metabolic disorders. *Reproductive toxicology*. 2017;68:3-33.
2. Derakhshan SM, Sehrig FZ, Sohrabi N, Shiva S, Baradaran B, Khaniani MS. The Association between Human Leukocyte Antigen Class II DR3–DQ2 Haplotype and Type 1 Diabetes in Children of the East Azerbaijan State of Iran. *Iranian Red Crescent Medical Journal*. 2015;17(9).
3. Al-Tu'ma FJ , Yassin AG and Al-Kayatt TH. Effects of Type-2 Diabetes Mellitus on Serum Leptin, Insulin, Interlukin-8, and Lipid Profile. *Karbala J. Med*. 2011 , 4 (1,2) : 1011-18.
4. Sayin N, Kara N, Pekel G. Ocular complications of diabetes mellitus. *World journal of diabetes*. 2015;6(1):92.
5. Maresch CC, Stute DC, Alves MG, Oliveira PF, de Kretser DM, Linn T. Diabetes-induced hyperglycemia impairs male reproductive function: a systematic review. *Human reproduction update*. 2017;24(1):86-105.
6. Chew B-H, Hassan N-H, Sherina M-S. Determinants of medication adherence among adults with type 2 diabetes mellitus in three Malaysian public health clinics: a cross-sectional study. *Patient preference and adherence*. 2015;9:639.
7. Summers RH, Moore M, Byrne J, Byrne C, Mullee M, Welbourn R, et al. Perceptions of Weight, Diabetes and Willingness to Participate in Randomised Controlled Trials of Bariatric Surgery for Patients With Type 2 Diabetes Mellitus and Body Mass Index 30–39.9 kg/m². *Obesity surgery*. 2015;25(6):1039-46.
8. Anhe FF, Roy D, Pilon G, Dudonné S, Matamoros S, Varin TV, et al. A polyphenol-rich cranberry extract protects from diet-induced obesity, insulin resistance and intestinal inflammation in association with increased Akkermansia spp. population in the gut microbiota of mice. *Gut*. 2015;64(6):872-83.
9. Al-Tu'ma FJ ; Ibraheem AA and Al-Khayatt TH. Adiponectin, Insulin and Interlukin-8 in Type-2 Diabetic Obese Patients in Kerbala Province: Iraq. *Karbala J. Med*. 2011 4 (3,4) : 1047-56.



**Amir F. Al-Tu'ma et al.**

10. Dhindsa S, Ghanim H, Batra M, Kuhadiya ND, Abuaysheh S, Sandhu S, et al. Insulin resistance and inflammation in hypogonadotropic hypogonadism and their reduction after testosterone replacement in men with type 2 diabetes. *Diabetes care*. 2016;39(1):82-91.
11. Donazar-Ezcurra M, López-del Burgo C, Bes-Rastrollo M. Primary prevention of gestational diabetes mellitus through nutritional factors: a systematic review. *BMC pregnancy and childbirth*. 2017;17(1):30. Al-Tu'ma FJ ; Ibraheem AA and Al-Khayatt TH. Adiponectin, Insulin and Interlukin-8 in Type-2 Diabetic Obese Patients in Kerbala Province: Iraq. *Karbala J. Med*. 2011 4 (3,4) : 1047-56.
12. Atkinson MA, Eisenbarth GS, Michels AW. Type 1 diabetes. *The Lancet*. 2014;383(9911):69-82.
13. Zaccardi F, Webb DR, Yates T, Davies MJ. Pathophysiology of type 1 and type 2 diabetes mellitus: a 90-year perspective. *Postgraduate medical journal*. 2015;postgradmedj-2015-133281.
14. Al-Ghamdi AH, Fureeh AA, Alghamdi JA, Alkuraimi W, Alomar F, Alzahrani FA, et al. High prevalence of vitamin D deficiency among Saudi children and adolescents with type 1 diabetes in Albaha Region, Saudi Arabia. *IOSR J Pharm Biol Sci*. 2017;12:5-10.
15. Katsarou A, Gudbjörnsdóttir S, Rawshani A, Dabelea D, Bonifacio E, Anderson BJ, et al. Type 1 diabetes mellitus. *Nature reviews Disease primers*. 2017;3:17016.
16. Kaur N, Bhadada SK, Minz RW, Dayal D, Kochhar R. Interplay between Type 1 Diabetes Mellitus and Celiac Disease: Implications in Treatment. *Digestive Diseases*. 2018;36(6):399-408.
17. Zhang J, Cao J, Nie W, Shen H, Hui X. Red Cell Distribution Width Is an Independent Risk Factor of Patients with Renal Function Damage in Type 1 Diabetes Mellitus of Children in China. *Annals of Clinical & Laboratory Science*. 2018;48(2):236-41.
18. Ganz T, Wainstein J, Gilad S, Limor R, Boaz M, Stern N. Serum asymmetric dimethylarginine and arginine levels predict microvascular and macrovascular complications in type 2 diabetes mellitus. *Diabetes/metabolism research and reviews*. 2017;33(2):e2836.
19. Al-Tu'ma FJ ,Dheyauldeen MH and Al-Saegh RM. Measurement of urinary kidney injury molecule-1 as a predictive biomarker of contrast-induced acute kidney injury *J Contemp Med Sci* 2017 , 3 (9) : 178–181.
20. Ferrannini E, DeFronzo RA. Impact of glucose-lowering drugs on cardiovascular disease in type 2 diabetes. *European heart journal*. 2015;36(34):2288-96.
21. Rand LI, Ferris FL. Long-term Contributions From the Diabetes Control and Complications Trial Cohort. *JAMA ophthalmology*. 2015;133(10):1107-8.
22. Sekar A, Bialas AR, de Rivera H, Davis A, Hammond TR, Kamitaki N, et al. Schizophrenia risk from complex variation of complement component 4. *Nature*. 2016;530(7589):177.
23. Sohrabi N, Khaniani MS, Derakhshan SM. Evaluation of Association Between HLA Class II DR4–DQ8 Haplotype and Type I Diabetes Mellitus in Children of East Azerbaijan State of Iran. *Advanced pharmaceutical bulletin*. 2015;5(1):137.
24. Pociot F, Lernmark Å. Genetic risk factors for type 1 diabetes. *The Lancet*. 2016;387(10035):2331-9.
25. Morran MP, Vonberg A, Khadra A, Pietropaolo M. Immunogenetics of type 1 diabetes mellitus. *Molecular aspects of medicine*. 2015;42:42-60.
26. Derakhshan SM, Sehrig FZ, Sohrabi N, Shiva S, Baradaran B, Khaniani MS. The Association between Human Leukocyte Antigen Class II DR3–DQ2 Haplotype and Type 1 Diabetes in Children of the East Azerbaijan State of Iran. *Iranian Red Crescent Medical Journal*. 2015;17(9).
27. Bergenstal RM, Gal RL, Connor CG, Gubitosi-Klug R, Kruger D, Olson BA, et al. Racial differences in the relationship of glucose concentrations and hemoglobin A1c levels. *Annals of internal medicine*. 2017;167(2):95-102.
28. Vashist SK, Schleicher E, Lupp PB, Luong JH. Glycated haemoglobin (HbA1c) monitoring for diabetes diagnosis, management and therapy. *Point-of-care Glucose Detection for Diabetic Monitoring and Management: CRC Press*; 2017. p. 107-34.
29. Ohtsubo K, Chen MZ, Olefsky JM, Marth JD. Pathway to diabetes through attenuation of pancreatic beta cell glycosylation and glucose transport. *Nature medicine*. 2011;17(9):1067.
30. Sherwani SI, Khan HA, Ekhzaimy A, Masood A, Sakharkar MK. Significance of HbA1c test in diagnosis and prognosis of diabetic patients. *Biomarker insights*. 2016;11:BMJ. S38440.





Amir F. Al-Tu'ma et al.

31.Gurram VC, Kapoor S, Polipalli SK, Karra VK, Ruttala R, Poludasu VM, et al. HLA DQA1-0501 AND DQB1-0201 ALLELES IN RHEUMATOID ARTHRITIS. International Journal of Chemical and Life Sciences. 2017;3(1):1265-8.

32. Olerup O, Zetterquist H. HLA-DR typing by PCR amplification with sequence-specific primers (PCR-SSP) in 2 hours: an alternative to serological DR typing in clinical practice including donor-recipient matching in cadaveric transplantation. HLA. 1992;39(5):225-35.

33.Thomson G, Valdes A, Noble J, Kockum I, Grote M, Najman J, et al. Relative predispositional effects of HLA class II DRB1-DQB1 haplotypes and genotypes on type 1 diabetes: a meta-analysis. Tissue antigens. 2007;70(2):110-27.

34.Howson J, Roy M, Zeitels L, Stevens H, Todd J. HLA class II gene associations in African American Type 1 diabetes reveal a protective HLA-DRB1* 03 haplotype. Diabetic Medicine. 2013;30(6):710-6.

35.El-Amir MI, El-Feky MA, Laine AP, Härkönen T, El-Badawy O, Eltayeb AA, et al. Risk genes and autoantibodies in Egyptian children with type 1 diabetes–low frequency of autoantibodies in carriers of the HLA-DRB1* 04: 05-DQA1* 03-DQB1* 02 risk haplotype. Diabetes/metabolism research and reviews. 2015;31(3):287-94.

36.Kiani J, Hajilooi M, Furst D, Rezaei H, Shahryari-Hesami S, Kowsarifard S, et al. HLA class II susceptibility pattern for type 1 diabetes (T1D) in an Iranian population. International journal of immunogenetics. 2015;42(4):279-86.

37.Oilinki T, Otonkoski T, Ilonen J, Knip M, Miettinen P. Prevalence and characteristics of diabetes among Somali children and adolescents living in Helsinki, Finland. Pediatric diabetes. 2012;13(2):176-80.

38.El-Ella SSA, Shaltout A, Tawfik MA, Deeb M, EL-Lahony DM, Khatab ES, et al. Non HLA genetic markers association with type-1 diabetes mellitus. Egyptian Journal of Medical Human Genetics. 2011;12(1).

39.Lebenthal Y, De Vries L, Phillip M, Lazar L. Familial type 1 diabetes mellitus–gender distribution and age at onset of diabetes distinguish between parent-offspring and sib-pair subgroups. Pediatric diabetes. 2010;11(6):403-11.

40.Wägner AM, Santana Á, Herrández M, Wiebe JC, Nóvoa J, Mauricio D. Predictors of associated autoimmune diseases in families with type 1 diabetes: results from the Type 1 Diabetes Genetics Consortium. Diabetes/metabolism research and reviews. 2011;27(5):493-8.

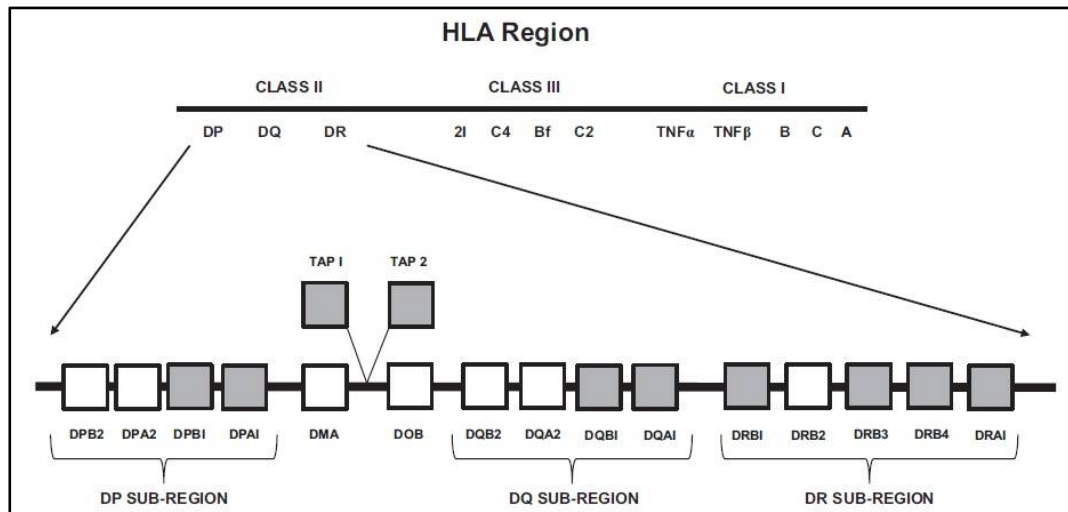


Figure 1: Schematic representation of the human leukocyte antigen (HLA) complex on chromosome 6. The genes that encode a protein product are indicated in grey color; the genes encoding non-functional products, or products that have not been characterized, are indicated in white color (25).





Amir F. Al-Tu'ma et al.

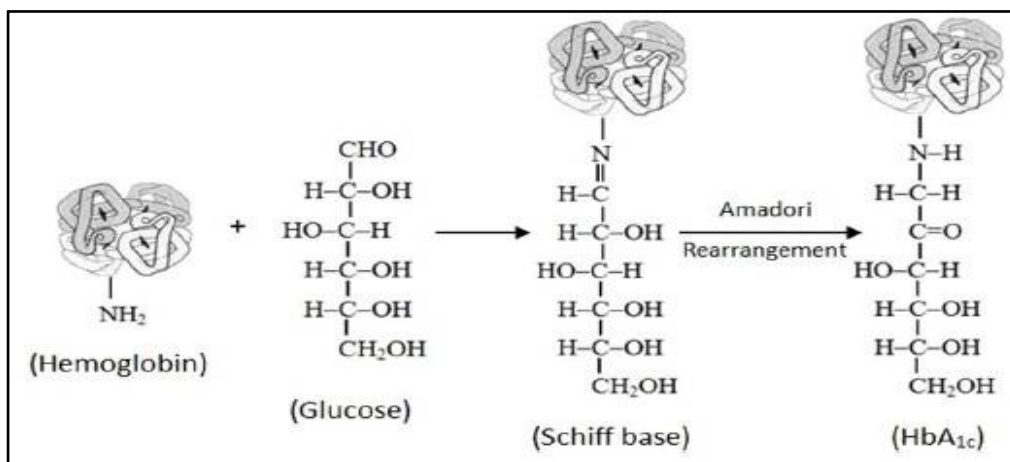


Figure 2: Formation of glycated hemoglobin (HbA1c) from the binding of glucose to hemoglobin (30).

Table 1: The program of PCR-SSP for three HLA genes.

Type of Cycle	Temperature °C	Time	No. of Cycles
Initial denaturation	95	5 min.	1
Denaturation	95	30 sec.	35 X
Annealing	61	35 sec.	
Extension	72	1 min.	
Final extension	72	5 min.	1
Hold	4	10 sec.	
Total time: 2 hours and 10 minutes			

Table 2: Primer sequence for alleles of HLA gene, number of base pair (bp) of primers, number of product size of three genes and the percentage of number of guanine and cytosine (GC)(26).

Alleles of HLA gene	Sequences of Primers	Number of bp in primers	Product Size	%GC
DRB1*0301	F: TACTTCCATAACCAGGAGGAGA	22 bp	151 bp	45%
	R: TGCAGTAGTTGCCACCCG	19 bp		58%

Table 3: The glycated hemoglobin levels compared with allele of HLA gene

Parameter	DRB1*0301		P value	
	T1DM (Mean ± SD) N = 125	Control (Mean ± SD) N = 100		
HbA1c	+	10.16 ± 2.63	4.78 ± 1.16	≤ 0.01
	-	9.83 ± 2.07	4.59 ± 1.25	≤ 0.01

Allele of HLA gene *DQB1*0201* correlated with T1DM patients and control groups





Amir F. Al-Tu'ma et al.

Table 4: HLA genotypes correlated with T1DM patients and control groups

Genes		T1DM No.(%)	Control No. (%)	Odd ratio(OR)	95% CI	P value
DRB1*0301	+	83 (66.4)	18 (18)	9.003	4.79 – 16.92	≤ 0.01
	-	42 (33.6)	82 (82)			

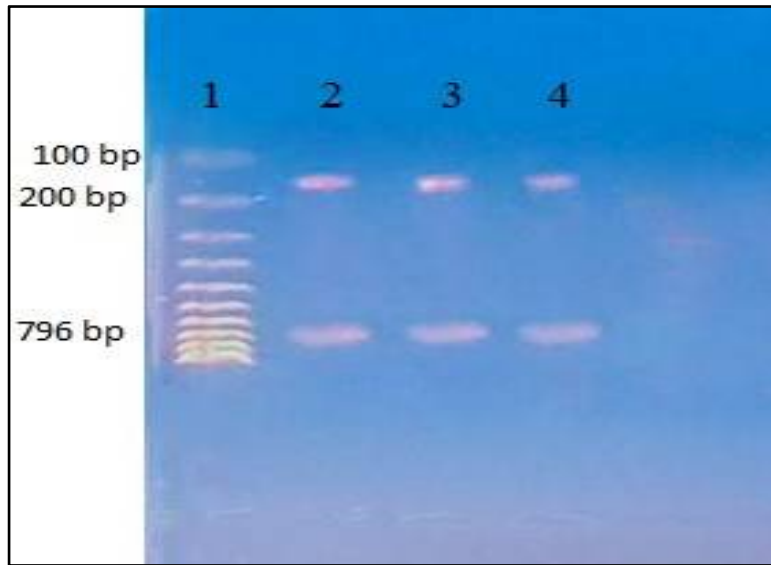


Figure 3: Amplification of *DRB1*0301* allele and internal control primer
 Line 1: Represented DNA marker (100-1000) bp.
 Line 2, 3 and 4: Represented *DRB1*0301* (151bp) and internal control primer (796 bp).

Table 5: Demographical characteristics compared with allele of HLA gene *DRB1*0301*

Demographical characteristics		DRB1*0301 allele		Statistical analysis
		T1DM patients (N=125)	Control (N=100)	
History of consanguinity	Homo +	56	15	$\chi^2 = 1.78$ P value = 0.18
	Hetro +	27	3	
	Homo -	26	52	$\chi^2 = 0.03$ P value = 0.87
	Hetro -	16	30	
History of family to T1DM	Father +	7	5	$\chi^2 = 0.07$ P value = 0.79
	Mother +	2	1	
	Father -	5	4	$\chi^2 = 0.07$ P value = 0.79
	Mother -	9	9	





Distinguishing of Housing Regions in the Original Basic Design of Baghdad City and Random Groups Using High-Resolution Satellite Images

Gheidaa Sabeeh Al-Hassany* and Alaa Hassan Harif

Unit of Remote Sensing, College of Sciences, University of Baghdad, Iraq.

Received: 23 Sep 2018

Revised: 25 Oct 2018

Accepted: 27 Nov 2018

*Address for Correspondence

Gheidaa Sabeeh Al-Hassany

Unit of Remote Sensing,

College of Sciences,

University of Baghdad, Iraq.

Email: gheidaa_sab@yahoo.com, AlaaHarif@Scbaghdad.edu.iq



This is an Open Access Journal / article distributed under the terms of the **Creative Commons Attribution License** (CC BY-NC-ND 3.0) which permits unrestricted use, distribution, and reproduction in any medium, provided the original work is properly cited. All rights reserved.

ABSTRACT

In this paper two scenes (from a satellite image) of housing group from the same region of Baghdad province will be studied to distinguish between them. The first group is combined of the basic design of the province of Baghdad and the second one is a random group. The used data is a high-resolution satellite image. The extracted scenes of a high-resolution satellite image will be analyzed to be able to distinguish between them directly through satellite images. The results will be obtained by using Geographic Information System (GIS Ver. 9.2) program.

Keywords: High-resolution, satellite images, ArcGIS, PCA, Baghdad, classification, change detection, random regions, sprawl.

INTRODUCTION

Suburban Sprawl (SS) means the spread of families away of city centers homes into low densities, in a case called sub-urbanization. As well as the term describes an especially forms of urbanization, it is associate with the public and environmentally effects related with these developments. A wide difference of opinion is appearing for knowing what comprises stretch and the way of quantifying it. Several Interested people measuring it just with the probable numbers of habitation unit / acre, in a location. However the other interested people associated sprawl with decentralizing (sprawl of families with not fully defining centre), uses segregation, and so forth. Urban Sprawl expression is a high politicization, and it is mostly has a negative conceptions. Urban Sprawl is unwanted because it leads to environment degradation, concentrating disconnection, and attacked the existing urban areas on aesthetic grounds. For these rezones and others, few of interested people still supporting Urban Sprawl. [1]



**Gheidaa Sabeeh Al-Hassany and Alaa Hassan Harif****Causes****Urbanization**

The density gradient of industrial cities has tended to have specifically patterns: the city center may be rise while urbanization and population would still concentrated with a rapidly declining in dominion towards the outskirts. [2]. Sprawl land may be were agricultural spaces, which are mostly located surrounding cities; the extension of recent Sprawl has wasted a large areas of the most fertile land, so as desert, forest and other types of land cover[3],

SS Environmentally Effects

SS is related with many of unfavorable environmental consequence. Land loss is one of the main problems related with Sprawl; it is causing habitats loss which leads to reduction in biodiversity. [4] The high birth rates and emigration regions have environmental problems caused by not planned urban growth and emerging megacities [5] Flooding is one of the other problems, which occurs for a rezone of increasing tiled surfaces and parking; increasing temperature of heat islands, which causes a significant risk increasing of mortality in Great ages. Because of the vast area occupied by most of the suburbs compared to urban in the center of the city, moreover wildlife habitats and farms are sizing and replaced by resident. Other disadvantage of SS, when forests removed and replaced with asphalt and concrete surfaces in the suburbs, then a reduction in rainfall absorption into the groundwater aquifers is occur. [6] This reduces the quantity and quality of groundwater. SS mostly leading to water pollution as rainwater mixing with gasoline, heavy metals, and other pollutants coming from parking lots and roads [7].

High Resolution Images Classification

Classification of Very High Resolution (VHR) imagery of urban regions is a very difficult task. For urban in VHR imagery: buildings, roads, and parking lots and other impervious land covers have closely spectrally resolution to be separated using only the spectral information. Therefore, a requirement to further information for separating such regions by the classifier is very necessary. Since 1999, VHR imagery with spatial resolution less than one meter was obtainable, urban classification of such data becomes an emerging field of researches in the remote sensing communities. Because of the less than one meter spatial resolution for VHR images, this type of image data has a high potential in mapping of more details and accurate of urban land cover [8]. To distinguish among impervious covers like buildings, roads, and parking, more information must be incorporated into the classification operation. [9]. A considerable amount of researches, over the past decade, have utilized spatial measures extracted from the scene such as morphology, texture and context in the classification operation of VHR images. [10].

Principal Component (PC) Analysis Concepts in ArcGIS Program

Theoretically, utilizing a raster of two layers, shift and rotate of the axes and transform of the utilize data is achieved as follows:

- A scatter plot for the data is plotted.
- A calculation of an ellipse is done to surround the points in the plotted scatter plot as shown in figure 1.
- The ellipse major axis is specified (the right part of figure 1). It becomes the new x-axis, for the PC1. PC1 portrays the utmost variance. The direction of PC1 represents the Eigenvector and the Eigen value represents its magnitude. The angle between the x-axis and PC1 is the rotation angle that is utilized in the transformation.
- A calculation of orthogonal perpendicular line to PC1 is done. This line represents the PC2 and the new transform axis for the original y-axis as shown in figure 2. It is describe the second most variation not represented by PC1. Utilizing the Eigen Values, the Eigenvectors, and the calculated covariance matrix of the input of the multi-band raster, a creation of a linear formula defining the shift and rotation is done. This formula is used to transform each





Gheidaa Sabeeh Al-Hassany and Alaa Hassan Harif

cell value relative to the new axis [11]. After the extraction of shadows, they would be added to their corresponded features class. Some of buildings have level roofs then shadows of the top covers parts of the lower levels. Shadows may be covering the roads, but mostly of shadows in the scenes are cast by houses, most of the shadow areas belong to streets or upper floor surfaces. It should be noted that this rule may not be necessary responsible to other locations have differences urban structures [12].

Study region

In the present work, urban sprawl of the Hey Ur city (situated in Baghdad province) has been studied and comparison with the basic design in surrounding , to extract the information related to sprawl, area of different feature surfaces and their percentage from total area of the two groups. Statistical classification approaches have been used for the classification of the remotely sensed image obtained from LandSat – 8 ETM+ sensor of a year 2017. Urban sprawl and its characteristics have been derived from the classified satellite images . Figure 3 shows the remotely sensed image obtained from LandSat – 8 ETM+ sensor of a year 2017 after surrounding the regular region and the studied block by yellow color line and random region with its studied block by green color line.

METHODOLOGY

The high resolution image is having a huge correlated data. To apply the classification technique the principal component analysis was applied first to avoid the redundancy in scene data on each block after applying Extraction technique.Extraction technique (A technique in the Tools of ArcGIS program) is applied in the study region taken from a Landsat-8 satellite image (high resolution image) in order to reduce the mix with unstudied features to let the classification process gives a best results as possible when classify and distinguish the features of each selected block,

The following steps were followed to apply the methodology

1. An image from Google Earth program was selected **for the year 2017 of the study region** then anticipates in ArcGIS program.
2. UTM project was chosen for the coordinates because it is a convenient for small spaces (lease than one zone).
3. A geo-reference technique was applied to the image to give their real coordinate.
4. The two blocks random and typical of Hey Ur was extracted from the original LandSat satellite image by using the techniques of spatial analyst tools, as following:
 - A. A zooming command was activate on the interested region (the studied area) to let the recognition of the selection of the boundaries be possible. As shown in Fig.3.
 - B. A polygon shape file is created to detect the boundaries lines points as a vertex of the created polygon to be a mask to extract the studied region. As shown in Fig.4. Then the extracted study region was result as shown in figure5.
5. Applying the PCA technique on each of the extracted raster as shown in figure 6.
6. Perform classification technique (i.e. Using symbology Criterion) on the resulted raster of collection process pixel values (collection between each resulted PCA pixel raster with symmetry real scene pixel) to produce different ranges of classes and then unify them into three classes: 1. Green class to recognition the green areas, 2. Whiteness orange color for the urban areas (mostly houses), 3. White class for wall shadows, to make the account process of each class be possible. As shown in figure 7
7. The account of each class pixels was multiplied by the spatial resolution value for each satellite image to calculate class area for each of them. These calculations are illustrated bellow.

The resolution of pixel= (0.5*0.5) m²

For the typical block:

The total area of block =9450.3m²





Gheidaa Sabeeh Al-Hassany and Alaa Hassan Harif

The count number of block pixels=37816 pixel

For the random block:

The total area of block =4585.32 m²

The count number of block pixels=18341 pixel

RESULTS AND DISCUSSION

The utilized Google earth image data is an image captured by Landsat-8 satellite were chosen to be the studied regions for this paper. Google earth image is a high spatial resolution images (0.5 meter*0.5 meter for the pixel). When the process of PCA was done, a raster of de-correlated data was resulted as shown in figure 6. It contains three bands. After applying a collection process between each resulted PCA pixel raster with symmetry real scene pixel to consecrate the de-correlate among values of image data pixels to avoid mixing among classes or make it at the lowest levels after classification to make the classification process successful and possible. In order to focus on the subject of the study, which is to show the bad consequences of the urban sprawl, the two groups were classified separately to three classes :white is the shadows of buildings to avoid mixing with the green areas, which are highlighted with green, and all other features are painted in light orange. Table- (1) and Table2 represents the calculation of each block typical and random: represents the area of each class and the percentage of classes' areas obtained by implementing the PCA technique and classification method.

CONCLUSION

The percentage of green areas for each group has been documented some of the disadvantages of urban sprawl in terms of it is overcrowded and unhealthy housing due to lack of green areas, internal gardens or sidewalks and through experience in the interpretation of satellite images can distinguish the slums in the outskirts of Baghdad, Most often directly.

REFERENCES

1. James, Paul; Holden, Meg; Lewin, Mary; Neilson, Lyndsay; Oakley, Christine; Truter, Art; Wilmoth, David (2013). "Managing Metropolises by Negotiating Mega-Urban Growth". In Harald Mieg and Klaus Töpfer. Institutional and Social Innovation for Sustainable Urban Development. Routledge
2. Bruegmann, Robert (2006). Sprawl: A Compact History. University of Chicago Press. p. 24. Retrieved November 9, 2013
3. Krannich, Jess M. (2006). "Modern Disaster: Agricultural Land, Urban Growth, and the Need for a Federally Organized Comprehensive Land Use Planning Model". *Cornell Journal of Law and Public Policy*. 16 (1): 57. Retrieved June 8, 2015
4. CZECH, BRIAN; KRAUSMAN, PAUL R.; DEVERS, PATRICK K. (2000). "Economic Associations among Causes of Species Endangerment in the United States". *BioScience*. 50 (7): 593. doi:10.1641/0006-3568 (2000) 050 [0593: EAACOS] 2.0.CO;2. Retrieved September 3, 2015
5. Fenger, J: 1999, "Urban air quality", *Atmospheric Environment*, vol.33, no.29, pp 4877-4900
6. Frumkin, Howard (May–June 2002). *Urban Sprawl and Public Health*. Centers for Disease Control and Prevention. Retrieved on February 7, 2008
7. Gordon, Peter; Richardson, Harry (Summer 2001). "The Sprawl Debate: Let Markets Plan" (PDF). *Publius: The Journal of Federalism*. 31 (3): 131–149. doi:10.1093/oxfordjournals.pubjof.a004901. Retrieved June 11, 2015
8. Pacifici, F.; Chini, M.; Emery, W.J. A neural network approach using multi-scale textural metrics from very high-resolution panchromatic imagery for urban land-use classification. *Remote Sens. Environ.* 2009, 113, 1276–1292.





Gheidaa Sabeeh Al-Hassany and Alaa Hassan Harif

9. Salehi, B.; Zhang, Y.; Zhong, M.; Dey, V. A review of the effectiveness of spatial information used in urban land cover classification of VHR imagery. *Int. J. Geolnf.* 2012, 8, 35–51
10. www.mdpi.com/journal/remotesensing] [*Remote Sens.* 2012, 4, 2256-2276; doi:10.3390/rs4082256, ISSN 2072-4292] [Object-Based Classification of Urban Areas Using VHR Imagery and Height Points Ancillary Data, Bahram Salehi 1,* , Yun Zhang Received: 10 June 2012; in revised form: 20 July 2012 / Accepted: 26 July 2012 / Published: 3 August 2012.
11. Jensen, John R. Introductory Digital Image Processing: A Remote Sensing Perspective. Prentice–Hall. 1986
12. Al-Hassany, Gheidaa Sabeeh; Harif, Alaa Hassan. Classification of Residential Group in the City of Baghdad from Trees and Green areas using High-Resolution Satellite Images. *Indian Journal of Natural Sciences.* Vol. 9 / Issue 50/ October 2018, pp 15011-15020.

Table1: The calculations of the typical blocks are illustrated below

	Number of pixels in region	The area of each class m ²	The percentage from the total area
The green regions	10215	2553.75	27%
The shadow regions	4190	1047.5	11.082%
The other regions	23413	5853.25	61.91%

Table2: The calculations of the random blocks are illustrated below

	Number of pixels in region	The area of each class m ²	The percentage from the total area
The green regions	3410	852.5	18.6%
The shadow regions	4064	1016	22.16%
The other regions	10867	2716.75	59.24%

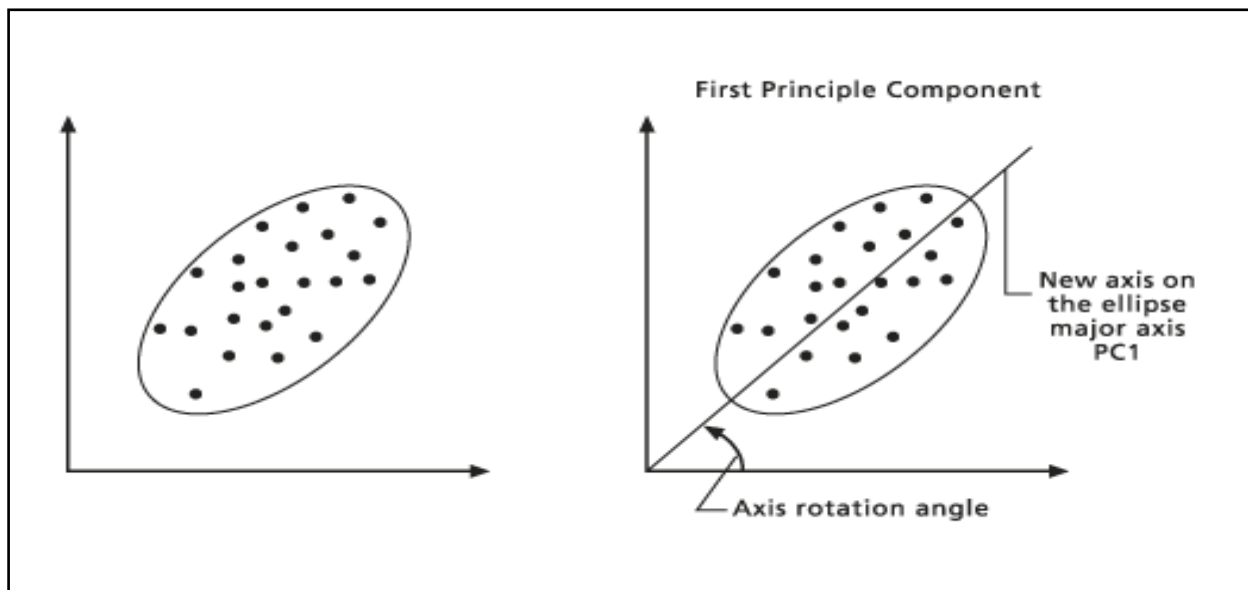


Figure1: An ellipse is calculated to bound the points in the scatter plot





Gheidaa Sabeeh Al-Hassany and Alaa Hassan Harif

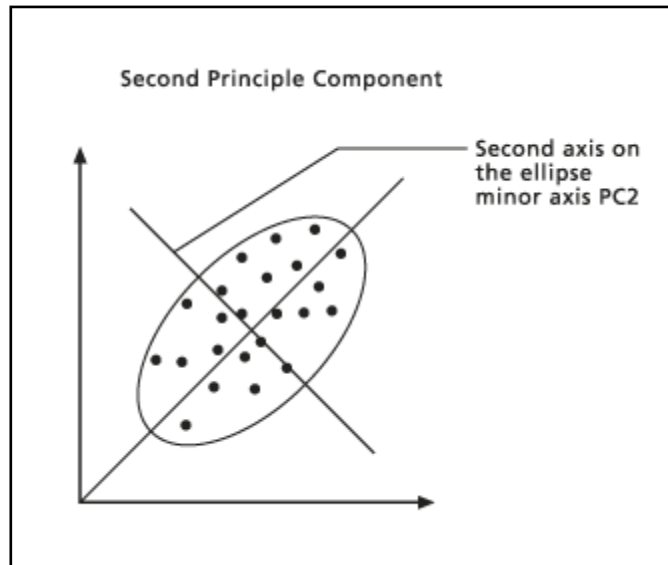


Figure2: An orthogonal perpendicular line to PC1 is calculated. This line is the second principal component (PC2) and the new axis for the original y-axis.



Figure 3 Illustrates the remotely sensed image obtained from LandSat – 8 ETM+ sensor of a year 2017 after surrounding the regular region with its studied block by yellow color lines and random region with its studied bClock by green color lines.





Gheidaa Sabeeh Al-Hassany and Alaa Hassan Harif

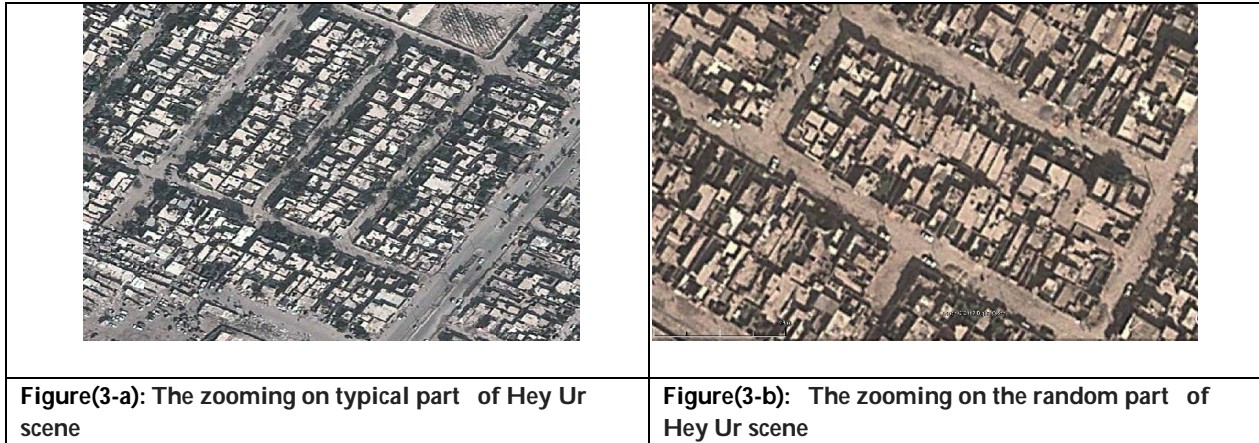


Figure 3: The activation of zooming command on each interested region

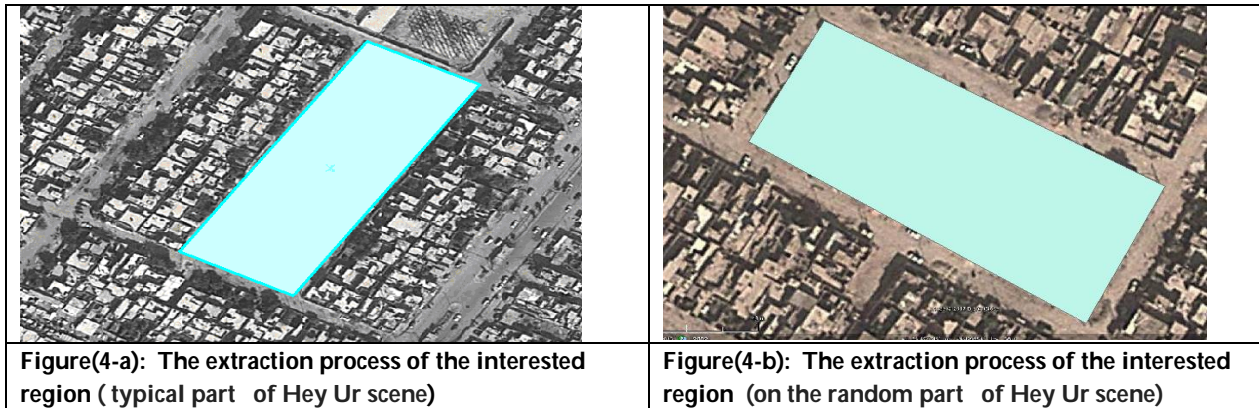


Figure4: The extraction process of the interested region in each scene

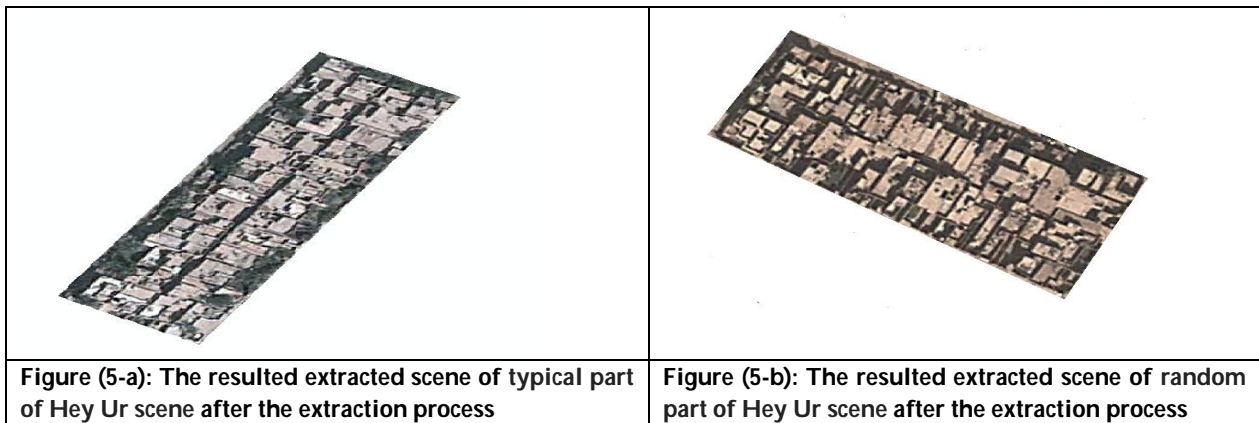


Figure5: The resulted two extracted scenes after the extraction process





Gheidaa Sabeeh Al-Hassany and Alaa Hassan Harif



Figure (6-a): The resulted raster of the PCA application technique on the extracted scene of typical part of Hey Ur scene

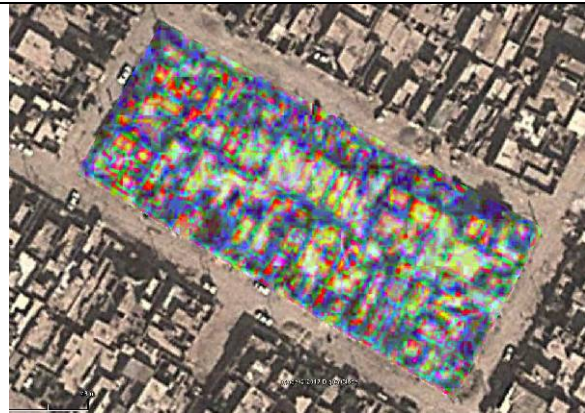


Figure (6-b): The resulted raster of the PCA application technique on the extracted scene of random part of Hey Ur scene

Figure 6. Applying the PCA technique on each of the extracted raster



Figure (7-a): The resulted three classes' raster after the application of classification technique of the resulted raster from the collection process of typical part of Hey Ur scene.

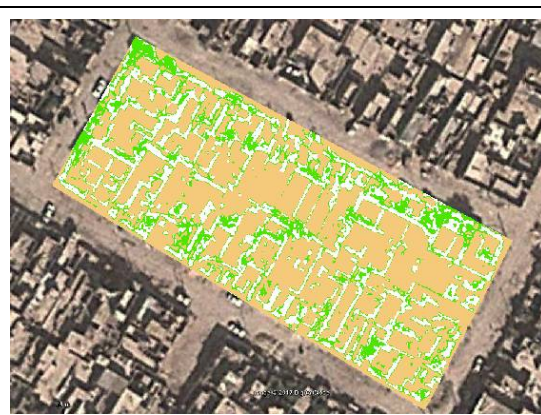


Figure (7-b): The resulted three classes raster after the application of classification technique of the resulted raster from the collection process of random part of Hey Ur scene

Figure 7: The classification application technique of each resulted raster from the collection process





Assessment of Vascular Endothelial Growth Factor-A and Insulin Resistance in Sera of Ischemic Heart Diseases with Type-II Diabetic Patients

Fadhil J. Al-Tu'ma^{1*}, Baqer A. Joda² and Raghad A. Al-Yassiry²

¹Department of Biochemistry, College of Medicine, University of Kerbala, Kerbala, Iraq.

²Department of Chemistry, College of Science, University of Kerbala, Kerbala, Iraq.

Received: 19 Sep 2018

Revised: 23 Oct 2018

Accepted: 27 Nov 2018

* Address for Correspondence

Fadhil J. Al-Tu'ma

Department of Biochemistry,

College of Medicine,

University of Kerbala,

Kerbala, Iraq.

Email: fadhil.jawad@uokerbala.edu.iq



This is an Open Access Journal / article distributed under the terms of the **Creative Commons Attribution License** (CC BY-NC-ND 3.0) which permits unrestricted use, distribution, and reproduction in any medium, provided the original work is properly cited. All rights reserved.

ABSTRACT

Background: Diabetes mellitus and hypertension are reported as the common risk factors for ischemic heart diseases that coexist with each other. Vascular Endothelial Growth Factor is act as promoter for angiogenesis, and induces new blood vessel formation. **Aim:** To investigate the role of vascular endothelial growth factor-A and insulin resistance and various biochemical markers with pathogenesis of ischemic heart diseases in type 2 diabetic patients. **Materials and Methods:** The study was conducted at Al-Zahraa Teaching Hospital, Holy Karbala-Iraq. A total number of 87 patients were used and they have classified into three groups: (40) type 2 diabetic patients without any marco-complications, (27) diabetic patients with ischemic heart disease (unstable angina and myocardial infarction) and (20) case of ischemic heart disease without diabetes mellitus. Fasting blood glucose, lipid profiles, insulin levels, HOMA-IR and vascular endothelial growth factor-A have been determined. **Results:** Serum levels of each of Vascular Endothelial Growth Factor-A, total cholesterol and low density lipoprotein-cholesterol were highly significantly elevated in all patients and a positive correlation between Vascular Endothelial Growth Factor-A and insulin ($p = 0.05$) in non-diabetic ischemic heart disease patients was observed.

Conclusion: Vascular Endothelial Growth Factor-A concentration may be used as an indicator of ischemic heart disease pathogenesis in type 2 diabetes mellitus.

Keywords: Vascular Endothelial, Growth Factor-A, Fasting Blood Glucose, Lipid profile, Insulin, Type 2 Diabetes Mellitus; Ischemic Heart Disease.



**Fadhil J. Al-Tu'ma et al.**

INTRODUCTION

Ischemic heart diseases (IHD) were the major cause of death in the world among men and women. It was responsible for nearly half of all deaths from cardiovascular disease, causing many complications as chronic obstructive pulmonary disease, liver cirrhosis, diabetes mellitus, lung cancer, and liver cancer combined. Ischemic heart disease (IHD) is a complex of clinical symptoms of various pathogenesis caused by insufficient supply of oxygen and nutritional compounds relative to the actual need of the myocardium. However the most risk factors for increased incidence of ischemic heart disease is the presence of predisposing factors like age, gender, atherogenic, diet, smoking, lack of physical activity, obesity, excessive consumption of alcohol, dyslipidemia, hypertensive, hyperglycemia, elevated concentration of homocysteine, fibrinogen and the genetic factor [1]. Diabetes mellitus and hypertension are reported as the common disease that coexist with each other, and constitute the most common risk factors for coronary heart disease (CHD). Diabetes mellitus (DM) is one of a metabolic syndrome diseases that marked by hyperglycemia resulting from defects in insulin action, insulin secretion or both. The long-term of uncontrolled high blood sugar of diabetic patient is caused chronic dysfunction, damage, and failure of various organs, especially the eyes, heart, blood vessels, kidneys, and nerves that enforce tremendous problems on diabetic patient and on the health care system [2].

Vascular endothelial growth factor-A (VEGF-A) is considered to be the main proangiogenic factor as it participates in the formation of new blood vessels. In patients with peripheral arterial disease (PAD), an angiogenic impulse is ischemia of tissues caused by narrowed vessels as a result of atherosclerotic plaque. Through hypoxia inducible factors (e.g. hypoxia inducible factor 1 α (HIF-1 α)), endothelial cells produce VEGF-A which participates in several angiogenesis stages. As clinical and laboratory data indicate, impaired angiogenesis can be observed [3]. Angiogenesis is an important process in the development of diabetes mellitus which is controlled and promoted by Vascular Endothelial Growth Factor-A (VEGF-A) which is a specific mitogen that stimulates new blood vessel formation by aiming growth and differentiation of endothelial cells [4]. Available studies suggest that soluble vascular endothelial growth factor receptors type 1 and type 2 (sVEGFR-1 and sVEGFR-2) may be regarded as angiogenic inhibitors.

In blood of patients with atherosclerosis and diabetic individuals, higher levels of VEGF-A caused by tissue hypoxia can be found. However, the role of different concentrations of sVEGFR-1 and sVEGFR-2 in the process of angiogenesis is still unknown [5]. The aim of this study is to investigate the level and relationship of VEGF-A with various biochemical markers such as (fasting blood glucose, lipid profile, insulin and HOMA-IR) in type 2 diabetic patients with the pathogenesis of ischemic heart disease.

MATERIALS AND METHODS

This cross-sectional study was carried out at Al-Zahraa Teaching Hospital - Al-Hussein Medical City - Kerbala Health Directorate/ Holy Kerbala – Iraq during Nov., 2016 to Dec. 2017. This study was approved by research ethical committee, college of medicine, university of Kerbala which includes (87) patients of diabetes type 2 and ischemic heart disease, all patients were undergoing therapy (Aspirin, Metformin, and Atrovastatin) and were classified in three groups. All the participants were interviewed with a special questionnaire form include age, gender, health habits, diet habits, smoking habit and exercise. The weight and height measurements for each patient were taken to determine their body mass index (BMI). Fasting blood glucose (FBG) and lipid profiles were investigated directly by reflotron technique (Reflotron plus, Roche, Germany), while insulin and VEGF-A levels were determined by using enzyme linked immune sorbent assay ELISA, (biotech instruments, USA). Qualitative data were expressed as number (N) and Percentages (%), while quantitative data were expressed as mean \pm standard deviation (SD). Quantitative variables were analyzed for linearity using the One-Sample Kolmogorov-Smirnov test, while the insulin, insulin resistance index (HOMA-IR) and VEGF-A were not normally distributed. ANOVA (F) test is used to estimate



**Fadhil J. Al-Tu'ma et al.**

significant difference between means of quantitative variables, while the non-normally distributed variables were assessed using Kruskal-Wallis test. Also spearman correlation coefficient test were used to assess the correlation between quantitative variables. A p value of ≤ 0.05 considered statistically significance, and p value of < 0.01 considered highly significant.

RESULTS

The patients of the presented work were classified into 3 groups (T2DM, IHD only, T2DM + IHD) as shown in table (1). The (Mean \pm SD) levels of biochemical marker test in the three patient groups were compared by using ANOVA test and Kruskal-Wallis test as shown in table (2). The results show highly significant ($p < 0.01$) in the levels of FBG, total cholesterol, LDL-C, and VEGF. The correlation data observed indicated that there is no significant correlation between VEGF-A with other parameters among all patient groups, except with insulin ($p = 0.05$) in IHD group, see table (3).

DISCUSSION

The results show highly significant ($p < 0.01$) increase in FBG in diabetic ischemic heart disease patient group (T2DM + IHD) as compared with diabetic patients (T2DM) and ischemic heart disease patients (IHD only). These results were in agreement with previous studies performed by others. High level of FBG is often associated with both qualitative and quantitative abnormalities of lipoproteins which are responsible for increased incidence of vascular complications [6]. Hyperglycemia is also closely associated with cardiovascular diseases (CVD). These are the main cause of death in both types of diabetic patients. Apart from the conventional risk factors such as obesity, dyslipidemia, and arterial hypertension, hyperglycemia are the independent risk factors for the development of (IHD), and for long-term leads to vascular damage through several mechanisms [7]. Total cholesterol and LDL-C are statistically highly significant ($p < 0.01$) in all patients group and the highest value of mean is in the T2DM group compared with the two others patients groups, these findings were in agreement with others [6], while TG and VLDL-C were non-significance in T2DM with IHD group as compared to the others ($P > 0.05$).

Also HDL-C level was low in all patients group but there are no significant differences and disagreement with other study which found that triglyceride and HDL-C are in highly significant, and the highest value of TG was in diabetic patients with CAD than in non-diabetic, while the level of HDL-C was low in patient groups [8]. This may be due to the patients which were undergoing therapy. Chan. *et al.* in (2002) found that the patients who were undergoing statin drugs reduced triglycerides by 14%, but when combined with omega-3 reduced triglycerides by 40% [9]. High level of total cholesterol, is believed to be a major factor in promoting atherosclerosis, which characterized by the deposition of cholesterol and cholesterol from the plasma lipoproteins into the artery wall. It also is recognized that triglycerides are an independent risk factor [10]. Although the highest mean value of insulin level was in diabetic ischemic heart disease patients group, there were no significant differences among all patients groups. This result disagrees with Inchiostro *et al.* study (1994) who found that significant increase in the level of insulin in diabetic ischemic heart disease patients compared with patients of without ischemic heart disease and suggest Insulin resistance is associated with IHD, a higher insulin resistance seems to be related to an earlier clinical onset of IHD [11], whereas, others suggest that the fasting plasma insulin level measurement may provide further information about the risk of IHD.

This discrepancy in the result between the previous studies and this study may due to exhaustion of pancreas that may occur in diabetic obese patients who are in a long duration of diabetes. Where the obesity stimulates the development of insulin resistance, increased insulin secretion, insulin gene expression and β -cell mass. Although these compensatory mechanisms can succeed to maintain glucose homeostasis and avoid the risk of diabetes mellitus, the long-term of increasing insulin secretion (relation to the degree of IR) cause reduction in insulin gene





expression, production, β -cell mass, and increased levels of glucose and free fatty acids [12]. The highest mean value of homeostatic model assessment (HOMA-IR) which is a method used to quantify insulin resistance IR was higher in diabetic ischemic heart disease group; there are no significant differences between all patients group. These data were disagree with previous study by (Gayoso-Diz) that showed a positive association between CHD and HOMA-IR in men, but in women it was not significant [13].

This may due to the effect of genetic or environmental factors (age, obesity and lack of physical activity), where IR increase with increasing the age and BMI [14]. Also, Ce Tan *et.al.* reported that IR and hyperinsulinemia are related to the risk of IHD and IR combine with hyperinsulinemia may be best predictor for ischemic heart disease case, while other study show a significant association between HOMA-IR and coronary artery diseases (CAD), and the patient group of CAD had higher value of HOMA-IR than patient group without CAD [15]. The present study was indicated that vascular endothelial growth factor A (VEGF-A) as a biomarker is highly significant increase in all patients group and the highest mean value was observed in (IHD only) group compared with other groups. While, a Nakajima *et.al.* study (2010), was reported the higher level of VEGF-A in diabetic macro-complication group than diabetic patients without complication [16]. These findings may be indicating that the diabetic patients were undergoing therapy that may affect the level of VEGF-A. Other study done by Alber *et.al.* (2005), shows that the concentrations of VEGF-A in plasma do not correlated with the severity and extent of CAD, and the patients who were taking statin therapy have lower VEGF-A concentrations compared to untreated patients [17]. Nakajima *et.al.* (2004), suggest that the plasma VEGF-A level may be associated with only severe coronary ischemia such as multiple coronary vessel diseases [18]. In general, the main role of VEGF is stimulating vascular endothelial cell division and enhance vascular endothelial cell permeability, thus promoting vascular endothelial cell proliferation, differentiation, and angiogenesis [19]. Elevated of plasma VEGF has been shown in patients with hypertension and diabetes, with levels correlating with measures of endothelial damage and / or dysfunction and overall cardiovascular risk in hypertensive patients, there is increasing evidence suggests a role for VEGF-A in the pathophysiology of cardiovascular disease (CVD) [20].

The present study shows a positive significant correlation between VEGF and insulin in non-diabetic IHD group in agreement with the study done by He *et.al.* (2006), which found that insulin regulates VEGF-A gene expression and vascularization in the myocardium via the response of insulin receptors to the insulin. Insulin resistance inhibits this process and may lead to the decreases in VEGF-A expression and capillary density in the myocardium [20,21]. While there is no correlation between VEGF and insulin show in diabetic patients groups, this may due to insulin resistance. Insulin has been shown can regulate the migration, proliferation, and tubular structure formation of endothelial cells through the response of insulin receptors and activation of intracellular phosphorylation cascades. Furthermore, the insulin that induces pro-angiogenic state is potentiated by vascular growth factors, such as VEGF-A, which produced by endothelial cells [22]. Diabetic ischemic heart disease patients have a reduction in micro vessel density in the myocardium as compared with those with IHD alone or healthy subjects, and this increases morbidity and mortality rates. This partly caused by reduced collateral vessel formation in response to ischemia in the myocardium, whereas ventricular cardiomyocytes are a rich source of VEGF-A production that significantly affects the development and function of cardiac vasculature [23]. The previous study has shown that diabetes and insulin resistance are associated with weaken cardiac VEGF-A expression, which may decrease capillary density in the myocardium in diabetes and insulin resistance states leading to cardiac dysfunction [24].

This study shows no significant correlation between VEGF-A with fasting blood glucose in all patients groups, also show no significant correlation between VEGF-A with lipid profile in all group patients, however, these data were disagree with other study done by Ciastek *et.al.* (2014) that showed a positive correlation between VEGF-A with TG, and suggested that lipid abnormalities occurring in diabetes may be involved in the angiogenesis process [25]. Also a non-significant correlation between VEGF and HOMA-IR was reported in this study in all patients groups which is in agreement with other study showed a non-significant correlation between VEGF-A and HOMA-IR in non-diabetic myocardium infarction ; while, Mokhtar *et.al.* show a significant correlation between VEGF-A and HOMA-IR in T2DM patients group [26]. The decreases in VEGF-A levels directly inhibits angiogenesis may be due to aspirin intake



**Fadhil J. Al-Tu'ma et al.**

of all patients studied [27]. The diabetic patients included in this study were taking metformin drug, which acts as anti-angiogenesis and lowers VEGF-A levels in diabetic patients. Various reports shown that metformin could inhibit VEGF-mediated pathological angiogenesis and also significantly inhibited VEGF-A mRNA expression and endothelial cell migration [28]. All ischemic heart disease patients and almost hyperlipidemic patients were taking statin therapy, which has an action of lowering cholesterol and prevent heart attack. Atrovastatin is one type of statin drugs, which may lower the plasma level of VEGF-A in CAD patients. Sergienko *et.al* (2015), found that IHD patients who were undergoing high-dose of atorvastatin significantly reduce VEGF-A in patients with diabetic CVD [29]. Also, the diabetic patients who may suffer from proteinuria may cause depletion in the level of VEGF-A. Cha *et.al* was found a significant increase in excretion of VEGF-A in urine according to the degree of proteinuria in diabetic patients. A weak significant correlation was found between the amounts of excretion VEGF-A in urine and the levels of serum proteinuria, microalbuminuria, creatinine, and creatinine clearance. These findings related to a fact which suggests that urinary VEGF-A may be used as a sensitive biomarker in the diagnosis of early diabetic nephropathy [30].

CONCLUSION

1. Vascular endothelial growth factor (VEGF) level was highly significant in all patients groups (T2DM, IHD only, T2DM + IHD) and the highest was observed in non-diabetic ischemic heart disease (T2DM + IHD).
2. There is no significant difference in the level of insulin among patients groups; the highest levels of insulin were observed in diabetic ischemic heart disease (T2DM + IHD).
3. Homeostasis model assessment of insulin resistance (HOMA-IR) value was showed a non significant difference among patients groups; the highest value of (HOMA-IR) was in type II diabetic with ischemic heart disease (T2DM + IHD).
4. A positive correlation was found between vascular endothelial growth factor (VEGF-A) and insulin in non-diabetic ischemic heart disease group (IHD only).
5. Vascular Endothelial Growth Factor A (VEGF-A) level may be an indicator of pathogenesis of ischemic heart disease in type 2 diabetes mellitus but its level also affected by drugs.

ACKNOWLEDGMENTS

The authors wish to thank to Dr. Rana M. Hameed, Department of Biochemistry, College of Medicine, University of Kerbala and Dr. Jawad F. Al-Tu'ma, Al-Zahraa Teaching Hospital, Al-Hussein Medical City, Kerbala Health Directorate, Kerbala – Iraq for their excellence technical assistance and supporting this work.

REFERENCES

1. Swanberg M. MHC2TA is associated into differential MHC molecule expression and susceptibility to Rheumatoid arthritis, multiple sclerosis and myocardial infarction. *Nat. Genet* 2005 ; 37(5): 486 - 94.
2. Tchaicaya A, Braun M, Lorenz N, Delagardelle C, and Beissd J. "Social inequality in awareness of cardiovascular risk factors in patients undergoing coronary angiography". *Eur J prev cardiol* 2013; 20 (5) : 872 – 879.
3. Drela E, Kulwas A, Jundził A, et al. VEGF-A and PDGF-BB—angiogenic factors and the stage of diabetic foot syndrome advancement. *Endokrynol Pol.* 2014; 65(4) : 306–312.
4. Craig ME, Hattersley A, and Donaghue KC. Definition epidemiology and classification of diabetes in children and adolescents. *J. Pediatr Diabetes* 2009; 12: 3-12.
5. Botti C, Maione C, Dogliotti G, et al. Circulating cytokines present in the serum of peripheral arterial disease patients induce endothelial dysfunction. *J Biol Regul Homeost Agents.* 2012; 26(1):67–79.





Fadhil J. Al-Tu'ma et al.

6. Ahmed KA, Muniandy S, Ismail IS (2007). Role of Nε-(carboxymethyl) lysine in the development of ischemic heart disease in type 2 diabetes mellitus. *Journal of clinical biochemistry and nutrition*. 41(2): 97-105.
7. Dresslerova I and Vojacek J. Diabetes mellitus and ischemic heart disease. *Vnitr. Lek.* 2010April; 56(4):301-6.
8. Abeid ZK, Al-Tu'ma FJ and Al-Naffi KO. Polymorphism of HFE Gene in Ischemic Heart Diseases and its Relation with Iron Overload. *Ijppr, Human* 2017; 8 (3): 31-41.
9. Chan DC, Watts GF, Mori TA, Barrett PH, Beilin LJ and Redgrave TG. Factorial study of the effects of atorvastatin and fish oil on dyslipidaemia in visceral obesity. *European journal of clinical investigation* 2002; 32(6):429-36.
10. Sreenivas RA, Meera S, Ebenezer W Correlation between glycemic control and lipid profile in type 2 diabetic patients: HbA1c as an indicator of dyslipidemia. *Asian J Pharm Clin Res.* 2014; 7:153-5.
11. Marchetti P, Dotta F, Lauro D, Purrello F. (2008) an overview of pancreatic beta-cell defects in human type 2 diabetes: implications for treatment. *Regulatory peptides.* 7;146 (1) : 4-11.
12. Yabe D, Seino Y, Fukushima M, Seino S. β-cell dysfunction versus insulin resistance in the pathogenesis of type 2 diabetes in East Asians. *Current diabetes reports* 2015; 15(6):1-9.
13. Gayoso-Diz P, Otero-González A, Rodríguez-Alvarez MX, Gude F, García F, De Francisco A, Quintela AG. Insulin resistance (HOMA-IR) cut-off values and the metabolic syndrome in a general adult population: effect of gender and age: EPIRCE cross-sectional study. *BMC endocrine disorders* 2013; 13(1) : 1-10.
14. Tan C, Sasagawa Y, Mori M. The association between insulin resistance, metabolic syndrome, and ischemic heart disease among Rumoi residents. *Journal of General and Family Medicine* 2017; 18(6):360-4.
15. Singh B and Saxena A. Surrogate markers of insulin resistance: A review. *World journal of diabetes* 2010; 15:1(2):36-47.
16. Nakajima K, Tabata S, Yamashita T, Kusuhara M, Arakawa K, Ohmori R, Yonemura A, Higashi K, Ayaori M, Nakamura H and Ohsuzu F. Plasma vascular endothelial growth factor level is elevated in patients with multivessel coronary artery disease. *Clinical cardiology* 2004; 27(5):281-6.
17. Shinohara K, Shinohara T, Mochizuki N, Mochizuki Y, Sawa H, Kohya T, Fujita M, Fujioka Y, Kitabatake A and Nagashima K. Expression of vascular endothelial growth factor in human myocardial infarction. *Heart and vessels* 1996; 11(3):113-22.
18. Nakajima K, Tabata S, Yamashita T, Kusuhara M, Arakawa K, Ohmori R, Yonemura A, Higashi K, Ayaori M, Nakamura H, Ohsuzu F. (2004). Plasma vascular endothelial growth factor level is elevated in patients with multivessel coronary artery disease. *Clinical cardiology.* 27(5):281-6.
19. Yeung SL, San Lam HS and Schooling CM. Vascular Endothelial Growth Factor and Ischemic Heart Disease Risk: A Mendelian Randomization Study. *Journal of the American Heart Association* 2017; 6(8):1-15.
20. He Z, Opland DM, Way KJ, Ueki K, Bodyak N, Kang PM, Izumo S, Kulkarni RN, Wang B, Liao R and Kahn CR. Regulation of vascular endothelial growth factor expression and vascularization in the myocardium by insulin receptor and PI3K/Akt pathways in insulin resistance and ischemia. *Arteriosclerosis, thrombosis, and vascular biology* 2006; 26(4):787-93.
21. Yarom R, Zirkin H, Stämmler G, Rose AG. (1992). Human coronary microvessels in diabetes and ischaemia. Morphometric study of autopsy material. *The Journal of pathology.* 166(3):265-70.
22. Haffner SM, Lehto S, Rönnemaa T, Pyörälä K and Laakso M. Mortality from coronary heart disease in subjects with type 2 diabetes and in nondiabetic subjects with and without prior myocardial infarction. *New England journal of medicine* 1998; 23:339(4):229-34.
23. Chou E, Suzuma I, Way KJ, Opland D, Clermont AC, Naruse K, Suzuma K, Bowling NL, Vlahos CJ, Aiello LP and King GL. Decreased cardiac expression of vascular endothelial growth factor and its receptors in insulin-resistant and diabetic states. *Circulation* 2002; 22;105(3):373-9.
24. Westergren HU, Svedlund S, Momo RA, Blomster JI, Wähländer K, Rehnström E, Greasley PJ, Fritsche-Danielson R, Oscarsson J and Gan LM. Insulin resistance, endothelial function, angiogenic factors and clinical outcome in non-diabetic patients with chest pain without myocardial perfusion defects. *Cardiovascular diabetology* 2016; 15(1):1-12.





Fadhil J. Al-Tu'ma et al.

25. Ciastek BR, Sokup A, Socha MW, Ruperecht Z, Halas L, Goralczyk B, Grażyna Gadomska G and Rosc D. A preliminary evaluation of VEGF-A, VEGFR1 and VEGFR2 in patients with well-controlled type 2 diabetes mellitus. *Journal of Zhejiang University-Science B (Biomedicine & Biotechnology)* 2014; 15(6):575-581
26. Mokhtar A, Attia FA, El-Seid SS, Abd EL Kader MA, Mousa SG, Khalid MM, Mahmoud AK, and Amen AE. Vascular Endothelial Growth Factor Serum Level In Patients With Diabetic Retinopathy. *AAMJ* 2013; 10(4): 90-122.
27. Gerrah R, Fogel M and Gilon D. Aspirin decreases vascular endothelial growth factor release during myocardial ischemia. *International journal of cardiology* 2004; 31;94(1):25-9.
28. Pichandi S, Pasupathi P, Rao YY, Farook J, Ambika A and Ponnusha BS. The role of statin drugs in combating cardiovascular diseases—A review. *Int J Cur Sci Res.* 2011; 30;1(2):47-56.
29. Jaumdally RJ, Goon PK, Varma C, Blann AD and Lip GY. Effects of atorvastatin on circulating CD34+/CD133+/CD45- progenitor cells and indices of angiogenesis (vascular endothelial growth factor and the angiopoietins 1 and 2) in atherosclerotic vascular disease and diabetes mellitus. *Journal of internal medicine* 2010; 267(4):385-93.
30. Kim NH, Kim KB, Kim DL, Kim SG, Choi KM, Baik SH, Choi DS, Kang YS, Han SY, Han KH and Ji YH. Plasma and urinary vascular endothelial growth factor and diabetic nephropathy in type 2 diabetes mellitus. *Diabetic Medicine* 2004; 1;21(6):545-51.

Table (1): Classification of patients groups

Type of groups	Frequency	Percent
*T2DM	40	46.0 %
*IHD	20	23.0%
T2DM + IHD	27	31.0%
Total	87	100.0%

*T2DM : Type II diabetes mellitus ; *IHD : Ischemic heart diseases

Table (2): Data of various biochemical markers of all patient groups T2DM (N = 40); IHD (N = 20); T2DM + IHD (N = 27).

Biomarkers	Group	No.	Mean ± SD	P value*
*FBG mg/dl	*T2DM	40	218.83 ± 88.13	< 0.001
	*IHD only	20	132.35 ± 32.43	
	*T2DM + IHD	27	241.97 ± 108.66	
Total Cholesterol mg/dl	T2DM	40	199.28 ± 45.67	< 0.001
	IHD only	20	147.80 ± 40.98	
	T2DM + IHD	27	176.19 ± 44.34	
*TG mg/dl	T2DM	40	188.12 ± 97.74	0.436
	IHD only	20	183.36 ± 126.41	
	T2DM + IHD	27	218.84 ± 109.66	
*HDL-C , mg/dl	T2DM	40	32.85 ± 9.94	0.187
	IHD only	20	38.88 ± 15.43	
	T2DM + IHD	27	37.20 ± 15.25	
*LDL-C , mg/dl	T2DM	40	129.16 ± 46.91	< 0.001
	IHD only	20	76.36 ± 33.39	
	T2DM + IHD	27	95.77 ± 42.86	





Fadhil J. Al-Tu'ma et al.

*VLDL-C, mg/dl	T2DM	40	37.61 ± 19.55	0.330
	IHD only	20	36.68 ± 25.28	
	T2DM + IHD	27	44.98 ± 23.59	
Insulin	T2DM	40	7.76 ± 17.24	0.166
	IHD only	20	13.76 ± 22.39	
	T2DM + IHD	27	17.30 ± 34.00	
*VEGF-A, pg/ml	T2DM	40	34.68 ± 93.04	< 0.001
	IHD only	20	49.76 ± 96.06	
	T2DM + IHD	27	33.86 ± 27.50	
*HOMA-IR	T2DM	40	4.22± 9.07	0.189
	IHD only	20	5.16± 8.96	
	T2DM + IHD	27	12.57 ± 35.95	

*FBG: Fasting blood glucose; *HDL-C: High density lipoprotein-cholesterol; *HOMA-IR: Homeostatic model assessment-insulin resistance; *IHD: Ischemic heart disease; *LDL-C: Low density lipoprotein-cholesterol; *T2DM: Type 2 diabetes mellitus; *T2DM + IHD: Diabetic ischemic heart disease; *TG: Triglyceride; *VLDL-C: Very Low density lipoprotein-cholesterol; *VEGF-A: Vascular endothelial growth factor.

Table (3): The correlation between VEGF-A with studies parameters among all patient groups.

Patient group	T2DM patients		T2DM + IHD patients		IHD only	
	Correlation Coefficient	Sig. (2-tailed)	Correlation Coefficient	Sig. (2-tailed)	Correlation Coefficient	Sig. (2-tailed)
Insulin	0.283	0.077	0.123	0.540	0.439	0.053*
*FBS	-0.055	0.737	0.159	0.429	-0.064	0.790
*TC	-0.227	0.159	0.027	0.895	0.200	0.399
*TG	0.253	0.116	0.224	0.260	-0.050	0.835
*HDL-C	-0.303	0.058	-0.302	0.126	-0.160	0.502
*LDL-C	-0.258	0.109	0.193	0.335	0.023	0.922
*VLDL-C	0.249	0.121	0.185	0.356	-0.050	0.835
*HOMA-IR	0.243	0.131	0.427	0.060	0.135	0.501

*P = 0.05 ; *FBG: Fasting blood glucose ; *HDL-C: High density lipoprotein-cholesterol; *HOMA-IR: Homeostatic model assessment-insulin resistance; *LDL-C: Low density lipoprotein-cholesterol ; *VLDL-C: Very Low density lipoprotein-cholesterol ; *VEGF-A: Vascular endothelial growth factor.





Leishmanicidal Activity of Methotrexate against *Leishmania tropica* Promastigotes

Buraq Abdulameer fingan* and Hayder Zuhair Ali

Department of Biology, College of Science, University of Baghdad, Baghdad, Iraq.

Received: 18 Sep 2018

Revised: 20 Oct 2018

Accepted: 27 Nov 2018

*Address for Correspondence

Buraq Abdulameer fingan

Department of Biology,

College of Science,

University of Baghdad,

Baghdad, Iraq.

E-mail: buraq40@yahoo.com



This is an Open Access Journal / article distributed under the terms of the **Creative Commons Attribution License** (CC BY-NC-ND 3.0) which permits unrestricted use, distribution, and reproduction in any medium, provided the original work is properly cited. All rights reserved.

ABSTRACT

Leishmaniasis is one of the neglected parasitic diseases, which belongs to the family *Trypanosomatidae*. Cutaneous leishmaniasis is endemic in Iraq and the available drugs are of side effect or resistant by the parasite. In this study, cytotoxicity of methotrexate was investigated on the promastigotes proliferation of the Iraqi strain of *L. tropica*. The results showed a significant ($p \geq 0.05$) difference in growth of treated groups at all concentration (1000, 500, 250, 125.5, 62.5, 31.25, 15.6) μM , after 24 and 48 hours of follow up, while after 72 hours, significant difference was observed at concentration (1000, 125, 62.5) μM . The IC_{50} measured after 24 and 48 hours and it was 40.366 and 44.452 μM , respectively. The present study showed the cytotoxic effect of methotrexate on the proliferation of two stages of the cutaneous form of *Leishmania*.

Keywords: Leishmaniasis, *Trypanosomatidae*, cytotoxicity, methotrexate.

INTRODUCTION

Leishmania parasites are obligate intracellular protozoa that cause Leishmaniasis, a neglected tropical disease responsible for extensive morbidity and mortality in the developing world. (1). Leishmaniasis is considered the third-most common cause of morbidity after malaria and schistosomiasis, especially children under 15 years of age suffering most of the disease burden (2). It is classified into three primary clinical forms: cutaneous, muco-cutaneous, and visceral leishmaniasis (VL); the latter being the most severe and potentially fatal form (3). Leishmaniasis disease is divided into: Old World Leishmaniasis found in Africa, Asia, the Middle East, the Mediterranean, and India (produces cutaneous or visceral) and New World Leishmaniasis found in Central and South America (produces cutaneous, mucocutaneous, and visceral) (4, 5). *Leishmania* is transmitted through bite sandflies of the genus *Lutzomyia* in the new world and *Phlebotomus* in the Old World (6). The parasite usually reside within the macrophage of the



**Buraq Abdulameer fingan and Hayder Zuhair Ali**

vertebrate host; to enter the macrophage, *Leishmania* utilizes a variety of cellular receptors to mediate endocytosis. Once inside the macrophage, *Leishmania* is protected from phagolysosome degradation by a variety of adaptations to inhibit cellular defense mechanisms (7). No vaccines are presently available against *Leishmania* infection and treatments rely primarily on chemotherapy (2). The chemotherapeutic arsenal is limited and includes pentavalent antimonial sodium stibogluconate (Sb) or (Pentostam) as first-line drugs exhibited some problems such as prolonged systemic therapy, less effectivity against various forms and high toxicity and the second-line drugs amphotericin B and pentamidine have limitations for use because of, prolonged length of therapy, high cost and adverse reactions. Current research is looking for new treatments including methotrexate. *Leishmania* is sensitive to MTX, the drug is not used clinically to treat leishmaniasis (8-10). Methotrexate, folate anti-metabolite used since more than 40 years as a potent anticancer agent in cases of leukemia, sarcoma and rheumatic disorders, it was less toxic than the then-current treatments (11, 12). MTX has been found toxic on some parasites, such as malaria spp. and thus, more investigation are currently on process for screening of this drug on other parasites, such as *Leishmania* (13). In this study, different concentrations of MTX were screened on the procyclic forms of *Leishmania tropica* and follow-up was made for up to 72 hours.

MATERIAL AND METHODS

Parasite culture

Leishmania tropica isolate was kindly provided by the department of Biology, College of Science, University of Baghdad. The isolate were previously diagnosed as *L. tropica* by PCR (14). Parasite culture was routinely maintained *in vitro* in cell-culture media (M199) and incubated at 26°C with continuous passages.

Methotrexate concentrations

Methotrexate was purchased from Sigma/USA and was dissolved according to the manufacturers'. The following concentrations (15.6, 31.25, 62.5, 125, 250, 500, 1000) μM of were diluted and investigated for cytotoxicity screening against *L. tropica* promastigotes in 96 micro-plate of 96 flat bottom wells. follow up was made for 24, 48 and 72 hours. Control was made by following the same procedure above but pentostam was added instead of MTX. Triplicates were made for each concentration.

Colorimetric assay

Alamar Blue (Resazurin) was added to wells in a ratio of 1:10 and incubated for 4 hours at 26°C prior reading the plates by ELISA reader (Avusturya®) at 570/600 nm wavelength (15).

Statistical analysis

The t test was used to determine the significance of methotrexate effect and IC50 was calculated as previously described by (16).

RESULTS AND DISCUSSION

Procyclic insect stage promastigotes of *L. tropica* was treated with different concentrations of methotrexate to detect the cytotoxicity of this drug on the parasite viability. Methotrexate is anticancer drug, antimetabolite and antifolate drug, it has been deemed to be less toxic, high potent effect against *Malaria*, *Echinococcus* spp. and *Leishmania* (17, 18). The use of promastigote form is of limited value; because the parasite exists naturally in the vertebrate host as amastigote intracellular form (Chang and Fish, 1983; Molyneaux and Killick-Kendrik, 1987). The first study of



**Buraq Abdulameer fingan and Hayder Zuhair Ali**

investigating the leishmanicidal activity of MTX against *L.tropica* was by (13). The results showed significant ($p \geq 0.05$) difference in growth of treated groups at all concentration after 24, 48 hrs., while at 72 hrs. Significant difference was observed at concentration (1000, 125, 62.5) μM . The mean of cell viability measured at the highest concentration of 1000 μM was (27.65, 38.27, 56.73) % after 24, 48 and 72 hours, respectively. Furthermore, the mean of cell viability measured at the lowest concentration of 15.6 μM was (83.05, 55.20, 155.30) % after 24, 48 and 72 hours respectively, Figures (1, 2 and 3). According to the cytotoxicity and cell viability results, the IC_{50} was calculated after 24 and 48 hours of follow up and demonstrated a time-dependent inhibition of the parasite growth to 50 % and it was 40.366 μM and 44.452 μM , respectively.

MTX (Dihydrofolate reductase inhibitors) established drugs with novel compounds, have been tested against *Leishmania* species in culture as amastigotes or promastigotes (19). The folate derivatives folic acid and folinic acid decrease the *in vitro* and *in vivo* activities of antifolate drugs in *Plasmodium falciparum* (Nduati, et al. 2008). A Previous study indicated the MTX (anticancer) is a potent inhibitor against *P. falciparum*, with $\text{IC}_{50} < 50$ nM, in comparison to other drugs, IC_{50} value to new world leishmaniasis of the reference drugs Amphotericin B (nM), Miltefosine (μM) and Pentamidine (μM) against *L. braziliensis* (61, 17.5, 1.23), *L. Mexicana* (57.5, 27.5, 2.61) and *L. amazonensis* (56, 12.25, 1.32) respectively (20). MTX has many advantages such as its half-life, which at low doses is 3-10 h, which is approximately shorter than those of available anti-leishmanial drugs, therefore, resistance to this drug is less likely to develop. MTX is taken by oral, intravenous and intramuscular, which is another advantage over many currently anti-leishmanial drugs. The major concern in the use of MTX as treatment of leishmaniasis is its side effects because side effects in long-term and high-dose of MTX use are numerous. However, side effects of MTX in short-term treatment, even at relatively high doses are few and rare (18).

Mahmoudvand et al. (2017) indicated the IC_{50} values of Sb(V) for sensitive and Sb(V) resistant strains were 52.2 and 170 $\mu\text{g/ml}$, respectively. Whereas the IC_{50} values of MTX alone for sensitive and Sb (V) resistant strains were 22.2 and 51.4 $\mu\text{g/ml}$, respectively. These values are significantly ($P < 0.05$) higher than the measured IC_{50} values for various concentrations of MTX along with Sb(V) against sensitive and Sb(V) resistant strains of *L. tropica* (16.1 and 39.8 $\mu\text{g/ml}$, respectively), indicating less effectivity of Sb(V) or MTX alone as compared with combination of MTX+ Sb(V) on promastigotes of both strains of *L. tropica*. On the other hand, the IC_{50} values to *L. tropica* of the reference drugs Amphotericin B, Miltefosine and Pentamidine was 46.5 nM, 18 μM , 1.04 μM respectively and *L. major* 36 nM, 11.5 μM , 2.83 μM respectively (13, 20).

The traditional therapy of cutaneous leishmaniasis is usually carried out by the glucantime drug but it is known for its toxicity and leading to broad side effects (21). Miltefosine and Paromomycin are two drugs that have been introduced in the last decade for the therapy of leishmaniasis disease (22). While the IC_{50} to relative drug such as miltefosine for amastigotes *L. donovani* was 52.0 μM . Methotrexate is a potent inhibitor of the enzyme dihydrofolate reductase and causes a depletion of the cellular tetrahydrofolate pools. Despite the insensitivity of *L. mexicana* promastigotes to methotrexate, the dihydrofolate reductase from this organism was inhibited 50% by MTX at a concentration of only 2×10^{-9} M (19). Tetrahydrofolates are necessary for both purine and thymidylate nucleotide biosynthesis in eukaryotic and mammalian cells (12). Another study by (23) indicated the IC_{50} values of *L. donovani* was measurable after 24, 48 and 72 hours and it was 174.238, 52.283 and 109.175 μM , respectively, and the results showed a significant ($p \geq 0.05$) difference in growth of treated groups at high concentrations (1000, 500, 250, 125.5) μM after 24, 48 hrs., while after 72 hours, significant difference was observed at all concentration. However, promastigote of cutaneous leishmaniasis was found to be resistant to some classical drugs such as pentavalent antimony and pentamidine (13)





Buraq Abdulameer fingan and Hayder Zuhair Ali

CONCLUSION

Methotrexate inhibited the proliferation of the Iraqi strain of *L. tropica* promastigotes and it is recommended to study the efficacy of this drug in animal model.

ACKNOWLEDGMENTS

Great thanks to the Dept. of Biology, College of Science, University of Baghdad for giving the opportunity to work in Parasitology lab.

REFERENCES

1. Carlsen ED. Neutrophil interactions with Leishmania amastigotes: implications for chronic leishmaniasis 2018.
2. Savoia D. Recent updates and perspectives on leishmaniasis. The Journal of Infection in Developing Countries. 2015;9(06):588-96.
3. Trigkidis K, Geladari E, Kokkinakis E, Vallianou N. Visceral Leishmaniasis in a patient with rheumatoid arthritis undergoing treatment with methotrexate: Case report and review of the literature. European journal of rheumatology. 2017;4(2):139.
4. AlSamarai AM, AlObaidi HS. Cutaneous leishmaniasis in Iraq. The Journal of Infection in Developing Countries. 2009;3(02):123-9.
5. David JR. The successful use of radiofrequency-induced heat therapy for cutaneous leishmaniasis: a review. Parasitology. 2018:1-10.
6. Stoops CA, Heintshcel B, El-Hossary S, Kaldas RM, Obenauer PJ, Farooq M, et al. Sand fly surveillance and control on Camp Ramadi, Iraq, as part of a leishmaniasis control program. Journal of Vector Ecology. 2013;38(2):411-4.
7. Ali HZ. Cytotoxicity of Miltefosine against Leishmania major Promastigotes. Advances in BioResearch. 2012;3(4).
8. Kóczán G, Ghose AC, Mookerjee A, Hudecz F. Methotrexate conjugate with branched polypeptide influences Leishmania donovani infection in vitro and in experimental animals. Bioconjugate chemistry. 2002;13(3):518-24.
9. Ouellette M, Drummelsmith J, El Fadili A, Kündig C, Richard D, Roy G. Pterin transport and metabolism in Leishmania and related trypanosomatid parasites. International journal for parasitology. 2002;32(4):385-98.
10. Noor SM, Bhatti MZ, Majid Paracha M, Ullah GU. EFFICACY OF COMBINED INTRALESIONAL MEGLUMINE ANTIMONIATE AND CRYOTHERAPY VERSUS CRYOTHERAPY ALONE FOR THE TREATMENT OF CUTANEOUS LEISHMANIASIS. Journal of Postgraduate Medical Institute (Peshawar-Pakistan). 2018;32(1).
11. Sneader W. Drug discovery: a history: John Wiley & Sons; 2005.
12. Díaz E, Köhidai L, Ríos A, Vanegas O, Silva A, Szabó R, et al. Leishmania braziliensis: Cytotoxic, cytostatic and chemotactic effects of poly-lysine-methotrexate-conjugates. Experimental parasitology. 2013;135(1):134-41.
13. Mahmoudvand H, Sharifi I, Fasihi Harandi M, Shokohi M, Shakibaie M, Rezaei Rabani T, et al. Anti-leishmania effects of methotrexate (MTX) alone and in combination with meglumine antimoniate (MA) against Iranian isolate of sensitive and MA-resistant Leishmania tropica: An invitro assay. Asian Pacific J Trop Med. 2014;4:412-20.
14. Kamil MM, Ali HZ. Using PCR for detection of cutaneous leishmaniasis in Baghdad. Iraqi Journal of Science. 2016;57(2B):1125-30.
15. O'brien J, Wilson I, Orton T, Pognan F. Investigation of the Alamar Blue (resazurin) fluorescent dye for the assessment of mammalian cell cytotoxicity. The FEBS Journal. 2000;267(17):5421-6.
16. Abe Y, Sasaki H, Osaki T, Kamiya K, Kawano R, Miki N, et al., editors. Rapid and accurate IC 50 determination using logarithmic concentration generator. Chemical and Biological Microsystems Society; 2012.



**Buraq Abdulameer fingan and Hayder Zuhair Ali**

17. Dar O, Khan M, Adagu I. The potential use of methotrexate in the treatment of falciparum malaria: in vitro assays against sensitive and multidrug-resistant falciparum strains. Japanese journal of infectious diseases. 2008;61(3):210-1.
18. Mahmoudvand H, Kheirandish F, Mirbadie SR, Kayedi MH, RIABI TR, Ghasemi AA, et al. The Potential Use of Methotrexate in the Treatment of Cutaneous Leishmaniasis: In Vitro Assays against Sensitive and Meglumine Antimoniote-resistant Strains of Leishmania tropica. Iranian journal of parasitology. 2017;12(3):339.
19. Scott DA, Coombs GH, Sanderson BE. Effects of methotrexate and other antifolates on the growth and dihydrofolate reductase activity of Leishmania promastigotes. Biochemical pharmacology. 1987;36(12):2043-5.
20. Ganguly S, Bandyopadhyay S, Sarkar A, Chatterjee M. Development of a semi-automated colorimetric assay for screening anti-leishmanial agents. Journal of microbiological methods. 2006;66(1):79-86.
21. Kip AE. Clinical pharmacology and bioanalysis of antileishmanial drugs: Towards improved treatment strategies for leishmaniasis: Utrecht University; 2017.
22. Mosimann V, Neumayr A, Paris DH, Blum J. Liposomal amphotericin B treatment of Old World Cutaneous and Mucosal Leishmaniasis: A literature review. Acta tropica. 2018.
23. Fingan, B. A;and Ali, H. Z.(2018).Cytotoxic effect of Methotrexate on Leishmania donovani promastigotes.ISOR Journals of pharmacy and biology sciences5(13):65-69.

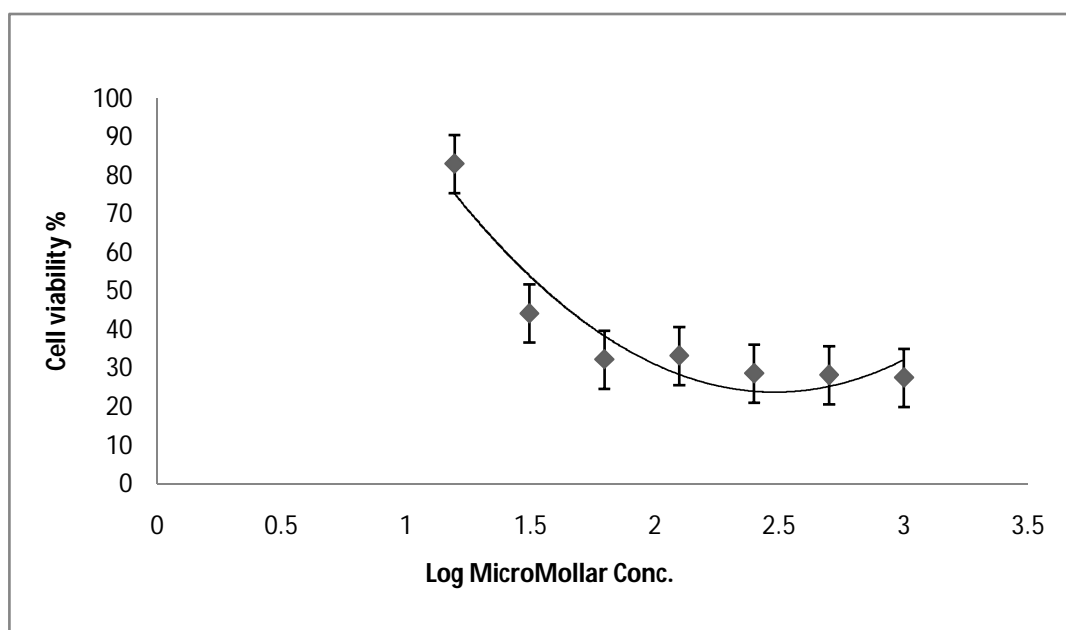


Figure (1) Cell viability of *L. tropica* treated with Methotrexate, after 24 hours of incubation.





Buraq Abdulameer fingan and Hayder Zuhair Ali

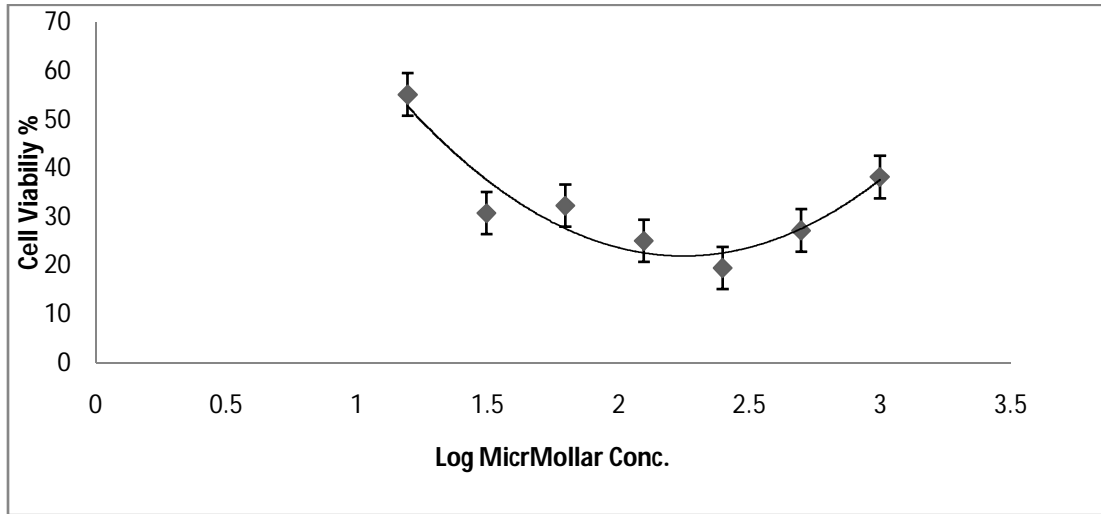


Figure (2) Cell viability of *L. tropica* treated with Methotrexate, after 48 hours of incubation.

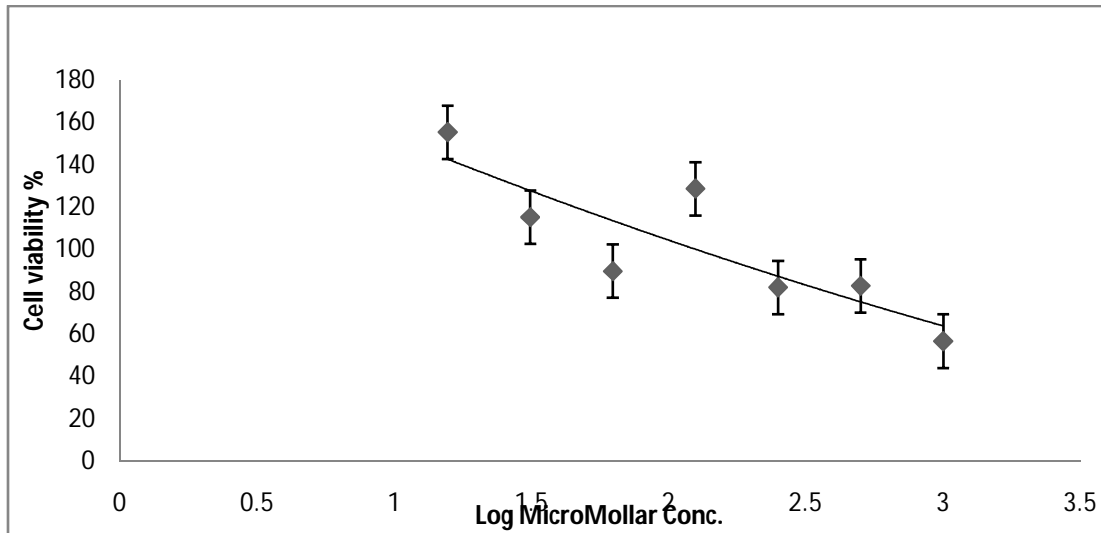


Figure (3): Cell viability of *L. tropica* treated with Methotrexate, after 72 hours of incubation.





Histopathological Study on Experimental Formation of Cholelithiasis in Lambs After Infection by *Salmonella typhimurium*

Basim M. jwad* and Bushra I. AL-Kaisei

Department of Pathology and Poultry Diseases, Collages of Veterinary Medicine, University of Baghdad, Baghdad, Iraq.

Received: 15 Sep 2018

Revised: 18 Oct 2018

Accepted: 27 Nov 2018

* Address for Correspondence

Basim M. jwad

Department of Pathology and Poultry Diseases,
Collages of Veterinary Medicine,
University of Baghdad,
Baghdad, Iraq.

E-mail: bassimpatho@yahoo.com , bassimpathology1979@gmail.com.



This is an Open Access Journal / article distributed under the terms of the **Creative Commons Attribution License** (CC BY-NC-ND 3.0) which permits unrestricted use, distribution, and reproduction in any medium, provided the original work is properly cited. All rights reserved.

ABSTRACT

Despite major effect for a subset of experimental infected lambs, *Salmonella enterica* subsp. *enterica* serovar *typhimurium* colonized the gallbladder, that represent as a reservoir for the spread of the bacterial infection in human and animal after long symptoms subside. So abdominal ultrasonography with histopathological examination was used to revealed pathological effects experimentally in gallbladder, consistent with cholelithiasis formation. Therefore, this study was designed to address this issue. Eight local lambs in 5-4 months old experimentally were taken (two for control), they were single dose, through orally administered lambs via stomach tube, with a volume of 0.5 ml contain (1×10^8 cfu/ml *S.typhimurium*). then animal became under observation, and weekly examined by abdominal ultrasonography until (30 day) duration of experience, associated with sacrificed of infected lambs, with control animal, after (7, 15 and 30 days), for bacterial culture detection on *Salmonella-Shegilla agar* (SS agar), and grossly & histopathological examination of the gallbladder. All results recorded a brown-pigment gallstone type after 30 day from infected animal, combined with bacterial nidus growing on culture media (SS agar). Histopathology revealed severe chronic cholecystitis associated with petechial hemorrhage and thickens in the wall of gallbladder grossly, and severe congestion of blood vessels with (xantic cells) formation in the mucosal layer surrounding with mono nuclear cells (MNCs) infiltration microscopically in the infected animal.

Keywords: cholelithiasis, lambs, *S.typhimurium*, pigment gallstones.





INTRODUCTION

Salmonella typhimurium causes systemic infection and gastroenteritis in human and animals (1). *Salmonella spp.* have been isolated from gallbladders from patients with acute and chronic disease (2). Although the majority of *S. typhimurium* is affect several animal species and birds, However, in acute infectin, bacterial colonized in gallbladder are scarcely diagnosed, but it may become apparent with the onset of acalculous cholecystitis (3;4). Cholelithiasis is the one of clinical causes that may represent risk factors for gallbladder cancer (5). Depending on their cholesterol content, kinds of gallstones are typically distributing as either pigment gallstones or cholesterol gallstones (6). Whereas cholelithiasis account for 10 - 15% of the total common disease, that affecting approximately adults in the United States (7; 8). From other hand, recent many cases of cholelithiasis was recorded in different countries that included several types of animal, so it has been reported spontaneous formation of cholelithiasis in a male African green monkey *Chlorocebus aethiops*, with infiltration of inflammatory cells within pathological observe in gallbladder, but the etiology formation cholelithiasis in gallbladder examined remains unknown (9).

In addition (10) noted spontaneous cholelithiasis during routine semiannual examinations, in amature female squirrel monkey *Saimiri sciureus*, show as echogenic, shadowing debris appear in the gallbladder during in ultrasonography abdominal test. Also (11 ; 12) demonstrated that (*S. typhimurium*, *S. typhi*, and *S. Enteritidis*) have ability bile-dependent mature biofilm formation, combined with characteristic (ECM production) occurs on human gallstones and on cholesterol-coated Eppendorf tubes in vitro. Depending on their cholesterol content, kinds of gallstones are typically distributing as either pigment gallstones or cholesterol gallstones (13). Furthermore, condition of gallbladder like mucus hypersecretion, or gallbladder stasis may promote to growth and formation cholelithiasis (14). Therefore 80% of types gallstones in the western hemisphere was cholesterol gallstones, which occur when cholesterol rates exceed the solubilising capacity of bile (15). A present study was aimed to investigate the pathological feature of experimental cholelithiasis in lambs gallbladder caused by infection *S.typhimurium*.

MATERIAL AND METHODS

Experimental animal and management

Eight local lambs in 5-4 months old, (5.250 - 6.750 Kg) were obtained from (animal market at Al-Shu'ala neighborhoods) in Baghdad-Iraq ; then kept in animal house, range in dimensions (10x7) meter, under conditions were maintained at $20 \pm 2^{\circ}C$, the air of the room was changed by air vacuum and animals were fed on animal pellets of concentrated food and water. The study was conducted in department of pathology, at college of veterinary medicine/University of Baghdad, during a period extended from septumber into October 2017. Lambs was treated by [Oxytetracylin 50% water soluble powder, in which 250 m.m dissolved in one liters of drinking water, with subcutaneous (S/C) injected with 0.02 ml/kg Ivermectin solution (each ml contain 10 mg Ivermectin) as single dose, for 6 days. after that animals gives (Trisulpha-Nad, 1ml/2 liters of drinking water) for 3 days, as a preventive treatment], then animal was left for (15 days) without treatment, as adaptation. The divided into:-

1- Control group, included two animals.

2- Infected group included six animals, infected by 0.5 ml contain (1×10^8 cfu/ml *S.typhimurium*), given as single dose, through orally administered lambs by stomach tube. Animal became under observation, and weekly examined by abdominal ultrasonography until (30 day).

Dose preparation

Infected bacterial dose and concentration, was preparation by (Department of Microbiology/College of Veterinary Medicine /Baghdad University).





Basim M. jwad and Bushra I. AL-Kaisei

Salmonella-Shigella agar (SS agar) prepare

Salmonella-Shigella agar (SS agar):-Salmonella-Shigella agar represent as selective and differential medium for thecultivation, isolation and differentiation of Salmonella spp. and some strains of Shigella spp. And it prepared according to manufacturer instructions by suspend 63.02 g. in 1000 ml of D.W. Then boiling the mixture with regular shakeup until the medium dissolve completely then cooled, to about 50°C and poured into sterile petri plates.

Animal sacrifice

Lambs are sacrificed (infected and control groups), that occur via slaughtering animal after (7, 15 and 30 days) duration of experiment, linked with small pieces of gallbladder were taken "after each sacrificed period". For bacterial cultuer isulation, and the others was fixed in 10% buffered formalin saline (16) for 72 hour, and embedding tissue preparation according to whom (17), and slide were stained with (Hematoxylin and Eosino), then examined under light microscope.

RESULTS AND DISCUSSION

Bacterial isolation

The result of culture media founded, growing of Salmonella on (SS agar) colonies will appear as a colorless with black centers (Figure: 1). This occur due to produce hydrogen sulfide (H₂S) gas by *Salmonella*, as a result for non lactose fermented, that differs from sveral *Enterobacteriaceae*, like *E.coli* spp. will ferment the lactose, with pink color colonies growth in culture media. From other hands, the *Salmonella* colonies differ from *Shigella* spp. that was appear as resulting a colorless colonies because it not produce (H₂S) gas and non lactose fermented. Whereas it differs from *Klebsiella* spp. colonies appears mucoid, pale, and larger than *E. coli*, opaque cream to pink. This result was agreement with (18), who isolated the *S.typhimurium* from different food sources. Also (19), diagnosis *S.typhimurium* from gastroenteritis in lambs (in control groups). Al-Khayat (20) was reported growing *Salmonella* enterica serovar *typhimurium* on culture media when insulated from chicken.

Pathological results

(grossly) an ultrasonography examination was appear in the (figure:2) show thickening of the wall of gallbladder that visible, with gallstone formation in gallbladder, that development during, that associated with bouts of acute cholecystitis may be complicated to chronic cholecystitis of gallbladder. That connected with (Figure: 3), that show multi focal from necrotic area that appear in the liver after (7 day) from oral infected lambs by (1x10⁸ cfu/ml *S. typhimurium*), associated with enlargement and dilation of gallbladder. Also gross appearance of the gallbladder that appear in (Figure: 4), thickening of gallbladder wall, with petechial hemorrhage that recorded after seven day from infected lambs, too necrotic with hemorrhagic area were seen after slaughter animal at end of (15 day) with mucoid texture, whereas at end of experiment, view a hard, rounded pigment stones with irregular border, dark yellowish-brownish in color when extracted from the gallbladder after month from infection, leaving severe necrotic area, ulcerated and sloughing of the tissue when touch it. These occur due to inflammatory responses against endotoxin that release from bacterial infection, despite to normally gallbladder rich by the bile salts, that was provide sources of calcium, carbon and nitrogen that required for essential for bacterial growth, causes an imbalance of biliary components, then supersaturating and subsequent precipitation.

These results have the same investigation of (10) intramural edema within the gallbladder wall, and cystic duct dilated, at abdominal ultrasonography in squirrel monkey (*Saimiri sciureus*), and with (9) in an (African green monkey),through recorded a cholelithiasis, with multiple echogenic, shadowing structures consistent with



**Basim M. jwad and Bushra I. AL-Kaisei**

cholelithiasis, correlated with gross necropsy finding of liver and gallbladder that recognized with distention and cobblestone texture marked in gallbladder, in addition multiple light brown gallstones measuring (5x5x3 mm) each, when incision gallbladder, of monkey, characterized by partially solid, several irregular black pinpoint, with black core, appear at varying stages of disintegration, after incision into the gallbladder.

Histopathological examination

The specific structural lesions observing in the parenchyma of the gallbladder, at (7 day) was characterized by the severe hemorrhage and congestion of blood vessels, also mild aggregation of mononuclear cells in some of blood vessels, and slight hyperplasia of epithelial cell with lamina propria, incorporated with induced obstructive cholestasis, that appear within epithelial cells (Figure: 5). Furthermore the pathological lesion of *S. typhimurium* on the gallbladder parenchyma, after (15 day) characterized by extensive sloughing of the epithelial cells, associated with sever congestion of blood vessels (Figure: 6), besides that an extensive infiltration from mononuclear cells mainly lymphocyte and macrophages (Figure: 7). The (Figure: 8) show the histopathological picture of gallbladder after (30 day) from infected lambs by (1×10^8 cfu/ml *S.typhimurium*), was manifested by mild infiltration of inflammatory cells in muscular layer, accompanied with thickening of muscular propria, some areas, they were separated from mucosal layer, in addition, severe sloughing of the epithelial cells, with severe infiltration of mononuclear cells macrophages and lymphocytes (Figure: 9). Furthermore, "xantic cells" were formed, that represented types from macrophages, which it through examination, consisted from polygonal and larger cells, with hyperchromatic small central nucleus, with foamy cytoplasm, that appear in the mucosal layer surrounding with MNCs infiltration (Figure: 10).

Our results revealed severe inflammatory reaction of gallbladder with chronic cholangitis and cholecystitis, this may be due to severe infiltration of neutrophils with, associated with MNCs infiltration, which indicated by engulfing bile pigment to destroy them, that appear as brown-yellowish color. This observation was in acceptance with those previously reported it's several investigators(10), severe inflammatory cell infiltration, with brown granular material within macrophages, representing intra-cytoplasm bile, this demonstrating bile duct hyperplasia at the liver section in mature female squirrel monkey. However (9), explained that moderate chronic diffuse hyperplasia of the gallbladder epithelium, also moderate to diffuse infiltration of lymphocytes in epithelial layer of gallbladder, with severe chronic-active diffuse cholecystitis and severe chronic-active hepatic degeneration, necrosis with severe cholestasis (22). However, result was similar to that recorded by (19) with the findings regarding, infected sheep via intraperitoneal injection by (1×10^{11} cell/ml) exhibited severe mucinous secretion associated with severe destruction and sloughing of mucosal folds epithelium, as well as shortening of mucosal folds and tissue debris in the lumen of tissue after (6 & 14 day), combined with focal necrotic and ulceration with collagen fibers fragmentation of glandular lamina propria. Occasionally, pathological lesion, characterized by existence (xantic cells) in cholelithiasis that was recorded in gallbladder after month from infected lambs via (1×10^8 cfu/ml *S.typhimurium*), this may occur due to that the xantic cells represent as macrophages -2, for phagocytized the excess calcium bilirubinate or calcium carbonate or cholesterol composition, that was passed into the lamina propria, so this type of cell considered as hallmark of late stage cholelithiasis lesion formation. This evidence was provided established previously investigation. Villous mucosal hyperplasia with foamy macrophages was seen in the epithelium and lamina propria of gallbladder or near from tips of villi and this changes are restricted to gallbladder and don't involve extrahepatic bile ducts (23).

We have verified in present study investigated that the *S. typhimurium* causes Cholelithiasis in lambs gallbladder when experimental infection orally by 0.5 mm. contain (1×10^8 cfu/ml *S.typhimurium*).

Conflict of Interests Statement

The authors declare that there is no conflict of interests regarding the publication of this article.





Basim M. jwad and Bushra I. AL-Kaisei

Financial Disclosure Statement

This study was not funded by any funding agency and was conducted at the expense of the researcher. As part of the research requirements for the degree of Doctor of Philosophy in the department of Pathology.

Animal Rights Statement

The experiments and procedures involving local lambs, were approved by scientific committee of department of pathology; in the College of Veterinary Collages of Veterinary Medicine, University of Baghdad, Iraq, and were conducted according to the guidelines of the committee.

REFERENCES

1. Aseel Jasim Mohammed.: Study the role of grape seeds polyphenols as anti-bacterial, anti-inflammatory, anti-apoptotic and immunomodulatory agent in mice Infected with Salmonella typhimurium . A dissertation degree of doctor of philosophy veterinary medicine/microbiology; Collage of veterinary medicine, University of Baghdad. Iraq. **2017**.
2. Doerr R.: Experimentelle untersuchungen u'ber das fortwuchern von typhusbacillen in der gallenblase. Centralbl f Bakt. **1905**, 39: 624–34.
3. Helm RA. ; Porwollik S.; Stanley AE. ; Maloy S. ; McClelland M. ; Rabsch W. and Eisenstark A.: Pigeon-associated strains of Salmonella enterica serovar typhimurium phage type DT2 have genomic rearrangements at rRNA operons. Infection Immunity. **2004**, 72, 7338–7341.
4. Alfredo Menendez ; Ellen T. Arena ; Julian A. Guttman ; Lisa Thorson ; Bruce A. Vallance ; Wayne Vogl and Brett Finlay B.: Salmonella Infection of Gallbladder Epithelial Cells Drives Local Inflammation and Injury in a Model of Acute Typhoid Fever. Journal of Infectious Diseases. **2009**, 200:1703–13.
5. Vineeta Mittal; Surendra Kumar ; Anshuman Pandey and Saurabh Singh.: Is Salmonella enterica serovar Typhi associated with carcinoma gall bladder?. Biomedical Research. **2018**, 29 (8): 1617-1620.
6. Chowdhury, A. H. and Lobo, D. N.: Gallstones, Surgery (Oxford), 29, 610–617, doi:10.1016/j.mpsur. **2011**.09.008, **2011**.
7. Venneman NG and van Erpecum KJ.: Pathogenesis of gallstones. Gastroenterol Clin North Am. **2010**, 39:171–183.
8. Portincasa P. ; Ciaula AD. ; Bonfrate L. and Wang DQ.: Therapy of gallstone disease: what it was, what it is, what it will be. World J. Gastrointest Pharmacol Ther. **2012**, 3:7–20.
9. Dina Kleinlützum and Roland Plesker.: A case of gallstones in an African green monkey (Chlorocebus aethiops). Primate Biol. 2017, 4, 33–37.
10. Mia T. Lieberman ; Lynn M. Wachtman ; Robert P. Marini ; Vasu Bakthavatchalu and James G. Fox. (2016). Case Report Spontaneous Cholelithiasis in a Squirrel Monkey (Saimiri sciureus). Division of Comparative Medicine. 2002, 66(1):63–67.
11. Prouty AM. ; Schwesinger WH. and Gunn JS.: Biofilm formation and interaction with the surfaces of gallstones by Salmonella spp. Infect Immun; 70:2640–2649.
12. Crawford RW. ; Gibson DL. ; Kay WW. and Gunn JS.: Identification of a bile-induced exopolysaccharide required for Salmonella biofilm formation on gallstone surfaces. Infect Immun; 2008, 76:5341–5349.
13. Prevot, S.: Pathology of the gallbladder and extra-hepatic bile ducts, Cases 2 and 3, Chronic cholecystitis, Ann. Pathol., 34, 279–287, doi:10.1016/j.annpat.2014,06.007.
14. Kumar, V. ; Abbas, A.K. ; Aster, J.C. and Perkins, J.A: Robbins and Cotran pathologic basis of disease, Ninth edition, Elsevier/Saunders, Philadelphia, PA, xvi; 2015, 1391.
15. Wang, H.H. ; Portincasa, P. and Wang, D.Q.H.: Molecular pathophysiology and physical chemistry of cholesterol gallstones, Frontiers in bioscience a journal and virtual library. 2008, (13) 401–423.





Basim M. jwad and Bushra I. AL-Kaisei

16. Carson F L, and Hladik Ch. Histotechnology.: A Self-Instructional Text. Third Ed., Chicago ASCP Press, 2009. P:400.

17. Luna, L.G.: "Manual of histologic staining methods of the armed force institute of pathology" 3rd Ed. McGraw-Hill, New York. USA. , 1968.

18. Ali Karim Husuni Al-Bakri : Molecular and Conventional detection of Salmonella typhimurium in different food sources. Degree of master in genetic engineering and biotechnology GEB. Genetic engineering and biotechnology institute for postgraduate studies/ University of Baghdad. Iraq.2015.

19. Roaa Adnan Hussein : Comparison study for treatment of enteritis in lambs induced by Salmonella typhimurium as compared colicin E1 or enterocin A1 with enrofloxacin. Degree of doctor of philosophy in veterinary medicine ; College of veterinary medicine/University of Baghdad. Iraq.2016.

20. Lujain Dhiaa Nasser Al-Khayat.: Molecular identification by using multiplex PCR to detect some Salmonella serotypes from chicken. Degree of Master of Science in Veterinary Medicine / poultry diseases. College of veterinary medicine/University of Baghdad. Iraq.2017.

22. Gonzalez-Escobedo G. and Gunn J.S.: Gallbladder epithelium as a niche for chronic Salmonella carriage. Infect. Immun. 2013, 8(1):2920– 2930.

23. Hanni Gulwani.: Gallbladder miscellaneous nontumor cholesterolosis :Surgical Pathology of the GI Tract, Liver, Biliary Tract and Pancreas "Odze and Goldblum" 3rd 2018. edition. Pathology Outlines. comwebsite. <http://www.pathologyoutlines.com/topic/gallbladdercholesterolosis.html>.

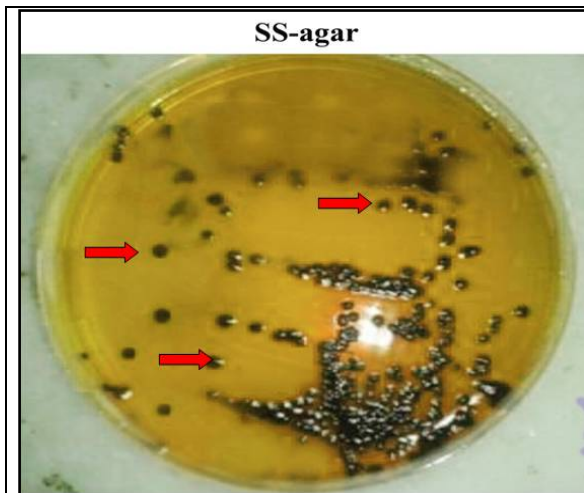


Figure: 1 show colorless colonies, with black centers that grown of *S. typhimurium* on (SS agar), after isolated from lambs after infected by (1×10^8 cfu/ml *S. typhimurium*).

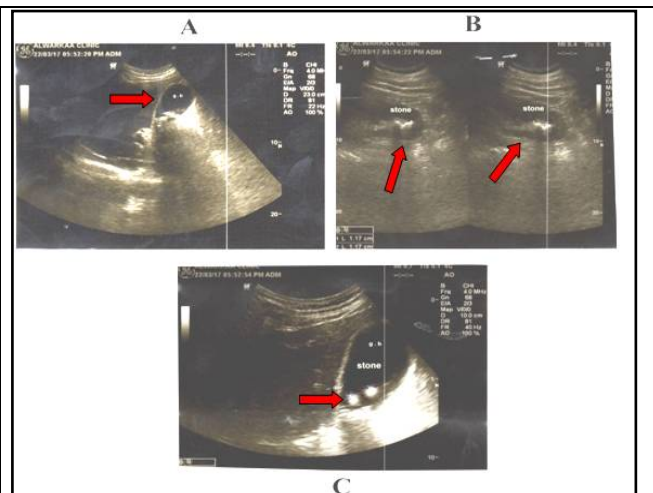


Figure: 2 show Abdominal ultrasonography. (A: at 7 day), (B: at 15 day), (C: at 30 day), was show formation & development of gallstones in gallbladder of lambs after infected by (1×10^8 cfu/ml *S. typhimurium*)



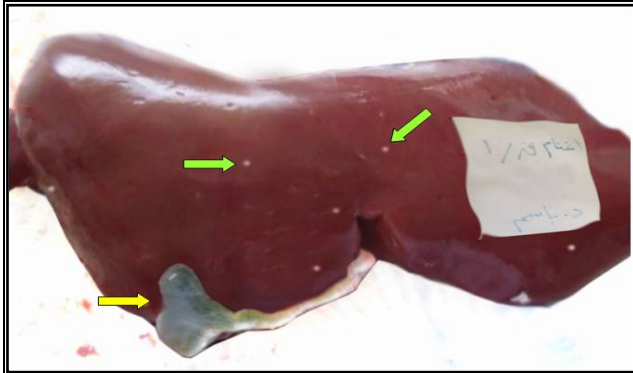


Figure:3 show gross appearance of infected liver at (7 day) appear multifocal necrotic with enlargement and dilated of gallbladder of lambs after infected by (1×10^8 cfu/ml *S. typhimurium*).

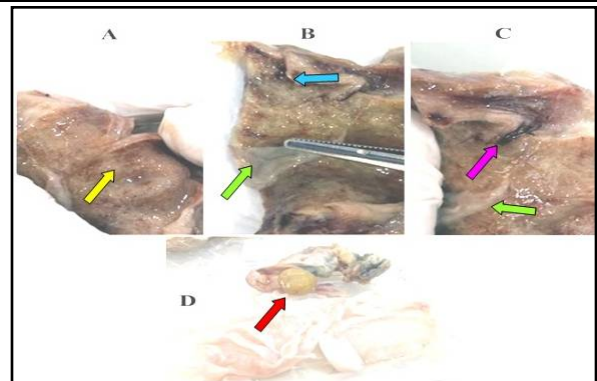


Figure:4 grossly appearance of gallbladder of infected lambs with (1×10^8 cfu/ml *S. typhimurium*) .show petechial hemorrhage was seen in (A: 7day),whereas necrotic with hemorrhagic area and mucoid were seen in (B:15 day) within tissue organ. Severe necrotic area in (C), and gallstones in (D) after 30 day.

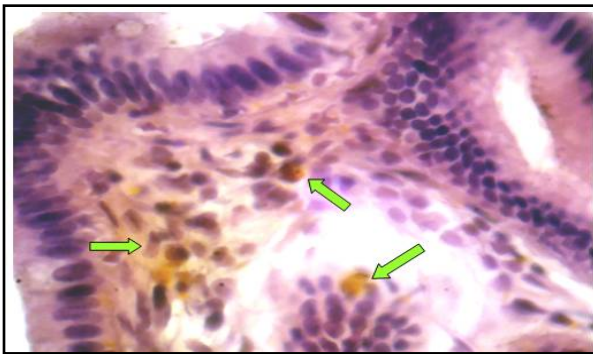


Figure: (5): Histopathological section in gallbladder epithelial cell of lambs at (7 day) after infected (10^8 *S. typhimurium*) show yellowish-brown color within epithelial cells obstructive cholestasis (H&E stain 40X).

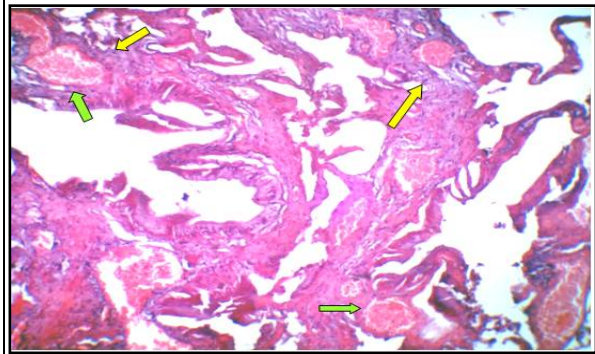


Figure: (6): Histopathological section in gallbladder epithelial cell of lambs at (15 day) after infected (10^8 *S.typhimurium*) show severe congestion of blood vessels with MNCs infiltration (H&E stain 10X).

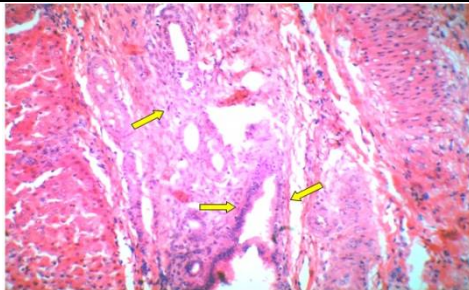


Figure: (7): Histopathological section in bile duct of lambs at (15 day) after infected (10^8 *S.t*) show proliferation of fibrocytes in the wall of bile duct (H&E stain 10X).

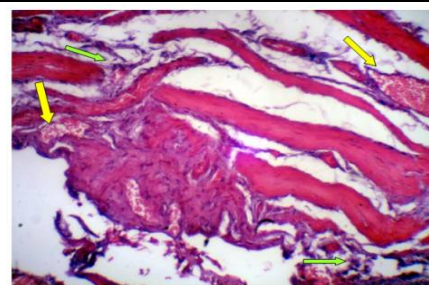


Figure: (8): Histopathological section in gallbladder epithelial cell of lambs at (30 day) after infected (10^8 *S.t*) show congestion of BV. with mild inflammatory cells infiltration in muscular layer (H&E stain 10X).



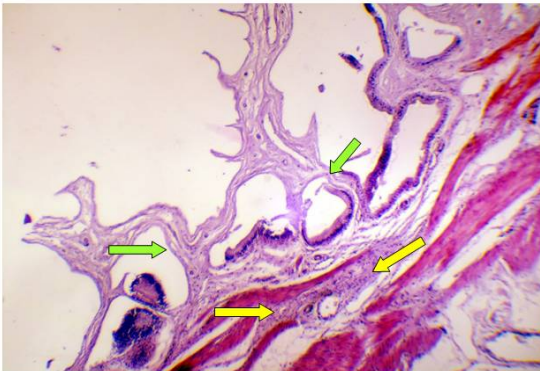


Figure: (9): Histopathological section in gallbladder epithelial cell of lambs at (30 day) after infected (10^8 *S.typhimurium*) show sloughing of the epithelial cells,  with severe infiltration of MNCs  (H&E stain 10X).

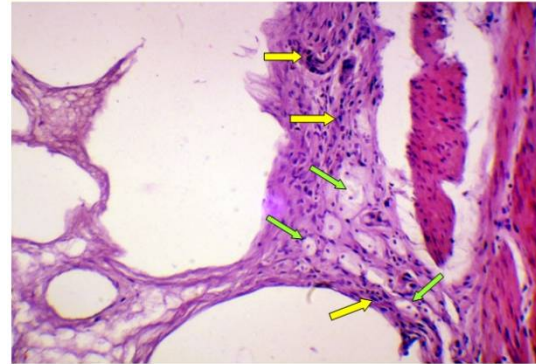


Figure: (10): Histopathological section in gallbladder epithelial cell of lambs at (30 day) after infected (10^8 *S.typhimurium*) show xanthic cells  formation in the mucosal layer surrounding with MNCs infiltration  (H&E stain 10X).





A General Overview on *Staphylococcus* and Betalactamase Enzyme

Reem Zuhair Shinashal*

Department of biology, College of Girls Education, University of Mosul, Iraq

Received: 20 Aug 2018

Revised: 22 Sep 2018

Accepted: 27 Oct 2018

*Address for Correspondence

Reemzuhairshinashal

Department of Biology,
College of Girls Education,
University of Mosul, Iraq
Email: reemzhyr1970@gmail.com



This is an Open Access Journal / article distributed under the terms of the **Creative Commons Attribution License** (CC BY-NC-ND 3.0) which permits unrestricted use, distribution, and reproduction in any medium, provided the original work is properly cited. All rights reserved.

ABSTRACT

The current review focused on the *Staphylococcus* spp and Betalactamase Enzyme. *Staphylococcus* contains at least 30 species. There are three main types of clinical significance: *S.aureus*, *S.epidermidis*, *S. saprophyticus*. The first to be named *S.saprophyticus* on non-coagulase-producing *Staphylococcus aureus* (Coagulase) was the World Fair brother in 1940. In 1951, Shaw and his group were able to classify isolated *Staphylococcus* from different sources such as humans, animals, dairy products. The soil and the sewers were divided into five subgroups of the *Staphylococcus* genus. *S.saprophyticus* was called the second group, which was characterized by acetone production; acid from the fermentation of the cocose, non-couculase or pigment, as well as its nitrate reduction Analysis of urea. In 1962, Torres recorded the presence of groups similar to the *S.epidermidis* strains that cause urinary tract infection. These strains possess 51 serotypes and show resistance to the antibiotic Novobiocin. In 1963, these bacteria were re-categorized as *Micrococcus* and classified as a subset of this species. They were called *Micrococcus* Subgroup3 because they shared this species as non-coagulase and Phosphatase.

Keywords: *Staphylococcus* spp., Betalactamase Enzyme, fermentation, *Micrococcus*

INTRODUCTION

Several studies have shown that there is a significant difference between *Staphylococci* and *Micrococci* since this type of *Staphylococcus aureus* is not an optional antenna, and its content is from 39 to 30% G + C which is similar to G + C in the *Staphylococci* these isolated bacteria were then re-categorized as anthrax in 1973 and were associated with *Staphylococcus* species. The *micrococcus* subgroup 3 was also found to be similar to the *S.aureus* or *Staphylococcus aureus*, and it can produce acid from an aerosol-free fermentation. Thus, *S.saprophyticus*, isolated from non-coagulase-induced urinary tract infections, and resistance to the antibiotic Novobiocin (Novobiocin).



**Reem Zuhair Shinashal*****Staphylococcus saprophyticus***

S.saprophyticus is the most common cause of urinary tract infection in young women. The most important characteristic of these bacteria is their inability to produce coagulase. This enzyme is one of the most important enzymes that distinguish between the types of *Staphylococcus* produced and non-productive *Staphylococcus aureus* (CONS) Coagulase Negative Staphylococci. The colonies of this type of *Staphylococcus* are circular and smooth. The diameter of the colony varies from 5-9 mm to the solid media. It does not possess the ability to produce the DNase. However, it is characterized by its production of mucus, which is an important fermentation agent. It facilitates the adhesion of bacteria to the epithelial cells of the urinary system, as well as the bacterial resistance to many antibiotics.

It also has the ability to produce the enzyme Urease, which is also an important ferment factor for these bacteria, and has a role in its diseases. These bacteria can grow under anaerobic conditions and grow in high salinity conditions with concentrations of up to 10% or 15% of NaCl. They can also grow in different temperatures ranging from 15-45 m. *S.saprophyticus* can be distinguished from the rest of the other non-producing coagulants of the blood coagulase enzyme, which is characterized by the inability to ferment the manganese sugar while *S. epidermidis* can ferment. *S. capitis* is unable to produce urease while *S.saprophyticus* can produce this enzyme. *S. hominis* are characterized by their inability to grow in anaerobic conditions while *S.saprophyticus* grows in such conditions. This type of *Staphylococcus aureus* is characterized by its inability to produce phosphatase, and its resistance to the antibiotic Novobiocin 5 µg and diameter of 14 mm, is required for the test of Catalase, and is non-blood analysis.

Sensitivity of *S.saprophyticus* bacteria to antibiotics

It was found that the resistance of many types of bacteria, including *S.saprophyticus* for many antibiotics, and found that the sensitivity of bacteria to antibiotics depends on the type of amino acids found in the wall of the cell, the types containing the amino acid Serine in bridges between the peptide such as: *S. apaphyticus* and *S. haemolyticus* and *S. hominis* are more resistant to antibiotics.

A study in London hospitals showed that *S. apapyticus* isolates were all sensitive to Vancomycin and Rifampicin and were sensitive to Clindamycin and Ciprofloxacin at 4%. The same study indicated that of the 194 isolates of *S. aprophyticus*, the resistance of penicillin, methicillin and Oxacillin was 57%, 80% and 20%, respectively. It was found that the resistance of all isolates of Cefotaxim was equal to their resistance to penicillin, and the value of MIC was 2 µg / ml. Based on the NCCLs results, the isolates were considered to be moderately sensitive to Cefotaxim and it was observed that bacterial resistance to Methicillin was associated with the presence of mecA gene. Methicillin-resistant isolates were <MIC16 mg / L.

Coagulase resistance to quinolones is determined by the presence of a region called gyr genes. About 15 isolates of *S. apaphyticus* have been shown to be sensitive to quinolones commonly used to treat urinary tract infections, including Ciprofloxacin and Norfloxacin. MIC for 0.39 mg / L and 1.56 mg / l respectively. Oxacillin-resistant isolates may be resistant to anti-betelactam, including penicillins and cephalosporins, and many other antibiotics are contraindicated. Vancomycin can be considered the most common treatment for these isolates. *Staphylococcus aureus* of Oxacillin and Methicillin is associated with the protein associated with penicillin binding (PBP2a), and that a change in penicillin-bound protein does not allow the drug to bind to the bacterial cell wall, causing resistance to the betelactam antibodies.

The resistance of *S. apaphyticus* to penicillin was not limited to isolates isolated from the blood. Bacteria isolated from other sources of the body, such as cough and blood, were resistant to antibiotics such as Penicillin, Oxacillin and other antibiotics such as Chloramphenicol and Erythromycin. They were sensitive to Vancomycin antagonist. *S. saprophyticus* isolates, all isolated from urinary tract infection, have demonstrated high resistance to Nalidixic acid.



**Reem Zuhair Shinashal**

Genetic Nature of Antibiotic Resistance

The emergence of antibiotic resistance by *Staphylococcus aureus* over the past 50 years is a genetic response due to the indiscriminate use of antibiotics. The rapid emergence of resistance after the use of any antibiotic indicates the ability of these microorganisms to adapt to environmental changes. Antibiotics in bacteria initially develop at Mutation. Staphylococcal resistance to a number of antibiotics, including Fusidic acid, Rifampicin, Streptomycin, and Novobiocin appears to be a result of a chromosome mutation, but sometimes this Chromosomal antibodies that lead to the emergence of antibiotic resistance are harmful to the bacteria itself, leading to the emergence of less virulent bacteria, so this type of mutations is not enough to illustrate the rapid emergence of antibiotic resistance, and found that bacteria can acquire genetic material in the form of DNA located Outside the chromosome, plasmid, it has been shown that the appearance of resistance in *Staphylococcus aureus* is due to the presence of plasmids carrying resistance genes.

These plasmids contribute to the emergence of resistance through two mechanisms

- 1 - Through the possibility of the union of plasmid bacterial chromosome.
- 2 - Through the transmission of plasmids with bacterial bacterium, this can act as the carrier of genes

And that there are many mechanisms, by which microbes can show antibiotic resistance (Jawetz et al., 1998; 2001), including:

1. Microsurgery produces active antagonist enzymes such as Penicillin-G-*Staphylococcus aureus* (PEN), which produces the Betalactamase enzyme that destroys the antibody.
2. Microcellular cells or microscopic microorganisms change their antimicrobial efficacy, such as tetracycline, which is collected in sensitive bacteria but not in resistant bacteria.
3. Microorganisms change Target structure, for example chromosomal resistance to amino glycosides, is associated with the loss or alteration of a specific protein in unit 30S in the bacterial ribosome, which acts as a binding site in sensitive microbes. Microorganisms develop different metabolic pathways, thus allowing the antidepressant to continue to interact with the antagonist. Microorganisms develop heterozygous enzymes, thus leaving their metabolic function and being less affected by the antimicrobial.

Betalactamase enzyme

The first enzyme was found to be able to break down anti-betalactam early before purification of penicillin G antibiotic and its actual use in the treatment of *Staphylococcus aureus*. This enzyme was known as Penicillinase. This enzyme is produced by many pathogenic bacterial strains, and on this basis the bacterial strains produced by it resist anti-betalactam containing the beta lactam ring (Richmond, 1965).

These enzymes are specialized for the protection of bacteria from anti-betalactam inhibitors that inhibit the formation of myorin or peptidoclique in the cell wall of bacteria (Pollock, 1971). Studies have created the possibility that these enzymes may be dispersed from one of the enzymes involved in the manufacture of this sensitive layer to anti-betalactam (Ambler, 1980). Betalactamines contain the amino acid Serine, the essential component of the active site (Sanders, 1992). There is a significant difference between the beta-enzymes produced by the Gram-positive bacteria and those produced by the Gram-negative bacteria. The first group is extracellular enzymes, while the second group is cell-bound enzymes. The production of Gram positive bacteria is greater, and the antibody is decomposed in the medium surrounding the cell, as is the case with *Staphylococcus aureus*, while the antibody within the bacterial cell is destroyed in the Gram-negative bacteria as in *E. coli*.





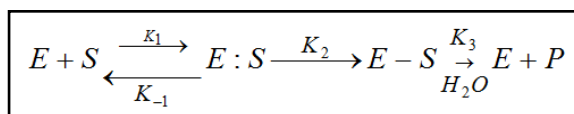
Reem Zuhair Shinashal

The effectiveness of the betalactamase enzyme to inhibit penicillin G but also be effective against many types of penicillin such as Amoxicillin, Carbenicillin and other antibiotics containing the betalactam ring. A study of different strains of sensitive *Staphylococcus aureus* resistant to penicillins showed that there was a significant difference in thickness of the outer layer of the wall Cellular cell thickness of the sensitive strain (70 μstrom), whereas in the resistant strains it was about 140 μm . The degree of resistance to penicillin depends on the amount of enzyme produced, as the strains produced for a small amount are classified as non-produced by the enzyme. Resistance to *Staphylococcus aureus* bacteria is due to their ability to produce the stimulated beta-actamase. Because *Staphylococcus aureus* produces high resistance to penicillins compared with cephalosporins, the enzyme is usually called Staphylococcal penicillinase and most *S.aureus* strains carry the genetic determinants of the enzyme that are located on the extracellular plasmid DNA .

Mechanisms of the action of the enzyme albitalactamase

When the bacteria produce the betalactamase enzyme, the enzyme attacks the pylactamase ring in the nucleus of penicillins and cephalosporins and analyzes the peptide (CN) in the betalactam ring. The antibody then turns into a compound that is ineffective. The compound, called penicillic acid, And this acid is stable Stable, and can be estimated to contain two groups of acid instead of one group was found in the base material (antifreeze), while the compound composed of cracking Cephalosporin unstable, called (Cephalosporic acid), which breaks into two molecules, It found that one enzyme molecule stopped the effectiveness of more than one molecule of the counter through the broken counter and then re-link with another anti-molecule.

The betalactamase enzyme analyzes the anti-beta-actam antibody with a two-step reaction, Michaelis-Menten, then acylation of the enzyme, followed by deacylation of the decomposition reaction by the following equation:



Chromosomal B-lactamase Enzymes

This type of enzymes is produced by most types of positive and negative bacteria. This type of enzyme favors cephalosporins as a base material.

These enzymes are divided into two types

A. Constitutive enzymes: These enzymes are produced continuously by the bacterial cell and do not need to be stimulated by the base material. The enzyme is determined by enzymatic activity known as the amount of enzyme that can convert one micromol from the base material in a single time unit, under standard experimental conditions of heat and pH (Bell et al., 1985). Enzyme activity was defined as the amount of enzyme that analyzes 1 micromol of anti-betalactam in one hour at 30 ° C .Among the bacterial species produced for this type of enzyme are Klebsiellaoxytoca.

B. Inducible enzymes: These enzymes are important in their ability to increase their production by the presence of an inductor called high inducible enzymes for their transformation from low production to high enzymatic production. These enzymes are characterized by a high number of cephalosporins that break down 100 times faster than penicillins and are not affected by normal inhibitors such as Clavulanic acid, Sulbactam, and Tazobactam, but are also affected by other inhibitors such as Cloxacillin (Bush, 1989). Many types of Gram-negative bacteria can produce this



**Reem Zuhair Shinashal**

type of enzyme such as *Pseudomonas aeruginosa* and spp. *Providencia* and *Preteus vulgaris*. Enzymes encoded have structural genes controlled by other genes, control genes through repressor, activation of control genes due to a genetic mutation or as a result of inhibitory inhibition leads to an increase in the synthesis of synthetic genes and And increased enzyme production .

The production of these enzymes can be increased by the presence of a catalyst in the medium in which the bacteria live. A number of catalysts such as Clavulanic acid, Sulbactam and Tazobactam, which increase production significantly, become antibiotic despite the presence of the inhibitor with little efficacy against bacteria. Studies show that strains of *S.aureus* produce penicillin, which controls the production of hereditary factors on the chromosome and its production is induced.

Bactalactamase-based enzymes on plasmid

Which act as antiperspirants and cephalosporins as their basis and effectiveness inhibits most known inhibitors such as Clavulanic acid, Sulbactam and Tazobactam as opposed to chromosome enzymes. These enzymes are produced by many types of bacteria such as *P. aeruginosa*, *P.mirabilis* and *Klebsiella*. Staphylococci and Enterococci were found to produce the betalactamase enzyme, which controls the production of a plasmid that is non-conjugative and also has resistance to heavy metals. The resistance of *S.aureus* to penicillin G is usually the production of the enzyme exogenous betalactamase. In most *S.aureus* strains, the genetic determinants of penicillin production are located on the plasmid .The risk of these plasmids comes with multiple resistance to more than one antagonist from different groups.

Bactalactamase-based enzymes on poplar genes

Real and primitive organisms possess sequences of nucleotides or pieces of DNA that are able to move from place to place within the genetic material, called the transposable element .The jumping genes contain resistance genes for many antibiotics such as Ampicillin, Kanamycin, and Tetracyclin. The excretion of the jumping genes in the new sites results in the appearance of traits at the expense of the disappearance of other traits. Inhibition of the Tnc gene carrying the antimicrobial resistance of Trimethoprim and Streptomycin in RP4 controlling the resistance to Kanamycin, Tetracyclin and Ampicillin inhibited the resistance of Tetracyclin and Kanamycin, Self-transport in the plasmid mentioned and then resistance to Streptomycin and Trimethoprim.

Extended Spectrum B-lactamase (ESBL)

In recent years, several intestinal family strains have shown a new pattern of resistance to anti-betalactam derivatives, especially cephalosporins. The resistance is due to the production of enzymes controlled by plasmids capable of destroying antibiotic groups. This type of enzyme was called the BSA. The production of these enzymes is due to genetic mutations in the synthetic genes controlling the production of TEM-1, TEM-2, and SHV-1 enzymes. The bacteria that produce this type and many of the antimicrobials available are currently being treated. I am currently using a new generation of treatments such as: Iminomethoxycephalosporins, including Ceftriaxone, Cefotaxim and Ceftacidin, as well as other antibiotics such as Imipenem, Cefoxitin, Aztreonam and other Cephalosporins.

P.aeruginosa bacteria have been found to produce TEM-type betalactamases, which analyze narrow-spectrum penicillins and extended-spectrum cephalosporins, as well as Aztreonam. These enzymes, called broad-spectrum betalactamase enzymes, are inhibited by Clavulanic acid, most of which are due to Class A of the Ambler classification scheme, and are resistant to many broad-spectrum cephalosporins. This type was found in the enterobacteriaceae family during the 1980s, recently in *P.aeruginosa*. Most ESBLs are under the control of conjugative plasmids. These plasmids are large in size, resistant to various antimicrobials, as well as heavy metals such as mercury, zinc and zinc



**Reem Zuhair Shinashal**

.Carbapenem antagonists, such as Imipenem, are used to treat infections caused by ESBLs. These enzymes have high association with Calvulanic acid, Azotobactam and Sulbactam inhibitors. The combination of penicillins and cephalosporins is used to inhibit the effectiveness of these enzymes.

Purification of the enzyme Pitalactamase

Enzymes are purified for the purpose of studying their properties because the presence of other substances can lead to incorrect results. The first attempts to purify the penicillins enzyme from some isolates of P-penicillin-resistant *Staphylococcus aureus* were carried out in the 1940s. The enzyme was purified from *S.aureus* bacteria by absorbing the enzyme on Cellulose phosphate, which is directly added to the bacterial suspension or to the entire plant. It absorbed about 80-90% of the enzyme's efficacy within one hour at room temperature, and then used gelatin filtration chromatography using Se gel phadex G-75 as a second step of purification. The protease of *E.coli* bacteria could be purified using ion exchange chromatography using the DEAE-cellulose exchanger, using 0.1 M Phosphate Phosphate pH = 7. The CM-cellulose exchanger was used as a second step for purified purification in the same way. Just as gel filtration was used using the Sephadex G75 gel as a final step of purification, the specific efficacy of the enzyme in the final step was 201.78 units / mg. The enzyme was purified from *S.aureus* bacteria using gel filtration using gelatin sulfide gel instead of using CM-cellulose. Purified alkaligenase enzymes produced by *alcaligenesfaecalis* were purified using the DEAE-Toyopearl transducer with dimensions (3 x 35 cm) with the tris-HCl triglyceride concentration of 0.1 mM. The parts that gave efficacy were added by adding glycol polyethylene, on the Toyopearl column, and the enzyme was recovered with the phosphorus buffer containing 0.1 molar of KCl. The final step of the purification was done using electrofocussing.

Properties of Betalactamase

Betalactamase or penicillinase is an effective enzyme used as a defense by bacteria to protect itself from other harmful microbes. Antibacterials attack bacteria and kill them by inhibiting their enzymes in the irreversible structure of the cell wall. The work of betalactamides is very complex, which is the destruction and digestion of anti-betalactam. This is accomplished through the production of enzymes and enzymes associated with the wall that contribute to the resistance of bacteria to antibiotics. The production of betalactamase is affected by the presence of penicillin, since the manufacture of betalactamides will increase but the amount of output will vary greatly depending on the type of strain and antimicrobial used. Betaactylase production is doubled when induced by ampicillin compared with penicillin G, but if methicillin is used, the production of betalactamides will increase continuously. The molecular weight of the betalactamase enzyme was determined by 28,779 using gelatin filtration chromatography method and electrostatic transfer method using SDS-polyacrylamide. The molecular weight of Penicillinase produced by *S.aureus* calculated from the amino acid sequence was determined to be 28,823, and by the sedimentation method the molecular weight of the enzyme was estimated at 29,600.

The Betalactamis consists of 257 units and consists of two dimensions comprising five parallel cords with beta plates (B2, B1, B5, B4, B3) and three snails. The effective location of the Betactamase is Serine 70. Effectiveness of the betalactamase enzyme is affected by betalactamase inhibitors Clavulanic acid, Sulbactam, Tazobactam and other inhibitors such as Cloxacillin and Boronic acid and others. The isoelectric point of penicillin produced by *Staphylococcus aureus* was determined to be equal to 8.9. The enzyme-specific conditions, such as pH and optimum heat, were identified as the optimal pH for the enzyme activity produced by *Staphylococcus* is 7. As for the enzyme produced by *E.coli*, the optimal pH for its efficacy is 6.5, while the optimum temperature for the enzyme efficacy of the same bacteria is 45 m. It has been noted that there are many substances that inhibit the effectiveness of the enzyme Altealactamiz such as: EDTA, halogens, including: Iodine, iron ions, mercury and others. It was found that the enzyme *alcaligenesfaecalis* inhibits the presence of EDTA, iodine, Cu + 2 and Hg + 2, inhibiting enzymatic efficacy of EDTA at a concentration of 3 molar and the original enzymatic activity can be restored by using dialysis towards distilled water. It was found that the different charge ion ions, such as Fe + 2 and Zn + 2 ions but Cu





Reem Zuhair Shinashal

+ 2 copper ions, had no effect on the enzymatic activity of the enzyme produced by the *E. coli* bacteria. However, halogens and nitrite at high concentrations were found to be higher than 1.4 mM Enzyme inhibitors, while sulfates, phosphates and esters have no effect on the enzyme, as it is observed that sodium ions have an inhibitory effect on enzymatic activity and different concentrations.

Betalactamase inhibitors and their types

The increase in the production of Bactalactamase, which is one of the most important antimicrobial resistance in clinical isolates, has been observed for more than 90% in recent years. To reduce this problem, several attempts were made to develop compounds that inhibit the effectiveness of β -lactamase inhibitors. It was found that some semi-manufactured penicillins, such as Penicillin Isoxazolyle and Methicillin, had an inhibitory effect of Bactalactase enzymes by *Staphylococcus aureus*. Methicillin was used to inhibit Bactalactamase enzymes produced by *Staphylococcus aureus*. Penicillin Isoxazolylepenicillins were used with high concentrations to inhibit enzymes produced by intestinal family, and the search for the possibility of producing these inhibitors naturally from microorganisms began, and this led to the discovery of Clavulanic acid.

Bactalase inhibitors include Tazobactam, Sulbactam and Clavulanic acid, which have low efficacy as an antibiotic against bacteria. But they are associated with a number of beta-actamines, inhibited by a non-inverse reaction. These compounds are therefore called suicidal. They are fixed complexes between them and the enzyme with a chemical reaction of several. Thereby blocking the enzyme and preventing it from breaking the effective anti-beta -actactam molecule. These inhibitors with anti-betelactam are effective, wide-spectrum compounds against the Gram-negative bacteria and the fungal spores, and despite the effectiveness of the inhibitor + antagonist. However, resistant strains soon emerged, so it became necessary to pay attention to the use of these compounds and to determine their ideal doses (Launay et al., 1997). Other inhibitors such as: HgCl₂, EDTA, Boronic acid, and Cloxacillin.

REFERENCES

1. Ambler, R., P. (1975). The amino acid Sequence of *Staphylococcus aureus* Penicillinase. *Biochem. J.* 151 : 197-218.
2. Ambler, R., P. (1980). The structure of β - Lactamase. *Philos. Trans. Soc. London. Biol. Sci.* 289:321-331.
3. Anderws, J.; Ashby, J.; Jenovs, G; Linesand, N.; Wise, R. (1999). Antimicrobial resistance in gram positive pathogens isolated in the UK between October 1996 and January 1997. *J. Antimicrob. Chemother.* 43:689-698.
4. Arakwa, Y.; Ohta, M.; Kido, N.; Mori, M.; Ito, H.; Komatsus, T.A. and Kato, N. J. (1985). Chromosomal β -lactamase of *Klebsiella oxytoca* new class A enzyme that hydrolyzes broad -spectrum β -lactam antibiotics. *Antimicrob. Agents Chemother.* 33(1) : 63 -70.
5. Asheshow, B.H. (1969). The Genetics of penicillinase production in *Staphylococcus aureus* strain Ps 80. *J. Gen. Microbiol.* 59(2) :289-301.
6. Atlas, R. M. (1995). Prokaryotes In: Principle of Microbiology. P.669. 3rd ed. McGraw -Hill Companies INC
7. Atmaca, S.; Saffet, E.; Nezahat, O.A. (2000). Differential production of slime by *Staphylococcus Saprophyticus* aerobic and anaerobic condition. *J. Med. Microbiol.* 49: 1051-1052..
8. Audrey R.W. and Barbara, E.M. (1990). Comparison of *Enterococcal* and *Staphylococcus* β - Lactamase Plasmids. *J. Infect. Dis.* 161 : 54-58.
9. Ausubel, F.U.; Bernt, R.; Kingston, R.E.; Moore, D.D.; Seidman, J.D. and Struhl, K. (1987). Current protocols in molecular Biology. John Wiley and Sons, Inc. New York.
10. Baird - Parker, A.C. (1963) A classification of *Micrococci* and *Staphylococci* based on Physiological and biochemical test. *J. Gen. Microbiol.* 30: 409-427.
11. Balows, A; Hauster, WJ. Jr. and Herman, K.L. (1991). Manual of clinical Microbiology Washington, De, American Society for Microbiology. p P:1194-1195.
12. Barber, M. (1962). Resistance of Bacteria to Penicillins In: Ciba foundation study. Group No.13 (A.V.S., Renck





Reem Zuhair Shinashal

- and M. P. Cameron eds.), P.89. J and A. Churchill. London.
13. Bonfiglio, G. and Livermore, D.M. (1994). Beta – lactamase types amongst *Staphylococcus aureus* isolates relation to Susceptibility to Beta – lactamase inhibitor combination. J. Antimicrob. Chemother. 33 (3) : 465 – 481.
 14. Bonomo, R.A. and Louis, B.R. (1999). Inhibitor resistant class A Beta – lactamase. (Internet). www. Yahoo.com.
 15. Brath, P.T.; Grinter, N.J. and Bradley, D.E. (1978). Conjugal transfer system of plasmid RP4. analysis by transposon 7 insertion. Molec. Gen. Genet. 133 (1) : 43-52
 16. Brown, M.R. (1975). Resistance of *Pseudomonas aeruginosa*. 1st ed. John Wiley and Son. London
 17. Brummer, W. and Gunzer, G. (1987). Laboratory techniques of enzymes recovery In: Biotechnology. (Rehm, J.H. and Read, G. eds.) pp:213 -278. vch- Derrfield Beach.
 18. Burns, W. and Keplere, H. (1987). Extracellular and membrane bound β -Lactamase for *Staphylococcus aureus*: Their importance for the expression of penicillin resistance. J. Med. Microbiol. 23:133-139.
 19. Bush, K. (1989). Characterization of β - lactamase. Antimicrob. agents Chemother. 33(3):529-563.
 20. Bush, K.; Jacoby, G. A. and Medeiros, A.A. (1995). A functional classification scheme for β - lactamase and its correction with molecular structure. Antimicrob. Agents Chemother. 39 (6):1211-1233.
 21. Christensen, G. D.; Simpson, W.A.; Bisno, A.L. and Beachey, E.H. (1982) Adherence of slime production strain of *Staphylococcus epidermidis* to smooth surface. Infect. Immun. 37 : 318 – 326.
 22. Collee, J. G.; Fraser, A.G.; Marimion, B.R; Simmons, A.S. (1996). Laboratory strategy in the diagnosis of infective syndromes In: Practical Medical Microbiology. (Mackie and Macartuney eds.) method 14th ed. Churchill Living Stones.
 23. Collins, C.H. and Lyne, P.M. (1987). Microbiological Methods. 5th ed. London.
 24. Coppoe, G.L. (2002). Penicillin derivative. (internet) www. Yahoo.com.
 25. Cowders, W.M.; Timothy, R.W.; Linda, B.; Margaret, P. and James, S. (1998). Over expression, purification, and characterization of the cloned Metallo- β Lactamase II from *Stenotrophomonas maltophilia*. Antimicrob. Agents Chemother. 42(2) : 921-926.
 26. Cruickshank, R.; Duguid, J.P.; Marmion, B.P. and Sawin, R.H. (1975). Medical Microbiology. Vol 2 12th ed. Churchill livingstone. Edinburgh. London.
 27. Cown and Steel's (1974). Manual for the Identification Medical Bacteria. 2nd ed. Cambridge University Press.
 28. Davis, B.D; Dulbeco, R.; Eisen, H.W and Wood, W.B. (1974). Microbiology. 2nd ed. Howper International edition. New York.
 29. Deighton, M.A. (1988). Species Identification, antibiotic sensitivity and slime production of coagulase– negative *Staphylococci* isolated from clinical specimens. Epidem. Infect. 101:99-113.
 30. Easmon, C.S.F. and Aldam, C. (1983). Extracellular Enzyme In: *Staphylococci and staphylococcal infections*. Vol 2. P768-775. Academic Press Inc. London.
 31. Garrod, L.P.; Lambert, H.P.; Ogrady, F. and Water Worth, P.M. (1973) Antibiotic and chemotherapy. 4th ed. Edinburgh and London, Churchill Living Stone.
 32. Gatermann, S. (1986) Virulence factor of *Staphylococcus saprophyticus*, *Staphylococcus epidermidis* and *Micrococci* In: Molecular pathogens and clinical management. (Harry, L.T. and John, W. eds.) P. 313-340. American Society for Microbiology.
 33. Gay, P., Goq, L.; Steinmetz, M.; Berkelman, T. and Kado, I. (1985). Positive selection producing for entrapment of insertion sequence elements in Gram-negative bacteria. J. Bacteriol. 164(2): 918-921.
 34. Gillipse, W. A.; Margret, A. S.; Praticia, G.; Mary, F. L. A. and Tuckwell, Hilton, A. L. (1978). Urinary tract infection in young women, with special reference to *Staphylococcus saprophyticus* J. Clin. Pathol. 31: 348-350.
 35. Grace, M. E.; George, F. J.; Hung, P. P.; and Fu, K. P. (1986). Purification and properties of a β - lactamase from *Proteus penneri*. J. Antibiotics. (7): 938-942.





An Evaluation of Renal Function among Abortive Iraqi Women Diagnosed With Toxoplasmosis and Urinary Tract Infection

Sabeeha A. Al – Sarray^{1*}, Salah M. Muhsin² and Mouruj A. Al Aubydi^{1*}

¹Department of Biotechnology, College of Science, University of Baghdad, Iraq.

²Biotechnology Research Center, University of Al-Nahrain, Iraq.

Received: 19 Sep 2018

Revised: 24 Oct 2018

Accepted: 27 Nov 2018

*Address for Correspondence

Mouruj A. Al Aubydi

Department of Biotechnology,

College of Science,

University of Baghdad, Baghdad, Iraq.

Email: mourujrabea@gmail.com



This is an Open Access Journal / article distributed under the terms of the **Creative Commons Attribution License** (CC BY-NC-ND 3.0) which permits unrestricted use, distribution, and reproduction in any medium, provided the original work is properly cited. All rights reserved.

ABSTRACT

Toxoplasma gondii and urinary tract infection (UTI) are the most prevalent infectious agents in pregnancy. This study is focused on the determination of several physiological parameters related directly or indirectly with renal function among (75) abortive women diagnosed with Toxoplasmosis and bacterial UTI in the eastern side of Baghdad city, Iraq. The results revealed that 48% of aborted women infected with *T. gondii* at the first trimester of pregnancy, as well as 48% of abortive women infected with both infection (bacterial UTI and *T. gondii*). Urea concentration was significantly increased in aborted women infected with *T. gondii* (24.75 ± 1.54) mg/dl, infected with UTI (21.37 ± 1.34) mg/dl and infected with both infection (34.69 ± 3.01) mg/dl compared to the control group (13.78 ± 0.66) mg/dl, according to gestational age, urea concentration verified significant elevation (21.06 ± 1.77 , 25.61 ± 1.98 and 26.91 ± 2.29) mg/dl in first, second, and third trimester respectively for all groups. Whereas significance rises was recognized for creatinine concentration in blood samples of aborted women infected with UTI (1.465 ± 0.95) mg/dl, and according to gestational period, creatinine concentration results showed increases in the first trimester in all abortive women (1.19 ± 0.55) mg/dl. Moreover the pH and several ions (Ca, K, Na) concentration were measured, the results revealed, no significant differences were verified in all groups except for group infected with UTI and group infected with both infection in case of Ca concentration (9.20 ± 0.19 and 9.87 ± 0.31) mg/dl respectively, but according to gestational age, the results showed there was a significant elevation in pH value for abortive women in second (7.52 ± 0.01) and third (7.52 ± 0.01) trimesters than the first one (7.34 ± 0.03).

Keywords: *Toxoplasma gondii*, UTI, urea, creatinine, pH, electrolytes, renal functions





Sabeeha A. AI – Sarray et al.

INTRODUCTION

Abortion is defined as the termination of a pregnancy before the twentieth week of gestation, while the delivery of a dead baby after twenty-four weeks of pregnancy is referred to as stillbirth. Abortion is considered one of the most stressful problems during gestation period, particularly in those who have no successful pregnancy. Abortion has an approximate prevalence of 15% worldwide [1]. *Toxoplasma gondii* is a causative agent of abortion; this parasite is an obligate intracellular protozoan which infects a wide range of warm-blooded animals. Infection in humans is usually asymptomatic, but a severe manifestation can occur in cases of congenital toxoplasmosis and immune-compromised individuals, with treatment being directed in such cases [2]. The importance of the parasite to obstetricians lies in the fact that although the great majority of infants born to mothers acquiring toxoplasmosis during pregnancy are asymptomatic, effects such as abortions, early infant mortality, and blindness are known to be associated with this zoonotic disease when mothers are infected during the first and second trimesters [3].

Throughout the gestation period, a woman undergoes several physiological changes which can be grouped as predominantly hematological, cardiovascular, hormonal, and renal. The hemodynamic profile of pregnancy is characterized by an increase in intravascular volume, cardiac output, and heart rate. Yet although maternal physiological systems undergo adjustment as a result of pregnancy, the greatest upheaval is to the renal system [4].

An evaluation of renal function is therefore necessary for women during their pregnancy. Blood urea nitrogen (BUN) and serum creatinine levels are critical indicators of renal function. The most useful tool for screening is urinalysis. Further testing is necessary if changes in renal status are detected [5]. Renal function during pregnancy can be adequately assessed by measuring the levels of serum urea and creatinine.

The decline in the normal range values of urea and creatinine during pregnancy has clinical consequences; normal urea and creatinine levels in pregnant women may indicate an underlying renal disease [6]. Pregnancy is also associated with a substantial reduction in pCO₂ levels and this change is indicative of the diffusion between maternal and fetal circulations [7]. The possible causes of a rise in plasma/serum urea in observance with a normal glomerular filtration rate (GFR), or what is otherwise referred to as normal renal function, include both physiological and pathological factors; the two physiological components are ageing and increased dietary protein. Pathological causes include possible hemorrhage in the gastrointestinal region related to increased protein consumption (blood in the gastrointestinal tract is effectively a high-protein meal) which in turn leads to increased urea production and, subsequently, increased plasma/serum urea concentration [8]. As well as heart failure [9], hypovolemic shock and dehydration [10] necessarily enhance this adaptive response and may all be associated with slight increases in plasma/serum urea concentration in spite of a normal GFR. On the other hand, UTIs are indicative of bacteriuria and are more common (up to 7%) during pregnancy. It is found in approximately 2% of sexually active women; of those, 25% go on to develop pyelonephritis during pregnancy because of the dilatation of the calyces and ureter, which can cause intrauterine growth restriction (IUGR) due to reduced levels of maternal plasma protein, fetal death, or premature labor [11].

Furthermore, pregnancy has been identified as a period marked by intense change in a woman's electrolyte level [12]. The ability to regulate nutrients and balance electrolytes during pregnancy is critical to the health of both the mother and the growing fetus [13]. Levels of urea and creatinine observed in pregnant women who carry symptoms of toxoplasmosis and bacterial UTI have improved in recent years. This study is focused on several biochemical factors related to kidney function among abortive women native to the eastern side of the city of Baghdad, Iraq. However, a practical question arises when dealing with abortive women whom we will endeavor to unpack first; it entails the identification of the reasons which may lead to miscarriage and/or abortion.





Sabeeha A. Al – Sarray et al.

MATERIALS AND METHODS

Subjects of study

This study was carried out on 75 of abortive Iraqi women. The first group included 25 abortive women infected with *Toxoplasma gondii*; the second group involved 25 abortive women infected with a UTI; the third group included 25 abortive women infected with both toxoplasmosis and a UTI. In addition to these groups, an additional group of 25 apparently healthy pregnant (control group) with an age range of 18-41 years old. The samples obtained from participants in a period between 1 / 3 / 2017 to 1 / 7 / 2017 from three main hospitals related to gynecology and obstetrics located in the eastern side of Baghdad.

Sample collection

Five ml of venous blood sample was obtained from each patient and control subject by sterile syringe under sterile condition, put into sterile gel tube, after clotting the centrifugation was carried out at 3000 rpm for 5 minutes, then the serum was directly use for biochemical test

Measurement of serum urea and creatinine level

Measurements of serum urea and creatinine levels were carried out by using Fuji dry –chemistry analyzer (NX500i) from (Fuji film /Japan), uses dry – chemistry principle, with its quick, easy operation and higher sensitivity .

Measurement of serum pH and electrolyte levels

Measurement of serum pH and electrolyte levels were done by using HumaLyteplus 5 (Germany), this instrument uses ion-elective electrode principle.

RESULTS AND DISCUSSION

The results in (Table 1) showed that, most early abortions occurred due to *Toxoplasma gondii* infection, and particularly during the first trimester, as well as 48% of abortive women infected with both infection (bacterial UTI and *T.gondii*). In addition 48% of UTI group, the abortion occurred more through late period of pregnancy. *Toxoplasma gondii* apparently appeared to be the overriding factor responsible for abortions amongst our participants. In addition, the results presented in Table 1 also demonstrate that a higher percentage of abortions in the UTI group occurred later in the pregnancy. The results that were obtained for the purposes of this study are compatible with Seviet al. [14], who noted the role of infections in relation to systemic infections such as viral, parasitic, and bacterial vaginitis leading up to miscarriages.

Urea and creatinine concentrations

The results in (Table 2) showed that, a significant increase in urea concentration across all infected groups compared with the control group. Furthermore, the results do not indicate a significant difference between group 1 and 2. In fact, there appears to be a synergistic effect between both infections as can be observed from the results of group 3, which demonstrated a significant increase in urea concentration levels compared with each infected group (groups 1 and 2).



**Sabeeha A. AI – Sarray et al.**

Whereas a significant difference was observed for creatinine concentrations in blood amongst group 2 participants carrying UTIs, this was not the case across any of the other groups. These results revealed the impact of UTIs on kidney function. On the other hand, *Toxoplasma gondii* clearly does not have the same impact as UTIs on kidney function as demonstrated by the non-significant results recorded for creatinine concentration levels in group 3. These findings clarify the detrimental effect of bacterial UTIs on kidney function, particularly when it progresses to a chronic stage. Biliel *et al.* lend credibility to this result when stating that "the most important factor affecting fetal and maternal prognosis is the degree of renal function at conception" [15]. Moreover, according to gestational stage, urea concentration levels were significantly higher across all trimesters, particularly the third trimester (Table 3). Yukari *et al.* [16], mentioned the presence of substantial negative associations between the BUN level and gestational age in the latter cohort or the birth weight therefore it can be suggested that increasing blood urea levels during pregnancy is a worrying factor which may contribute to weakening the fetus and thus lead to abortion. The results also indicate higher creatinine levels in the first trimester in comparison with individuals in other trimesters across all abortive women (Table 3).

This increase in serum urea concentration reveals the equilibrium between urea production in the liver and urea elimination by the kidneys. During glomerular filtration, urea passes from blood to the glomerular filtrate, the fluid that is the precursor of urine. The concentration of urea in the filtrate as it is formed is similar to that in plasma so the amount of urea entering the proximal tube of the nephron from the glomerulus is determined by the glomerular filtration rate (GFR). Compromised kidney function, whatever its cause, reduces the GFR and there appears to be a strong correlation between the GFR and the severity of kidney diseases because glomerular filtration rate is the best test to measure level of kidney function and determine the stage of kidney disease. [10]. In comparison with urea, creatinine measurement is no more sensitive but is more indicative of kidney function. Urea and creatinine are good indicators of a normal functioning kidney and increase in the serum are indications of kidney dysfunction [17]. The decline in the concentration levels of apparently healthy pregnant women (the control group) as shown in (Table 4) has extensively reflected the functional impact of pregnancy on kidney physiology, including practically all features of kidney function (higher GFR with a subsequent decrease in serum creatinine, urea, and uric acid values). Abortion accompanied by *Toxoplasma gondii* and bacterial UTI has shown a rise in urea concentration, revealing the stress factors directed against kidney function due to these infections as well as other possible causative agents such as hormonal disturbances which can cause an abortion as Al-Kaissy *et al.* noted [18].

In addition to previous parameters, some serum electrolytes (Na, Ca, and K) and their relationship with blood/serum pH levels were measured for the studies groups and compared with the control group (Table 5). The main findings for these parameters, there appears to be no significant differences ($P \leq 0.01$) which can be observed across all groups except for group 2 and 3 in the case of Ca concentration. But when these parameters are evaluated according to gestational stage (Table 6), a notable increase in pH value is apparent for second and third trimester in abortive women as opposed to those in their first trimester. There also appears to be a correlation coefficient (inverse relationship) between pH and sodium ion levels (Table 7). This correlation suggests that when pH levels are raised, the Na ion level decreases while the K ion level increases in the blood. This may be directly associated with blood pressure, the consequences of which may also lead to abortion. This suggestion is confirmed by the results in Table 3, which depicts the dysfunctional nature of abortive women's kidney function during the first trimester. These findings indicate the high regulation of body liquid osmolality throughout acid-base homeostasis and pH regulation and stabilization; both are serious for normal physiology as well as cell metabolism and function. The importance of this regulation is demonstrated by a variety of physiological disorders that occur when plasma pH levels are either too high or too low. The kidneys play a major role in regulating the systemic bicarbonate concentration and, hence, the metabolic component of acid-base balance, as Hamm *et al.* described [19].

As shown in Table 5, pH values for the studies groups show little variation in comparison with the control group, these variations are critical in the language of pH analysis because a slight change in the pH level may significantly affect the function of various fetal organ systems such as the cardiovascular and central nervous systems, which can





Sabeeha A. Al – Sarray *et al.*

fuel fetal distress and induce a poor Apgar score, as Omo-Aghoja documented [20]. Therefore, our observation that abortions during first trimester are recorded more than other trimesters, because any disturbances in the acid-base may involve the complex interplays of different organ systems which include the brain, lungs, kidney, and liver. Compensations for acid-base disorders within the brain are more complete, while limitations of compensations are more apparent for most systemic disorders as Seifter and Chang reviewed [21].

On the other hand, the results concerning electrolyte levels across the different groups showed no significant differences in the levels of Ca, Na, and K concentrations in blood/serum, except for Ca concentration associated with group 3. This finding contradicts the findings of [22,23], who reported that electrolyte derangements among pregnant women is perhaps due to the variation in the pattern of infection. However, Barber *et al.* found normal electrolyte levels among pregnant women infected with the malarial intracellular parasite [24].

CONCLUSION

Kidney function assessment is essential to form a better understanding of electrolyte excretion and renal compensations in cases of abortion accompanied by toxoplasmosis and bacterial UTIs. Urea concentration levels in blood/serum were higher in all observed groups in comparison with the control group. Thus, we may conclude that bacterial UTIs have a notable impact on kidney function through the observation of increased creatinine concentrations in the blood/serum of aborted women. Furthermore, the different infections included in this study did not impact on the concentration of Ca, Na, K, and pH levels in the blood, with the exception of Ca. However, first trimester abortive women showed significant differences in their blood pH levels which carried an inverse relationship with Na levels. Since the blood samples used for the purposes of this study were directly collected post abortion, it can be concluded that the results delivered from the testing of these samples are credible in delivering worthwhile analyses about abortion and the causes of it.

REFERENCES

1. Gray, C. F. E. (2014). *Concise Williams Obstetrics*. New York: McGraw Hill.
2. Dubey, J. P., Lago, E. G., Gennari S. M., Su C., and Jones, J. L. (2012). *Toxoplasmosis in humans and animals in Brazil: High prevalence, high burden of disease, and epidemiology*. *Parasitology*; 10: 1–50.
3. Singh, M. (2016). *Seroprevalence of toxoplasmosis in pregnant females attending a Tertiary Care Hospital in Uttar Pradesh, India and its effect on perinatal morbidity and mortality*. *Acta Medica*; 3(1):50.
4. Isra, H. and Hamdani, A. L. (2006). *Measurement of serum uric acid urea and creatinine in pregnant women*. *Medical Journal of Tikrit*, 122(2): 31-35.
5. Airoidi J., Weinstein, L. (2007). *Clinical significance of proteinuria in pregnancy*. *Obstetrics and Gynecology Survey*, Vol. 62, pp. 117–24.
6. Patricia, O.O., Christiana, B. A., and Raphael, O. J. (2013). *Evaluation of changes in renal function of pregnant women* *lied Science Research*, 5 (4):111-116.
7. Spencer, J. A. (1999). *Intrapartum fetal monitoring*. In: Edmond, D. K., ditor. *Dewhurst Textbook of Obstetrics and Gynaecology for Postgraduates*. 6th ed. United Kingdom: Blackwell Sciences Ltd; pp. 259–76.
8. Witting, M. D. (2006). *Predictors of upper gastrointestinal tract bleeding in patients without hematemesis*. *Am J Emerg Med* 2006; 24, 3: 280-85.
9. Aronson, D. (2004). *Elevated blood urea nitrogen level as a predictor of mortality in patients admitted for decompensated heart failure*. *The Am J Med*; 116, 7: 466-73.
10. Mehta, A. R. (2008). *Why does the plasma urea concentration increase in acute dehydration? Advances in physiology education*; 32, 4: 336.
11. Bretelle, F., Arnoux, D., Shojai, R., D'Ercole, C., Sampol, J., Dignat, F., Camoin-Jau, L. (2005) *Protein Z in patients with pregnancy complications*. *Am J Obstet Gynecol*. 193(5): 1698-702.





Sabeeha A. AI – Sarray et al.

12. Zavalza-Gomez, A. B., Anaya-Prado, R., and Rinan-Sanchez, A. R. (2008). *Ipokinesand insulin resistance during pregnancy. Diabetes Research and Clinical Practices*; 80: 8-15 .
13. Mayne, D. P. (1994). *Sodium, Potassium and Water Metabolism: in Clinical Chemistry in Diagnosis and Treatment*. 6th edition; Arnold Euston Publishers, London (pp 25-78).
14. Sevi, G., Nick, W., Kate, C., Gary, E., Sarah, E., Howie, A., W. Horne. (2016). *The role of infection in miscarriage. Human Reproduction Update*, Volume 22, Issue 1, pp116–133.
15. Bili, E1., Tsolakidis D1., Stangou, S2., Tarlatzis, B. (2013). *Pregnancy management and outcome in women with chronic kidney disease. HIPPOKRATIA*, 17, 2:163-168.
16. Asamiya, Y., Otsubo, S., Matsuda, Y., Kimata, N., Kikuchi, K., Miwa, N., Uchida, K., Mineshima, M., Mitani, M., Ohta, H., Nitta, K., and Akiba, T. (2009). *The importance of low blood urea nitrogen levels in pregnant patients undergoing hemodialysis to optimize birth weight and gestational age*. 75, 1217–1222; doi:10.1038/ki.2009.48.
17. Lamb, E. *Kidney Function Tests (Chapter 25) In: Tietz Textbook of Clinical Chemistry and Molecular Diagnostics*. By: Burtis, C. A., Ashwood, E. R., Bruns, D. E. Elsevier Health Sciences; 2012.
18. Al-Kaissy, A. M., Eid, R. A. A., and Fahmy, B. G. A. (2010). *Biochemical studies on the effect of Toxoplasma infection on liver and kidney functions in mice*. Egypt. J. Comp. Path. & Clin. Path., 23(1), pp: 174–185.
29. Hamm, L., Lee, Nakhoul, N., and Hering-Smith, K. S. (2015). *Acid-Base Homeostasis*. Clin J Am Soc Nephrol. 7; 10(12): 2232–2242.
20. Omo-Aghoja, I. (2014). *Maternal and fetal Acid-Base chemistry: A major determinant of perinatal outcome*. Ann. Med. Health Sci. Res; 4(1):8-17.
21. Seifter, J. L., Chang, H. Y. (2016). *Disorders of Acid-Base Balance: New Perspectives*. Kidney Dis 2016; 2:170-186.
22. Elbadawi, N. E., E. K. Ibrahim, and Dawod, O. (2013). *The effect of malaria on biochemical renal function parameters in Sudanese pregnant women*. Journal of Cell Biology and Biochemistry Research, vol. 1, no. 1, pp. 4–7.
23. Brown, S., Azike, C. A., and Obisike, U. A. (2015). *Electrolyte imbalance in pregnant women with malaria parasitaemia*. American Journal of Biomedical Sciences, vol. 7, no. 3, pp. 148–155.
24. Barber, B. E., Bird, E., Wilkes, C. S., et al. (2015). *Plasmodium knowlesi malaria during pregnancy*. Journal of Infectious Diseases, vol. 211, no. 7, pp. 1104–1110.

Table 1: The percentage of abortions according to gestational stage

Groups	1 st trimester	2 nd trimester	3 rd trimester	Chi-Square
Infected with Toxoplasmosis(25)	48%	40%	12%	10.66 **
Infected with UTI(25)	20%	32%	48%	8.41 **
Infected with Toxoplasmosis and UTI(25)	48%	28%	24%	8.07 **
Chi-Square	8.38 **	7.62 **	10.74 **	---

** (P<0.01)

Table 2: Serum levels of Urea and creatinine in aborted and healthy pregnant women

Groups	Mean ± SE	
	Urea concentration (mg/dl)	Creatinine concentration (mg/dl)
Group 1 (toxoplasmosis)	24.75 ± 1.54 B	0.614 ± 0.05 A
Group 2 (UTI)	21.37 ± 1.34 B	1.465 ± 0.95 B
Group 3 (toxoplasmosis & UTI)	34.69 ± 3.01 A	0.704 ± 0.06 A
Group 4 (control group)	13.78 ± 0.66 C	0.778 ± 0.047 A
LSD value	5.200 **	0.497 **
P-value	0.0001	0.001

** (P<0.01), NS: non-significant.
Different letters indicates significant differences





Sabeeha A. AI – Sarray et al.

Table3 : Serum level of Urea and creatinine according to gestational stage in all aborted women

Gestational stage	Mean ± SE	
	Urea conc. (mg/dl)	Creatinine conc. (mg/dl)
First	21.06 ± 1.77 A	1.19 ± 0.55 A
Second	25.61 ± 1.98 B	0.596 ± 0.04 B
Third	26.91 ± 2.29 B	0.642 ± 0.07 B
LSD value	4.230 *	0.417 *
P-value	0.0498	0.0451

* (P<0.05), NS: Non-Significant. Different letters indicates significant differences.

Table4: Serum level of Urea ,creatinine in healthy pregnant women according to gestational stage

Pregnancy stage	Urea (mg/dl)	Creatinine (mg/dl)
First trimester	12.36 ± 0.55 b	0.25 ± 0.03 a
Second trimester	15.12 ± 0.63 a	0.33 ± 0.04 a
Third trimester	17.51 ± 0.67 a	0.35 ± 0.07 a
LSD value	2.951 **	0.118 NS
P-value	0.0046	0.084

Table 5: pH and electrolyte concentrations in aborted and healthy pregnant women

Group	Mean ± SE			
	pH	Ca concentration (mg/dl)	Na concentration (mEq/L)	K concentration (mEq/L)
Group 1 (toxoplasmosis)	7.45 ± 0.03 A	8.86 ± 0.14 B	132.12 ± 2.06 A	3.85 ± 0.09 A
Group 2 (UTI)	7.44 ± 0.04 A	9.20 ± 0.19 B	132.20 ± 2.70 A	3.93 ± 0.10 A
Group 3 (toxoplasmosis&UTI)	7.43 ± 0.04 A	9.87 ± 0.31 A	132.20 ± 2.33 A	3.83 ± 2.33 A
Group 4 (control group)	7.41 ± 0.04 A	8.68 ± 0.12 B	130.64 ± 2.33 A	3.96 ± 0.09 A
LSD value	0.108 NS	0.582 **	6.652 NS	0.279 NS
P-value	0.872	0.0006	0.957	0.778

** (P<0.01), NS: Non-Significant. . Different letters indicates significant differences

Table 6: pH and electrolyte concentrations according to gestational stage in all abortive women

Gestational stage	Mean ± SE			
	pH	Ca concentration (mg/dl)	Na concentration (mEq/L)	K concentration (mEq/L)
First	7.34 ± 0.03 B	9.08 ± 0.15 A	133.21 ± 1.76 A	3.81 ± 0.06 A
Second	7.52 ± 0.01 A	9.31 ± 0.19 A	130.00 ± 1.91 A	3.98 ± 0.08 A
Third	7.52 ± 0.01 A	9.05 ± 0.31 A	131.47 ± 2.65 A	3.93 ± 0.15 A
LSD value	0.091 **	0.599 NS	6.245 NS	0.263 NS
P-value	0.0001	0.598	0.467	0.292

** (P<0.01), NS: Non-Significant.
Different letters indicates significant differences





Sabeeha A. Al – Sarray et al.

Table 7: Correlation coefficient between pH and electrolyte levels in abortive women

Parameters	Correlation coefficient(r)with pH	Level of significance
Ca concentration	0.004	NS
Na concentration	-0.19	*
K concentration	0.12	NS
* (P<0.05), NS: Non-Significant.		





Determination of Yamama Reservoir Units Thicknesses by 3D Post Stack Seismic Data. (Abo-Amood Field in Southern Part of Iraq).

Nawal Abed Al-Ridha, Faleh Mahdi and Mazin R. Lafta*

Department of Geology, Collage of Science, University of Baghdad, Baghdad, Iraq

Received: 20 Aug 2018

Revised: 24 Sep 2018

Accepted: 27 Oct 2018

* Address for Correspondence

Mazin R. Lafta

Department of Geology,

Collage of Science,

University of Baghdad,

Baghdad, Iraq

Email: rasheedmazin@yahoo.com



This is an Open Access Journal / article distributed under the terms of the **Creative Commons Attribution License** (CC BY-NC-ND 3.0) which permits unrestricted use, distribution, and reproduction in any medium, provided the original work is properly cited. All rights reserved.

ABSTRACT

The study is an attempt to find out the thickness distribution of reservoir units of Carbonate Yamama Formation (early cretaceous) in (Abo-Amood) and east (Abo-Amood) field in southern part of Iraq by 3D post-stack seismic data of 1534.88 Km² survey area. Seven Isopach maps were prepared for the stratigraphic reservoir units by using isochron maps and interval velocity values which derived from 6 wells velocity survey, seven instantaneous frequency maps (seismic attribute) were drawn in order to confirm the distribution of thicknesses, Geo-frame software was used to detected top, bottom and seven reservoir units of Yamama Formation in (Abo-Amood) field.

Keywords: reservoir units, isopach maps, instantaneous frequency, Yamama Formation, Abo-Amood field, Iraq.

INTRODUCTION

The study is an attempt to find out the thicknesses distribution of reservoir units of carbonate Yamama Formation (early cretaceous) in (Abo-Amood) and east (Abo-Amood) field in southern part of Iraq by 3D post-stack seismic data of 1534.88 km² survey area. The importance of knowledge of the distribution of the reservoir units thicknesses come from the fact that it gives a picture of the facies improvement direction and helps in determining the location of thickness increasing which may represent the ideal locations of new wells [1]. In reservoir studies the knowledge of units thicknesses distribution contribute in directing of oil wells drilling sites selection and reducing risks and costs [2]. A new method used to confirm the acceptability of the results of seismic data analysis by using the knowledge of the thickness distribution of the stratigraphic carbonate units of Yamama Formation, and compare it to the thickness distribution derived from the wells information, which showed a high correlation at wells locations that indicating the certainty of the results of isopach maps derived from seismic data. The change in thickness reflects the change in



**Nawal Abed Al-Ridha et al.**

topography of sedimentary basin and its relation to sea level change .Which are controlled by the tectonic factor, the climate and the amount of sedimentary supplying. As by studying the range of the thickness of each unit of Yamama Formation and determine the relationship between the thickness of each unit and the others, we can identify and recognize the fluctuation occurring at sea level during the deposition of Yamama units, and this fluctuation caused by local tectonic activity, which led to the cycle of Yamama deposition within the early cretaceous cycle. The approach of this thesis also included the attempt to find a relationship between the distributions of high thickness of the carbonate units derived from the seismic data with the distribution of low frequency values, which showed acceptable compatibility in most units. In current study CPS program on Geo-frame software was used to detected top, bottom and reservoir units of Yamama Formation in (Abo-Amood) field. Seven Isopach maps were prepared for the stratigraphic reservoir units and seven instantaneous maps (seismic attribute) were drawn in order to confirm the thicknesses distribution over Yamama reservoir.

Location of the Study Area

Abo-Amood field is located at southern part of Iraq within the administrative boundaries of three provinces (Maysan, Thi-Qar, and Wasit) (figure1). The area of 3D seismic survey is 1534.88 km²) which is determined by coordinates according UTM WGS 84 system (figure -2), [3].

Tectonic Setting of Study Area

The study area is located in the south-eastern part of Iraq, which represents the northern and north-eastern parts of Arabian plate [4]. Abo Amood field located in Basrah Depression as a part of unstable shelf of Mesopotamian basin which is surrounded by Salman shelf at the west, Dezful Embayment and Lurestan platform of Iran at the East, Basrah Depression separated by Basrah Arch from Arabian Gulf at the South and surrounded by Tigris-Hilla Depression from the north[5] .The Basrah Depression axis have two directions, (NS) and (NW – SE) as a result of the salt movement in Mesozoic due to the effect of Zagros orogeny[6]. Abo Amood structure (study area) has axis in (NW – SE) directions and tectonically located in the southern part of the wing close to the platform flank of Mesopotamian within the Sub – Euphrates Zone of the sedimentary plain which represents the largest unit of unstable shelf units [7].

Stratigraphic Setting of Study Area

The sedimentary history of the study area refers to the dominance of calcareous sediments on stable areas and appearance of large-scale platforms boarded by the (Neo- Tethys) from the east and clastic sediments replace the carbon – limestone sediments in the western direction of Arabian plate due to being close to supplying area which was severing from uplifting in the Arabian shield region. The sediments developed after Hercienic movement, so that the dominance of shallow carbonate sedimentary platforms covering large areas of Arabian Plate which accompanied by an abundance of evaporation sediments that observed with invasion of clastic incursions which is originated from the Arab Shield during the late Carboniferous – Early Jurassic. During the middle Jurassic – Turonian age the limestone platforms became more distinctive (Differential Platforms) through the presence of Intra-Shelf Basin, while during the early cretaceous the climate conditions became more humid causing the disappearance of evaporation sediments from stratigraphic column of this age with presence of the ramp type of carbonate platforms which represents the sediments of Yamama formation during (late Berriasian –Valangian sediments),[8].



**Nawal Abed Al-Ridha et al.**

Geology of the Study Area

Surface Geology

The study area consists of the flat and board plains of the Tigris and Euphrates rivers. Abo Amood and Eastern Abo Amood field is part of the sedimentary plain of the Mesopotamian plain in its southern part, located between Tigris and Euphrates rivers. Most parts of the region are large flat lands covered with the sediments of the Holocene age which is composed of river deposits that filled the depressions with channels sediments formed of sand and silt, which are deposited as a result of river floods. The majority of the fields and structures in the Mesopotamian basin are not characterized by existence of any natural surface features that can indicate the effects of the subsurface structural conditions such as anticlines and fault [9].

Subsurface Geology

Six wells were drilled in the study area (Abo Amood and Eastern Abo Amood), four were ended at Yamama Formation and AAm1 well ends at Najma Formation in the late Jurassic, while Eastern AAm end at Yamama Formation. The exploratory drilling of the AAm1 well was carried out in 1980 at the crest of the structure shows the stratigraphic column which starts from the upper Miocene (Upper Fars Formation).

Yamama Formation

This formation was defined by Steint and Biamkainp in (1952) as being exposed on the surface (outcrops) in Saudi Arabia, and described by (Van Bellen et.al 1959) as (257 m) interval in Ratawi -1 well in the south of Iraq as Yamama - Sulaiy Formation. The upper (203 m), now assigned to the Yamama Formation comprises (12 m) of spicular and brown detritus limestone with thin shale beds overlain by (191 m) of micritic limestone and oolitic limestone. Yamama Formation is of Berriasian-Volanganian age .It was deposited in alternating oolitic shoal and deep inner shelf environments, probably controlled by subtle structural highs within a carbonate ramp [10].The thickness and depth of Yamama Formation in Abo Amood and eastern Abo Amood field were determined from the wells (AAM1 – and EAA1), (table 1).

Synthetic Seismogram Generation

The process of generation of six synthetic seismograms which were carried out for six drilled wells of AAm and EAA field including the using of all formations of well logs (marker, sonic, and velocity) to identify reflectors of seismic data and for seismic correlation purposes. The deterministic method has been adopted in the calculation of the wavelet from seismic data. In line seismic section number (53850) with AAm1 well, synthetic seismogram projection was taken to identify the reflection on seismic data (VA) (variable Amplitude section), The synthetic seismogram of the sixth wells were projected on the seismic data for seismic stratigraphic correlation overall seismic cube area. Arbitrary line pass through (AAM 4, 1, 2 and EAA1) wells on seismic section shows the seismic correlation between synthetic seismograms of these wells and seismic data with good matching (figure 3).

Reflectors Definition

After completion of reflectors defining process on seismic data which represent top, bottom and reservoir units of Yamama Formation over all post-stack seismic cube by picking it in (5) inline and (5) cross-line interval, an interpolation for picking process has been applied to fill the interval spaces to become on whole seismic cube at Yamama reflectors level (figure 4 and 5).The information of 6 wells (marker log) was used to determine the depth of Yamama Formation and to detect Yamama units on seismic section at wells location .





Nawal Abed Al-Ridha et al.

Isopach Maps from Seismic Data

Isopach maps were prepared for stratigraphic units of Yamama reservoir in (Abo-Amood) and east (Abo-Amood) field by using the isochron maps and interval velocities which derived from the information of wells survey for the purpose of the conversion process from the time domain to the depth domain to extract the isopach maps, seven units isopach maps were drawn as follow:

Top Yamama Unit

The thickness increasing occurred in NW direction with the presence of two anomalies of thickness decreasing in the middle of study area. Unit thickness ranges from (27) m to (67) m (figure 6).

Yamama B1 Unit

The thickness increasing occurred in NW direction around wells sites as well as to the SE direction, unit thickness ranges from 5m to 68m (figure 7).

Yamama B2 Unit

Thickness increased in the middle area between the crest of (Abo-Amood) structure and the east (Abo-Amood) structure. There is also an increase in thickness in area around east (Abo-Amood) well, as well as the area around the wells of (Abo-Amood) unit thickness ranges from 5m to 93m (figure 8).

Yamama B3 Unit

The highest increasing is located in the south eastern region where the thickness reaches to 90m; there are significant decreases in the area surrounding (Abo-Amood) wells. Unit thickness ranges from 10m to 95m (figure 9).

Yamama C1 Unit

The highest thickness located in (Abo-Amood) wells area which is extended to the center of area and then begin to decreases in the area of east (Abo-Amood), unit thickness ranges from 10m to 55m (figure 10).

Yamama C2 Unit

The thickness increases significantly in the far NW of (Abo-Amood) field to reached 130m in the middle of the study area the thickness rate ranges from (45 – 55)m and continues at the same rate towards the east (Abo-Amood) field. Unit thickness ranges from 30m to 130m (figure 11).

Yamama C3 Unit

The highest increases concentrated at the far SE of the study area in the entire study area the thickness rate is almost equal and ranges from 10m to 85m (figure 12).

Seismic Attribute

Seismic attribute are specific measurements of geometry, kinematic, dynamic or statistical features derived from seismic data [11].





Nawal Abed Al-Ridha et al.

Instantaneous Frequency Attribute

Instantaneous frequency is the time derivative of phase, i.e., the rate of change of the phase: $F(t) = d(\phi(t)) / dt$. [12]. The seismic cube of study area was processed and converted to the frequency domain to calculate the instantaneous frequency attribute in order to identify the low instantaneous frequency zones within Yamama reservoir. The compatibility between the high thickness area of the reservoir units and the low frequency values were evident.

Top Yamama Unit

Abo-Amood field wells (2, 5, and 4) are located at low frequency anomaly of 30Hz, while other wells are at range (36 to 38) Hz (figure 13).

Yamama B1 Unit

Abo-Amood field wells (1, 2, 3, 4, and 5) fall within low frequency anomaly of 20Hz. Also could notice the presence of two low frequency anomalies one in the NW and the other in the SE of the study area, (figure 14).

Yamama B2 Unit

This unit is characterized by the same frequency behavior of (B1) unit, where the wells of Abo-Amood fields fall within low frequency anomalies are of 20Hz, while east Abo-Amood well is located within 35Hz frequency zone, (figure 15).

Yamama B3 Unit

Abo-Amood wells as well as east Abo-Amood well are located within the low frequency range from (25-30) Hz (figure 16).

YamamaC1 Unit

It is possible to observe that the area of the wells within this unit is still in the low frequency zone (13-25) Hz and this range has expanded east wards to the center of study area (figure 17).

Yamama C2 Unit

The low frequency zone in this unit continues with the same direction and expansion of C1 unit (figure 18).

Yamama C3 Unit

Its barrier unit, that's why we note that the area of the wells does not exist within the low frequency zone and the low frequency anomalies that have been marked in the above reservoir units have disappeared in this unit (figure 19).

CONCLUSIONS

The isopach maps were drawn for the stratigraphic units, which were calculated in two approaches, from wells and post - stack seismic data, showed a significant matching in the calculated thickness of the two methods at the wells





Nawal Abed Al-Ridha et al.

locations and that this match indicates that the isopach maps derived from the seismic data can be adopted in determining the distribution of thicknesses along the study area at the level of Yamama Formation.

1. There is a clear matching between high thicknesses distribution of stratigraphic units and low instantaneous frequency values.
2. The thickness increasing starts from north western at top and B1 units to concentrate in the middle of study area at B2 unit to record a marked increasing in the SE region at B3 unit. While thickness increasing trend turn to N W at C1, C2 units to become almost in one level at C3 unit.
3. The change in thickness reflects the change in topography of sedimentary basin and its relation to sea level change .Which are controlled by the tectonic factor, the climate and the amount of sedimentary supplying. As by studying the range of the thickness of each unit of Yamama Formation and determine the relationship between the thickness of each unit and the others, we can identify and recognize the fluctuation occurring at sea level during the deposition of Yamama units, and this fluctuation caused by local tectonic activity, which led to the cycle of Yamama deposition within the early cretaceous cycle. The results showed that: the change in the sea level is began with a sea regression towards the south–east direction represented by (Top, B1, B2, and B3) Yamama units, and then the sea began to transgression towards the north–west starting from the C1 unit to the end of Yamama Formation. This diagnosis is important and useful in the calculation of oil reservoirs in the future studies of Abu– Amoud and east Abu–Amoud fields.

ACKNOWLEDGEMENTS

The researchers are pleased to thank the administration of the oil exploration company of the Iraqi Ministry of Oil for provided all three-dimensional seismic data as well as wells information in the study area. We also thank the employees of the company who contributed in providing the necessary assistance.

REFERENCES

- 1- Aqrabi, A. A. M., Goff, J. C., Horbury, A. D., & Sadooni, F. N. (2010). The petroleum geology of Iraq. Cambrian Printers, Aberystwyth, 424.
- 2- Beydoun, Z. R. (1993). Evolution of the north-eastern Arabian plate margin and shelf: Hydrocarbon habitat and conceptual future potential. *Revue de l'Institut Français Du Pétrole*, 48(4), 311–345.
- 3- Buday, T., & Jassim, S. Z. (1987). The Regional geology of Iraq, vol. 2: Tectonism, Magmatism and Metamorphism. Publication of GEOSURV, Baghdad, 352.
- 4- Buday, T. (1980). The regional geology of Iraq: stratigraphy and pale geography. State Organization for Minerals, Baghdad, Iraq, Vol.1.
- 5- Chen Q., and Sidney, S. (1997), seismic attributes technology for reservoir forecasting and monitoring leading Edge. 16, 445-448.
- 6- Jassim, S. Z., & Goff, J. C. (2006). Phanerozoic development of the northern Arabian Plate. Geology of Iraq, Publication of Dolin, Prague and Moravian Museum, Brno.
- 7- Maheucci, G., 1996, seismic attributes analysis and calibration: A general procedure and a case study: annual meeting abstracts, society of exploration Geophysicists, 373,376
- 8- Mitchum, R.M.Jr., 1977, seismic stratigraphic and global changes of sea level, part 1: glossary of terms used in seismic Stratigraphy application of petroleum geologists, Memoir 26, p, 205-212
- 9- Murriss, R. J. (1980). Hydrocarbon Habitat of the Middle East.
- 10- OEC, 2013, final field report of 3D seismic survey for Abo-Amoud field, internal report.
- 11- Partyka, G, Gridley, J., and Lopez J. 1999, interpretational applications of spectral decomposition in reservoir characterization: the leading Edge, vol. 18(3), pp.353-360.





Nawal Abed Al-Ridha et al.

12- Sadooni, F. N. (1993). Stratigraphic sequence, microfacies, and petroleum prospects of the Yamama Formation, Lower Cretaceous, southern Iraq. AAPG Bulletin, 77(11), 1971–1988.

Table 1. thickness and depth of Yamama Formation in study area

Well	Depth (m)	Thickness (m)
AAM1	3865.6	232.5
EAA1	4055.1	342.0

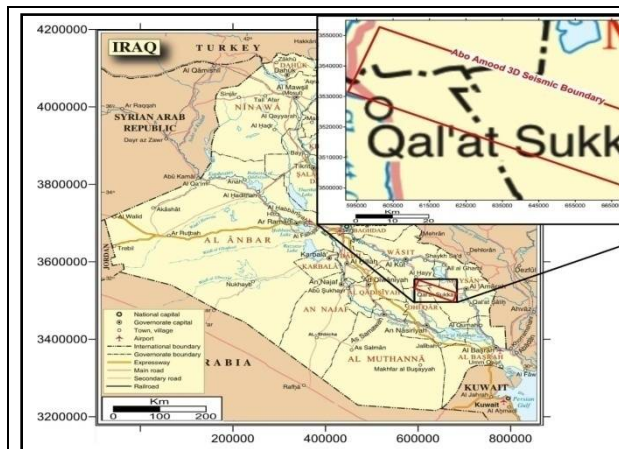


Figure 1: Location map of study area.



Figure 2: Base map of study area with surface boundaries and well locations

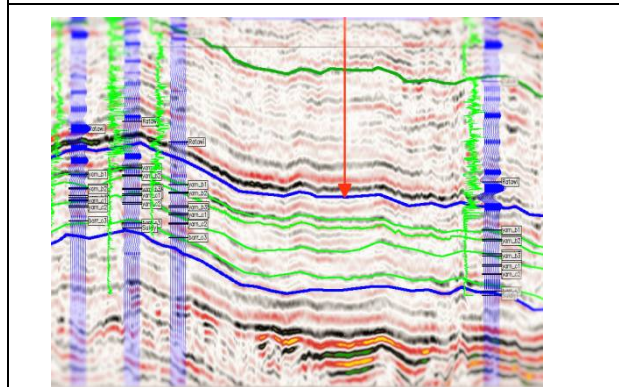


Figure 3 : Arbitrary line through AAM4, 1, 2 and EAA1wells on seismic section.

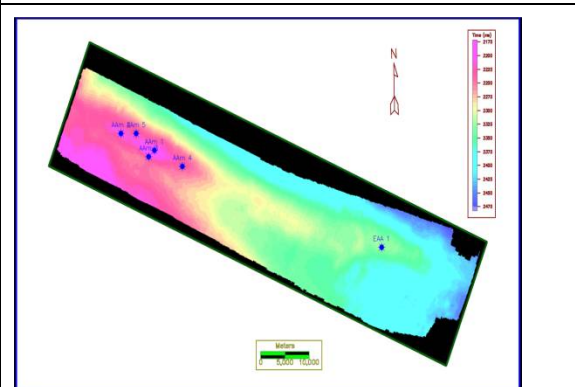


Figure 4: Top Yamama Formation picking in (5) inline and (5) crossline interval.





Nawal Abed Al-Ridha et al.

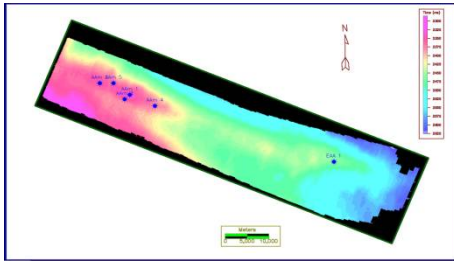


Figure 5: Bottom Yamama Formation picking in (5) inline and (5) crossline interval.

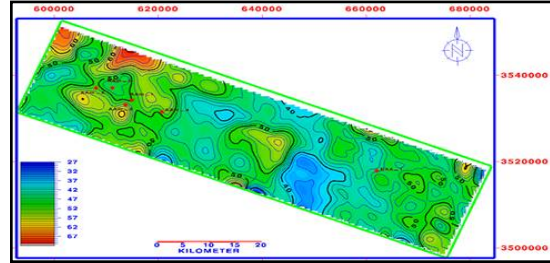


Figure 6: Top unit isopach map from seismic data

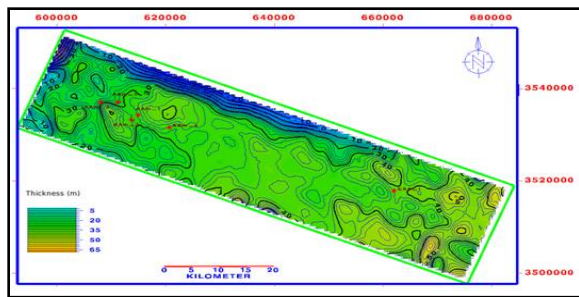


Figure 7: Yamama B1 unit isopach map from seismic data.

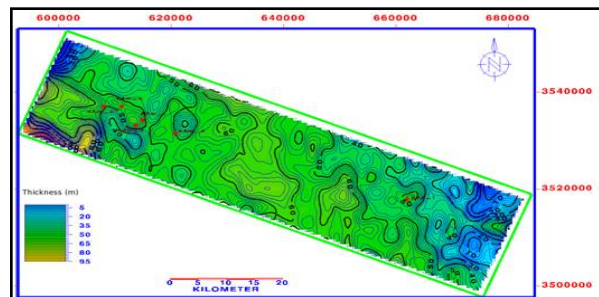


Figure 8: Yamama B2 unit isopach map from seismic data.

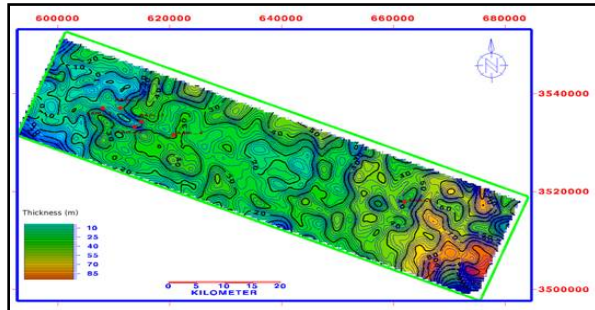


Figure 9: Yamama B3 unit isopach map from seismic data

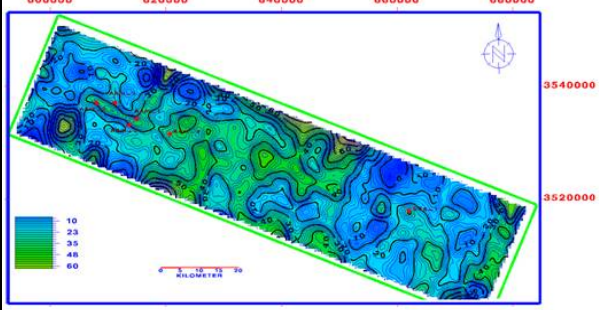


Figure 10: Yamama C1 unit isopach map from seismic data.

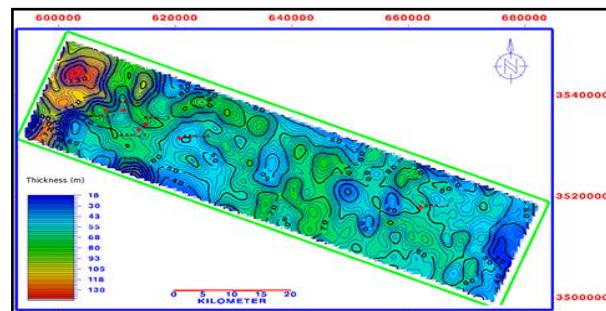


Figure 11: Yamama C2 unit isopach map from seismic data.

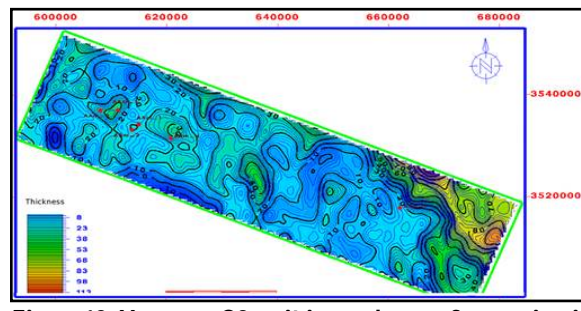


Figure 12: Yamama C3 unit isopach map from seismic data





Nawal Abed Al-Ridha et al.

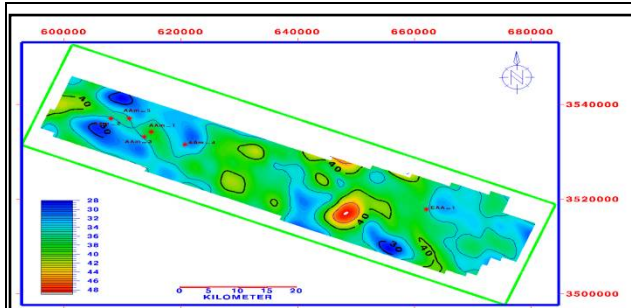


Figure 13: Top Yamama unit instantaneous frequency map.

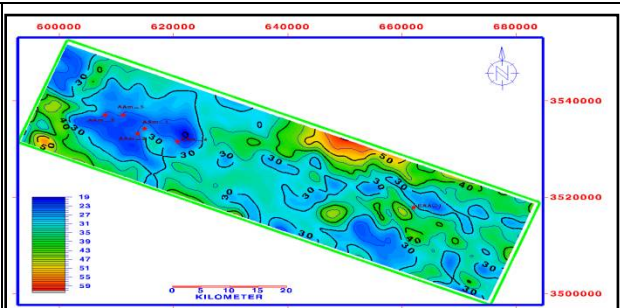


Figure 14: Yamama B1 unit instantaneous frequency map.

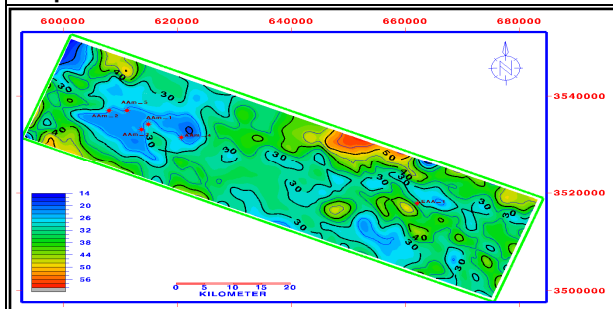


Figure 15: Yamama B2 unit instantaneous frequency map.

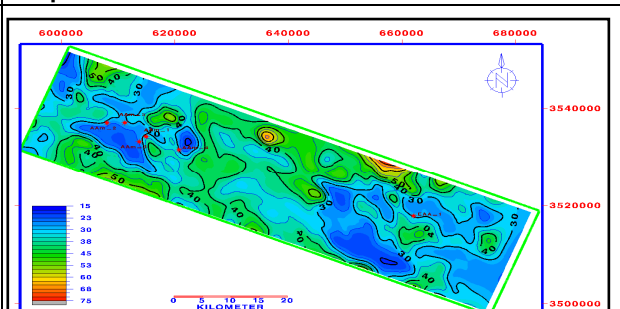


Figure 16: Yamama B3 unit instantaneous frequency map.

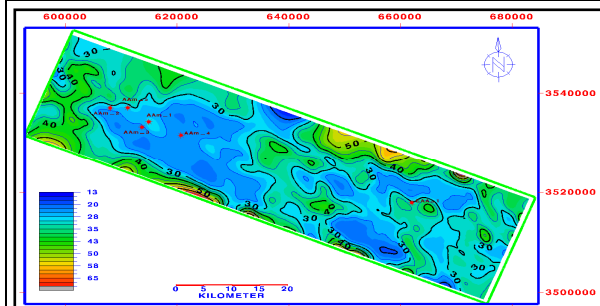


Figure 17: Yamama C1 unit instantaneous frequency map.

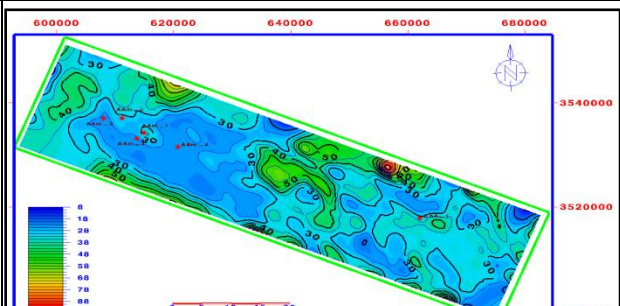


Figure 18: Yamama C2 unit instantaneous frequency map.

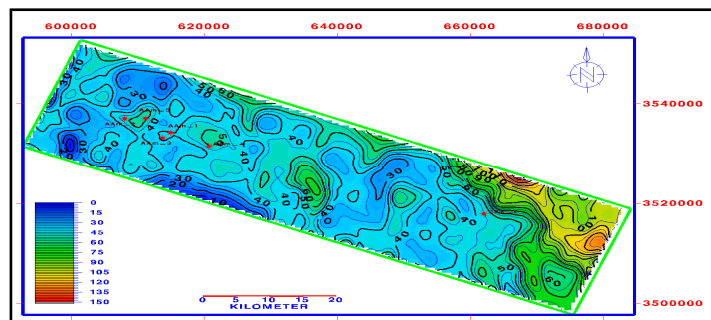


Figure 19: Yamama C3 unit instantaneous frequency map.





Stratigraphic Model of Upper Cretaceous in Samawa-Diwan Area (South of Iraq)

Suhail U. Muhsin^{1*}, Nawal Abed Al-Ridha¹ and Ghazi H. AL-Sharaa²

¹Department of Geology, College of Science, University of Baghdad, Baghdad, Iraq.

²Oil Exploration Company, Baghdad, Iraq.

Received: 17 Sep 2018

Revised: 22 Oct 2018

Accepted: 27 Nov 2018

* Address for Correspondence

Suhail U. Muhsin

Department of Geology,

College of Science,

University of Baghdad, Baghdad, Iraq.

Email: Suhail_ubaid@yahoo.com



This is an Open Access Journal / article distributed under the terms of the **Creative Commons Attribution License** (CC BY-NC-ND 3.0) which permits unrestricted use, distribution, and reproduction in any medium, provided the original work is properly cited. All rights reserved.

ABSTRACT

A 3D seismic data was used for stratigraphic interpretation of Hartha and Shiranish Formations which represent Upper Cretaceous period (upper Maastrichtian-Campanian) by using 1914.72 km² 3D seismic data covered Samawa-Diwan area, it located in the south part of Iraq with in Muthna governorate. Tectonically, the study area locates in the exterior margin of Salman subzone and represents a contact between the stable and unstable shelves as well as between Mesopotamian basin and Salman Subzone. In the area, Hartha Fn. was deposited in an inner shelf to lagoonal environment, while Shiranish Fn. was deposited in an outer shelf to basinal environment. These formations were defined in time domain and picked over the 3D seismic cube and mapped in time and depth domains by using average velocity. A 3D stratigraphic model was constructed and converted to facies model by using Samawa-1 and Dewan-1 wells data. Stratigraphically, the models showed that Shiranish Fn. sequence consist of four units which formed as a mound which sets on-laps relation on Hartha Fn. The mound is surrounded by two unconformity surfaces; top of Hartha Fn. represents the lower boundary and top of Shiranish Fn. represents the upper boundary. This configuration confirms that the area was uplifted and Hartha was exposed and eroded, it forms the Rim margin (platform) which Shiranish sequence was deposited on it. Hartha sequence represents high stand system tracks at end of sequence cycle and the Shiranish units represent the late stage of high stand system tracks of the same sequence cycle.

Keywords: Mound, Ramp, On-laps relation, Stratigraphic model, Facies model, Unconformity surface.



**Suhail U. Muhsin et al.**

INTRODUCTION

The term "stratigraphy" means "the study of the rocks and their variations". Eustatic sea level changes controlled development of the sequence stratigraphy. Tectonism primarily defined the sites of platform development that complicated the architectural heterogeneity of the depositional sequences (Posamentier et al., 1988). Sequence stratigraphy is the subdivision of sedimentary basin fill into genetic packages bounded by unconformities and their correlative conformities, these genetic packages are chronostratigraphic markers that describe periods of relative sea level changes. Depositional sequence boundaries are recognized on seismic data by identifying reflections caused by lateral terminations of strata which termed top-lap, on-lap, down-lap and truncation. The stratigraphic signatures and strata patterns in the sedimentary rock record are the result of the interaction of tectonics, eustasy and climate (Mitchum, 1977).

Basically, changes in rock type produce changes in the reflectivity, which affect the wave shape seen in seismic data. Also inferring stratigraphic changes and their occurrence which is based on characteristics of seismic data is an objective of seismic stratigraphy. Seismic stratigraphy is a technique for interpreting stratigraphic information deduced from seismic data. Seismic Sequence Analysis based on the identification of stratigraphic units composed of relatively conformable succession of genetically related strata termed depositional sequence (Sheriff, 1980). Seismic reflections are believed to follow gross bedding surfaces, and impedance contrasts which are abrupt across bedding planes and gradual across facies boundaries. Stratigraphic modeling is a powerful solution that allows modeling the development of stratigraphic sequences at regional scale or at field scale. The model solves the equation of sediment transport as a function of basin topography, sea level variations, and accommodation space. It ensures calibration against existing well data and seismic data. The result is a more robust and internally consistent prediction of 3D stratigraphic sequences as well as a prediction of facies distribution laterally and vertically (Ziegler, 2001). The current research is stratigraphic analysis study of top Cretaceous Formations of Samawa-Diwan area by using 3D seismic reflection data carried out by the Iraqi seismic 3D crew in 2015.

Location of the study area

The study area is located to the south part of Iraq within Muthna governorate, approximately 40 Km to the southwest of Samawa city (OEC, 2015). Surface topography shows the area is flat and there is no structural feature appear on the surface, and elevation rises towards southeast where it's about 10m above sea level in the northeast and about 120m above sea level in the southeast. The area bounded by Euphrates river from the northeast as shown in the figure-1.

Synthetic seismograms

Generation and extraction of the wave let help Interpreter to fill the gap between geology and geophysics by creating the most accurate time to depth relationships for the wells in the field. Sonic calibration required to reduce interval velocities of acoustic models to well velocity survey curve. Therefore, seismic well tie divided into several stages: sonic calibration, wavelet extraction, synthetic trace production and tying synthetic to seismic data (Meckel and Nath, 1977). Synthetic seismograms were generated for two wells (Samawa-1 and Diwan-1) using IESX software package. A fundamental element in transformation from seismic to geological boundaries is a stratigraphic well tie of seismic data to define reflectors (figures-2, 3, 4, 5).

The main steps of synthetic seismogram generation are (Dedman et al., 1975):

- 1- Computing the reflection coefficients of the vertical incident wave on reflector separating two series time intervals such (i) and $(i+1)$ that have values of acoustic impedance (ρ_i, v_i) and (ρ_{i+1}, v_{i+1}) respectively. According to





Suhail U. Muhsin et al.

Lindseth, 1979, reflection coefficients computed as the following:

$$Rc_i =$$

$$\frac{(\rho_{i+1})(v_{i+1}) - \rho_i v_i}{(\rho_{i+1})(v_{i+1}) + \rho_i v_i}$$

Where: (ρ_i, ρ_{i+1}) the density at the interval $(i), (i+1)$.

(v_i, v_{i+1}) the velocity at the interval $(i), (i+1)$.

2- Convolution process between the reflection coefficient values and experimentally selected wavelet which is made to obtain the synthetic seismogram by using wavelet was extracted from the closest seismic trace of seismic data (Corso et al., 2003).

Seismic Reflection Configuration

The seismic section represents the end product of seismic work (field work and data processing), so the accuracy of the interpretation depends on the accuracy of previous works. The geophysicist uses interpretation work station to map the structural and stratigraphic seismic features correlating them with geological settings in the subsurface (Bacon, 2003).

Configuration of reflections provides the best guide to interpret stratigraphic seismic facies (Neidell, and Poggiagliolmi, 1977). Interpret these reflection configurations to have a better understanding of Upper Cretaceous sedimentary basin in the Samawa-Diwan area.

The Hilbert transform is a kind of filtering which does not affect the amplitude of the spectral component, but it causes changes in the phases of these components by 90° to obtain the imaginary part of the complex function that we get from knowledge of the real part which represents the conventional seismic section (Taner et al., 1979). The seismic instantaneous phase attribute is considered as various aspects of the seismic data (Yilmaz., 1987); it's obtained by complex trace analysis (figure-6).

The imaginary trace is calculated from real trace by using Hilbert transform (Robertson and Nogami, 1984).

The analytic trace is given by: $F(t) = g(t) + h(t) \dots\dots\dots(1)$

The instantaneous phase is: $\varphi(t) = h(t) / g(t) \dots\dots\dots(2)$

Where: $g(t) = A(t) \cos \varphi(t), h(t) \sin \varphi(t) \dots\dots\dots(3)$

Mounded reflection configurations are interpreted as strata-forming elevations rising above the general level of the surrounding strata. Most mounds in the carbonate rocks like Shiranish Fn. deposited in shelf platform it's associated with Reefal buildups. The mounds were divided as the following stratigraphic features (Brown, 2011):

- Carbonate build-ups together with their talus deposits (organic growth).
- Submarine fan complexes.
- Volcanic eruption cones.

In the current research, structurally, the instantaneous phase attribute sections showed the study area was affected by two normal fault formed a graben appear at west side of these sections, affected at Hartha Fn. and reflectors beneath it, while Tertiary reflectors not affected by any type of fault systems. Stratigraphically, Shiranish progradational mound was pointed and picked on seismic data (figure-7). The seismic sections show that Shiranish mound sequence consist of four unites which set on-laps relation at top of Hartha Formation. In addition, seismic sections show that Shiranish mound sequence was surrounded by two unconformity surfaces, top Hartha reflector represents the lower boundary which formed the anti-form (eroded Rim) that Shiranish units set on, while top of Shiranish reflector represents the upper eroded surface boundary.





Suhail U. Muhsin et al.

Maps of top Hartha and Shiranish Formations and its sequence units are drawn in time domain (figures-8, 9, 10), then by using average velocity (figures-11) these maps converted to depthdomain (figures-12, 13, 14). After that, 3D stratigraphic models were constructed for each domain, (figures-15, 16).

The following velocity equation ($V=V_0+K*Z$) was chosen in this research to calculate average velocity values, where:

V:Average velocity.

V_0 :Instantaneous velocity.

K:Constant Ratio of Time/Depth.

Z:Depth.

This equation means, at each XY location, the velocity changes in the vertical direction by a factor of k. Typical values used in modelling work range from around (100 to 5000) m/s for V_0 and -0.2 to 1.8 s^{-1} for K (AL-Chalabi, 1979).

The average velocity values calculated by using time of interest horizons which were picked on seismic data and their markers in Sa-1 and Dn-1 well check-shot logs. Then, a 3D velocity model has been constructed in Petrel software which explains the distribution of velocities in both vertical and horizontal direction that is equivalent to wells check-shot velocities.

Vertically, one observes high velocity values at shallow reflectors with low positive gradient with the depth throughout the area. This due to high consolidation of rocks. Horizontally, at Shiranish reflector velocity values increase toward northwest and decreased toward east and southeast of study area, while at Hartha reflector velocity values increase toward northeast and decreased toward south and southwest of study area. In addition, at deep reflector the velocity values increase toward southeast and decreased toward northwest of study area.

The stratigraphic maps show that Shiranish units distribute in the north and northeast of study area with general dip to northeast and depth increase to the northeast and this deal with the Mesopotamian direction in Samawa-Diwan area. In addition, the maps show there is a clearly increase in the space of units with the depth due to the erosion part of Shiranish upper units as a result of their exposure. Also, the maps of units three and four take a form that resembles the elongated fold which consist of three domes extend to northwest-southeast. A 3D models show that configuration of sedimentary shape of Hartha and Shiranish sequences confirms that the area was uplifted then Hartha was exposed and eroded, it forms the Rim margin (platform) which Shiranish units were deposits on it. Hartha sequence represents high stand system tracks at end of sequence cycle and Shiranish sequence represents the late stage of high stand system tracks at next sequence cycle.

Facies Model

Facies model is a general summary of a particular depositional system, involving many individual examples from recent sediments and ancient rocks. It's controlled by sedimentary processes that operated in particular areas of the depositional environments (Walker, 1990). Hence, understanding of facies as a critical element for the reconstruction of paleo-depositional environments, it helps to interpret of Syn-depositional processes. In turn, such reconstructions are one of the keys for the interpretation of sequence stratigraphic surfaces.

In the current research, a 3D Lithofacies model was constructed to reveal the stratigraphic attitude in the depth domain of Shiranish and Hartha Formations in the Samawa-Diwan area. Figure-17 represents Lithofacies dip section passes near Sa-1 well, this section was derived from the structural, stratigraphic interpretation and lithology of Sa-1 and Dn-1 wells. Consequetelly, one observe that there may be distinct stratigraphic trap within Shiranish Formation. This trap probably can be high prospective areas to investigate the presence of hydrocarbons and the probability of prospecting exploration wells in this areas.

In addition, a good seismic attribute is either directly sensitive to the desired geological feature or reservoir property of interest (Chopra and Marfurt, 2007). Consequently, seismic data cube is converted from amplitude domain to seismic reflection strength attribute. Figure-18 represents reflection strength attribute section, this type of





Suhail U. Muhsin et al.

attributes sensitive to reservoir property of interest. The section shows there is variation in strength values at unit-3 of Shiranish sequence boundary, it represents high negative amplitude and reflects high probability of hydrocarbon accumulation.

CONCLUSION

1. Top Cretaceous was studied Stratigraphically in Samawa-Diwan area, it's representing by Shiranish and Hartha Formations. Shiranish sequence were picked and mapped in time and depth domains.
2. Structurally, seismic sections have been confirmed the study area during upper Jurassic and lower Cretaceous period was seated within a contact boundary between stable and unstable shelves (Mesopotamian basin and Salman subzone). While Seismic sections show that there is no indication to any tectonic effect on Tertiary succession. It's characterized by low with regular thicknesses and no structural features. Tectonically, it's reflect the area quit at that time. Stratigraphically, a sequences feature observed on seismic sections, represents Shiranish progradational mound. It's consist of four unites which set on-laps relation and surrounded by two unconformity surfaces. Top Hartha reflector represents the lower boundary which formed eroded Rim margin that Shiranish on-laps relation set on, while top of Shiranish reflector represents the upper eroded surface boundary, it interpreted as shelf margin setting and Hartha represents high stand system tract at sequence cycle and Shiranish represents the late stage of high stand system track of the same sequence cycle.
3. The maps show that Shiranish units distributes in the north and northeast of study area with general dip to northeast. In addition, the maps show there is a clearly increase in the space of units with the depth due to the erosion top part of Shiranish units as a result of their exposure. Also, units three and four show a stratigraphic features take a form that resembles the elongated fold which consist of three domes extend to northwest-southeast.
4. A3D model in time and depth domains show that shape of Shiranish Fn. was established on the edge of shelf platform near the shoal and deposited in neritic environment.
5. Facies model shows that study area at top Cretaceous reflects the exterior margin of Salman subzone and represents a contact between the stable and unstable shelves as well as between Mesopotamian basin and Salman Subzone. Tectonically, it's interpret that the separation of Arabian plate from the African continent and collision it with the Eurasian plate at the end of Cretaceous was caused the rotational motion of Arabian plate toward the north and north-east. Seismic data have been showed that the study area influenced by these events, where is noted the stratigraphic succession affected by normal fault system which formed a graben. In addition, the stratigraphic features extend northwest-southeast trend due to Arabian plate rotational motion, it's consistence with general trend of Zagros Mountains belts.
6. Seismic reflection attribute observed that distinct stratigraphic trap within Shiranish Formation. This trap probably can be high prospective areas to investigate the presence of hydrocarbons and the probability of prospecting exploration wells in this areas.

ACKNOWLEDGMENTS

We offer our highest thanks, gratitude, appreciation and love to those who carry the most sacred message in life. Those who paved the way for us the path of science and knowledge. Also the greatfull to all our illustrious professors and I would like to express my special appreciation and thank to my supervisor Prof. Dr. Nawal Abed Al-Ridha, and Dr. Ghazi H. AL-Sharaa for all his patience, guidance and continuous support of my Ph.D. study and related research.





Suhail U. Muhsin et al.

REFERENCES

1. AL-Chalabi, M., 1979, Velocity determination from seismic reflection data, Volume I.A.A., pp. 1-68.
2. Bacon, R.S. Redshaw T., 2003, 3-D Seismic Interpretation, Printed in United Kingdom at the University press, Cambridge, 212p.
3. Brown, A.R., 2011, Interpretation of Three-Dimensional Seismic Data, seventh edition. American Association of Petroleum Geologists Memoir 42.646p.
4. Chopra S. and Marfurt K. J., 2007, Seismic Attributes for Prospect Identification and Reservoir Characterization, Seg Geophysical development series No: 11, 463p.
5. Corso, G., Kuhn, P.S., Lucena, L.S., Theme, Z.D., 2003, Seismic ground roll time–frequency filtering using the Gaussian wavelet transform, Departamento de Física Teórica Experimental, International Center for Complex Systems, Universidade Federal do Rio Grande do Norte, Natal CEP 59078-970, Brazil, 11p.
6. Lindseth, R., 1979, Synthetic sonic logs - a process for stratigraphic interpretation: Geophysics, 44, 3-26.
7. Meckel, L. D., Jr., and Nath, A. K., 1977, Geologic considerations for stratigraphic modeling and interpretation: Am. Assoc. Pet. Geol. Special Memoir 26, 417-438.
8. Mitchum Jr., R. M., (1977), Seismic Stratigraphy and Global Changes of Sea Level: Part 11. Glossary of Terms used in Seismic Stratigraphy: Section 2. Application of Seismic Reflection Configuration to Stratigraphic Interpretation, Memoir 26 Pages 205 - 212.
9. Neidell, N. S., and Poggliogliomi, E., 1977, Stratigraphic modeling and interpretation-geophysical principles and techniques: Am. Assoc. Petr. Geol. Special Memoir 26, 389-416.
10. OEC, 2015, Final field report of 3D seismic survey for Samawa-Diwan area, Oil Exploration Company, internal report, 53P.
11. Posamentier, H.W., Jervey, M.T., Vail, P.R., 1988, Eustatic controls on clastic deposition. I. Conceptual framework. In: Wilgus, C.K., Hastings, B.S., Kendall, C.G.St.C., Posamentier, H.W., Ross, C.A., Van Wagoner, J.C. (Eds.), Sea Level Changes-An Integrated Approach, vol. 42. SEPM Special Publication, pp. 110- 124.
12. Robertson, J. D., and Nogami, H. H., 1984, Complex seismic trace analysis of thin beds: Geophysics, 49, 344-352.
13. Sheriff, R.E., 1980, Seismic Stratigraphy, IHRDC, Boston, 277 p.
14. Shetty, S., Liang, L., Habashy, T., Simoes, V., Boyd, A., Sinha, B., Zeroug, S., Sirju, C., Pritchard, T., Glassborow, B., 2014, Inversion-based method integrating sonic and resistivity logging data for estimation of radial water saturation and porosity near the wellbore, Annual Technical Conference, 27–29 October.
15. Taner, M.T., Kohler, F. and Sheriff, R.E., 1979, Complex trace analysis, Geophysics, V. 44, No. 6, p. 1041-1063.
16. Walker, R.G., 1990, Perspective, facies modelling and sequence stratigraphy. Journal of Sedimentary Petrology. v. 60, p. 777-786.
17. Yilmaz., 1987, seismic data processing, SEG series: Investigation Geophysics, V.2 526 p.
18. Ziegler, M., 2001. Late Permian to Holocene Paleofacies evolution of the Arabian Plate and it hydrocarbon occurrences. GeoArbia, 3, p. 445-504.





Suhail U. Muhsin et al.

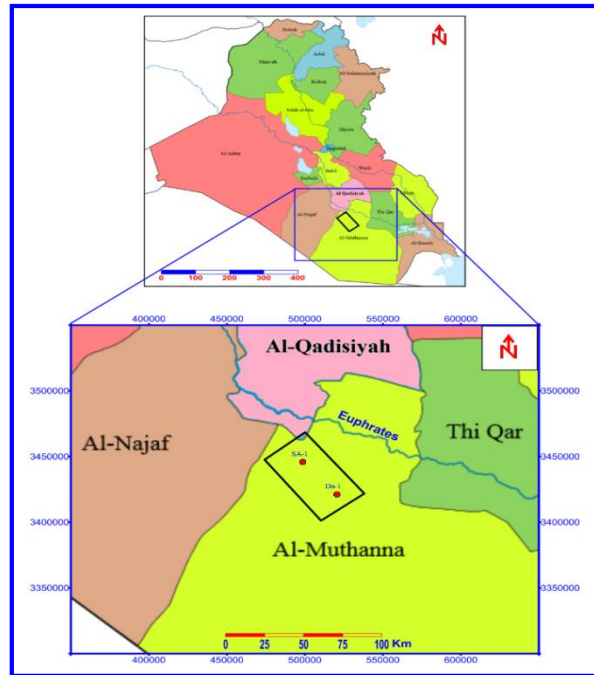


Figure-1. Location map of the study area.

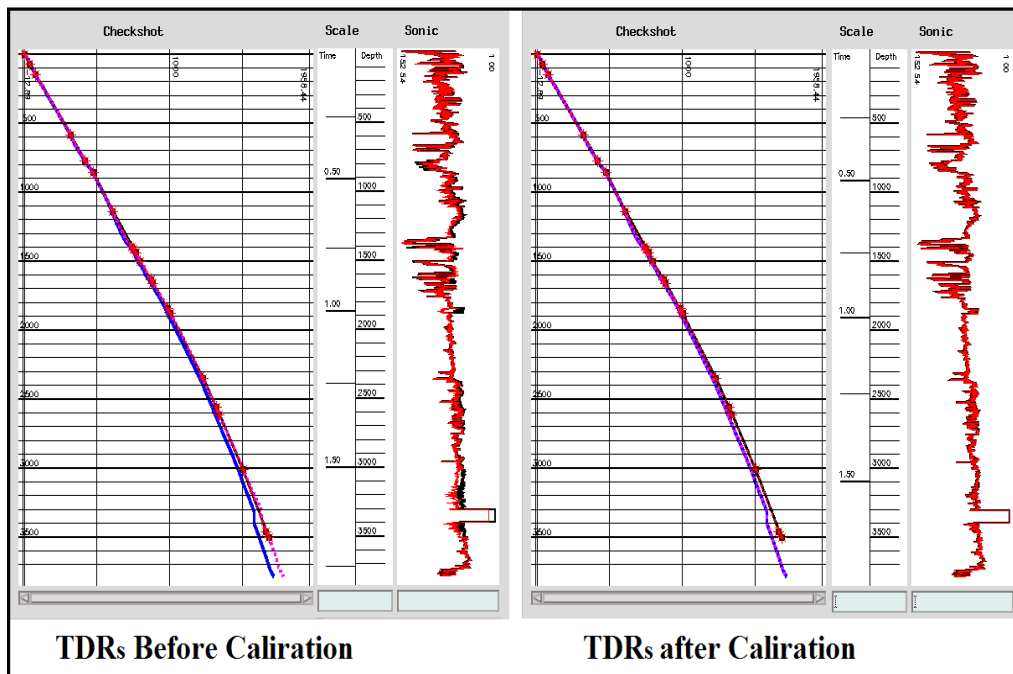


Figure-2. The calibration processes by time-depth relation of sonic and check-shots curves in Samawa-1 well.





Suhail U. Muhsin et al.

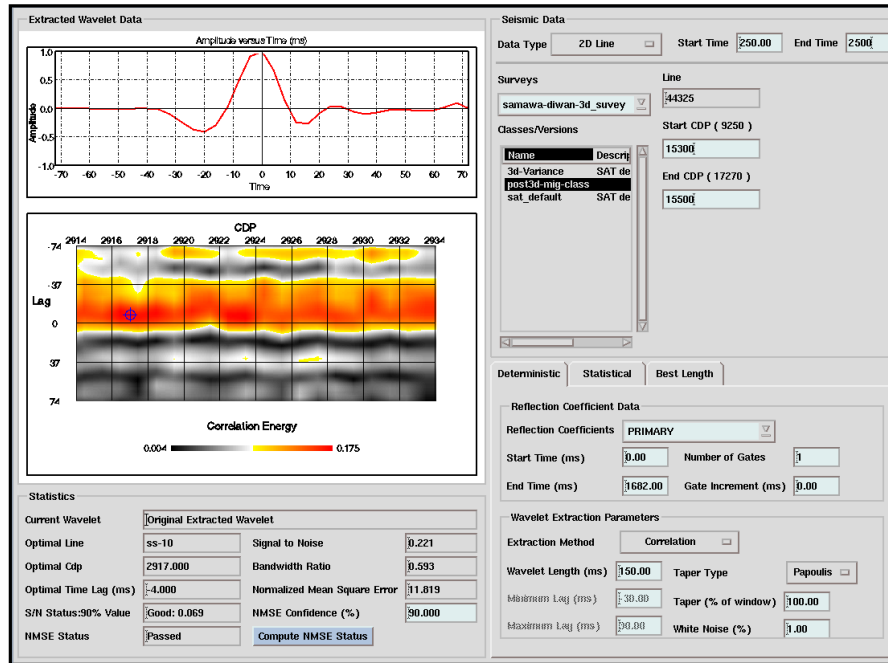


Figure-3. An extracted wavelet window of Samawa-1 well from seismic data with matching 69%.

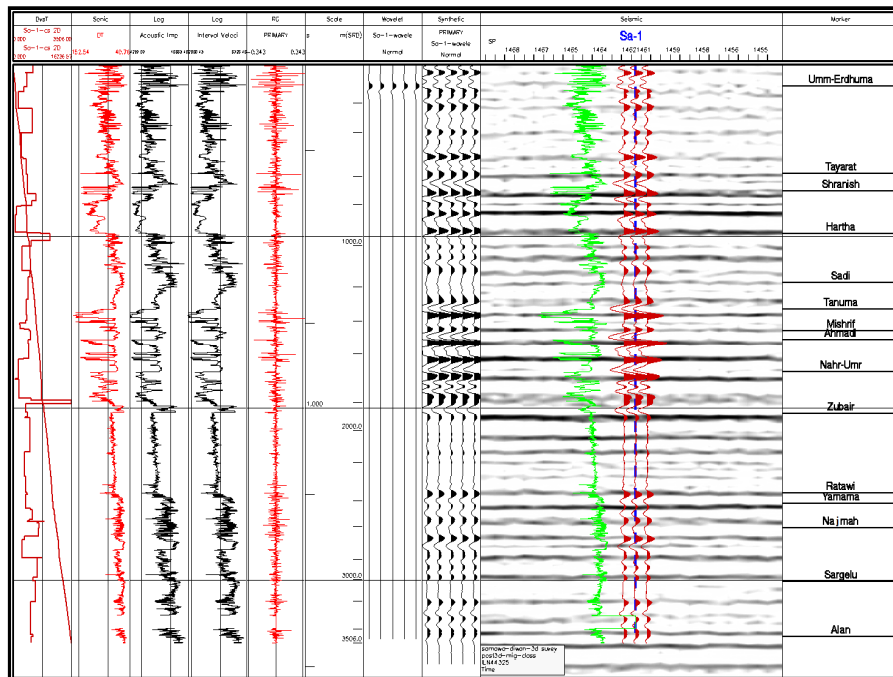


Figure-4. Samawa-1 well synthetic seismogram window.





Suhail U. Muhsin et al.

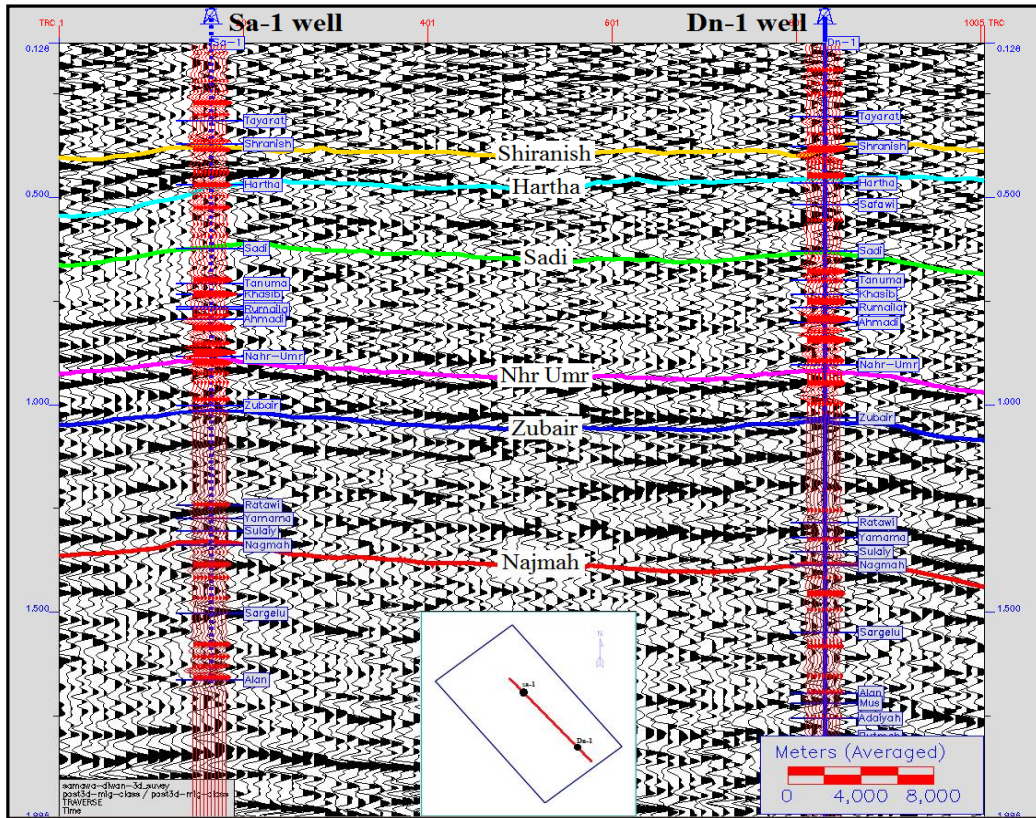


Figure-5. An arbitrary seismic section shows seismic correlation of picked reflectors between synthetic traces of Sa-1 and Dn-1 wells.

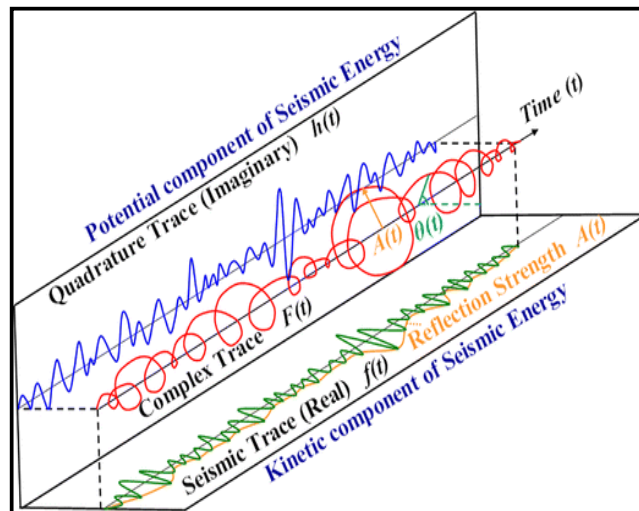


Figure-6. The complex seismic trace and seismic attributes.





Suhail U. Muhsin et al.

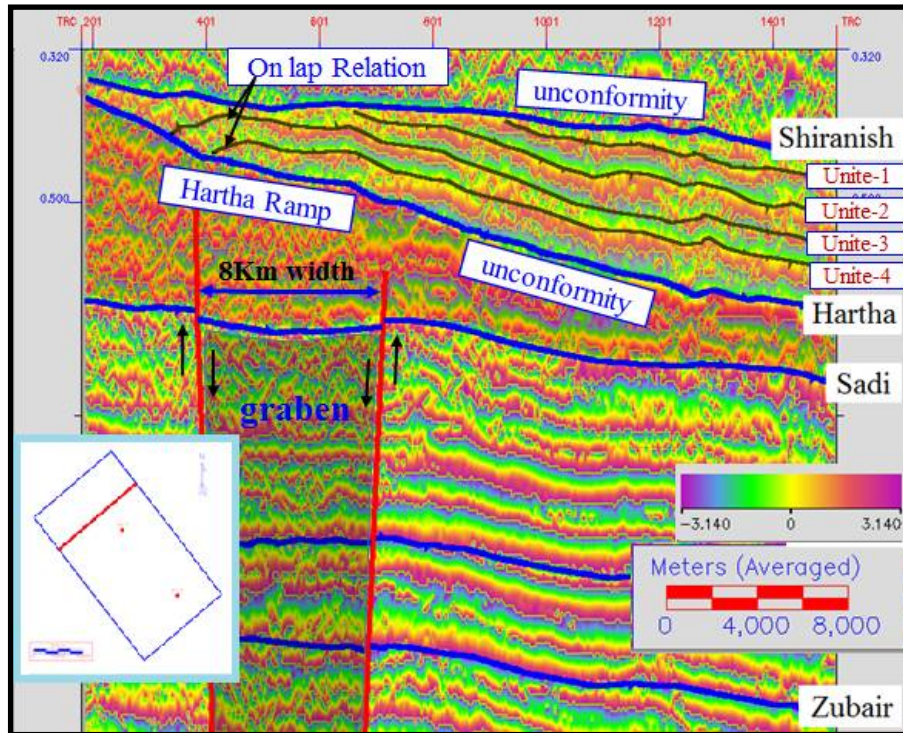


Figure-7. An instantaneous phase section inline no. 45375 shows Shiranish Progradational mound (on-lap relation sequence).

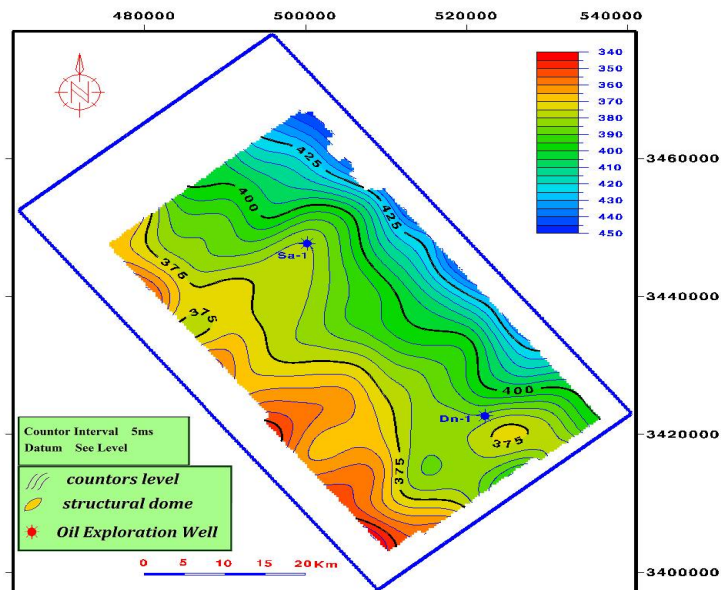


Figure-8. Time map of top Shiranish horizon.





Suhail U. Muhsin et al.

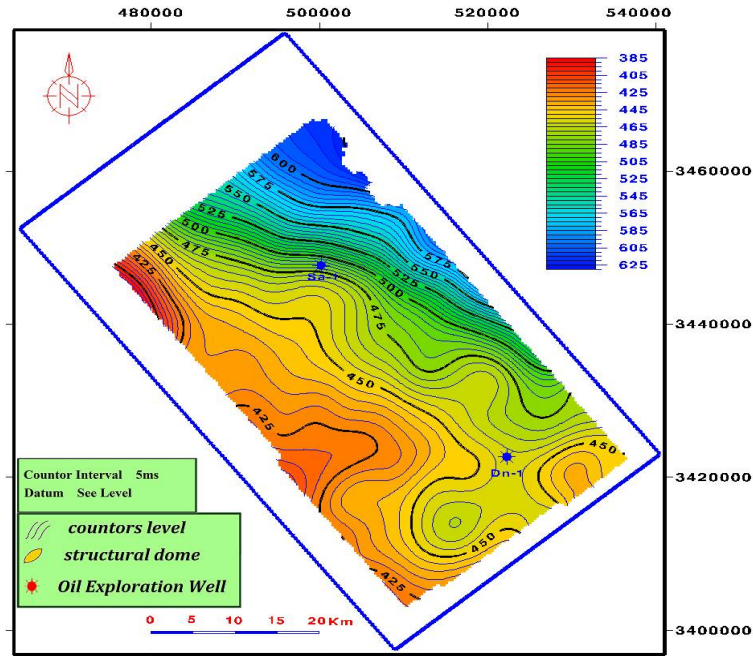


Figure-9. Time map of top Hartha horizon.

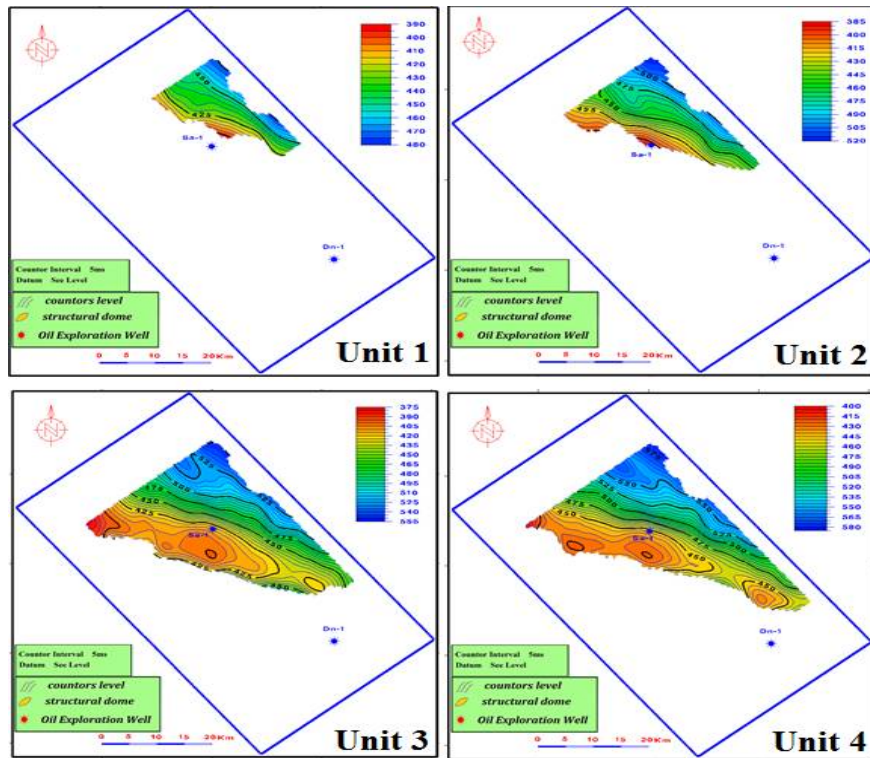


Figure-10. Time maps of Shiranish Fn. mound





Suhail U. Muhsin et al.

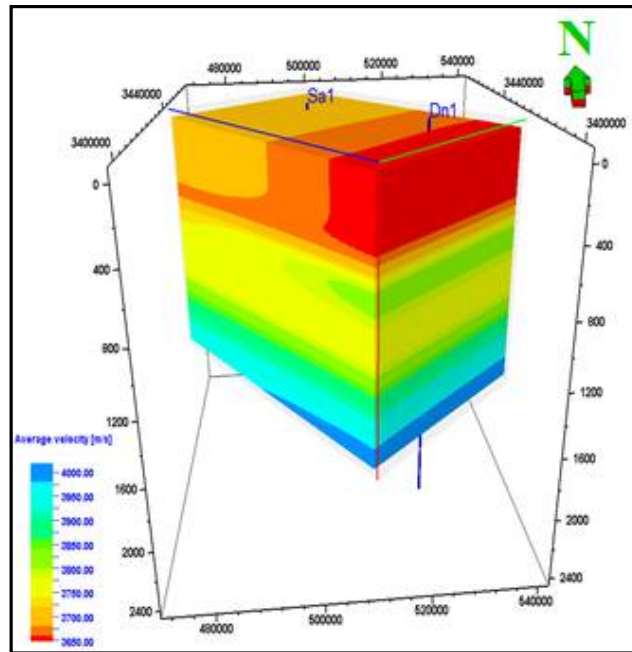


Figure-11.A 3D view of average velocity model throughout study area.

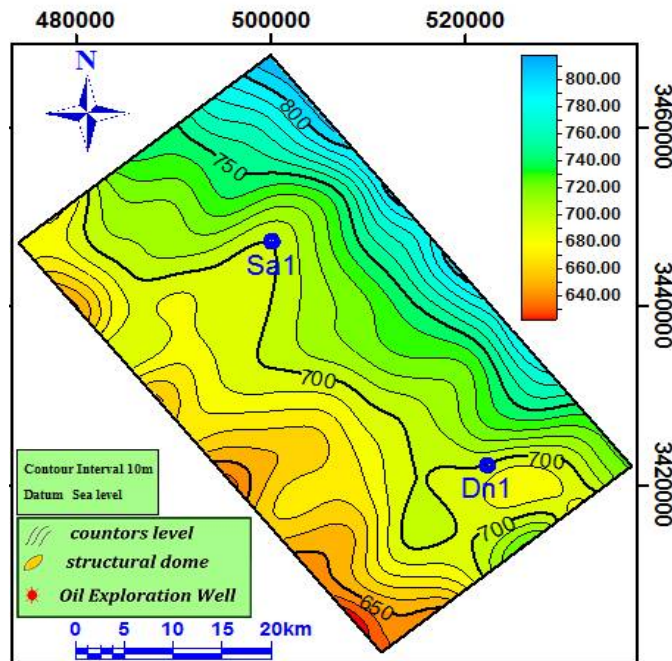


Figure-12.Depth map of top Shiranish Fn.





Suhail U. Muhsin et al.

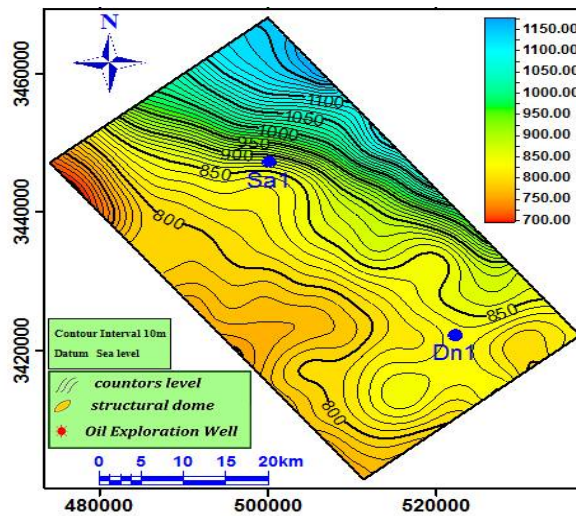


Figure-13.Depth map of top Hartha Fn.

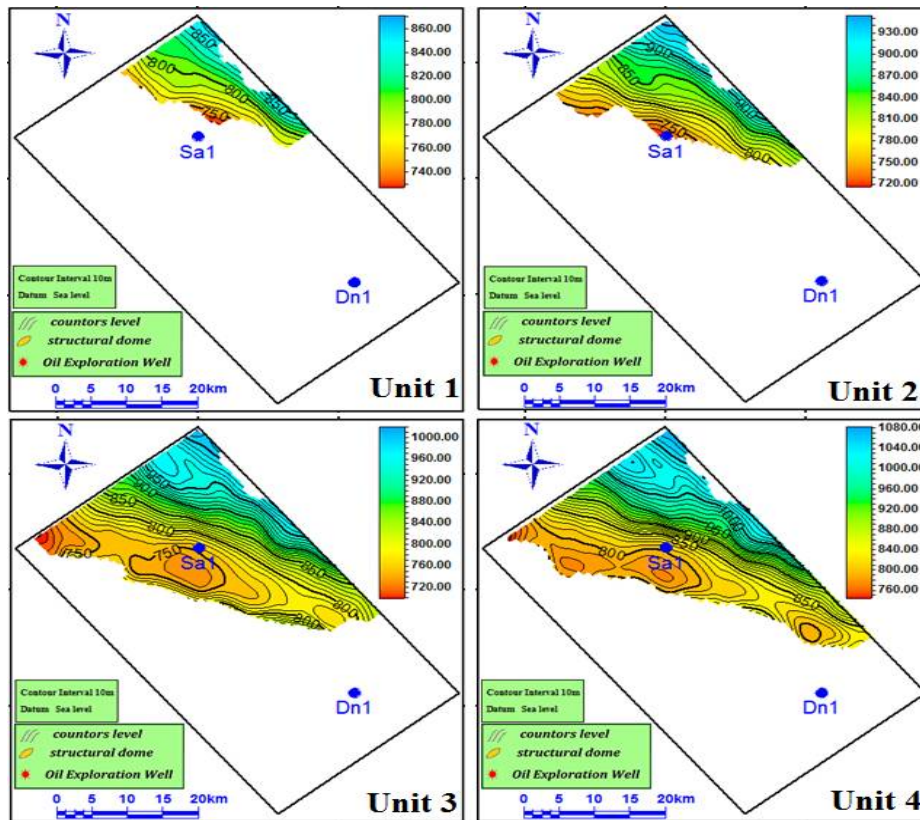


Figure-14.Depth maps of Shiranish Fn. mound units.





Suhail U. Muhsin et al.

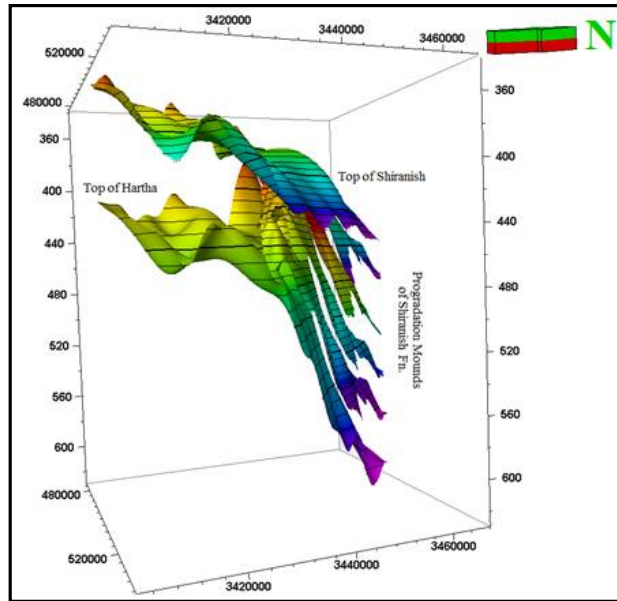


Figure-15 A 3D model of Shiranish progradational mound sequence in time domain

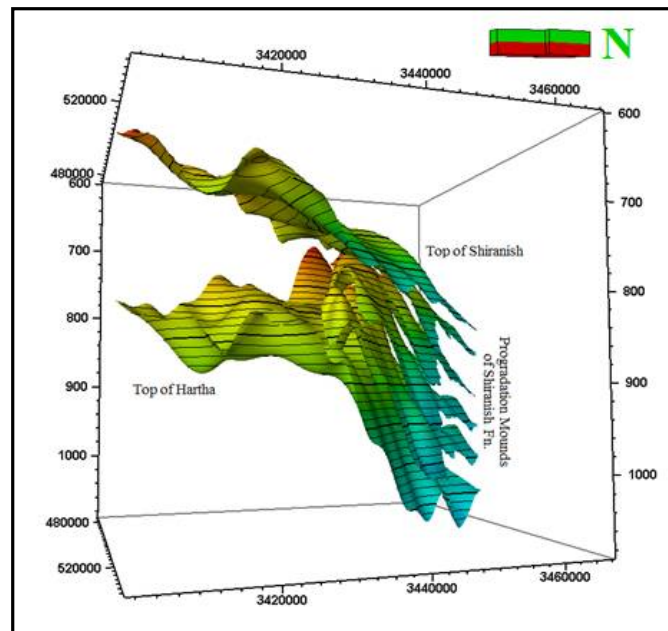


Figure-16 A 3D model of Shiranish progradational mound sequence in depth domain





Suhail U. Muhsin et al.

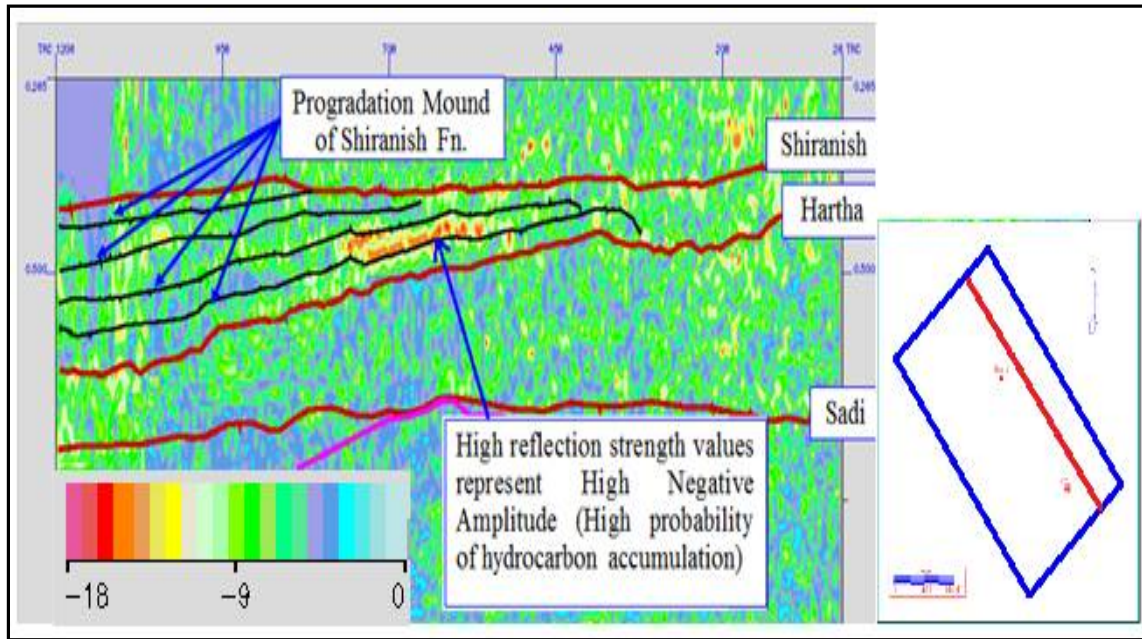


Figure-17.Lithofacies dip section derived from a seismic interpretation and wells data in the study area.

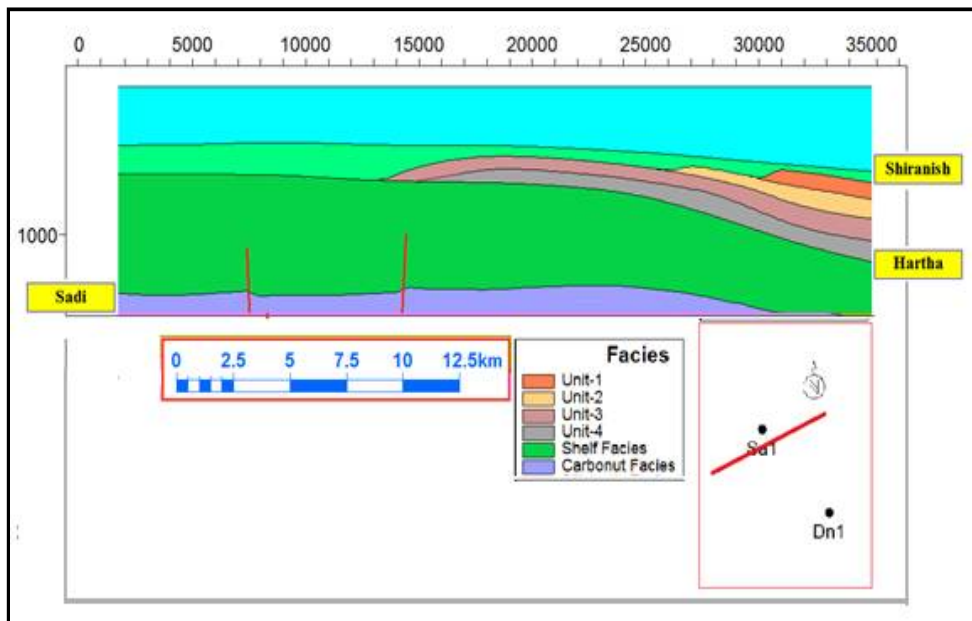


Figure-18.Reflection strength attribute section shows high negative of amplitude values at unite-3 of Shiranish Fn.





A Comprehensive 3D Seismic Study and Logs Interpretation to Delineate the Stratigraphic Depositional Model for the Upper Cretaceous Reef in Merjan-West Kifl Oil Fields – Central of Iraq

Mohammed Sadi Fadhil^{1*}, Ali, M. Al-Rahim² and Jameel R. Kamoona¹

¹Oil Exploration Company, Baghdad, Iraq.

²Earth Science Department, College of Science, University of Baghdad, Iraq.

Received: 19 Sep 2018

Revised: 21 Oct 2018

Accepted: 27 Nov 2018

* Address for Correspondence

Mohammed Sadi Fadhil

Oil Exploration Company,

Baghdad, Iraq.

Email: mohammedal_hamdai@yahoo.co.uk



This is an Open Access Journal / article distributed under the terms of the **Creative Commons Attribution License** (CC BY-NC-ND 3.0) which permits unrestricted use, distribution, and reproduction in any medium, provided the original work is properly cited. All rights reserved.

ABSTRACT

Seismic stratigraphic study of an upper cretaceous reef within Hartha formation (L Maestrichtian, 550-658M) and 108m thick in the Merjan oil field. The Merjan 3D seismic survey is a vibroseis survey of 1026.17 km² area located in the central Iraq. Two exploration wells were drilled in the area Me-1 and Wkf-1 wells, the distance between them is 15.82 km. Results of Me-1 well proved that Hartha formation is a carbonate reservoir and production test was gave 650 bbl /day of oil and water of formation. Depending on the study of the internal reflection configuration and reflection termination, the mound seismic facies has been determined and adopted to reconstruct the depositional model. It illustrates that formation is carbonate pinnacle reef which is developed on the margin of sub-basin. It is overlain by a regional unconformity. The main goal of this work is suggest a stratigraphic model to determine the nature of the oil entrapment mechanism in the Merjan-1 well. Spatial modeling by mapping of stratigraphic traps is the first step of solution and other step is study behavior of physical properties of a multi phases anisotropic carbonate build up system. logs interpretation, seismic attributes and seismic inversion techniques have been applied. Reservoir has been divided into three main zones which are diagnosed zone A, zone B and zone C where the latter zone is water charge, while the other produce oil with water. Low instantaneous frequency and high reflection magnitude values across stratigraphic trap indicate to presence hydrocarbon zones. Acoustic impedance results reveal the impedance which reflects high porous calcareous rocks through the reef seismic anomaly.

Keywords: Depositional model, carbonate buildup, pinnacle reef, Seismic attribute, Seismic inversion



**Mohammed Sadi Fadhil et al.**

INTRODUCTION

3D seismic survey becomes essential method for hydrocarbon exploration (Brown, 1996). To exploration of depositional model of carbonate sedimentation, it is not always adequate to follow a standard interpretation routine and more advanced techniques are demanded (Skirius et al., 1999). Carbonate buildup is very important target for hydrocarbon exploration in both frontier and mature basins (Peter et al., 2013). Carbonate reservoirs is widespread, but still its identification is a major challenge, so synthetic models with computational experiments have been used to demonstrate the possibility seismic diffraction imaging, Luke Decker et al., 2015. The main agents to develop the carbonate build-up stratigraphy are antecedent geomorphology, sea level fluctuations which controls the geometry of Carbonate buildups, Nordaunet et al., 2015, Matthew Rine et al., 2016, RuiZhai et al., 2017. Significantly, a change from a carbonate ramp to a rimmed platform have been recorded during the Cenozoic, with regional data documenting the contiguous growth of carbonate buildups in the shallowest parts of the North West Shelf after the early Oligocene, Rosleff-Soerensen et al., 2012; Belde et al., 2017; Rankey, 2017. In sequence stratigraphic framework, 3-D seismic geometric attributes provide important information for understanding the facie variation on siliciclastic-carbonate dominated shelf margin, RuiZhai et al., 2017. Brightened seismic reflections, dim spots, and other evidence of fluid accumulation can occur in carbonate build up, James Van Tuyl et al., 2018. The stratigraphic model for complex reef requires the core, thin section, wireline logs and biostratigraphic data, to construct the facies distribution and depositional history, that model will allow to better predictability to potential unconventional resources Matthew Rine et al., 2016, Keelan F. Umbarger et al., 2016. An integrated geological and geophysical analysis of carbonate reservoir presents an effective method to better understand of paleogeographic evolution and distribution of geological reservoir and barriers layers, Vincentelli et al, 2017 which applied method includes the use of petrographic and qualitative description from the integrated reservoir with seismic interpretation of attribute's map. The well Merjan-1 was drilled as an exploration wildcat between May and August 1983 to a depth of 2777m. Hartha formation (L Maestrichtian, 550-658M, and 108m thick, it consists of limestone on top underlain by dolomite, which is alternating with limestone and shale. Porosity and permeability of the wackestone and carbonate mudstone facies have been affected by diagenetic processes. The environment of deposition of the Hartha Formation is deep continental shelf margin or the sedimentary basin margin, O.E.C, Documents, 1984, O.E.C, Documents, 1989. The well encountered moveable hydrocarbons only in the Upper Cretaceous Hartha Formation. Production test show that the well-produced up to 650 bbl/day of oil and formation water. Results of electrical logs interpretation show that the oil column reaches to 49m at top Hartha formation, Reservoir and field development Directory, 2010. The results of reinterpretation studies of the 2D seismic survey data of Merjan-West Kifl show a small structural enclosure at Hartha Formation (10m) in the Merjan area, thus, the oil column in the well was greater than the mapped closure at Hartha level, O.E.C, 1984. These studies indicate that oil was retained due to a reefal stratigraphic trap. But they can't determine the nature of this trap and its extension and the trapping mechanism for the oil discovered in the Hartha Formation reservoir in the ME-1 well remains unresolved, also they recommended a seismic stratigraphic study, O.E.C, 2000, O.E.C, 2005, Petrel Resources plc. 2007, O.E.C, 2014. The understanding the geology of reservoir will help us to determine the locations of drilling thus less risk and benefit in quality and quantity of production. The principal aim of this study is to determine the depositional system, nature of the oil entrapment mechanism, confirmation of hydrocarbon presence and areal distribution of the stratigraphic trap for exploration and developing the Merjan field.

Geological setting

The West-Kifl-Merjan Oil fields are located in the middle of Iraq, west the Euphrates River within Al- Najaf – Karbala province as shown in (Figure 1) (O. E. C., 2014). Stratigraphic column of drilled well in the area (Me-1 well), (Figure 1), were taken as a good instance to identify stratigraphy of Hartha formation. Study area is located in the western boundaries of the Mesopotamian basin (near platform flank of Mesopotamian fore deep adjacent to the north eastern slope of African-Arabian platform. It lies in the critical area between the stable and unstable shelf, Geoserve, 1996,



**Mohammed Sadi Fadhil et al.**

(Figure 1). Regionally, Ziegler, M. 2001, indicates the Late Turonian -Danian (89-61 ma) period, encompassing the Tanuma, Sadi, Hartha and Shiranish, was dominated by shallow marine platform carbonate over much of Arabia. The Hartha and Shiranish represent transitional facies between shallow marine and deeper marine facies.

Available data

3D seismic data covering an area of 1026.17 km² of the Merjan –West Kifl Oil field has been acquired in 2013. Wire line log data which includes logging data of Me-1 well, and check shot of 2 wells (Me-1, Wk-1). Depth of top Hartha formation from sea level is 488m in Me-1 and 593m in Wk-1.

METHODOLOGY**Synthetic Seismogram**

The synthetic seismogram was generated using the Seismic to Well Tie module in GeoFrame Software. The sonic data was first edited for any spiky noise and calibrated to check shot and any gap in the sonic data was filled by interpolating the nearby data. The correlation of synthetic seismogram and 3D seismic data is very good and it was easy to identify well markers on seismic data, (Figure 2).

Horizon picking of Hartha formation and determine the biohermal shape. The geophysical criteria to recognition of reef signature were applied which has been referred in Bubb and Hatlelid, (1977). Log behavior study and petrophysical analysis were conducted. Some seismic attributes have been generated for Merjan field, such as Amplitude, Instantaneous Frequency, Instantaneous phase, and so on. Inversion was adopted to convert PSTM to AI (Acoustic Impedance) volume using Me-1 well data. The last important step is search for analogues of the known objects.

RESULTS AND DISCUSSION**Construction of Depositional Model**

The upper cretaceous is a regional sequence boundary separates Tectonostratigraphic Megasequences (TMS) Arabian Plate (AP9) and (AP10), and ends by Shiranish formation. Hartha formation is below Shiranish and it represents carbonate system with evaporate system which characterizes the supratidal and intertidal environment. Carbonate buildup is formed in these environments, and due to these bodies, the topography of top Hartha reflector does not consistent with general trend of structure in the field. Consequently, the lower parts of Shiranish formation intersect with the carbonate buildup, also its units form the seal to Hartha formation. Seismic facies study are showed the mound features and other associated indicators such reflection termination. The lithological data and seismic characteristics associated with mounds confirm the presence of biohermal shape or carbonate buildup. The kind of reef of interest is pinnacle reef which is approximately circular shaped to slightly elongate steep-sided organic accumulations. The model proposes the trapping is by carbonate pinnacle reef, (Figure 3).

Picking top of carbonate buildups in the Hartha formation was conducted. Two way time (TWT) map of top the biohermal shape in the Hartha formation was drawn to delineate the extension of reef in the area, and it is presented as part of (Figure 4). The proposed depositional model in this paper depicts the puzzle of the nature of oil entrapment in the Hartha formation.





Mohammed Sadi Fadhil et al.

It is well known that younger reef is good exploration targets because of their larger potential. The reason for this is that the younger upper cretaceous reefs have usually much greater porosity than the older Paleozoic ones. This coincides with our reef of interest because it nearly shallow. A depositional model for the Hartha carbonate buildup that would produce pinnacle reef is a prograding shelf as illustrated in (Figure 4).

This model comprises a variety of depositional environments, including Pinnacle reef which are surrounded by deep water during deposition. The geological time of this model is late Campanian–Maastrichtian and this period represent rise global in sea level according to global sea level change, Haq et al., 1977. Van Bellen et al., 1959 pointed that Hartha formation is deposited on a regional erosional surface overlay the Sadi formation. Sadi formation comprises of deep environment facies while the Hartha formation is shallow environment facies, O.E.C, Laboratory documents, 1984, this sharp change in facies indicates the unconformity episode. This means that Hartha formation is deposited during the regional flooding of the sea level and it is represents high stand system tract. Transgressive system tract facies is far from the study area toward east. 2D seismic data were used to track the depositional setting toward east. The seismic line Mz-20p1 shows the seismic facies of barrier reef. It is located within Musyibe area 140 km east Merjan field, (Figure 5). Figure also shows the karst feature which could be conduit for hydrocarbon leakage. The important thing to say that barrier reef has regional extension accompanied the regional break up between Tectonostratigraphic Megasequences (TMS) Arabian Plate (AP 9 & 10). (Figure 5) shows the relation between pinnacle reef and barrier reef. This feature represents barrier reef which indicate to sub-basin ward, also it is water charge in Musyibe-1 exploration well (84.9 km east me-1) while in Me-1 well, the reef is oil reservoir.

Structurally Merjan area is higher than Musyibe area; consequently, this may be leads to conclude that oil may be migrated laterally to Merjan area after vertical migration from deep source rocks through fault and karst features.

Hartha Formation Anatomy

Depositional model was showed that Hartha facies is considered promising reservoir facies. System tract have been distinguished using gamma ray log pattern. The upward-fining successions are interpreted to represents transgressive system tract (TST) the upward-coursing successions are interpreted to represents high stand system tract (HST). System tracts are useful in reservoir distribution.

Hartha has been divided into reservoir and barrier units which distributed in three zones, (Figure 6).

- 1- Zone (A): It is occupying the depth interval (575–560) m. The upper part comprises of packstone and lower part comprises of mud limestone with planktonic fossils.
- 2- Zone (B): It is occupying the depth interval (575–630) m. This zone is the most important reservoir unit.
- 3- Zone (C): It is occupying the depth interval (628–655) m. It comprises of mud dolomite and benthonic foraminifera (*Monolepidorbis*) which is index fossils for Hartha formation.

Studies of well logs behavior of ME-1 well for Hartha reservoir are showed the following:

1. Gamma ray (GR) and sonic logs indicates to shale presence where high reading of both them is correlated with shale. Shale is high porous, impermeable and cause high reading of sonic log. It contain high amounts of radioactive material which cause high reading of GR, consequently, Hartha reservoir is dirty, where, most of Hartha section. GR values not less than 20 API.
2. Neutron log (NPHI) indicate to good porous for Hartha interval, thus, Hartha reservoir zone.
3. Bit Size (BS) is useful to determine the permeable zones where when the well diameter equal bit size, this reflect impermeable bed and vice versa. In interval of interest, well diameter is less than bit size, this mean that the interval is permeable. The difference between well diameter and bit size due to forming of mud cake which is





Mohammed Sadi Fadhil et al.

forming as result. Logs interpretation and cross-plot for Me-1, (Figure 7) indicate domination of dolomitic limestone for the Hartha formation.

To investigate the permeability, fluid content and type of fluid, the resistivity logs were used. Separation of resistivity logs indicates to permeability of Hartha formation and there are fluids in the reservoir. It is clear that reading of ILD log are high, that indicates to presence of hydrocarbon in the reservoir. DST data and separation of ILD at depth interval 628 m indicate the OWC level, where, production test at (600 – 615) m show flow of oil, gas and salty water 320 barrel/day with water percentage 40%. Oil indicator in the Hartha reservoir and porosity is summarized within the (Figure 8).

A number of DSTs and production tests were carried out on the Merjan-1 well. Study of the reservoir potential of the Hartha reservoir was made using the available test and log data drilling, log and test data are consistent and demonstrate that

- 1- The only one zone has good oil shows in this well is the Upper Hartha, which tested oil. Movable oil is evident on the interpreted logs opposite the tested zone, which also includes intervals that could have been responsible for the water production.
- 2- The logs of the lower zones that tested water and mud indicate high water saturations, little hydrocarbon and reasonable porosity
- 3- Those zones that did not flow on test generally have low porosities, suggesting poor permeability, and no movable oil.

The porosity and matrix lithology were determined together from a combination of the Sonic, Density, Neutron data curves with the defined minerals being anhydrite, dolomite, limestone and sandstone. Hydrocarbon saturation was based on the computed values of porosity, and the Induction resistivity (ILD) was taken as the true formation resistivity (R_t). In order to compute R_w it is necessary to assume a value for the cementation exponent (m) within the Archie equation. In the absence of any measurements, the value 2 was used. A log-derived value over the lower interval of the Hartha determined that an appropriate value for R_w was 0.34 ohm m at 60°F (equivalent to 20 g/l NaCl). Oil saturation was divided between "movable/immovable" based on the MSFL. Not too much confidence should be placed in this division because R_{mf} is often very inaccurate: MSFL reads beyond the flushed zone and for various other reasons. Water saturation (SW) is estimated by using well log interpretation, Archie equation was used to calculate SW. SW nearly become equal to 1 at depth 628 m, which indicate to oil water contact, (Figure 8).

Seismic attributes analysis and results

Seismic attributes application is becoming mandatory for successful reservoir evaluation in many oil and gas fields. Seismic attributes have been studied to explain the geometry of reef, (Figure 9), physical properties and confirm the hydrocarbon (H.C) content. Some of one dimension complex seismic traces were calculated which include instantaneous phase, instantaneous, frequency and reflection strength for study interval of interest.

1. **Instantaneous Frequency** : It is the time or depth derivative of the instantaneous phase. It is a measure of the frequency of the waveform at every sample. Low frequency anomaly can be correlated by fluid zones, (Figure 10). Red color represents low frequency, this indicates to reservoir facies and porous zones. These low frequency anomalies are linked by reef in Hartha formation.
2. **Instantaneous Phase**: It is the measurement of the position on the waveform. It is very useful for determination of reflection termination and lateral variation of reflector geometry (Figure 11). The Phase display show clearly stratigraphic boundaries of reef, and flat spot which represents the seismic response of hydrocarbon – water contact.



**Mohammed Sadi Fadhil et al.**

- 3. Reflection Strength:** Determination of total energy of seismic signal is useful for discrimination of geological features such as unconformity and fluid content. These features cause observed changes in the reflection energy as a response to acoustic impedance contrast across surfaces of these features. High contrast across geological surface gives high reflectivity. (Figure 12) shows reflection inline strength section across Me-1 well. It explains the lateral variation of reflection strength of reservoir reflectors. It is clear that red color represents negative high reflection strength which indicates the H.C accumulation. It shows that high values correlate with high attenuated areas which indicate fluid content within a mound seismic facies and the latter represent seismic response of pinnacle reef. The arrows in the figure points to migration of the fluids toward up dip direction. The unit of measurement is the decibel and negative sign indicate to the reverse polarity of the amplitude.

Seismic Inversion analysis and results

In carbonate facies, diagenesis play important role in seismic velocity changes, thus changes in acoustic impedance, therefore, the seismic facies it may be difficult to diagnose changes in acoustic impedance (Masferro, J.I., R. Bourne, and J. C. Jauffred, 2004). The Seismic inversion was performed to confirm the depositional model and oil prospectively. Log data told us good information about nature of reservoir and seismic data is explained the depositional setting of reef and now as final step will be confirm the reservoir characterization via inversion data to determine the porosity property. Generally it is assumed that the density is invariant and that the impedance variation is determined by velocity variation. Al-Rahim and Hashim, (2016), used the flow chart to invert seismic data to acoustic impedance which adopted here to perform the inversion, (Figure 13). In sedimentary rocks dominated by a single mineral the velocity is normally correlated directly with porosity. Inversion of the seismic trace can therefore be used to detect porosity variations within a given reservoir section. For a given reservoir this hypothesis can be tested by cross-plotting impedance and porosity well logs. The technique has been widely used for many years in carbonate, chalk and some sandstone reservoirs. The seismic, seismic velocity, horizon and well data are loaded into the HSR-9 system. Petrophysical conditioning of the well log data is performed to remove artefacts in the data created by borehole (or other) problems during the logging run. Quality log data are essential to the wavelet estimation, model building and interpretation of final results.

Wavelet has estimated from the well by using sonic log to estimate both the amplitude spectrum and phase spectrum of the wavelet. The time-depth relationship of the well is updated and a new wavelet is estimated as iteration process until a stable wavelet and a reasonable time-depth relationship are established. The log correlation window, (Figures 14) has been showed that the synthetic trace well matching in character with the seismic traces, also it illustrates a very good nearly symmetric cross-correlation with peak value of about 80%. The symmetric correlation shape means that extracted zero-phase wavelet is probably very accurate.

Low Frequency Model Building and Data inversion

Seismic data lack low frequencies. In order to generate absolute values of impedance a low frequency model must be generated. The low frequency model is call initial model and it is a combination of information from stacking velocities and well log data, (Figure 15). The stacking velocities constrain the low frequency model in the 0-2Hz range and the well log data provide the information from 2 Hz up to the lowest seismic frequencies. Low frequency has added (up to 12Hz). P-impedance versus effective porosity cross plots from the ME-1 well in the Hartha to Safawi interval showed P-impedance to be clearly related to effective porosity, with a relationship close to linear, (Figure 16). The inversion of the seismic data to acoustic impedance could, therefore, be transformed directly to porosity. The results of the inversion project revealed widespread porosity within the Hartha interval, (Figure 17). Now the results present support to us to locate the exploration well in the field which nearly far from Me-1 well 11 km toward west as shown in (Figure 22). Farther more works can be carried in the futures in this field.



**Mohammed Sadi Fadhil et al.**

Impedance slices were extracted from inverted cube through the Hartha reservoir to depict the porosity property, (Figure 18). Brown color indicates low impedance values which correlates high porous zones. Slices Show the low AI in the mound area, indicated higher porosity, while, the blue color point to high AI in the Safawi formation.

The Oil Fields – Analogues

The analogy has referred to support the result of the work, the first is national and the other is foreign. Area is located at the south-west part of Iraq, (Figure 19). The drilling is achieved on buildups reef and a result is 1billion barrel of light oils. In North Africa, (Figure 19), seismic line shows anomaly interpreted as pinnacle reef, this pattern is so-called "eye effect". Location A was first to be drilled, based on poorer seismic data, on closure at Eocene level above Paleocene reef unit. Well encountered about 60 m of gas-filled pay in Paleocene and was abandoned; acreage in area was subsequently dropped. Another company picked up acreage, obtained high-quality seismic data that showed Paleocene reef, and drilled well B as discovery well. Well encountered about 300m of porous algal-foraminiferal and coralline limestone. Pay section was 293m thick. Oil flowed on test at rate of more than 40,000 bbl/day. Estimated recoverable reserves in this field are approximately 1.5 billion bbl of oil, (Bubb and Hattelid, 1977). In our area of interest, pinnacle reef, is important prospective target to drilled show the proposed location for wellsdrilling, (Figure 19).

CONCLUSION

3D seismic data provide fantastic performance to make seismic facies analysis of pinnacle reef in the Merjan oil field. Reef seismic anomaly is mapped in all 3D area allowing us to develop a plan for exploratory drilling. Me-1 well data with seismic data help us to determine the depositional supratidal and intertidal flat environment. The seismic stratigraphy and well log data are robust controls to capture the most reliability subsurface model. Although seismic attributes and inversion algorithms are not sufficient to confirm the hydrocarbon potential of target because it suffers from non-uniqueness, but they good support to fluid content in the depositional model especially if they are confirmed same result as in current paper. Low instantaneous frequency, high reflection strength, clear flatspot and reflection termination provide good indicators are added to results of depositional setting and fluid content. Logs interpretation has been proved that Hartha is reservoir and they help us to anatomy it into reservoir units. The important thing which we want to say that location of Me-1 well lies in ends of reef body, if it were located farthest to west ward, The results would have been much better than the previous production results. Seismic inversion is another guide to determine the porous zones which are coincide with reef locations. Acoustic impedance inversion of the seismic data produced a well-defined correlation with effective porosity, as observed in the well ME-1. In the end, the combination of results and the final outcome of this paper made us able to locate the exploratory well in the green oil field. The results will change ideas about the nature of oil entrapment and developing plans which will take into consideration the model submitted here, also will open up a new opportunity to go step forward to explore the barrier reef 140 km east of Me-1 well. Structurally Merjan area is higher than Muysibe area; consequently, this may leads to conclude that oil may be migrated laterally to Merjan area after vertical migration from deep source rocks (Sulaiy and Sargelue formations) through fault and karst features.

REFERENCES

- 1- Al-Ameri, T.K., Al-Marsoumi, S.W., and Al-Musawi, F.A., 2014: Crude oil characterization, molecular affinity, and migration pathways of Halfaya oil field in Mesan Governorate, South Iraq. Arabian Journal of Geosciences, pp2-4, DOI 10.1007/s12517-014-1733-z.
- 2- Al-Rahim, Ali, M. and Hashem, H., A., 2016, Subsurface 3D Prediction Porosity Model from Converted Seismic and Well Data Using Model Based Inversion Technique, Iraqi Journal of Science, Vol. 57, No. 1A, PP: 163-174.





Mohammed Sadi Fadhil et al.

- 3- Belde, J., Back, S., Bourget, J., and Reuning, L., 2017, Oligocene and Miocene carbonate platform development in the Browse Basin, Australian Northwest Shelf: *Journal of Sedimentary Research*, v. 87, no. 8, p. 795– 816, <https://doi.org/10.2110/jsr.2017.44>.
- 4- Brown, A., 1996, Interpretation of Three-Dimensional seismic data: AAPG Memoir 42, 424p.
- 5- Bubb and Hatlelid, 1977, Seismic Stratigraphy and Global Changes of Sea Level, Part 10, Seismic Recognition of Carbonate Buildups, in *Seismic Stratigraphy applications to hydrocarbon exploration: AAPG Memoir 26*, p.185-204.
- 6- Haq, B. U., Vail, P. R., Hardenbol, and Van Wagoner, J.C., 1977, Sea Level History, *Science*, 241, p. 596-602.
- 7- James Van Tuyl, Tiago M. Alves, and Lesley Cherns, 2018, Pinnacle features at the base of isolated carbonate buildups marking point sources of fluid offshore Northwest Australia, 3D Seismic Laboratory, School of Earth and Ocean Sciences, Cardiff University, Main Building, Park Place, CF10 3AT Cardiff, UK, This paper is published under the terms of the CC-BY license.
- 8- Keelan F. Umbarger¹ and John W. Snedden¹, 2016, Delineation of post KPg carbonate slope deposits as a sedimentary record of the Paleogene linkage of De Soto Canyon and Suwannee Strait, northern Gulf of Mexico, *Society of Exploration Geophysicists and American Association of Petroleum Geologists, Interpretation*, Vol. 4, No. 1 (February 2016); p. SC51–SC61, <http://dx.doi.org/10.1190/INT-2015-0086.1>.
- 9- Luke Decker, Xavier Janson, and Sergey Fomel, 2015, Carbonate reservoir characterization using seismic diffraction imaging, *Published in Interpretation*, 3, no. 1, SF21-SF30.
- 10- Masferro, J.I., R. Bourne, and J. C. Jauffred, 2004, Three-dimension of seismic visualization of carbonate Reservoirs and Structures, in *seismic imaging of carbonate reservoirs and systems: AAPG Memoir 81*, P. 11-41.
- 11- Matthew Rine, Jon Garrett, Stephen Kaczmarek, David Barnes, and William Harrison, 2016, A New Model for Niagaran “Pinnacle” Reef Complexes of the Michigan Basin, *Search and Discovery Article #51319* (2016), Adapted from oral presentation given at AAPG 2016 Annual Convention and Exhibition, Calgary, Alberta, Canada, June 16-22, 2016.
- 12- Nordaunet-Olsen, E. M. 1,2, Escalona, A.1, Skar, T.2, Pedersen, L.2, 2015, Controls on upper Paleozoic Carbonate Build-up Development in the SC Barents Sea, publisher
- 13- Oil Exploration Company, 1984, final geological report on exploration well no. Me-1, 33p. (In Arabic).
- 14- Oil Exploration Company, 1984, preliminary paleontological study of Jurassic-Cretaceous succession of Merjan-1 well, Department of Geological Laboratories, 42p. (In Arabic)
- 15- Oil Exploration Company, 2000, re-interpretation study of seismic data in the Merjan Oil Field, 44P. (In Arabic).
- 16- Oil Exploration Company (O.E.C), 2005, geological study of Merjan field, O.E.C documents, 34p. (In Arabic).
- 17- Oil Exploration Company, 2014, geological and geophysical study of 3D seismic survey of Merjan field, p. 293, (In Arabic).
- 18- Peter M. Burgess, Peter Winefield, Marcello Minzoni, and Chris Elders, 2013, Methods for identification of isolated carbonate buildups from seismic reflection data, *AAPG Bulletin*, v. 97, no. 7 (July 2013), pp. 1071–1098
- 19- Petrel Resources Plc, 2007, Merjan project: final report, 377p.
- 20- Rankey, E.C., 2017, Seismic architecture and seismic geomorphology of heterozoan carbonates: Eocene–Oligocene, Browse Basin, Northwest Shelf, Australia: *Marine and Petroleum Geology*, v. 82, p. 424–443, <https://doi.org/10.1016/j.marpetgeo.2017.02.011>.
- 21- Reservoir and field development Directory, 2010, Reservoir study of the Merjan, West kifl and Kifl oil fields, North Reservoir department, 96p.(In Arabic)





Mohammed Sadi Fadhil et al.

- 22- Rosleff-Soerensen, B., Reuning, L., Back, S., and Kukla, P. 2012, Seismic geomorphology and growth architecture of a Miocene barrier reef, Browse Basin, NW-Australia: Marine and Petroleum Geology, v. 29, p. 233– 254, <https://doi.org/10.1016/j.marpetgeo.2010.11.001>.
- 23- RuiZhai, and John D. Pigott Conoco-Phillips, 2017, Integrated Seismic Stratigraphic and Reservoir Characterization of Leonardianreefal carbonates on the Eastern Shelf of Midland Basin, School of Geology and Geophysics, University of Oklahoma, SEG International Exposition and 87th Annual Meeting. p. 1955–1959, <http://library.seg.org/>
- 24- Skirius, C., S. Nissenm N. Haskell, K. Marfurt, S. Hadley, D. Ternes, K. Michel, I. Reqlar, D. D’Amico, F. Deliencourt, T. Romero, R. D’Angelo, and B. Brown, 1999, 3D seismic attributes applied to carbonates: Leading Edge (March), P. 384-393.
- 25- State Establishment of Geological Survey and Mining (GEOSURV), 1996, Tectonic Map of Iraq, printed and published by the GEOSURV, Baghdad, Iraq. (Arabic ref.).
- 26- Van Bellen, H.V., R. Wetzel, and D.M. Morton, 2005, 1959-2005 Stratigraphic Lexicon of Iraq. LexiqueStratigraphique International, Asie (Iraq), reprinted electronically and on paper by Gulf PetroLink in 2005.
- 27- Vincentelli M. Gabriela Castillo, Julia Favoreto J., Roemers-Oliveira E., 2017, Paleogeographic evolution of carbonate’s reservoirs: geological and geophysics analysis at the Albian of Campos Basin – (Brazil), Sinopec Geophysical Research Institute, Journal of Geophysics and Engineering, Vol.15, No.1, 21p.
- 28- Ziegler, M. 2001, Late Permian to Holocene paleofacies evolution of the Arabian Plate and its hydrocarbon occurrences. GeoArabia, 3, p. 445-504.

Table (1) summarizes divisions of Hartha reservoir.

Litho zone	Depth interval (m)	Unit Name	Interval (m)	Unit Type	Lithology	Thickness(m)
A	575 – 560	Rese-1	560 - 568	Reservoir	Packstone	8
		Barr-1	568 - 572	seal	Lime mudstone	4
B	575 - 630	Rese-2	572 – 582	Reservoir	Packstone, benthonic forminifera and algae	10
		Barr-2	582 – 585	seal	Lime mudstone	3
		Rese-3	585 – 592	Reservoir	Packstone	7
		Barr-3	592 – 593	seal	Lime mudstone	1
		Rese-4	593 – 597	Reservoir	Packstone	4
		Barr-4	597 – 598	seal	Lime mudstone	1
		Rese-5	598 – 607	Reservoir	Packstone	9
		Barr-5	607 – 609	seal	Lime mudstone	2
		Rese-6	609 – 623	Reservoir	Packstone	14
		Barr-6	623 – 625	seal	Lime mudstone	2
C	628 - 655	Rese-7	625 - 628	Reservoir	Packstone	3
		Rese-8	628 - 655	Water Reservoir	Mud Dolomite	27





Mohammed Sadi Fadhil et al.

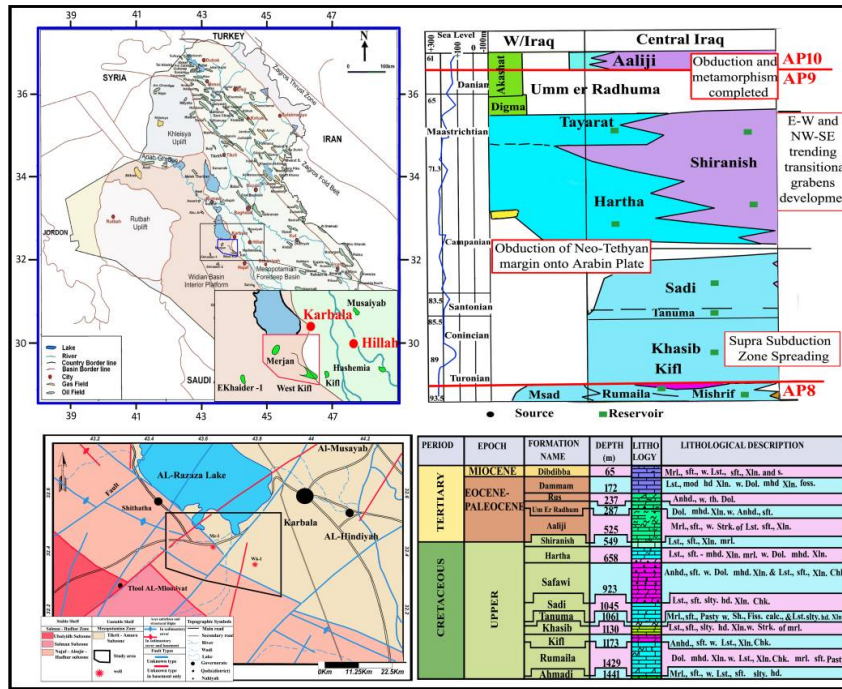


Figure 1. Location map after Al-Ameri et al., 2014, stratigraphic correlation of formation of Megasequences Ap9 after Jassim et al, 2006, Stratigraphic section of Me-1 well, after O.E.C., 2005 and tectonic map of a study area, after Geosurve, 1996.

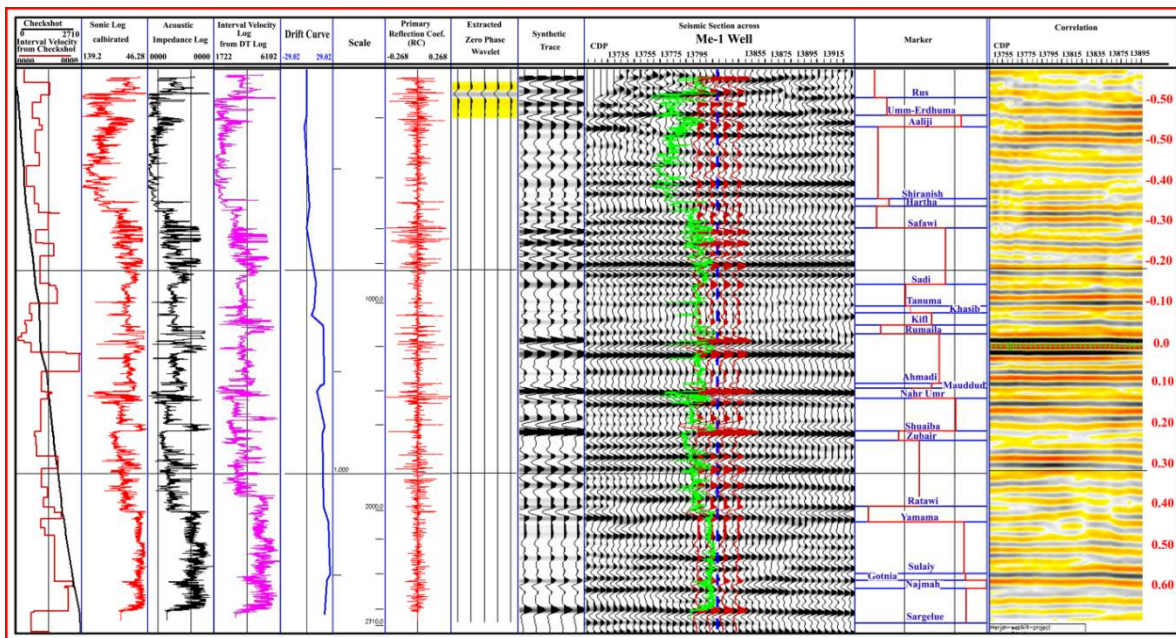


Figure 2. Synthetics seismogram of Me-1 which shows a good tie with seismic data.



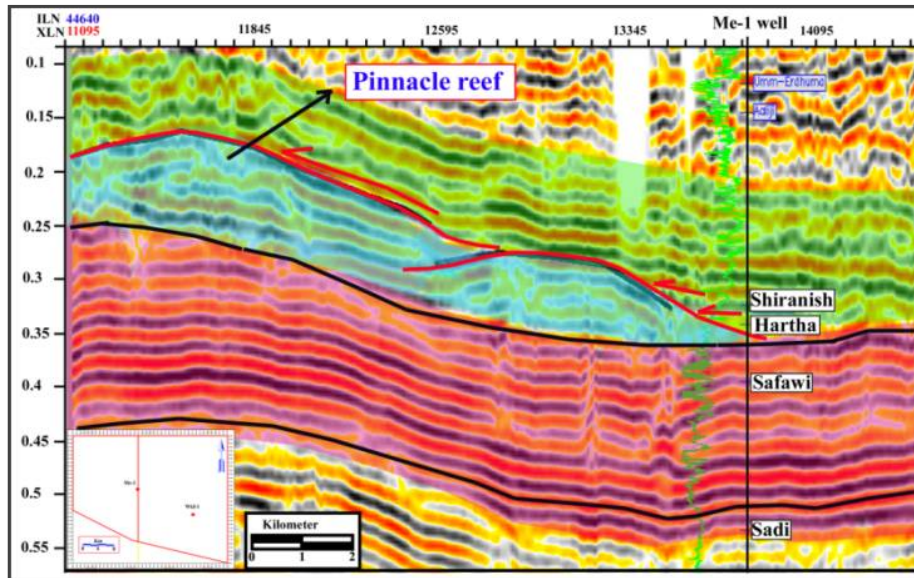


Figure 3. Seismic section show mound seismic facies which indicates biohermal shape in the Hartha formation.

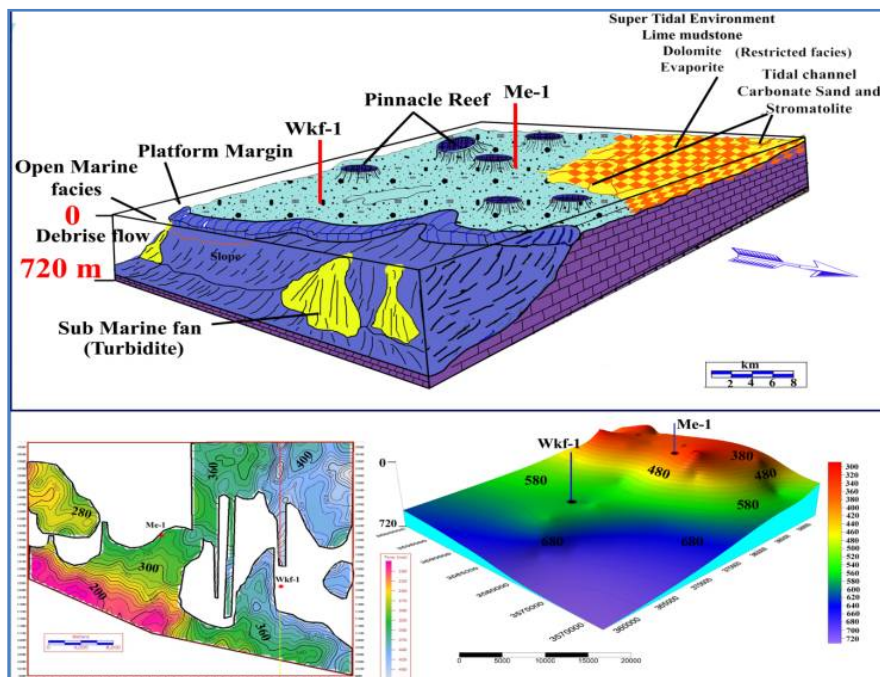


Figure 4. Model of facies distribution of Hartha carbonate buildup and two way time map of mound feature.





Mohammed Sadi Fadhil et al.

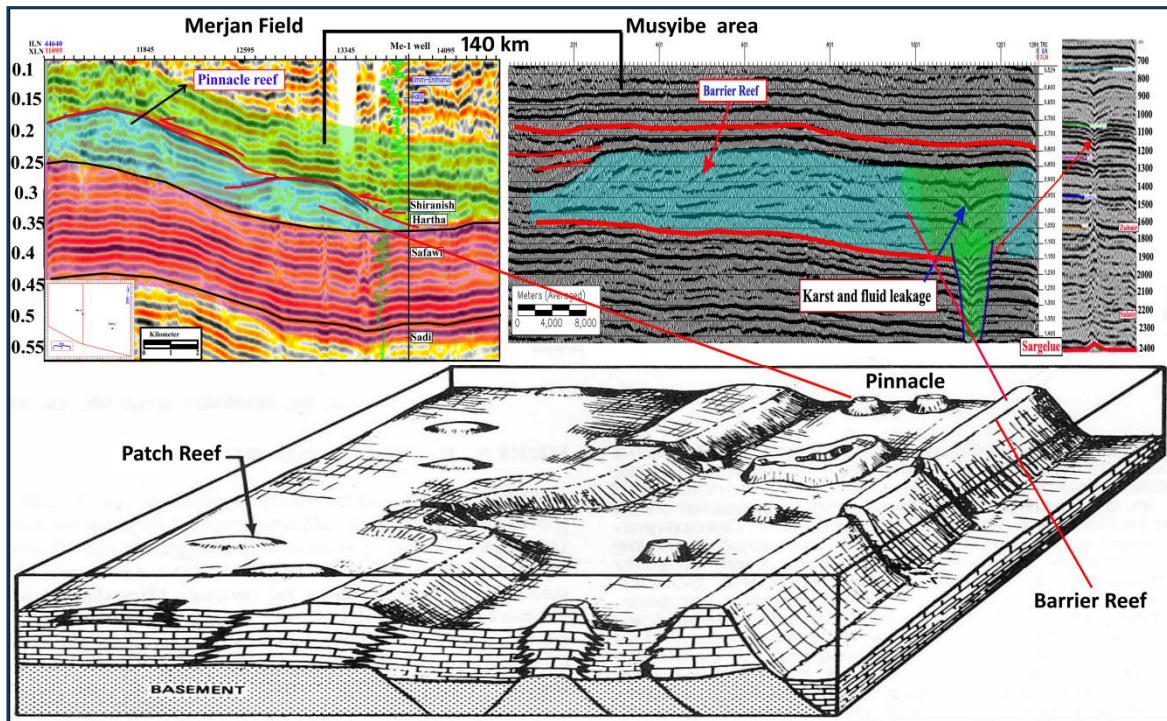


Figure 5. Illustrates distribution of the reef types and seismic sections show the pinnacle reef seismic facies in the Merjan and the barrier reef seismic facies accompanied with karst and fluid leakage in the Musyibe area.

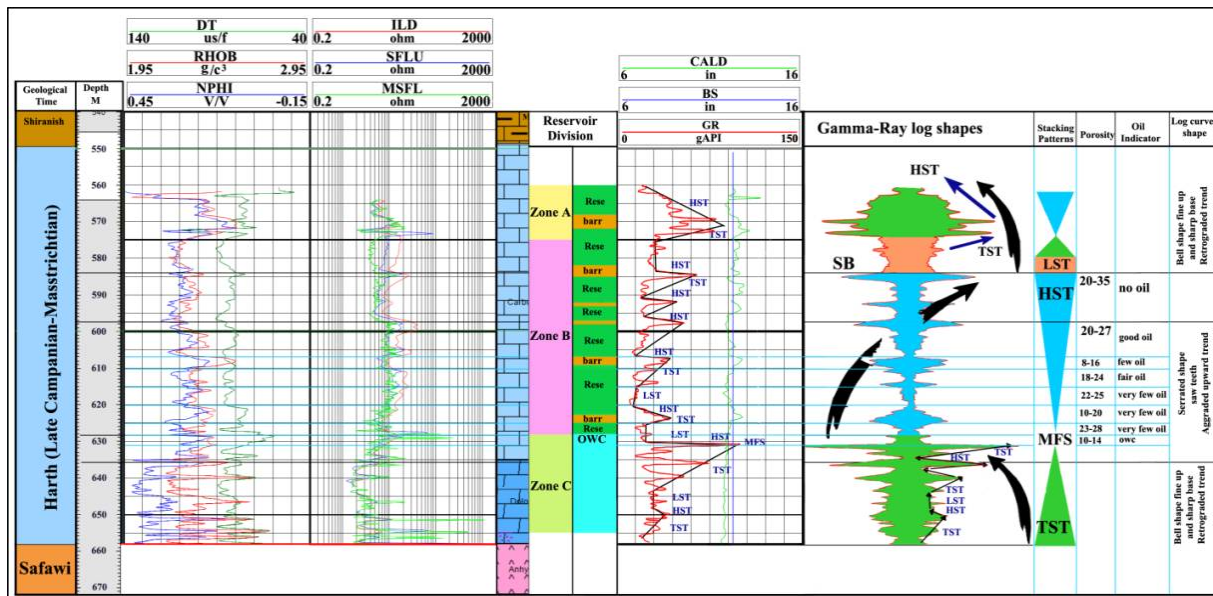


Figure 6. Sequence stratigraphic section and reservoir division of Hartha formation of the Me-1 well.





Mohammed Sadi Fadhil et al.

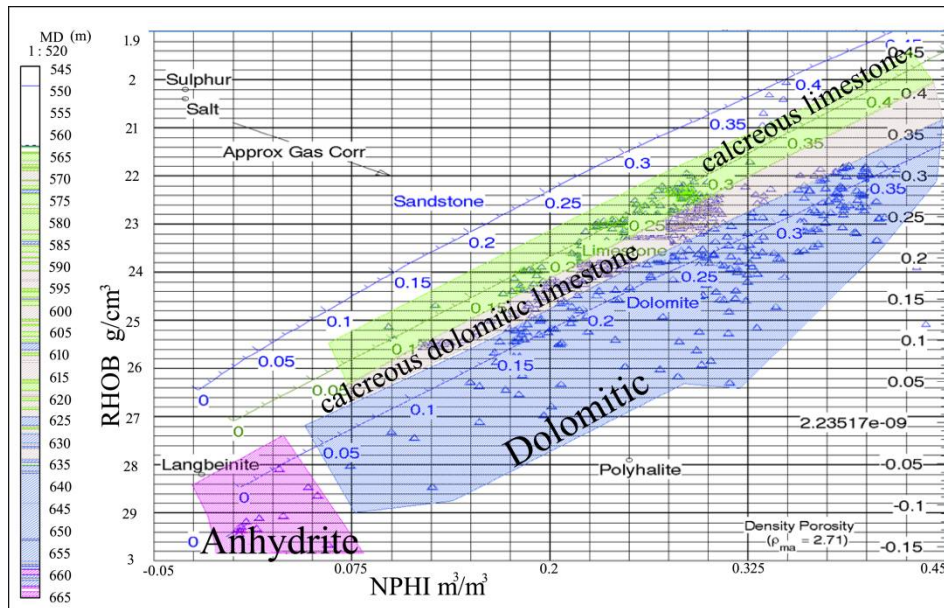


Figure 7. Neutron-Density Cross-Plot illustrates the Lithology distribution of Hartha formation in well Me-1

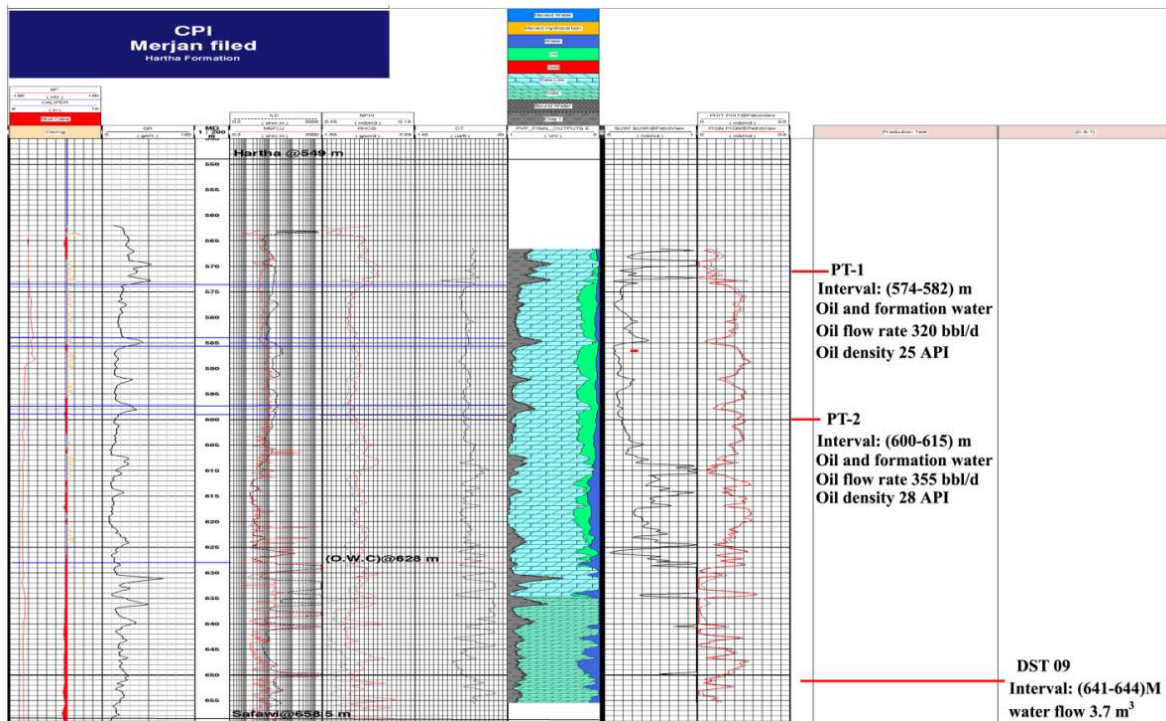


Figure 8. Computer Processed Interpretation (CPI) showing a hydrocarbon charged reservoir of Hartha formation in the Me-1 well.





Mohammed Sadi Fadhil et al.

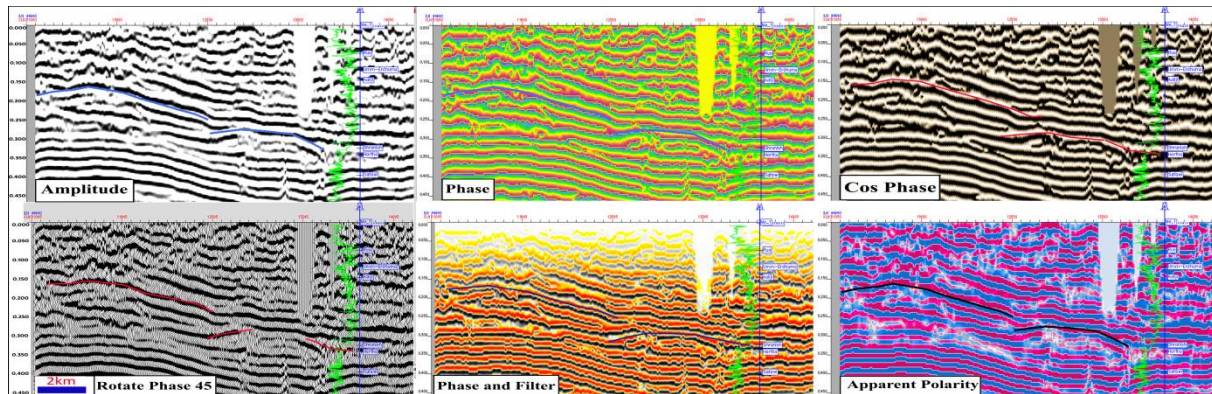


Figure 9. 3-D seismic attributes sections through mound seismic facies in the Hartha formation.

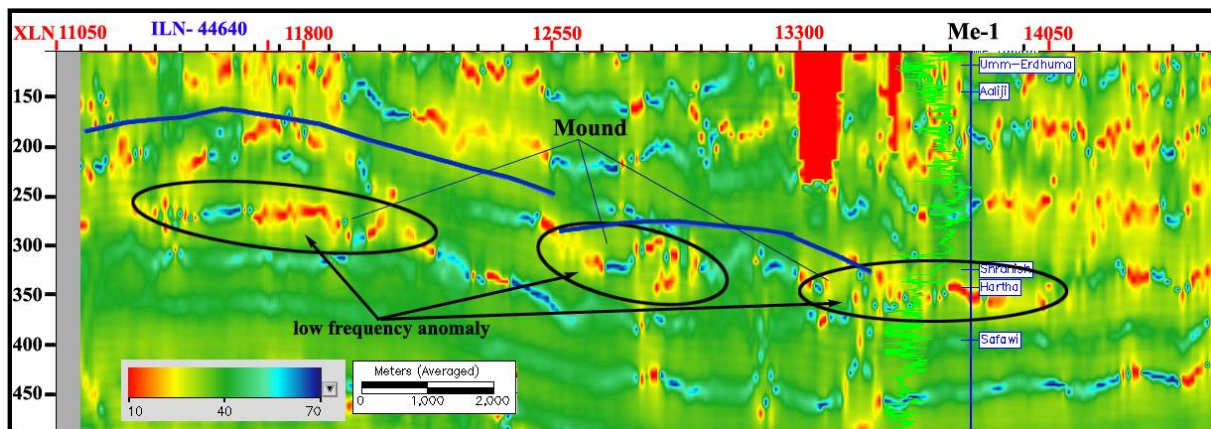


Figure 10. 3-D seismic in-line section shows the low instantaneous frequency through mound seismic facies in the Hartha formation.

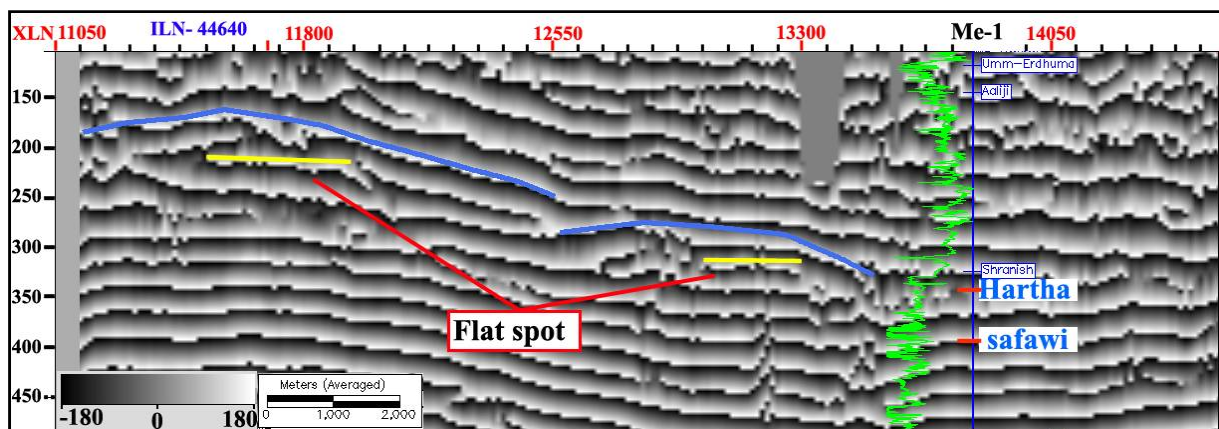


Figure 11. 3-D In-line instantaneous phase section shows flat spot features through mound seismic facies in the Hartha formation.





Mohammed Sadi Fadhil et al.

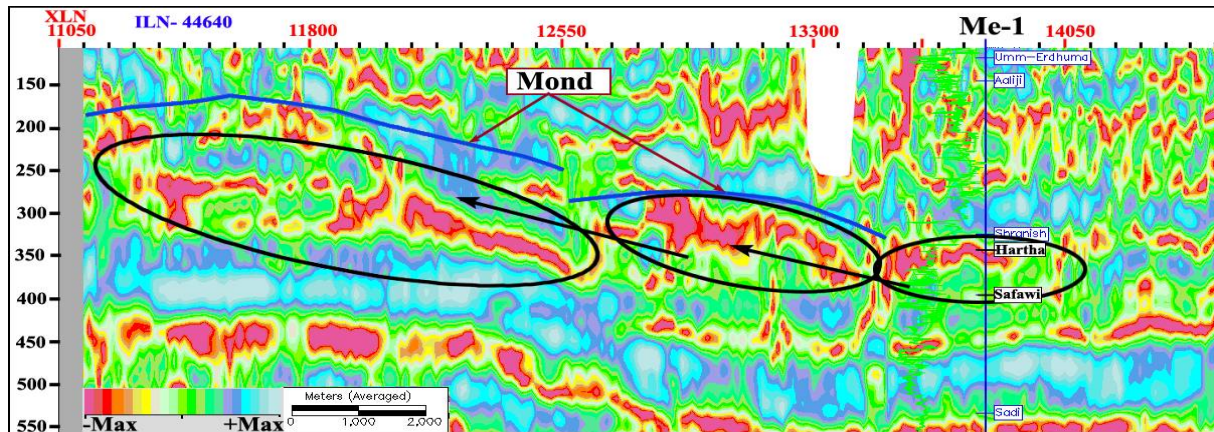


Figure 12. Inline reflection strength section show high reflection through mound seismic facies in the Hartha formation.

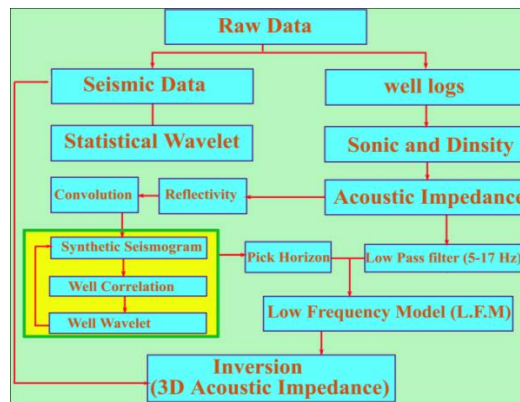


Figure 13. Flow chart summarized the main steps of inversion process, after Al-Rahim and Hashim, 2016.

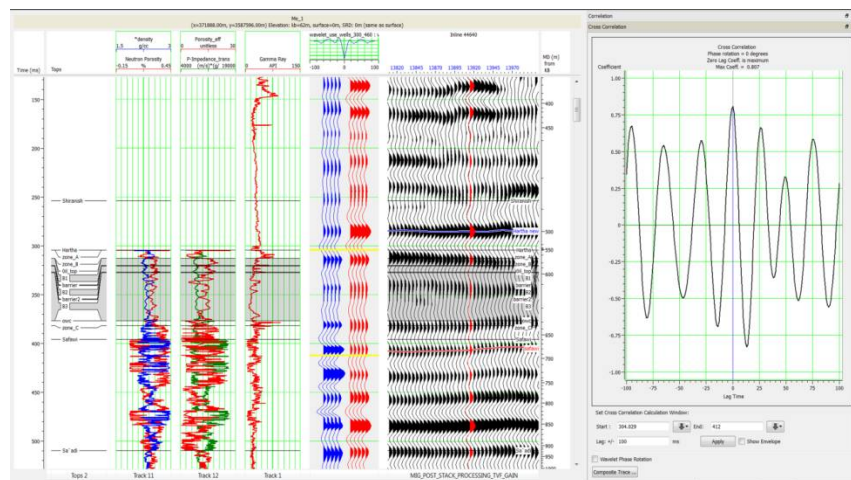


Figure 14. Well-Seismic Correlation, blue is the synthetic; red is trace around the well.





Mohammed Sadi Fadhil et al.

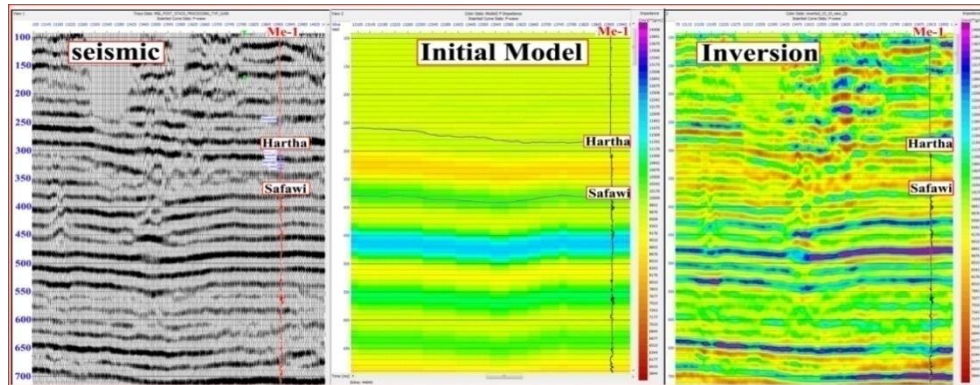


Figure 15. Shows seismic section, low frequency initial model LFM and inverted section matching well logs.

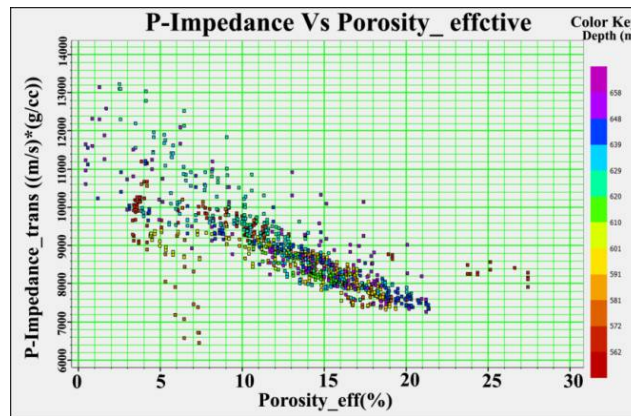


Figure 16. P-impedance versus porosity cross plot from Hartha to Safawi formation.

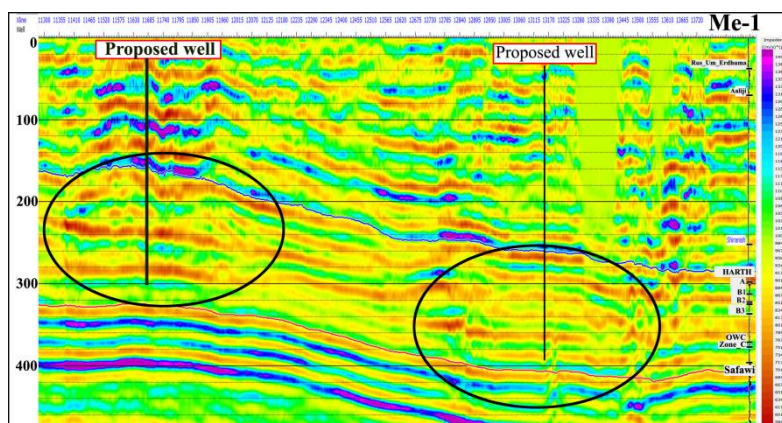


Figure 17. Acoustic impedance (AI) section shows a low AI throughout the entire interval of mound in the Hartha formation, which indicated a high porosity.





Mohammed Sadi Fadhil et al.

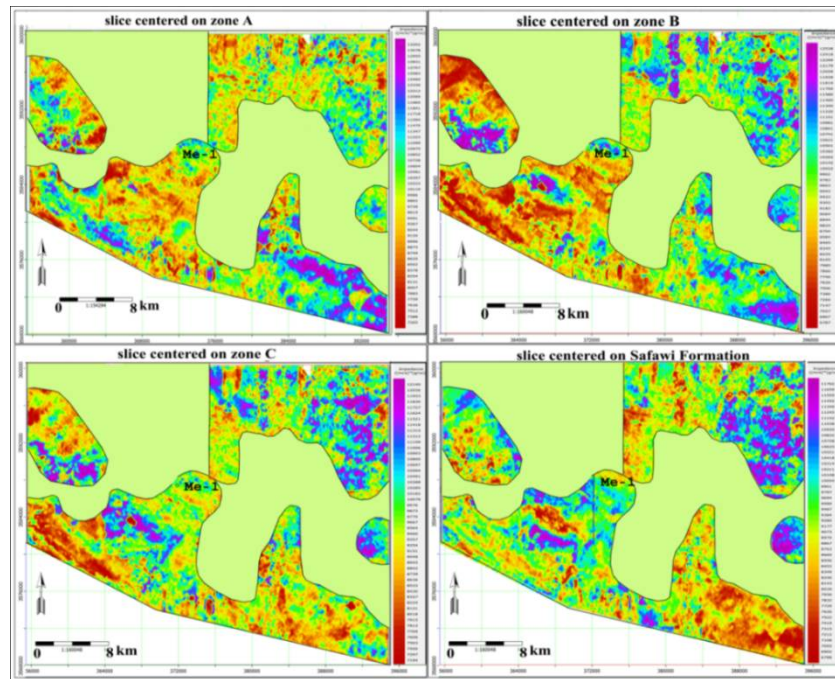
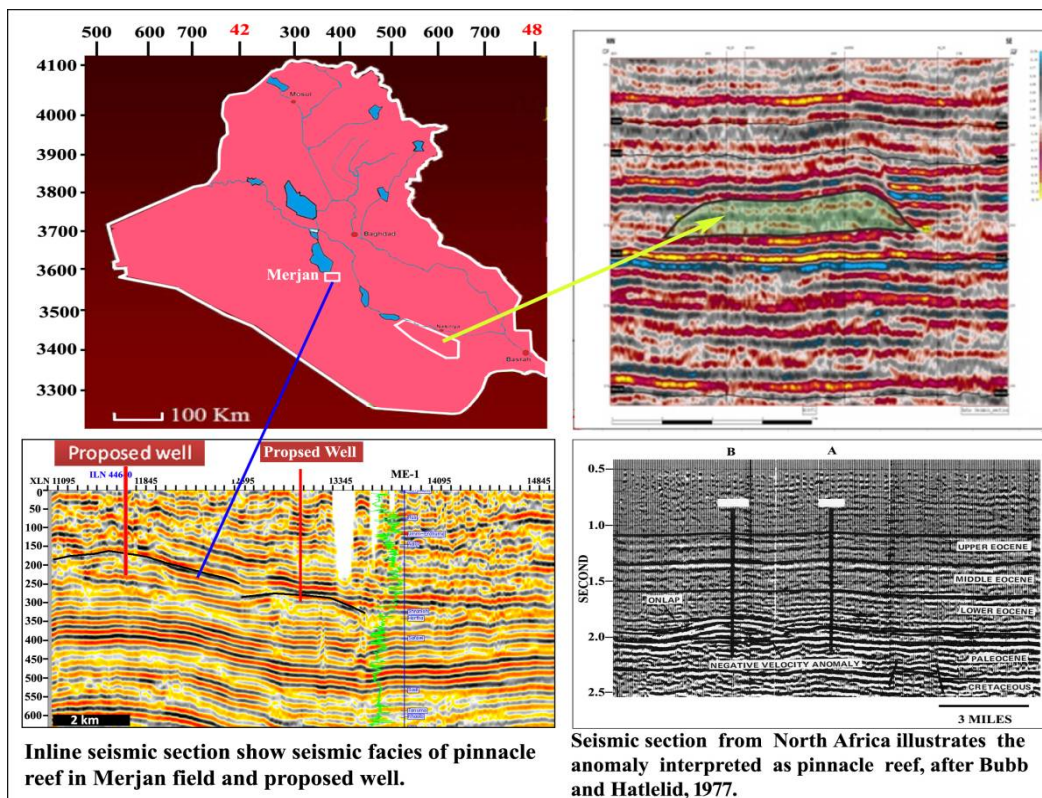


Figure 18. AI inverted Time slice distributed vertically through the reservoir of Hartha to Safawi formation.



Inline seismic section show seismic facies of pinnacle reef in Merjan field and proposed well.

Seismic section from North Africa illustrates the anomaly interpreted as pinnacle reef, after Bubb and Hatlelid, 1977.

Figure 19. Distribution of organogenic buildups, the Mishrif formation.





A General Overview on the Adsorption

Amal H. Mhemeed

College of Pharmacy, University of Misan, Iraq.

Received: 15 Sep 2018

Revised: 19 Oct 2018

Accepted: 27 Nov 2018

* Address for Correspondence

Amal H. Mhemeed

College of Pharmacy,

University of Misan, Iraq.

Email: ahamya12486@yahoo.com



This is an Open Access Journal / article distributed under the terms of the **Creative Commons Attribution License** (CC BY-NC-ND 3.0) which permits unrestricted use, distribution, and reproduction in any medium, provided the original work is properly cited. All rights reserved.

ABSTRACT

Adsorption is a phenomenon that collects gas or liquid matter in molecules, atoms or ions on the surface of another solid substance. Or is a physical or chemical association of material molecules in the active sites of a surface through the weak Vander Waals or by forming chemical bonds with effective sites on the surface(1), Adsorption can also include removal of dissolved solids in a solution or solvent by a solid surface or recovery of dissolved solvents by that surface A process called blackmail (Desorption)(2), The adsorption process usually involves a decrease in free energy(Surface Free Energy ΔG), Of the surface that occurs on it as accompanied by a lack of entropy (ΔS) Because adsorbed molecules become restricted because of their association with surface atoms , And thus lose the degrees of freedom compared to the situation that was before the adsorption, It results in a decrease in energy free ($G\Delta$) and entropy ($S\Delta$) At one time decrease in thermal content (Heat content ΔH) Under the thermodynamic relationship that binds the three amounts together at a certain temperature (3). The adsorbate is called adsorbate, whereas adsorbent adsorbents such as Charcoal, Silica gel, Zeolite and Porous clays are called (4). Adsorption may be limited to the formation of a single molecular layer on the surface of the atom. The phenomenon is then called unimolecular adsorption. Adsorption sometimes involves the formation of several molecular layers on the mass surface. The process is then called multimolecular adsorption. Adsorption and absorption are often combined on the surface with sorption (5). This process often occurs on the surfaces of porous adsorbents. This process is most positive for the need for propagation within the Surface of the surface to the energy, the process is endothermic (6) this condition indicates that the absorption process is greater than the adsorption process.

Keywords: Phenomenon, Chemical, Temperature, Adsorbent, Charcoal, Silica gel.





Amal H. Mhemeed

TYPES OF ADSORPTION

Both physical and chemical forces enter solvent adsorption from the solvent. Physical forces include van der Waals and electrostatic forces. The chemical forces result from a short inter-union rate involving the formation of internal compounds, which include a mechanism for the exchange of bonds and symbiotic bonds, and hydrogen bonds (7). On this basis adsorption can be divided into two types: The first is called natural adsorption or physical (8) (physical adsorption) or (9) (physisorption). This adsorption is also called Vander Waals adsorption, which is a natural attraction between the surface of the atom and the atoms, particles or ions that adsorb on the surface. Physical adsorption is not specific (10) because the atom or molecule that suffers from physical adsorption is not chemically bound to the surface atoms but occupies a certain area of the surface. The occupied area depends on the size of the atoms, molecules or evaporated ions, and the heat of physical adsorption is Low. Physical adsorption does not require activation energy, which is an inverse process (11, 12, 13), and the atom, molecule or ions that adsorb on the surface have the ability to move within a specific surface area, this is not nonlocalized. This type of adsorption also incorporates many layers on the surface.

The second type is called chemical adsorption or chemisorptions. Hydrogen bonds are formed in this type between the surface and the atoms, molecules or ions that adsorb on the surface. Chemical adsorption is characterized by privacy (specific). As happens in certain conditions and adsorption may not occur on another surface at the same conditions or on the surface itself when changing surrounding conditions. Chemical adsorption. With a higher heat emission than that emitted by physical adsorption may reach the level of heat emitted when the normal chemical bonds are developed. Chemical adsorption needs energizing energy (Activation Energy). The adsorption is quick and low and the reaction is often irreversible and sometimes has strong chemical bonds (13, 14, 15). It also has a location (localized) because it is done on adsorption sites that are inherently low - energy. The adsorbent energy requires chemical adsorption to a constant activation energy relative to the homogeneous surface and variable in relation to the heterogeneous surface (16). Chemical adsorption consists of a single layer of adsorbent adsorption on the surface of the adsorbent.

HEAT ADSORPTION

Heat is released when a molecule is adsorbed onto a certain amount of adsorption surface. Adsorption heat is used to determine the strength of the barrier formed by adsorption. The adsorption temperature decreases as the amount of adsorption increases. Effective sites are associated with high adsorption heat and other less efficient sites that are less heat-absorbing. In addition, there is a dissonance factor that arises between the absorbed minutes and this increase is increased with increasing adsorption due to the convergence of the minutes that are absorbed by each other. Heat emitted or associated with the adsorption process is called heat of adsorption. Temperature plays an important role in adsorption. Physical adsorption may occur at a low temperature and turn into chemical adsorption at high temperature, as in the case of hydrogen adsorption on nickel surface (17).

Factor Influencing on Adsorption Process

PH Effect

The pH of the solution is one of the most important factors affecting the adsorption and ionic exchange processes in clay minerals (18). In the case of surfaces containing polarized or charged locations, the amount of adsorption increases if the surface acquires a charge that exceeds the charge of the minutes absorbed by the effect of acidity. Conversely, the amount of adsorption decreases if the surface and the evaporated minutes acquire a similar charge (19).



**Amal H. Mhemeed**

If the pH of the solution is low, the adsorption levels may decrease because of the competition shown by the protons for the active sites in the soil granules and the amount of adsorption of the elements from the aqueous solutions increases by increasing the pH (34). Stem and Morgan (35) showed that the lead ions in the water solution turned into PbOH at pH = 5.9 and Pb (OH) 2 at pH = 7.9 and Pb (OH) 3 at pH = 9.5.

Temperature Effect

As mentioned previously, adsorption is a heat-generating process while absorption is a heat-absorbing process (Endothermic). Absorption is through adsorption, which is often accompanied by energy emission. As is evident, the increase in temperature caused a decrease in adsorption due to increased desorption. While the adsorption process, which is accompanied by the process of absorption or spread inside the pores, is absorbent to the heat and thus the kinetic energy of the molecules absorbed increases the ability to enter the pores of the steel phase and increase the speed of spread in it, so increase the adsorption process by increasing the temperature (20), Al-Haj Ali et al. (21) showed that the percentage of nickel removal from the water solution increased by increasing the temperature of the solution due to the absorption process associated with adsorption. The adsorption speed increases exponentially with the absolute temperature while the absorption process increases with the speed of absorption.

Initial concentration Effect

The adsorption process is affected by the primary concentration of the adsorbent material because the largest amount of ions or absorbable molecules is exposed to the active sites in the maze at the high concentration, which increases the adsorption speed while the percentage of adsorption.

Nature of Adsorbate

The size of the ion plays an important role in the adsorption process, affecting the amount of adsorption of a certain ion on the surface of the atom with the presence of more than one ion of different size in the solution. Altine et al. (22) has shown that under certain conditions lead ion is twice as dense as the ion of cadmium because of the large lead ion volume. The solubility of the adsorbent in the solvent also has an effect on the adsorption process where the amount of the adsorbent is reduced by increasing its solubility in the solvent (23). The soluble solubility is increased and the adsorption of the solvent.

Surface Area Effect

Adsorption is significantly affected by the rate of granularity of the mazze material because adsorption occurs mainly on the outside of the granules and slightly inside the granules because only a few of the internal effective sites allow the element ion to propagate within. Therefore, the decrease in grain size increases the surface area of adsorption, which increases the availability of suitable sites for adsorption.

Adsorption Isotherms

Isotherm is defined as the relationship between the amount of material absorbed on a surface and the equilibrium concentration of the substance absorbed in the solution at a constant temperature. It can also be defined as a description of the relationship between the amount of adsorbate on the surface of adsorbent and the primary concentration of the solution at a constant temperature (24) the first isomerization of solvent adsorption from the solvent was described by Van Bumber (1888) who described experimental data using adsorption isomerization. The reliability of the isotherm depends on the temperature in extracting useful information about the nature of the





Amal H. Mhemeed

adsorption process because it provides important information in describing the nature of adsorption and its conditions. Adsorption also helps to obtain thermodynamic amounts of adsorption.

REFERENCES

- 1- Saleh, Jalal Mohammed, ("Selective Auxiliary Function of Zeolite Molecular Sieves and its Uses in the Manufacture of Lead " Free Gasoline" Journal of the Scientific Complex, Vol. II, vol. 5, Baghdad (2004).
- 2- Stumm, W., "Chemistry of the solid water interface". John Willey & sons, New York, (1992).
- 3- Saleh, Jalal Mhammed,, "Surface chemistry and adjuvants". College of Science Press - University of Baghdad (1980).
- 4- Adam, N. K., "Physical chemistry". Oxford University press, London, 3rd ed., P. 559, (1962).
- 5- Maron, S. H. and Lando, J. B., "Fundamentals of physical chemistry". Macmillan publishing Co., London, (1974).
- 6- Doming, M., Fernandez, I. and Morals, F. G., J. chromatog., 29, 14, (1984).
- 7- Stumm, W. and Morgan, J. J., "Aquatic Chemistry". John Wiley & sons, New York, (1981).
- 8- Glasstone, S. and Lewis, D., "Elements of physical chemistry". Macmillan & Colted, 2nd ed., London, pp. 560 – 565 (1963).
- 9- Moor, W. J., "Physical Chemistry". Prentice Hall, 4th ed., Inc., p. 495 (1972).
- 10- Scharf, A., in Rica, F., "Adsorption – Desorption phenomena". Academic Press, London and New York, p. 57 (1972).
- 11- Adamson, A. W., "Physical Chemistry of Surfaces". Wiley Interscience, 3rd ed., (1976).
- 12- Yong, D. M. and Crowell, A. D., "Physical adsorption of gasses on porous solids". Butter Worths, (1962).
- 13- Gregg, S. J. and Sing, K. S. W., "The adsorption of gasses on porous solids". William Clowes & Sons, (1979).
- 14- Hayward, D. O. and Tranpell, B. M. W., "Chemisorption". Butter Worths, 2nd ed., (1964).
- 15- Tompkins, F. C., "Chemisorption of gasses on metals". Academic Press, (1978).
- 16- Szabo, Z. G. and Kallo, D., "Contact Catalysis". Vol. 1, Elsevier Scientific publishing comp., Copenhagen, p. 134 (1976).
- 17- Al-Grawi, E.D.C., and G.R.L. Al-Awsi. 2018. "Expression of CDKN2A (P16/Ink4a) among Colorectal Cancer Patients: A Cohort Study." Journal of Pharmaceutical Sciences and Research 10 (5).
- 18- Saleh, Jalal Mohammed, "Surface Chemistry and Assistive Factors". College of Science Press - University of Baghdad (1980).
- 19- Garcaya-Miragaya, J. and Dage, L. A., "Influence of ionic strength and inorganic complex on the sorption of trace amount of Cd by montmorillonite". Soil Sci Soc. Am., 740 : 458 – 663 (1976).
- 20- Awad, K. M., "The principle of soil chemistry". Basrah University Press, Basrah (1986).
- 21- Al – Haj Ali, A. and El – Bishtawi, R., "Removal of Lead and Nickel ions using zeolite tuff". J. chem. Tech. Biotechnol., 69, 27 – 34 (1997).
- 22- Stumm, W. and Morgan, J. J., "Aquatic chemistry". John Willey & Sons, New York, (1970).
- 23- Shamran, A. R, Shaker, Z. H, Al-Awsi, G. R. L, Khamis, A. S, Tolaifeh, Z. A. and Jameel, Z. I, 2018. RAPD-PCR IS A GOOD DNA FINGERPRINTING TECHNIQUE TO DETECT PHYLOGENETIC RELATIONSHIPS AMONG STAPHYLOCOCCUS AUREUS ISOLATED FROM DIFFERENT SOURCES IN HILLA CITY, IRAQ. Biochemical and Cellular Achieves. Vol. 18, Supplement 1, pp. 1157-1161.
- 24- Ibraheem, Lujain Hussein, and S. A. A. 2017. "Accumulation Detection of Some Heavy Metals in Some Types of Fruits in the Local Market of Al-Diwaniyah City, Iraq." *Rasayan Journal of Chemistry* 10 (2) 339–43. doi:10.7324/RJC.2017.1021641.
- 25- Al-Thahab, Azhar Omran and Al-Awsi, Ghaidaa Raheem Lateef, 2018. DETECTION OF HELOCOBACTER PYLORI IN PREGNANT WOMEN BY STOOL CULTURE METHOD. Biochemical and Cellular Achieves. Vol. 18, No. 1, pp. 49-54.
- 26- Doming, M., Fernandez, I. and Morals, F. G., J. chromatog., 29, 14, (1984).





Amal H. Mhemeed

- 27- Altin, O., Hozbelge, O. and Dogu, T., "Effect of pH, flow rate and concentration on the sorption of Pb and Cd on montemorillonite: 1- Experimental". *J. Tech. Biotech.* , 74: 1131 – 1138 (1999).
- 28- Thomas, M. and Robert, P., *J. Agr. Food chem.*, 13 (4), 334 (1965).





Petrography and Diagenetic Development of the Zubair Formation in the Kifl Oil Field, Southern Iraq

Aiad Ali Al-Zaidy^{1*} and Mohammed Jamal Ahmed²

¹Department of Geology, College of Science, University of Baghdad, Baghdad, Iraq.

²Geotechnical Engineering Department, Faculty of Engineering, University of Koya, Erbil, Iraq.

Received: 13 Sep 2018

Revised: 16 Oct 2018

Accepted: 18 Nov 2018

*Address for Correspondence

Aiad Ali Al-Zaidy

Department of Geology,

College of Science,

University of Baghdad,

Baghdad, Iraq.

Email: dr.aiad.alzaidy@gmail.com



This is an Open Access Journal / article distributed under the terms of the **Creative Commons Attribution License** (CC BY-NC-ND 3.0) which permits unrestricted use, distribution, and reproduction in any medium, provided the original work is properly cited. All rights reserved.

ABSTRACT

The Barremian succession in the present study is represented by the Zubair Formation which is the most significant sandstone oil reservoir in Iraq. The studied area is located in the southern part of Iraq at the Kifl oil field, within the Mesopotamian basin. The petrographic study showed that quartz mineral is the dominated component of the sandstone in Zubair Formation with minor percentage of feldspar and rare rock fragments which classified as quartz arenite. The Zubair formation in the study area was affected by many diagenetic processes during and after deposition. The main diagenetic processes impressed the succession with different intensity are cementation, compaction, dissolution, and dolomitization. These processes affected porosity in many ways and stages. There are three diagenetic zones; the lower part of the Zubair Formation was characterized by three effected porous zone separated by high compacted and cemented sandstone. The middle part of this formation was showing high compacted sandstone with appearing of overgrowth quartz and micro-quartz cementation. Whereas the upper part of the Zubair Formation was seemed as alternative compaction shale with high compaction and overgrowth of quartz. The clean sandstone was deposited and affected by the compaction with chemical dissolution lead to form the secondary quartz precipitated on the original grains this decrease the primary porosity. The increasing of compaction process destroyed the quartz and rock fragment grains this associated with chemical solution lead to precipitate extra grains of quartz as a small grain decreasing the porosity. After this process the changing in chemical and physical properties of depositional basin leads to precipitate the calcite cements, and finally as results of organism activity calcite was dissolved and produced the secondary porosity.

Key words: Petrography, Diagenetic development, Zubair Formation, Kifl oil field, Southern Iraq.



**Aiad Ali Al-Zaidy and Mohammed Jamal Ahmed****INTRODUCTION**

The Zubair Formation was introduced by Glynn Jones in 1948 from the Zubair oil field and amended by Nasr and Hudson in 1953 (Bellenet *et al.*, 1959). It is the most significant sandstone oil reservoir in Iraq, is composed of fluvio - deltaic, deltaic and marine sand stones. It covers wide areas of the Arabian Plate including northern Saudi Arabia, Kuwait and most of southern and part of Central Iraq. The formation correlates with the Biyadah (Riyadh) Formation in Saudi Arabia (Powers *et al.*, 1966 in Aqrawi *et al.*, 2010). The studied area (Kifl oil field) is located in south of Baghdad to the south-west of Hilla city at a distance approximately (35km), and lies within the Mesopotamian Zone between the Zagros fold to the north and the Stable Shelf To the west. The study area lies in the middle of Iraq between Najaf and Karbala governorates (west of the Euphrates River) (Fig.1), it limits from east the Euphrates River to the north Karbala city and to the north-west the Razaza lakes.

During the Hauterivian to Early Aptian age the Zubair Formation was deposited with 380-400m of alternating shale, siltstone and sandstone (Bellen *et al.* 1959). This formation was assumed to represent a prograding delta originating from the Arabian shield (Zeigler, 2001). Zubair Formation is overlying with the Shuaiba Formation are mostly gradational and conformable (Fig.2). The lower boundary is, however unconformable with Ratawi Formation (Buday, 1980), and this unconformity described by Douban and Al-Medhadi (1999).

Petrography**Petrography of Sandstone**

The composition of sand can be controlled by many factors such as the composition of source rocks, transportation distance of detritus before it reaches its final site of deposition, the residence time that detritus is held in environment so other than its final deposition position, the climate in the source area and diagenetic effect following final deposition (Suttner and Dutta 1986). Texture is used when describing sedimentary rocks (sandstones) with a view to determining their depositional mechanism and environment. It is also a means of assessing the degree of porosity and / or permeability which has proved to be a valuable tool in the analysis of potential hydrocarbon rich sand-bodies. The recognized components in Zubair Formation sand stone are shown below:-

Quartz

Quartz has the most abundant mineral ratio among main component grains (quartz, feldspar and lithic grains only) ranging from more than 95% in the well sorted, rounded quartz-arenite sandstone unit of Zubair Formation to the less of 25% in the shale dominated unit of the same Formation. The predominance of quartz can be result by recycling, long transportation distance or tropical weathering predominance (Dickenson, 1988). Quartz grain size ranges from medium to very fine according to Wentworth, 1932 (in Pettijohn *et al.* 1973). Grains roundness ranges from subangular to rounded according to visual chart of Powers (1953) (Fig.3). This variation in size and roundness lead to form many types of contact between quartz grains such as long, concavo – convex and Y-contact type, but in some slides there are few of floating contact sand point contact which increase in slides with high ratio of calcite cement related to the growth of carbonate cement which leads to forceful wedging apart of the grains (Waldschmidt, 1941 in Pettijohn, 1975).

There are two types of quartz recognized in Zubair Formation they are: the first, Monocrystalline Quartz (Plt.1-A, B) as a dominant type. This type of quartz shows two types of extinction: sharp extinction and slightly undulating extinction. Monocrystalline quartz refers to granitic source rock (Folk, 1968). and the second, Polycrystalline Quartz (Plt.1-C, D) as a small percentage as a reason for that is the lack of stability during long-distance transport or lack of presence in the source (Pettijohn, *et al.*, 1973). The polycrystalline quartz can develop from monocrystalline quartz



**Aiad Ali Al-Zaidy and Mohammed Jamal Ahmed**

during metamorphism under the influence of increasing pressure and temperature. Non-undulatory monocrystalline quartz changes progressively to undulatory quartz, then to polygonized quartz (quartz that shows distinct zones of extinction with sharp boundaries), and finally to polycrystalline quartz (Young, 1976).

Feldspar

Like quartz, feldspar has low relief and low first-order interference colors (white to gray), and it can be easily misidentified as quartz where it lacks twins. But so many feldspar grains are recognized by complex twinning (plagioclase) (Plt.1-E), while the orthoclase has occasionally a simple twin (Plt.1-F). Feldspar ratio is less than (1%), due to the weak stability as it decomposes and eroded when transported to long-distance, Therefore the presence or absence of feldspar is a result of balance occurring between rate of decomposition and rate of erosion (Pettijohn, 1975).

Rock Fragments

Rock fragments are detrital particles made up of two or more mineral grains depending upon source-rock composition. It can provide the most direct lithological evidence (Boggs, 1995). **Chert** is microcrystalline quartz and therefore occurs as a mass of very fine crystals with low first-order interference colors (gray and white) and low relief (Plt.2-A). **Rock fragments** are fine-grained sedimentary rock fragments. They are often brown, with silt-sized quartz grains and disseminated opaque iron-oxide or iron-sulfide (pyrite) grains (Plt.2-F). Because they are mechanically soft, shale fragments are commonly deformed during compaction. They are thus often confused with matrix and sometimes known as pseudo-matrix (Plt.2-B). Composed of various metal components such as shale or flint and the proportion of their presence and a few are almost non-existent long distance transported (Pettijohn *et al.*, 1973).

Petrography of Shale

The shale continues as a thinly laminated, weakly calcareous, pyritic, silty shale with abundant organics as is represented in the lower and upper parts of Zubair Formation. This shale contains moderate to abundant bands quartz grains (Plt.2-C), less of calcite and dolomite, and bands with long calcite strands (Plt.2-D), often with scattered pyrite crystals. Pyrite within the shale occurs as microcrystals, framboidal aggregates, or as nodules that formed within the laminated shale (Plt.2-E). Whereas, the middle part characterized by lenses and false bands of shale within sandstone unit (Plt.2-E).

Maturity

The textural maturity determined by relative abundance of matrix and the degree of rounding and sorting of framework grains. Textural maturity can range from immature (much clay, framework grain poorly sorted and poorly rounded) to super mature (little or no clay, framework grain well sorted and well rounded). That reflects the degree of sediment transport and reworking (Boggs, 2009). In this study represented a high percentage of quartz about 90% represented super maturity and according to classification of Pettijohn, *et al.*, 1973 represented quartz arenite that composed of more than 90 percent siliceous grains that may include quartz (Plt.1-A & B). The rocks in the upper sand member are mature physically and chemically. This evidenced by the presence of the high percentage of quartz and by the medium to good sorting. This support the concept that rock of Zubair Formation passes in many cyclic depositions and transport to a far distance.



**Aiad Ali Al-Zaidy and Mohammed Jamal Ahmed****Diagenetic Processes**

Diagenesis alters the original pore type and geometry of a sand stone and therefore controls its ultimate porosity and permeability. Early diagenetic patterns correlate with environment of deposition and sediment composition. Later diagenetic patterns cross facies boundaries and depend on regional fluid migration patterns (Stonecipher and May, 1990). Effectively predicting sandstone quality depends on predicting diagenetic history as a product of depositional environments, sediment composition, and fluid migration patterns. Diagenesis may also play an extremely important role in post-depositional modification of porosity, causing either decrease in porosity as a result of compaction and cementation or increase in porosity owing to solution processes. Accordingly, the economic importance for a particular sandstone body as a reservoir rock for petroleum (Boggs, 2009). Diagenesis refers primarily to the reactions which take place within sediment between one mineral and another, or between one or several minerals and the interstitial or supernatant fluids (Selley, 2000). There are four types of diagenesis were distinguished in the studied succession, as follows:

1. Compaction
2. Cementation
3. Dissolution
4. Dolomitization

The effects of diagenesis on sandstone reservoirs include the destruction of porosity by compaction and cementation, and enhancement of porosity by solution for that it is control regional variations of reservoir quality the main processes include:-

Compaction

This is the process of volume reduction and consequential pore- water expulsion within sediments (Burley, 2003). The degree of compaction dependent on sorting, clay content, percentage of ductile fragments and burial depth or tectonic stresses (Blatt, 1982).

Compaction of Sandstone

There are two types of sandstone compaction, physical and chemical (pressure solution) (Boggs, 1995).

Physical compaction

The physical compaction can be notes from his effects: -

- a. Ternary concourse to grain of quartz that is contact relation between grains in ideality state on impact of mechanical precision (Plt3-A).
- b. Quotient deformation to wake grains (Plt. 3-B).
- c. The fissures are happening to grains (Plt. 3-C).

Chemical compaction

It can continue during burial. The solubility of silicate minerals tends to increase with increasing pressure and temperature (Burley, 2003). After the initial physical rearrangement of grains, chemical compaction can continue during burial in further porosity loss. The solubility of silicate minerals tends to increase with increasing pressure and temperature (Robin, 1978, in: Burley, 2003). Pressure dissolution is thus compaction response of sandstone during burial to increase the surface area of grain – grain contacts. Thus point – contacts evolve through straight – elongate to concave–convex and even sutured contacts (Burley, 2003)(Plt. 4 A & B).



**Aiad Ali Al-Zaidy and Mohammed Jamal Ahmed****Compaction of Muds**

Modern muds contain > 60% water, which can be squeezed out by exerting little pressure. Muds can be compacted because grains are ductile (flexible) and can pack easily (Rieke and Chilingarian, 1974). This type of compaction is common in the all shale units in the studied succession (Plt. 5-A&B).

Cementation

Refer to growth or precipitation of minerals in pore spaces (Burley, 2003) so it have special important in reservoir studied. In the studied area, there are four types of cement: Silica cement, Carbonate cement, Iron oxide cement, Clay cement. (Plt.5-A&B)

Silica Cement**Quartz Overgrowths**

Quartz overgrowths develop by the precipitation of silica directly from aqueous solution as well-ordered, low (alpha) quartz. The most common form of quartz cement is an overgrowth, a syntaxial rim with the same crystallographic orientation and optical continuity as that of the detrital grain. Overgrowths are one variety of Krynine's (1946) sedimentary (low-temperature) quartz and are megaquartz in Folk's (1968) size classification of sedimentary quartz. This type of cement is abundant in the sandstones of Zubair Formation in the studied sections (Plt. 6-A & B).

Micro-Crystals Quartz Cement

Other polymorphs of silica that occur as cements in sandstones are fibrous microcrystalline quartz. Almost all occurrences of these polymorphs are in silcretes, indurated products of surface silica diagenesis (Plt. 7-A & B).

Clay Cement

The average of this cement is less than 1% (Plt. 8-A). The source of this cement is partly from dissolution to rock fragment and feldspar. This cement has an important effect on permeability (Burley, 2003).

Carbonate Cement

The carbonate cement is also uncommon in sandstone of Zubair Formation. Some sandstone has carbonate cement with silica and iron cement. The average of it is 1% in the studied wells. Sometimes it is appearing as patches between quartz grains. The source of this carbonate cement is from Ratawi and Shuaiba Limestone Formations (Plt. 8-B).

Dissolution

Rock fragments and low stability silicate minerals dissolved because of increasing burial temperatures. There are two types of dissolution; the first is the pressure solution (see compaction) and the second is the dissolution which leads to increase in secondary porosity (Boggs, 1995) (Plt. 9-A & B).





Aiad Ali Al-Zaidy and Mohammed Jamal Ahmed

DISCUSSION AND CONCLUSION

The concept of diagenetic regimes is a broad framework that relates diagenetic processes to the evolution of sedimentary basins. Three conceptual regimes are commonly recognized: early diagenesis (eogenesis), burial diagenesis (mesogenesis) and uplift-related diagenesis (telogenesis). This terminology was adopted from a scheme developed initially by Choquette & Pray (1970) to describe limestone diagenetic processes, but is now more generally applied: correctly so, as the same fundamental processes and controls operate in clastic diagenesis and in carbonate diagenesis. Alternative schemes (e.g. the Russian system including such terms as catagenesis and epigenesis) have been used but are less commonly applied now (Prozorovich, 1970). This is because systems and classifications defined by the maximum temperature of burial run into the difficulty of the effect of varying time spent at a given temperature—a direct consequence of the kinetic control on the rate of diagenetic reactions.

The Zubair formation in the study area is affected by many diagenetic processes through deposition represented by (Fig. 4). There are three diagenetic zones; the lower part of the Zubair Formation is characterized with three effective porous zone (Fig. 4) separated by high compacted and cemented sandstone. The middle part of this formation is showing high compacted sandstone with appeared the overgrowth quartz and micro-quartz cementation. While the upper Zubair Formation is appeared as compaction shale alternative with high compaction overgrowth quartz. The quartz arenite sandstone affected by the compaction in low amount follows by chemical dissolution lead to made the secondary quartz precipitated on the original grains this decrease the primary porosity, the increase of compaction process destroyed the quartz and rock fragment grains this associated with chemical solution lead to precipitate extra grains of quartz as a small grain decreasing the porosity. After this process the changing in chemical and physical properties of depositional basin lead to precipitate the calcite cements, and finally as a results of organism activity calcite were dissolved and produced the secondary porosity.

REFERENCES

1. Aqrawi, A.A.M., Goff, J.C., Horbury, A.D. and Sadooni, F.N., 2010. The petroleum Geology of Iraq. Scientific Press Ltd., 424pp.
2. Bellen, R.C., Dunnington, H.V., Wetzel, R. & Morton, D.M., 1959: Lexique stratigraphic international, Asia, Fascicule 10, Iraq, 333pp. (center national de la Recherche scientifique, Paris).
3. Blatt, H., Middleton, G., Murray, R., 1980: Origin of Sedimentary Rocks: Prentice-Hall, New Jersey.
4. Boggs S., 2009, Petrology of Sedimentary Rocks, Cambridge University Press, United States of America.
5. Boggs, S., 1995: principles of sedimentology and stratigraphy, prentice Hall, New Jersey, 774p.
6. Buday, T., 1980: The Regional geology of Iraq, VI: Stratigraphy and Paleogeography, state organization for minerals, Mosul, Dar Al-Kutab publication House, 445P.
7. Burley S. D. and Worden H., 2003: Sandstone Diagenesis: Recent and Ancient, Blackwell Publishing, P649.
8. Choquette, P.W. and Pray, L.C., 1970. Geologic Nomenclature and Classification of Porosity in Sedimentary Carbonates, AAPG Bulletin, Vol. 54, No. 2, 1970, pp.
9. Dickinson, W.R., 1985: Interpreting provenance relation from detrital modes of sandstones, in Zuffa, G.G. (ed.), Provenance of Arenites: NATO ASI Series, C 148, D. Reidel Publishing Company, Dordrecht, 333–363.
10. Douban, A.F. and Medhadi, P., 1999. Sequence Cretaceous Megasequences, Kuwait. AAPG International.
11. Folk, R., 1968: Petrology of Sedimentary rocks, Hemphill, Texas, P182.
12. Pettijohn, F. J. 1975: Sedimentary Rocks. (3rd Edition), Harper and Row New York, 628p.
13. Pettijohn, F. J; Potter, P.E. and Siever, R., 1973: Sand and Sand Stone. Springer-Verlag. New York, 618p.
14. Powers, M. C., 1953: A new roundness scale for sedimentary particles: J.Sediment. Petrol. 23,117–119.
15. Prozorovich, G.E. Determination of the time of oil and gas accumulation by epigenesis studies. Sedimentology, 15, 41–52, 1970.





Aiad Ali Al-Zaidy and Mohammed Jamal Ahmed

16. Rieke, and Chilingarian, 1974. Compaction of Argillaceous Sediments. Developments in Sedimentology V.16. xiv + 424 pp.
17. Selley R. C., 2000: Applied Sedimentology, Academic press. P523.
18. Stonecipher, S.A. and May, J.A.: "Facies Controls on Early Diagenesis: Wilcox Group, Texas Gulf Coast," in Prediction of Reservoir Quality Through Chemical Modeling: AAPG Memoir 49, I.D. Meshri and P.J. Ortoleva, eds. (1990) 25-44.
19. Suttner, L.J. and Dutta, P.K., 1986. Alluvial Sandstone Composition and Palaeoclimate Framework Mineralogy. Journal of Sedimentary Petrology, 56, 329-345.
20. Young, S.W., 1976: Petrographic textures of detrital polycrystalline quartz as an aid to interpreting crystalline source rocks. Journal of Sedimentary Petrology, 46, 595-603.
21. Ziegler, M. 2001. Late Permian to Holocene paleofacies evolution of the Arabian Plate and its hydrocarbon occurrences. GeoArabia, 3, p. 445-504

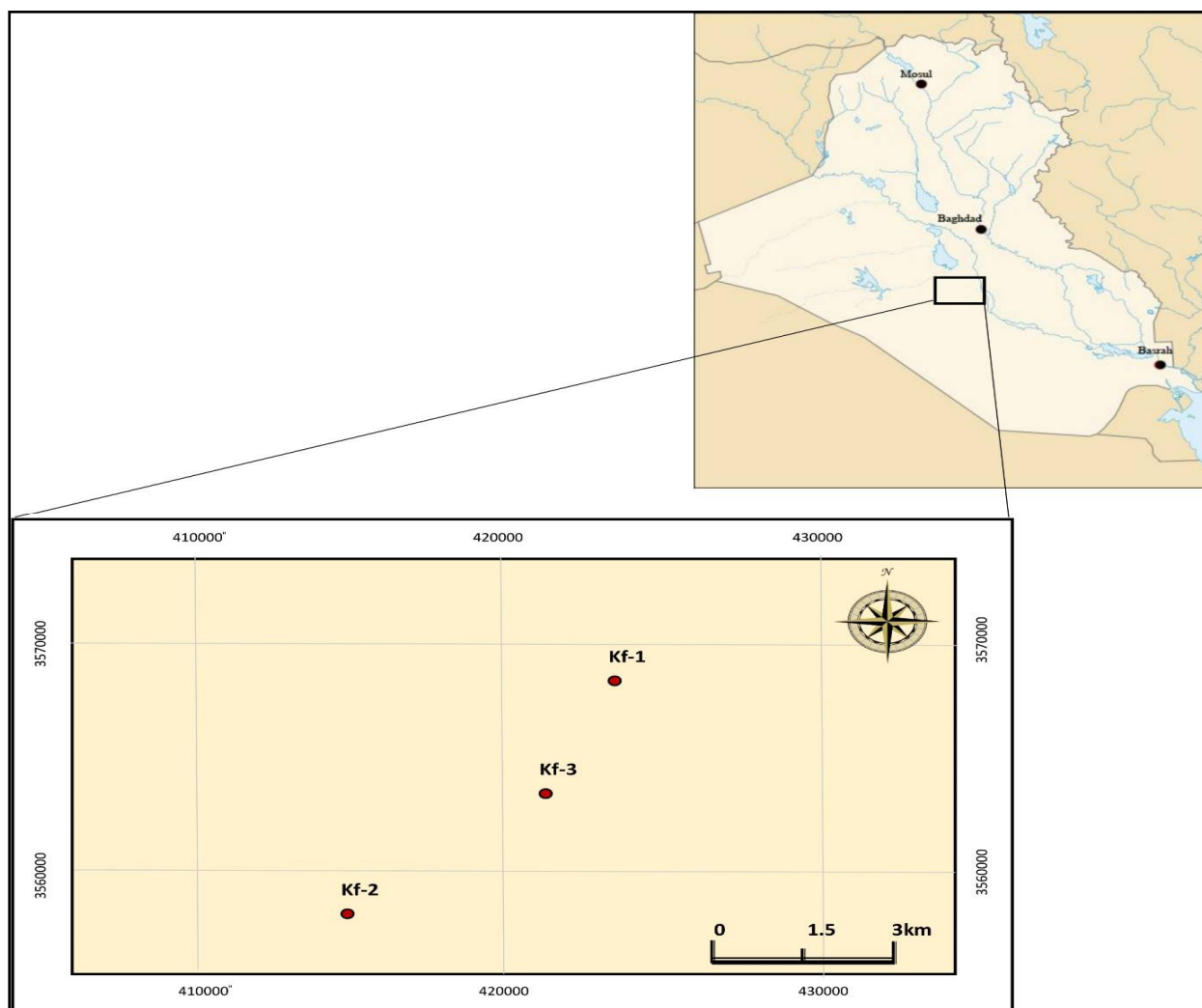


Fig.1. The study area west of the Euphrates River





Aiad Ali Al-Zaidy and Mohammed Jamal Ahmed

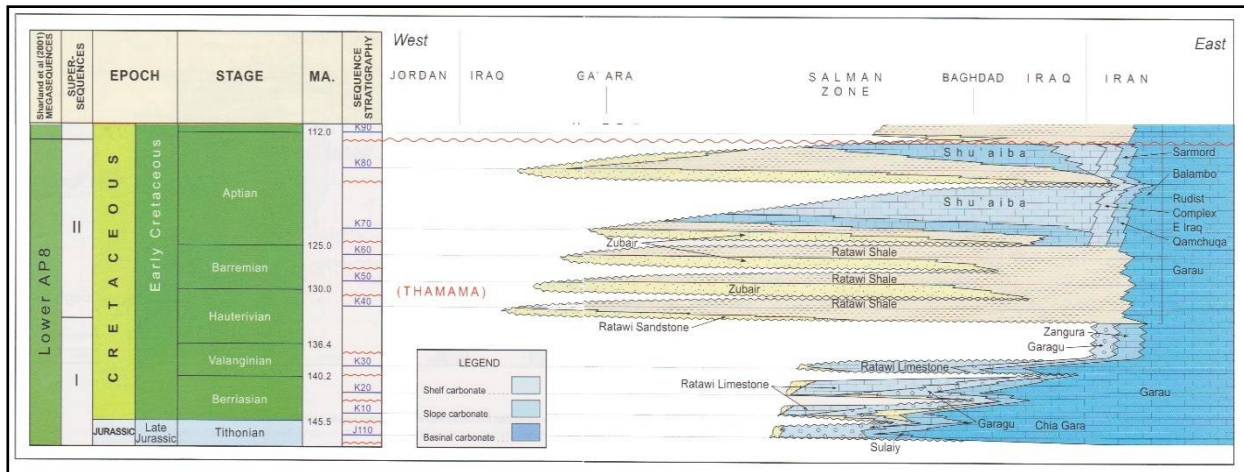


Figure 2. Schematic west-east profile across Southern/ Central Iraq illustrating stratigraphic position of Zubair Formation (Aqrawi, et al. 2010)



Figure 3. Standard dimensions used in the description of sedimentary particle size





Aiad Ali Al-Zaidy and Mohammed Jamal Ahmed

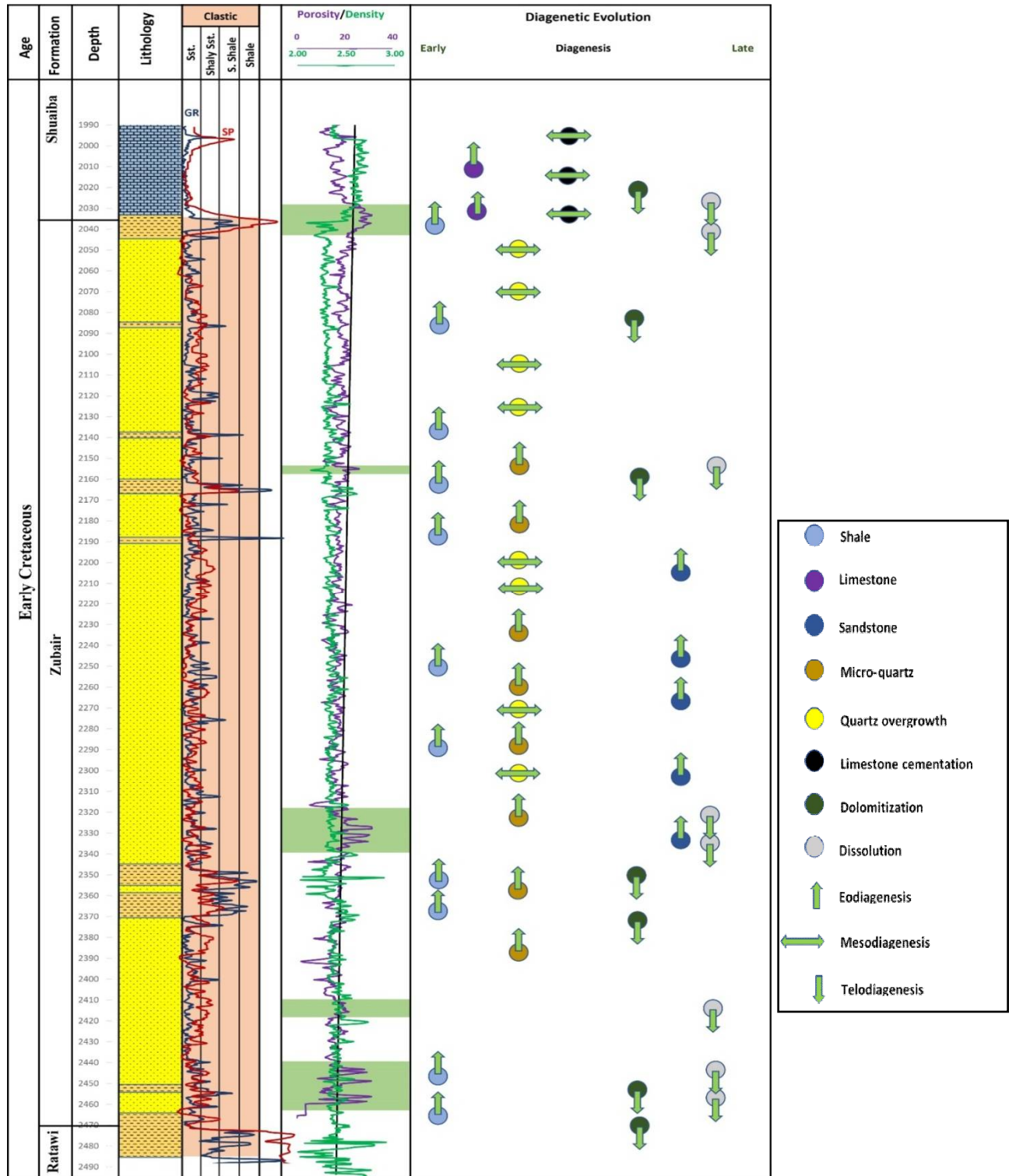
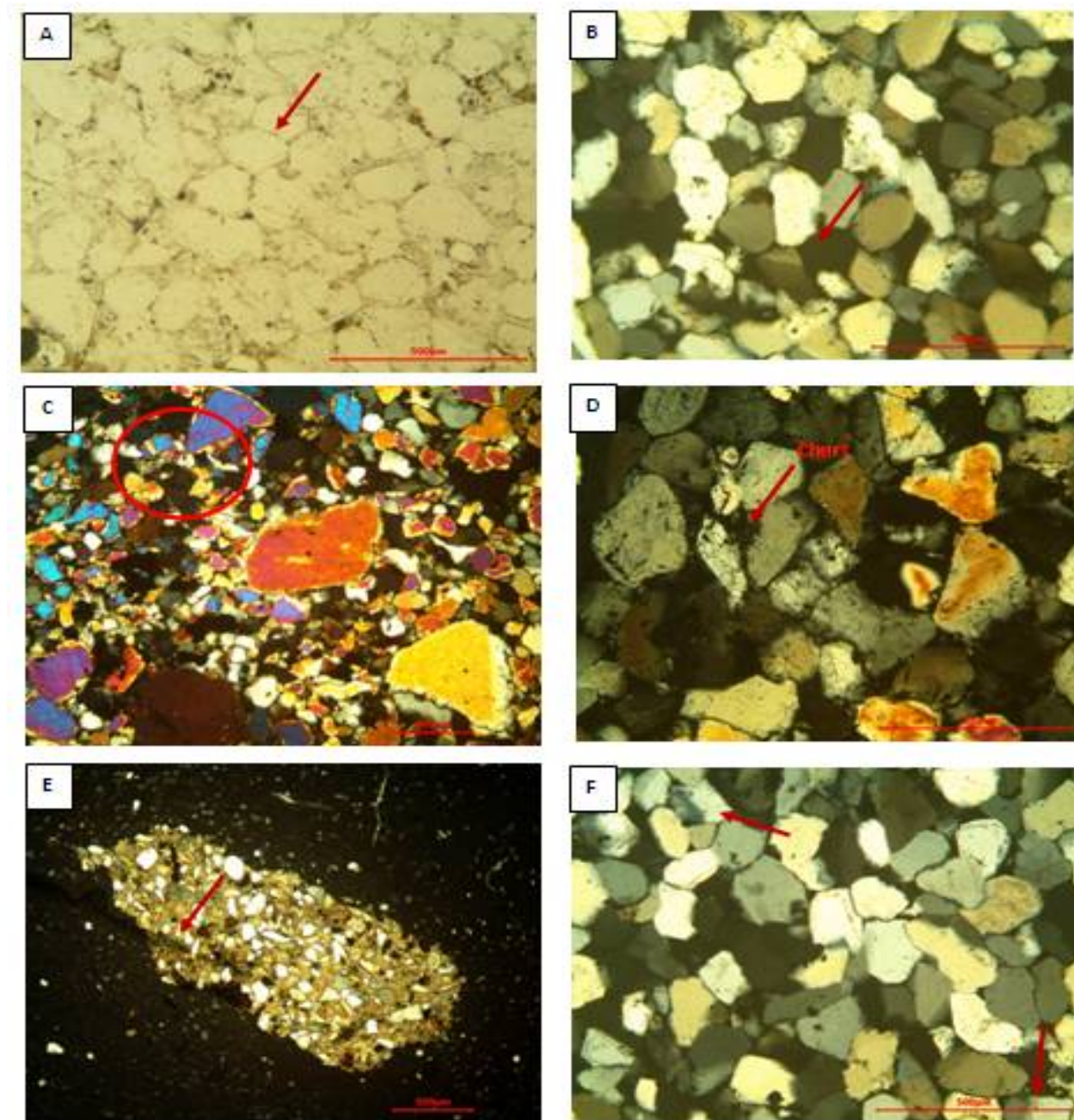


Figure 4. Diagenetic history of Zubair Formation in the study area





Aiad Ali Al-Zaidy and Mohammed Jamal Ahmed



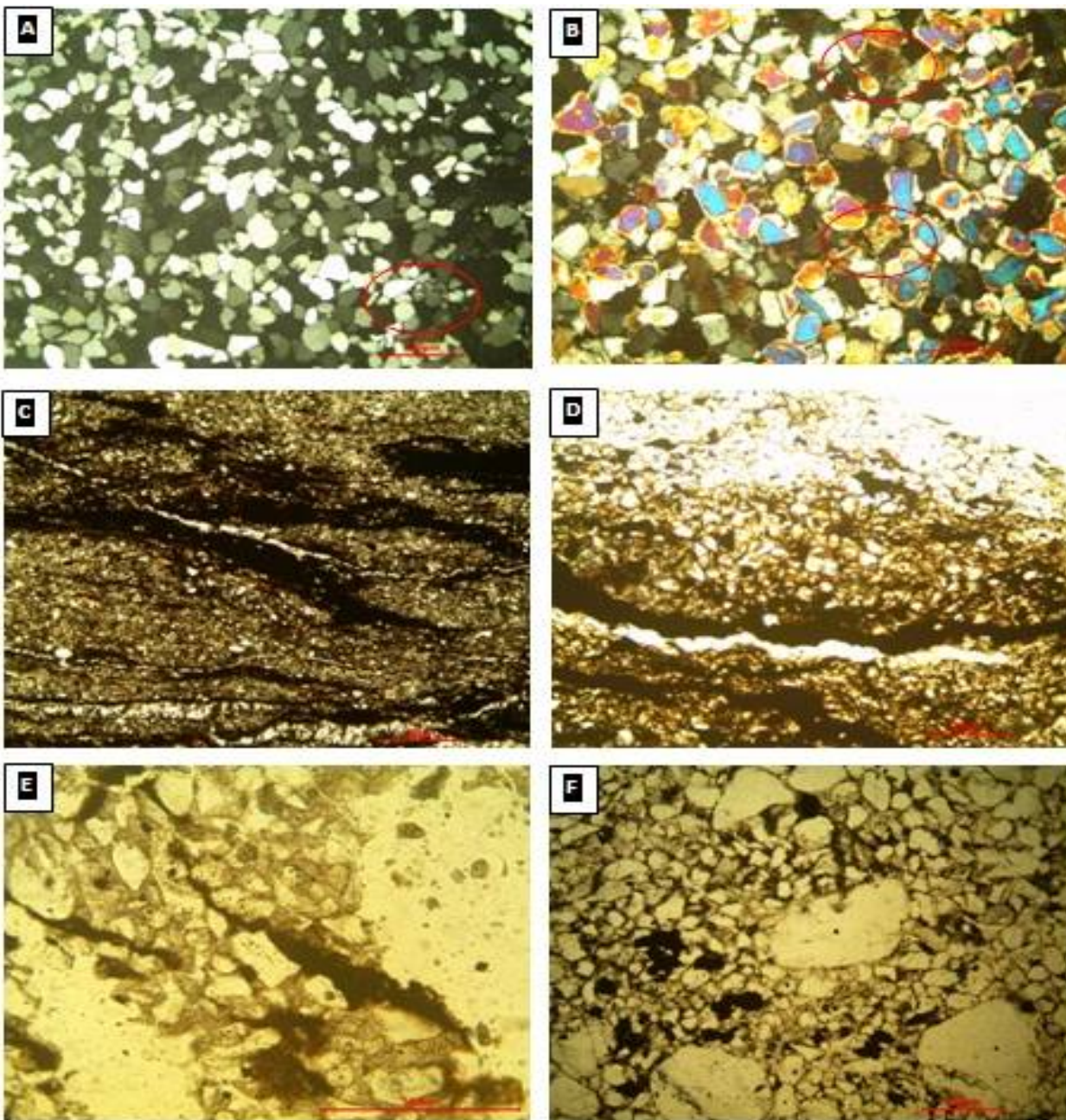
Plat 1.

- A. Monocrystalline Quartz. Kf-1 (2200m)
- B. Monocrystalline Quartz under the polarized. Kf-1 (2200m)
- C. Polycrystalline Quartz. Kf-1 (2450m)
- D. Polycrystalline Quartz and chert under the polarized. Kf-1 (2200m)
- E. Plagioclase. Kf-1 (2435m)
- F. Orthoclase. Kf-1 (2090m)





Aiad Ali Al-Zaidy and Mohammed Jamal Ahmed



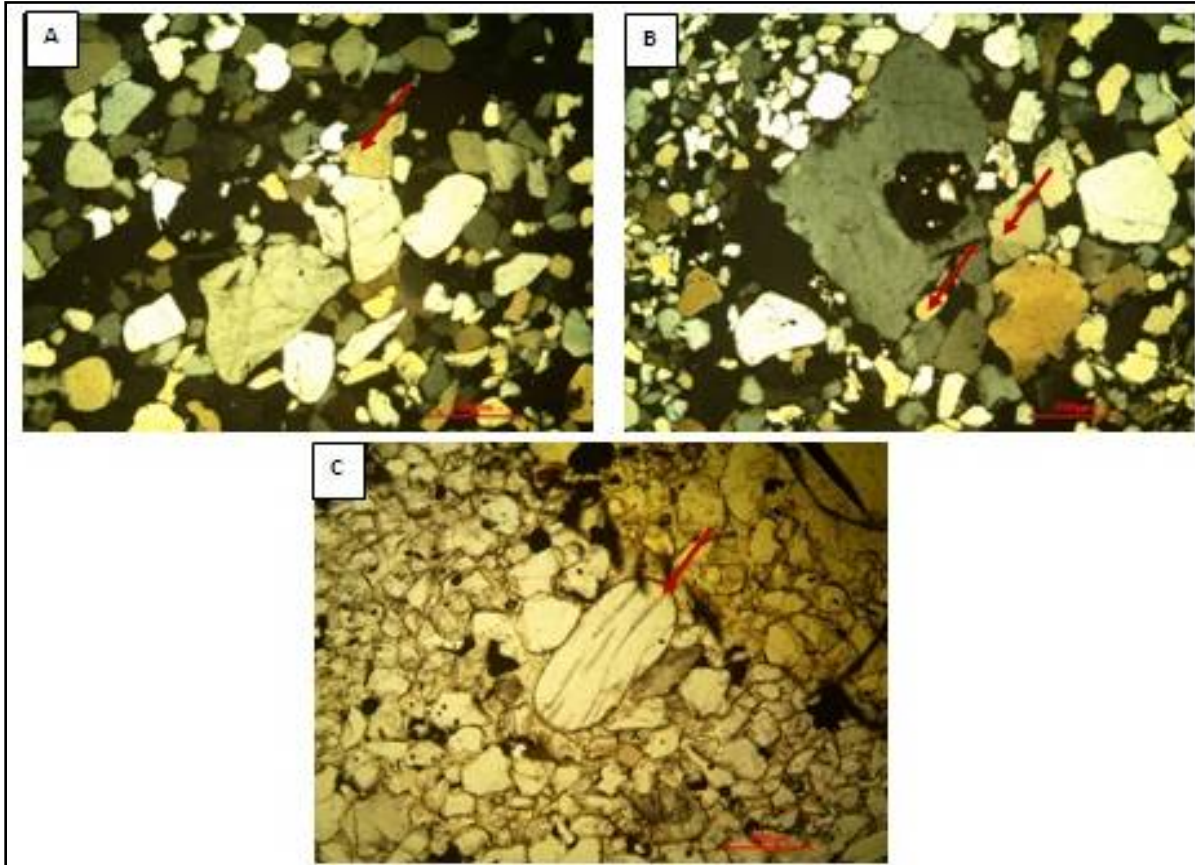
Plat 2.

- A. Chert fragment under the polarized.Kf-1 (2090m)
- B. Rock fragments under the polarized. Kf-1 (2250m)
- C. Shale with sand bands.Kf-3 (2350m)
- D. Shale with sand lenses and calcite bands.Kf-3 (2365m)
- E. Sandstone with shale bands.Kf-3 (2138m)
- F. Pyrite mineral in shale rocks.Kf-1 (2010m)



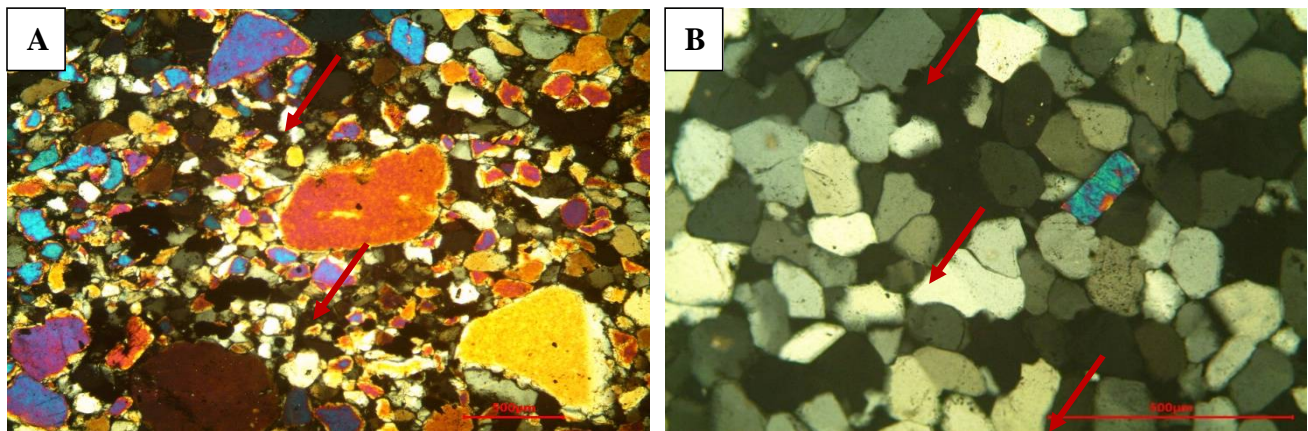


Aiad Ali Al-Zaidy and Mohammed Jamal Ahmed



Plat 3.

- A. Ternary concourse to grain of quartz contact relation between grains.Kf-1(2200m).
- B. Quotient deformation to wake grains. Kf-1 (2010m)
- C. The fissures are happening to grains. Kf-1 (2010m)

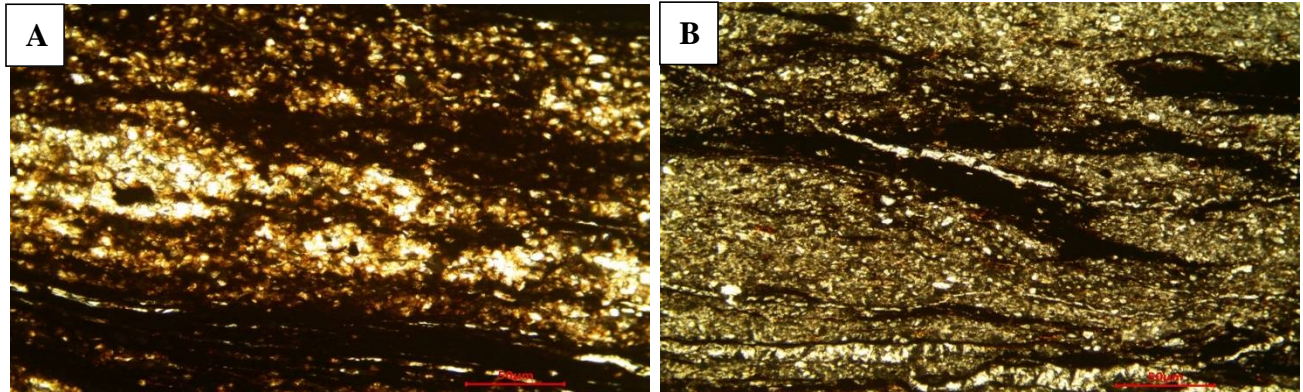


Plat (4) A & B Chemical compaction, point – contacts evolve through straight – elongate to concave – convex and even sutured contacts.A. Kf-1 (2450) B. Kf-1(2200m).

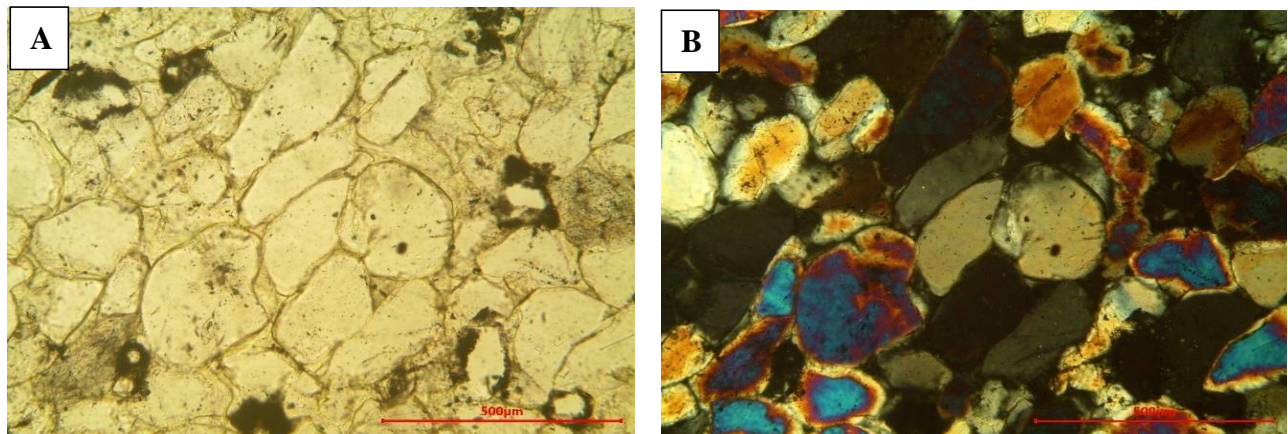




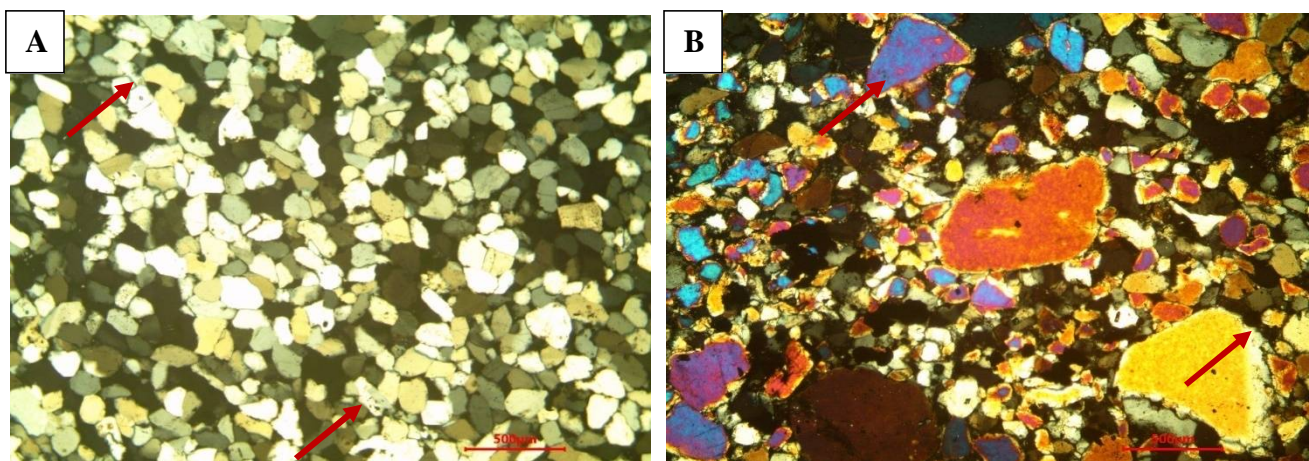
Aiad Ali Al-Zaidy and Mohammed Jamal Ahmed



Plat (5) A & B shale compaction in Zubair Formation.Kf-3 (2350m).



Plat (6) A. Quartz overgrowths.Kf-1 (2200m) B. Quartz overgrowths under the polarized.Kf-1 (2450m)



Plat (7) A & B Micro Crystalline Quartz cement.A.Kf-1 (2090m) B.Kf-1(2450m).





Aiad Ali Al-Zaidy and Mohammed Jamal Ahmed

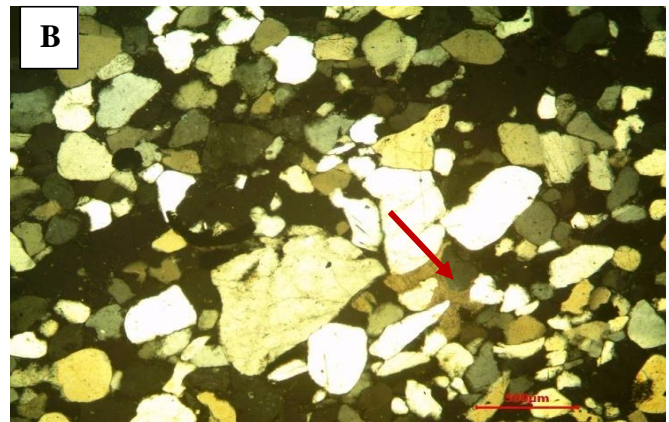
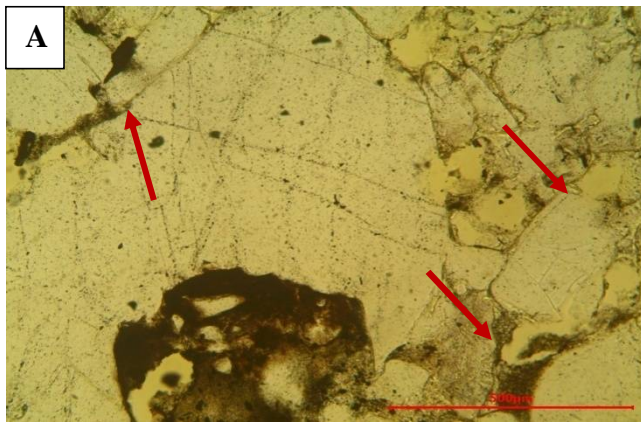


Plate 8. A. Clay Cement. Kf-1 (2010m) B. Calcite Cement. Kf-1 (2200m)

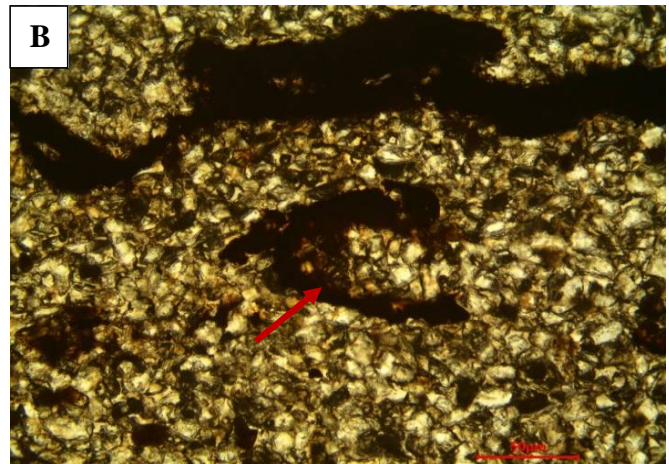
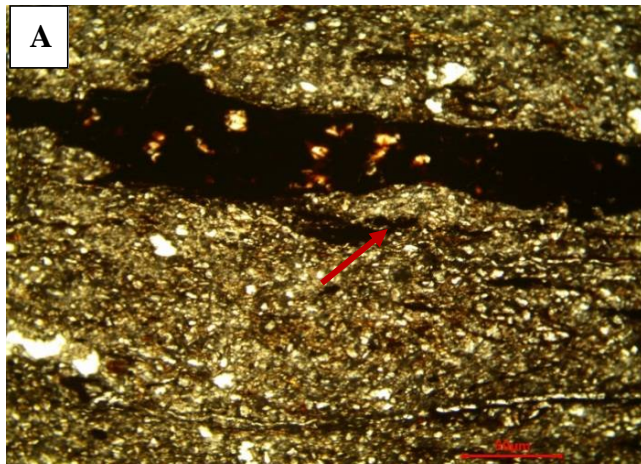


Plate 9.A & B Dissolution in shale unit of Zubair Formation.Kf-3 (2350m)





Pathological Effects Associated with Parasitic Infections

Hiba Riyadh Jameel Al-abodi

Department of Environment, College of Science, University of Al-Qadisiyah, Iraq.

Received: 20 Sep 2018

Revised: 23 Oct 2018

Accepted: 27 Nov 2018

*Address for Correspondence

Hiba Riyadh Jameel Al-abodi

Department of Environment,
College of Science,
University of Al-Qadisiyah, Iraq.
Email: Hiba.Al-abodi@qu.edu.iq



This is an Open Access Journal / article distributed under the terms of the **Creative Commons Attribution License** (CC BY-NC-ND 3.0) which permits unrestricted use, distribution, and reproduction in any medium, provided the original work is properly cited. All rights reserved.

ABSTRACT

Intestinal parasites that infect humans are widespread health problems, especially in tropical and semi-tropical zone, is no less important than other microscopic pathogens because it has the ability to infect most of the body's organs and lead to sometimes fatal complications that end in death, in addition to its ability to reproduce and in great numbers, which led to the failure to eliminate it completely, parasitic protozoa and helminthes intestinal are a large variety of parasites that live in the intestine, either this parasite is unsatisfactory or satisfactory symptoms causes and its vary in their resistance to the steroidal and macrophages, this infection is dependent on the type and number of parasites in addition to the duration of infection, age, gender, and health habits have an important and prominent role in the spread of infection. Infection of intestinal parasites is not limited to the local infection of the digestive system, but rather to cause many pathological changes in the values of normal blood components (hematological changes), causing diseases in the other, or it can cause biochemical changes resulting in a deviation from natural values such as the rise or fall of the liver enzymes, the total protein, cholesterol, sugar, fat and others, as well as other diseases will be associated with intestinal infection, parasites may not cause high a And low standards in the body of the infected person, but also to the occurrence of various pests and infections outside the digestive system, as in the appendicitis, which has parasitic infections a large role in the occurrence.

Keywords: intestinal parasites, parasitic protozoa, parasitic helminthes.

INTRODUCTION

Intestinal parasites are widespread pathogens, its divided into parasitic protozoa and parasitic helminthes [1,2], the prevalence of parasitic infections are widespread in tropical and semi-tropical areas, due to their climate conditions are suitable for a permanence and evolution of parasites, for example, humidity, temperature, and many



**Hiba Riyadh Jameel Al-abodi**

environmental factors, so the economic and social conditions have a great effect on the epidemiology of intestinal parasites [3]. people in crowded places are more likely to be infected than others by intestinal parasitic infections, because the lack of municipal services and lack of adequate housing are common the causes of incidence of intestinal parasites [4], children are more susceptible to intestinal parasites in particular, because decrease in the immune body response and lack of health awareness and lack of hygiene etc.. [5].

Intestinal parasites are infected human in several ways according to the type of parasite, some of them transmitted by mouth through contaminated drink and food such as *Entamoebahistolytica*, case of oral-fecal transmission such as *Giardia lamblia* [6,7,8], *Cryptosporidium parvum* does not differ from the Entamoeba and Giardia, as the method of transmission and the resistance of this parasite to chlorine also contributes to its widespread transition [9,10], the pinworm transferred from person to another after ingestion of their eggs, and fingernails, hands are sources of transmission, in addition, Pets for example cats, when carrying eggs of a parasite in their fur and thus contribute to incidence of infection by the parasite transition [8,11], due to it can be carried by dust, the dust is considered a source of infection, in addition, another form of transmission of the parasitic infection to the rest of the other intestinal worms such as bovine tapeworms, Ascaris worm, etc.. [11,12].

Pathological changes associated with intestinal parasitic infection in humans

Infections of intestinal parasites include many pathological changes, including changes in blood components, where anemia is a health problem affecting public health, and has several studies have been conducted that have shown the effect of intestinal parasites on blood components worldwide, its cause many health problems, such as anemia, which affects a high proportion of people worldwide, with about 1 billion people, anemia in the case of parasitic infection, where iron deficiency occurs in the blood of the infected person either due to a deficiency of folic acid or vitamin B12 [13], and of the serious pathological conditions that also result from intestinal parasitic infections, diarrhea, which causes more than 3.2 million deaths of children under the age of 20 years, especially in developing countries, and the infection of people intestinal parasites make the body vulnerable to other diseases associated with Such as appendicitis or hepatitis and biochemical changes in the blood parameters of infected patients [14,15] a study to determine the relationship of anemia to intestinal parasites [16], and in a study in the province of Maysan in southern Iraq to determine the incidence of pin worm and the effect of this parasite on the host, and there was a significant decrease in the concentration of hemoglobin and blood cell volume in children, a significant increase in the number of white blood cells was observed, the number of neutrophils and leukocytes increased and the number of lymphocytes decreased, while no effect was observed on the number of basal cells and monocytes [17].

A study on the effect of intestinal parasites [18] on blood image in Hilla city center of Babylon, tests were conducted to measure the level of hemoglobin and number white blood cells and counting the number of follicle cells, and there was observed a significant increase in the rate of white blood cells and eosinophilic cells, while the researcher did not notice a significant decrease in the mean value of hemoglobin and the impact of the intestinal parasites on the blood parameters in [19] when he noted a decrease in the number of red blood cells respectively, and hemoglobin level while recording an increase in the number of white blood cells and differential blood cells, as shown by [20] in the study of the blood variables of people with amoebic dysentery in Wasit province, the incidence of anemia was high (60%) among the infected and the rate of hemoglobin and the size of blood cells were lower in children under the age of 20 years compared to other age groups, Note that the number of white blood cells increased significantly among people aged between 30 and 22 years., and study of [21] in Tikrit in their study which aimed to compare microscopy and ELISA in the diagnosis of Giardia parasite infection with epidemiological and biochemical study among children under age the tenth in Tikrit and they recorded (9.1 gm/dl) rate of concentration of hemoglobin and (31%) PVC and (8973) of WBC.

Many researchers have also noted that there have been chemical changes due to some parasitic worms, where [22] parasites urge changes in fat values, but the mechanisms that cause them to occur the changes are not yet



**Hiba Riyadh Jameel Al-abodi**

understood, and a study on the effect of *Giardia lamblia* infection, by study of [23] the biochemical variables in human serum among children in Al-Mansour Educational Hospital in Baghdad, the variables included primary hepatic enzymes and total protein ratio of diarrheal children. The researchers observed elevated liver enzymes compared to control group for all age groups and observed a change in overall protein level but less., the study of [24] in northern Iraq, where they pointed out the negative effects of *Giardi* parasites on some biochemical parameters in children and the results of the study showed a decrease in the rate of blood sugar, low cholesterol, and decrease in the total protein albumin and reached as well as a decrease in magnesium, the researchers were interested [25] to study the effect of both *Giardia* parasites and amoeba parasites on some of the biochemical parameters among children in the province of Sulaymaniyah in northern Iraq, and included the parameters of the total protein albumin, zinc, cobalt and iron and observed a decrease in the values of total protein and albumin in children with amoeba slightly higher than those with *Giardia*, the researchers also observed a higher total-concentration of total globulin in children with *giardia*, while it was less concentrated in children with amoeba, and the concentration of zinc, iron and cobalt decreased significantly in children with both types, researchers have noted in study of [26] increase in concentrations of GPT and GOT in people with Echinococcosisin Babylon province in central Iraq.

Prevention, control and treatment of parasites in general and intestinal in particular requires knowledge parasite relationship to the external environment and host as well as detailed knowledge of the life cycle of the parasite itself to identify the weakness in the life cycle of that parasite and eliminate it and contribute to the washing of vegetables and fruits with soap and water 42% and may prevent the spread of infection to - before eating and clean as good as washing hands in preventing infection by 41% [27,28] the treatment of parasites requires the use of medical or chemical means such as the use of drugs or physical use UV, X-ray or biological radiation, such as eradication of insects and intermediates of the parasite infections of intestinal parasites occur by entering the infectious stages of eggs or stages stimulation of the mouth with water, food, or contaminated hands to the host's digestive system so preventive measures can be used to prevent infection. An important means of prevention is improving the health and nutrition situation and caring for hygiene [29,30]. Treatment used for severe injuries differs from that used for light injuries, cases that do not show symptoms in which treatment should be used so that the condition does not develop into severe injury, especially patients use of drugs that are not absorbed by the host as immune deficiency drugs [31], it helps in the elimination of infection as is the case of furate or Diloxanide, Iodoquinol, Paromomycin in nitroimidazole or metronidazole in amoeba parasites, and in acute cases, drugs are used Nitazoxanide is a treatment [32,33] in cases of severe diarrhea or treatment-resistant infections, *Giardia* parasites are used Thiazolides Nitazoxanide In some parasites such as phagocytosis, anti-parasitic drugs are used which is given Azithromycin which relieves diarrhea by attacking the metabolic processes of the parasite and treating for people whose immune system is at risk [34].

Treatments may slow bowel movements and increase and its derivatives sometimes treatment with Loperamide is the absorption of fluids to reduce diarrhea and these treatments during the replacement of fluids and minerals such as potassium and sodium by mouth or intravenous injection and lost result for continuous nitazoxanide diarrhea to maintain fluid balance in the body, sometimes, in cases of acute abdominal pain caused by amoebic colitis, surgical intervention is used [35] any type of infection can be prevented by using sterile water and treatment and avoiding drinking tap water, lake water, rivers and other untreated or sterile water sources, since the methods used in treatment of drinking water involves heating the contaminated water to boiling point for at least one minute or filtering the water using filters with holes of no more than 2 microns, The use of chlorine or iodine may contribute to the destruction of infectious bags, but it is considered ineffective as it depends on the degree of temperature, acidity, and the turbidity of water [36], infection persons should not swim in the pool for two weeks after the end of the event, as well they must leave the wrong sexual practices that contribute significantly to the transfer of infectious cysts because of the possibility of spread of these parasites among the family members, so all individuals must conduct the necessary tests in case of injury to any one of them. In study of [1] for children showed to a breast milk plays an important role in protecting the host from *Giardia* and there are a number of studies which demonstrated the protection of newborns from *giardia* [37], parasitic worms may differ in their treatment from the parasite, but not





Hiba Riyadh Jameel Al-abodi

very significantly in terms of prevention. Diphtheria can be treated with one dose (22 mg / kg) of body weight, Pyrantel pamoate can be used with one dose and with a capsule weighing 200 mg. Mebendazole is a treatment of tapeworms [38]. The dwarf worm can be treated with Praziquantel or Niclosamide also used in the treatment of parasitic infections, but Nitazoxanide has proven to be very effective in the treatment of ASKA in Mexico [39] that the prevention for worms is not different from the parasitic protozoa through the treatment of family members, all in the presence of injury or confirmation of the absence of food and water from any fecal contaminants may be infected with eggs. Parasites block the appendix cavity either by infecting the parasite with tissue, leading to scar formation in the area of infection, such as in the case of parasitic infection or *Enterobius vermicularis*, *Entamoeba histolytica*, the catch may occur due to the collection of worms and the opening of the appendage, as in the case of large numbers of worms such as *Ascaris lumbricoides* [40], many studies and scientific research have confirmed the role of bacterial, viral and parasitic pathogens in the occurrence of this inflammation, and because the appendix is clogged, the contents of the appendix are rapidly replenished and thus become the site of acute and chronic inflammation that progresses towards the cavity [41].

CONCLUSION

Since infection with intestinal parasites acts as a cause of other diseases associated with them may be more serious than the diseases caused by the infection intestinal parasites themselves, so it is recommended to try to prevent exposure to intestinal parasites and the speed of treatment in the event of injury to prevent the development of the disease.

REFERENCES

- 1- Haque, R. (2007). Human Intestinal Parasites. *J Health Popul Nutr.* 25(4):387–391.
- 2- Al – Shalah , S. A. J. (2014). Diagnostic study of *Entamoeba histolytica* and attenuated of parasitic by Gamma radiation ,Msc. Thesis. College of medicine . University of Babylon .PP. 94.
- 3.- Al-Abodi, H. R. J.; Al-Mayali, H. M. H. and Ali, M. J. (2015). Molecular study to most important virulence factor of *Entamoeba histolytica* in Diwaniyah province. *International Journal of Advanced Research*, Volume 3, Issue 8, 231-236.
- 4- Al-Mayali, H. M. H. and Al-abodi, H. R. J. (2017). Molecular characterization of *Entamoeba spp.* In Al-Qadisiyah province, Iraq. *Al-Kufa University Journal for Biology*, VOL.9 / NO.1 : 374-386.
- 5- AL-Khalidy, K.A.H. (2016). Detection of *Entamoeba histolytica* in patients an infected infants with diarrhea in born and children's hospital by classic methods and Real time Polymerase Chain Reaction. *Al -Qadisiyah Journal of Pure Sciences*, Vol. 21, No. 2.
- 6- Al-Abodi, H. R. J. (2018). USE OF RAPID CASSETTE TEST AND POLYMERASE CHAIN REACTION TECHNIQUE TO INVESTIGATE TOXOPLASMOSIS IN *Columba livia* BIRDS IN AL- MUTHANNA GOVERNORATE. *Basrah Journal of Veterinary Research*, Vol.17, No.3: 45-50.
Proceeding of 6th International Scientific Conference, College of Veterinary Medicine
- 7- AL-Khalidy, K.A.H. (2015). Diagnostic study of *Giardia lamblia* associated with contamination of drinking water in some residential neighborhoods in AL-Diwaniyah city using the method of flotation and polymerase chain reaction. *Al -Qadisiyah Journal of Pure Sciences*, Vol. 20, No. 2.
- 8- Al-abodi, H. R. J. (2015). Phylogenetic sequencing for some species of *Entamoeba sp.* in Al-Qadisiyah Province. Ph.D. thesis, College of Sciences, University of Al-qadisiyah.
- 9- Bradley, E. H., Taylor, L. A. And Cuellar, C. J. (2015). Management matters: a leverage point for health systems strengthening in global health. *Int J Health Policy Manag.*;4(7):411–415.
- 10- Obada, S. R. K. (2015). Effect extract *Allium sativum* and *Punicagranium* on white rat Experimental infection *Cryptosporidium parvum* and Comper with Metranidazole, Ms. thesis, College of Science University of Al-Qadisiyah.





Hiba Riyadh Jameel Al-abodi

- 11-Ziadi, Saba Abdul Ameer (2018) .PREPARATION OF CULTURE MEDIA FOR GROWTH TRICHODERMA HARIZANUM FROM RESIDUES OF BLACK TEA (WASTE TEA).*Biochem.Cell. Arch.* Vol. 18, No. 1, pp. 197-200
- 12-Cook, Gordon C. and Zumla, Alimuddin I. (2009). *Manson's tropical diseases* (22nd ed.). Saunders Elsevier. pp. 1515–1519.
- 13- AL-Shaibani, K. T. M. , Al-abodi, H. R. J. and Mahmood, H. R. (2018). Effect of Two Species of Ticks and Lice on Some Blood and Biochemical Parameters and their Role in the Transmission of *Toxoplasma Gondii* to Turkey MeleagrisGallopavo during Spring and Summer Seasons in AL-Diwaniyah Province – Iraq. *Journal of Global Pharma Technology*, 10(06):273-280.
- 14- AL-Khalidy, K.A.H.(2015).Identification study of *Giardia lamblia* which associated with drinking water in some areas in AL-Diwaniyah city by flotation methods and conventional-PCR. *Al -Qadisiyah Journal of Pure Sciences*, Vol. 20, No.
- 15- Hamzah, H. M. and Jameel, H. R. (2017). Epidemiology study of *Entamoebaspecies* in AL-Qadisiya governorate.*Al-qadisiyah Journal for pure science*, Vol.9, No. 3.
- 16-Mahmood H.R. &Ziadi S. A. (2017). Toxicity of golden nanoparticles synthesized by Insects pathogen *Entomophthraculicis* versus mosquito *Anopheles stephensi* (Diptera:Culicidae) *Advance Research Journal of Multidisciplinary Discoveries.* , Vol. 8.0, C7, PP. 44-48. ISSN-2456-1045.
- 17-Jabir, A. K.(2007). The prevalence of infection with *Enterobiusvermicularis* among the children of three kindergartens in Maysan governorate and the impact on some blood parameters;*Maysan Research Journal*, 3:(6)302-186.
- 18-Al-Mosa, A. H. and Al-Taie, H. H. (2007).Effect of infection with intestinal parasites on blood picture. *AL-TAQANI Journal*, Foundation of technical education, 20 (1):1-7.
- 19- Adday, L. (2009). Hematological test in patients with intestinal parasites in Al-Hashimiah village.*Biology Journal of Al-Kufa University, Kufa University*, 1(1):145-148.
- 20- Abdul-Sada, A. R. (2011). The Blood Variables of People with Amebious Sickness, *Science and Medicine, Wasit University*; 4(2):1-7.
- 21- Shamran, A. R, Shaker, Z. H, Al-Awsi, G. R. L, Khamis, A .S , Tolaifeh, Z. A. and Jameel, Z. I, 2018. RAPD-PCR IS A GOOD DNA FINGERPRINTING TECHNIQUE TO DETECT PHYLOGENETIC RELATIONSHIPS AMONG STAPHYLOCOCCUS AUREUS ISOLATED FROM DIFFERENT SOURCES IN HILLA CITY, IRAQ. *Biochemical and Cellular Achieves.* Vol. 18, Supplement 1, pp. 1157-1161.
- 22- Bansal, D.; Harinderpal, S. B. and Rakesh, S. (2005). Role of cholesterol in parasitic infections.*BioMed Central Ltd. Lipids in Health and Disease*, 4:10.
- 23- Al-abodi, H. R. J. (2018). SUSPICION IN THE FORM OF INFECTION IS THE BASIS FOR SELECTING THE APPROPRIATE METHOD FOR EXAMINING THE TOXOPLASMOSIS DISEASE OF BENDS THAT HAVE NO SYMPTOMS FROM PATIENTS. *Int. J. Adv. Res.* 6(9), 655-662.
- 24- Yahya, G. S.; Esraa, A. M. and Majida, N. I. (2007). Effect of *Giardia lamblia* on some biochemical changes of the human.*Tikrit Journal of Pure Science, Tikrit University*, 12(1):29-32.
- 25- Kadir, Mohammed A. and Mohammad-Ali, Sirwan M. (2011). Nutritional status of children infected with *Giardia lamblia* and *Entamoebahistoltyica* infections in Kalar town, Iraq. *Tikrit Journal of Pharmaceutical Sciences, Tikrit University*, 7 (2):162-170.
- 26- Al-Yasari, H. F.; Ali, K. and Al-Jaddoa, Najim A. (2012). A Study of Human Hydatidosis: Demographically and Clinically In Hilla City. *Journal of Babylon University*, 22 (4).
- 27 Al-abodi, H. R. J. (2017).Serological and molecular detection of *Toxoplasma gondii* in Columba livia hunting pigeons of AL- Qadisiyah province.*AL-Qadisiyah Journal of Vet. Med. Sci*; 16 (1):128-133
- 28- Curtis, V. and Cairncross, S. (2003). Effect of washing hands with soap on diarrhea risk in the community: a systematic review. *Lancet Inf. Dis.*; 3:275-81.
- 29- Shaker, E. M., Al-Shaibani, K. T. M. and Al-abodi, H. R. J. (2018). Effect of Alcohol extract of green tea plant *Camellia sienensis* as a therapeutic of parasite *Entamoebahistoltyica*. *Plant Archives* Vol. 18 No. 1, pp. 953-959.
- 30- Al-Abodi, H. R. J. (2018). EFFECT AND SPREAD OF GIARDIA PARASITE ON CHILDREN IN PRIMARY DEVELOPMENT STAGES IN SOUTHERN IRAQ.*Biochem.Cell. Arch.* Vol. 18, No. 2, pp: 1537-1541



**Hiba Riyadh Jameel Al-abodi**

- 31-Heymann, DL. (2004). Amoebiasis: Control of communicable diseases. America Public Health Association,; 11–15.
- 32- Al-Abodi, H. R. J. (2018). Suspicion in the form of infection is the basis for selecting the appropriate method for examining the toxoplasmosis disease of bends that have no symptoms from patients. *Int. J. Adv. Res.* 6(9), 655-662.
- 33- Rosenthal, PJ. (2011). Protozoal and helminthic infections. In: McPhee SJ, Current Medical Diagnosis and Treatment (50th ed.). New York; The McGraw-Hill Companies.
- 34-Savioli, L.; Smith, H. and Thompson, A. (2006). Giardia and Cryptosporidium join the 'Neglected Diseases Initiative'. *Trends Parasitol* 22:203-208.
- 35-Al-Grawi, E.D.C., and G.R.L. Al-Awsi. 2018. "Expression of CDKN2A (P16/Ink4a) among Colorectal Cancer Patients: A Cohort Study." *Journal of Pharmaceutical Sciences and Research* 10 (5).
- 36-Gardner, TB.and Hill, DR. (2001). Treatment of giardiasis. *ClinMicrobiol Rev.*;14:114-28.
- 37- Al-Ammash, M. S. J.; KhaledThamerMatar Al-Shaibani, K. T. M. and Al-Abodi, H. R. J. (2018). INVESTIGATING THE PREVALENCE OF INFECTION WITH *TOXOPLASMA GONDII* IN MEN AND WOMEN IN SAMARRA CITY, IRAQ. *Plant Archives* Vol. 18 No. 2, pp. 2501-2508.
- 38- Medical Letter Organization (2010). Drugs for Parasitic Infections (2nd ed.). The Medical Letter, Inc.
- 40- AL-NASHI, A.P.AliAbed Raheem; AL-AOSI, Ghaidaa Raheem Lateef (2013). Isolate and diagnose the bacteria present in the hospital in the city of Diwaniyah and the statement of the mechanisms to control the use of antibiotics and antiseptics. *Al-Qadisiyah Journal Of Pure Science*, V. 18 (3): 11-20.
- 41- G. R. L. Al-Awsi, 2012. Isolation and Identification of microbiological from AL-Diwanya hospitals and Controlled by Antiseptic and Antibiotic, M.Sc. Thesis, University of Al-Qadisiyah.
- 42- Al-Sammarai, A.S.M. (2015). Diagnosis study of parasites that cause appendicitis and histological changes accompanying her in Sammara city. *Al-Anbar J. Vet. Sci.* 8(2): 46-53.





Depositional Environments and Microfacies Analysis of Yamama Formation in Luhais, Subba and Ratawi Oil Field, South Iraq

Naseem Sh. ALhakeem^{1*}, Medhat E. Nasser¹ and Ghazi Hassan AL-Sharaa²

¹Department of Geology, College of Science, University of Baghdad, Baghdad, Iraq.

²Oil Exploration Company, Baghdad, Iraq.

Received: 17 Sep 2018

Revised: 21 Oct 2018

Accepted: 27 Nov 2018

*Address for Correspondence

Naseem Sh. ALhakeem

Department of Geology,

College of Science,

University of Baghdad,

Baghdad, Iraq.

Email:naseemshehab@yahoo.com



This is an Open Access Journal / article distributed under the terms of the **Creative Commons Attribution License** (CC BY-NC-ND 3.0) which permits unrestricted use, distribution, and reproduction in any medium, provided the original work is properly cited. All rights reserved.

ABSTRACT

The study involves 1 borehole in Luhais field (Lu-12), 3 borehole in Subba field (Su-7, Su-8, and Su-9), and 5 borehole in Ratawi field (Rt-3, Rt-4, Rt-5, Rt-6 and Rt-7), the Luhais, Subba, and Ratawi fields located in Mesopotamia zone (Zubair subzone), South of Iraq. Petrographic examination of (76) thin sections of core sample from (Rt-3, Rt-5, and Rt-7 wells), and Electrofacies study leads to microfacies analysis and Sedimentary environment of the lower cretaceous Yamama succession revealed to six cyclic type of microfacies have the characteristics that distinct ramp depositional environment of multiple transgression–regression stages. In Subba and Luhais fields the formation comprises five reservoirs (YR-A, YR-B, YR-C, YR-D, YR-E) ranging in thickness from 70 to 80 m for each of them, separated by five barriers (YB-2, YB-3, YB-4, YB-5), deposited by five sedimentary cycles. In Ratawi field the formation was divided into three reservoir units (YR-A, YR-B, and YR-C) separated by two barrier units (YB-2 and YB-3).

Keywords: Depositional Environments, Microfacies Analysis, Yamama Formation units.

INTRODUCTION

The Yamama Formation, which is a heterogeneous carbonate reservoir, is one of the most important oil production reservoirs in southern Iraq and neighboring area, which is deposited during the Lower Cretaceous period, within the main retrogressive depositional cycle (Berriasian - Aptian) [1]. And From its stratigraphic position an age range of Late Berriasian to Early Hauterivian age is expected [2], it is assigned a Valanginian age [3].



**Naseem Sh. ALhakeem et al.**

The Yamama Formation was defined by Steinke and Bramkamp in 1952 from outcrops in Saudi Arabia. They mentioned that the Yamama Formation represents the Thamama Group. The Formation underlain conformably by the Sulaiy Formation and grades upward into the Ratawi Formation which is considered the cap rock of the Yamama reservoir. The Formation is made up mainly of limestone, but some dolomitic limestone and shale have been reported [4].

The Study Area

The study area is located south of Iraq, to the South West of Basra governorate that includes the three oil fields Luhais, Subba, and Ratawi. Which accrue within the Zubair subzone, that forms the southernmost unit in the Mesopotamian zone, and has a uniform structural style controlled by the underlying basement because of the faulting and uplifting, figure (1).

MATERIALS AND METHODS

- 1-Petrographic examination of (76) thin sections of core sample from (Rt-3, Rt-5, and Rt-7 wells), Microfacies Analysis using Dunham's classifications (1962) of carbonate rocks figure (2), to classify Yamama formation in the study area.
- 2-The study of electrofacies depending on (Sonic, Neutron, Density, Spontaneous Potential (SP.), and Gamma Ray logs) and comparing the results with the thin sections using GeoFrame software.
- 3-Analysis (core and cutting description from Final geological reports) of the studied boreholes in Subba (Su-7, Su-8, Su-9), Ratawi (Rt-3, Rt-4, Rt-5, Rt-6, and Rt-7), and Luhais oil field (Lu-12).
- 4-Environment interpretation.
- 5-Facies distribution within the three studied fields using petrel software (version 2013).

Electrofacies (Facies Prediction by Logs)

Facies and the Rock Type Prediction of the sub-surface formations and reservoir rocks, for most of the logs are combinations of physical response of logging tools against formations. In other words, physical records have been regarded as inefficient data to analyze macro- and micro-textural facies of formations. It is still expected to analyze sedimentary facies by the use of conventional suite of logs, for no other record than core and seismic data are available. The understanding of facies distribution in the field is important to delineate and develop the heterogeneous carbonate reservoir efficiently [5]. For the un-cored interval of the formation in the Ratawi field, Subba and Luhais oil field, many references mentioned latter will be used [6], and connect cores inspection and porosity with conventional log set, to conducted facies and rock typing Prediction of carbonate reservoirs in the three studied Fields.

Formation Units

The formation consists of three reservoirs in Ratawi field (YR-A, YR-B, YR-C), and five in Subba and Luhais fields (YR-A, YR-B, YR-C, YR-D, YR-E), separated by tight barrier units which are formed of mudstones and shale (YB-2, YB-3) in Ratawi, and (YB-1, YB-2, YB-3, YB-4, YB-5) in Subba and Luhais fields. Each reservoir unit shallows up into either an oolitic-peloidal shoal or a patchy reef. A new scheme has been adapted to vertically subdivide, the Yamama Formation in southern Iraq into a series of reservoirs and barrier units. The formation was divided in (Ratawi field) into three reservoir units (YR-A, YR-B, and YR-C) separated by two barrier units (YB-2 and YB-3), but in Subba and Luhais fields the formation began with barrier YB-1 and represent three order cycle with five barriers and five reservoirs. The first cycle was missing in Ratawi field, due to it was structurally higher during the deposition than the adjacent fields, this subdivision has made it possible to correlate the formation over study area [7].





Naseem Sh. ALhakeem et al.

The top and bottom of each Yamama units are sharp lithological boundaries;table (1) shows the depth and thicknesses for each unit in the three studied fields.The formation thickness in Ratawi field is about 270 m, 310 m in Subba field, and 262.8 in Luhais field.

Barrier Unit YB-1

This unit is located at the uppermost succession of the Yamama Formation in Subba and Luhais fields and consider as cap rock for the formation, the unit consist of impermeable mudstone, the thickness is almost equally distribute on Subba field, (20, 21, 22.5 m) in (Su-7, Su-8, Su-9) wells respectively, and about 7 m in Lu-12 table (1), this unit is missing in Ratawi field as mentioned before.

Reservoir Unit YR-A

This unit shows a wide variation in thickness in the three studied wells as below:

- ❖ In Ratawi field this unit represents the upper lithology part, and higher in both thickness and reservoir quality than the other two fields, its greatest thickness (126 m) at the Ratawi-4 well, (123 m) at Rt-5, (119, 118, 119.5 m) in (Rt-3, Rt-6, Rt-7) respectively. In general, crestal well (Rt-3) has purer sections of the unit than flanking wells, the order of the Microfacies is the same in most of Ratawi wells, except a little change in Rt-7 and a bigger changes in Rt-4.
- ❖ In Subba oil field the thickness of the unit is (11, 9, 8 m) in (Su-7, Su-8, Su-9) wells respectively.
- ❖ In Luhais oil field the thickness of this unit is (13 m) in (Lu-12) well.

Barrier Unit YB-2

This unit separates the two reservoir units YR-A and YR-B. This unit over the studied wells is made of argillaceous Lime mudstone, Fossiliferous lime mudstone and shale. It ranges in thickness from (12, 11, 11, 12, 12 m) in (Rt-3, Rt-4, Rt-5, Rt-6, Rt-7) respectively, to (40, 45, 38.5 m) in (Su-7, Su-8, Su-9) wells respectively, and (23 m) in Lu-12.

Reservoir Unit YR-B

The unit YR-B is characterized by high reservoir quality, and it is the highest oil-bearing unit especially in Ratawi field, which is related to the dominance of packstone and grainstone shoal facies that have high effective porosity and very low clay volume, the unit thickness is (84.5, 88, 93, 84, 81.5 m) in (Rt-3, Rt-4, Rt-5, Rt-6, Rt-7) respectively, (29, 32, 30.4 m) in (Su-7, Su-8, Su-9) wells respectively, and (22 m) in Lu-12.

Barrier Unit YB-3

This unit separates the two reservoir units YR-B and YR-C. YB3 is less consistency than YB-2 and its argillaceous content is lower. This unit is made of Fossiliferous lime mudstone and shale in most of the studied wells, the thickness of the unit is (13.5, 14, 12, 19, 12 m) in (Rt-3, Rt-4, Rt-5, Rt-6, Rt-7) respectively, (16.5, 17, 12 m) in (Su-7, Su-8, Su-9) respectively, and (17 m) in Lu-12, the maximum thickness in well Rt-6.

Reservoir Unit YR-C

This unit represents the bottom of Yamama formation with the lower Sulaiy formation in Ratawi oil field, YR-C has varied lithology in the studied wells ranging from algal–foraminiferal packstone with zones of oolitic and peloidal limestone, it's also ranging in thickness between 58.5 in well Rt-7 which is the maximum thickness, and 25 m in Lu-12. The open marine facies of this unit show better reservoir properties than restricted marine facies as indicated by





Naseem Sh. ALhakeem et al.

higher effective porosity values and low clay volume especially in Subba oil field, Although similar facies is observed in both units YR-D and YR-E the contact between them is distinguished by sharp changes in porosity and resistivity logs pattern, which reflect the changes in reservoir properties associated with transition from open to restricted marine facies.

Barrier Unit YB-4

YB-4 separates the two reservoir units YR-C and YR-D, (the unit is missing in Ratawi oil field, so as YR-D, YB-5, YR-E as mentioned earlier), YB-4 in in Subba wells, and Lu-12 well is made of argillaceous lime mudstone, with low shale content (as compared with the other 4 barriers within the formation), the thickness of the unit is (7, 10 m) in Su-7, Su-8 respectively, (4 m) in Su-9, and (14 m) in Lu-12 well, table (2–10), so it's the thinnest barrier unit within the formation.

Reservoir Unit YR-D

The unit YR-D is composed of inter-bedded succession of open and restricted marine facies, the thickness of this unit is (33, 37, 37.5 m) in (Su-7, Su-8, Su-9) respectively, and the maximum thickness (40 m) in well Lu-12.

Barrier Unit YB-5

The thickness of the unit is (92, 90, 93 m) in (Su-7, Su-8, Su-9) respectively, and (70 m) in Lu-12, which consider the maximum thickness among the other four barriers of the formation in Subba and Luhais fields, this unit is made of Fossiliferous lime mudstone and shale, and separates the two reservoir units YR-D and YR-E.

Reservoir Unit YR-E

This reservoir unit is located at the lowermost unit of Yamama Formation in Subba and Luhais fields, and the contact with the Sulaiy formation below, the unit is represented by a succession of open marine, restricted marine and shoal facies. The thickness ranges between (92, 90, 93 m) in (Su-7, Su-8, Su-9) respectively, and (70 m) in well Lu-12.

Microfacies Analysis and their environments of the Yamama Formation

Microfacies of Yamama formation reflects deposition within different types of subenvironments recognizing from shallow to deep water conditions as it indicated by the type of depositional textures and type of carbonate grains.

From the petrographic analysis and Electrofacies study, six microfacies deposited from restricted area platform interior to deep water environments that have been identified. From these microfacies and the depositional environment, imply that one microfacies can have one or more group of similar pore attributes, and also one similar pore attributes could be derived from (one or more) microfacies. These Microfacies may be corresponding to Wilson's Standard Microfacies Types (SMF), (1975), and according to Flugel classification (2004) of standard facies Zones (FZ), figure (2). Six microfacies are present in Yamama Formation rocks and their association environments are:

1- Mudstone microfacies which are divided into

A- Aargillaceous lime mudstone submicrofacies

And as this submicrofacies compared with Wilson's Standard Microfacies Types (SMF), indicated that it is similar to (SMF-23), and (FZ-7) according to Flugel classification (2004) of standard facies Zones (FZ), which refer to shallow open marine environment, plate (A and B).





Naseem Sh. ALhakeem et al.

B- Fossiliferous lime mudstone submicrofacies

This submicrofacies is similar to Wilson's (SMF-20), facies zone (FZ-7), which refers to shallow open marine conditions and accumulated by setting out of the water column indicating deposition below storm wave base, plate (C).

2- Algal wackestone – packstone microfacies

This microfacies may reflect shallow marine waters with open circulation (open marine environment). It may be corresponding to Wilson's (SMF-8), (FZ-7), plate (D).

3- Foraminiferal wackestone – packstone microfacies

This facies could be indicated a transgressive system tract. It may be correspond to Wilson's (SMF-8), (FZ-2), which indicated Shelf lagoon with circulation, low-energy environments below wave base, plate (E).

4- Bioclastic wackestone – packstone microfacies

It may be corresponding to Wilson's (SMF-10), (FZ-7). Because of the abundant of packstone over wackestone, which indicating shallow open marine environment (middle ramp setting) without reef or any restricted to water circulation, plate (F).

5- Oolitic –Peloidal grainstone microfacies

When compared this microfacies with Wilson's Standard Microfacies Types it indicates that it is similar to (SMF-15), and (FZ-6) according to Flugel classification (2004) of standard facies Zones, which indicates shoal environment, plate (G).

6- Peloidal packstone microfacies

This facies formed in a low-energy sheltered environment and could be correspond to Wilson's Standard Microfacies (SMF-15), and (FZ- 8) according to Flugel classification (2004) of standard facies Zones, which indicating inner ramp setting with restricted water circulation, plate (H).

Figure (5 and 6) shows the correlation sections of facies distribution in the nine studied wells within the three fields, using petrel software (version 2013).

Depositional System and Paleoenvironments

Within this succession, Yamama facies constitutes a prominent carbonate sequence deposited on the platform during a high-stand period. The dominant components of the facies deposits, such as Bioclastic–Wackestone–Packstone and in the studied area are not materials that derived from the reefal facies but detrital oolitic / Pelletal grains. Therefore the Yamama Formation was regarded as a deposit in the carbonate sand shoal environment. The oolitic sediments are deposited on the shallow ramp and create the carbonate sand shoal complex along the shorelines. Currents and wave actions also, contributed a great deal in redistributing of the oolites to other parts of the basin including both landward lagoons and seaward open marine areas. The sea-level fluctuation was the cause of the repeated vertical occurrences of tight and porous carbonates in the Yamama succession, figure (3) [8].

The Yamama Formation in SE Iraq comprises three depositional cycles later interpreted by Sharland et al., (2001) as equivalent to third-order sequences. Cycle tops contain oolitic grainstone inner-ramp facies which passes down into finer-grained peloidal facies and middle-ramp bioclastic packstone – wackestones. Outer-ramp cycle bases comprise thick grey shale with stringers of chalky micrite. Twelve to 14 sub-cycles may occur, bounded by low-stand horizons containing plant remains [8]. Facies belts indicate an easterly – facing ramp system [4] with limited development of up-dip marly limestone of the Lower Ratawi formation [5]. The same environment repeated after a regressive system and the deposition of Mudstone Microfacies.





Naseem Sh. ALhakeem et al.

Cycle tops (YR–A, YR–B, and YR–C) and bases (YB–1, YB–2) represent late high-stand and transgressive / early high-stand systems tracts, respectively. They are organized into a series of NW–SE oriented [4], interpreted as "depocentre"[8].

RESULTS

Yamama is a gentle carbonate ramp dominated by inner ramp facies, consists of a sequence of shallow–water limestone which have a thickness about 300 m. The formation represents one of the principal reservoirs in southern Iraq. 5 sedimentary cycles in Yamama, considered as 3 order sequences ranging from 70 to 80m thick each of them and can be subdivided in several 4th order depositional sequences, except in Ratawi field which was structurally higher during the deposition than the adjacent fields as mentioned above. Best reservoir properties appear in the upper part of the high-stand systems tracts (HST) oolitic shoals below the sequence boundary and the worst reservoir properties occur in the barriers mudstones which were deposited in the deeper parts of the foredeep. In general reservoir quality is good; porosities are about 20%. Outer ramp setting Characterized by mudstone Microfacies, Algal Wackestone to Packstone Microfacies, Foraminiferal Wackestone – Packstone Microfacies. Middle ramp setting Characterized by Bioclastic Wackestone – Packstone Microfacies. Inner ramp setting Characterized by the Oolitic – Peloidal Grainstone Microfacies, Peloidal Packstone Microfacies.

CONCLUSION

The high reservoir quality is related to the dominance of packstone and grainstone shoal facies that have high effective porosity and low clay volume, open marine facies on the other hand shows better reservoir properties than restricted marine facies as indicated by higher effective porosity values and low clay volume within open marine facies. The reservoir units (YR-C and YR-D) in Subba oil field, and YR-B in Ratawi oil field represent the major reservoir units that characterized by the high reservoir quality, due to the dominance of packstone inner ramp and grainstone shoal facies that have high effective porosity and low clay volume. Otherwise, the Luhais oil field has low oil bearing in YR-A, YR-B and YR-C units, and produce heavy oil and salt water from YR-D and YR-E as indicated by low resistivity log reading, and according to DST test with the description of cutting in final geological reports.

REFERENCES

- 1- Buday, T., 1980; The regional geology of Iraq, Stratigraphy and Paleogeography, State Organization for minerals, Baghdad, P. 242-245.
- 2- AL–Sharaa, Ghazi, Mutlak, 2004. Facies Architecture and Sequence Stratigraphy of the Yamama Formation in Rafedain field correlated with Distal and Proximal oil fields, M.Sc. Thesis, University of Baghdad.
- 3- Jassim S. Z., and Goff J. C., 2006. Geology of Iraq . Dolin, Prague and Moravian Museum, Brno. P. 124-127.
- 4- Sadooni F. N., 1993, a, b. Stratigraphic Sequence, Microfacies, and Petroleum Prospect of the Yamama Formation, Lower Cretaceous, Southern Iraq. The American Association of Petroleum Geologists, P. 1971-1988.
- 5- Schlumberger, 1972. Log Interpretation, Vol. I—Principles: New York, Schlumberger Limited, P. 124.
- 6- Serra, O., 1984. Fundamentals of well-log interpretation. Elsevier, Amsterdam, P. 7, 122.
- 7- Alsharhan, A. S. and Nairn A. E. M., 2003, Sedimentary Basins and Petroleum Geology of the Middle East, Elsevier. The Netherlands, p. 232
- 8- Aqrabi, A.A.M., J.C. Goff, A.D. Horbury, and F.N. Sadooni, 2010, The Petroleum Geology of Iraq: Scientific Press, P. 168-173.
- 9- Sharland, P.R., Archer, R., Casey, D.M., Hall, S.H., Heward, A.P., Horbury, A.D. and Simmons, M.D., 2001., The Arabian Plate Sequence Stratigraphy. Geo Arabia Special Publication 2, by Gulf Petrolink, Bahrain, P. 269-271.





Naseem Sh. ALhakeem et al.

Table (1): Tops and Thickness of the lithostratigraphic units for Yamama Formation in Ratawi, Subbaand Luhais oil fields (measured by meter from sea level).

Yamama Formation		Ratawi					Subba			Luhais
		Rt-3	Rt-4	Rt-5	Rt-6	Rt-7	Su-7	Su-8	Su-9	Lu-12
YB-1	Top	—	—	—	—	—	3384.5	3406.8	3379.8	3443.14
	Thick.	—	—	—	—	—	20	21	22.5	7
YR-A	Top	3499.9	3639.2	3645.3	3618.5	3616.5	3404.5	3427.8	3402.3	3450.14
	Thick.	119	126	123	118	119.5	11	9	8	13
YB-2	Top	3618.9	3765.2	3768.3	3736.5	3736	3415.5	3436.8	3410.8	3463.14
	Thick.	12	11	11	12	12	40	45	38.5	23
YR-B	Top	3630.9	3776.2	3779.3	3748.5	3748	3455.5	3481.8	3448.8	3486.14
	Thick.	84.5	88	93	84	81.5	29	32	30.5	22
YB-3	Top	3715.4	3864.2	3872.3	3832.3	3829.5	3484.5	3554	3479.3	3508.14
	Thick.	13.5	14	12	19	12	16.5	17	12	17
YR-C	Top	3728.9	3878.2	3884.3	3851.5	3841.5	3501	3530.8	3491.3	3525.14
	Thick.	40	38	48	43	58.5	53.5	45	42.5	25
YB-4	Top	—	—	—	—	—	3554.5	3575.8	3533.3	3550.14
	Thick.	—	—	—	—	—	7	10	4	14
YR-D	Top	—	—	—	—	—	3561.5	3585.8	3537.8	3564.14
	Thick.	—	—	—	—	—	33	37	37.5	40
YB-5	Top	—	—	—	—	—	3594.5	3622.8	3575.3	3604.14
	Thick.	—	—	—	—	—	12	14.5	14	31
YR-E	Top	—	—	—	—	—	3606.5	3637.4	3589.3	3635.14
	Thick.	—	—	—	—	—	92	90	93	70
Top of Sulaiy		3768.9	3916.2	3932.3	3894.5	3900	3698.5	3724.8	3682.3	3705.34
Total Thick. of the Formation		269	277	287	276	283.5	314	318	302.5	262.2





Naseem Sh. ALhakeem et al.

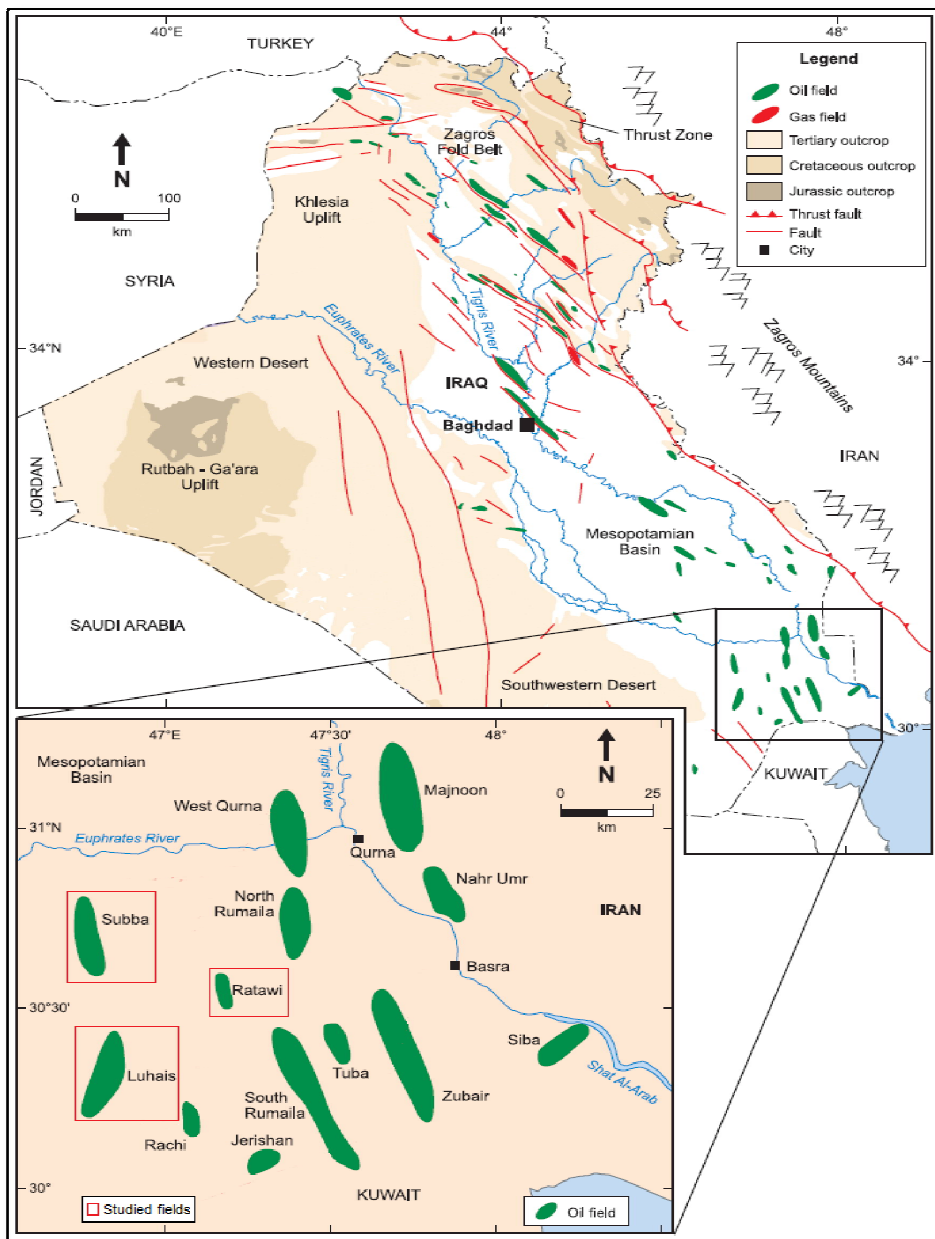


Figure 1. Map of the study area with larger site in southern Iraq showing the locations of the three studied oil fields, modified from the map of Iraq, South Oil Company (S.O.C).





Naseem Sh. ALhakeem et al.

Mudstone	Wackestone	Packstone	Grainstone	Boundstone	Crystalline
Less than 10% grains	More than 10% grains	Grain-supported	Lacks mud and is grain-supported	Original components were bound together	Depositional texture not recognizable
Mud-supported					
Contains mud, clay and fine silt-size carbonate					
Original components not bound together during deposition					
Depositional texture recognizable					

Figure 2. Dunham Classification for carbonate rocks (After Dunham, 1962).

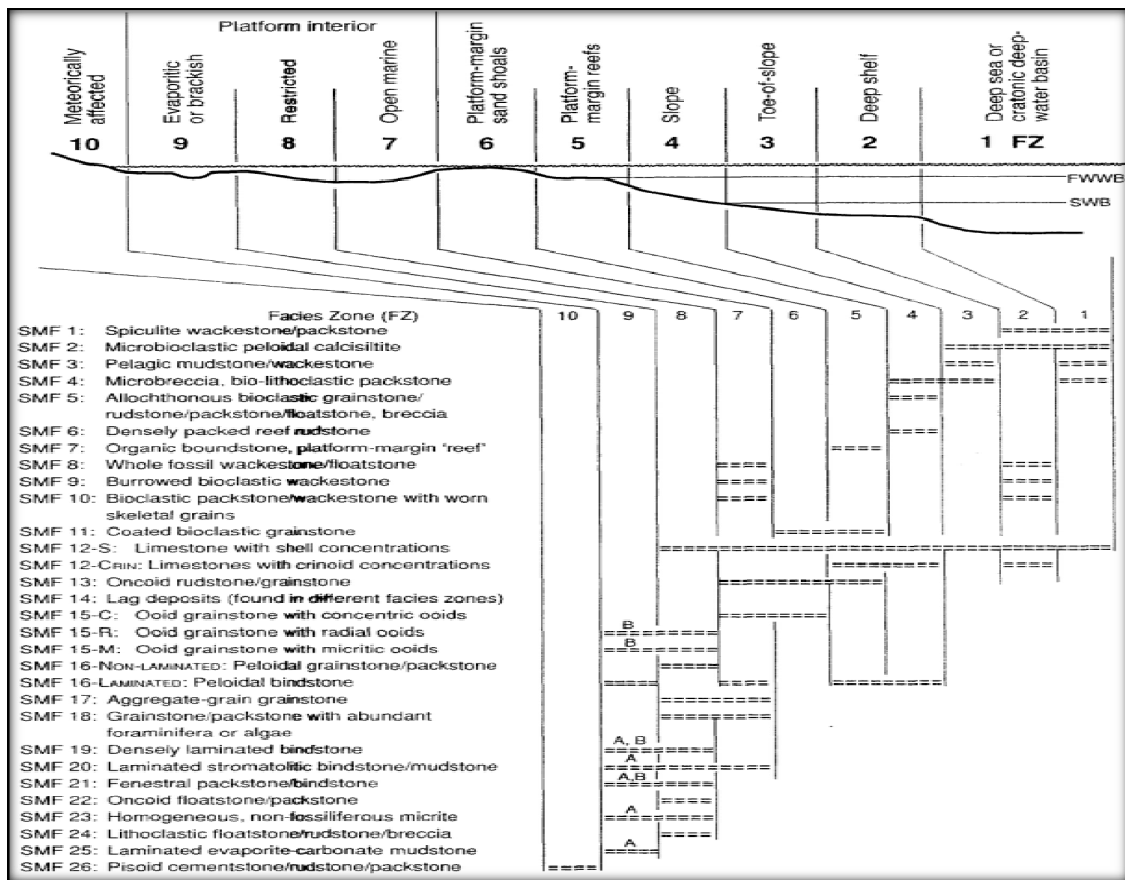


Figure 3. Distribution of SMF Types in the Facies Zone (FZ) of the carbonate platform model (Flügel, 2004).





Naseem Sh. ALhakeem et al.

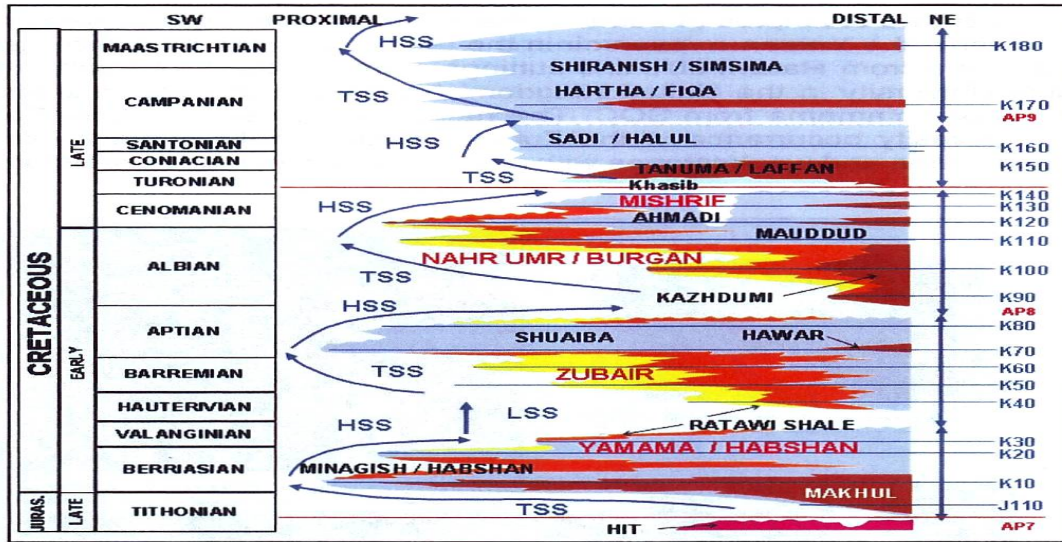


Figure 4 Sequence stratigraphy of the Cretaceous age with Sea level fluctuation [9].

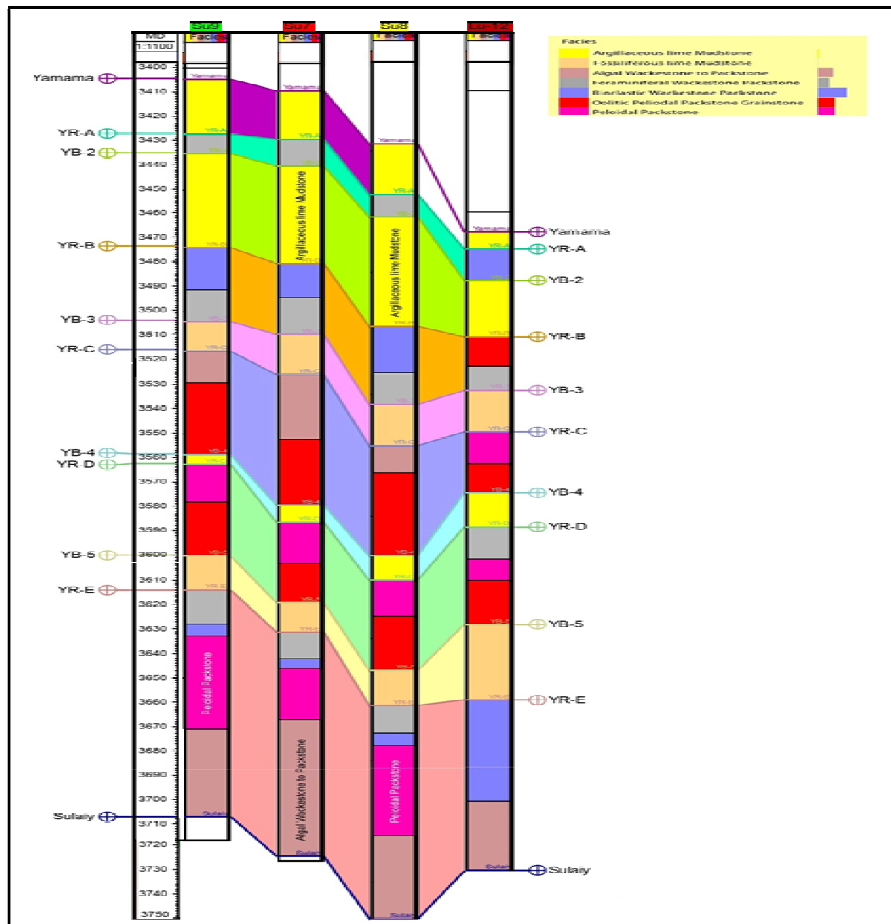


Figure 5 Correlation section of facies distribution within Subba and Luhais fields.





Naseem Sh. ALhakeem et al.

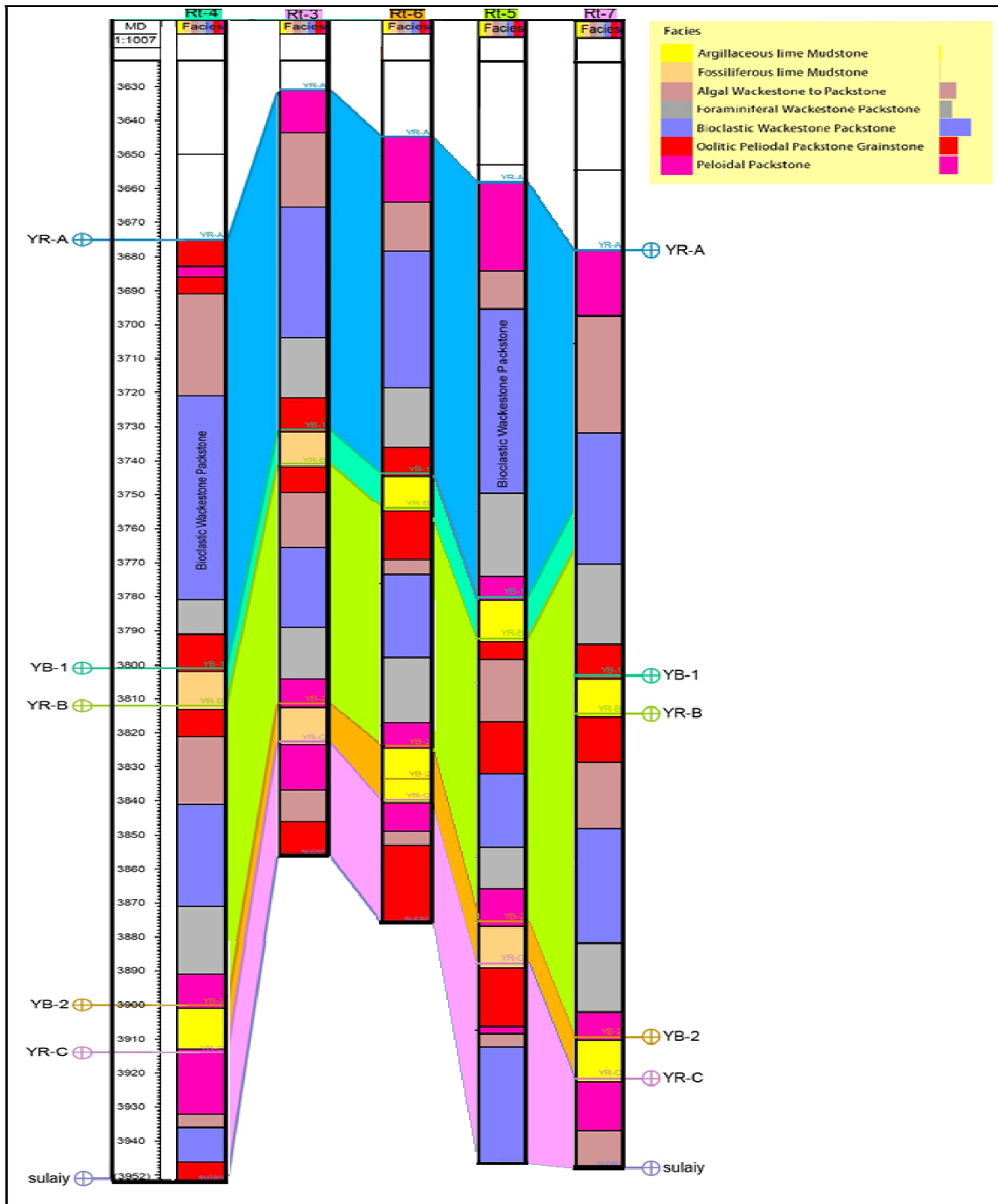


Figure 6 Correlation section of facies distribution within Ratawi field.



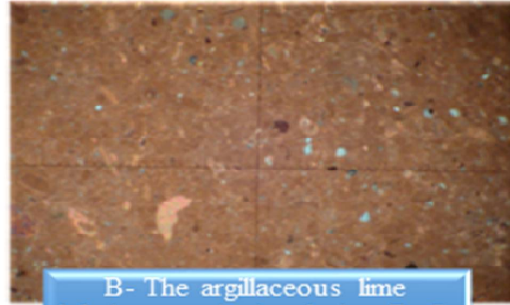


Naseem Sh. ALhakeem et al.

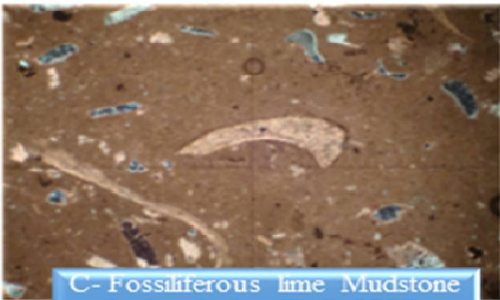
Plates



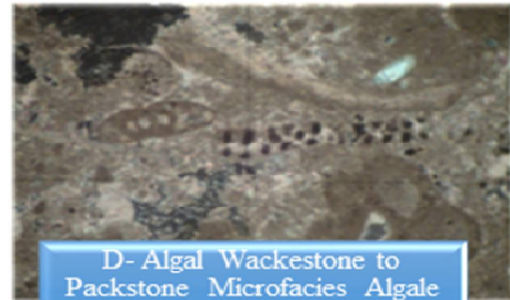
A- Transverse section through a single, gastropod, in Argelleouse Mudstone, Rt-7, 3782.75 m, YB-1.



B- The argillaceous lime Mudstone submicrofacies Rt-7, 3333m, YB-1.



C- Fossiliferous lime Mudstone submicrofacies Rt-7, 3778m, YB-1, (40X), XPL.



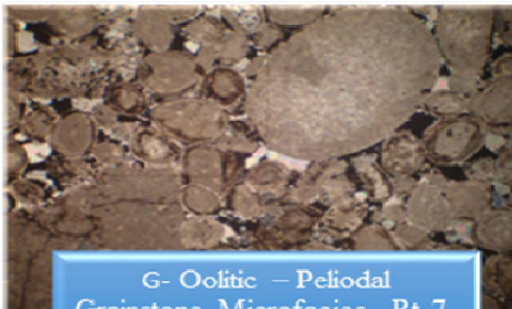
D- Algal Wackestone to Packstone Microfacies Algae Wk. to Pk. Rt-7, 3806.40, YR-B, (10X), XPL.



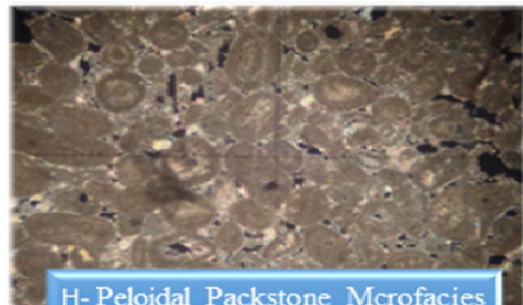
E- Foraminiferal Wackestone – Packstone Microfaciese, Rt-5, 3896 m, YR-C, (10X).



F- Milioids in Bioclastic Wackestone - Packstone Microfaciese, Rt-3, 3697.5 m, YR-B, (10X).



G- Oolitic – Peloidal Grainstone Microfacies Rt-7, 3810.5 m, YR-B, (40X).



H- Peloidal Packstone Mcrofacies Rt-5, 3895 m, YR-B, (40X).





A Review on the Urease Enzyme that Produced From *Staphylococcus saprophyticus*

Eqbal Dohan Challap* and Ghaidaa Raheem Lateef Al-Awsi

Department of Radiological Techniques, Al-Mustaqbal University College, Hilla, Babylon, Iraq.

Received: 20 Sep 2018

Revised: 24 Oct 2018

Accepted: 27 Nov 2018

* Address for Correspondence

Eqbal Dohan Challap

Department of Radiological Techniques,
Al-Mustaqbal University College,
Hilla, Babylon, Iraq.

Email: Dr.Ghaidaa.R@mustaqbal-college.edu.iq



This is an Open Access Journal / article distributed under the terms of the **Creative Commons Attribution License** (CC BY-NC-ND 3.0) which permits unrestricted use, distribution, and reproduction in any medium, provided the original work is properly cited. All rights reserved.

ABSTRACT

Fairbrother is the first to be named *S. saprophyticus* on non-producing coagulase *Staphylococcus aureus* isolated from humans and animals. These isolates were found to be unable to ferment mannitol sugar (Fairbrother, 1940). In 1951, Shaw and his group were able to classify isolated strains of *Staphylococcus aureus* from different sources. These bacteria are an important cause of urinary tract infection in females between the ages of 15 and 45. Studies have shown that these bacteria have the potential to infect some males with sewage. In addition, these bacteria have the potential to cause bacteremia (Gatermann et al., 1989). These bacteria are an important cause of urinary tract infection in women after *E. coli* is the second cause of urinary tract infection after *E. coli*. The enzyme urease is a metal enzyme containing the nickel at the active site of the enzyme (Won et al., 2004). Nickel is associated with the amino acids in the effective sites of the enzyme, called the metal enzyme (Dixon et al., 1980). The nickel-containing enzymes all contain nickel in the active site. The enzyme is purified for the purpose of studying its properties because the presence of other substances can lead to the results of the real, the purification process means the separation of the enzyme from the rest of the components of the center, and include several steps increase during the qualitative effectiveness.

Keywords: humans, animals, *S. saprophyticus*, *Staphylococcus aureus*, urinary tract, infection, enzyme

History of *Staphylococcus saprophyticus* bacteria

Fairbrother is the first to be named *S. saprophyticus* on non-producing coagulase *Staphylococcus aureus* isolated from humans and animals. These isolates were found to be unable to ferment mannitol sugar (Fairbrother, 1940). In 1951, Shaw and his group were able to classify isolated strains of *Staphylococcus aureus* from different sources. This classification included five subgroups of *Staphylococcus* and *S. saprophyticus* was called the second group, isolated from different sources such as humans, animal and water products, soil and sewage. It has been characterized by its non-production of cacaools, acetoin, and acid from glucose, and has been described as reducing nitrates and can



**Eqbal Dohan Challap and Ghaidaa Raheem Lateef Al-Awsi**

analyze urea (Shaw et al., 1951). This type of *Staphylococcus aureus* was first isolated from women with urinary tract infections for the first time in 1962. These bacteria were identified by traditional serological techniques and based on the resistance of these bacteria to the Novobiocin antibody (Torres-Perriera, 1962).

In 1963, these bacteria were re-classified as Micrococcus and classified as a subset of this species called Micrococcus subgroup 3 because they share the Micrococcus species with several characteristics such as the inability to produce the enzyme and the Phosphatase In 1974, Buchanen and Gibbon observed that some groups of the Micrococcus belonged to *Staphylococcus* depending on the content of the DNA bases. This led to the researcher Baird-Parker in 1974 to modify the scheme and so Micrococcus subgroup 3 was renamed *S. saprophyticus* biotype (1-4) (Baird-Parker, 1974). These bacteria have received widespread interest from many researchers, possessing the ability to metabolize the red blood cells of the sheep (Hovelius et al., 1979). Recent studies have shown that lysopotoxic acid plays an intermediate role in the *S. saprophyticus* adhesion process. This acid is composed of a fatty part that is correlated with the phosphorylation chain and by its ability to adhere to eukaryotic cells. The occurrence of infection with these bacteria. This type of *Staphylococcus* is the ability to produce lectin, which is a factor in the adhesion of cytotoxic cells to eukaryotic cells. This substance protects the *Staphylococcus* from the effect of macrophages (Gatermann et al., 1992).

The most important characteristic of *Staphylococcus saprophyticus* bacteria

These bacteria are an important cause of urinary tract infection in females between the ages of 15 and 45. Studies have shown that these bacteria have the potential to infect some males with sewage In addition, these bacteria have the potential to cause bacteremia (Gatermann et al., 1989). The coagulase is called coagulase negative (Kloos and Smith, coagulase positive), which is called coagulase positive. 1980; Kloos and Jorgensen, 1985). These bacteria are not able to produce phosphatase, which is an important characteristic of the diagnosis of *Staphylococcus aureus* (Pickett and Welch, 1985). 83% of *S. epidermidis* are derived from this enzyme, Saprophyticus is not a product of this enzyme, so it is an important diagnostic feature of these bacteria (Geary and Stevens, 1989). *S. saprophyticus* colonies are circular, smooth, and uniform. The diameter of the colony varies between 9-5 mm in solid circles and has the ability to produce a white dye that becomes yellow by the age of the colony (Sneath et al., 1986). It is characterized by its inability to produce the enzyme DNase (DNase), but is characterized by the production of mucus (Slime), which consists of multiple sugars only, and are important in helping bacteria to adhere to host tissue, and is one of the factors of virility of these bacteria (Hjelm and Lundell -Etherden, 1991; Atmaca et al., 2000). Bacteria have a high ability to produce urease, which plays an important role in the pathogenesis of these bacteria, and is one of the factors of virulence of these bacteria (Gatermann and Marre, 1989). These bacteria have two types of proteins, which are considered the factors of virility of these bacteria: Surface Associated Protein (Ssp), which accelerates the process of adhesion of cells to the cells of the eukaryotic cells, and estimated the molecular weight of this protein in the isolates produced by 95 kelodalton (Gatermann, 1992).

(Hemagglutinin), which is one of the surface proteins produced by this bacteria, which gives the bacteria the ability to link to the cells of the eukaryotic, the use of the phenomenon of blood balance of red blood cells of sheep as a model to study the adhesion of this bacteria, and that it can recognize the double sugars located on the surface of pellets (Geynarsson et Meyer, 1994; Meyer et al., 1997). The molecular weight of this protein is estimated at 160 kelodalton (Meyer et al., 1995) 1996), and the most important diagnostic feature of these bacteria is their resistance to antibiotic nuclear (Goldstein et al., 1983).

Pathogens of *Staphylococcus saprophyticus*

The presence of non-producing coccylase *staphylococci* (CONS) in the droplet sample is contaminated and therefore neglected. However, at the beginning of 1970, these species became common causes of urinary tract infection, especially *S. saprophyticus* (Hovelius and Mardh, 1984). These bacteria are an important cause of urinary tract infection in women after *E. coli* is the second cause of urinary tract infection after *E. coli* (Baily, 1973; Anderson et al.,



**Eqbal Dohan Challap and Ghaidaa Raheem Lateef Al-Awsi**

1981; Marrie et al., 1982; Price and Flournoy, 1982; Schneider and Riley, 1996; Finhn et al., 1998). It was found that 10-30% of urinary tract infections occur as a result of infection with these bacteria, especially in females (Stamm, 1998). In the study, 607 migraine samples were taken from women with urinary tract infection. It was noted that 477 samples were due to *E. coli* and 67 samples were due to *S. saprophyticus* (Latham et al., 1983). The incidence of urinary tract infection due to these bacteria undergo seasonal changes, as the infection is at the peak in the late summer and early spring, and less in winter and autumn (Jordan et al., 1980), and the incidence of infection of these bacteria varies from one age to another, 1973 A study of 172 women with urinary tract infection and different ages found that the presence of bacteria varies from one age to another (Wallmark et al., 1978).

The most common types of urinary tract infections caused by these bacteria include cystitis, urethritis, and pyelonephritis, usually accompanied by bacteriuria (Hovelius and Mardh, 1977; Lee et al. (1983), and Hovelius and his group noted the susceptibility of these bacteria to cause urethritis in men (Kauffman et al., 1983; Hovelius et al., 1984). Prostatitis can also cause meningitis (Carson et al., 1982; Bergman et al., 1984). These bacteria cause bacteremia, a rare condition that is associated with obstruction of the urinary tract (Goleddege, 1988; Kloos and Bannerman, 1994). In addition, these bacteria cause sepsis after urinary surgery Gillespie et al., 1978).

Enzymes that degrade urease

Urea is a nitrogenous product that is secreted from both the human and animal body. It is produced in the liver and then released into the circulatory system, so all the tissues of the body, as well as the natural microorganisms present in it, are susceptible to urea as they pass through blood vessels feeding the tissues (McLean et al., 1988). The urea enzyme stimulates hydrolysis of urea to release ammonia and carbamate. This molecule is automatically decomposed to form a second molecule of ammonia and carbonic acid, which in turn changes to bicarbonate and hydrogen ions. Ammonium and water molecules are also balanced with ammonium hydroxide, To high pH (Song et al., 2001).

Physiology of urease in living organisms**The location of ureases in the cell**

The urease enzyme is sometimes an exogenous enzyme, but some studies have indicated that it is concentrated in the cytoplasmic fluid part of the bacterial cell and yeasts (Mobley and Husinger, 1989). The researcher Jeffries said that the enzyme urease in 22 species of bacteria is associated with the extracts of intracellular Urease, which needs to be derived from the breakdown of sonic bacterial cells (Sonication) or glass beads (Jeffries, 1964). While the electron microscopy studies showed the association of the periplasmic urease with the outer membrane in *P. mirabilis* cells (Rozalsi et al., 1997), as well as between the electron microscopy and the intracellular binding of the inner membrane (Inner Membrane) of *Staphylococcus* cells (McLean et al., 1985). *Helicobacter pylori* is characterized by its enzyme in the cytoplasm and on the surface of the cell in one, because its outer membrane has the ability to adsorb the enzyme released from the adjoining neighboring cells (Dunn et al., 1997).

Regulate the production of urease in bacteria**Urease Regulation in Bacteria**

The enzyme urease is either constitutive or induced, depending on the type of bacteria and surrounding environmental conditions. The production of the urease enzyme is linked to the nitrogen regulation system. For example, the production of the urease enzyme inhibits the repressed in case of ammonia. The presence of nitrogen-rich compounds, including chlorine, and the effect of braking is reduced when the amount of nitrogen is limited in



**Eqbal Dohan Challap and Ghaidaa Raheem Lateef Al-Awsi**

the environment, while other bacterial species respond directly to the concentration of urea as a catalyst, the enzyme is made in the induction (induced), and in some other bacterial species are synthesized urease, Its manufacturing is influenced by Addition or lack of nitrogen compounds and urea or ammonia (Mobley and Hausinger, 1989). Falkinham and Hoffman observed a difference in the efficiency of urease in the swarming cells of *Proteus* in non-swarming cells, which is more effective in cells Timing (Falkinham and Hoffman, 1984).

In *Streptococcus salivarius*, the production of urease is regulated by the pH of the surrounding environment (Sissons et al., 1992). In *Proteus rettgeri* bacteria, the urease enzyme is produced when bacteria are grown in the center of the urea (Magana-Plaza and Ruize Herrera, 1967). In *Klebsiella* bacteria, urease is not synthesized when cells are grown in a rich medium of nitrogenous compounds such as ammonia. The enzyme is produced when cells are grown in a medium of limited nitrogen compounds such as histidine, arginine and proline. The enzyme is produced in *Providencia* bacteria in the case of urea (Mobley et al., 1995). In *S. saprophyticus*, the urease is synthesized by adding or not adding urea to the medium (Gatermann et al., 1989). In *S. xylosus* bacteria, its production is also synthesized without the presence or absence of urea (Jose et al. 1991). There are three main enzymes responsible for controlling the production of urease: Glutamate dehydrogenase (GDH) E.C.14.1.4, Glutamine Synthetase (GS) E.C.6.3.1.2 and Glutamate Synthase (GOGAT) E.C.2.6.1.53 (Mclean et al., 1988).

When the bacteria are grown in nitrogen-rich conditions, GDH is the preferred pathway for nitrogen representation, and when nitrogen is limited, GS-GOGAT is preferred to represent nitrogen. Friedrich and MagaSanick noted that the efficacy of urea from *Klebsiella aerogenes* was directly related to the efficacy of GS (Friedrick and MagaSanick, 1977). Janssen and his group found in 1984 that the efficacy of *Pseudomonas aeruginosa* produced positive relationship with the effectiveness of Glutamine synthase.

Urease Structure

The enzyme urease is a metal enzyme containing the nickel at the active site of the enzyme (Won et al., 2004). Nickel is associated with the amino acids in the effective sites of the enzyme, called the metal enzyme (Dixon et al., 1980) The nickel-containing enzymes all contain nickel in the active site. Studies indicate that there is ion of nickel for each active site. No other metal can replace nickel to give the active form of the enzyme (Schaffer and Kaltwasser, 1994). If this is done, it will reduce or inhibit Enzyme activity (Park and Hauser, 1996). There are some urease enzymes for some types of bacteria such as: *S. saprophyticus*, *S. xylosus*, and *H. pylori* contains small amounts of nickel that may reach up to one ion per active site, due to the incomplete mobilization of protein in mineral ions (Mobley et al., 1995). The initial protein synthesis was identified by nucleotide sequence analysis of DNA, or amino acid sequence of protein. The results of the studies, which included several types of bacteria, showed that there are similarities in the initial structure of some bacteria and differences in other types of bacteria, indicating variance in urease enzymes, although there is similarity in the triangular structure. The quadruple structure of the urease enzyme for *S. saprophyticus* is composed of three subunits: Schaffer and Kaltwasser (1994). The quadruple structure of the purified urease of all bacteria consists of 3 subunits Except *H. pylori* it consists of two units (Mobley and Hausinger, 1989).

Urease Mechanism

The other role is to connect and activate the water molecule . The urea is correlated consistently with nickel ions and with the help of the histidine group 219. A base at the active site (B and Hestden-320) activates the water molecule, which in turn is linked to the second nickel ion. When the carboxyl group, which is connected to the second nickel ion, is attacked by the carbon atom of the substrate (urea) Which links the two mineral sites , The proton moves to the central compound, while ammonia is released and the water molecule replaces the carbamate that is automatically decomposed into a second molecule of ammonia and carbon dioxide to complete the cycle (Mobely et al., 1995) as shown in the following diagram.



**Eqbal Dohan Challap and Ghaidaa Raheem Lateef Al-Awsi****Role of Urease in Pathogens**

Recent studies indicate the importance of this enzyme because it is a virulence factor for many bacteria. The role of the enzyme in the various diseases can be classified according to the following:

Urinary Tract Infection

Bacteria such as *Ureaplasma Proteus*, *Pseudomonas*, *Staphylococcus*, *Klebsiella*, *Morganella*, *Corynebacterium* sp. Group D2 to urinary tract infection and formation of bladder and kidney stones (Urolithiasis) (Rosenstein et al., 1981). These stones occur as a result of pH elevation of 6.5 to 9 for the environment in which the enzyme works. It analyzes urea, produces CO₂ and ammonia, Mg + 2, Ca + 2, which are insoluble in base pH in the form of struvite salts and Carbonate apatite (Senior et al., 1980; Kralden et al., 1984; Mclean et al., 1988). These are deposited in a cellular structure called polysaccharide, which facilitates the adhesion of bacteria to the surface of the tissue (Rozisk et al., 1997). It is also noted that there is a glycoprotein in the gravel in patients treated with antibiotics (Mobely and Hausinger, 1989). In addition, this enzyme causes inflammation of the renal tubules. The role of this enzyme in the pathogenesis of *Proteus mirabilis* was studied by Braude and Siemianski, who infected these bacteria in the rats, noting that the enzyme of this bacteria leads to infection of the renal tubules and elevates the kidney pH to 8.2, which leads to the necrosis of the renal tubules and the sedimentation of salts (Braude and Siemianski, 1960).

Johnson and his group injected mice with *P. mirabilis*, which is a product of urease, and non-urea-producing *P. mirabilis*. They were injected separately by transurethrally. A week later, ulceration of the renal epithelial cells with the leachate pool Exudate) in the alveolar cavity, with severe necrosis of the epithelial tubules near the kidney pelvis, as well as the formation of kidney stones, along with a large number of neutrophil cells. The non-producing *P. mirabilis* bacteria showed a simple trigemination of the epithelial cells of the embryo, and a moderate number of neutral cells and epithelial epithelial cells in the ventricle cavity (Johnson et al., 1993). Urease also causes the obstruction of the catheter. This catheter is an excellent focal point for colonization by organisms such as *Proteus*, *Providencia*, and *Morganella* (Mobley and Hausinger, 1989).

Gastrointestinal Tract Infections

H. pylori is the main cause of infectious infections by producing urease, which increases the ammonia hydroxide ratio at the site of inflammation, thereby protecting the bacteria from the acidic environment of the stomach, which gives birth to the tissue that has been colonized by bacteria (Mobley et al., 1995). The bacteria produced by these bacteria cause peptic Ulceration due to the production of the enzyme in large quantities, which increases the pH of the stomach, prevents the transfer of hydrogen ions from the gastric glands to the gastric cavity, and allows the reverse diffusion of hydrogen ions, Concentration of ammonia changes the mucosal permeability of the stomach and thus breaks down the mucous membrane of the stomach, and the formation of peptic ulcer (Mobley and Hausinger, 1989).

Methods of measuring the effectiveness of urease**Urease Activity Assay**

Several methods for detecting the effectiveness of urease were included: Quantitative methods, Qualitative methods, and the latter based on the change in the pH value with a redolent Phenol redshift detected by ammonia release (Magana-Plaza and Ruiz-Herrera, 1967). Quantitative methods are more accurate in detecting the presence of the enzyme, but vary in their degree of sensitivity, and the estimation of the reaction products. A quantitative method for the determination of the effectiveness of the urease enzyme, based on ammonia release, is the Nessler Reagent method or the Indophenol measurement method, which is the result of the ammonia reaction released from



**Eqbal Dohan Challap and Ghaidaa Raheem Lateef Al-Awsi**

the enzymatic reaction with the hypochlorite reagent and the presence of phenol in a base environment (Weatherburn, 1967). In addition to these two methods, there is a more accurate and cost-based method of estimating the absence of nicotinamide adenine dinucleotide (NADH) and in conjunction with the enzyme Glutamic dehydrogenase. This method is called the Coupled Assay, so it is of little use (Kaltwasser and Schlegel, 1966).

Another method is dependent on the change in pH on the polyacrylamide gel, where the effective beams of the urea enzyme only appear. There is a method in which a ion-selective electrode is used to measure the continuous emancipation of ammonia ions, Or the use of the Urea substrate in which carbon is the radioactive counterpart C14-urea in the enzymatic reaction, and the liberated bicarbonates are estimated by the Scintillation Counting (Swanberg et al., 1978). Other methods depend on the carbon dioxide containing the radioactive isotope C13-urea (Graham et al., 1987), or the estimate of the carbon dioxide that contains the radioactive C14 from the reaction, using the urea substrate containing the radioactive isotope C14 They are estimated by mass spectrometry (Bell et al., 1987). Both methods are used to detect the presence of *H. pylori* in the human intestinal mucosa.

Purification of uric acid

The enzyme is purified for the purpose of studying its properties because the presence of other substances can lead to the results of the real, the purification process means the separation of the enzyme from the rest of the components of the center, and include several steps increase during the qualitative effectiveness (Whitaker and Bernhard, 1972). Various methods were used to purify the urease. The first attempt to purify this enzyme was to purify urease from *Bacillus pasteurii* bacteria in 1954. Since then, urease has been purified from many bacteria. Urea has also been purified from *Aspergillus nidules* but without homogenization Homogeneity) in most of them (Mobley and Hausinger, 1989). The purification of urease from *Bacillus pasteurii* bacteria was a series of simple separation steps such as ammonium sulphate deposition: precipitation with protamine sulfate for nucleic acid deposition and calcium phosphate treatment; subsequent ammonium sulphate deposition and acetone treatment. In order to improve the purification process, the treatment was introduced with ethanol and heat treatment for partial purification of the enzyme (Christians and Kaltwasser, 1986). Other separation methods were also used, including gel filtration, ion exchange chromatography and Affinity chromatography, The efficacy of *Bacillus Pasteurii*-purified Urea enzyme by using gel filtration has decreased compared with the previous one (Mobley and Hausinger, 1989).

The separation columns then evolved to include many types of urease resins, because the urease enzyme carries a negative charge at the pH. (*Proteus mirabilis* (Breitenbach and Hausering, 1988) and *Providencia stuartii* (Mulrooney et al., 1988) were purified in a homogeneous manner using Mono-Q- resins. *Ureaplasma urealyticum* was synthesized using Affinity Chromatography, which is mediated by binding the acetyhydroxamic acid free group with the CH group of the Sepharose column and the purity of the urease enzyme produced by *H. pylori* using Superose 12 gel (Dunn et al., 1990). The urease extracted from the *Schizosacchomyces pomb* yeast was pure by sedimentation with acetone, ammonium sulphate deposition, and the use of the ion exchanger column DEAE-Sepharose (Lubbers et al., 1996). In addition, the enzyme purified from *Morganella morganii* was extracted using several ion exchangers such as DEAE-Sepharose, Phenyl-Sepharose, Mono-Q, Superose-6 . Uryiz, the product of the rest, was the first isolating enzyme and was synthesized in a simple way by the treatment of Sumner (1926). No method of purification was applied until 1941 as it was recrystallized in Dounce to give a pure enzyme (Bailey and Boulter, 1969). The method of rheumatoid chromatography was successful in purifying urease from the rest (Shobve and Brosseau, 1974).

REFERENCES

- 1- Atmaca, S.; Elci, S. and Akpolat, N. O. (2000). Differential production of slime by *Staphylococcus saprophyticus* under aerobic and anaerobic conditions. J. Med. Microbiol. 49: 1051-1052.
- 2- Bailey, C. J. and Boulter, D. (1969). The subunit structure of Jack bean urease. Biochem. J. 113: 669-677.




Eqbal Dohan Challap and Ghaidaa Raheem Lateef Al-Awsi

- 3- Breitenbach, J. M. and Hausinger, R. P. (1988). Partial purification and inhibition by boric acid and boronic acid. *Biochem. J.* 250: 917-920.
- 4- Christians, S. and Kaltwasser, H. (1986). Nickel-Content of urease from *Bacillus pasteurii*. *Arch. Microbiol.* 145: 51-55.
- 5- Dixon, N. E.; Gazzola, C.; Asher, C. J.; Lee, D. S. W.; Blakeley, R. Z. and Zerner, B. (1980). Jack bean urease (Ec. 3. 5. 1. 5) II. The relationship between nickel enzymetic activity and the abnormal ultraviolet spectrum. The nickel content of Jack bean urease. *Can. J. Biochem.* 58: 474-480.
- 6- Dunn, B. E.; Campbell, G. P.; Perez-Perez, G. T. and Blaser, M. J. (1990). Purification and characterization of urease form *Helicobacter pylori*. *J. Biol. Chem.* 265 (16): 9464-9469.
- 7- Fairbrother, R. W. (1940). Coagulase production as a criterion from the classification of the Staphylococci. *J. Path. Bacteriol.* 50: 83-85.
- 8- Gatermann, S.; Kerft, B.; Marre, R. and Wanner, G. (1992). Identification and characterization of a surface-associated protein of *Staphylococcus saprophyticus*. *Infect. Immun.* 60 (3): 1055-1060.
- 9- Geary, C. and Stevens, M. (1989). Detection of phosphatase production by *Staphylococcus* species: a new method. *Med. Lab. Sci.* 46 (4): 291-494.
- 10- Graham, D. Y.; Klein, P. D.; Evans, D. J.; Alpert, L. C.; Opekun, A. R. and Boutton, T. W. (1987). *Campylobacter pyloridis* detected by the C13-urea test. *Lacet* 1: 1174-1177.
- 11- Hovelius, B.; Thelin, I. and Mardh, P. A. (1979). *Staphylococcus saprophyticus* in the etiology of nongonococcal urethritis. *Br. J. Vener. Dis.* 55 (5): 369-347.
- 12- Johnson, D. E.; Russell, R. G.; Lockett, C. V.; Zulty, J. C.; Warren, J. W. and Mobley, H. L. T. (1993). Contribution of *Proteus mirabilis* urease to persistence, urolithiasis, and acute pyelonephrities in a mouse model of ascending urinary tract infection. *Infect. Immun.* 61 (7): 2784-2754.
- 13- Kaltwasser, H. and Schlegal, H. G. (1966). NADH-dependent coupled enzyme assay for urease and other ammonia-producing systems. *Anal. Biochem.* 16: 132-138.
- 14- Kloos, W. E. and Bannerman, T. L. (1994). Update on clinical significance of coagulase-negative Staphylococci. *Clin. Microbiol. Rev.* 7 (1): 117-140. (Internet).
- 15- Kloos, W. E. and Jorgensen, J. H. (1985). Staphylococci. In manual of clinical microbiology. P: 143-153. 4th ed. (Balows, A.; Hausler, W. J. R. and Shadomy, H. J.). American Society for Microbiology. Washington.
- 16- Kloos, W. E. and Schleifer, K. H. (1975). Simplified scheme for routine identification of human *Staphylococcus* species. *J. Clin. Microbiol.* 1 (1): 82-88.
- 17- Kloos, W. E. and Smith, P. B. (1980). Staphylococci. In manual of clinical microbiology. P: 83-87. 3rd ed. (Balows, A.; Hausler, W. J. R. and Iruant, J. P. eds). American Society for Microbiology. Washington.
- 18- Kloos, W. E. and Wolfshohe, J. F. (1982). Identification of *Staphylococcus* species with the Api Staph. Ident. System. *J. Clin. Microbiol.* 16 (3): 509-516.
- 19- Latham, R. H.; Grootes-Reuvecamp, G. A.; Zeleznik, D. and Stamm, W. E. (1983). Use of a novobiocin-containing medium for isolation of *Staphylococcus saprophyticus* from urine. *J. Clin. Microbiol.* 17 (6): 1161-1162.
- 20- Lubbers, M. W.; Rodriguez, S. B.; Honey, N. K. and Thornton, R. J. (1996). Purification and characterization of urease from *Schizosaccharomyces pombe*. *Can. J. Microbiol.* 42 (2): 132-140.
- 21- Magana-Plaza, I. and Ruiz-Herrera, J. (1967). Mechanisms of regulation of urease biosynthesis in *Proteus rettgeri*. *J. Bacteriol.* 93 (4): 1294-1301.
- 22- Mobley, H. L. T. and Hausinger, R. P. (1989). Microbial ureases: Significance, regulation and molecular characterization. *J. Microbiol. Rev.* 53 (1): 85-108.
- 23- Mulrooney, S. B.; Pankratz, H. S. and Hausinger, R. P. (1988). Regulation of gene expression and cellular localization of cloned *Klebsiella aerogenes* (*Klebsiella pneumoniae*) urease. *J. Gen. Microbiol.* 135: 1769-1776.
- 24- Park, I. S. and Hausinger, R. P. (1996). Metal ion interactions with urease and D-urease apoproteins. *Biochemistry.* 35 (6): 5345-5352.
- 25- Rozalsi, A.; Sidorczyk, Z. and Kotelko, K. (1997). Potential virulence factors of *Proteus bacilli*. *Microbiol. and Molecular Biol Rev.* 61 (1): 65-89.



**Eqbal Dohan Challap and Ghaidaa Raheem Lateef Al-Awsi**

- 26- Senior, B. W.; Bradford, N. C. and Simpson, D. S. (1980). The urease of *Proteus* strains in relation to virulence for the urinary tract. *J. Med. Microbiol.* 13: 507-512.
- 27- Shaw, C.; Still, J. M. and Cowan, S. T. (1951). *Staphylococci and their classification.* *J. Gen. Microbiol.* 5: 1010-1023.
- 28- Sneath, P. H. A.; Mair, N. S.; Sharpe, M. E. and Holt, J. G. (1986). *Bergey's Manual of Systematic Bacteriology.* Vol. 2. The Williams and Wilkins Co., Baltimore.
- 29- Song, H. K.; Mulrooney, S. B.; Huber, R. and Hausinger, R. P. (2001). Crystal structure of *Klebsiella aerogenes* Ure E, a nickel-binding metallochaperone for urease activation. *J. Biol. Chem.* 276 (52): 49359-49364.
- 30- Stamm, W. E. (1998). Urinary tract infections and pyelonephritis. In: *Harrisons principle of internal medicine.* P: 817-823. 14th ed. (Fauci, A. S.; Brauwold, E.; Isselbacher, K.; Wilson, J. D.; Martin, J. B.; Kasper, O. L.; Hausinger, S. L. and Longo, D. L. eds). McGrawc Hill. New York.
- 31- Teti, G.; Chiofalo, M. S.; Tomasella, F.; Fave, C. and Masteroeni, P. (1987). Mediation of *Staphylococcus saprophyticus* adherence to uroepithelial cells by lipoteichoic acid. *Infect. Immun.* 55 (3): 839-842.
- 32- Ghaidaa Raheem Lateef Al-Awsi, 2017. Immunological and Molecular Study on *Helicobacter Pylori* in Pregnant Woman, Ph.D. thesis, College of Science, University of Babylon, Iraq. DOI: 10.13140/RG.2.2.36634.54726.
- 33- Ghaidaa Raheem Lateef Al-Awsi, 2012. Isolation and Identification of microbiological from Al-Diwanya hospitals and Controlled by Antiseptic and Antibiotic, M.Sc. Thesis, University of Al-Qadisiyah. DOI: 10.13140/RG.2.2.14299.87844.
- 34- Azhar Omeran Al-Thahab, and Ghaidaa Raheem Lateef Al-Awsi, 2017. Relationship between *H. pylori* infection and IL-1 β polymorphism in pregnant women, *Research Journal of Pharmaceutical, Biological and Chemical Sciences*, 8 (4) P. 858-866.
- 35- Torres-Pereira, A. (1962). Coagulase negative strains of *Staphylococcus* processing antigen 51 as agents of urinary infection. *J. Clin. Path.* 15: 252-253.
- 36- Weatherburn, M. W. (1967). Phenel-hypochlorite reaction for determination of ammonia. *Anal. Chem.* 39 (8): 971-974.
- 37- Al-Grawi, E.D.C., and G.R.L. Al-Awsi. 2018. "Expression of CDKN2A (P16/Ink4a) among Colorectal Cancer Patients: A Cohort Study." *Journal of Pharmaceutical Sciences and Research* 10 (5).
- 38- LATEEF, Ghaidaa Raheem; AL-THAHAB, Azhar Omeran; CHALAP AL- GRAWI, Eqbal Dohan. Linkage between *H. pylori* Infection and TNF- α polymorphism in The Pregnant Women. *International Journal of Research in Pharmaceutical Sciences*, [S.I.], v. 9, n. SPL1, apr. 2018. ISSN 0975-7538. Available at: <<https://www.pharmascope.org/index.php/ijrps/article/view/1298>>. Date accessed: 27 july 2018. doi: <https://doi.org/10.26452/ijrps.v9iSPL1.1298>.
- 39- Shamran, A. R, Shaker, Z. H, Al-Awsi, G. R. L, Khamis, A .S , Tolaifeh, Z. A. and Jameel, Z. I, 2018. RAPD-PCR IS A GOOD DNA FINGERPRINTING TECHNIQUE TO DETECT PHYLOGENETIC RELATIONSHIPS AMONG *STAPHYLOCOCCUS AUREUS* ISOLATED FROM DIFFERENT SOURCES IN HILLA CITY, IRAQ. *Biochem. Cell. Arch.* Vol. 18, Supplement 1, pp. 1157-1161.
- 40- Williams, D. A.; Lund, M. E. and Blazevic, D. J. (1976). Significance of urinary isolates of coagulase-negative micrococaceae. *J. Clin. Microbiol.* 3 (6): 556-559.





Eqbal Dohan Challap and Ghaidaa Raheem Lateef Al-Awsi

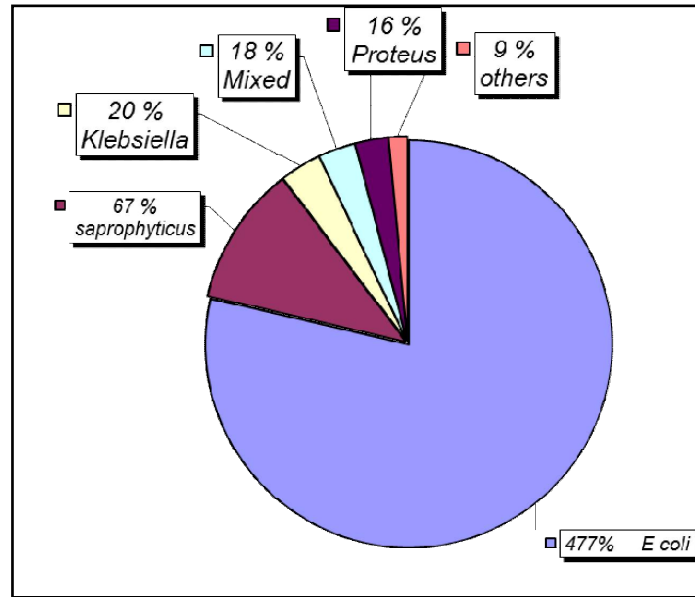


Fig.1: Rates of different types of bacteria in urine samples

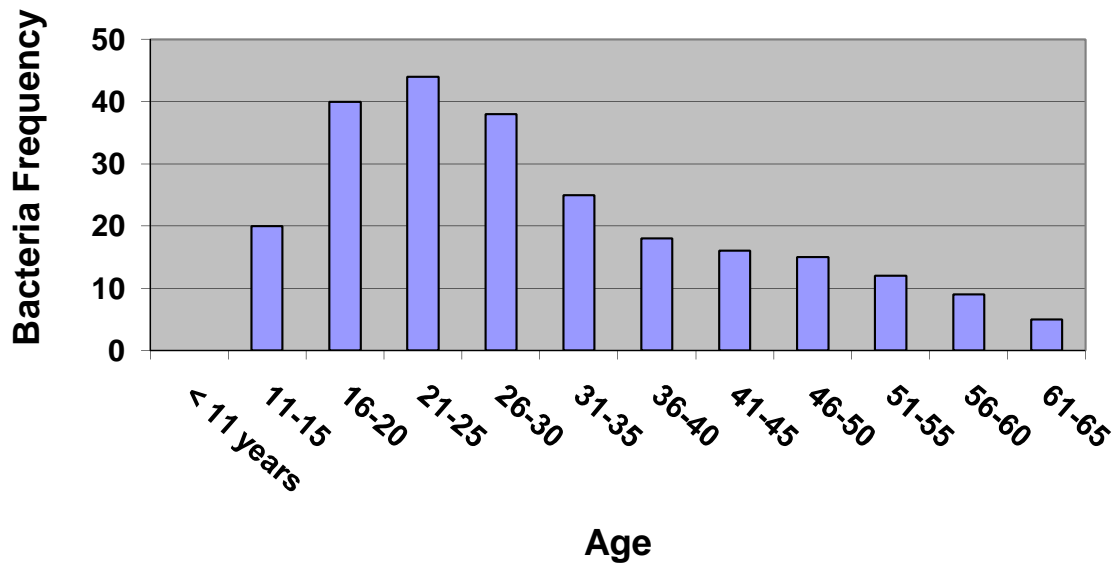


Fig.2: The frequency of *Staphylococcus saprophyticus* in different age groups





Eqbal Dohan Challap and Ghaidaa Raheem Lateef Al-Awsi

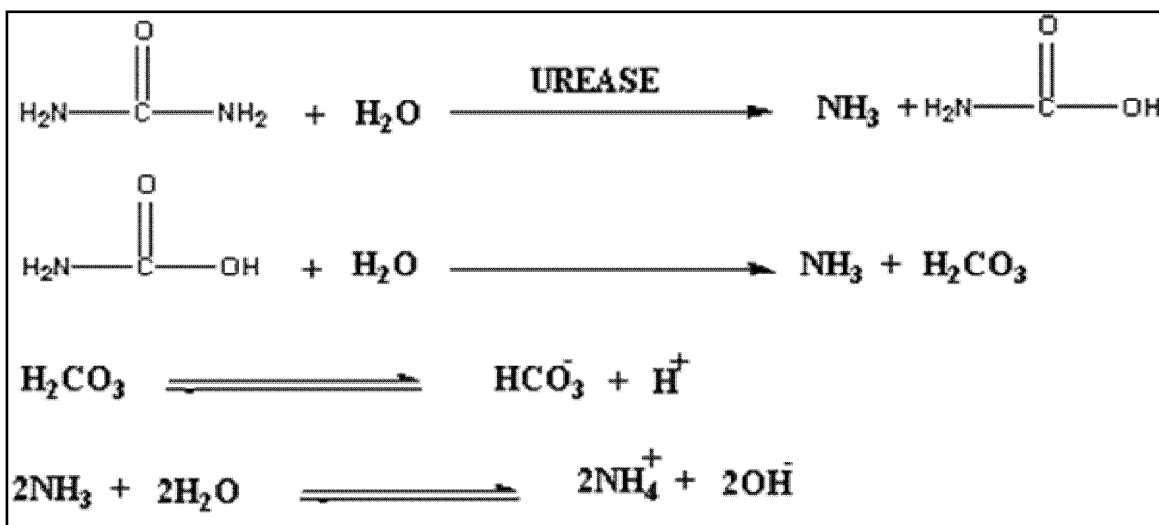


Diagram.1: showing the breakdown of urea molecule

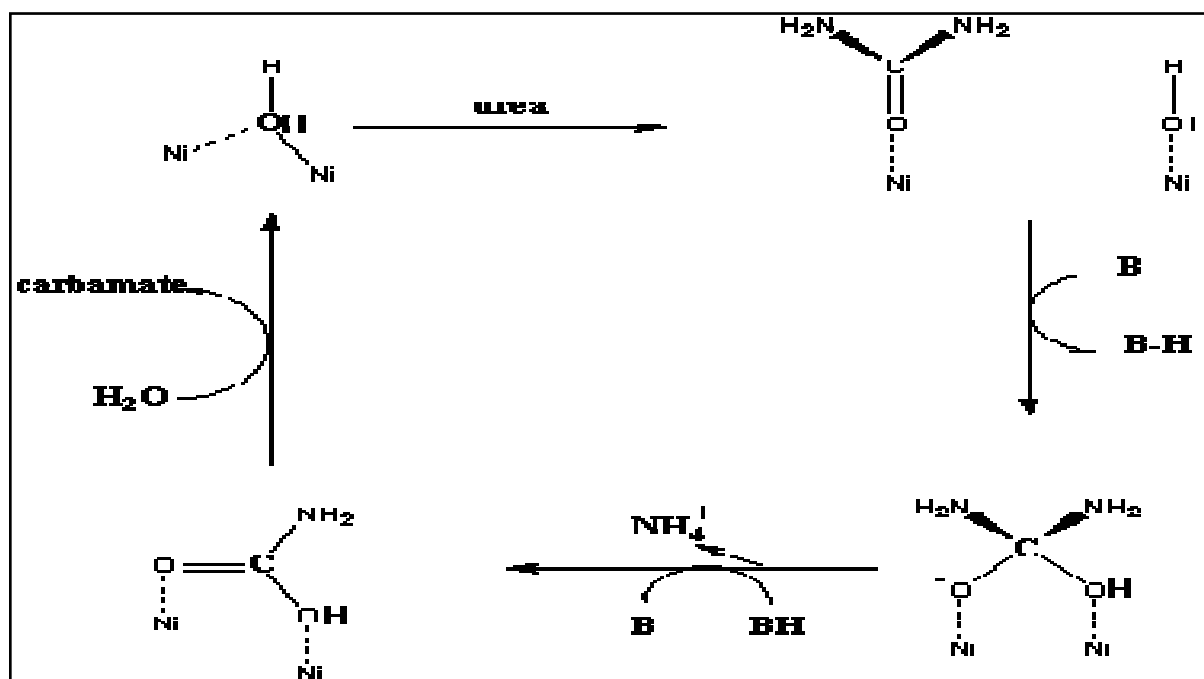


Diagram.2: showing the mechanism of action of urease enzyme





Role of Fat Mass and Obesity Associated Genotype in Type 2 Diabetic Obese Patients of Karbala Province, Iraq

Fadhil J. Al-Tuma^{1*}, Dhuha H. Al-Safah² and Hassan M. Al-kutubi³

¹Department of Biochemistry, College of Medicine, University of Kerbala, Iraq.

²Department of Chemistry, College of Science, University of Kerbala, Iraq

³Department of Internal Medicine, Al-Zahraa Teaching Hospital, Imam Al-Hussein Medical City, Kerbala Health, Iraq.

Received: 27 Aug 2018

Revised: 20 Sep 2018

Accepted: 27 Oct 2018

*Address for Correspondence

Fadhil J. Al-Tu'ma

Department of Biochemistry,

College of Medicine,

University of Kerbala, Iraq.

Email: f_altoma_56@yahoo.com



This is an Open Access Journal / article distributed under the terms of the **Creative Commons Attribution License** (CC BY-NC-ND 3.0) which permits unrestricted use, distribution, and reproduction in any medium, provided the original work is properly cited. All rights reserved.

ABSTRACT

Background: Fat Mass and obesity associated gene is one of the factors to development obesity where it's located in chromosome 16. Single nucleotide polymorphism was selected in the current study to see its association with obese type 2 diabetes mellitus (T2DM). **Aim:** To detect any association between fat mass and obesity associated (*FTO*) rs9939609 variant (mutation of allele T to allele A) with the pathogenesis of type 2 diabetes mellitus in obese patients of Kerbala population. **Materials and Methods:** This across-sectional study in which *FTO* gene variant rs9939609 was genotyping in a total 180 male subjects, 92 subjects of them were obese with T2DM and the other 88 subjects were obese without T2DM during Nov., 2017 to Sep., 2018 and both age were matched between the range 40-70 years. The patient's group was enrolled from Al-Husain medical city in Kerbala province based on WHO guidelines of T2DM. Body mass index (BMI), fasting blood sugar (FBS), lipid profile, insulin level and HOMA-IR were measured; DNA was extracted from whole blood and genotyped by using ARMS-PCR technique with using specific primers. Multinomial logistic regression was applied to compare the proportions of genotypes or alleles. The odds ratio, t-test, and P-value at 95% confidence interval (CI) were measured. Also in the present study, the Hardy Weinberg equilibrium was tested. **Results:** Our results showed that there are no association between the minor allele A at rs9939609 of the *FTO* and increase T2DM risk with an allelic odd ratio (OR) of 1.45, (95%CI [0.73 - 3.24] P=0.25). While Stratified data revealed an association between the *FTO* A variant and body mass index (BMI) in the diabetic group (P=0.001), and non-diabetic group (P=0.001). Furthermore, no significant association was observed between *FTO* genotypes and covariates of insulin level and HOMA-IR or any tested metabolic trait in both diabetic and non-diabetic individuals (P>0.05).



**Fadhil J. Al-Tu'ma et al.**

Conclusion: Our results showed no association between *FTO* gene (rs9939609) variant and T2DM, insulin level and HOMA- IR. As well, no significant association was observed between this variant and other biochemical parameters. But there is a strong association between *FTO* gene (rs9939609) variant and BMI in obese (diabetic and non-diabetic) Iraqi males

Keywords: T2DM, fat mass and obesity-associated (*FTO*) gene, rs9939609, HOMA-IR.

INTRODUCTION

Obesity is a health problem worldwide and is the fifth risk factor for global mortality and it is a very complex medical condition. The condition is characterized by the accumulation of excess fat in the body (1). It is described as having a body mass index (BMI) exceeding 30 kg / m². Obesity has been shown to be a risk factor for many chronic diseases including diabetes, hypertension, non-alcoholic fatty liver disease, metabolic syndrome and cardiovascular disorders (2). The "Diabesity" epidemic (obesity and type 2 diabetes) is likely to be the biggest epidemic in human history (3). Obesity is also associated with insulin resistance and impaired insulin secretion, the two key features in the development of type 2 diabetes (4). Studies on inheritance have found that genetic differences account for 40% to 70% of the variation in individual susceptibility to obesity, affecting more than 10% of the world's population. In 2007, the fat mass and obesity associated gene (*FTO*) became the first gene identified by large-scale genomic correlation studies to correlate with high body mass index (BMI) and increased risk of obesity (5). Although the function of such a gene has not been clearly explained, a recent study has linked this to insulin secretion in a laboratory model of pancreatic β -cell (6). Insulin resistance has been shown to be a major link between obesity and type 2 diabetes. Clinically, insulin resistance refers to a condition in which a particular concentration of insulin is associated with an abnormal glucose response. The homeostasis model assessment of insulin resistance (HOMA-IR) is a simple method to measure insulin resistance (6). Insulin resistance is associated with numerous health risks. For one thing, it causes hyperinsulinemia, or high circulating insulin levels, which may be directly damaging to blood vessels (7).

Fat Mass and Obesity gene (*FTO*) reduces insulin action as a secondary effect, with the primary effect of its common variants being to influence adiposity (8). It is an enzyme that affects development of human obesity and energy homeostasis, Also known as alpha-ketoglutarate-dependent dioxygenase (9). It is also a polymorphic gene which is located on chromosome 16 and its molecular weight is 58 kDa (10). It is a very large gene with nine exons span more than 400 kb located on the long (q) arm at position 12.2 and its expressed in a wide range of tissues, including the adipose tissue and specific areas of the brain and muscles, suggesting its potential role in body weight regulation (11). The rs9939609 single nucleotide polymorphism (SNP) with nucleotide position "53786615", identified with the T to A missense mutation, located within the first intron of *FTO* was found to have a strong association with body mass index (BMI) (12). The A risk allele in the rs9939609 polymorphism was associated with increased consumption of fat and carbohydrates. This polymorphism has also been associated with a high amount of energy, both in adults and children but with no control over energy expenditure. The presence of the risk allele looks to reduce the toxicity after eating (13). The aim of this study was to detect any association of Fat Mass and Obesity associated (*FTO*) rs9939609 variant (mutation of allele T to allele A) with metabolic and anthropometric parameters and insulin level in Kerbala obese men with T2DM.

MATERIAL AND METHODS

This across-sectional study in which *FTO* gene variant rs9939609 was genotyping in a total 180 male subjects, 92 subjects of them were obese with T2DM and the other 88 subjects were obese without T2DM during Nov., 2017 to Sep., 2018 and both age were matched between the range 40-70 years. The patient's group was enrolled from Al-





Fadhil J. Al-Tu'ma et al.

Husain medical city in Kerbala province based on World Health Organization(WHO)guidelines of T2DM(14). All participants gave written informed consent after approval of the ethical committee.The inclusion criteria for selecting obese participations were: BMI ≥ 30 kg/m², FBS > 126 mg/ dl in T2DM and FBS <126 mg/ dl in non-diabetic obese, no family relationship between the subjects with non-diabetic group, no specific disease or chronic history. The exclusion criteria included the participants had no history of kidney disease or using cortisol and lipid lowering drugs.

Five milliliters of venous blood were collected from all individuals participated in this study. The blood was divided into two parts: The first part was used for molecular analysis. It included two milliliters of blood collected in EDTA containing tube and used for DNA extraction, then were analyzed directly to obtain high purity of DNA. The second part included three milliliters of blood placed in serum tube. Blood was centrifuged for 15 minutes at 3000 xg. Serum was collected then stored at -20°C serum that used for determination of different biochemical parameters such as Glucose, TG, HDL-C, LDL-C, VLDL-C, TC and serum insulin. DNA was isolated from the whole blood by using the genomic DNA mini kit (Geneaid /China). Then, DNA concentration and purity were measured by UV absorption at 260 and 280 nm (Nano-drop, USA). Genotyping was carried out using tetra-primer amplification refractory mutation system-polymerase chain reaction (ARMS-PCR) for FTO gene using the thermocycler (Cleaver, USA). The list of primers sequences and PCR condition used in current study for the SNP (rs9939609) of FTO gene obtained from Muller (15), as following:

Fout: 5'-TGG CTC TTG AAT GAA ATA GGATTC AGA A-3'

Rout: 5'-AGC CTC TCT ACC ATC TTA TGT CCA AAC A-3'

Fin: 5'-TAG GTT CCT TGC GAC TGC TGT GAA TAT A-3'

Rin: 5'-GAG TAA CAG AGA CTA TCC AAG TGC ATCTCA-3'

Amplification was performed by addition 10 μ l master mix, 1.5 μ l MgCl₂, 1.5 μ l from each primer, 5 μ l of extracted DNA in PCR tube, and completed the volume to 25 μ l by distilled water. Cycling conditions were 93°C for 5 min followed by 30 cycles of 93°C for 30 sec, 53 cycles of 72°C for 25 sec, and the final extension of 72°C for 5 min. Amplification product of FTO gene was 321 bp. Amplification product of FTO gene was run on 1.5% agarose gel by using ethidium bromide stain. Phenotypes data expressed as mean \pm SD and genotypes data expressed as frequencies, ANOVA test and Student t-test used to compare phenotypes data between diabetic and non-diabetic groups using SPSS windows software version 23 (SPSS Inc., Chicago, IL). Genotype frequencies were tested for Hardy-Weinberg equilibrium by χ^2 test. Multi-nominal logistic regression analysis was used to further test the association of SNP with T2DM measured by odds ratio (OR) and corresponding 95% confidence interval (CI) as covariates.

RESULTS

The clinical and biochemical characteristics of study individuals are presented in table 1. It revealed significant differences in FBS, HOMA-IR, and serum insulin between two groups. Genotypes did not deviate from Hardy-Weinberg equilibrium in obese T2DM individuals ($p = 0.102$), but in obese non T2DM individual ($P = 0.003$) as shown in table 2.

PCR Product

The amplification product of FTO gene polymorphism (rs9939609), the amplicon size is 321 bp it is described by Müller (15). Results of this study are shown in figure 1. The Genotype and allele frequencies of FTO gene variant are shown in table 3.





DISCUSSION

The two selected groups were found to be different with respect to FBS. The mean values of both the variables (FBS and HOMA-IR) are significantly higher in the diabetic compared to that of without diabetic (Table 1). The two groups do not seem to be differing with respect to the rest of the variables, body Mass Index, lipid profile. Both the groups exhibit means BMI, TC, TG, LDL-C VLDL-C value higher than the normal range, whereas except for HDL-C, which is within the lower than the normal range. Interestingly the presently studied populations exhibit similar distribution, with BMI and age. FBS is found to be significantly higher among the diabetic group compared to non-diabetic. So, we observed that there is significant correlation when compared between clinical and biochemical characteristics of the two groups obese T2DM, obese non- T2DM group with P-values ($P < 0.05$) in insulin, HOMA-IR, but there is no significant association with other parameters (cholesterol, TG, HDL-C, LDL-C, VLDL-C) ($P > 0.05$). this results consistent with the findings (16-18).

The results show significant differences among the codominant genotypes models and BMI ($p=0.001$) only. but no significant association with other biochemical parameters .Our results demonstrate in the Karbala population a strong association between rs9939609 SNP of the *FTO* gene and BMI in concordance with previously published studies in other Italian, China and Indian populations(19-21). A significant difference in BMI showed in genotype TA and AA groups of rs9939609 higher than the TT group ($P < 0.05$), indicating that the rs9939609 SNP was correlated with the obesity in Iraqi males and this results agreed with Iraqi studies have shown that there is a relationship between rs9939609 and BMI (22). In this study, we were unable to show any significant association between *FTO* gene polymorphism (rs9939609) common variant and insulin resistance. It should be noted that although not statistically significant, fasting glucose level, fasting insulin level, HOMA-IR, TC, TG, LDL-C and VLDL-C are higher in individuals with genotype (AA) and (TA) compared to those with genotype (TT). Our results were identical with another study conducted in Kerbala by (22). Others also showed that there was no association between *FTO* rs9939609 polymorphism and biochemistry parameters such as HOMA-IR, serum insulin levels and blood sugar in obese female adolescents in Indonesia(23). But other work found statistically significant difference polymorphism of rs9939609 in *FTO* gene with insulin level, HOMA, FBS and TG in Iranian Women(17). The discrepancy in findings concerning the association between *FTO* rs9939609 variants and insulin resistance among other studies including our results indicates that the effect of *FTO* rs9939609 variants on insulin resistance may be influenced by other variables including: gender, age and ethnic(24). The differences in our results may also be due to the limitations created by the small sample population.

CONCLUSION

In conclusion, our findings suggest that *FTO* gene variant rs9939609 is not associated with the pathogenesis of T2DM, but associated with obesity through its effect on BMI. We also did not note any correlation between this SNP of *FTO* gene with insulin resistance represented by HOMA-IR.

Conflict of interest

This research is a personal non-profit work and there is no conflict of interest.

Source of funding

None.





Fadhil J. Al-Tu'ma et al.

Ethical Clearance

Ethical clearance was obtained from the Faculty Scientific Committee (Faculty of Veterinary Medicine, University of Kerbala) to study the role of fat ass and obesity associated genotype in Typ 2 Diabetic obese patients of Kerbala Province, Iraq

REFERENCES

1. Ergören MC, Söyler G, Sah H, Becer E. Investigation of potential genomic biomarkers for obesity and personalized medicine. *Int J Biol Macromol* [Internet]. 2018;122:493–8.
2. Khan SM, El HajjChehadeh S, Abdulrahman M, Osman W, Al Safar H. Establishing a genetic link between FTO and VDR gene polymorphisms and obesity in the Emirati population. *BMC Med Genet*. 2018;19(1):1–9.
3. Zimmet PZ. Diabetes and its drivers: The largest epidemic in human history? *Clin Diabetes Endocrinol* [Internet]. 2017;3(1):1–8.
4. de Mutsert R, Gast K, Widya R, de Koning E, Jazet I, Lamb H, et al. Associations of Abdominal Subcutaneous and Visceral Fat with Insulin Resistance and Secretion Differ Between Men and Women: The Netherlands Epidemiology of Obesity Study. *Metab Syndr Relat Disord* [Internet]. 2018;16(1):met.2017.0128.
5. Dang LC, Samanez-Larkin GR, Smith CT, Castrellon JJ, Perkins SF, Cowan RL, et al. FTO affects food cravings and interacts with age to influence age-related decline in food cravings. *Physiol Behav*. 2018;192(December 2017):188–93.
6. Saber-Ayad M, Manzoor S, El Serafi A, Mahmoud I, Hammoudeh S, Rani A, et al. The FTO rs9939609 “A” allele is associated with impaired fasting glucose and insulin resistance in Emirati population. *Gene* [Internet]. 2018.
7. American Diabetes Association (ADA). Introduction: Standards of Medical Care in Diabetes—2018. *Diabetes Care* [Internet]. 2018;41(Supplement 1):S1–2.
8. Tobias ES, Connor M, Ferguson-Smith M. *Essentials: Essential Medical Genetics* (6). 2011.
9. Frayling TM. A Common Variant in the FTO Gene Is Associated with Body Mass Index and Predisposes to Childhood and Adult Obesity Timothy. *Science* (80-). 2007;316.
10. Gerken T, Girard CA, Tung YCL, Webby CJ, Saudek V, Hewitson KS, et al. The obesity-associated FTO gene encodes a 2-oxoglutarate-dependent nucleic acid demethylase. *Science* (80-). 2007;318(5855):1469–72.
11. Al-Tu'ma, F. J. ; Farhan N. H. and Al-Safi, W. G.. Association between Fat Mass and Obesity Geners9939609 Polymorphism with PCOS Women in Iraqi Population. *IJPPR Humanjournals*. 2015;5(1):62–72.
12. Luis DA de. Association of the rs9939609 gene variant in FTO with insulin resistance, cardiovascular risk factor and serum adipokine levels in obese patients. *Nutr Hosp*. 2016;33(5):1108–15.
13. Steemburgo T. The rs9939609 polymorphism in the FTO gene is associated with fat and fiber intakes in patients with type 2 diabetes. *J Nutrigenet Nutrigenomics*. 2013;6(2):97–106.
14. WHO. Obesity and Overweight. National Center for Health Statistics. 2016.
15. Müller TD, Hinney A, Scherag A, Nguyen TT, Schreiner F, Schäfer H, et al. “Fat mass and obesity associated” gene (FTO): No significant association of variant rs9939609 with weight loss in a lifestyle intervention and lipid metabolism markers in German obese children and adolescents. *BMC Med Genet*. 2008;9:1–6.
16. Younus LA, Algenabi AHA, Abdul-Zhara MS, Hussein MK. FTO gene polymorphisms (rs9939609 and rs17817449) as predictors of Type 2 Diabetes Mellitus in obese Iraqi population. *Gene* [Internet]. 2017;627:79–84.
17. Majdi MA, Mohammadzadeh NA, Lotfi H, Mahmoudi R, Alipour FG, Shool F, et al. Correlation of Resistin Serum Level with Fat Mass and Obesity-Associated Gene (FTO) rs9939609 Polymorphism in Obese Women with Type 2 Diabetes. *Diabetes Metab Syndr Clin Res Rev*. 2017;11:S715–20.
18. Ghafarian-Alipour F, Ziaee S, Ashoori MR, Zakeri MS, Boroumand MA, Aghamohammadzadeh N, et al. Association between FTO gene polymorphisms and type 2 diabetes mellitus, serum levels of apelin and androgen hormones among Iranian obese women. *Gene* [Internet]. 2018;641:361–6.
19. Sentinelli F, Incani M, Coccia F, Capoccia D, Cambuli VM, Romeo S, et al. Association of FTO polymorphisms





Fadhil J. Al-Tu'ma et al.

- with early age of obesity in obese Italian subjects. *Exp Diabetes Res.* 2012;2012.
20. Yang M, Xu Y, Liang L, Fu J, Xiong F, Liu G, et al. The effects of genetic variation in FTO rs9939609 on obesity and dietary preferences in Chinese Han children and adolescents. *PLoS One.* 2014;9(8).
21. Srivastava A, Srivastava N, Mittal B, Prakash J. Association of rs9939609 and rs1421085 with Obesity Risk in North Indian Population. *Int Physiol.* 2017;4:1-5.
22. Al-Tu'ma F. J. and Obed and KH. Association between Fat Mass and Obesity Associated (FTO) gene polymorphism (rs9939609) and lipid profile in type 2 diabetic obese Iraqi male. *Iraq Medecal J.* 2018;2:15-9.
23. Iskandar K, Patria SY, Huriyati E, Luglio HF, Julia M, Susilowati R. Effect of FTO rs9939609 variant on insulin resistance in obese female adolescents. *BMC Res Notes [Internet].* 2018;11:1-5.
24. Luczynski W, Zalewski G, Bossowski A. The association of the FTO rs9939609 polymorphism with obesity and metabolic risk factors for cardiovascular diseases in polish children. *J Physiol Pharmacol.* 2012;63(3):241-8.

Table 1: Clinical and biochemical characteristics of study subjects.

Parameters	Obese T2DM N=92	Obese without T2DM, N=88	P Values
Age (year)	53.26 ± 8.63	53.18 ± 9.25	0.959
BMI (kg/m ²)	34.78 ± 2.50	34.26 ± 2.56	0.196
FBS(mg/dl)	223.62 ± 43.08	97.93 ± 6.48	< 0.001
Total Cholesterol (mg/dl)	241.00 ± 20.34	240.08 ± 12.76	0.738
Triglycerides (mg/dl)	243.46 ± 42.11	231.27 ± 38.78	0.057
HDL-cholesterol (mg/dl)	37.90 ± 5.21	39.17 ± 4.74	0.92
LDL-cholesterol (mg/dl)	153.56 ± 25.89	152.31 ± 14.39	0.71
VLDL-cholesterol (mg/dl)	48.69 ± 8.22	46.25 ± 7.75	0.57
Insulin(μU/ml)	10.45 ± 4.00	14.12 ± 4.95	< 0.001
HOMA-IR	5.77 ± 2.53	3.42 ± 1.23	< 0.001

BMI, body mass index; FBS, fasting blood sugar; TC, total cholesterol; TG, triglycerides; HDL-C, high-density lipoproteins cholesterol; LDL-C, low-density lipoproteins cholesterol; VLDL-C, very low density lipoproteins cholesterol. Data were expressed as mean ± SD. P < 0.05 is considered as significant level.

Table 2. Analysis of Hardy–Weinberg equilibrium

Subjects	χ^2	P value
Obese diabetic	2.671	0.102
Obese non diabetic	8.732	0.003





Fadhil J. Al-Tu'ma et al.

Table 3. Genotype and allele frequency of rs9939609 polymorphism of *FTO* gene and association of this variant with T2DM in the study individuals

SNP rs 9939609 (A/T)	Non-T2DM N = 88	T2DM N = 92	OR (95%CI)	P-Value
Codominant				
TT(Reference)	32	24		
TA	30	38	1.69 (0.83-3.45)	0.14
AA	26	30	1.45 (0.73-3.24)	0.25
Dominant				
AA+TA	56	68	1.62 (0.86-3.06)	0.136
Recessive				
TT+TA(Reference)	62	62		
AA	26	30	1.15 (0.61-2.17)	0.657
Minor Allele frequency	46.65%	53.26%		

OR: Odd Ratio; p<0.05 statistically significant

Table 4: Clinical characteristics of obese T2DM subjects according to *FTO* gene rs9939609 genotype

Clinical characteristics	TT N=24	TA N=38	AA N=30	P value
Age	52.70 ± 8.90	52.50 ± 8.29	54.75 ± 8.97	0.54
BMI(kg/m ²)	32.41 ± 1.05	34.68 ± 2.20	35.60 ± 2.48	0.001
FBS(mg/dl)	214.17 ± 39.66	231.49 ± 45.61	221.04 ± 41.89	0.28
TC (mg/dl)	235.23 ± 21.11	241.30 ± 18.47	245.54 ± 21.56	0.19
TG(mg/dl)	235.46 ± 41.12	245.32 ± 43.64	247.79 ± 37.93	0.52
HDL- C (mg/dl)	40.64 ± 6.22	38.58 ± 5.78	37.34 ± 4.65	0.10
LDL- C (mg/dl)	147.50 ± 28.95	153.65 ± 23.05	158.64 ± 26.60	0.30
VLDL- C (mg/dl)	47.09 ± 8.22	49.06 ± 8.72	49.55 ± 7.58	0.52
Insulin(μU/ml)	10.05 ± 3.16	10.21 ± 4.45	11.10 ± 4.05	0.58
HOMA-IR	5.23 ± 1.59	5.83 ± 2.75	6.15 ± 2.85	0.42

p<0.05 statistically significant





Fadhil J. Al-Tuma et al.

Table 5: Clinical characteristics of obese without T2DM subjects according to *FTO* gene rs9939609 genotype

Clinical characteristics	TT N=32	TA N=30	AA N=26	P value
Age	52.63 ± 9.41	54.78 ± 9.29	52.05 ± 9.19	0.59
BMI(kg/m ²)	32.80 ± 1.80	34.95± 2.65	35.55 ± 2.17	0.001
FBS(mg/dl)	95.82 ± 5.50	96.44 ± 5.67	97.14 ± 2.93	0.10
TC (mg/dl)	237.78 ± 13.55	241.55 ± 12.84	242.02 ± 11.30	0.43
TG (mg/dl)	216.90 ± 13.65	228.00 ± 40.90	233.06 ± 36.54	0.11
HDL- C(mg/dl)	41.40 ± 4.59	42.46 ±6.06	40.45 ± 6.24	0.51
LDL- C(mg/dl)	155.59 ± 11.95	149.89 ± 15.03	149.95 ± 16.86	0.26
VLDL- C(mg/dl)	40.78 ± 2.73	42.20 ± 8.18	42.61 ± 7.30	0.61
Insulin(μU/ml)	12.63 ± 4.30	13.92 ± 4.98	14.30 ± 5.40	0.58
HOMA-IR	3.12 ± 1.01	3.56 ± 1.17	3.67 ± 1.40	0.47

p<0.05 statistically significant

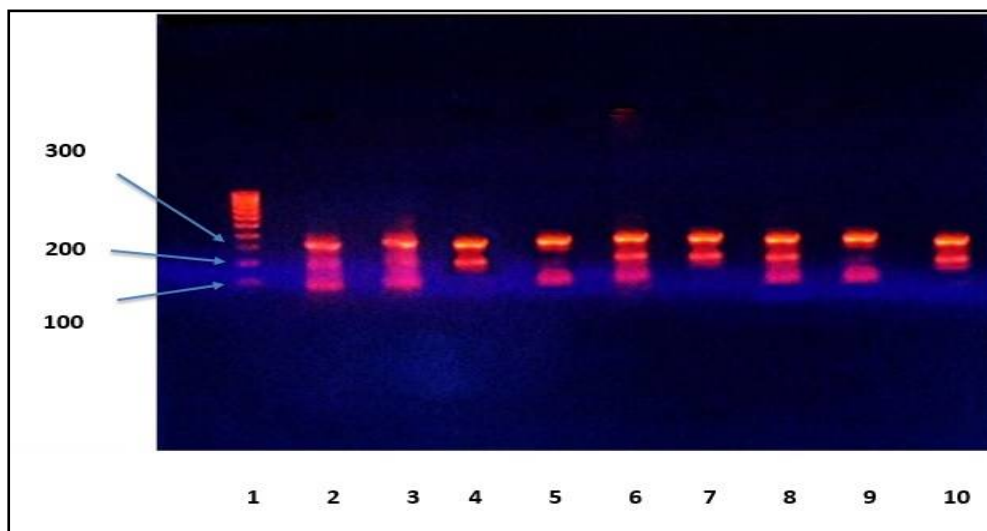


Figure1: PCR- ARMS analysis of the *FTO* gene by the rs9939609 in obese individuals (with T2DM and without T2DM). The wild type homozygote (TT) showed 2 bands (321, 210) bp, heterozygote (TA) showed 3 bands (321,210,178) bp, homozygote (AA) showed 2 bands (321, 178) bp. The product was electrophoresed on 1.5 % agarose gel at 70 volts for 90 min, stained with ethidium bromide, and then visualized under U.V light (Ladder = 100-1000) bp.





Building 3-D Geological Model for Rumaila Formation of Ahdeb Iraqi Oil Field and Its Importance in Simulation Study

Aya Ali Al-hamdi * and Jalal A.Al-Sudany

Petroleum Engineering Department, Collage of Engineering, University of Baghdad, Iraq.

Received: 19 Aug 2018

Revised: 23 Sep 2018

Accepted: 27 Oct 2018

* Address for Correspondence

Aya Ali Al-hamdi

Petroleum Engineering Department,

Collage of Engineering,

University of Baghdad, Iraq.

Email: ayaali9494@yahoo.com



This is an Open Access Journal / article distributed under the terms of the **Creative Commons Attribution License** (CC BY-NC-ND 3.0) which permits unrestricted use, distribution, and reproduction in any medium, provided the original work is properly cited. All rights reserved.

ABSTRACT

A 3D geological model including structural model and petrophysical model is the basis of building simulation model that must represent the under study field performance accurately in order to reach the required development plans results. In this paper a 3D geological model for Rumaila formation in Ahdeb Iraqi oil field has been built using Petrel 2015 simulator and some geoscience software (Didger5, Surfer14). Rumaila formation is one of middle cretaceous carbonate Ahdeb's formations. Ten wells from the field have been selected in order to build the structural and petrophysical models that represent Rumaila formation. This formation is divided into five sub-formations (units) named RU1, RU2a, RU2b-U, RU2b-L and RU3 each one of these units represent as a separated reservoir due to the existence of dry barrier between them. Structural model represents Rumaila formation is built using surface contour map of each unit in the formation. This model has been built only along AD-1 dome from the field this is due to the fact that Rumaila is oil bearing only along this dome of Ahdeb field; also this model has been built with no fault or fractures. Layering process is made after zonation in order to capture reservoirs heterogeneities. After that petrophysical modelings of (porosity and water saturation properties) have been made using some algorithm distribution methods. Petrophysical modeling results in identifying the good hydrocarbons Rumaila formation zones from the bad one, which is considered as the start of understanding the behavior of each zone in the formation and ultimately result in take important decisions for development stages of any simulation study. Volumetric calculations also have been made to calculate the OOIP for each zone in Rumaila formation and compared to petrophysical modeling results.

Keywords: - Ahdeb field, Rumaila formation, Geological model, Petrophysical modeling.





Aya Ali Al-hamdi and Jalal A.Al-Sudany

INTRODUCTION

Reservoir simulation is defined simply as this tool that engineers use to model the flow performance of the reservoir through the solving of fundamental flow equations in sufficient details in order to predicate the consequences of changes in operating practice, using numerical simulator for this purpose. Therefore from this define its clearly obvious that the purpose of doing simulation studies could be two things which are: - Those studies may use in order to develop new fields, where it helps in deciding how many wells the field is required and where they should be, or the simulation studies could use for an established field that has unexpectedly poor performance, where it helps in find ways to improve performance. In either way those studies is used to specifically address some decision that must be done on the field in the future[1]. The question now, what is the proper why of doing simulation study that could represent the field?

The common work flow of doing such study is to build dynamic model representing the flow behavior of the reservoir. The basic input to start building such model is the geological reservoir model which is established based upon explicit modeling of known geological properties[2]. Building a proper and accurate 3D grid geological model that include all important petrophysical properties and geological features which control or influence fluid flow and hydrocarbon storage capacity within the reservoir (e.g. porosity and permeability contrast among and within the zones and layers of the reservoir formation) is the first stone that must be established in order to estimate a probable hydrocarbon volumes and achieve a realistic and usable simulation results (history match results) that can describe the specific field under study properly[2].

So what's the proper way of describing the field accurately using geological model? This start with building the stratigraphic and structural compartments of a field where fluid is flowing, and then moving for modeling the lithological features and petrophysical properties of formation (facies and property modeling) depends on data such as Seismic data ,mud logs, open-hole wireline logs, core description and petrophysical analysis[3]

Case Study: Rumaila formation of Ahdeb field

The area under study is Rumaila formation which is middle cretaceous carbonate formation, located at 2800m depth of Ahdeb field. This field is an Iraqi oil field lies on a 303 km² block in Iraq's Wasit province. It is located between NOMINA town and KUT town, about 180 km southeast of Baghdad. This field has been discovered at 1979, with length of 29 km and width of 8 km, its area is about 200 km² and similar to most fields in Iraq; it is a NW-SE trending anticline, with three structural domes along its length, which are AD-1, AD-2 and AD-4. AD-1 is the highest dome in the field. To date, four carbonate formations saturated with oil has been discovered in the field which are: (A) Late Cretaceous Khasib Formation, this formation composed of shaly micritic limestone with sand grain limestone. (B) Middle Cretaceous Mishrif Formation, this formation is mainly bioclastic limestone. (C) Middle Cretaceous Rumaila formation; this formation is mainly bioclastic limestone with green algae limestone. (D) Middle Cretaceous Maaddud Formation, composed of bioclastic limestone intercalated with dolomitic limestone. Rumaila formation which is the area under study is mainly divided into five oil bearing layers (units), which are RU1, RU2a, RU2b-U, RU2b-L and RU3. Each one of these beds is considered as one separated reservoir due to the existence of dry barrier separating one from each other, only for RU2b-L and RU3 layers which are considered as one single reservoir (no barrier between them)[2, 4].

METHODOLOGY

Schlumberger software PetrelRE (v. 2015) is the simulator that used in building the 3D geological model for Rumaila formation. This software is 3D geo-cellular modeling software. The input data for building this model comprise well coordinates, formation tops, depth structure surfaces, well logs and cores data. The 3D built grid model dimensions





Aya Ali Al-hamdi and Jalal A.AI-Sudany

area is approximately 10 km by 10 km, where the geologic model area for Ramaila formation is limited to AD-1 dome as illustrated in figure (2). The main input data that must be imported into the simulator in order to start in building the model include:

- Well head: - which is the position of each well in x-y-z direction.
- Well survey: - include the data of measured depth, true vertical depth, inclination and azimuth of each well. (Rumaila wells are all directionally drilled wells but vertical in producing intervals).
- Well tops: - these include the data of the depths at which wells penetrate the units of formation.
- Well logs: - data of effective porosity and water saturation values along the well path.
- Counter maps: -A map showing elevations and surface configuration by means of contour lines.

The steps for building the geological model

The main steps of building a static model of a petroleum reservoir using petrel software are

Structural modeling

Structural modeling is the first step in building the geological model. It is subdivide into three processes which are: fault modeling, gridding and layering. Structural modeling can be defined as the process of reconstruction the geometric and structural properties of the reservoir by importing and interring a map with structural tops and the sets of faults along it if they found[5]. At first a 3D structural contour map for top of first unit in Rumaila formation (RU1) were built using Didger program for digitizing process of this map. Then the resulted map used as a basis for the building of the following units surfaces maps with adjusting these maps to well tops. The constructed structural maps for each unit of Rumaila formation can be shown in figures below. 3D Grid Construction: this process consist of three sub-processes which are:

Gridding

gridding is the main first step in building a 3D grid static model. In a simple term building a 3D grid means dividing a model up into boxes, each box is called cell[6]. A simple grid model is used because no faults exit along the formation, and this can be done by using make simple grid option in petrel simulator. The grid which used in Rumaila formation was represented by three dimensional grid systems of 167 grid along the x-axis, 133 grid along the y-axis. The dimensions for the grid are 100m in the x direction and 100m in the y direction. The size of the grid was chosen depending on the area of the field and to specify correctly the variation of the petrophysical properties. The result from gridding process is a skeleton of a top, mid and bottom as can be shown in figure below.

Make Horizons and layering

Make horizon step is the beginning step of defining the vertical layering of the 3D grid. Rumaila formation as noted consists of five oil bearing units, these five main units are defined in Petrel program as horizons. After this step comes layering step which is the process of dividing reservoir units into several sub-layers in order to retain geological heterogeneity in the model[2]. The layering step of Rumaila formation has been done as shown in table (1) below. The resulted grid model size in three dimensions is 167×133×65.

Scale up well logs

Scale up means averaging and scale up well logs means averaging the log values to the cells in the 3D grid. This means that each grid cell will take one value per up scaled logs[6]. This process must be done before starting with the



**Aya Ali Al-hamdi and Jalal A.AI-Sudany**

petrophysical modeling process. Petrel has a lot of averaging methods to use. Porosity and water saturation values have been scaled up using the arithmetic averaging method. Figure below shows the scale up of porosity, saturation for one of the field wells as an example on this process.

Property modeling

Petrophysical modeling is the process of giving petrophysical property values (porosity, water saturation, and permeability) to each grid cell in 3D grid model. Petrel software has several algorithms for modeling the distribution of log values for each reservoir zone in the model. Porosity, water saturation property modeling has been done using the Statistical Sequential Gaussian Simulation Algorithm distribution method which fits with the amount of the available data[7]. Figures below show the property modeling process results.

Net to gross modeling (NTG)

Net to gross modeling is done based on the values of net to gross that have been inserted into the simulator by an equation. This equation established according to cut off values that has been estimated according to a certain calculations. Where this equation is built in the form so that NTG property is set equal to a value of 1 if porosity \geq porosity cut-off value and water saturation \geq water saturation cut-off value.

Volumetric calculations

one of the main purposes of building geological model is to estimate how much the hydrocarbons that is stored in the formation. Volume calculation option in petrel simulator is used to calculate the total volume of hydrocarbons stored in a reservoir prior to production. Reserves estimates from this method of calculation often high because this method does not consider the problems of reservoir heterogeneity.

Note: - Volumetric calculations step need accurate estimate for the positions of water-oil contact of each reservoir in the formation, these positions can be estimated from Well tests, petrophysical analysis and production data. These data were reviewed in number of wells penetrate producing zones to constrain the position of the OWC by the accurate identification of The oil down to (ODT) and water up to (WUT) subsea depths in each well[3]. The values of oil-water contact setting positions have been estimated and used in volumetric calculations for Rumaila units are:-

Oil- water contact TVDSS for RU1=-2810 m.

Oil- water contact TVDSS for RU2a=-2910 m.

Oil- water contact TVDSS for RU2b-U =-2945 m.

Oil- water contact TVDSS for RU2b-L&RU3=-2970 m.

Up- scaling

Most flow simulators cannot cope with the typical size of geological models (millions of active model cells). Up scaling is the concept of creating a coarse simulation 3D grid from a fine- scaled geological 3D grid. This process consists of two sub-processes which are: - scale up structure and scale up property. Scale up structure is to change the number of 3D grid cells vertically and/or aerially to result in a smaller geological model size that is more suitable to the latter dynamic flow simulation processes. While property scales up is the process of averaging the original model petrophysical properties to suit the cells of new up scaled model using different scale up property methods. Porosity, NTG and water saturation are up scaled using the arithmetic mean method[8].





Aya Ali Al-hamdi and Jalal A.AI-Sudany

RESULTS AND DISCUSSIONS

from the above work of building a 3D geological model the following results are estimated:-

Porosity values in RU1 zone as shown in figure (9) is relatively higher than other formation zones, where it ranges from 16% to 28% with an average of 23%. Water saturation model for this zone is characterized as shown in figure (15) with relatively lower values than other formation zones. The values for this property are ranges from 17% to 91% with an average of 74%. From petrophysical modeling it obvious that RU1 zone is represented as a good hydrocarbons bearing reservoir with relatively higher hydrocarbons contents than the other lower zones. Porosity modeling of RU2a zone in the formation as shown in figure(10) is characterized with moderate to low values in relative to RU1 zone, where these values ranges from 3% to 25% with an average of 16%. Water saturation values as shown in figure (16) is higher than RU1 water saturations values, where it ranges from 20% to 97% with an average of 77%. This zone is characterized with moderate hydrocarbons content which is much lower than the content of upper Rumaila's formation zone.

RU2b zone in Rumaila is divided into two subzones separated from each other with dry barrier. Each zone with a different water-oil contact. The upper RU2b zone which is RU2b-U is characterized with low porosity values than other Rumaila zones. The values of this property are ranges between 1% and 24% with an average of 14% while water saturation for this zone is range between 2% to 90% which is lower than RU2a water saturation. This zone represents as a good reservoir with high to moderate hydrocarbons content in relative to other Rumaila reservoirs and most of Rumaila production is from this zone (most Rumaila wells are perforated in this zone). The lower RU2b zone which is RU2b-L is characterized with very poor hydrocarbons content where the values of its porosity is low range from 3% to 17% with an average of 11% and the higher water saturation content in relative to other zones which is range between 3% to 98% with an average of 95%.

The last Rumailas' hydrocarbon zones is RU3, this zone is characterized with good porosity values range from 9% to 25% with an average of 21%. But due to the high water saturation found in this zone which is range from 20% to 98% with an average of 77% this zone is represented as a poor oil reservoir zone. Volumetric calculations results of OOIP is matched with the results concluded from petrophysical modeling of each zone, where RU1 zone have the higher hydrocarbons content compared to other zones, while RU2b-L and RU3 are characterized as the lower oil bearing zones in Rumaila formation. The total OOIP results from geological model has been built for Rumaila formation is equal to $109 \times 10^6 \text{ m}^3$ as shown in table (2) below. Up scaled process results in decreasing the number of grid cells of original 3D grid model has been built for Rumaila formation from 144,000,000 grid cell to 495,264 grid cell with slightly change in the OOIP estimated from each zone in the formation (total OOIP after up- scaling is $106 \times 10^6 \text{ m}^3$), in turn this considered as a good up-scaled process that helps in increasing the storage capacity of the software while lowering the time of processing run by the simulator which is very important for development stages of simulation study. The results of volumetric calculations for each zone in the formation after up-scaling process are shown in table (3) below.

CONCLUSIONS

Geological model is the first main step that simulation study must start with; as this model consider as the start towards understanding reservoir performance and uncertainties, and ultimately to field development planning decisions which is the purpose of doing simulation studies. Reservoir evaluation study prior to starting with building geological model is very important, where understanding the behavior of petrophysical properties (e.g. porosity and water saturation) along formation from logs and cores data is very helpful, this is due to the fact that these properties control fluid contents and flow within the reservoir layers. Therefore layering process is based on accurate reservoir evaluation process. Petrophysical modeling process gives simulation engineers a good insight toward identifying the good oil bearing reservoir zones from the bad zones in the formation, where it will help with simulation results in the





Aya Ali Al-hamdi and Jalal A.AI-Sudany

development stages on knowing the zones where more wells should be drilled to increase hydrocarbons recovery and the zones that should avoiding them. (For Rumaila formation petrophysical modeling shows that RU2b-U is the better zone for drilling while RU2b-L is the worst zone). Increase geological model accuracy is important to reduce field development uncertainty. This accuracy increased with additional accurate reservoir data collected which will add value by increasing the chance that field development decisions lead to expected ultimate recovery. up-scaled process is very helpful step where it helps in increasing the storage capacity of the software and lowering the time of processing run by the simulator while in the same time keeps the built geological model properties unchanged.

REFERENCES

1. Exploring the role of Reservoir Simulation Roundtable: Reservoir simulation. Oilfield Review, October, 11, 1989. volume 2 number 2.
2. Al-Waha Petroleum Co., L., FIELD DEVELOPMENT PLAN—2013 UPDATE AHDEB OIL FIELD IRAQ SECTION 2: G&G December 2013.
3. Al-Waha Petroleum Co., L., SECTION 2: G&G All Appendices 12-01-2013 December 2013.
4. Al Waha Petroleum Co., L., AHDEB OIL FIELD IRAQ FIELD DEVELOPMENT PLAN—2013 UPDATE Section 6- Surface_Engineering December 2013.
5. Hartline, C.S., M.A. Walters, and M.C. Wright, Three-dimensional structural model building, induced seismicity analysis, drilling analysis, and reservoir management at The Geysers Geothermal Field, Northern California. Geotherm. Resour. Coun. Trans, 2015. 39: p. 603-614.
6. Al-Baldawi, B.A., Building A 3D Geological model Using Petrel Software for Asmari Reservoir, South Eastern Iraq. Iraqi Journal of Science, 2015. 56(2C): p. 1750-1762.
7. Golaleh Zandkarimi*, A.R.R., Static Model Construction for Lower Shuaiba Formation (Lower Dariyan). 2016.
8. Durlofsky, L.J., Upscaling and Gridding of Fine Scale Geological Models for Flow Simulation. June 20-24, 2005.

Table 1. Number of Layers in Rumaila Reservoir.

Zone	Layers per zone
RU1	20
RU2a	10
RU2b-U	15
RU2b-L	10
RU3	10

Table 2. Volumetric Calculations of Rumaila units final results.

Unites	Bulk volume (*10 ⁶ m ³)	HCPV (*10 ⁶ rm ³)	OIIP (*10 ⁶ sm ³)
Zone1 (RU1)	676	61	47
Zone2 (RU2a)	626	19	15
Zone3 (RU2b-U)	488	31	24
Zone4 (RU2b-L)	432	16	13
Zone5 (RU3)	160	15	12





Aya Ali Al-hamdi and Jalal A.AI-Sudany

Table 3. Volumetric Calculations final results after UP- Scaling of Geological model

Unites	Bulk volume (*10 ⁶ m ³)	HCPV (*10 ⁶ rm ³)	OIIP (*10 ⁶ sm ³)
Zone1 (RU1)	674	59	45
Zone2 (RU2a)	625	19	14
Zone3 (RU2b-U)	487	30	23
Zone4 (RU2b-L)	431	16	12
Zone5 (RU3)	159	15	11

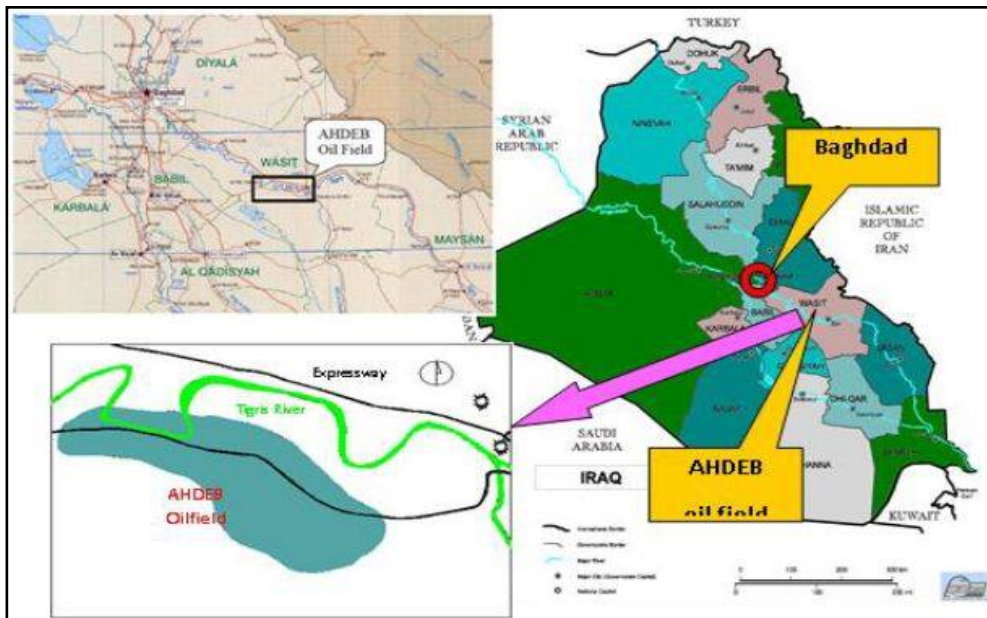


Figure 1. Ahdeb field location.[4]

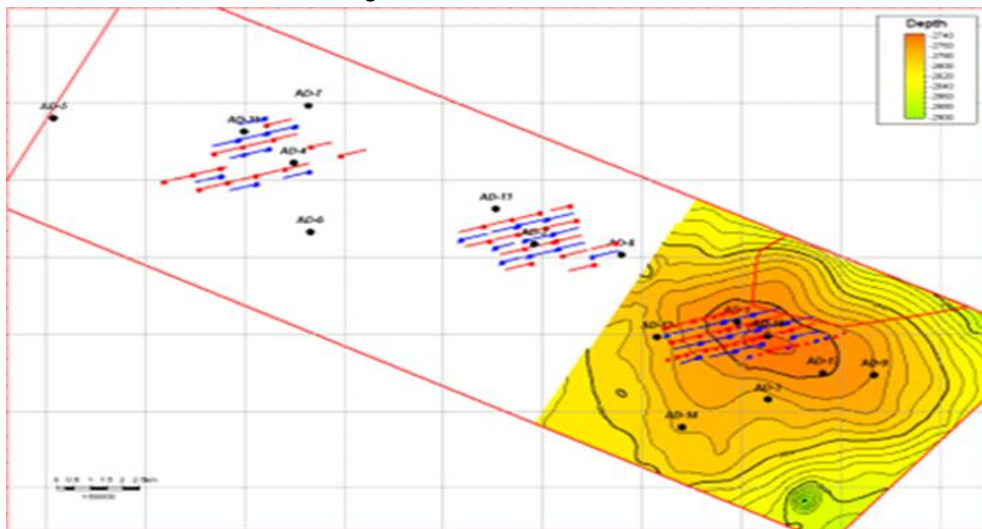


Figure 2. Model areas for Mi4-Ma1. [2]





Aya Ali Al-hamdi and Jalal A.AI-Sudany

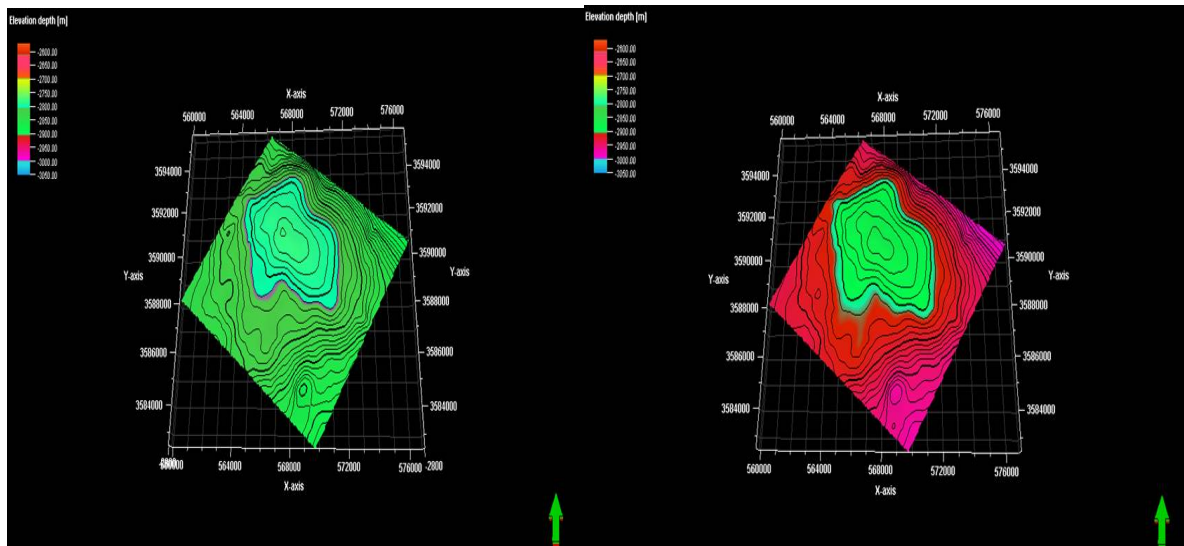


Figure 3. 3D structural modeling of two units from Rumaila reservoir in Ahdeboil field.

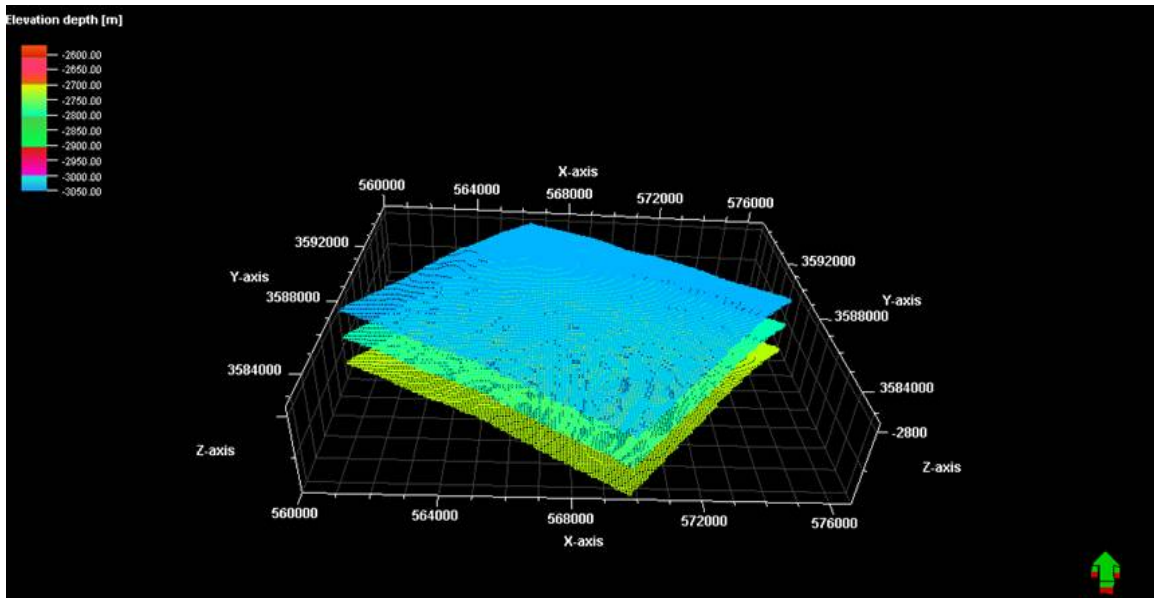


Figure 4- The skeletons of Rumaila reservoir in Ahdeboil Field.





Aya Ali Al-hamdi and Jalal A.AI-Sudany

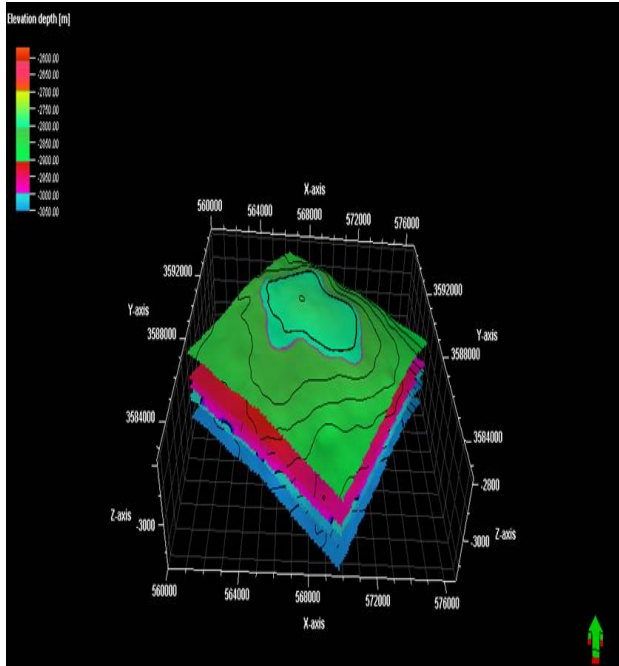


Figure 5. Main Horizons of Rumaila reservoir

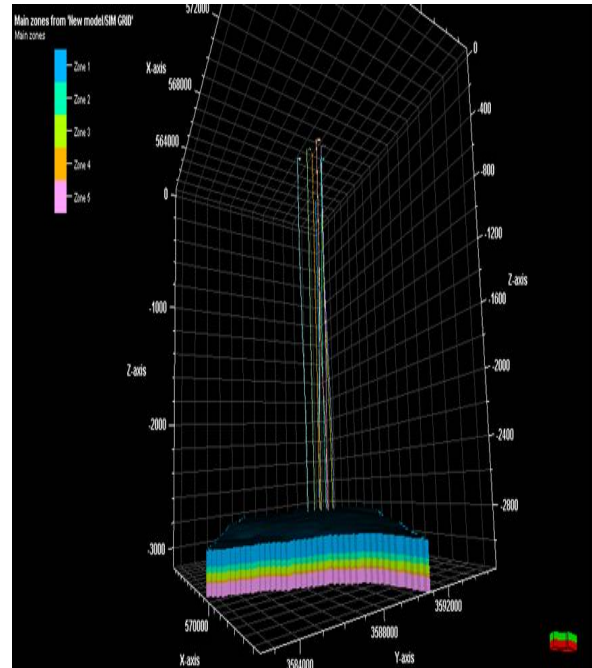


Figure 6. Main Zones of Rumaila formation

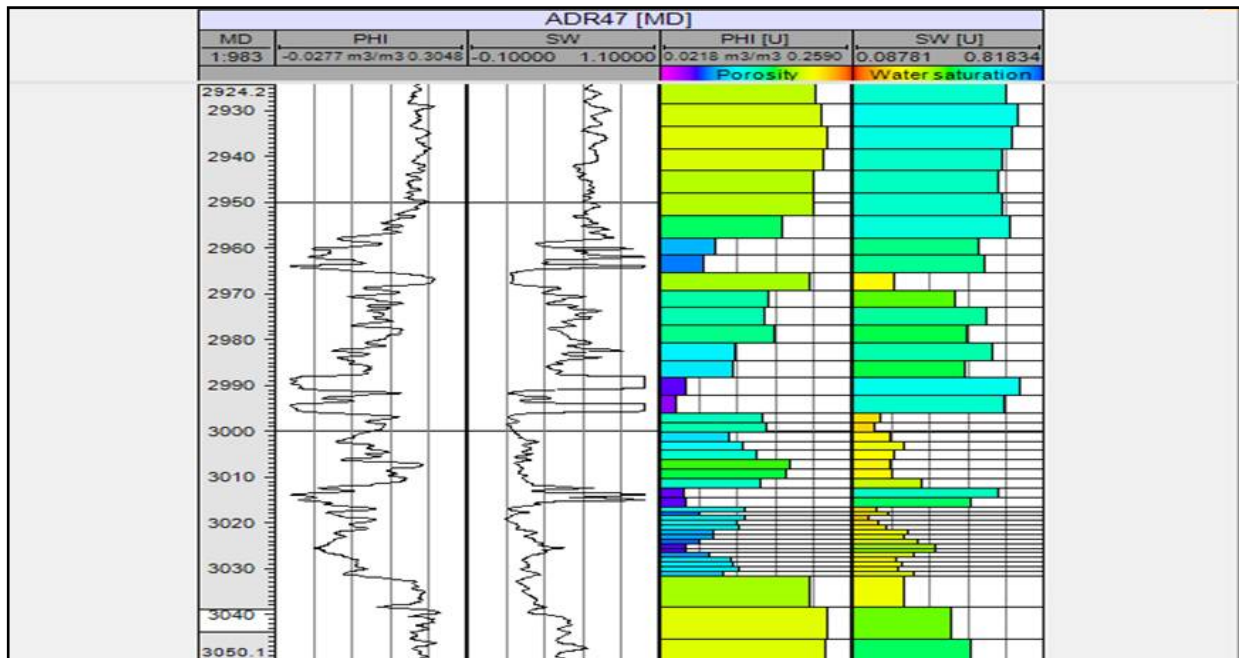


Figure 7. Scale up of porosity and water saturation for well ADR47





Aya Ali Al-hamdi and Jalal A.AI-Sudany

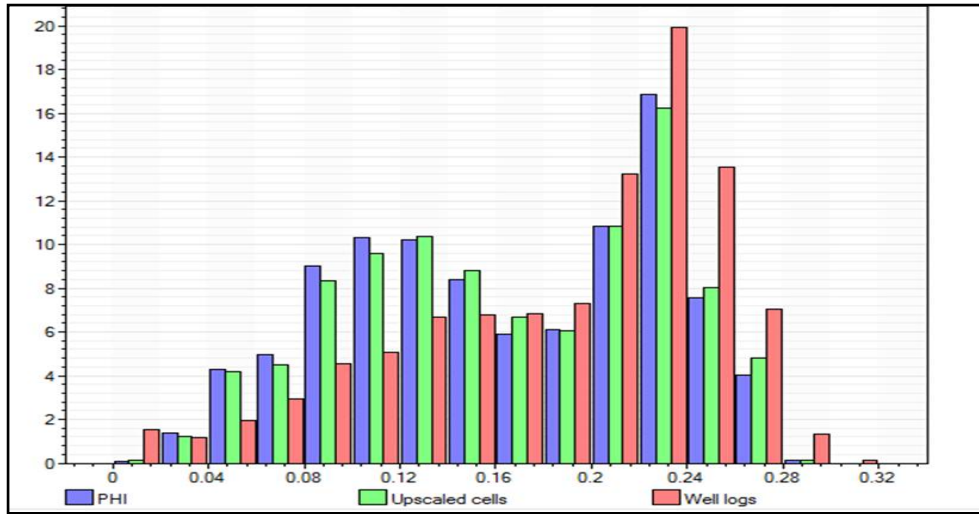


Figure 8- Histogram for Porosity Model of Studied Area.

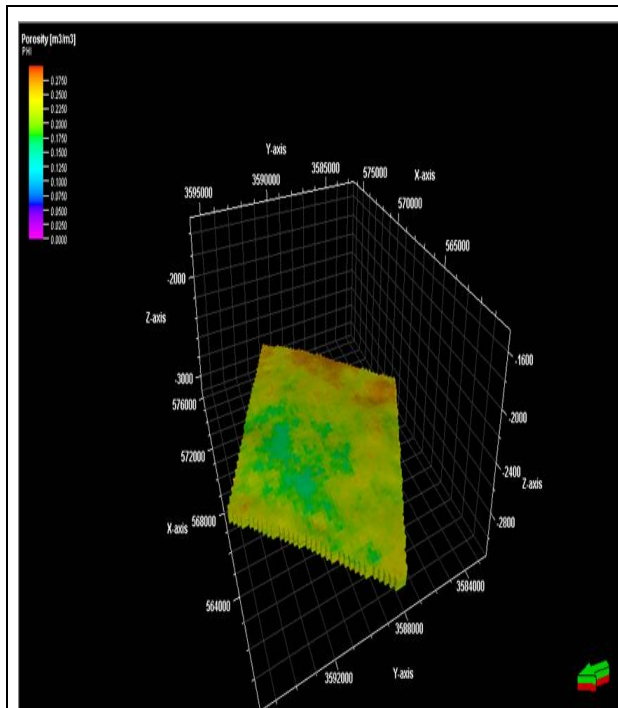


Figure 9- Final porosity model for RU1 unit

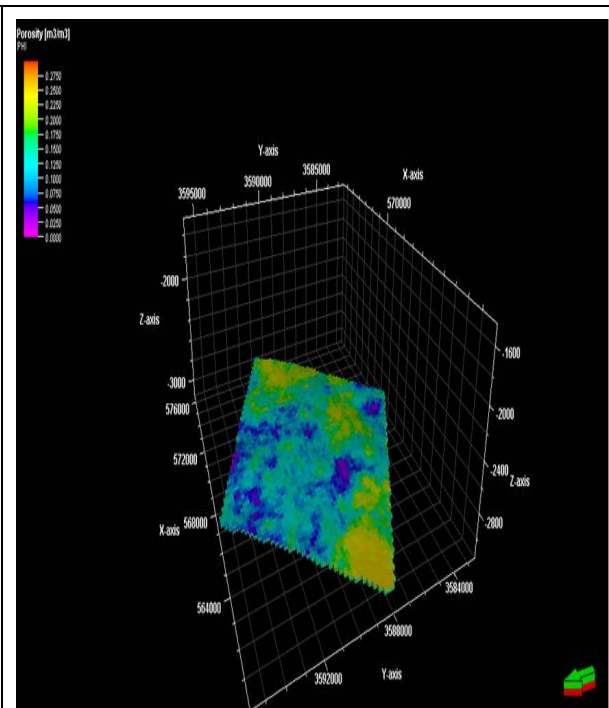


Figure 10- Final porosity model for RU2a unit



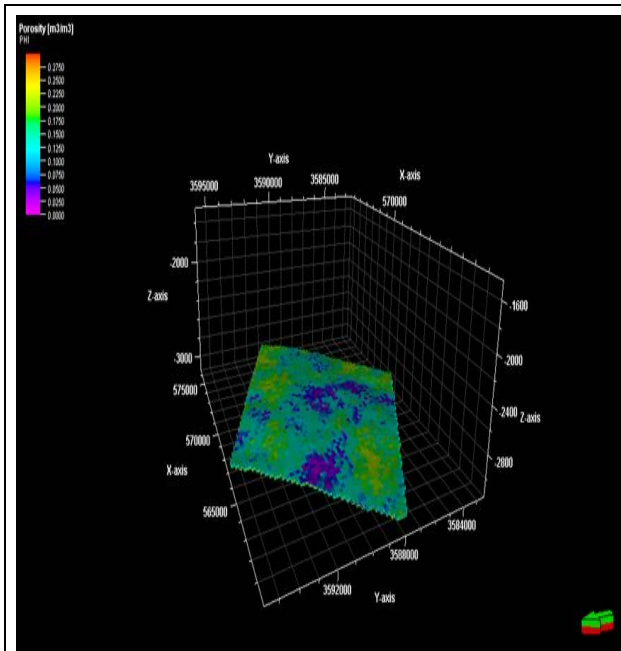


Figure 11- Final porosity model for RU2b-U

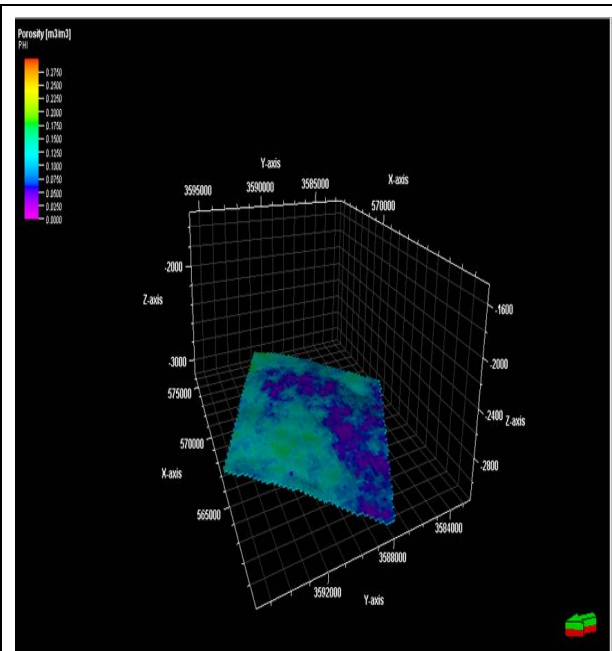


Figure 12- Final porosity model for RU2b-L

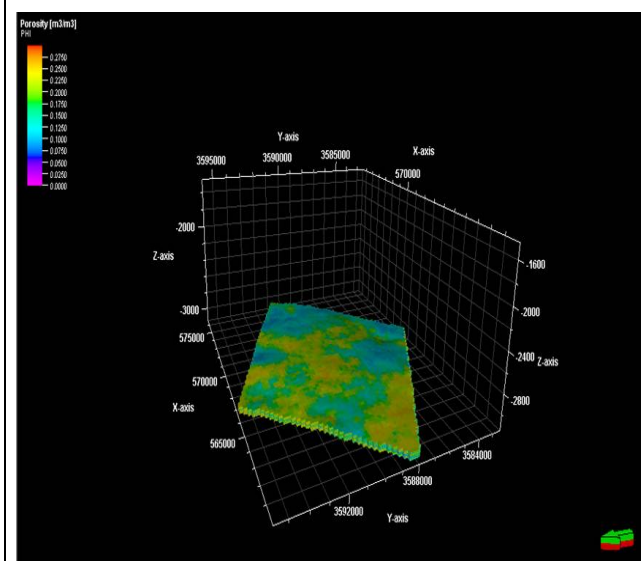


Figure 13- Final porosity model for RU3 Water saturation modeling

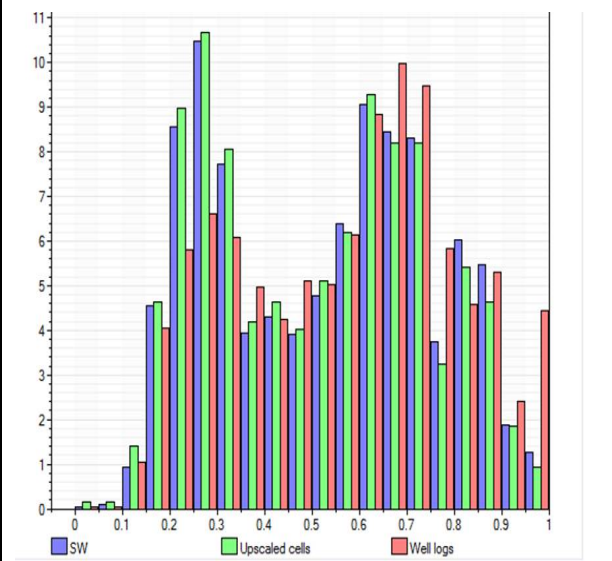


Figure 14- Histogram for Water saturation Model of Studied Area





Aya Ali Al-hamdi and Jalal A.AI-Sudany

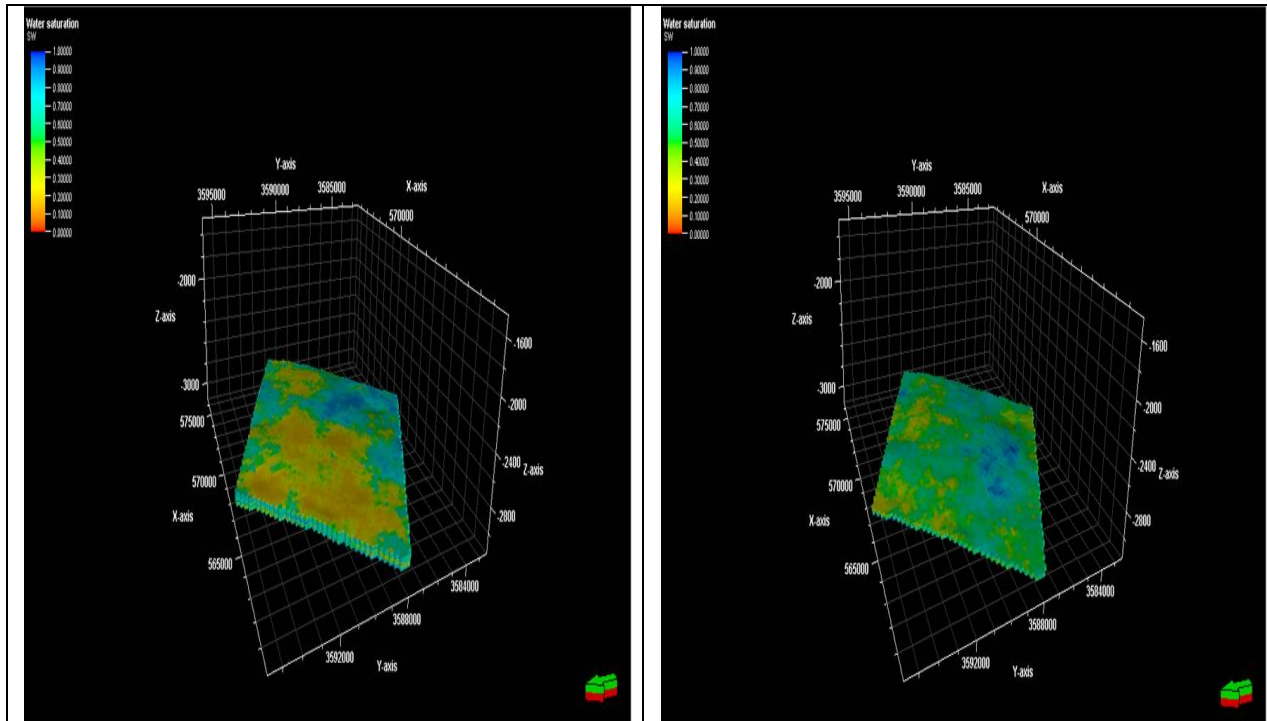


Figure 15, 16 - Final Water Saturation models of RU1, RU2a units respectively

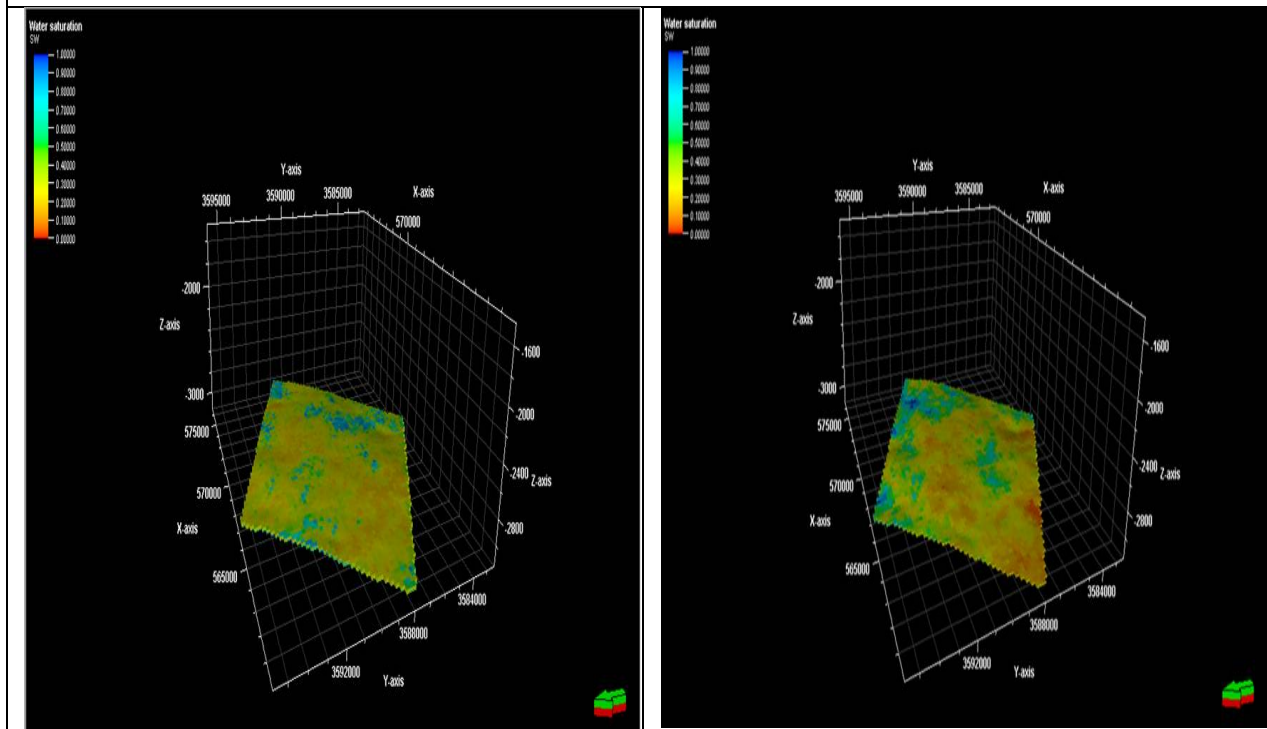


Figure 17, 18- Final Water Saturation models of RU2b-U, RU2b-L units respectively





Aya Ali Al-hamdi and Jalal A.AI-Sudany

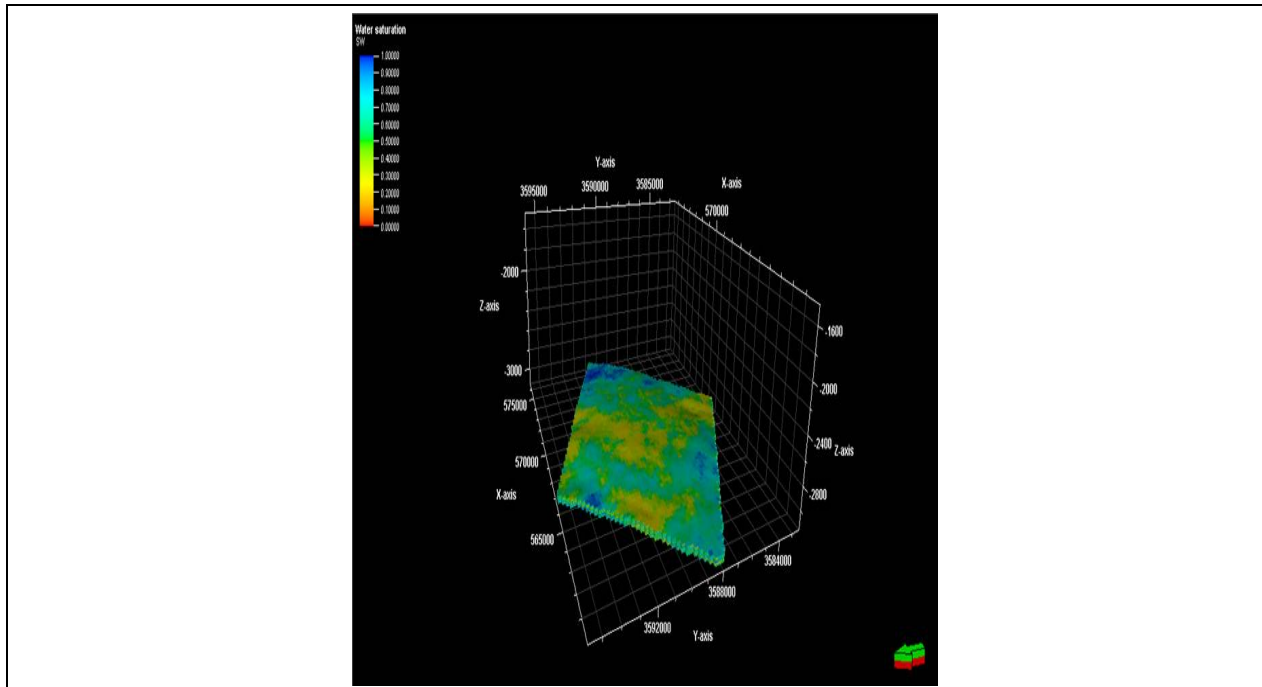


Figure19- Final Water Saturation model of RU3 unit.

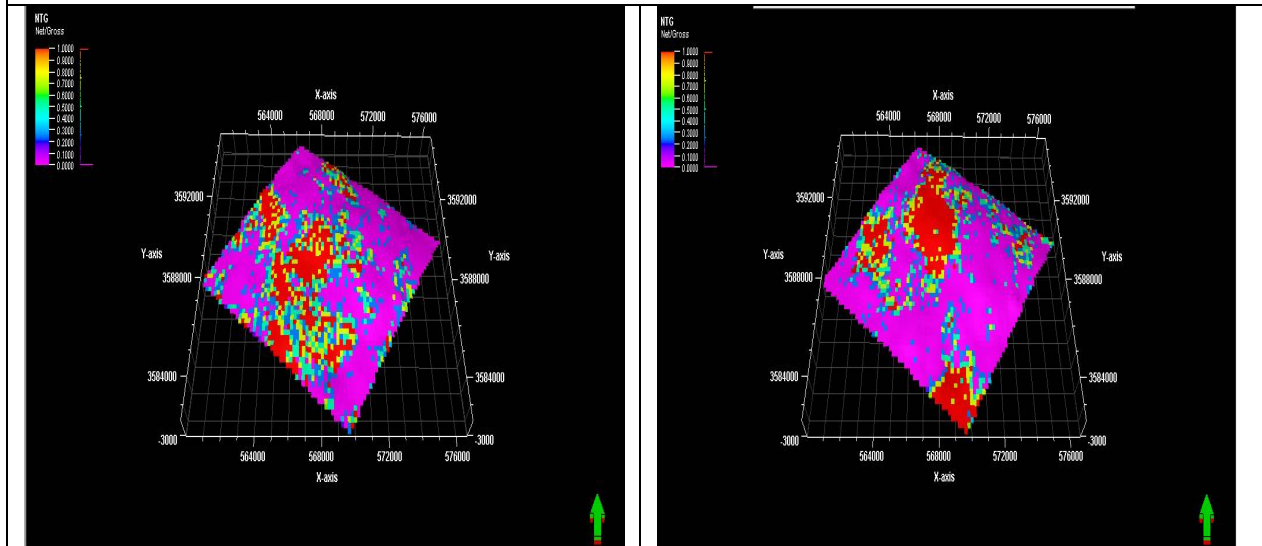


Figure 20, 21- Final NTG modeling for some RU2b-L layers in the formation





Biotechnology and Stress Tolerance

Intedhar Abbas Marhoon^{1*}, Ebtessam kadem khudher² and Khitam Abbas Marhoon³

^{1,2}Biology Department, Faculty of Science University of Al-Qadisiyah ,Iraq.

²Environment Department, Faculty of Science University of Al-Qadisiyah ,Iraq

Received: 17 Aug 2018

Revised: 21 Sep 2018

Accepted: 27 Oct 2018

* Address for Correspondence

Intedhar Abbas Marhoon

Biology Department,

Faculty of Science University of Al-Qadisiyah ,Iraq.

Email: Intedhar.Abbas@qu.edu.iq ; Khitam.Abbas@qu.edu.iq



This is an Open Access Journal / article distributed under the terms of the **Creative Commons Attribution License** (CC BY-NC-ND 3.0) which permits unrestricted use, distribution, and reproduction in any medium, provided the original work is properly cited. All rights reserved.

ABSTRACT

Environmental stresses are the main risk affecting plant activity and agricultural production.. Abiotic stresses are the most dangerous for plants, from these stresses: water stress, salinity stress, temperature change, and intensity of lighting stress, as well as the accumulation of heavy metals in the soil.The mechanisms that occur in plants when exposed to stress, including many of the activationsignal factors and changes in gene expression, the Synthesis of stress protein within cells and the construction of antioxidants as Pox, APx, CA_t, GR, DHAR and SoD, in addition to a hormonal balance within the plant tissues.Biotechnologies have been used to reduce the damage caused by these stresses on plants, including plant breeding and improvement techniquesand hybridization of plants. The method of genes transport of stress tolerance is one of the most important methods used.

Keywords: stress tolerance, stress protein,genes transport,Abiotic stresses, Thermal stress.

INTRODUCTION

Environmental stresses are the main threat to agricultural activity, given the magnitude of the losses caused by these strains in reducing agricultural productivity. Water scarcity alone accounts for 64%, and the temperature factor is 27%. Other stress factors are coming from immersion with water, light, and soil and air pollutants (Luan, 2002)⁽¹⁾. In view of the importance of the subject, scientific research has been more and more directly developed in recent years (Figure 1) to double the number of published research to tens of times, demonstrating the importance of the subject and its threat to food security(Shahbazi, et.al. 2009)⁽²⁾. Plant breeding and improvement technologies and proper management strategies continue to play an important role in plant improvement (Hasegawa, et al. 2000) ⁽³⁾. Formerly employed traditional plant hybridization methods continue to be used for the transfer of genes responsible for carrying one or more environmental stresses from vegetation to plant and the susceptibility of hybridization between plants based on plant affinity(Srinivas J., et al. 2013) ⁽⁴⁾.





Intedhar Abbas Marhoon *et al.*

The rapid development of bio-technologies has been positively reflected in the development of sustainable agriculture and in the production of stress-tolerant plants in particular after the availability of gene transport and the crossing of plant boundaries (distant gene pools) provided by modern technologies in comparison with traditional methods (Siedlecka, et al., 2001)⁽⁵⁾. It is known that plants cannot escape the stresses and are constantly exposed to them without any protection unlike the animals that move to avoid them (Vanaja, et al. 2011)⁽⁶⁾. At the same time, plants have developed different mechanisms to cope with the difficult conditions that they are exposed to, such as avoiding the stresses of morphological mutations and unfortunately not all plants do so (Blikhina, et al. 2003)⁽⁷⁾. The choice of plants is to change their mechanisms, such as accumulation of iodine and increased gene expression. The products of the gene Act play a role in stress-bearing mechanisms (Lungu, et al. 2011)⁽⁸⁾. Transgene silencing is one of the determinants of gene transfer that causes the genetic expression to decrease (Feizi, et al. 2007)⁽⁹⁾. The cultivation of plant cells, tissues and organs has contributed to the fact that they are easy, economical and workable, and have greatly facilitated and accelerated programmes to obtain durable or stress-resistant crops. It is necessary to understand the mechanisms of endurance or resistance and the accompanying changes, thereby promoting increased endurance (Athar and Ahmad, 2010)⁽¹⁰⁾.

Abiotic stresses

Abiotic stresses negatively affect plant growth, development and productivity (Tewari, et al., 2002)⁽¹¹⁾. The plant developed mechanisms for endurance (for certain limits), including the avoidance of stress Avoidance through which the plant's appearance and anatomical form to reduce the impact of stress with the difficulty of transferring such qualities and introducing them in plant improvement programs, which requires a focus on the mechanisms of endurance (Zhao, et al., 2009)⁽¹²⁾. Benefiting from this heterogeneity is important in developing stress-tolerant plants. Most stress factors produce inter-plant partnerships, although each factor has its own specific effects (Shalata, et al., 2001)⁽¹³⁾. Abiotic stress factors are often common to cellular membranes that operate under normal conditions to perpetuate vital events (Figure 2). Active oxygen species (ROS) is always associated with aerobic conditions and that stress factors Abiotic accelerate their production ROS in plants causing damage to cellular membrane systems and other cellular processes (Tan, et al., 2008)⁽¹⁴⁾. Antioxidants, whether enzymatic or non-enzymatic, play an important role in preventing oxidative damage, although the production and efficacy of antioxidant systems depend on plant type and genetic composition (Unyayar, et al., 2004)⁽¹⁵⁾. For the purpose of minimizing the impact of stress, plants have developed different bearing mechanisms that can be summarized in the following points (table 1).

The most important mechanisms that plants adopt when exposed to stress (Islam, et al., 2007)⁽²²⁾:

- 1- Active of signaling factor.
- 2- Altered genes expression
- 3- Accumulation in compatible solutes
- 4- Synthesis of stress protein
- 5- Enhanced antioxidant metabolisms.
- 6- Ion homeostasis and compartmentation
- 7- Membrane transport
- 8- Polyamines
- 9- Hormonal balances.

Given the importance of producing plant-tolerant plants under the threat of salinization of agricultural land, as well as the need to develop drought-tolerant plants in conditions where water warfare has become a reality in the near term. Vital pathways for signal transmission that reveal stress play an essential role in stimulating the stress-bearing mechanism (Cavalcanti, et al., 2004)⁽²³⁾. Gene transfer technologies are important methods of conveying stress tolerance (Tammam, 2003)⁽²⁴⁾.





Intedhar Abbas Marhoon et al.

Development of drought-tolerant crops

Traditional plant improvement programmes require the research of the genetic variability of drought tolerance in cultivated crops, especially their sexual compatibility, and the introduction of drought-bearing characteristics into desirable field characteristics, taking into account the limitations of species and gene carriers bearing Drought (Ghaffari, et al., 2012)⁽²⁵⁾. Traditional plant improvement methods have increased drought tolerance (albeit limited) in rice, wheat and mustard crops, and in the development of yellow maize hybrids for this characteristic while continuing with election processes (Selection) (Majeed, et al., 2011)⁽²⁶⁾. On the other hand, there is a need for drought-bearing genes in a number of cultivated and terrestrial plants for the purpose of isolating them and transferring them to strategic crops through genetic engineering methods (Liu, et al., 2017)⁽²⁷⁾. Dehydration causes many physiological responses that in turn affect the activity of a number of genes, as experiments have indicated that genetic manipulation may succeed in diagnosing several hundred genes that have been stimulated or discouraged when the plant is dehydrated (Vanaja, et al., 2011)⁽²⁸⁾. Tissue farming technologies have opened up wide horizons from sifting through the cells of different plant species under controlled conditions and electing the ending of the cell to a complete plant and a field-borne test (Geetha, et al., 2012)⁽²⁹⁾.

CONCLUSIONS

Plants are exposed to different stress that affect the physiological processes within the cell. Many mechanisms occur within the cell to resist or tolerant stress. Gene transfer technology is one of the most important techniques for producing resistant or tolerant plants

REFERENCES

1. Luan, S. 2002. Signalling drought in guard cells. *Plant Cell Environ.* 25: 229–237.
2. Shahbazi, H., M. Taeb. B. hamte . M.R. and F. Darvish . 2009. In heritage of antioxidant activity of bread wheat under terminal drought stress *J. agricandenviron Sci.* 6(3) : 298-302.
3. Hasegawa, P. M., Bressan, R. A., Zhu, J. K., & Bonhert, H. J. (2000). Plant cellular and molecular responses to high salinity. *Annu. Rev. Plant Physio. PlantMol.Biol.*, 51, 463-499. <http://dx.doi.org/10.1146/annurev.arplant.51.1.463>
4. Srinivas J., Purushotham A.V. and Murali Krishna K. (2013) The effects of Heavy metals on Seed Germination and Plant Growth on *Coccinia*, *Mentha* and *Trigonella* Plant Seeds in Timmapuram, E.G. District, Andhra Pradesh, India. *Int. Res. J. Environment Sci.* 2(6), 20-24
5. Siedlecka, A., Tukendorf, A., Skórzyńska-Polit, E., Maksymiec, W., Wójcik, M., Baszyński, T., Krupa, Z., 2001. Angiosperms (Asteraceae, Convolvulaceae, Fabaceae and Poaceae; other than Brassicaceae). In: Prasad, M.N.V. (Ed.), *Metals in the Environment*. Marcel Dekker Inc., New York, pp. 171–215.
6. Vanaja, M., S.K. Yadav, G. Archana, J.N. Lakshmi, P.R. Ram Reddy, P. Vagheera, S.K. Abdul Razak, M. Maheswari, and B. Venkateswarlu. 2011. Response of C4 (maize) and C3 (sunflower) crop plants to drought stress and enhanced carbon dioxide concentration. *Plant Soil Environ.* 57:207-215.
7. Blikhina, O., Virolainen, E., Fagerstedt, K.V., 2003. Antioxidants, oxidative damage and oxygen deprivation stress: a review. *Ann. Bot.* 91, 179–194.
8. Lungu, L, Popa, C., Morris, J., & Savoiu, M. (2011). Evaluation of phytotoxic activity of *Melia azedarach* L. extracts on *Lactuca sativa* L. *Romanian Biotech. Letters*, 16(2), 6089- 6095.
9. Feizi, M., Aghakhani, A., Mostafazadeh-Frad, B., & Heidarpour, M. (2007). Salt tolerance of wheat according to soil and drainage water salinity. *Pakistan J. Biol. Sci.*, 10(17), 2824-2830. [http:// dx.doi.org/ 10.3923/ pjbs. 2007. 2824. 2830](http://dx.doi.org/10.3923/pjbs.2007.2824.2830)
10. Athar Rana and Ahmad M. (2010). Heavy Metal Toxicity: Effect on Plant Growth and Metal Uptake by Wheat, and on Free Living Azotobacter. *water Air pollution* .v.138.N.1-4.P:165-180.





Intedhar Abbas Marhoon et al.

11. Tewari, R.K., Kumar, P., Sharma, P.N., Bisht, S.S., 2002. Modulation of oxidative stress responsive enzymes by excess cobalt. *Plant Sci.* 162, 381–388.
12. Zhao, X., Tan, H. J., Liu, Y. B., Li, X. R., & Chen, G. X. (2009). Effect of salt stress on growth and osmotic regulation in *Thellungiella* and *Arabidopsis callus*. *Plant Cell Tissue Organ Cult.*, 98, 97-103. <http://dx.doi.org/10.1007/s11240-009-9542-x>
13. Shalata, A., Mittova, V., Volokita, M., Guy, M., Tal, M., 2001. Response of the cultivated tomato and its wild salt-tolerant relative *Lycopersicon pennellii* to salt-dependent oxidative stress: the root antioxidative system. *Physiol. Plant.* 112, 487–494.
14. Tan, J., H. Zhao, J. Hong, Y. Han, H. Li and W. Zhao. 2008. Effects of exogenous nitric oxide on photosynthesis, antioxidant capacity and proline accumulation in wheat seedlings subjected to osmotic stress. *World J. Agric. Sci.* 4(3):307- 313.
15. Unyayar, S., Y. Keles, and E. Unal. 2004. Proline and ABA levels in two sunflower genotypes subjected to water stress. *Bulg. J. Physiol.* 30(3-4):34-47.
16. Gunes, A., Soylemezoglu, G., Inal, A., Bagci, E.G., Coban, S. and Sahin, O. 2006. Antioxidant and stomatal response of grapevine (*Vitis vinifera*L.) to boron toxicity. *Sci. Hort.* 110:279-284.
17. Shinohara, T. and D. Leskovar. I. 2014. Effects of ABA, anti transpirants, heat and drought stress on plant growth, physiology and water status of artichoke transplants. *Scientia Horticulturae.* 165 : 225–234.
18. Al-Grawi, E.D.C., and G.R.L. Al-Awsi. 2018. "Expression of CDKN2A (P16/Ink4a) among Colorectal Cancer Patients: A Cohort Study." *Journal of Pharmaceutical Sciences and Research* 10 (5).
19. Hussain, s., A. Muhammad. A. Saeed. I. Javaid. S. Muhammad. N. Sajid Sagheer. and I. Muhammad .2013. Improvement of Drought Tolerance in sunflower (*Helianthus annuus* L.) By Foliar Application of Abscisic Acid and Potassium Chloride. *Pak. J. Nutr.*12(4): 345-352.
20. Saleem, M. F., S. Hussain. M. A. Cheema. M. Y. Ashraf. and M. A. Haq.2010. Abscisic acid, a stress hormone helps in improving water relations and yield of sunflower (*Helianthus annuus* L.) hybrids under drought. *Pak. J. Bot.* 42 (3): 2177-2189.
21. Heged, A., Erdei, S., Horvath, G., 2001. Comparative studies of H₂O₂ detoxifying enzymes in green and greening barley seedlings under cadmium stress. *Plant Sci.* 160, 1085–1093.
22. Munne-Bosch, S. and Alegre, L. 2002. Plant aging increases oxidative stress in chloroplasts. *Planta* 214:608-615.
23. Islam MZ, Mia MA, Islam MR, Akter A (2007) Effect of different Saline levels on growth and yield attributes of mutant rice. *J. Soil. Nature* 1(2): 18-22.
24. Cavalcanti, F.R., Oliveira, J.T.A., Martins-Miranda, A.S., Viegas, R.A., Silveira, J.A.G., 2004. Superoxide dismutase, catalase and peroxidase activities do not confer protection against oxidative damage in salt-stressed cowpea leaves. *New Phytol.* 163, 563–571.
25. Tammam AA (2003) Response of *Vicia faba* plants to the interactive effect of sodium chloride salinity and salicylic acid treatment. *Acta Agronomica Hungarica* 51(3): 239-248. <https://doi.org/10.1556/AAgr.51.2003.3.1>
26. Ghaffari, M., M. Toorchi. M. Valizadeh. M. R. Shakiba.2012. Morpho-physiological Screening of Sunflower inbred lines under drought stress condition CO. *Turkish Journal of Field Crops.* 17(2):185-190.
27. Majeed, A. A., Bano. M. Salim. M. Asim. and M. Hadees .2011. Physiology and productivity of rice crop influenced by drought stress induced at different developmental stages. *African Journal of Biotechnology.* 10(26): 5121-5136.
28. Liu, S., Jia-guo Li, Hua X., and Xiao-feng W.(2017) Super absorbent polymer seed coatings promote seed germination and seedling growth of *Caraganakorshinskii* in drought. *J Zhejiang Univ Sci B;* 18(8): 696–706.
29. Vanaja, M., S.K. Yadav, G. Archana, J.N. Lakshmi, P.R. Ram Reddy, P. Vagheera, S.K. Abdul Razak, M. Maheswari, and B. Venkateswarlu. 2011. Response of C4 (maize) and C3 (sunflower) crop plants to drought stress and enhanced carbon dioxide concentration. *Plant Soil Environ.* 57:207-215.
30. Geetha, A., J. Suresh. and p. Saidaiah. 2012. Study on response of sunflower (*Helianthus annuus*L.) genotypes for root and yield characters under water stress. *Current Biotica.* 6(1): 32-41.





Intedhar Abbas Marhoon et al.

Table 1. Some of the environmental stresses and their subsequent effects and plant responses to them.

Stress type	The effect	Plant responses
Thermal stress	High temperature (T) leads to high evaporation and lack of water. This results in an increase in the enzyme transformation and thus the death of the plant(Gunes,et al., 2006) ⁽¹⁶⁾ .	Work the protein repair systems efficiently and try to stability, which increases the chance of survival of the plant. T can lead to plant acclimatization
Cold stress and freezing.	The biochemical reactions are slowed, the photosynthesis increases, the slower the CO ₂ fixation, resulting in damage to the oxygen roots. The freezing formation of ice crystals causes damage to cell membranes.	Plant growth ceased. In species that adapt, they may be overtaken by secondary metabolism change. The formation of ice crystals can be avoided by the accumulation of osmotic solutions and the manufacture of cells for water-loving proteins(Shinohara and Leskovar, 2014) ⁽¹⁷⁾ .
Drought stress	The inability of the plant to transfer water to the leaves, causing a reduction in the speed of photosynthesis(Hussain, et al., 2013) ⁽¹⁸⁾	Wrapping of leaves and other morphological adaptations. Closing the stomata will reduce the result of the ABA buildup. The accumulation of secondary metabolic compounds reduces the internal water.
Stress immersion with water and flooding	Reduces oxygen levels (anoxia) and anaerobic conditions interfere with mitochondrial respiration(Saleem, et al., 2010) ⁽¹⁹⁾ .	Developments in the spaces within the roots which facilitates the exchange of O ₂ and ethylene between the vegetative and roots growth (aerenchyma).
Mineral accumulation stresses	In the case of increased mineral accumulation, detoxification reactions may be insufficient and accumulation may be more than the cell's ability to store	Increased accumulation of mineral ions may be controlled by transferring them to the gaps and may generate free oxygen roots(Heged,et al., 2001) ⁽²⁰⁾ .
High-light stresses	Increased light increases the production of high intermediate compounds for interaction and the formation of accidental products that cause damage as a result of photooxidation and the discontinuation of photosynthesis	Increased exposure to light caused inhibition of manufacturing and production of ROS. The latter oxidizes fats, proteins, and enzymes necessary for the performance of the cell's functions(Munné-Bosch,et al., 2002) ⁽²¹⁾ .





Intedhar Abbas Marhoon et al.

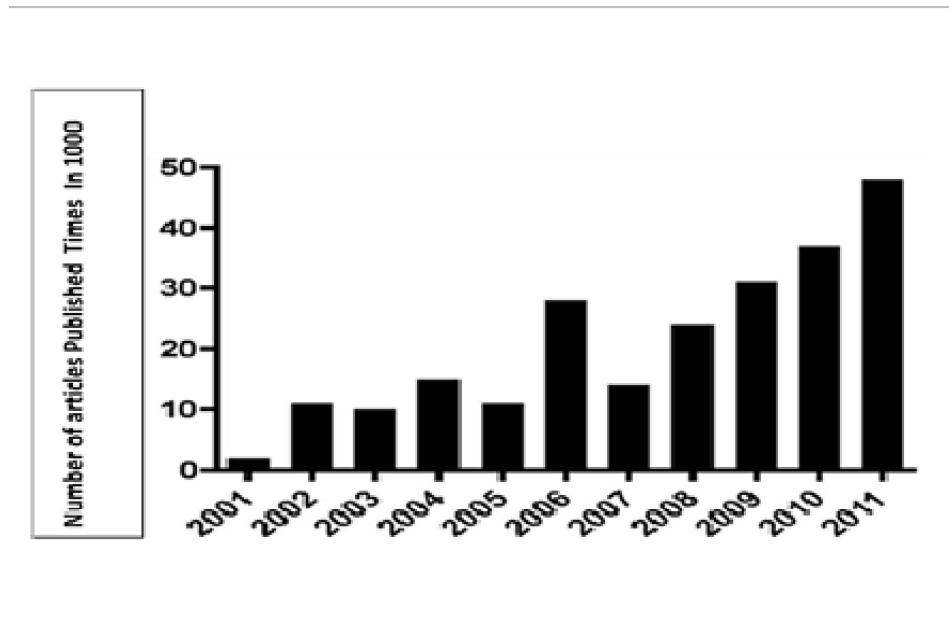


Figure.1. The number of publications in the years 2001 through 2011 published in international magazines regarding the election of plants for stress-tolerant.

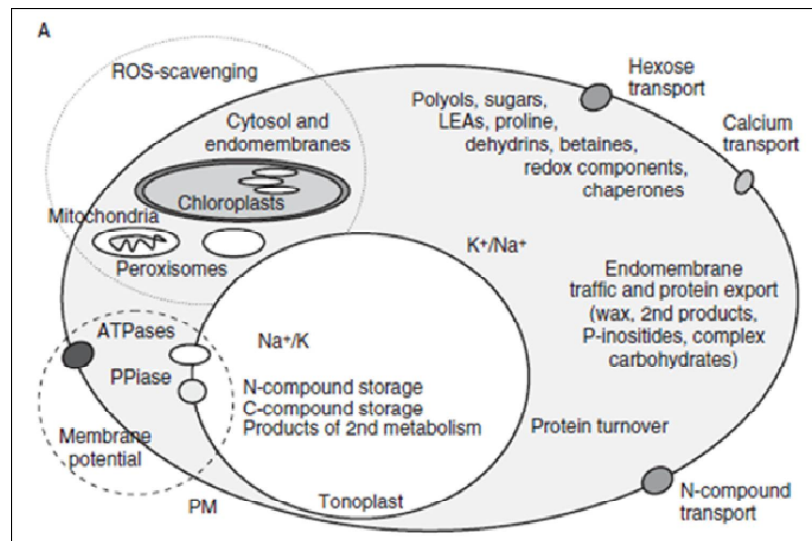


Figure 2: Biochemical determinants to stress tolerance

